Relationships Between Organic Maturity and Inorganic Geochemistry in Upper Jurassic Petroleum Source Rocks from the Norwegian North Sea and the United Kingdom.

by

Bryn Jones

A thesis submitted in fulfilment of the requirements for the degree of Doctor of Philosophy.

Department of Geology, The University of Newcastle upon Tyne.

March 1991.

Contents

Abstract

The aim of this study was to examine the relationship between organic maturity and trace element geochemistry of organic rich mudstones, to assess their behaviour as sources or sinks of metals during diagenesis, and their role in mineral deposit genesis. The suite studied consisted of 193 samples from the Draupne, Heather, and Kimmeridge Clay Formations from the Norwegian North Sea and onshore UK.

All three formations had above average contents of C and S, and the Draupne and Heather Formations had a low carbonate content. The Draupne Formation was particularly enriched in a number of trace elements but only Cr, Mo, Nb, and U were enriched in all three formations. After transformation of the data to avoid difficulties in interpretation, correlation analysis allowed the trace elements to be divided into three groups on the basis of their mineralogical residences.

The use of a battery of geochemical and mineralogical indices demonstrated that variation in sedimentological and environmental factors were significant within the formations studied, and that the relationship between organic maturity and trace element content could not be investigated in isolation. The technique of path analysis was used to assess the strength and nature of this relationship relative to the variation due to other causes.

Pb and Zn were found to increase with increasing maturity in both the Draupne and Heather Formations, and Mo was found to decrease. U was seen to decrease, and Cd to increase, in the Draupne Formation only, where they were especially abundant. It is believed that Pb and Zn were supplied by migrating basinal brines which may have acted to remove Mo and U. Other processes which may have mobilised these elements are the in situ generation of organic acids and hydrocarbons..

Acknowledgements

I would like to express my appreciation firstly to David Manning who supervised this work, and with whom I have had numerous interesting discussions. I am also grateful to Nils Telnaes of Norsk Hydro for access to the North Sea samples, facilities, and data, and to Charles Curtis for supplying the onshore samples studied.

Thanks are due to the staff and students of the departments of geology of Newcastle University (now sadly no more), and Oxford Polytechnic, for their continuous encouragement and assistance during the completion of this thesis, and particularly to the late Peter Oakley whose advice benefitted greatly the analytical component of the project.

Financial assistance was provided by N.E.R.C.

Finally I would like to thank my family, especially my wife, Heather, for the support given during the completion of this volume.

Chapter One

Introduction

1.0 Introduction

1.1 Aims of this project

As described below mudstones and especially metal rich black shales may be linked in a number of ways with sediment hosted Pb-Zn deposits, and may have acted either directly as a source of metals, or indirectly as a source of solvents which may liberate metals from elsewhere. It is also possible that mudstones retain their ability to fix metals during burial diagenesis and may fix metals from migrating solutions, becoming recipients of metals as well as possible donors, and having the potential to become ore deposits themselves.

The aim of this project is to investigate the nature of the relationships existing between black shale petroleum source rocks and ore deposits, particularly of the sediment hosted Pb-Zn variety. This aim was to be achieved by means of geochemical analysis of a suite of organic rich mudrocks of known organic maturity with a view to examining the strength of the relationships between organic maturity and the inorganic geochemistry. Particular reference was paid to those elements, present in trace amounts in shales, but which when concentrated by ore forming processes produce the deposits of interest namely Pb and Zn.

Ideally for a study of this nature one requires a set of samples where the maturities are known, and where they are distributed evenly over the maturity range relevant to diagenesis and catagenesis during which the processes linking shales to ore deposition are believed to operate. Again ideally the sample suite should be otherwise entirely uniform, that is, that over the period during which the samples were deposited, and over the geographical area studied there should be no variation in factors such as source area, nature of source rock, extent of weathering, transport and sedimentary processes, depositional environment etc, all of which may contribute to variation in the geochemistry which at best would lead to increased noise in the data set if the effects were only random, and which at worst might lead to a systematic

bias if the variation occurred in some manner such that it was correlated with organic maturity of the samples.

Such an ideal sample set would be difficult if not impossible to achieve and the sample set involved in this study does not meet these ideal requirements in their entirety. In order that the data produced might be usefully interpreted some means of removing the noise or bias due to differences in the samples not caused by organic maturity variation must be employed. The methods used here are those of multivariate statistical analysis, the methodology employed being discussed in the appropriate chapter.

The sample suite available for this study comprises samples from three Upper Jurassic mudstone formations from the Norwegian sector of the North Sea and the United Kingdom. From the North Sea 72 samples of the Draupne Formation and 69 of the Heather Formation were obtained all from core and sidewall core. These samples were provided by Norsk Hydro. In the United Kingdom 52 samples of the Kimmeridge Clay were obtained, these coming from boreholes. The effects of weathering should therefore be minimal. Small sample sizes particularly affected the North Sea sample suite and in some cases prevented a complete analysis from being performed resulting in variation in the total number of samples analysed for different elements. The maturity of the studied suite varies from vitrinite reflectances (R_o) of about 0.4% minimum to a maximum of about 1.1% which does effectively cover the range of diagenetic and catagenetic reactions of interest, but the maturity distribution is scattered, and is dominated by the lower values.

1.2 A summary of sediment-hosted Pb-Zn deposits

Sediment hosted Pb-Zn deposits have historically been a major source of world Pb and Zn and remain important today, accounting for half of world production of these metals. The deposits have recently been summarised in a number of papers (eg Macqueen, 1979; Ohle, 1980; Gustafson and Williams, 1981; Anderson and Macqueen, 1982; Sangster, 1990). Two

main sub-types can be identified, the carbonate hosted and generally epigenetic Mississippi Valley Type (MVT), and the usually clastic hosted syngenetic sedimentary exhalative type (Sedex type). The differences between the two sub-types are mainly a result of the differing timing of mineralisation relative to host rock deposition, and in reality the two types are likely to be end members of a continuum of deposit types rather than having a discrete existance (Gustafson and Williams, 1981; Lydon, 1986; Sangster, 1990).

The MVT deposits (eg Tri-State, Upper Mississippi Valley, Pine Point) are usually found in relatively undisturbed and unmetamorphosed shallow-water carbonate platform host rocks, which in most cases are dolomitic. In age they range from Proterozoic to Mesozoic but deposits are most common in the Palaeozoic. They are usually located adjacent to the margins of intracratonic basins, or within such basins on structural highs. Often numerous individual ore bodies may be concentrated in districts which can be located over a wide geographical area. The deposits are stratabound but not stratiform in nature and are usually found as cements in solution collapse breccias or palaeokarst. The association between ore and pre-existing porosity illustrates the importance of this factor on this type of mineralisation. The ore bodies are also often associated with reef structures or with facies changes between carbonate and shale, although deposits in uniform lithologies are also common.

Sedex Pb-Zn deposits (eg McArthur River) are also found in intracratonic settings, usually in fault bounded basins, from the Proterozoic onwards. The ore bodies are generally stratiform and may be associated with a stockwork type deposit beneath. The ores are found in host rocks deposited in a variety of environments, with varying amounts of clastic input, and in both deep and shallow water conditions (eg greywackes, shales, marls, carbonates, and locally derived breccias and conglomerates of these rock types). Some but by no means all Sedex deposits may have been associated with anoxic depositional conditions.

The mineralogies of both types of deposit are relatively simple. MVT deposits are composed of galena and sphalerite as the main ore minerals with pyrite and marcasite (sometimes with

chalcopyrite), and less commonly with fluorite and barite, although these may be important in some localities. The galena is usually low in Ag, and the sphalerite low in Fe. Other elements which may be present include Cd, Co, Cu, Ge, and Ni. The grain size of the ore minerals is relatively coarse suggesting a low rate of precipitation but some deposits have much finer textures. Organic matter (as bitumen) is also common in some deposits. Pb and Zn are the main elements of economic interest with Ag sometimes making up a useful by-product. Some deposits are now worked for barite and fluorite. The dominant sulphide minerals of the Sedex type are pyrite, pyrrhotite, sphalerite, and galena, and the deposits are usually richer in Fe and Ag than are MVT deposits. The major minerals may be accompanied by chalcopyrite and arsenopyrite, with or without barite, while some Ag rich deposits may include Ag minerals. The grain size is usually fine. Pb and Zn (sometimes plus Ag and Ba) are once more the main economic targets. Ore types may be massive, interlayered with the host, or disseminated.

Sedex type deposits are generally larger that their MVT counterparts (some have over 10,000,000 tonnes Pb+Zn) and are similar in size to the larger MVT districts. Zn/Pb ratios in the majority of MVT deposits are about 4, and ore grades of 2-6% Zn and 1-3% Pb are common. In Sedex types the Zn/Pb ratios are more variable but are usually 1-4, with the higher values occuring in carbonate hosts. Zn concentrations are usually 2-10%, and Pb 1-4%.

1.3 Genesis of sediment hosted Pb-Zn deposits

Both types of sediment hosted Pb-Zn deposits show a conspicuous lack of association with any local igneous activity, which usually precludes this as being a major factor in the ore forming process. Sverjensky (1984) has remarked on the great similarities existing between the chemical and isotopic composition, and P-T range, of fluid inclusions (Hall and Friedman, 1963) from MVT deposits (and hence by implication the ore fluids themselves), and oilfield brines (Billings et al, 1969; Carpenter et al, 1974; Kharaka et al, 1987; Saunders and Swann, 1990) which are the dominant means by which deep formation waters may be sampled. The

limited fluid inclusion data from Sedex deposits (Gustafson and Williams, 1981) suggest that these too are similar, if trapped at slightly higher temperatures. This has led to current theories on the genesis of these deposits which favour a sedimentary origin for the ore forming fluids (Gustafson and Williams, 1981; Anderson and Macqueen, 1982; Lydon, 1983, 1986; Sverjensky, 1984, 1987; Sangster, 1990).

The popular genetic model for MVT ore deposits remains the the basinal brine mechanism first proposed in the 1960s by workers such as Noble (1963), Beales and Jackson (1966), and Jackson and Beales (1967). This has recently been restated by Anderson and Macqueen (1982). The fundamental points of this model are that hot, saline brines, derived from sedimentary basins acquire metals by some process, and are laterally expelled from the basin by compaction. The brines migrate via aquifers to the basin margins where the accumulated base metals are precipitated in the carbonate host rocks of the interbasin platform areas. Precipitation mechanisms may involve cooling, dilution, or contact with sulphide bearing solutions (Anderson, 1975).

While the main points of the model are still generally accepted it has been modified in detail by a number of workers since it was first proposed. Thermal modelling by Cathles and Smith (1983) demonstrated that in order for the migrating brines to maintain a temperature of 100-150°C (indicated from fluid inclusion studies of the ore deposits) after migration over distances running into hundreds of kilometers the flow must have been episodic, with pulses of rapid fluid movement interspersed with periods of quiescence. These authors supported the proposal of Sharp (1978) that the episodic brine movement was a result of the progressive development of geopressurised zones, followed by rupture of these zones allowing rapid escape of hot saline fluids. An alternative to the compactional expulsion of fluids from sedimentary basins has been given by Garven (1984) and Garven and Freeze (1985a and b). These authors suggest that topographic uplift of part of a sedimentary basin will result in gravity driven groundwater movement away from the uplifted area, and that such movement can satisfy the thermal constraints imposed from ore deposit studies.

Models for the genesis of Sedex deposits also generally concentrate on basinal brines which are hot and metal rich (Gustafson and Williams, 1981; Badham, 1981; Lydon, 1983, 1986). Large scale lateral migration is not a necessity for the formation of Sedex deposits however, unlike their MVT counterparts. Instead brine migration must have a large cross stratal component allowing the hot metal rich brines to reach the sediment surface within the basin itself. Vertical migration in Sedex genetic models is usually accomplished via syn-sedimentary faults (Gustafson and Williams, 1981; Lydon 1983, 1986). As in MVT deposits the probability that fluid flow is episodic, and possibly related to the development and rupture of geopressurised zones has been noted (Lydon, 1983, 1986).

The main physical and morphological differences between the two types of deposit result from the differing timing and environment of mineralisation. In the formation of Sedex deposits it is likely that the mineralising fluids were episodically expelled onto the sea floor from hydrothermal mounds, which were probably above syn-sedimentary (growth) faults, and around which the sulphides precipitated, resulting in syn-genetic ore formation (Russell, 1978; Lydon, 1983, 1986). In contrast, for the formation of MVT deposits the metal bearing ore fluids must migrate for some considerable distance out of the basin of their origin prior to introduction into the carbonate host rocks in which the sulphides precipitate as pore filling cements in the shallow subsurface (Anderson, 1975; Anderson and Macqueen, 1982; Sverjensky, 1984, 1987).

1.4 Direct links between mudstones and Pb-Zn ore deposits

The metal source for sediment hosted Pb-Zn deposits is still controversial (Ohle, 1980; Anderson and Macqueen, 1982, Sangster, 1990). Mudstones, and especially the subset that is black shale, were amongst the first metal sources to have been suggested (Beales and Jackson, 1966; Dozy, 1970), and have also been proposed as the source of the metals of the oilfield brines of Canada and the Gulf Coast (Billings et al, 1969; Carpenter et al, 1974)

which have elevated metal concentrations. Factors in favour of shales as a potential source of metals for sedimentary ore deposits include their relative abundance in the sedimentary column, the often high content of metals present, the loosely bound nature of a large proportion of the metals, and their composition which may include large quantities of clay minerals and organic matter, both of which are relatively reactive under diagenetic and catagenetic conditions. One disadvantage which has been suggested is the relatively low permeability of mudstones which may prevent effective large scale interaction between rock and brine.

Further evidence in support of shales as a potential source rock for ore deposits has been gained from laboratory leaching experiments (Hirst, 1971; Hathaway and Galle, 1978; Hathaway et al, 1979; Long and Angino, 1982; Thornton and Seyfried, 1985). These experiments have been performed using a variety of solvents, both organic and inorganic, synthetic and natural, and show that metals such as Pb and Zn may be mobilised from shales in geologically significant amounts by concentrated brines. Pb/Zn ratios obtained in the experiments of Thornton and Seyfried (1985) are similar to the range of metal ratios observed in natural metal rich oilfield brines, and in sedimentary Pb-Zn ore deposits.

It is now accepted that sedimentary processes can account for the often elevated metal concentrations found in oilfield brines, and hence by implication for the metals in sediment hosted Pb-Zn deposits, and that the thick sequences of often metal rich mudstones found in most sedimentary basins are a likely source of these metals. However the processes responsible for production of brines of the necessary high salinity required for effective metal leaching and transport are not entirely clear (Hanor et al, 1988). Eugster (1985) has stressed the importance of evaporite dissolution as means of producing metal rich fluids especially where the evaporites and black shales have a close stratigraphic association. Carpenter et al (1974) and Kharaka et al (1987) believe that residual bittern brines resulting from salt deposition are the main cause of the high salinities of Gulf Coast brines, and Graf (1982) has

suggested that membrane filtration by overpressured shales may result in significant salinity increases in formation waters.

In summary mudstones, and especially black shales which may be very metal rich, provide a possible source for the metals of sediment hosted Pb-Zn deposits provided that solutions of high salinity capable of leaching and transporting them are present. In this sense there may be a direct connection between the mudstones as a source of metals and the ore deposits as eventual sinks.

1.5 Indirect links between mudstones and Pb-Zn ore deposits

Mudstones need not be directly related to Pb-Zn ore deposits as described above, where they are considered as metal sources, but may be related indirectly as a source of solvents which can increase the metal transporting ability of formation waters enabling them to leach metals from formations interbedded with the mudstones themselves.

The role of organic acid anions has recently been recognised as an important consideration as a result of a number of recent studies (eg Carothers and Kharaka, 1978; Surdam et al, 1984; Surdam and Crossey, 1985a and b; Kharaka et al, 1985; Fisher, 1987; MacGowan and Surdam, 1988; Surdam et al, 1989). Both mono- and di-carboxylic acids have been identified in oil field brines although in most cases acetate is by far the most abundant. The organic anions have been found in concentrations up to 10000ug/ml (Carothers and Kharaka, 1978; Surdam et al, 1984; Fisher, 1987; MacGowan and Surdam, 1988) and usually dominate the measured alkalinity. Carothers and Kharaka (1978) showed that acid concentrations in formation waters are low (<60ug/ml) at temperatures of <80°C, probably because of bacterial degradation. Above this temperature organic acid anion concentrations increase rapidly to maxima of several thousand ug/ml in the region of 80-100°C and then begin to decrease with increasing temperature as a result of thermal decarboxylation, approximately zero concentrations being reached at 200°C. Experimental work on the rate of decarboxylation

shows that considerable ranges may exist (Kharaka et al, 1983; Drummond and Palmer, 1986; Palmer and Drummond, 1986) and Shock (1988) has suggested that organic acids may exist in a metastable state.

The di-carboxylic acids present in oilfield waters may reach concentrations of up to 2500ug/ml in the 80-100°C temperature window with malonic and oxalic being dominant (Kharaka et al, 1985; Kawamura and Kaplan, 1987; Surdam and MacGowan, 1987; MacGowan and Surdam, 1988). They may make up a significant proportion of the total acid anion content over this interval, but concentrations fall rapidly above about 100°C because of the lower thermal stability of the di-carboxylic acids in relation to the mono-functional acids.

The high concentrations of mono- and di-functional acids are probably the result of thermal degradation of kerogen during burial (Kharaka et al, 1985; Surdam and Crossey, 1985a and b; Surdam et al, 1989) the carboxylic acids being attached peripherally to the kerogen core (Surdam and Crossey, 1985a and b; Surdam et al, 1989). Kerogen shows a particularly rapid decrease in atomic O/C ratios during early burial as the carboxylic acids are lost. Surdam and Crossey, 1985a and b, and Crossey et al, 1986 have suggested that further organic acids may be generated from kerogen during burial by oxidation by mineral oxidants such as Fe^{3+}. The smectite-illite clay transition may be important in this respect as it generally occurs at temperatures similar to those of acid generation and involves the release of Fe^{3+}.

Organic acid generation will be dominated by input from mudstones in mixed mudstone/sandstone sequences as the argillaceous rocks will generally contain the bulk of the kerogen in the sequence and may also have an abundance of smectite or mixed layer clays and other suitable mineral oxidants. Within the mudstones the concentrations of the organic acids may be very high. Hower et al (1976) have demonstrated the decrease to zero of K feldspar in Gulf Coast shales at temperatures in the 80-100°C range which may be a result of high acid concentrations (see below) but their data indicates that there is no bulk change in the chemical composition of the shales with the exception of Ca which is lost. The Si, Al,

and K released from the dissolved feldspar are apparently conserved within the shales, the K and Al being precipitated as illite and the Si probably as quartz.

The organic acids expelled from the shales are believed to be an important factor in the diagenesis of adjacent sandstones (Moncure et al, 1984; Surdam et al, 1989). The important role that organic acids may play in diagenesis stem from a number of properties summarised by Kharaka et al (1985). Firstly they can be the dominant source and sink of H^+ and are thus important in controlling the pH and buffer capacity of the pore waters, secondly they have the ability to control Eh and so the concentration of some multivalent ions in solution, thirdly they can be decarboxylated to CO_2 and hydrocarbons, and finally they can form soluble complexes with metals.

Organic acids may also play an important role in aluminosilicate diagenesis (Surdam et al, 1984; Surdam and Crossey, 1985a and b; Surdam and MacGowan, 1987; MacGowan and Surdam, 1988). Dissolution of minerals such as feldspar (a common feature in sandstones) is essentially a problem of aluminium mobility. In the inorganic system Al solubility is very low resulting in in situ alteration (eg to kaolinite, the framework grain alteration of Siebert et al, 1984). Laboratory experiments (Surdam et al, 1984; Surdam and Crossey, 1985a and b; MacGowan and Surdam, 1988) have shown that carboxylic acid anions especially dicarboxylic and aromatic acids are particularly effective at increasing Al solubility (by complexing), and can raise Al solubility by over 4 orders of magnitude over kaolinite saturation. MacGowan and Surdam (1988) have also shown experimentally that feldspars are unstable in the presence of some oilfield brines and organic acid destabilisation of feldspar has been suggested by Fisher and Boles (1990) to account for the concentrations of dissolved Al found in Californian sandstone reservoirs. MacGowan and Surdam (1988) have proposed that such measurements of Al concentrations in oilfield waters and many of the measurements of difunctional acid concentration may however be erroneously low because of sampling and analytical difficulties. Feldspar dissolution will occur in the 80-100°C temperature window when difunctional acid concentrations are at maximum (resulting in the framework grain

dissolution of Siebert et al), and corresponding to the period of potential carbonate dissolution.

Moncure et al (1984) and Siebert et al (1984) have shown from a study of a cored sandstone/shale sequence that feldspars were preferentially dissolved and porosity enhanced in sandstone close to the shale contact, and that sandstones with high original permeability showed the greatest feldspar dissolution. This was interpreted as being a result of the expulsion of brines from the shale and the removal of Al by complexing, brines being channelled through the more permeable sandstones. Near the sandstone/shale interface kaolinite was insufficient to account for the Al removed from decomposed feldspar, whereas at a greater distance the kaolinite present was far greater than that available from local feldspar dissolution suggesting movement of Al away from the zone of greatest feldspar dissolution and later precipitation.

Surdam et al (1989) have shown that a paragenetic sequence may be predicted on the basis of the reactions likely to occur as organic acids are released from mudstone source rocks into adjacent sandstones over the temperature interval 80-200°C. This sequence is consistent with observed paragenesis of many sandstones (MacGowan and Surdam, 1987). For maximum interaction to occur between organic acid rich brines from mudstone source rocks and sandstone reservoirs, and for optimum development of enhanced porosity a number of factors have been identified (Moncure et al, 1984; Surdam et al, 1989). The ratios of shale to sandstone in the basin should be high, the sandstones should have good permeability, be feldspar rich, and short migration routes should be available between source and reservoir, allowing maximum flushing of the sandstones by expelled fluids. The mudstone sources should contain large amounts of organic material and this should be of type II or III (or type I and include mineral oxidants).

The interactions described above between solutions expelled from mudstones (rich in organic acids) with surrounding sandstone aquifers resulting in the generation of secondary porosity

may also be important from the point of view of ore genesis. Secondary porosity is usually thought to result from the partial or complete dissolution of the detrital feldspar content of sandstones. Any such dissolution of feldspars, particularly K-feldspar but also plagioclase, will result in release of Pb to the formation waters. Those MVT deposits involving long distance migration through feldspar bearing aquifers may be particularly sensitive to ore fluid modification in this manner (Sverjensky, 1984). Both Pb and Zn and other metals may also be mobilised from reddened sandstones by leaching from oxide phases (Zielinski et al, 1983). Such a mechanism for metal mobilisation would result in a more indirect link between shale and ore deposit.

Mudstones may also be linked indirectly to ore deposit genesis by their contribution to the transport of metals from their source, whatever it may be, to the eventual sink which might be the ore body. This may occur in two ways. Firstly the high concentration of organic acids (particularly acetic) reported in some oilfield brines (Kharaka et al, 1987; Surdam et al, 1989) might significantly enhance the transport of base metals in aqueous fluids by complexation. Laboratory studies (Hennet et al, 1988; Yang et al, 1989; Giordano, 1989) have shown that acetate complexes of both Pb and Zn are stable at temperatures of up to 200-300°C, and have solubilities greater than the corresponding chloride complexes (Manning, 1986). Such complexes cannot be neglected in studies of oilfield (Na-Ca-Cl) brines and might even dominate the chloride complexes provided that acid concentrations are sufficient. Thermodynamic modelling of oifield brines (Kharaka et al, 1986, 1987) suggest that this may not be the case with chloride complexing being overwhelming. The results from such models depend however on assumptions made on parameters such as pH under reservoir conditions.

Secondly Pb and Zn may be to some extent transported in a mobile hydrocarbon phase (Manning 1986; Manning and Gize, in prep) possibly in porphyrin or related tetrapyrrole complexes. Indeed the metal contents of many petroleums are significant in comparison with the concentrations believed necessary in aqueous fluids for ore formation. This method of transport would favour Zn rather than Pb due to stability of the respective complexes, Pb

porphyrins being unlikely, however in co-existing brine/hydrocarbon fluids both metals are likely to be partitioned into the aqueous fluid. Most of the migrating hydrocarbons in a sedimentary basin would have a mudstone origin and the richest hydrocarbon source rocks are often those with elevated metal contents which might further enhance the possibilities of metal mobilisation.

1.6 Mudstones as ore deposits

Finally although mudstones have been considered above as possible sources of Pb and Zn for sedimentary hosted ore deposits, or as factors enabling elevated concentrations of the metals to be transported, the possibility also exists that they may continue to fix metals during burial diagenesis as they do during deposition and very early diagenesis (Coveney and Martin, 1983; Coveney et al, 1987). In some senses this would be the wheel come full circle, with mudstones fixing metals that have been mobilised from, or in association with, other mudstones. If this fixing was to occur during deposition then a mudstone would be a Sedex deposit in its own right. Similarly the Kupfershiefer Type of ore deposit (Eugster, 1985) would fall under this category.

1.7 Structure of this thesis

An introduction into the nature and aims of the current research has been given above. In Chapter 2 previous research on the Draupne, Heather, and Kimmeridge Clay Formations is reviewed. The data collected for this study is summarised on a mineral by mineral and element by element basis in Chapter 3, and comparison is made to published average shale compositions. Chapter 4 examines correlation matrices, the effects of closure being negated by the method of Aitchison (1986). The examination of correlations allows deductions to be made on the mineralogical residences of the elements. In Chapter 5 variations in the sedimentological properties of the sample suite are investigated employing a number of mineralogical and geochemical indices taken from the literature. In Chapter 6 the relative

importance of the differing factors controlling the trace element geochemistry of the suite is examined by means of path analysis (a variation of multiple linear regression) in order that the importance of organic maturity as an influence on the concentrations of the different trace elements be determined after removing the effects of variation in sedimentological factors. In Chapter 7 the results of these analyses are applied to possible economic uses in exploration for hydrocarbons and source rock evaluation. Results are discussed and conclusions presented in Chapter 8.

Chapter Two

Geological Setting

2.0 Geological Setting

2.1 Introduction

The samples investigated for this study are Upper Jurassic to Lower Cretaceous organic rich mudrocks from north-west Europe. Though being of broadly similar age the samples cover a wide geographical range (Fig. 2.1), and differing post-depositional histories have resulted in a

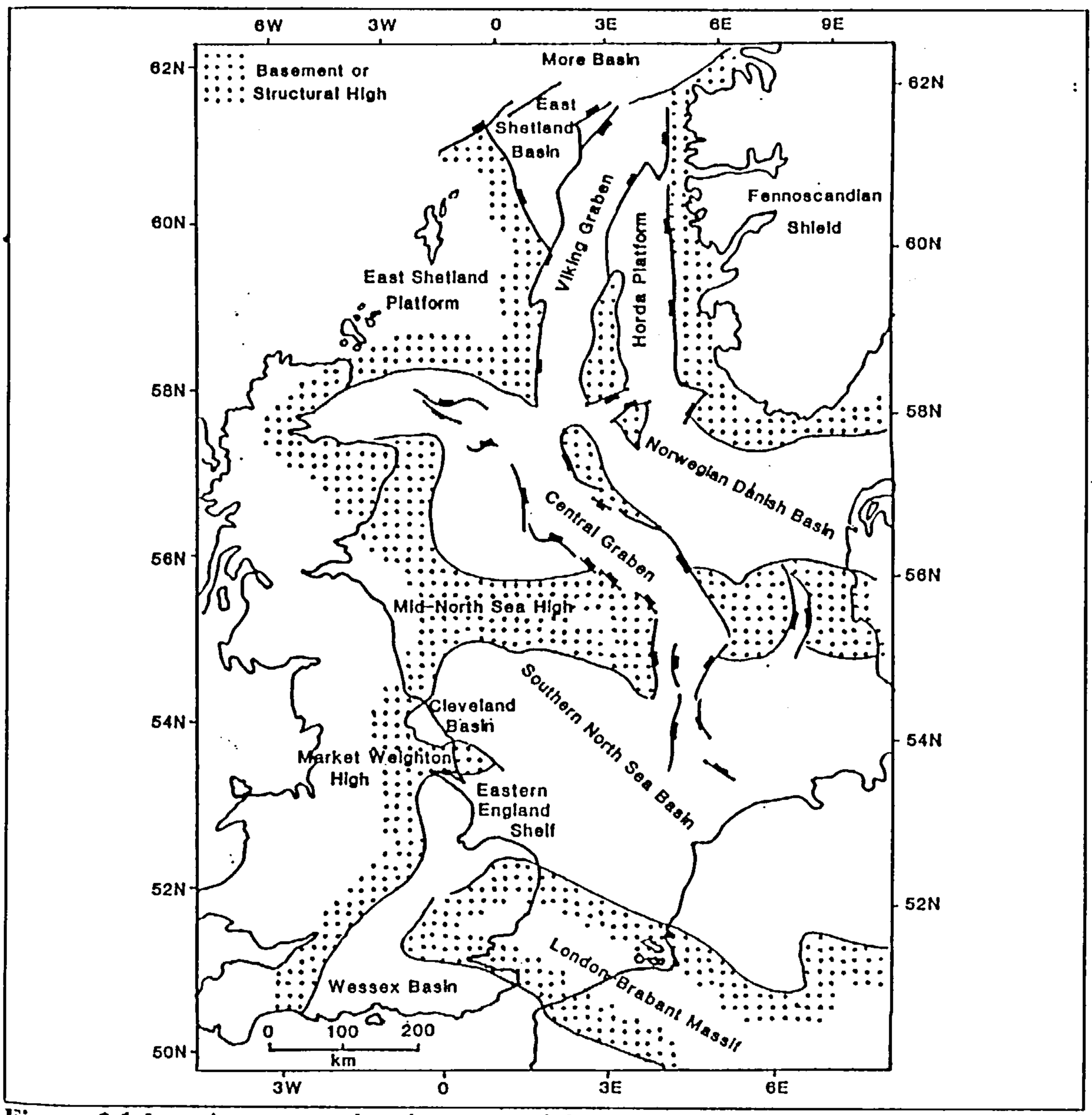

Figure 2.1 Location map and main structural features

wide range of thermal maturities. The suite comprises 72 samples of the Draupne Formation and 69 samples of the Heather Formation from wells in the Norwegian North Sea (core or side-wall core supplied by Norsk Hydro), and 52 samples of the Kimmeridge Clay Formation taken from boreholes throughout the length of the English outcrop.

2.2 Chronostratigraphic and lithostratigraphic nomenclature.

The Kimmeridgian stage was introduced by D'Orbigny (1842-1851) and was intended to be synonymous with the Kimmeridge Clay Formation of Dorset. In D'Orbigny's scheme the Kimmeridgian was followed by the Portlandian which was represented by the Portland Beds. A mistaken correlation of ammonites however led to much of the Dorset Kimmeridge Clay being included in the Portlandian as defined by D'Orbigny and this has led to a divergence in the meaning of the terms Kimmeridgian and Portlandian between English and European geologists, the Kimmeridgian Stage *sensu anglico* including the entire Kimmeridge Clay Formation whereas in European usage it includes only the Lower Kimmeridge Clay, the Upper Kimmeridge Clay being included in the Portlandian. Further complication arises from Upper Jurassic ammonite provinciality, with various claims being made in support of the Portlandian, Tithonian, or Volgian stages as the uppermost Jurassic stage. Boreal stage nomenclature will be used here as this follows normal usage in the Norwegian North Sea from where the majority of analysed samples originate. The Volgian Stage thus used overlaps with the Upper Kimmeridgian *sensu anglico* and is approximately equal to the Portlandian *sensu gallico*. Following the Volgian is the lowermost Cretaceous stage the Ryazanian.

As discussed above the Kimmeridge Clay Formation in its Dorset type area is Kimmeridgian to mid-Volgian in age but the use of the term Kimmeridge Clay Formation has more recently been extended offshore into the southern and northern North Sea (Rhys, 1974; Deegen and Scull, 1977) where its definition is substantially different from that onshore (Dore et al, 1984). The work of Rhys (1974) on wells off the coast of Yorkshire and Lincolnshire includes at the base of the formation the offshore equivalent of the Ampthill Clay which

underlies the lithologically similar Kimmeridge Clay throughout much of eastern England and thus lowers the base of the formation to the Upper Oxfordian. In the northern North Sea Deegan and Scull (1977) define the formation on the basis of its log responses. In the northern region it shows anomalously high gamma ray values and low sonic velocities, but due to lithological differences these are not seen in the southern North Sea wells of Rhys (1977). Chronostratigraphically the formation was extended still further, ranging from Oxfordian to Ryazanian (Dore et al, 1984) (Fig. 2.2).

In this thesis the lithostratigraphic scheme of the Norwegian Lithostratigraphic Nomenclature Committee (Vollset and Dore, 1984) will be followed. This suggests that in order to avoid ambiguity in the meaning of the name Kimmeridge Clay Formation its offshore use should be restricted to the southern North Sea following Rhys (1974). North of the Mid-North Sea High the Kimmeridge Clay Formation of Deegan and Scull (1977) is replaced by the Draupne

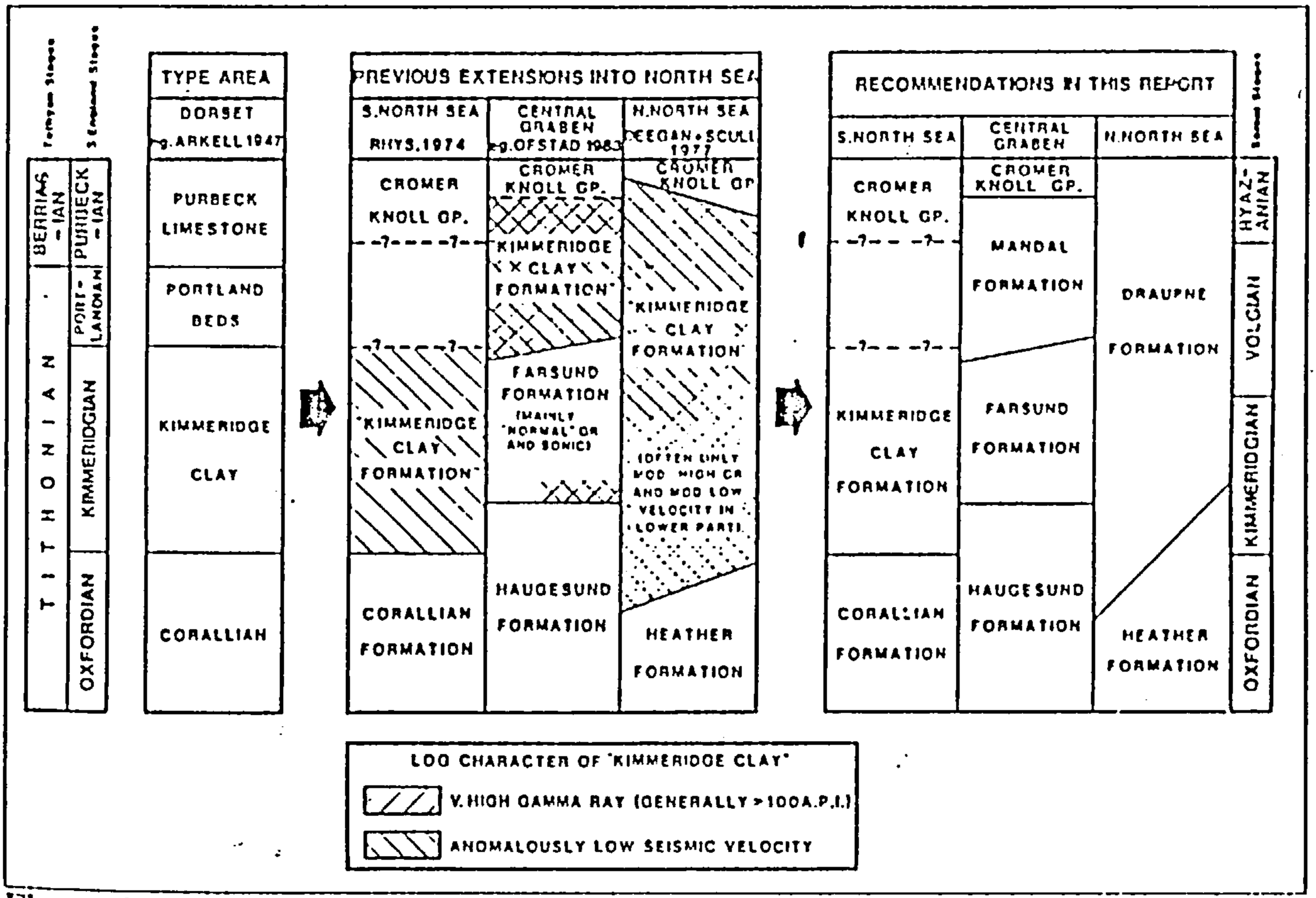

Figure 2.2 Lithostratigraphic recommendations of Vollset and Dore (1984) and their relationships with previous North Sea usage (Vollset and Dore 1984).

Formation retaining the definition based on log breaks, whilst in the Central Graben 'hot' shales commonly referred to as Kimmeridge Clay are named the Mandal Formation.

Below the Draupne Formation lies the Heather Formation (Deegen and Scull, 1977; Vollset and Dore, 1984) and this too is bounded by distinct log breaks. Its base is marked by the contrast with the underlying Brent sands and its top by the appearance of the 'hot' shale facies of the Draupne Formation. The Heather is Bathonian to Kimmeridgian in age and the Heather/Draupne contact is markedly diachronous. Vollset and Dore (1984) suggest that the name be applied only in areas north of the Mid-North Sea High.

Deegan and Scull (1977) included the widespread Kimmeridge Clay and Heather Formations together with the areally restricted Piper Formation in the Humber Group, which they extended from the southern North Sea where it was the offshore equivalent of the Oxford, Ampthill, and Kimmeridge Clays (Rhys, 1974). Vollset and Dore (1984) replaced the Humber Group in the northern North Sea by the Viking Group which consists of the Draupne and Heather Formations defined as above, together with three marginal sandy formations having restricted distributions on the Horda Platform, the Krossfjord, Fensfjord, and Sognfjord Formations.

2.3 The Mesozoic basins of North West Europe

2.3.1 Introduction

Between the Variscan Orogeny of the Carboniferous and the Tertiary Alpine Orogeny north west Europe underwent a period of crustal tension related to the breakup of Pangaea. This had two causes, the first being the late Triassic-Jurassic opening of the Tethys Ocean and the second being the opening of the North Atlantic which had begun in the mid-Carboniferous but was not complete until the late Palaeocene or early Eocene. A result of these crustal

stresses was the initiation in the late Carboniferous to Permian of a system of rift basins whose development was to dominate the post-Variscan evolution of the region.

McKenzie (1978) introduced a simple two stage model to describe the formation of intra-continental sedimentary basins by lithospheric extension. Continental lithosphere, initially in isostatic equilibrium and with its upper surface at sea level is instantaneously extended thinning the lithosphere and causing initial fault controlled subsidence due to isostatic disequilibrium. The upwelling of hot asthenosphere caused by extension results in a thermal anomaly which gradually decays causing further subsidence as isostatic equilibrium is maintained. This later phase of subsidence is achieved by lithospheric flexure and is regional in extent resulting in a steers head geometry. Subsequently many variations of McKenzie's (1978) model have been proposed to account for the nature of the North Sea basins and those of onshore England.

The sedimentary sequences in steers head basins contain numerous unconformities (Badley et al, 1984) which may be due to both local and regional tectonics or eustatic causes. Badley et al (1988) favour tectonics as the main cause though Rawson and Riley (1982) suggested sea level movement to be dominant. Sea levels are thought to have generally risen throughout the Jurassic and Cretaceous (Fig. 2.3), reaching a maximum Jurassic stand in the Kimmeridgian

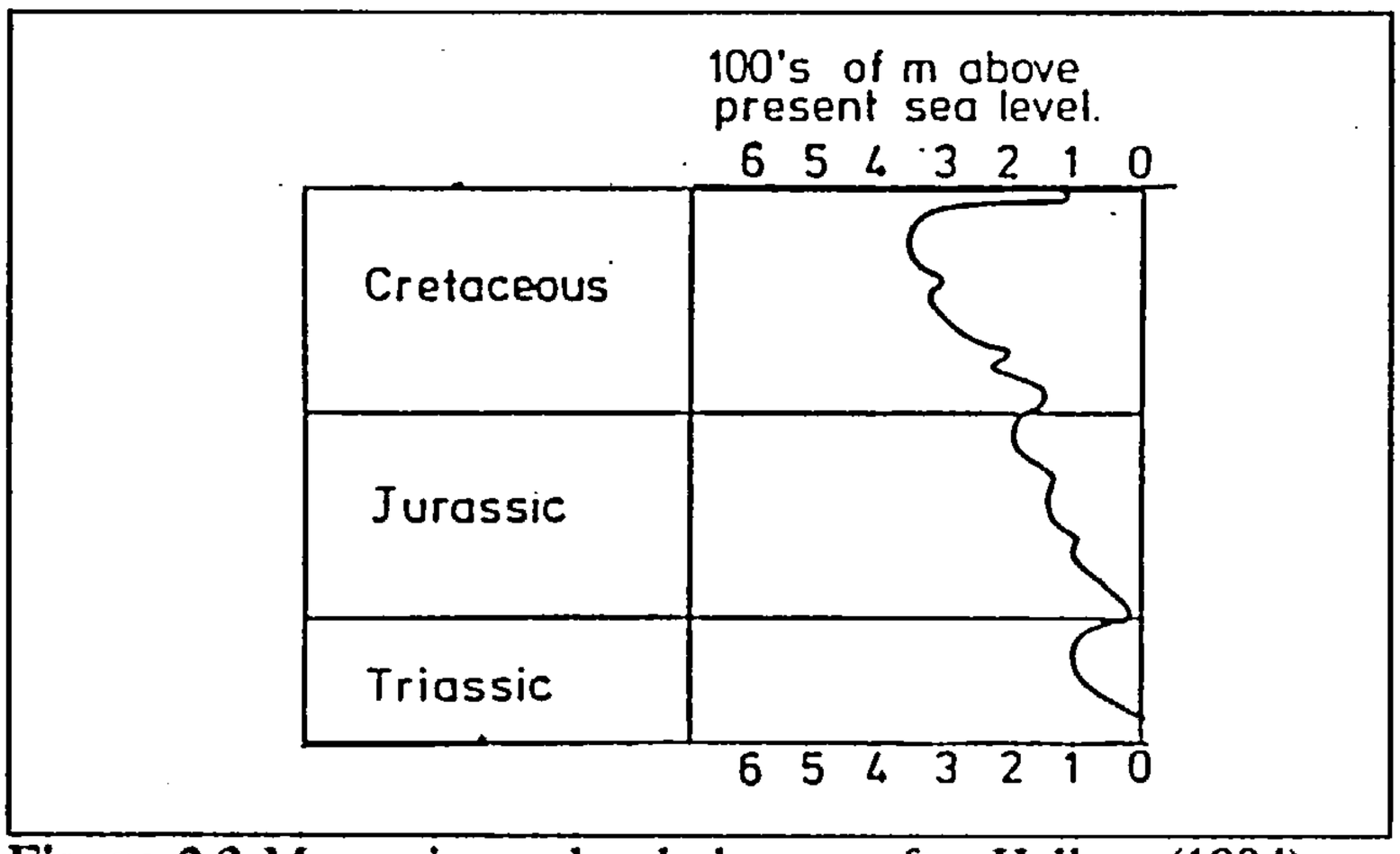

Figure 2.3 Mesozoic sea level changes after Hallam (1984).

and a maximum Mesozoic stand in the late Cretaceous prior to a sharp fall to early Mesozoic levels (Hallam, 1984).

2.3.2 Development of the Mesozoic basins of the Norwegian North Sea

2.3.2.1 Introduction

The North Sea between 60° and 62° north can be divided into three main basins: the East Shetland Basin; the Viking Graben; and the Horda Platform (Fig 2.1). The East Shetland Basin is bounded to the west by the East Shetland Platform, a lower palaeozoic block with a thin Tertiary cover, and to the east by the Viking Graben, though in Norwegian use the term includes the northern part of the graben. It consists of a terrace of generally westerly dipping fault blocks bounded by north-south or northeast-southwest trending faults with easterly downthrows. In the northeast of the basin lies the Tampen Spur, a high complex of rotated fault blocks with a westerly or north westerly dip. The East Shetland Basin is of major economic importance as an oil producing province and includes such fields as Brent, Statfjord, Ninian, Hutton, and North and South Alwyn, which occur along the ridges of the tilted fault block trends.

To the east lies the Viking Graben which north of 60°N has a north northeast-south southwest trend though to the south this becomes more nearly north-south. It extends from the East Shetland Platform and East Shetland Basin in the west to the Horda Platform in the east. Its main economic importance is as the location of a thick sequence of mature Upper Jurassic organic rich shales which are the source of most of the oil and gas in the reservoirs of the northern North Sea. The Horda Platform lies to the East of the Viking Graben and to the west of the Scandinavian Massif. It is separated from the graben by the variously named Vestland, Utsira, and Bergen Highs. There is only a relatively thin sequence of Mesozoic rocks over the platform, but a rather thicker Triassic sequence. Of economic importance in the area is the large Troll field.

2.3.2.2 The Viking Graben

The Viking Graben *sensu stricto* was probably formed in the late Carboniferous (Glennie, 1984) but the main extensional phases of basin development occurred in the Permian to early Triassic and in the mid-Jurassic (Badley et al, 1988). The first major rifting episode, that in the Permo-Trias, was associated with a series of north-south trending listric faults and was succeeded by a thermal relaxation regime lasting from the early Triassic to the mid or late Jurassic. Faulting continued throughout the thermal relaxation phase, but this later faulting was not associated with block rotation. Early basin development was probably asymmetric with the eastern graben faults being most active (Badley et al, 1988).

The second major rifting episode occurred in the mid-Jurassic to earliest Cretaceous (Badley et al, 1988) and was associated with local erosion on footwalls, such as those of the Brent Field trend, though regional uplift was not apparent. Despite reactivation of the older north-south faults the later rifting introduced a northeast-southwest trend to faulting which is best developed in the East Shetland Basin and the Horda Platform. Greatest subsidence in the graben occurred from the Bathonian onwards and was associated with block faulting and rotation. Active rifting and block tilting ceased in the Ryazanian and thermal relaxation began to dominate subsidence which was again associated with planar normal faulting along previously listric faults. The graben itself was the site of major thermal subsidence in the later Cretaceous and Tertiary and this extended outwards with time by fault migration and later by flexure.

2.3.2.3 The East Shetland Basin

As a result of the first rifting phase during the Permo-Triassic, and the subsequent thermal subsidence, some 0.5-1.5km of decompacted Permian to lower Jurassic sediments were deposited in the East Shetland Basin (Badley et al, 1988), considerably less than on the

Horda Platform. During the second rift phase block tilting continued along reactivated older faults, and some emergence and erosion of pre-rift sediments occurred on uplifted footwalls, especially those nearest the graben, such as in the Brent Field. In the Kimmeridgian there was some uplift of the western margins, but as elsewhere rifting ceased in the Ryazanian at the onset of thermal subsidence.

During thermal subsidence much of the East Shetland Basin acted as a single block and greatest sediment thicknesses were preserved in the west where faulting occurred against the East Shetland Platform. Faulting occurred in the east in order to accommodate the subsidence occurring in the Viking Graben, and after flexure of the western margin of the Horda Platform faulting occurred with a northeast-southwest trend on the southeast extremity of the Tampen Spur where uplift of footwall blocks caused erosion of block crests. These faults migrated westwards as time progressed with older fault lines becoming dormant.

2.3.2.4 The Horda Platform

Two rifting episodes are also apparent in the Horda Platform area. North-south faulting during the first (Permo-Triassic) phase resulted in a series of rotated fault blocks being formed. Subsidence associated with this early rifting and subsequent thermal relaxation was sufficient for the deposition of at least 3.5km of (decompacted) Triassic to mid-Jurassic sediments (Badley et al, 1988), a much greater thickness than the equivalent sequence in the East Shetland Basin illustrating the asymmetrical nature of the early basin development. Early rifting was followed by thermal subsidence until the onset of further rifting in the late Jurassic and early Cretaceous.

As elsewhere the second rifting stage was marked by the initiation of northeast-southwest trending faults in areas of previously north-south faulting, and reactivation of many of these earlier faults. The northern and western margins of the platform were complex, and despite overall subsidence some uplift and erosion occurred on the footwalls of the platform margin

faults. The northern edge of the platform was marked by a series of en echelon faults which possibly overlie a reactivated Caledonian thrust. Most of the platform away from its margins was tectonically quiet during the early part of the second rifting episode but during the Kimmeridgian this relatively inactive area suffered some extension and fault reactivation, which ceased in the Ryazanian, simultaneously with the Viking Graben, and thermal subsidence ensued.

Faulting over the platform reached a maximum during the early part of the thermal subsidence phase, with footwall uplift causing considerable exposure and erosion, particularly of the Draupne Formation (Badley et al, 1988), and the northern part of the platform remained exposed until the late Cretaceous. Subsidence of the Viking Graben was accommodated initially by faulting on the western margins, and later by flexure along the north western margin. By the early Tertiary faulting had ceased except at the basin edges and subsidence caused the entire platform to tilt gently westwards as thermal subsidence prevailed.

2.3.3 Development of the onshore Mesozoic basins of England.

2.3.3.1 Introduction

During the Kimmeridgian and throughout much of the Mesozoic sedimentation in England was controlled by the subsidence of two major basins in the southern and eastern parts of the country (Kent, 1949). The southern basin known as the Wessex Basin occupies the region between the Cotswolds, Dorset and Kent, while the North Eastern Basin lies between the Wash and east Yorkshire. Separating the two major basins, and contrasting with the fairly thick and continuous Permian to Early Cretaceous sequences preserved within them lies the north western extremity of the London Brabant Massif occupying the South Midlands, East Anglia and the home counties (Fig 2.4). From the Permian to the Triassic the North Eastern Basin formed a single tectonic unit but in the early Jurassic the appearance of the stable

Figure 2.4 Onshore Mesozoic basins of England (Chadwick, 1985).

Market Weighton Block north of the present Humber Estuary served to divide it into the northerly and rapidly subsiding Cleveland Basin, and the southerly shallow and gently subsiding area known as the Eastern England Shelf.

2.3.3.2 The Wessex Basin

The Wessex Basin occupies a large part of southern England and also extends southwards into the English Channel. Within the basin a series of often en echelon east-west trending

fault zones occur which downthrow to the south (Fig. 2.4). These fault zones subdivide the basin into a series of half graben basins and intervening highs, and closely coincide with the positions of variscan thrusts in the basement of southern England. The coincidence of faults and variscan thrusts is explained by Chadwick (1985a, 1986) as being due to reactivation of the thrusts during times of crustal tension, stress within the brittle upper crust causing fractures along preexisting lines of weakness, which in southern England are the thrusts. At greater depths the lower crust deforms by ductile thinning. The en echelon nature of the basin faults is probably related to the geometry of the thrusts in relation to the lithospheric stress field. Fault movement in the basin was greatest in the Permo-Trias, Early Jurassic, Late Jurassic and Early Cretaceous, while at other times little movement occurred (Chadwick, 1986), subsidence being greatest at times of active faulting, and decreasing exponentially during periods of fault quiescence, as the major cause of subsidence switched from fault control to regional thermal relaxation.

Extension began in the Permian and early Triassic with graben formation in the west of the basin, and movement of the Pewsey, Wardour and Winterbourne Kingston Faults, but in the east there was little contemporaneous subsidence in what would later become the Weald Basin. Lithospheric extension was renewed in the Late Triassic, and Early Jurassic as movement continued on many but not all of the Permo-Triassic faults. Rapid subsidence in the east with movement on the London Platform Faults signalled the beginning of the Weald Basin, and in the south movement of the Portland-Wight Faults initiated Channel Basin subsidence. In the Middle Jurassic subsidence was again controlled by thermal relaxation and the whole basin gently subsided with sediments once more overlapping the margins.

By the Kimmeridgian much renewed faulting and subsidence led to rapid deepening of the Weald and Channel Basins with subsidence continuing into the Cretaceous as the thermal relaxation regime was reestablished. Between the Ryazanian and Barremian however the combination of isostatic uplift and low sea level stand caused the widespread Late Cimmerian unconformity which was responsible for the removal of sediment from many of the highs

especially the London Brabant Massif. From the mid-Cretaceous subsidence in the basin was almost entirely due to thermal relaxation and was still rapid in the Weald and Channel Basins, until the Maastrichian sea level fall caused further erosion and removed much of the chalk.

2.3.3.3 The North East Basin

In contrast to the Wessex Basin described above the Eastern England Shelf shows little evidence of synsedimentary faulting. Permian subsidence in eastern England was initiated later than in the Wessex Basin and it has been suggested (Chadwick, 1985b) that it represents the thermal relaxation stage of earlier lithospheric extension in the southern North Sea. Subsidence increased somewhat in the Early Triassic but was not associated with significant faulting and subsequently slowed through the early and mid-Jurassic due to the exponential decrease in thermal relaxation. An Upper Jurassic subsidence increase was still unfaulted and probably represented the onshore effects of further extension in the North Sea (Chadwick, 1985b).

The first evidence of the emerging Market Weighton High appeared in the Rhaetian when sedimentation in the area became attenuated. North of the Market Weighton High greater but unfaulted subsidence began in the Early Jurassic in the east west trending trough of the Cleveland Basin. Active faulting began here in the mid-Jurassic and the initially gentle downwarping developed into a rapidly subsiding fault bounded basin, the southerly bounding faults having a shallow listric geometry and soling out in weak Permian evaporites (Chadwick, 1985b). The effects of Late Jurassic and Early Cretaceous erosion were greatest over the Market Weighton High in the north and the London Brabant Massif in the south. In the later Cretaceous the Market Weighton area underwent greater subsidence than in the Jurassic while the Cleveland Basin and its offshore extension, the Sole Pit Trough were uplifted and subjected to considerable erosion.

2.4 The Draupne Formation

2.4.1 Introduction

The Draupne Formation has a widespread distribution throughout the Norwegian North Sea, though its thickness varies and it may be locally absent due to erosion. It is thickest in the Viking Graben but thins on its flanks, thickening again in the East Shetland Basin and on the Horda Platform (Fig 2.5). The formation is notable as the major petroleum source rock of the North Sea.

2.4.2 Stratigraphy

The formation consists mainly of carbonate poor marine mudstones, with high radioactivity and a low sonic velocity. Its base is diachronous and usually Oxfordian to Kimmeridgian in age where the formation overlies Heather shales. Over the northern Horda Platform the Draupne overlies the marginal sands of the Sognefjord Formation and here the base is Volgian. Over highs the base may be sharp and unconformable and the Draupne may onlap pre-Heather rocks but in basins the sequence is usually continuous and the contact may be gradational. The Draupne was deposited at a time of active rifting during listric faulting and block tilting and tends to thicken towards major synsedimentary faults, and thin towards the uplifted block crests. The upper boundary of the formation is often unconformable or discontinuous, but may be conformable and isochronous in the Viking Graben. The upper age limit of the formation is usually Ryazanian but may be Volgian where Cretaceous erosion has removed later strata.

2.4.3 Sedimentation

The Draupne Formation was deposited during a high stand of world sea level (Fig. 2.3) when much of Europe formed a shallow epicontinental sea with poor connections to oceans in the

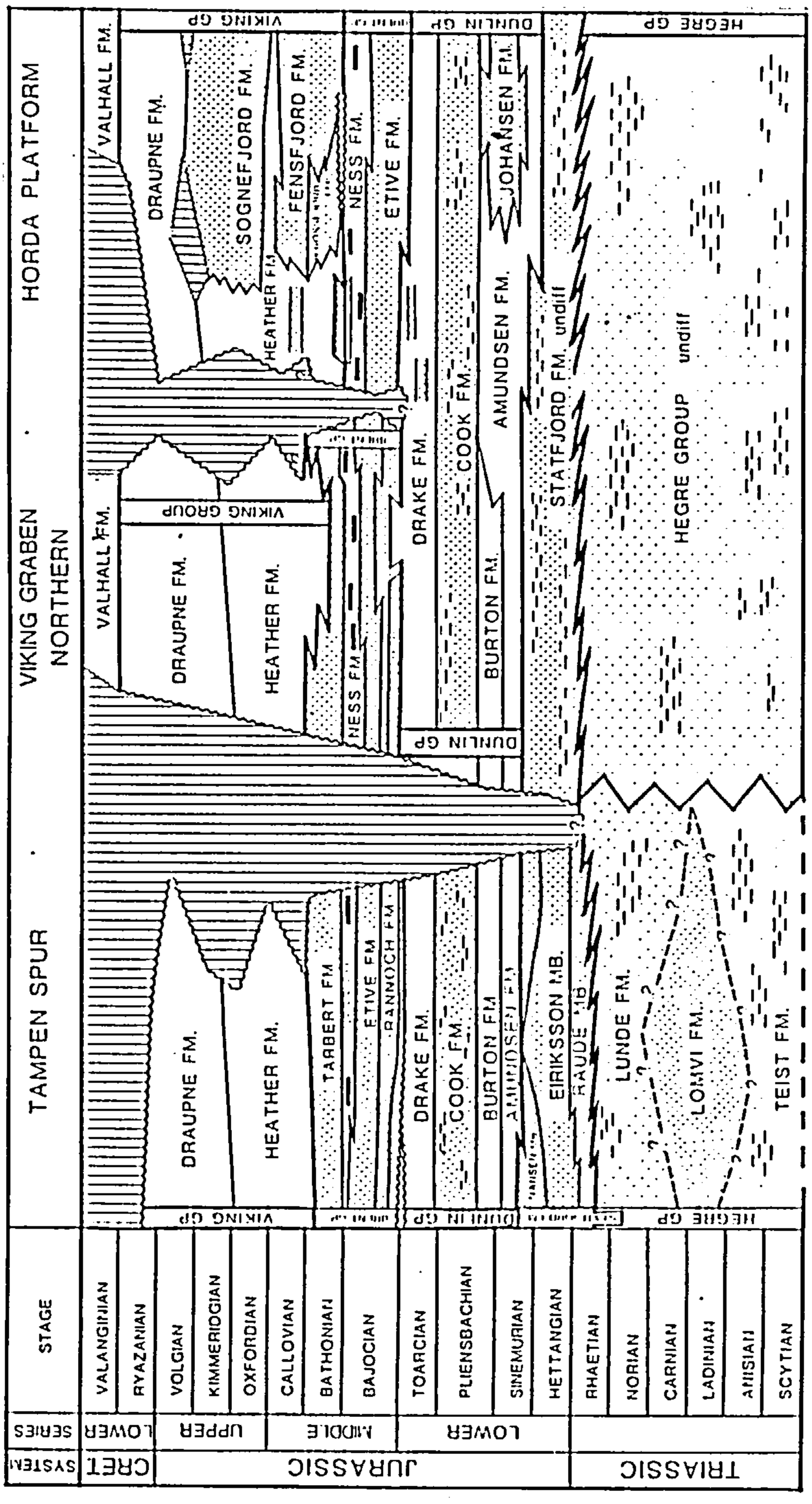

Figure 2.5 Northern North Sea lithostratigraphy (Vollset and Dore, 1984)

north and south, and at a time of rapid subsidence of the North Sea Basins (Badley et al, 1988). These conditions combined to minimise the supply of oxygen to the basin floors and resulted in the preservation of a thick sequence of organic rich sediments. The formation is usually developed in an anoxic black shale facies throughout the northern North Sea, though in more marginal settings such as on the Hordà Platform this may be less pronounced. Locally sandy facies may be apparent at some levels and these may have a turbiditic origin. The best developed lithology is a dark grey to black organic rich and highly radioactive mudstone with occasional fissile horizons. It is generally carbonate poor but calcareous streaks and concretionary horizons are found throughout. The Draupne is much more homogenous than the onshore Kimmeridge Clay and its log responses show none of the cyclic variations characteristic of the latter. This may be because the calcareous mudstones so common onshore represent a more marginal development which is not seen in the deeper North Sea basins (Scotchman, 1984).

2.4.4 Mineralogy and geochemistry

The published literature on the mineralogy and inorganic geochemistry of the Draupne Formation is very limited, though some authors report analyses of 'Upper Jurassic' or 'Kimmeridgian' sequences which may include Draupne Formation samples. Pearson and Small (1988) show the mineralogy of Upper Jurassic sediments from the East Shetland Basin to be dominated by clay minerals with quartz, carbonates, pyrite, and traces of feldspar being present. The clay mineralogy of the formation has been described by Pearson et al (1982, 1983), Huc et al (1984), Scotchman (1984, 1987a and b), Pearson and Small (1988) and Glasmann et al (1989c) and consists of illite, mixed layer illite/smectite, and kaolinite, with increasing amounts of chlorite in more deeply buried samples. The composition of the illite/smectites is seen to become more illitic with increasing burial depth due to the effects of diagenesis (Pearson and Small, 1988) though these effects are complex in this part of the North Sea (Glasmann et al, 1989c).

Bjorlykke et al (1975) report on the mineralogy and geochemistry of 'Kimmeridgian' shales from two wells in the Central Graben and Norwegian Danish Basin. These are not Draupne Formation but are probably similar in many ways. V increases upwards in both wells and is much higher (up to 450ppm) in the graben than the Norwegian Danish Basin (maximum about 160ppm) and may indicate a trend towards anoxia in the later sediments with generally more restricted conditions in the Central Graben. Conversely, Cr is much higher in the Norwegian Danish Basin (400-500ppm compared with up to 200) and may indicate a volcanic component to the sediment, which may also be responsible for some of the V as the two are correlated. Alternatively the high Cr values may be a result of concentration by weathering on the Scandinavian Shield.

Th/U ratios reported by these authors are about normal for marine shales in the Norwegian Danish Basin but in the Central Graben especially towards the top they are much lower, again suggesting more oxygen deficient deposition there. They suggest that trace element analyses may be useful in interpreting depositional conditions of apparently homogenous shale sequences. Dypvik and Brunfelt (1979) includes details of the REE distribution in 'Kimmeridgian' shales from another well in the Norwegian Danish Basin and conclude that they are similar throughout the North Atlantic area.

Rainey (1984) examined both the chemistry and mineralogy of the Magnus Fan sediments, including the associated shales and found these to be enriched in total C (which is about equal to TOC in these carbonate poor shales), Fe, S, Mo, As, V, Cu, Zn, and Ni relative to normal shales.

Stow and Atkins (1987) discuss aspects of the geochemistry of Upper Jurassic mudrocks, including Draupne Formation, from the southern Viking Graben and Witch Ground Graben. They identify three sedimentary facies of which the most organic rich, a fissile shale dominates the Volgian succession and is enriched in S, Fe, P, Mo, Ni, Se, U, and Ni, and to a lesser extent Co, Cr, Cu, and Zn. Inter element relationships are discussed and particularly

interesting is V which appears to be correlated with clay content in the more organic rich fissile sediments, but with loss on ignition and hence TOC in the organic poor facies.

The Draupne Formation has been the subject of numerous organic geochemical investigations as befits its economic importance (see Cornford, 1984) and many of these have studied the maturity of the formation, and its organic facies (eg Goff, 1983; Thomas et al, 1985; Field, 1985; Schou et al, 1985; Leadholm, 1985; and Baird, 1986). These have shown that the formation has reached a maturity of greater than 1.3% R_o in the deeply buried sections of the northern Viking Graben, but only 0.5% or less on the Horda Platform or in parts of the East Shetland Basin, spanning the range from immaturity to post peak dry gas generation. Thomas et al (1985) have shown the Draupne to have hydrogen indices in excess of 700 and to contain 2.1-12.5% TOC in the northern North Sea.

The kerogen in the Draupne also displays both lateral and vertical variations in type and hence in source potential. Present day lateral distributions have been mapped (Demaison et al, 1983), and the original distribution calculated by Baird (1986). These show that the best oil source rocks were deposited in the centre of the graben system and generally contained type II kerogen and that away from the graben the type II kerogen gives way to type III or IV as the dominant type. Barnard et al (1981) and Fisher and Miles (1983) both document vertical variation in kerogen type with the kerogen becoming more oil prone towards the top of each section. Barnard et al (1981) explained this as resulting from transgression, with Goff (1983) also suggesting that the richest source horizons were developed at maximum transgression.

2.5 The Heather Formation

2.5.1 Introduction

The Heather Formation is also found over a wide area in the North Sea though again it may have been removed over structural highs on the margins of the Viking Graben (Fig 2.5).

2.5.2 Stratigraphy

The lower boundary of the Heather Formation is the contact with the sands of the Brent Group, where it usually overlies the Tarbert Formation, or possibly the Ness Formation on the Horda Platform. The contact is clearly marked by log breaks and is Bathonian to Callovian in age. The thickness of the formation varies greatly from >1000m in the graben to only a few metres on the flanks, and it may be completely absent over eroded fault block crests. The formation may be further subdivided by an unconformity or disconformity. The diachronous upper contact is with the Draupne Formation, the youngest Heather being Kimmeridgian.

2.5.3 Sedimentation

The Heather was deposited in generally open marine conditions following the Bathonian transgression of the Brent Delta system. It consists mainly of grey silty mudstones with thin limestone streaks. At its base the Heather may be present in a black shale facies suggesting the development of anoxia in the Bathonian to Callovian, but these conditions gave way to normal marine oxygenation (Thomas et al, 1985) by the late Callovian. Black shale facies returned at least locally in the upper part of the formation prior to the widespread anoxia of the Draupne Formation.

2.5.4 Mineralogy and geochemistry

The literature on the mineralogy and geochemistry of the Heather Formation is very limited. Huc et al (1985) have published clay mineral analyses of the upper part of the formation in the Viking Graben and show the main clay minerals to be kaolinite, illite, and mixed layer illite/smectite. Their work shows that kaolinite and illite increase downwards at the expense of the illite/smectite, and that chlorite appears in the deeper samples. The increase in chlorite

and decrease in illite/smectite are attributed to the effects of diagenesis, but the increases in illite and kaolinite are thought to represent original depositional characteristics due to changing distances from the palaeoshoreline as transgression proceeded. These vertical changes were also expected to be seen as lateral changes across the basin.

Huc et al (1985) related their clay mineral interpretation to the organic geochemistry of the formation which shows a decrease in both TOC and hydrogen index down the section from the Draupne to the Heather. The TOC decreases from about 10% to 5% and the hydrogen index from about 600 down to around 200. The extractable alkane composition also changes from a maximum of low to medium molecular weights in the higher parts of the section to higher molecular weights downwards with increasing odd number dominance. These changes are thought to represent the increasing influence of terrestrially derived organic matter downwards into the Heather Formation due to the proximity of the palaeoshoreline.

Thomas et al (1985) have also analysed the Heather Formation and found hydrogen indices in excess of 600 giving type II kerogen though the majority of samples are much lower with type II/III kerogen dominating. These authors found TOCs to lie in the range 0.6-10.9% though Kirk (1980) reports an average value of only 2.24% TOC in the Statfjord Field. The Heather is generally considered a good potential gas source but in thicker sections and with type II kerogen it could also yield some oil.

2.6 The Kimmeridge Clay Formation

2.6.1 Introduction

The Kimmeridge Clay Formation in England has a narrow outcrop which runs almost continuously from the type area in Dorset through the south midlands, the Wash, and Lincolnshire, to Yorkshire, a distance of some 500km, broken only occasionally where post-depositional (Cretaceous) erosion has removed strata. Its subcrop is extensive, generally dips

to the south east, and underlies much of southern and eastern England. Exposure is good on the Dorset coast but inland it is poor and much modern work on the formation is based on material from cored boreholes.

The Formation is thickest in parts of the Wessex and Cleveland Basins and is somewhat thinner on the Eastern England Shelf. In the Cleveland Basin the greatest thicknesses are preserved in the north west, in the Vale of Pickering, and the formation thins south eastwards towards Market Weighton. On the Eastern England Shelf the formation is thickest in a north east-south west trending belt in Lincolnshire, thinning both northwards against the Market Weighton Block, and southwards against the London Brabant Massif. In the Wessex Basin the thicknesses vary considerably as a result of the presence of local highs and basins, but the greatest thicknesses are achieved in the east in the Weald Basin, and in the south in the Channel Basin. Elsewhere in the Wessex Basin the formation may be thinner or even absent over intra basinal highs.

Facies and thickness variations in the Jurassic of Britain were for many years related to a series of axes of uplift (Arkell, 1933), upon which sedimentation was slow and discontinuous. It was believed that these usually followed anticlines in the palaeozoic basement, that they were in turn followed by younger folds, and that they represented long standing lines of weakness in the crust. Hallam (1958), rejected this explanation and suggested his own concept of basins and swells to explain changes in facies and thicknesses. Basins were defined as zones of rapid downwarping and sedimentation while swells were zones of relative uplift which probably existed as submarine shallows. Causes of the swells and basins were not well understood however.

Further work also showed that the initially simple basin and swell concept was more complex, and that swell areas only acted as such during specific intervals while at other times they too subsided (Sellwood and Jenkyns, 1975). These authors put forward an explanation for the behaviour of the majority of swells involving periodic synsedimentary fault movement.

The swell in the Market Weighton area was noted as being unusual for its longevity however and has been related to the presence of an unexposed granite intrusion in the basement (Bott et al, 1978; Bott, 1988) though other suggestions have been salt diapirism (Sellwood and Jenkyns, 1975) or a Carboniferous graben in the basement (Arveschoug, 1986).

2.6.2 Stratigraphy

The Kimmeridge Clay Formation is a marine argillaceous unit composed mainly of a rhythmic sequence of mudstones with variable carbonate, silt and organic matter contents. In southern England the formation overlies the Corallian Beds, and in the north east the lithologically similar Ampthill Clay.

In the Wessex Basin the Kimmeridge Clay exists as a thick and complete succession, with the greatest thicknesses occurring on the southern (downthrown) sides of the major growth faults particularly in the easterly Weald Basin where the formation passes conformably into the Portland Beds. Again in south Dorset the succession is complete and the transition conformable. Over the highs the sequence is thinner because of slower subsidence, and low subsidence rates also occurred on the North Downs Shelf between the London Brabant Massif and the Weald, and on the shallow swell to the west of the London Brabant Massif and north west of the Wessex Basin. Here the low sedimentation rate was sufficient to cause local emergence.

On the Eastern England Shelf the Kimmeridge Clay is thickest in Lincolnshire where it occurs between the baylei and pectinatus zones (Penn et al, 1986). Towards the south east it thins close to the flanks of the London Brabant Massif probably because of slow sedimentation rates. Most of the thinning occurs in the lowermost (baylei and cymodoce) zones which overlap one another and onlap the upper part of the Ampthill Clay. In the north much of the formation has been removed by post depositional erosion, and it is progressively overstepped northwards by the Spilsby Sandstone, and Cretaceous sediments, so that on

Humberside in the Worlaby borehole only the baylei to mutabilis zones remain (Richardson, 1979). The thick Ampthill Clay succession recorded in this borehole suggests that the Market Weighton High was temporarily less important in the Oxfordian before reestablishing itself in the Kimmeridgian.

Recent work associated with a number of boreholes in the Wash area has enabled the formation between the baylei to pectinatus zones to be divided into a sequence of 48 beds on the basis of their fauna and lithology (Gallois and Cox, 1974, 1976; Cox and Gallois, 1979). These beds show great lateral continuity and it has proved possible to identify them in the Warlingham borehole, Surrey, and in the Dorset coastal exposures, distances of 180km and 300km respectively (Cox and Gallois, 1981).

In the Cleveland Basin the baylei to pectinatus zones are present in the centre and though the formation thins eastwards the same zonal sequence is present.

2.6.3 Sedimentation

The continued sea level rise throughout the Jurassic led to a much reduced land area in the Kimmeridgian and Volgian (Fig. 2.3), and the Kimmeridge Clay was deposited over a wider area than any of the preceding Jurassic sediments, originally extending to the west of its present outcrop, and with thinning, over the London Brabant Massif. The small land area remaining as a possible sediment source is puzzling in relation to the large volumes of sediment deposited as most of the islands in the British area seem only to have been local sources. North America and Scandinavia have been suggested as the major sources of Kimmeridgian sediment on the grounds of clay mineralogy (Sellwood and Sladen, 1981), the sources probably being weathered Palaeozoic sediments (Sellwood and Jenkyns, 1975).

The formation was deposited almost entirely in an argillaceous marine facies throughout the onshore area, though some development of a sandy facies with a north western derivation

occurs in the Upper Kimmeridge Clay over the shallow swell of the south midlands in the Oxford and Swindon areas and sandy sequences have also been recorded close to the stable positive Market Weighton Block (Richardson, 1979), and to the west and north east of the Wessex Basin (Gallois, 1979; Smart, 1966). In general sediments from the more slowly subsiding swell areas tend to be more calcareous and those from the basins more organic rich.

The formation exhibits a cyclic variation in lithology on a number of scales. On a large scale the character of the formation itself changes from being silty in its lower parts, to being organic rich, before becoming calcareous towards its top. This is similar to the Kellaways-Oxford Clay, and the West Walton Beds-Ampthill Clay sequences (Cox and Gallois, 1981). On a smaller scale there are variations in carbonate and kerogen content which may be correlated over distances such as the 300km between the Wash and the Dorset coast (Gallois and Cox, 1974), and even the smallest scale rhythms can still be correlated over tens of kilometres (Cox and Gallois, 1981).

A number of idealised cycles for these small scale rhythms have been proposed. Cox and Gallois (1981) suggest that in the Lower Kimmeridge Clay the sequence is siltstone passing upwards into dark grey mudstone and then into pale grey calcareous mudstone, while in the Upper Kimmeridge Clay the rhythms become oil shale based giving oil shale or bituminous shale overlain by dark grey mudstone which is in turn, overlain by pale grey calcareous mudstone with occasional limestones. For the wheatleyensis to pectinatus zones of the Upper Kimmeridge Clay Tyson et al (1979) favoured the sequence: mudstone, bituminous shale, oil shale, limestone. More recently House (1985) and Wignall (1989) have favoured a simpler alternation between the organic rich bituminous shales and oil shales and the organic poor and often calcareous mudstones (Fig. 2.6).

Most workers agree that the cyclic nature of the Kimmeridge Clay is related to vertical movements of the oxic/anoxic interface through the sediment and into the water column in an

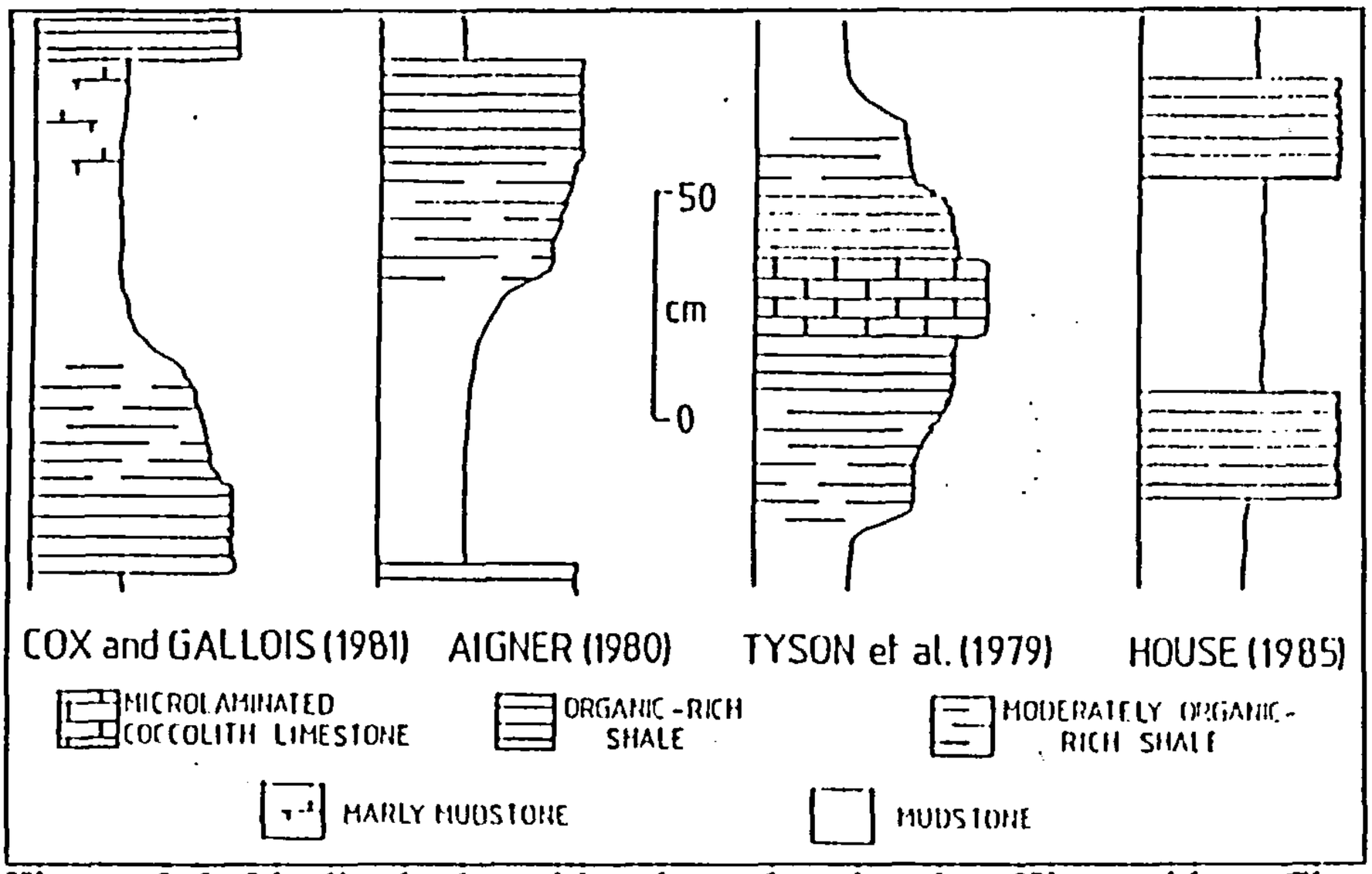

Figure 2.6 Idealised depositional cycles in the Kimmeridge Clay Formation (Wignall, 1989)

episodically thermally stratified basin (Gallois, 1976; Tyson et al, 1979; Irwin, 1979; Myers and Wignall, 1987; Wignall, 1989). Some debate has been centred on the detailed relationship between the lithology and the position of the oxic/anoxic interface with Gallois (1976) proposing that the oil shales represented the highest stand, but with Tyson et al (1979) supported by Farrimond et al (1984) believing the coccolith limestones are the result of maximum anoxicity.

Myers and Wignall (1987) and Wignall (1989) stressed the importance of storm induced mixing in the oxygenation of bottom waters and proposed that small, possibly climatically induced ascents of the oxic/anoxic interface may, by reducing the efficiency of water mixing, rapidly lead to a stratified basin within which organic rich sediments would be deposited. The shallower swell areas and basin flanks would be less prone to stratification and therefor leaner in organic matter, thus water depth and hence basin topography are shown to be important controls on the nature of Kimmeridge Clay deposition.

2.6.4 Mineralogy and geochemistry

The mineralogy of the formation consists chiefly of silty quartz, clay minerals, calcium and magnesium carbonates, and pyrite (Cox and Gallois, 1981; Morris, 1980; Dypvik, 1984) and in general the differing lithologies are composed of varying proportions of the same mineral components. Of the clay minerals the dominant species is ordered mixed layer illite/smectite, with varying but subordinate amounts of kaolinite, and minor chlorite (Scotchman, 1984, 1987a and b). Scotchman (1984, 1987a and b) has also discussed the changes in clay mineralogy due to diagenesis within the formation.

Publications detailing the inorganic geochemistry of the Kimmeridge Clay are scarce. Cosgrove (1970) reported trace element analyses for a number of samples taken from around the Blackstone Band in the hudlestoni, wheatleyensis, and pectinatus zones of the Upper Kimmeridge Clay at Kimmeridge Bay and identified three groupings of elements: C, Br, I, and Mo; Ga, Rb, Zr, Nb, and Y; and Sr and CO_2 which he interpreted as being due to organic matter, clastic, and carbonate components respectively. These samples are amongst the most iodine rich sedimentary rocks known.

Dunn (1974) also analysed samples from the bituminous sediments of the wheatleyensis and hudlestoni zones at Kimmeridge and associated Mo and P with organic matter, V, Cr, Zr, Ni, Cu, Ga, Li, Rb, Cs, and Sc with the detrital component of the sediment, and Mn and CO_2 with carbonates. Fourier analysis of his data revealed the presence of cycles of several periodicities which he related to climatic changes and tectonic pulses.

Dypvik and Brunfelt (1979) reported REE distributions in the Lower Kimmeridge Clay of Yorkshire and demonstrated that these were similar to other Upper Jurassic shales from the North Sea, northern Norway, and Svalbard despite the different sediment sources. This was attributed to the extensive reworking of the sediment prior to final deposition.

As part of a study of Upper Jurassic and Lower Cretaceous clays in Yorkshire Dypvik (1984) reported both major and trace element analyses of the Lower Kimmeridge Clay of the Cleveland Basin. These showed the formation to be enriched in Cr, V, Co, Ni, and Mo when compared to average shale, but depleted in Ba. The data collected allowed him to ascertain the mineralogical residences of the elements, and were interpreted as showing deposition of sedimentologically mature sediment within a basin of restricted circulation.

Recent work by Myers and Wignall (1987) and Wignall and Myers (1988) has used gamma ray spectrometry to determine U and Th in the Kimmeridge Clay of the elegans, wheatleyensis, hudlestoni, and pectinitus zones at Kimmeridge Bay in order to aid in the interpretation of benthic oxygen levels. 'Authigenic' U is suggested as being a useful parameter for indicating palaeo oxygen levels. Further recent work by Scotchman (1989) has concentrated on the chemistry of the carbonate phases illustrating their lateral variation which he relates to basin topography.

Many of the organic geochemical studies of the formation have concentrated on the distribution of organic facies, and the levels of organic maturity (Dypvik et al, 1979; Williams and Douglas, 1980; Douglas and Williams, 1981; Williams, 1986; Ebukanson and Kinghorn, 1985, 1986; Scotchman, 1984, 1987a and b). These studies have concluded that the majority of the kerogen in the Kimmeridge Clay is amorphous material with minor spores and vitrinite (Williams, 1986; Scotchman, 1987a and b) and that it is dominantly type I/II, II, or II/III, (Ebukanson and Kinghorn, 1985; Scotchman, 1984, 1987a and b; Williams, 1986) with type III present towards the basin margins.

Williams and Douglas (1980) and Douglas and Williams (1981) reported an increase in the maturity of the formation northwards from Dorset, finding Vitrinite Reflectance (R_o) to be 0.39-0.42% in Dorset, 0.47% in Lincolnshire, and 0.51% in Yorkshire. This was supported by consistent changes in the Carbon Preference Index (CPI), and in pentacyclic triterpane ratios. No values were recorded as high as the 0.70%R_o of Dypvik et al (1979) from South Ferriby

in Humberside, or the values of Barnard and Cooper, (1983) from the Cleveland Basin (0.7-0.9% R_o). This increase was also noted by Williams (1986) who reported R_o to be 0.30-0.39% in the southwest of the Wessex Basin, 0.31-0.48% in central Lincolnshire, and 0.39-0.51% in the deeper parts of the Cleveland Basin, but not by Scotchman (1984, 1987a and b) who commented on the difficulty of obtaining reliable R_o values where particle sizes are small and where the vitrinite has been reworked. Overall the formation onshore is generally immature but may be mature for oil generation in the deeper parts of the Cleveland Basin, and in the Weald and Isle of Wight areas (Williams, 1986; Ebukanson and Kinghorn, 1986).

Chapter Three

Summary of the Mineralogical and Geochemical Data

3.0 Summary of the Mineralogical and Geochemical Data

The aim of this chapter is to summarise the mineralogical and geochemical data collected during this study. In the first section the mineralogical data will be discussed, and this is followed in section two by a review of the 32 major and trace elements determined. In the following chapter the relationships between the mineralogical and chemical variables are examined by means of correlation analysis. The mineralogical and geochemical data collected during the study are summarised in Tables 3.1-3.4, 3.7 and 3.8, and in the following discussion. The descriptive statistics used below and in Tables 3.1-3.4, 3.7 and 3.8 are elementary and need no qualification save only to note that the median is a more reliable measure of the average than is the mean because of the susceptibility of the latter to perturbation by outlying observations with extreme values. For this reason the median is used in the following discussion in preference to the mean. Those variables with the most skewed distributions will show the greatest divergence between mean and median values.

3.1 The mineralogical data

The mineralogy of 61 samples of the Draupne Formation and 77 samples of the Heather Formation from the Norwegian sector of the North Sea was examined by means of X-Ray Diffraction (XRD) of randomly orientated bulk rock material. The analyses were performed at the Norsk Hydro Research Centre in Bergen and made use of the automated XRD system installed there. The system is calibrated with, and produces output in terms of, 13 common sedimentary minerals these being: quartz, plagioclase, K-feldspar, muscovite, biotite, chlorite, smectite, illite, kaolinite, calcite, dolomite, siderite, and pyrite. Further analytical details are found in Appendix A. The resulting mineralogical data are summarised in Tables 3.1 and 3.2 and are discussed below.

Table 3.1 Draupne Formation mineralogy.

Mineral	N	Mean	Median	Std.Dev.	Max.	Min.
Quartz	61	13.5	13.1	5.10	28.5	0.00
K-spar	61	5.06	5.00	1.20	8.11	0.14
Plag.	61	3.07	2.89	1.04	6.50	0.61
Musc.	61	0.11	0.00	0.16	0.74	0.00
Biot.	61	0.02	0.00	0.12	0.96	0.00
Calc.	61	2.71	0.66	11.4	89.3	0.00
Dol.	61	3.45	2.82	2.48	18.7	1.34
Sid.	61	0.46	0.31	0.50	1.99	0.00
Pyrite	61	12.5	11.1	9.75	72.5	0.00
Clay	61	53.6	56.5	10.2	65.8	11.8

Table 3.2 Heather Formation mineralogy.

Mineral	N	Mean	Median	Std.Dev.	Max.	Min.
Quartz	77	17.7	18.8	9.35	35.9	0.00
K-Spar	77	7.25	6.96	2.70	14.4	0.76
Plag.	77	4.16	3.96	2.65	12.7	0.00
Musc.	77	0.39	0.07	0.57	3.38	0.00
Biot.	77	0.17	0.00	0.59	4.87	0.00
Calc.	77	3.18	1.32	8.72	67.2	0.00
Dol.	77	3.10	2.63	3.46	28.8	0.00
Sid.	77	2.95	1.05	6.65	48.9	0.00
Pyrite	77	9.37	7.28	7.26	49.1	0.00
Clay	77	47.3	47.5	9.42	66.7	13.5

3.1.1 The bulk mineralogy

3.1.1.1 Quartz

The quartz contents of the Draupne and Heather Formations determined in this study are summarised in Tables 3.1 and 3.2. The Heather has the higher of the two median values with 18.8% quartz in comparison with 13.1% for the Draupne. Quartz distributions are shown in Fig. 3.1, both formations being positively skewed. The maximum recorded quartz content of 35.9% was from the Heather Formation, the corresponding value from the Draupne being 28.5%. Quartz in mudstones is usually present as silt sized particles (Pettijohn, 1975) and this is probably the case here. The average shales given by this author have quartz contents in the range 20.0-36.8%, the most recent value being the 36.8% quartz of Shaw and Weaver (1965). The quartz contents recorded in this study are considerably lower than 36.8% but are closer to the 22.1% quartz content recorded by Spears and Amin (1981) for the Namurian black shales of the Tansley borehole.

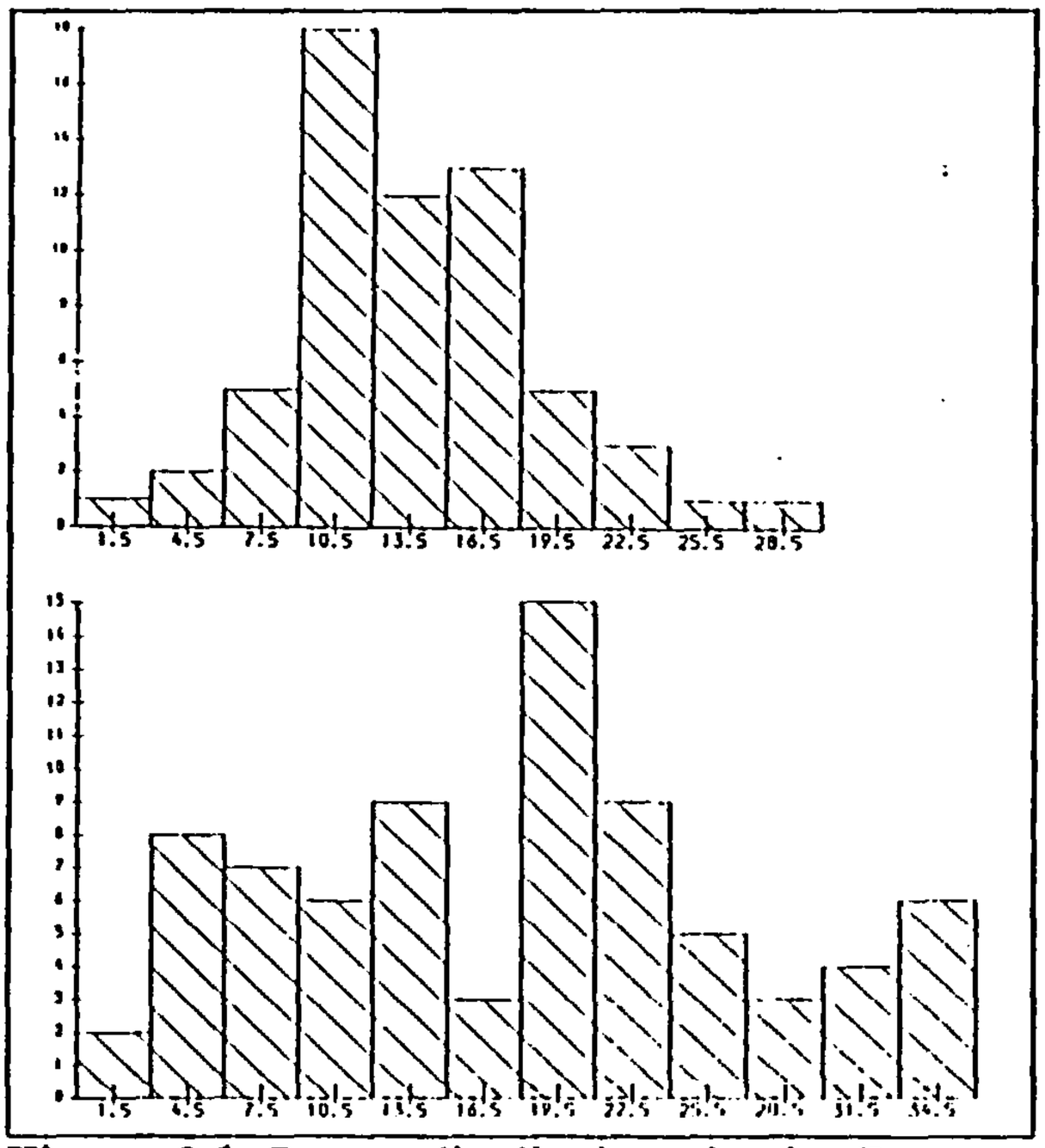

Figure 3.1 Quartz distributions in the Draupne (above) and Heather Formations

The mineralogy of the Kimmeridge Clay was not determined here but Morris (1980) states that the formation has 10-20% quartz of silt to fine sand grain size, which closely agrees with the shales of this study. In addition Merriman (1978) quotes the quartz content of Kimmeridge Clay samples as being 10-24%, while Cox and Gallois (1981) give various values for the different lithologies, stating that the quartz is mainly present as silt sized grains.

3.1.1.2 Feldspars

The feldspar data are summarised above and in Figs. 3.2 and 3.3. K-feldspar has an approximately normal distribution in both formations but plagioclase is positively skewed in both cases. Maximum recorded feldspar contents are 14.4% K-feldspar and 12.7% plagioclase, both from the Heather Formation. The Heather Formation also has the higher average content of both plagioclase and K-feldspar, having a median of 6.96% K-feldspar and 3.96% plagioclase. The Draupne Formation has 5.0% K-feldspar and 2.89% plagioclase but this still

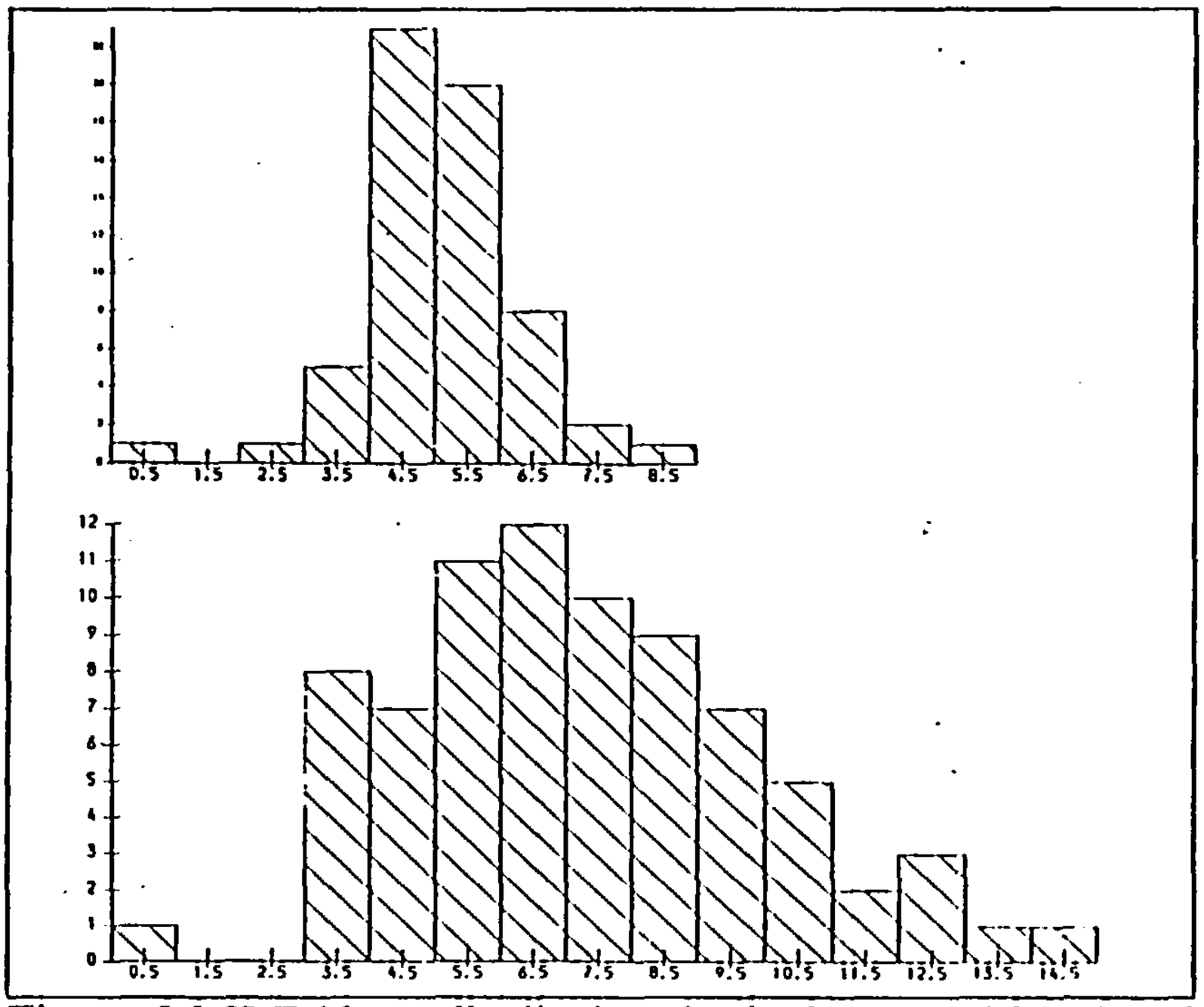

Figure 3.2 K-Feldspar distributions in the Draupne (above) and Heather Formations

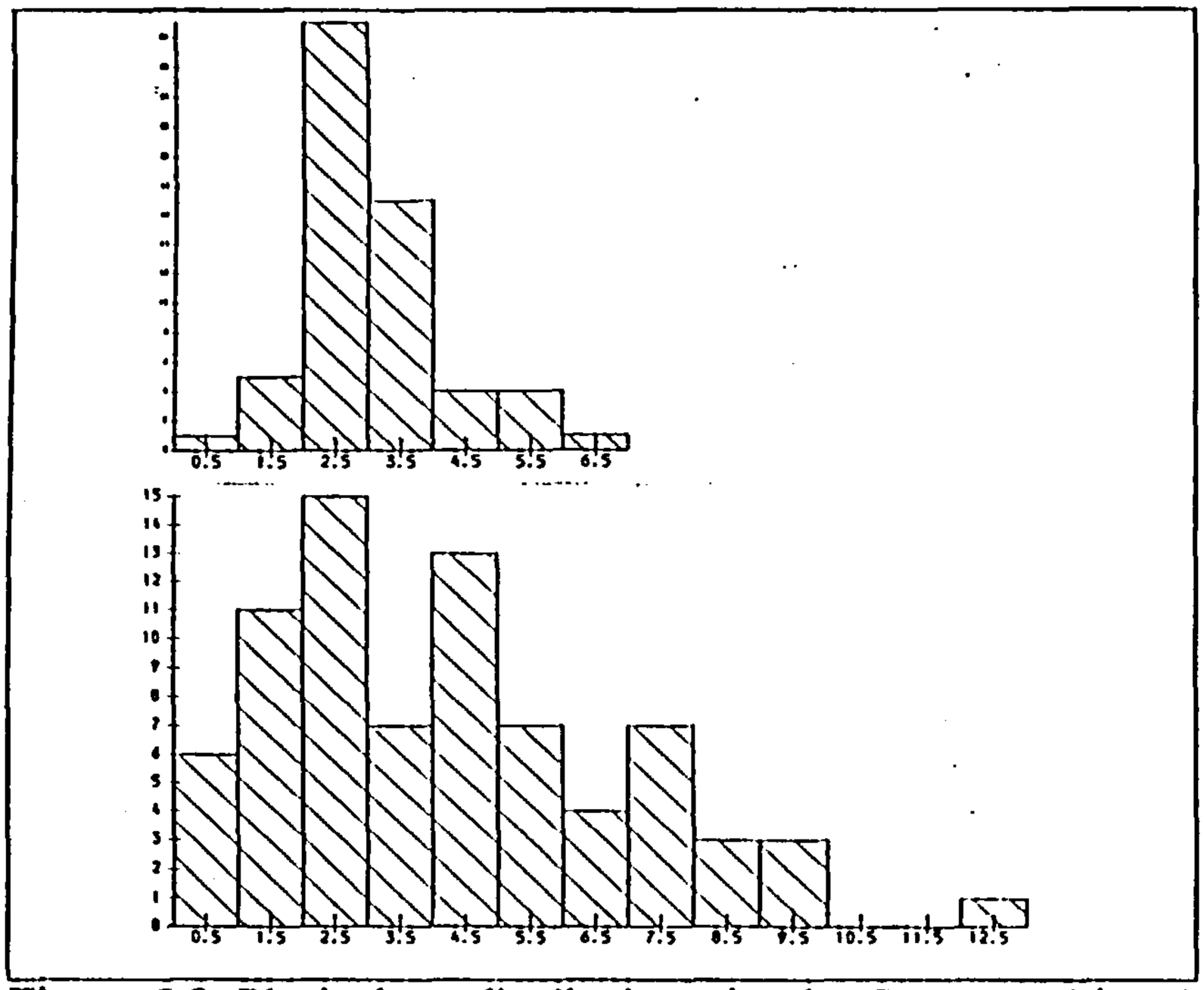

Figure 3.3 Plagioclase distributions in the Draupne (above) and Heather Formations

exceeds the 4.5% feldspar of Shaw and Weaver (1965) for average shale and the 3.5% recorded in the marine Tansley black shales (Spears and Amin, 1981). Feldspars are also concentrated in the silt fraction of mudstones. For the Kimmeridge Clay Formation Morris (1980) found 5% feldspar which was mainly microcline and orthoclase and feldspar has also been recorded in the Kimmeridge Clay by Merriman (1978), and by Dypvik (1984).

3.1.1.3 Mica

Both muscovite and biotite were only detected in small quantities in the Draupne and Heather Formations. The mica data are summarised in Tables 3.1 and 3.2. Morris (1980) states that muscovite is dominant in the Kimmeridge Clay and this is in agreement with the results of this study. The micas are not discussed further.

3.1.1.4 Carbonate minerals

Carbonate contents of the Draupne and Heather Formations are summarised above (Tables 3.1 and 3.2). Their distributions are not illustrated because of the difficulty of producing informative histograms from such strongly skewed data. The maximum recorded calcite contents were 89.3% for the Draupne Formation and 67.2% in the Heather Formation but the Heather Formation has the higher median calcite content. The maximum recorded dolomite values were 18.7% in the Draupne Formation and 28.8% in the Heather. The median dolomite contents are similar. Siderite contents reached a maximum of 48.9% in the Heather Formation but only 1.99% in the Draupne, the Heather Formation having the higher median value also.

Shaw and Weaver (1965) give 3.6% carbonate minerals in average shale which is similar to the Draupne but suggests that the Heather Formation is slightly carbonate rich which is not in accordance with the geochemical data discussed below. Morris suggests that the organic rich shales of the Kimmeridge Clay contain 10-15% carbonate, while Cox and Gallois (1981) state that up to 55% $CaCO_3$ is present in pale grey shales and up to 90% of Ca/Mg/Fe carbonate in the cementstones. Traces of dolomite and siderite were detected by Dypvik (1984) in the Kimmeridge Clay of Yorkshire.

3.1.1.5 Pyrite

The pyrite contents found in this study are summarised in Tables 3.1 and 3.2. Pyrite distributions are illustrated in Fig. 3.4.;, both formations are positively skewed. The maximum recorded pyrite contents are 72.5% in the Draupne and 49.1% in the Heather Formation. The Draupne Formation has the higher median pyrite content at 11.1%, but the Heather Formation has a median of 7.38% pyrite which is still considerably greater than the <2% 'other minerals' including pyrite of Shaw and Weaver (1965). Morris (1980) states that pyrite is ubiquitous in the Kimmeridge Clay both as framboids and larger crystals, and it has also been recorded by

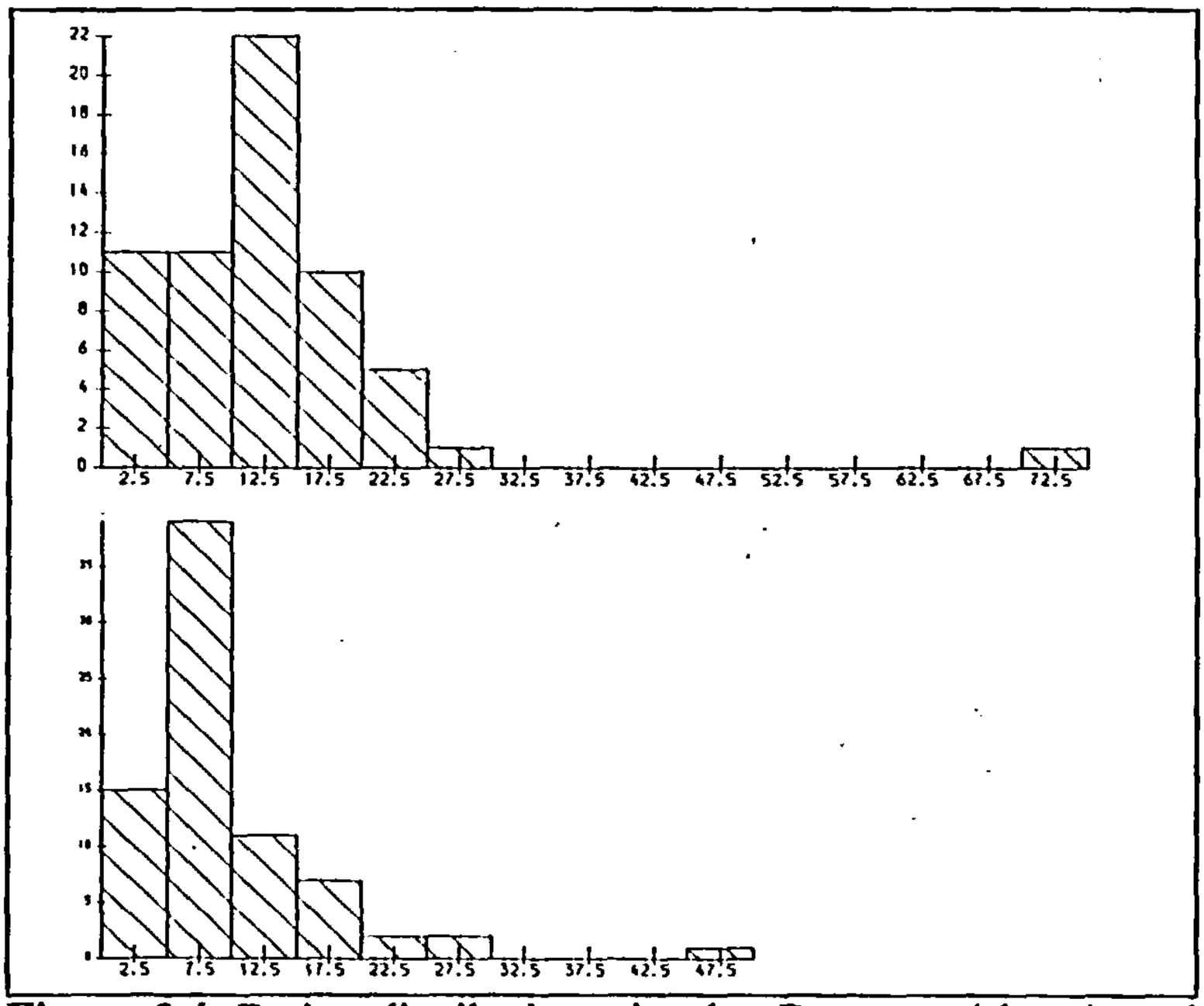

Figure 3.4 Pyrite distributions in the Draupne (above) and Heather Formations

Merriman (1978) and Dypvik (1984).

3.1.1.6 Clay content

Because of the likely inaccuracy of the determination of the clay mineralogy of the samples by the bulk XRD package the clays are here discussed as total clay. The clay mineralogy is discussed in greater detail below. The total clay contents of the Draupne and Heather Formations are summarised above (Tables 3.1 and 3.2). The distribution of the total clay is illustrated in Fig. 3.5. The Heather Formation has a nearly symmetrical distribution but the Draupne Formation is negatively skewed and is suggestive of a bimodal distribution. The Draupne has up to 65.8% total clay minerals in comparison with the Heather Formation maximum of 66.7%. The median clay content of the Draupne Formation is 56.5% and this exceeds that of the Heather Formation which is 47.5%. Shaw and Weaver (1965) give the total clay content of average shale as 66.9% which is rather higher than the formations studied here, but Spears and Amin (1981) detected on average 55.7% clay in the marine Tansley black shales.

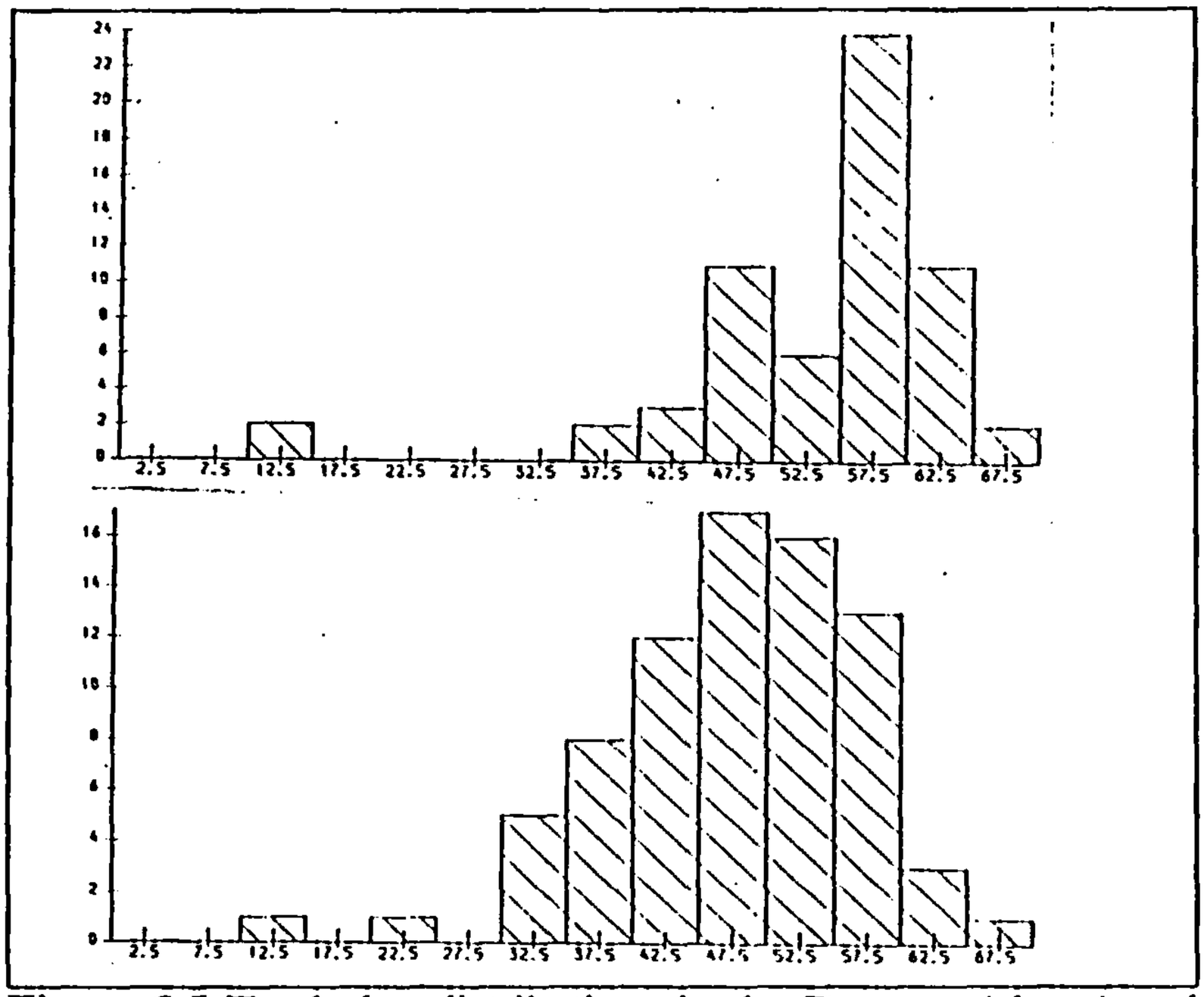

Figure 3.5 Total clay distributions in the Draupne (above) and Heather Formations

The Kimmeridge Clay Formation has 20-60% clay minerals according to Morris (1980) and 44-70% clays according to Merriman (1978) both of which are similar to the range of values recorded here for the offshore formations. Cox and Gallois give a clay content of 25-65% depending on lithology. The lower clay mineral content of the Draupne and Heather formations in comparison to average shales is probably due to the higher proportions of authigenic minerals, particularly pyrite.

3.1.2 The clay mineralogy

The clay minerals smectite, illite, kaolinite, and chlorite were determined by the bulk XRD package in the Draupne and Heather Formations. Of these smectite, illite and kaolinite were found in appreciable amounts but chlorite was present in much smaller quantities. To confirm the results obtained from the bulk XRD analysis and to obtain more detailed information on the clay mineralogy. the clay mineral fraction (<2 microns) was separated and analysed independently for 24 samples of the Draupne and Heather Formations. Where possible at least

one sample from each formation in each well was taken and including duplicate samples 37 analyses were made. Each sample was Mg saturated and analysed in an air dried state, after glycolation at 60°C and after ignition at 550°C (Appendix A for analytical details). Semi-quantitative clay mineral abundances were calculated from the resulting diffractograms by a method based on that of Weir et al (1975).

The clay minerals identified by the more detailed clay analyses were kaolinite, illite, mixed layer illite-smectite, and occasionally chlorite. The average composition of the clay mineral fraction is given in Table 3.3 for the Draupne and Heather Formations. From these data it can be seen that the Draupne Formation has a much lower kaolinite content than the Heather Formation but more illite and especially mixed layer illite-smectite. The chlorite contents of both formations are similar and much lower than the other clays.

In Fig. 3.6 a plot of (mixed layer illite-smectite)/kaolinite versus illite/kaolinite clearly illustrates the differing compositions of the two formations. The Heather Formation samples scatter about a central point in a seemingly random manner, some of which may be due to analytical imprecision. The samples of the Draupne Formation however are seen to lie on a distinct trend, becoming richer in both mixed layer illite-smectite and illite relative to the Heather Formation.

In order that these data may be compared with those from the bulk XRD analyses some recalculation is necessary. The bulk XRD package presents its clay output in terms of

Table 3.3 Clay mineralogy determined from clay XRD. Median values.

Formation	Chlorite	Kaolinite	Illite	Mixed Layer
Draupne	6.60	13.0	35.7	46.5
Heather	4.50	35.2	27.7	27.0

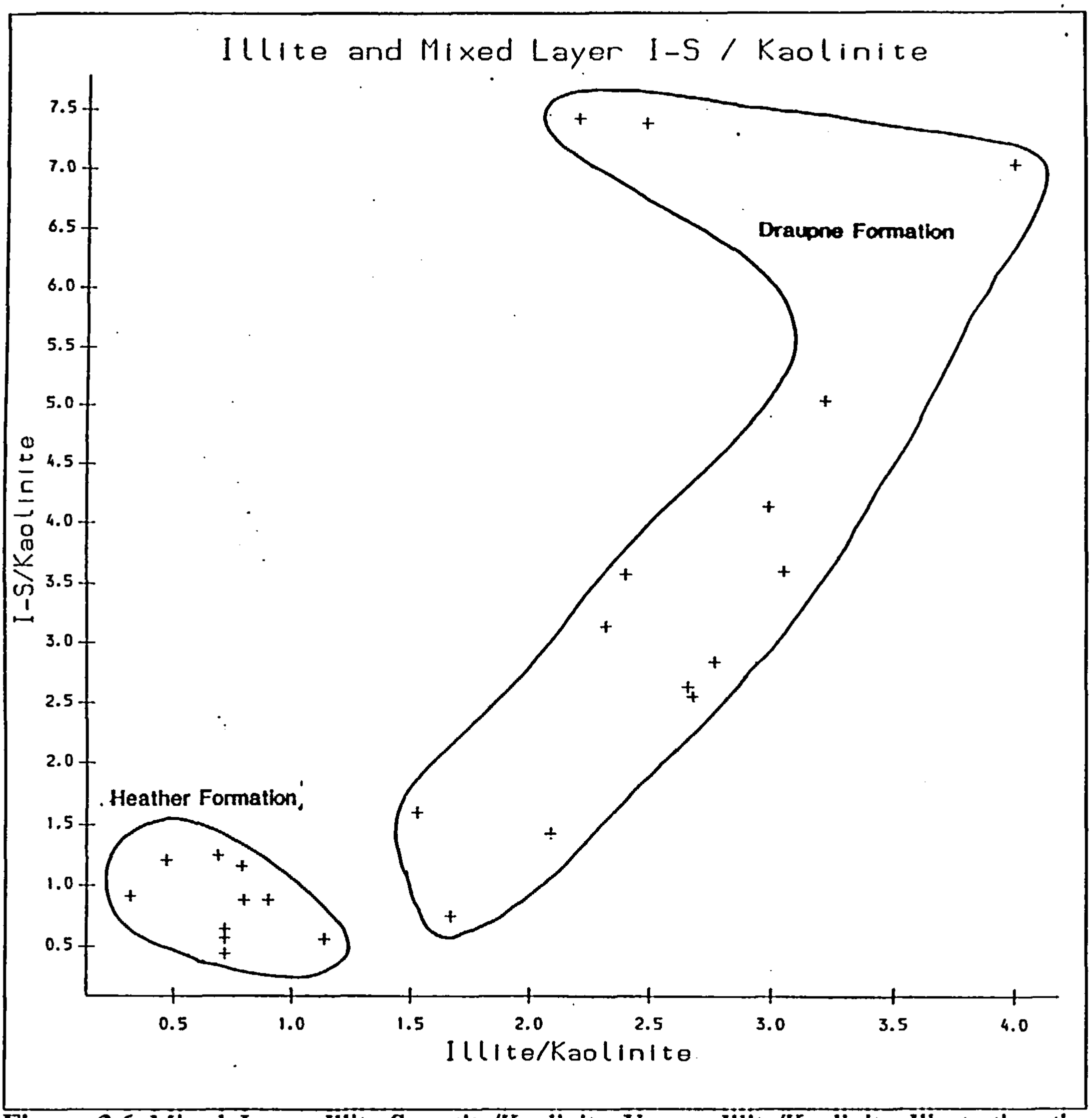

Figure 3.6 Mixed Layer Illite-Smectite/Kaolinite Versus Illite/Kaolinite Illustrating the Differing Clay Mineralogies of the Draupne and Heather Formations.

kaolinite, chlorite, and illite and smectite end-member clays. For a direct comparison therefore the mixed layer clays identified in the clay fraction analyses must be recalculated in terms of the illite and smectite end-members. This can be done provided the proportions of illite and smectite in the mixed layer clays can be estimated from the diffractograms. For the Draupne Formation, rich in the mixed layer clays this usually proved possible, but for the Heather Formation with little mixed layer material it was necessary to assume a likely value; 65% illite being chosen.

The recalculated clay mineralogy is given in Table 3.4, and may be compared with the results of the bulk XRD output recalculated to 100% clays in Table 3.5. The agreement between the two methods is surprisingly good for the Draupne Formation, given the levels of imprecision likely in clay mineral analysis. For the Heather Formation the agreement is poorer but both methods suggest that the Heather Formation is more kaolinitic than the Draupne and contains less illite and smectite which are present as illite and mixed layer illite-smectite.

The clay mineralogy of the Kimmeridge Clay Formation was not examined in this work but has recently been described by Scotchman (1984, 1987a, 1987b) who examined the <0.5 micron fraction and found it to be dominated by mixed layer illite-smectite with variable kaolinite. The fine fraction used might however be expected to be enriched in mixed layer illite-smectite relative to the <2 micron fraction studied in this work. Morris (1980) states that the Kimmeridge Clay is dominated by illite and mixed layer clays with subsidiary amounts of kaolinite whilst Merriman (1978) lists illite>kaolinite>mixed layer clays, with traces of chlorite sometimes detected. Cox and Gallois (1981) find mostly illite and kaolinite with minor smectite and chlorite. It would appear that the clay mineralogy of the onshore Kimmeridge Clay Formation lies somewhere between that of the Draupne and Heather Formations, lacking the high mixed layer content of the Draupne, but lower in kaolinite than the Heather Formation.

3.2 The geochemical data

The geochemical data collected during the study are discussed below. The raw compositions are summarised and compared with those of the other formations analysed, and with published average shale values (Turekian and Wedepohl, 1961; Pettijohn, 1975, based on Clarke, 1924; Krauskopf, 1979), and average black shale (Vine and Touterlot, 1970; Table 3.6). To overcome the interpretational difficulties caused by the variable dilution of the clastic sedimentary material by other components, such as organic matter or authigenic minerals,

Table 3.4 Clay mineralogy determined by clay fraction XRD. Recalculated to illite and smectite end members.

Formation	Chlorite	Kaolinite	Illite	Smectite
Draupne	6.60	13.0	61.4	17.8
Heather	4.50	35.2	49.3	9.20

Table 3.5 Clay mineralogy determined by bulk XRD, median values.

Formation	Chlorite	Kaolinite	Illite	Smectite
Draupne	0.83	15.3	59.7	24.5
Heather	2.46	26.2	55.0	18.5

Al_2O_3 normalised data are also discussed. In the case of the trace element discussion below the (element*10,000/Al_2O_3) ratio is used for convenience.

The ratio of an element deposited with the clastic detritus to Al_2O_3, which is itself dominantly resident in the detrital silicates, will remain approximately constant whatever the level of dilution of the clastics by non-detrital phases, and whatever the absolute concentration of the element. The ratio should take a value close to that of average shale. For elements fixed during diagenesis in non-detrital phases the ratio to Al_2O_3 will be an index of the extent to which the element has been concentrated above the level expected from the detrital input alone.

3.2.1 Major element geochemistry

The major rock forming oxides SiO_2, Al_2O_3, Fe_2O_3, MgO, CaO, Na_2O, K_2O, and MnO were determined on 72 samples of the Draupne Formation and 66 samples of the Heather Formation from the Norwegian sector of the North Sea, and 52 samples of the Kimmeridge

Table 3.6 Published average shales values: 1 Pettijohn, 1975; 2 Turekian and Wedepohl, 1961; 3 Krauskopf, 1979. Average black shale from Vine and Tourtelot, 1970.

Average Shale Analyses				
Element	Average 1	Average 2	Average 3	Average Black Shale
SiO_2	58.1	58.5	51.0	-
Al_2O_3	15.4	15.1	17.4	13.2
ΣFe_2O_3	6.74	6.74	6.71	2.86
MgO	2.44	2.49	2.32	1.16
CaO	3.11	3.09	3.50	2.10
Na_2O	1.30	1.29	1.21	0.94
K_2O	3.24	3.21	3.01	2.41
MnO	-	0.11	0.11	0.02
TiO_2	0.65	0.77	0.75	0.33
P_2O_5	0.17	0.11	0.17	-
S	0.26	0.24	0.25	-
TOC	0.80	-	-	3.20
CO_2	2.63	-	-	1.21

Clay Formation from along its English outcrop comprising samples from beds 44, 32, 24, and 18 (Cox and Gallois, 1981). Analysis was by Atomic Absorption following acid digestion based on the procedure of Bernas (1968). Analytical details are fully described in Appendix A. TiO_2 was also determined by Atomic Absorption after the trace element dissolution procedure outlined in Appendix A. P_2O_5 was determined colorimetrically (Appendix A for details).

S was determined on 72 Draupne Formation samples, 69 Heather Formation samples, and 52 Kimmeridge Clay Formation samples. S determinations were by two methods, the first being an ignition-titration wet chemical analysis, and the second using a Leco C+S analyser (Appendix A). The Leco C+S analyser was also used to analyse these Draupne, Heather and

Table 3.7 Major element composition of the Draupne, Heather, and Kimmeridge Clay Formations.

Draupne Formation						
Element	N	Mean	Median	Std. Dev.	Max.	Min.
SiO_2	72	50.3	51.6	7.46	59.5	8.20
Al_2O_3	72	16.4	17.1	2.81	23.8	2.82
ΣFe_2O_3	72	7.20	6.82	3.00	29.2	1.27
MgO	72	2.07	2.16	0.90	7.15	0.68
CaO	72	2.46	1.19	5.78	48.1	0.54
Na_2O	72	0.92	0.91	0.22	1.71	0.48
K_2O	72	3.39	3.55	0.80	4.98	0.34
MnO	72	0.04	0.03	0.04	0.34	0.01
TiO_2	72	0.57	0.58	0.11	0.81	0.14
P_2O_5	72	0.22	0.18	0.14	0.84	0.05
S	72	3.57	3.22	2.94	24.9	0.59
TOC	72	5.70	6.30	2.13	11.2	0.34
CO_2	72	1.89	0.33	5.18	38.5	0.00

Heather Formation						
Element	N	Mean	Median	Std. Dev.	Max.	Min.
SiO_2	66	50.1	52.4	12.8	68.0	7.82
Al_2O_3	66	16.8	17.9	4.87	24.1	1.68
ΣFe_2O_3	66	8.88	7.18	5.45	37.6	5.01
MgO	66	1.68	1.49	1.08	8.09	0.52
CaO	66	3.48	0.72	7.65	42.5	0.16
Na_2O	66	0.97	0.92	0.30	1.69	0.30
K_2O	66	2.83	2.92	0.91	6.66	0.28
MnO	66	0.27	0.05	0.51	2.79	0.02
TiO_2	66	0.71	0.78	0.19	0.98	0.13
P_2O_5	66	0.55	0.18	2.44	19.8	0.06
S	69	3.08	2.26	3.25	24.2	0.33
TOC	69	2.66	2.31	1.79	7.71	0.20
CO_2	69	3.62	0.29	7.55	35.9	0.00

Kimmeridge Clay Formation						
Element	N	Mean	Median	Std. Dev.	Max.	Min.
SiO_2	52	45.7	46.1	9.03	60.7	10.1
Al_2O_3	52	15.4	15.4	3.25	19.8	2.86
ΣFe_2O_3	52	5.75	5.14	2.60	16.5	1.18
MgO	52	1.75	1.62	0.69	4.63	0.93
CaO	52	10.6	9.08	7.51	42.6	0.83
Na_2O	52	0.99	0.94	0.40	2.11	0.38
K_2O	52	2.60	2.65	0.66	4.05	0.60
MnO	52	0.03	0.02	0.01	0.09	0.02
TiO_2	52	0.58	0.59	0.11	0.78	0.17
P_2O_5	52	0.16	0.15	0.07	0.48	0.07
S	52	1.90	1.49	1.52	8.85	0.31
TOC	52	4.14	3.75	2.78	15.2	0.31
CO_2	52	9.09	7.37	6.90	38.9	0.18

Kimmeridge Clay Formation samples for total organic carbon (TOC), and for total carbon, allowing carbonate carbon, and hence CO_2 to be calculated (Appendix A).

3.2.1.1 SiO_2

SiO_2 is the dominant oxide in the majority of samples analysed. Distributions are illustrated in Fig. 3.7. The Draupne and Heather Formation averages lie within the range of published averages for shales but the Kimmeridge Clay Formation is relatively deficient. The Draupne and Heather have similar SiO_2 contents (medians 51.6% and 52.4% respectively) and the distributions of SiO_2 in both are negatively skewed due to the presence of occasional samples with very high carbonate, pyrite, or phosphate contents. The Kimmeridge Clay Formation has a lower SiO_2 content with a median of only 46.1% and a more nearly normal distribution. The highest recorded SiO_2 value of 68.0% was from the Heather Formation.

SiO_2 in mudstones is present in the detrital silicate minerals, chiefly quartz, feldspars, and clays. The ratio of SiO_2 to Al_2O_3 will remain unchanged despite the varying effects of dilution

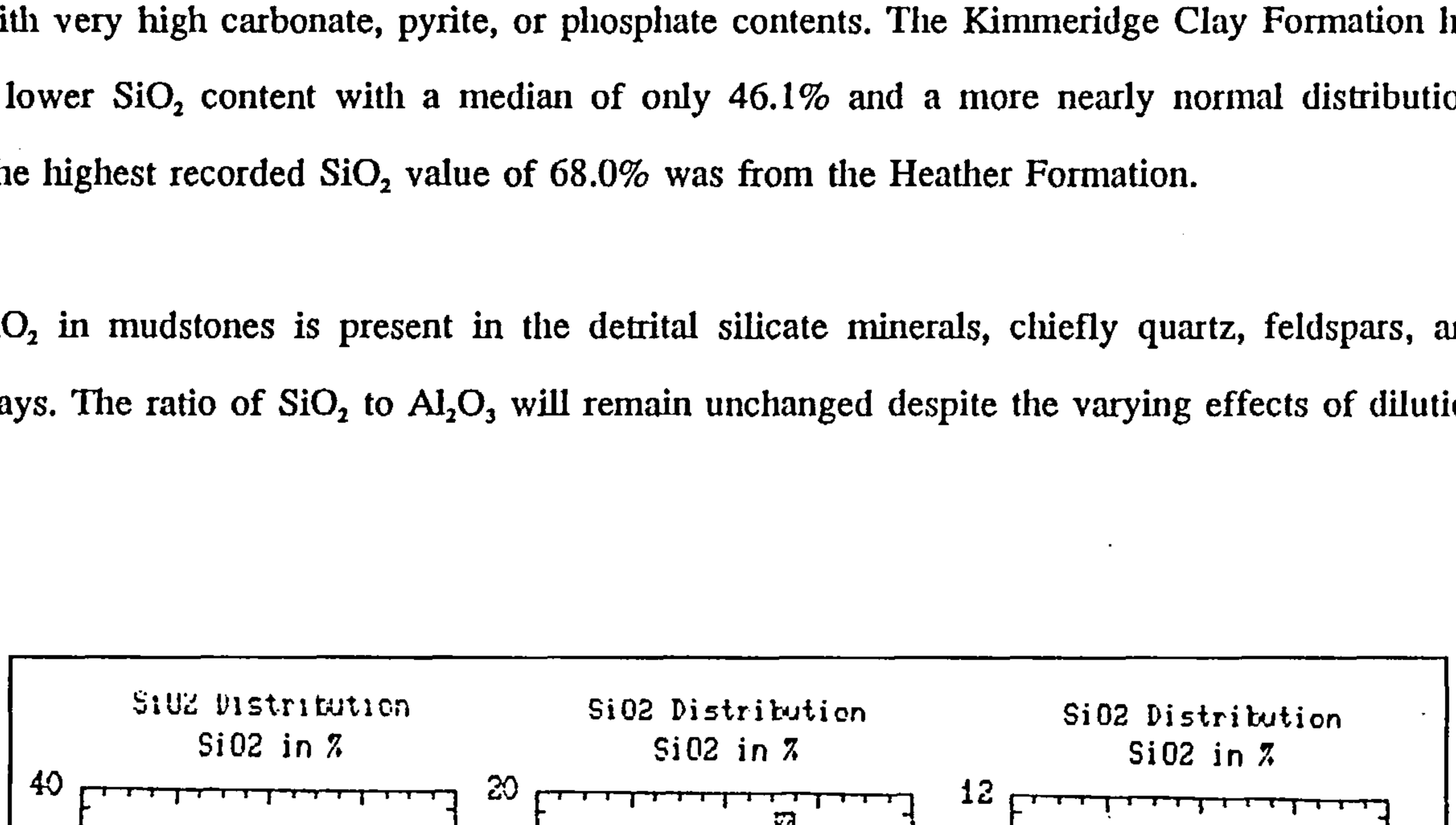

Figure 3.7 SiO_2 distributions in the Draupne, Heather, and Kimmeridge Clay Formations.

by carbonates or other minerals provided that the composition of this detrital fraction remains constant. The ratio will be most sensitive to variation in the proportions of quartz to total clays although changes in the clay mineralogy will also have an effect. The values of the SiO_2/Al_2O_3 ratios are similar for the Draupne, Heather, and Kimmeridge Clay Formations, with medians of 3.02, 2.95,and 2.97 respectively suggesting that the lower SiO_2 content of the Kimmeridge Clay Formation is due to a greater proportion of carbonate minerals (see below) and not to any change in the composition of the silicate detritus. These values are similar to the lowest of the published values for average shale where SiO_2/Al_2O_3 is 2.93.

3.2.1.2 Al_2O_3

Al_2O_3 is generally the second most abundant oxide in the samples, and in mudstones it is found mainly in clays, but also in feldspars and micas, and the distributions (Fig 3.8) are similar to SiO_2 in the corresponding formations. The Draupne and Kimmeridge Clay Formations are within the range of published shale averages, having median values of 17.1%, and 15.4% Al_2O_3 respectively, whilst the Heather Formation exceeds them slightly, having a median value of 17.9%. All are higher than the values published for average black shale.

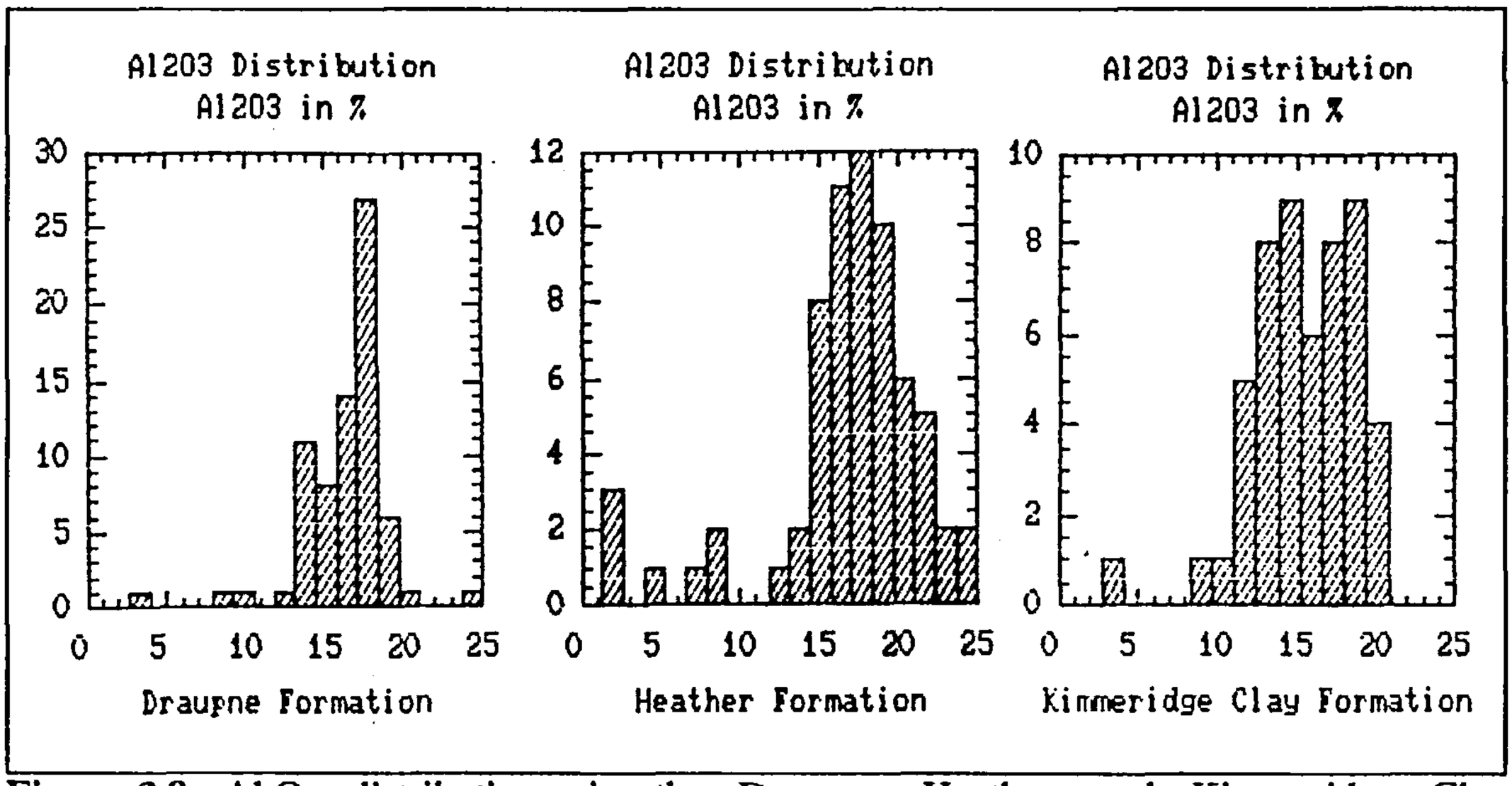

Figure 3.8 Al_2O_3 distributions in the Draupne, Heather, and Kimmeridge Clay Formations.

The Draupne and Heather Formations have similar Al_2O_3 contents, with the higher SiO_2 and Al_2O_3 of the Heather Formation indicating a slight dilution of the detrital silicates in the Draupne Formation possibly by organic matter and pyrite. The slightly lower SiO_2/Al_2O_3 ratio of the Heather Formation in comparison to the Draupne may be due to the increase in the abundance of kaolinite relative to other clays as noted above. The lower Al_2O_3 content of the Kimmeridge Clay is explained by its greater carbonate content, with a detrital component essentially similar to that of the Draupne and Heather Formations, and a SiO_2/Al_2O_3 ratio lying between the two.

3.2.1.3 Fe_2O_3

The Fe_2O_3 contents determined are summarised as EFe2O3 in Table 3.7, each formation having a positively skewed distribution (Fig. 3.9). None of the median values of the formations analysed in the present study lie within the limited range of the average shale analyses. The Draupne and Heather Formations both exceed the average shale values slightly, with median values of 6.82% and 7.18% Fe_2O_3 respectively, whilst the Kimmeridge Clay

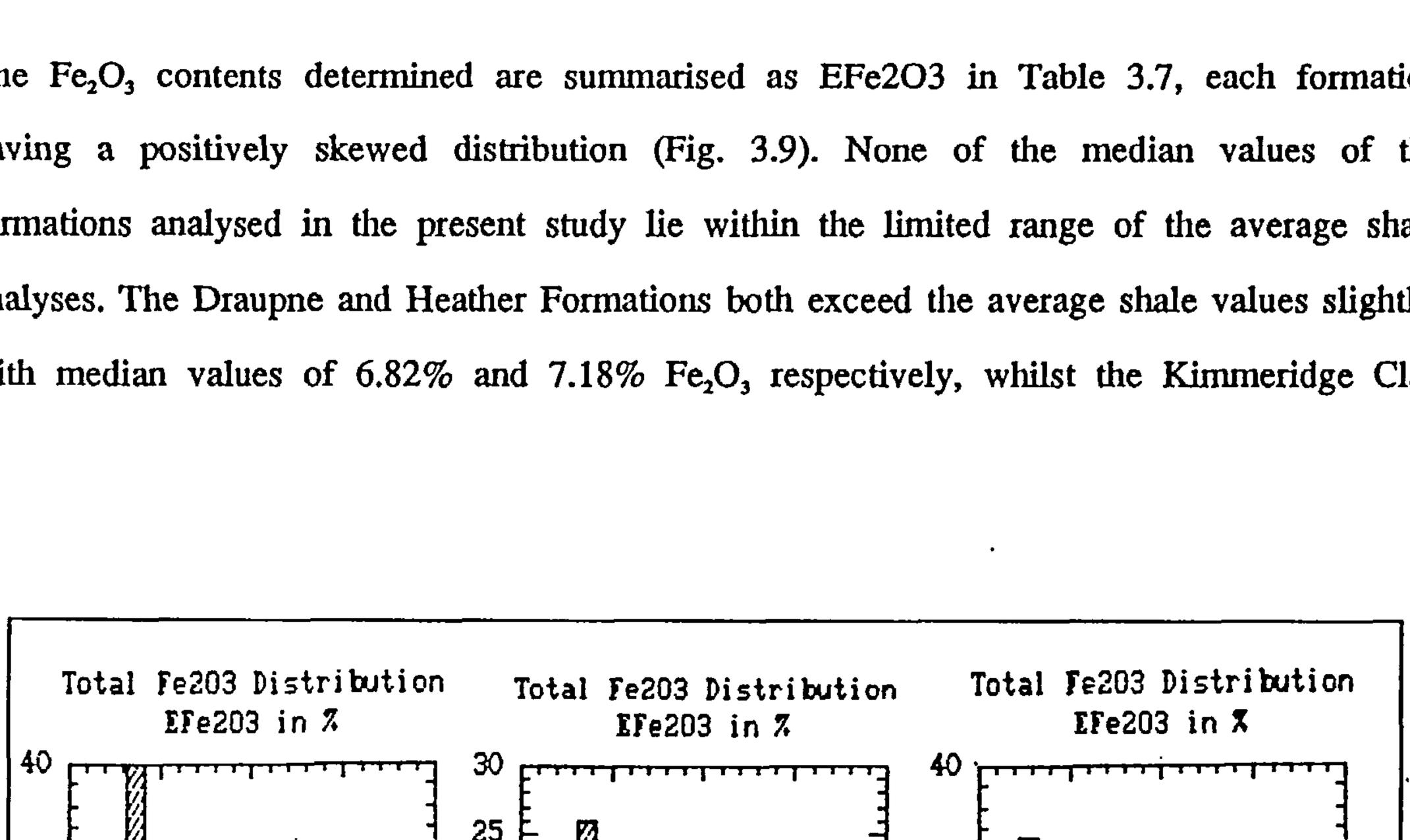

Figure 3.9 Total Fe_2O_3 distributions in the Draupne, Heather, and Kimmeridge Clay Formations.

Formation has less, its median being only 5.14%. All three have greater median Fe_2O_3 contents than the published average of black shales.

The main Fe bearing minerals in mudstones are pyrite, siderite, and clay minerals, the relative contributions depending on the depositional and diagenetic conditions. Originally, however much of the iron would have been supplied as oxide and hydroxide material. The Fe_2O_3/Al_2O_3 ratio measures the relative proportions of the iron bearing minerals to total clay. Median Fe_2O_3/Al_2O_3 ratios are 0.40, 0.39, and 0.32 respectively for the Draupne, Heather, and Kimmeridge Clay Formations. The Draupne and Heather Formations are very similar both to each other and to the average shales (0.45, 0.44, 0.39) but the Kimmeridge Clay is lower, though still above the Fe_2O_3/Al_2O_3 ratio of average black shale (0.22).

The proportion of Fe_2O_3 present as pyrite may be calculated from the S analyses if two assumptions are made, these being that the total S content of the samples represents total sulphide, and that all of the sulphide is present as pyrite. The first assumption relies on sulphate and organic S contributions being small in comparison with the sulphide S and is not unreasonable in unweathered shales in which sulphate reduction was probably very active during early diagenesis, and where the organic matter present is comparatively low in S (Nils Telnaes, personal communication). The second assumption also seems reasonable as no other sulphide minerals were detected by XRD and the combined total of other metal sulphides must be insignificant compared to that of Fe. If pyrite Fe is calculated in this way then non-pyrite Fe, which must reside in carbonates or clays can be found by difference.

The average pyrite Fe contents calculated in this way (note these are reported as Fe) are 2.81%, 1.98%, and 1.30% respectively for the Draupne, Heather, and Kimmeridge Clay Formations. Normalising to Al_2O_3 will represent the proportion of pyrite to clays in the sample, and when normalised in this manner the calculated pyrite Fe contents give values of 0.16, 0.11, and 0.09. This shows that the Draupne Formation has a considerably higher proportion of pyrite relative to clay minerals than do the others. The resulting non-pyrite

Fe_2O_3 contents have median values of 2.79%, 4.06%, and 3.07% for the Draupne, Heather, and Kimmeridge Clay Formations with Al_2O_3 normalised values of 0.16, 0.22, and 0.21 respectively. This non-pyrite Fe_2O_3 must reside in siderite or clays. Inspection of these data indicates that the Draupne Formation has the highest proportion of its total iron content as pyrite and the Kimmeridge Clay Formation the lowest. The Heather Formation is intermediate in composition. The relationships between pyrite and non-pyrite iron, and also sulphur and carbon are discussed in much greater detail in Chapter 5.

3.2.1.4 MgO

MgO distributions (Fig. 3.10) are all positively skewed and each of the formations in the present study (Table 3.7) is depleted in comparison to average shales (2.49%, 2.44%, 2.32%),

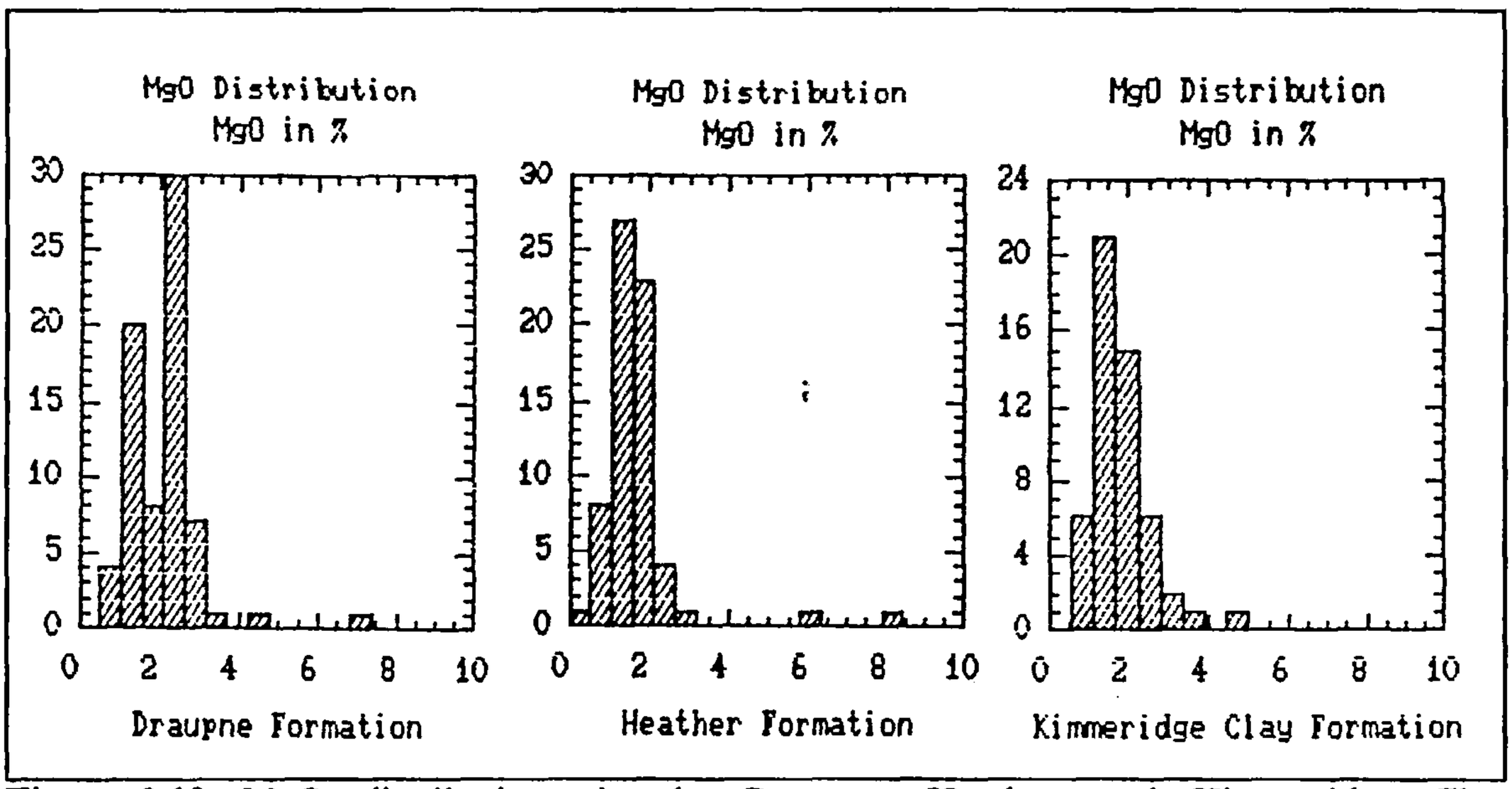

Figure 3.10 MgO distributions in the Draupne, Heather, and Kimmeridge Clay Formations.

but contain more than the average black shale (1.16%). The Draupne Formation (2.16%) is however richer in MgO than the Heather, and Kimmeridge Clay Formations (1.49% and 1.62% respectively). The MgO/Al_2O_3 ratio will be most sensitive to changes in the relative proportions of dolomite to clays, though changes in clay mineralogy may have a subsidiary effect as MgO is also likely to reside in the clays. The ratios take median values of 0.12, 0.08, and 0.10 for the Draupne, Heather, Kimmeridge Clay Formations, indicating the probable higher proportion of dolomite in the Draupne, or possible higher content of MgO bearing smectite and illite clays, and lower proportion in the Heather Formation in relation to the Kimmeridge Clay. These ratios are still below those of average shale, namely 0.16, 0.16, and 0.13 suggesting that all are depleted in dolomite compared to the average, but are similar to the value given for average black shale of 0.09.

3.2.1.5 CaO

The distributions of CaO (Fig. 3.11, Table 3.7) are positively skewed. Inspection of these values shows the Kimmeridge Clay to be some 10 times richer in CaO (9.08%) than the

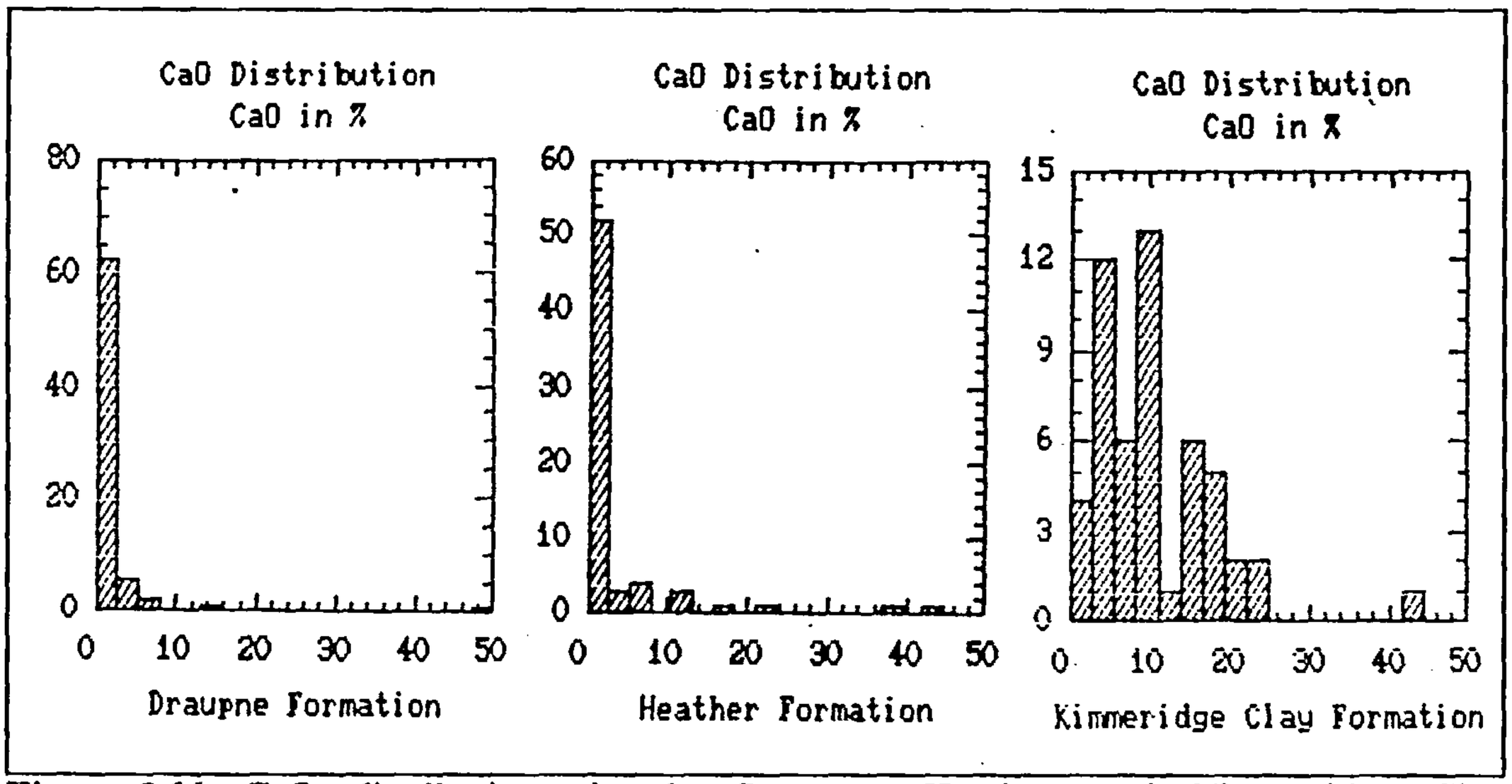

Figure 3.11 CaO distributions in the Draupne, Heather, and Kimmeridge Clay Formations.

Draupne (1.19%) and Heather (0.72%), and much richer than the published average shale values (3.09%, 3.11%, 3.50%), and the average black shale (2.10%). The Draupne and Heather Formations are very much depleted in CaO compared to these averages. CaO in these samples is likely to be controlled by the presence or absence of calcite and the CaO/Al_2O_3 ratio will indicate the relative proportions of calcite to clays. The median values of this ratio are 0.07, 0.04, and 0.58 for the Draupne, Heather, and Kimmeridge Clay Formations compared to average shale values of 0.20, and average black shale of 0.16. Thus it would appear that calcite in the Kimmeridge Clay Formation is much more common than in shales generally, and that conversely in the Draupne and Heather Formations calcite is much less abundant than the average. This conclusion differs somewhat from the XRD evidence but is considered to be more reliable.

3.2.1.6 Na_2O

The median Na_2O contents of the Draupne, Heather, and Kimmeridge Clay Formations, are very similar, 0.91%, 0.92%, and 0.94% respectively (Table 3.7), as are the distributions (Fig.

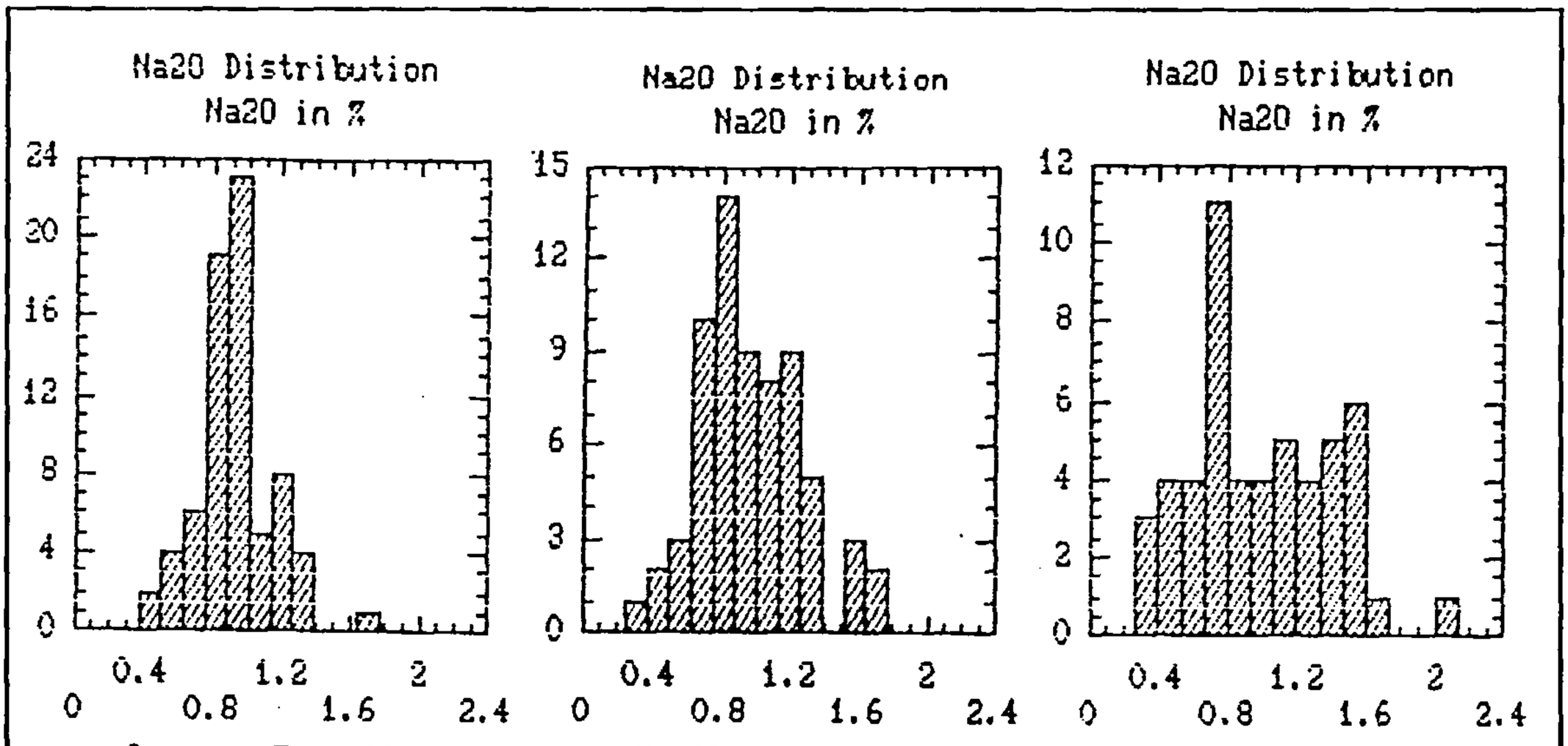

Figure 3.12 Na_2O distributions in the Draupne, Heather, and Kimmeridge Clay Formations.

3.12) which are symmetrical. The published average Na_2O contents for shales (1.30%, 1.21%, 1.29%) are all greater than those obtained in this study, but the average black shale value (0.94%) is in good agreement. Most of the Na_2O in these samples is probably resident in Na-feldspar so the Na_2O/Al_2O_3 ratio will indicate changes in the proportions of Na-feldspar present. The values of the Na_2O/Al_2O_3 ratio are 0.06 for the Draupne, Heather, and Kimmeridge Clay Formations, showing that their detrital components are similar.

3.2.1.7 K_2O

K_2O contents determined in this study are summarised above (Table 3.7). The distributions (Fig. 3.13) are negatively skewed with the exception of the Heather Formation and the Draupne Formation (3.55%) is enriched in K_2O relative to published averages (3.24%, 3.21%, 3.01%) with the Heather and Kimmeridge Clay Formations being depleted somewhat (2.92% and 2.65% respectively), though still above the black shale average (2.41%). K_2O is probably resident within both illitic clay and K-feldspar but probably has a smaller proportion of its content in feldspars than does Na_2O (Spears and Amin, 1981), so that the K_2O/Al_2O_3 ratio is

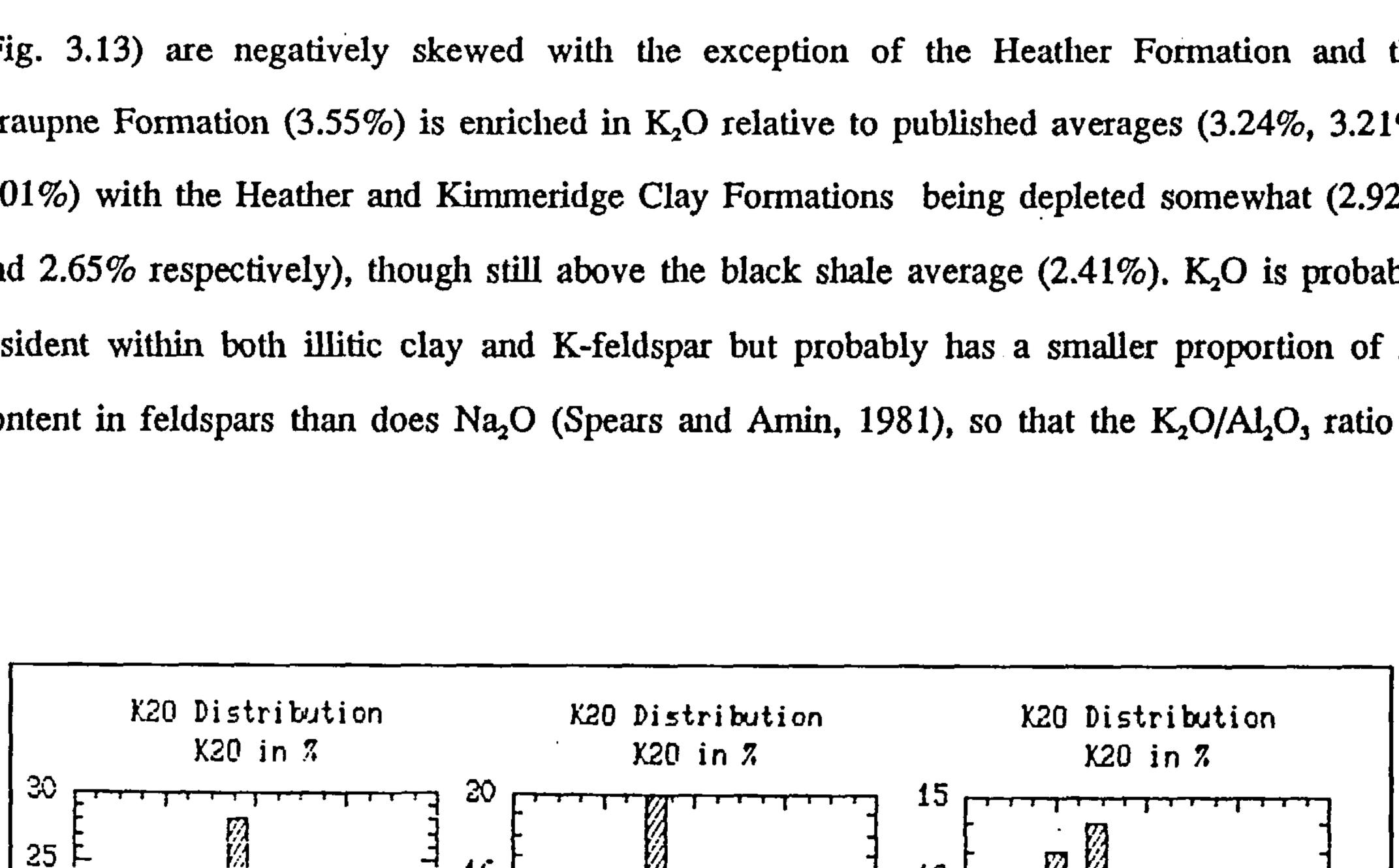

Figure 3.13 K_2O distributions in the Draupne, Heather, and Kimmeridge Clay Formations.

dependent upon both the clay mineralogy of the sediment and the K-feldspar content. The median ratios are 0.21, 0.16, and 0.17 for the Draupne, Heather, and Kimmeridge Clay Formations. The high K_2O/Al_2O_3 ratio of the Draupne formation is consistent with the more illitic clay mineralogy of that formation, and with the evidence from SiO_2/Al_2O_3 ratios for more kaolinitic clay in the Heather Formation. The Kimmeridge Clay occupies an intermediate position, but in both cases is more similar to the Heather than the Draupne. The similarity between the Heather and Kimmeridge Clay Formations indicates that the lower K_2O content of the latter is due to dilution of the silicate detritus by carbonate minerals, primarily calcite (see above).

3.2.1.8 MnO

The MnO distributions (Fig. 3.14) for the three formations studied are positively skewed. In comparison with the published average shale analyses (both 0.11% MnO) the median MnO contents in this study (Table 3.7) are all depleted, but are closer to the average of black shales (0.02%). The Heather Formation has the highest MnO content of the formations

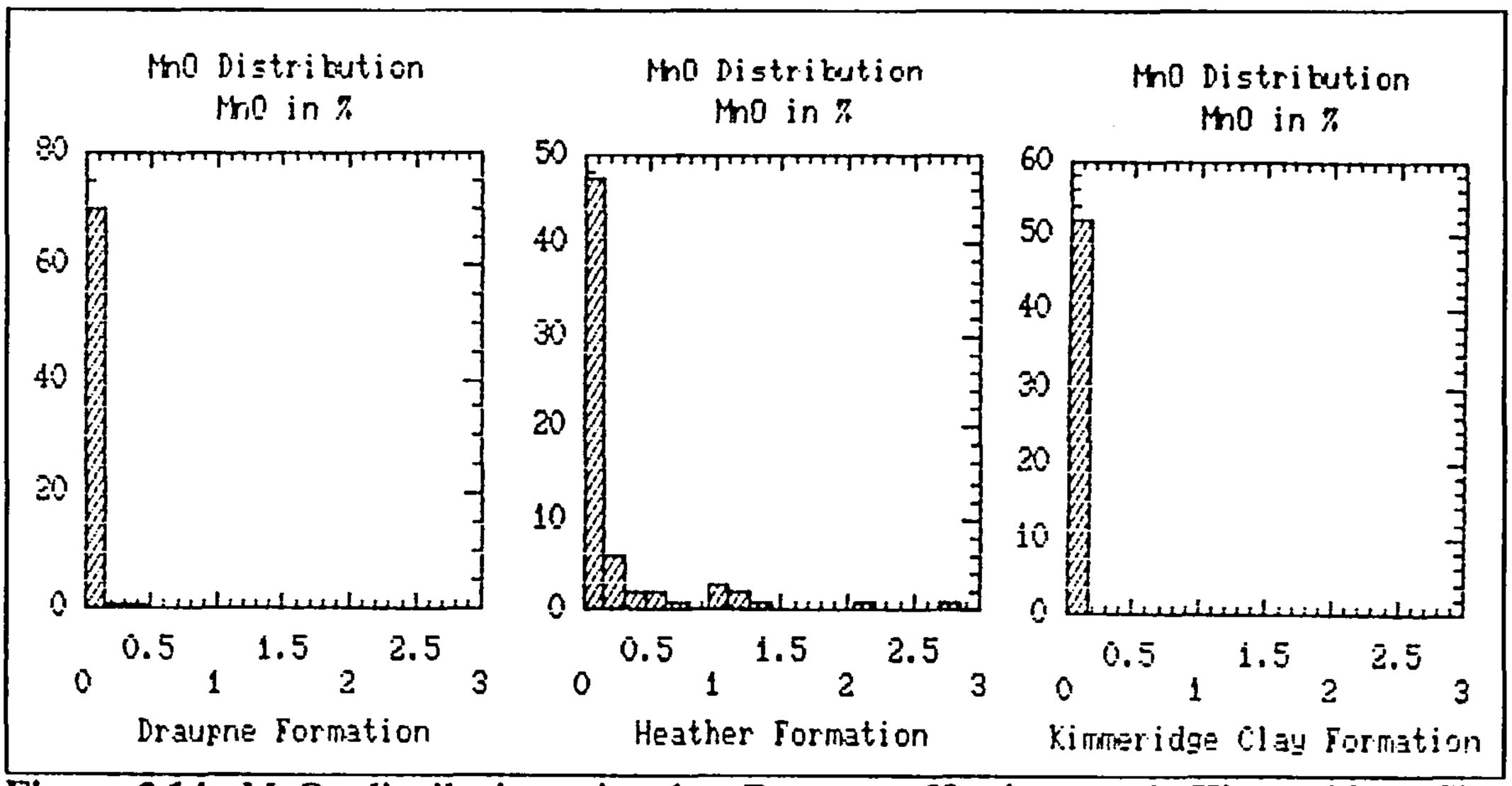

Figure 3.14 MnO distributions in the Draupne, Heather, and Kimmeridge Clay Formations.

analysed in the present study, with a median of 0.05% whilst the Draupne and Kimmeridge Clay Formations are similar with median values of 0.03% and 0.02% respectively. These low MnO contents are common in black shales and are due to loss of the mobile Mn^{2+} species to the pore water during deposition and diagenesis because of the reducing conditions. MnO is generally considered to reside in carbonate minerals but the very carbonate rich Kimmeridge Clay Formation is not especially abundant in MnO. Rather it is the Heather Formation with the highest MnO content, this also having the highest non-pyrite Fe content. When normalised to Al_2O_3 the MnO content of the Heather Formation (0.003) exceeds those of the other formations (both 0.002) although the difference is small. The normalised MnO contents are lower than the average shales (0.007, 0.006) but are similar to the average black shale (0.002).

3.2.1.9 TiO_2

All of the median values for the formations analysed here (Table 3.7, Fig. 3.15) lie outside the range of published shales (0.65%, 0.77%, 0.75%), though the Heather Formation whose

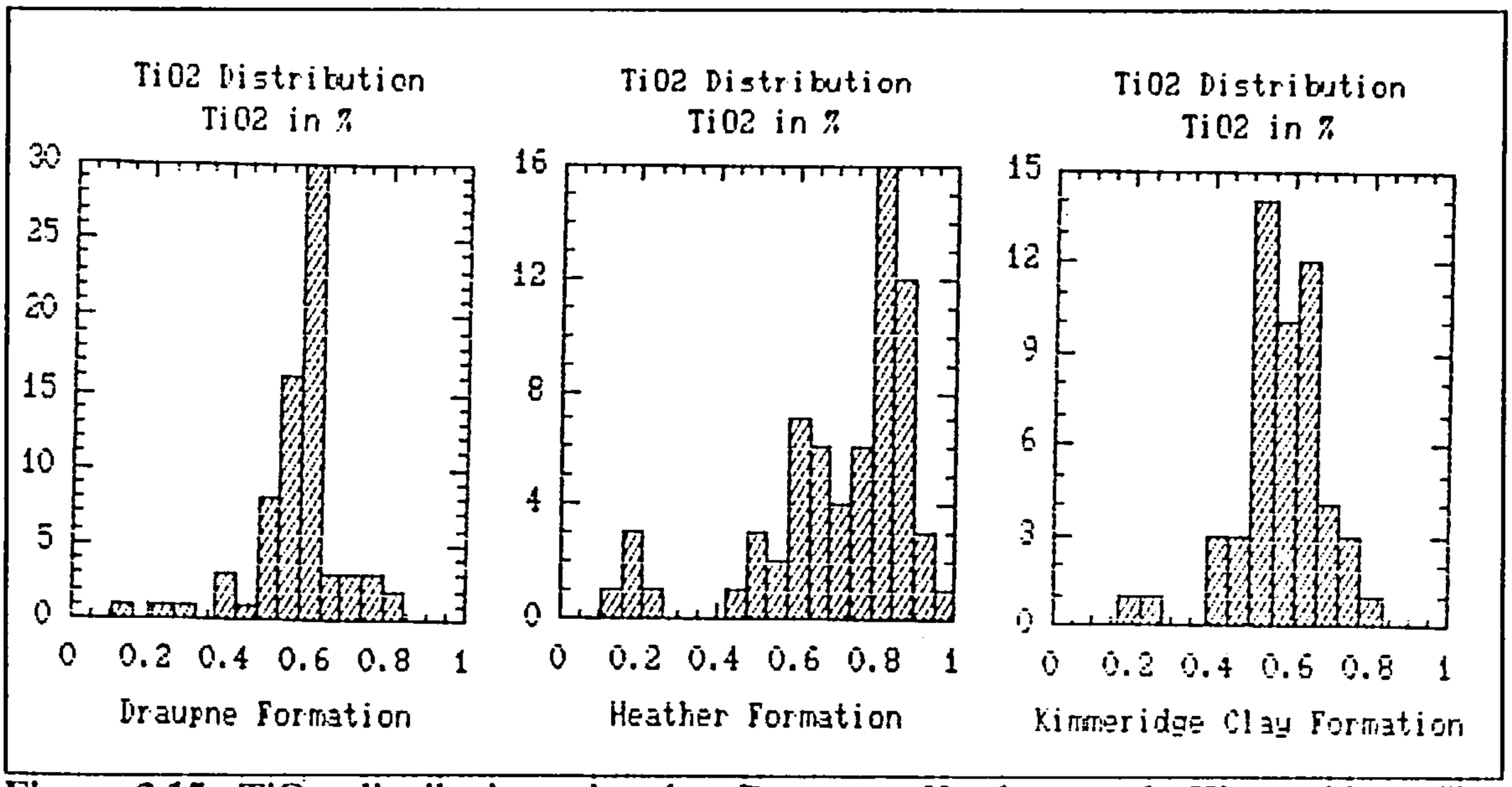

Figure 3.15 TiO_2 distributions in the Draupne, Heather, and Kimmeridge Clay Formations.

median is 0.78% lies just above. The Draupne and Kimmeridge Clay Formations both lie below the published shale averages with medians of 0.58% and 0.59%, but are above the value given for average black shale (0.33%). TiO_2 is probably present mainly in the resistant oxides anatase or rutile, but some is also likely to reside within clay mineral lattices. The ratio of TiO_2/Al_2O_3 increases as the proportion of quartz increases (Spears and Kanaris-Sotiriou, 1976) because the relative contribution from the Ti-oxides becomes greater than clay associated TiO_2 whose maximum TiO_2/Al_2O_3 ratio is about 0.025. In this study the median TiO_2/Al_2O_3 ratio is greatest in the Heather Formation (0.043) where it is similar to the average shales (0.042, 0.051, 0.043). The Kimmeridge Clay Formation (0.037) is intermediate and the Draupne Formation has the lowest average value (0.034), but this still exceeds the TiO_2/Al_2O_3 ratio of average black shale (0.025).

3.2.1.10 P_2O_5

P_2O_5 distributions (Fig. 3.16) are positively skewed especially the Heather Formation with a maximum of 19.8% and two others exceeding 1%. The Draupne and Heather Formations

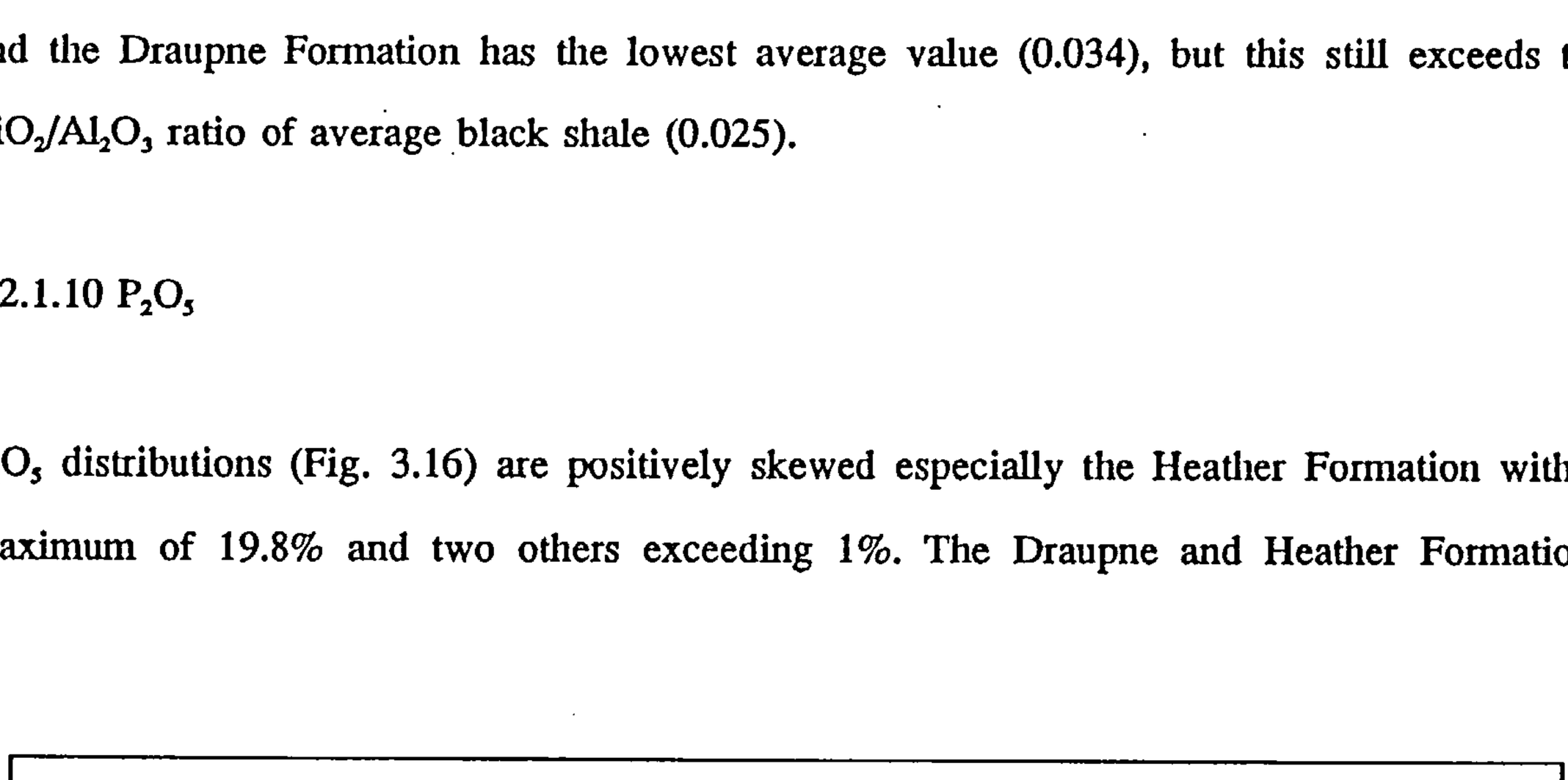

Figure 3.16 P_2O_5 distributions in the Draupne, Heather, and Kimmeridge Clay Formations.

have similar median P_2O_5 contents (0.18% P_2O_5 each) which are slightly higher than the published average shales (0.17%, 0.11%, 0.17%). The Kimmeridge Clay Formation has less (0.15%), and falls within their range. P_2O_5 in these samples is probably resident in apatite. The P_2O_5/Al_2O_3 ratio will represent the proportion of apatite to clay minerals present. The median Al_2O_3 normalised P_2O_5 contents for the three formations are all 0.010 suggesting that the lower total P_2O_5 content of the Kimmeridge Clay Formation is due solely to its greater dilution by carbonate minerals, chiefly calcite. Comparative Al_2O_3 normalised P_2O_5 contents for average shales are 0.011, 0.007, and 0.009 which are similar to those of this study suggesting that the slightly higher P_2O_5 contents of the formations in this work relative to average shale are due to the lower carbonate content of these shales relative to the average. It is likely that the source of the P_2O_5 in the majority of samples studied was decomposing organic matter, with perhaps some detrital phosphate material. A different origin must be proposed however for the very phosphoritic sample of the Heather Formation, possibly involving some reworking.

3.2.1.11 S

The distributions of the S contents (Fig. 3.17) are very positively skewed. Maximum values are 24.9% and 24.2% S respectively for the Draupne and Heather Formations. The median S content of the Draupne Formation (3.22%) is considerably higher than those of the other formations and the Kimmeridge Clay Formation has a rather lower median (only 1.49% S). The Heather Formation is intermediate (2.26%). These median S contents are about an order of magnitude greater than for average shale (0.26%, 0.24%, and 0.25% S). In mudstones and especially black shales the S content is probably held mainly in pyrite and this has been assumed above in the discussion of Fe_2O_3. The S/Al_2O_3 ratio will therefore be a measure of the pyrite content relative to clay minerals. The Draupne Formation has the greatest median S/Al_2O_3 ratio (0.18) and the Kimmeridge Clay Formation the smallest (0.10), with the Heather Formation having an intermediate value (0.13). As with the raw S contents these are roughly ten times higher than the average shales (0.017, 0.016, 0.014).

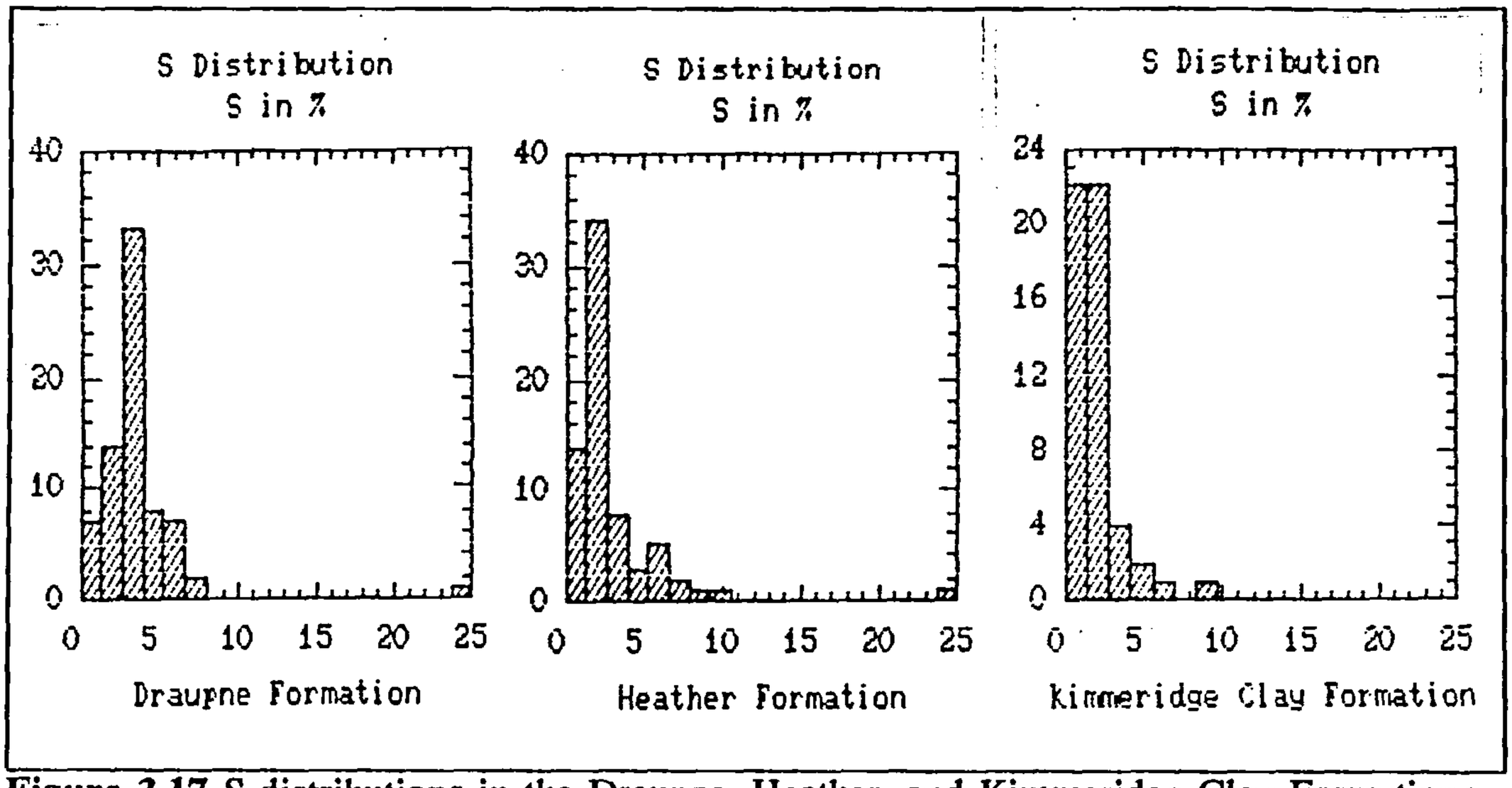

Figure 3.17 S distributions in the Draupne, Heather, and Kimmeridge Clay Formations.

3.2.1.12 TOC

The distributions of TOC are illustrated in Fig. 3.18. The Draupne Formation has by far the greatest average TOC content (6.30%) and exceeds both the Kimmeridge Clay Formation

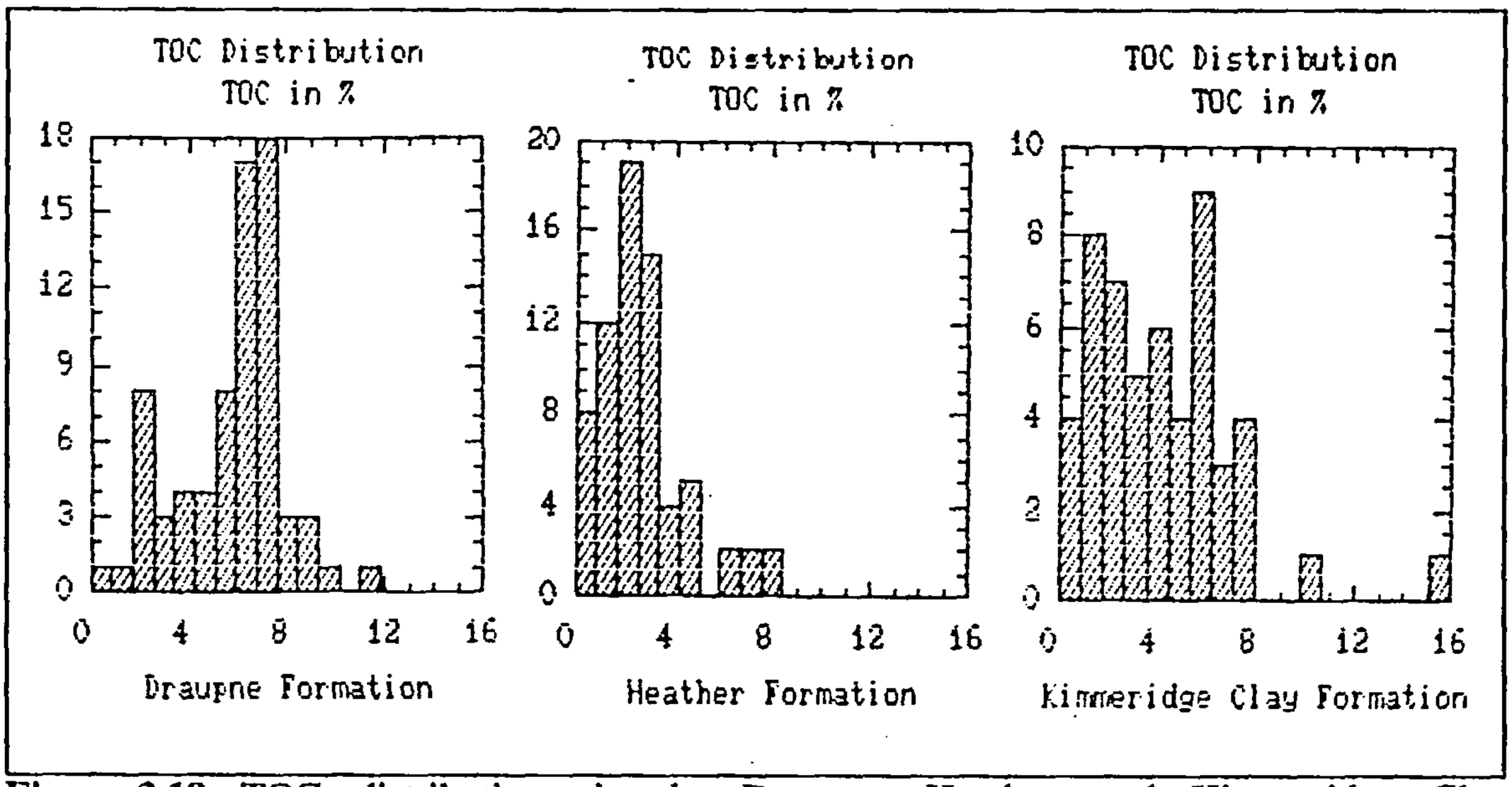

Figure 3.18 TOC distributions in the Draupne, Heather, and Kimmeridge Clay Formations.

(3.75%) and the Heather Formation (2.31%). Both the Draupne and Kimmeridge Clay Formations have a higher average TOC than the average black shale (3.2%), but the average shale (0.80% TOC) is much lower than even the Heather Formation. Although the median value of the Draupne Formation is the highest the greatest TOC value recorded, 15.2% C is from the Kimmeridge Clay Formation. Normalising to Al_2O_3 will indicate TOC to clay proportions, these being 0.37, 0.13, and 0.24 for the three formations and may be compared to a value of 0.052 for average shale, and 0.242 for average black shale.

3.2.1.13 CO_2

The distributions of CO_2 (Fig. 3.19) are all positively skewed, the maximum recorded values being 38.5%, 35.9%, and 38.9% respectively for the Draupne, Heather, and Kimmeridge Clay Formations. These are approaching the CO_2 content of pure calcite (44%). The median CO_2 content of the Kimmeridge Clay Formation (6.90%) is the greatest, and exceeds both average shale (2.63%) and average black shale (1.21%). The Draupne and Heather Formations (0.33% and 0.29% respectively) and have considerably less CO_2 than the average shales and black

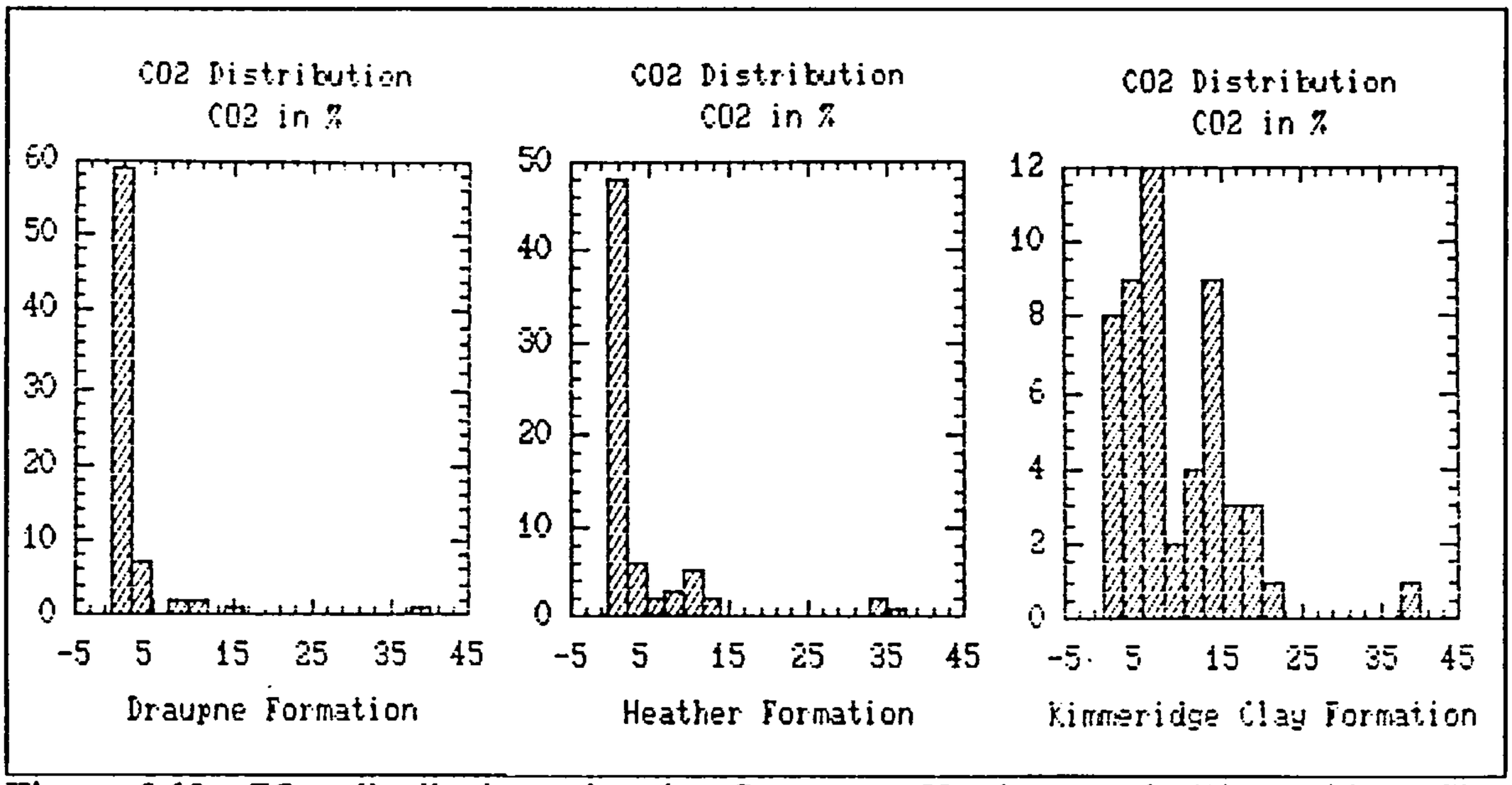

Figure 3.19 CO_2 distributions in the Draupne, Heather, and Kimmeridge Clay Formations.

shale. The CO_2/Al_2O_3 ratio represents the relative proportions of carbonate minerals, of which calcite is most common in these samples, to clay minerals. The Kimmeridge Clay has the highest median value (0.439) which exceeds the published average shale (0.171) and black shale (0.092). The Draupne and Heather Formations have very low values (0.016 and 0.010) emphasising their low carbonate contents.

3.2.2 Trace element geochemistry

The trace elements Ag, Cd, Co, Cr, Cu, Li, Ni, Sc, V, and Zn were determined for 72 samples of the Draupne Formation, 66 samples from the Heather Formation, and 52 samples of the Kimmeridge Clay Formation by Atomic Absorption following the acid dissolution procedure outlined in Appendix A. The additional trace elements Mo, Nb, Pb, Rb, Sr, Th, U, Y, and Zr were analysed by X-Ray Fluorescence on pressed powder pellets (Appendix A) for 67 of the Draupne Formation samples, 49 of the Heather Formation samples, and all 52 of the Kimmeridge Clay Formation samples. The remaining samples could not be analysed in this manner because of their small sizes. The trace element data are summarised in Table 3.8.

3.2.2.1 Ag

In most samples Ag was not detected although a maximum of 8ppm was recorded for the Heather Formation. Because of the very small number of reliable non-zero analyses Ag is not considered further.

3.2.2.2 Cd

The Cd distributions are positively skewed (Fig 3.20), the maximum recorded value being 27ppm from the Heather Formation. The median Cd content of the Draupne Formation (4ppm) is considerably higher than average shale (0.3ppm), and the other formations studied here. The average Cd contents of the Heather Formation (mean=1ppm, median=0ppm), and

Table 3.8 Trace element concentrations in the Draupne, Heather, and Kimmeridge Clay Formations

Draupne Formation						
Element	N	Mean	Median	Std. Dev.	Max.	Min.
Cu	72	67	63	21.9	123	10
Li	72	71	79	21.7	139	8
Co	72	24	22	11.5	59	1
Zn	72	472	328	397.8	1890	24
Cd	72	7	4	6.8	26	0
Cr	72	150	138	54.9	414	29
Ag	72	1	0	0.9	5	0
Ni	72	166	162	73.8	436	8
V	72	579	592	217.7	1087	74
Sc	72	13	13	3.6	23	6
Pb	67	24	22	12.0	83	3
Th	67	15	15	2.9	21	3
Rb	67	147	160	37.2	197	8
U	67	22	20	11.5	76	0
Sr	67	237	238	39.4	338	148
Y	67	34	34	8.2	66	7
Zr	67	138	136	42.0	375	27
Nb	67	22	20	7.2	50	12
Mo	67	91	85	81.1	609	4

Kimmeridge Clay Formation						
Element	N	Mean	Median	Std. Dev.	Max.	Min.
Cu	52	39	37	19.5	143	10
Li	52	81	79	22.1	121	14
Co	52	14	12	6.9	48	5
Zn	52	125	79	141.0	770	20
Cd	52	1	0	2.1	13	0
Cr	52	120	118	33.7	247	24
Ag	52	1	1	0.6	3	0
Ni	52	80	60	103.6	727	12
V	52	147	140	106.2	860	31
Sc	52	10	9	3.0	19	5
Pb	52	20	20	7.1	53	4
Th	52	14	14	2.8	17	2
Rb	52	150	146	39.1	226	27
U	52	6	5	2.5	13	0
Sr	52	336	332	96.8	577	157
Y	52	26	27	4.1	32	9
Zr	52	135	135	33.8	206	27
Nb	52	18	17	3.8	26	5
Mo	52	15	7	26.5	182	1

Heather Formation						
Element	N	Mean	Median	Std. Dev.	Max.	Min.
Cu	66	45	44	23.5	127	12
Li	66	112	119	44.9	230	13
Co	66	32	17	107.5	890	6
Zn	66	286	131	828.1	6720	32
Cd	66	1	0	4.3	27	0
Cr	66	165	135	109.5	765	18
Ag	66	0	0	1.3	8	0
Ni	66	99	78	166.0	1395	23
V	66	228	200	147.4	752	38
Sc	66	11	10	4.0	24	1
Pb	49	31	25	35.8	264	12
Th	49	15	15	5.6	26	2
Rb	49	106	113	27.3	196	12
U	49	6	5	10.2	73	0
Sr	49	236	179	233.8	1293	53
Y	49	37	31	26.8	206	11
Zr	49	239	187	118.4	575	41
Nb	49	21	20	5.2	43	9
Mo	49	7	4	8.7	56	2

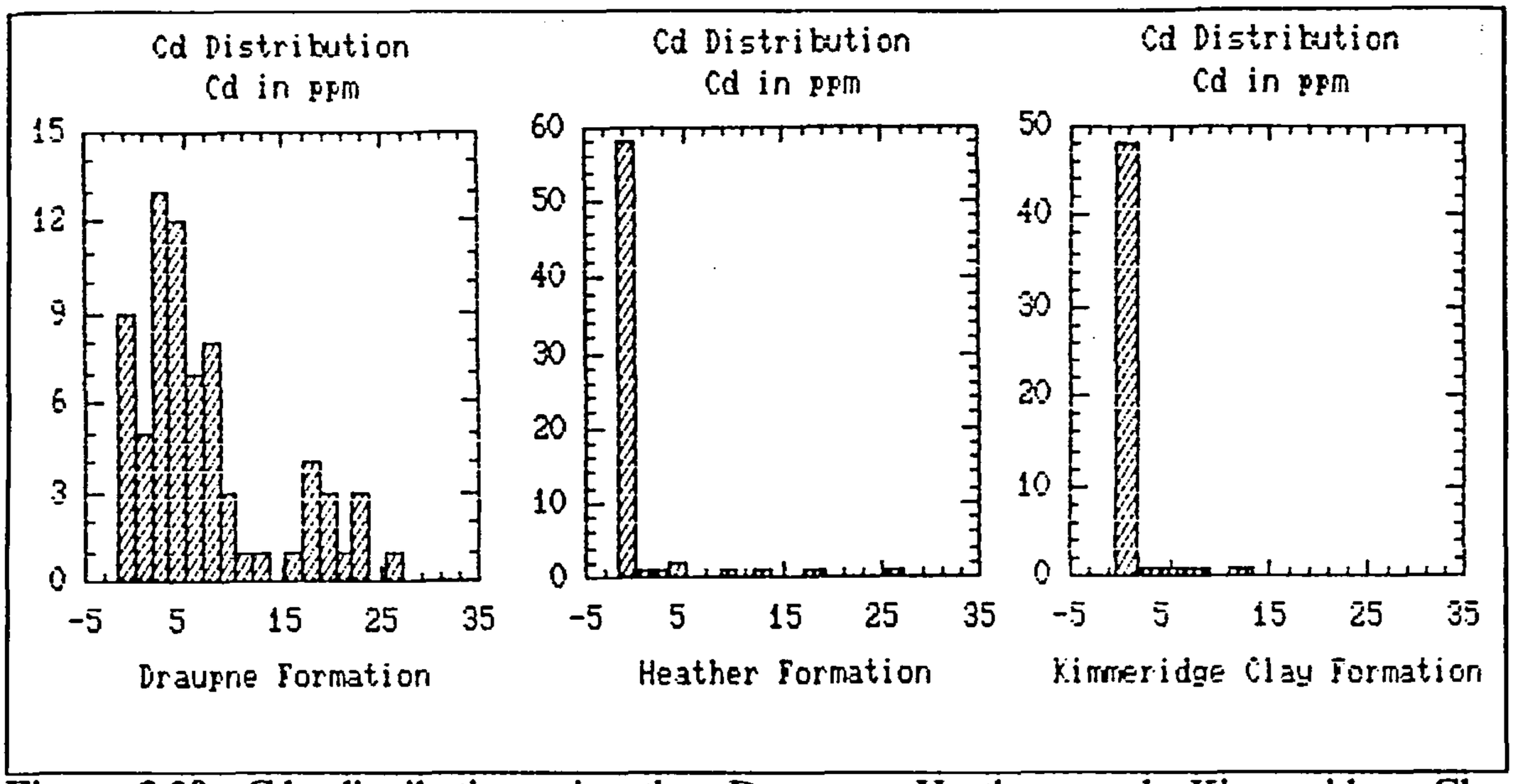

Figure 3.20 Cd distributions in the Draupne, Heather, and Kimmeridge Clay Formations.

Kimmeridge Clay Formation (mean=1ppm, median=0ppm) are much lower but the maximum values reached in each of these formations (27ppm, 13ppm, and 13ppm) are well above the detection limits. The median Al_2O_3 normalised Cd content of the Draupne Formation (0.26) greatly exceeds the average shale value (0.02) but the Heather and Kimmeridge Clay Formations are similar but lower with median normalised values of 0.00.

3.2.2.3 Co

The distributions of Co are positively skewed (Fig. 3.21; note the scale difference for the Heather Formation). The highest Co content recorded in this study is 890ppm in a phosphatic sample from the Heather Formation, the next highest being only 59ppm from the Draupne Formation. The medians of the Draupne and Heather Formations (22ppm and 17ppm respectively) are similar to average shale (19ppm, 20ppm) being slightly higher and lower respectively, but the Kimmeridge Clay Formation is depleted in Co (only 12ppm). All are greater than the published average black shale Co content (10ppm). The Draupne Formation has a similar median Al_2O_3 normalised Co content (1.26) to the average shales (1.26, 1.15), whilst the Heather Formation (0.99) is slightly lower. As with the raw Co contents the

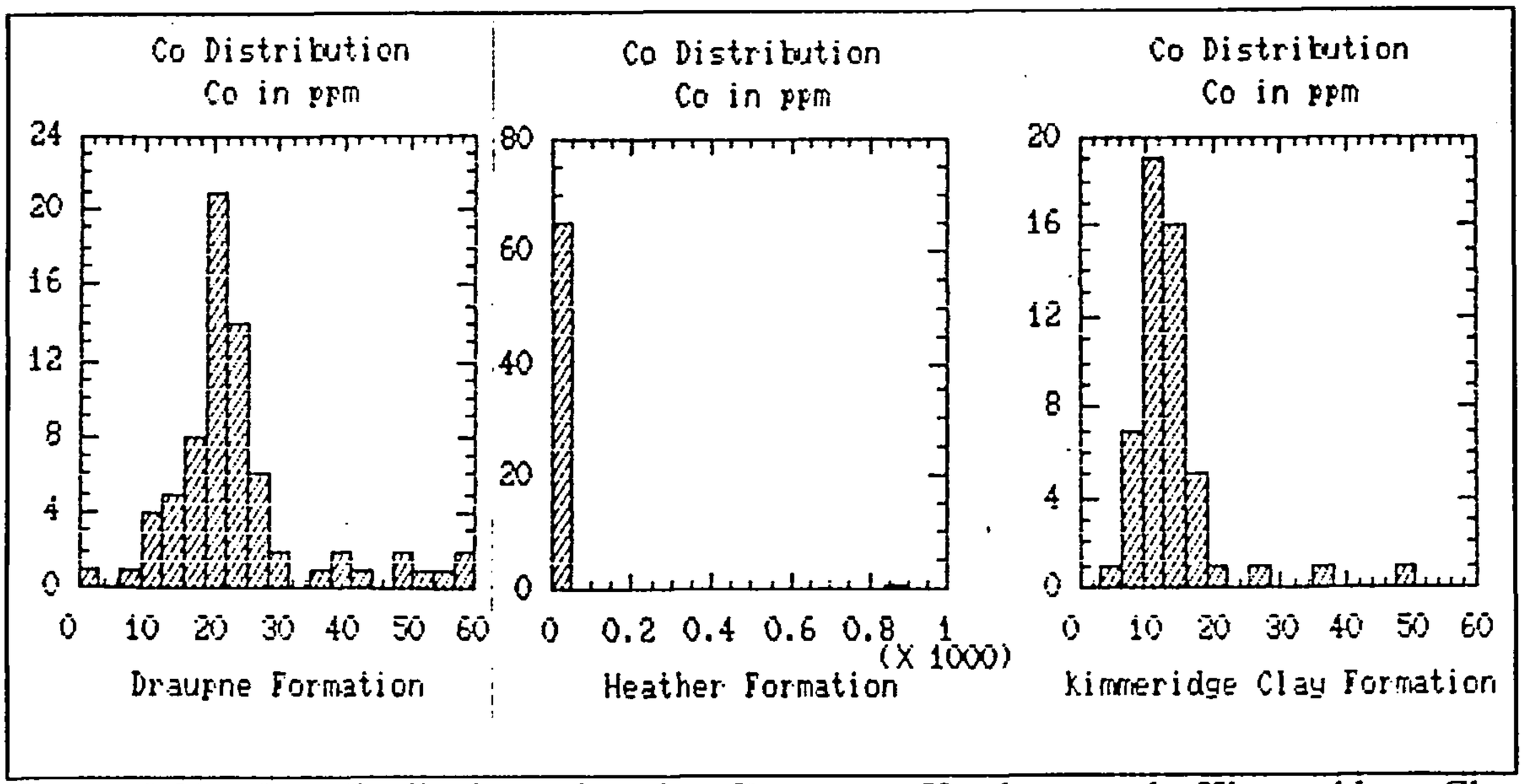

Figure 3.21 Co distributions in the Draupne, Heather, and Kimmeridge Clay Formations.

median normalised Co content of the Kimmeridge Clay Formation (0.78) is lower than the other three sample sets, and the average shales, but is similar to the average black shale (0.76). The lower Co content of this formation cannot then be attributed to the high carbonate content.

3.2.2.4 Cr

The distributions of Cr in each of the formations (Fig. 3.22) are positively skewed, the maximum recorded Cr content being 765ppm in the Heather Formation. The Draupne and Heather Formations have similar median Cr contents (138ppm and 135ppm respectively) which are higher than the Kimmeridge Clay Formation (118ppm). All of the Cr averages in this study exceed the published average shale values (90ppm, 100ppm) and average black shale (100ppm). The Draupne Formation has the highest median Al_2O_3 normalised Cr content of the formations studied (8.37), and this exceeds both average shales (5.96, 5.75) and average black shale (7.58). The Heather and Kimmeridge Clay Formations have very similar normalised Cr medians (7.75 and 7.72 respectively) suggesting that the lower Cr content of the latter is due to dilution by the large amounts of calcite present.

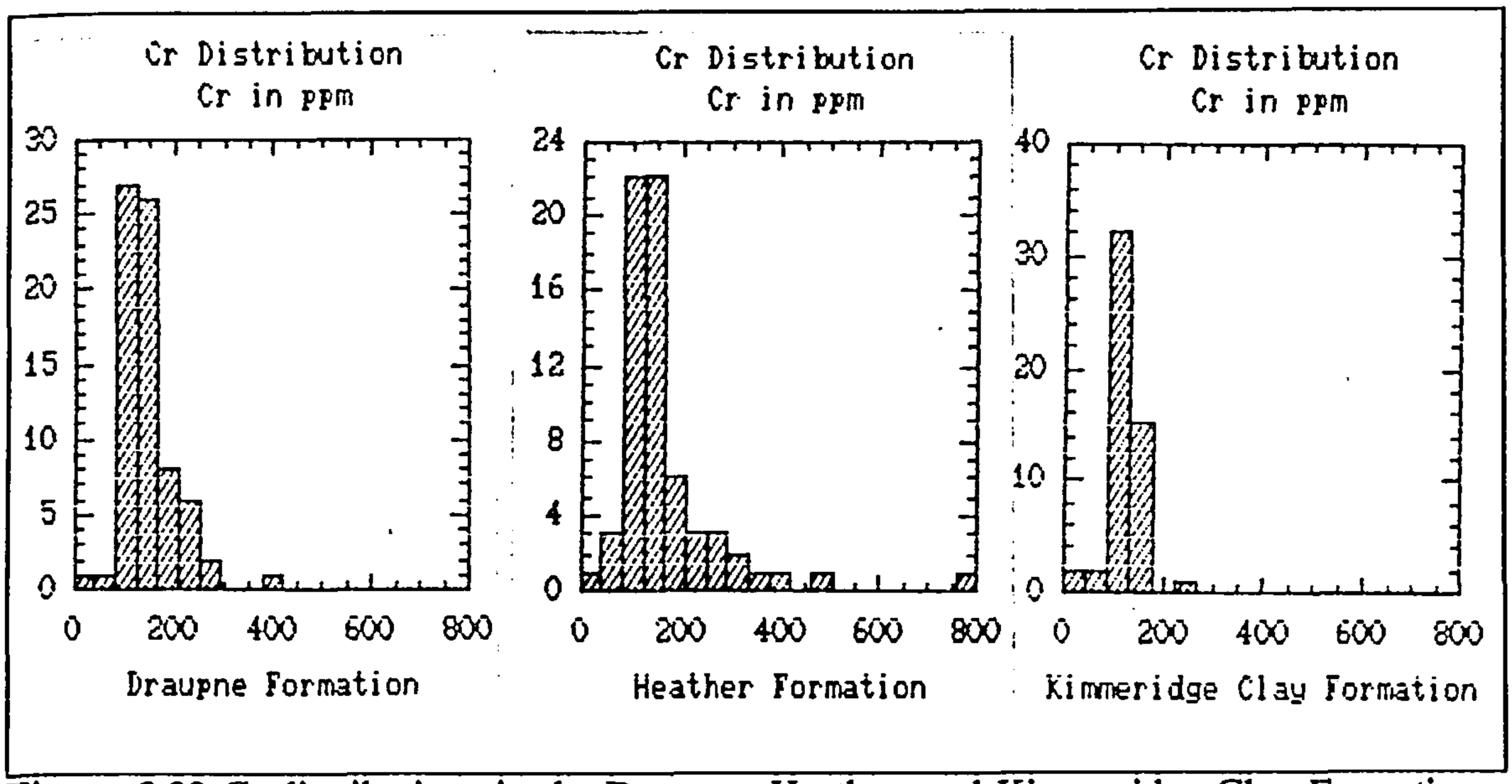

Figure 3.22 Cr distributions in the Draupne, Heather, and Kimmeridge Clay Formations.

3.2.2.5 Cu

The distributions of Cu (Fig. 3.23) are almost symmetrical in the Draupne Formation, but the Heather and Kimmeridge Clay Formations are both positively skewed. The highest individual Cu content recorded in this work was 143ppm in the Kimmeridge Clay Formation. The

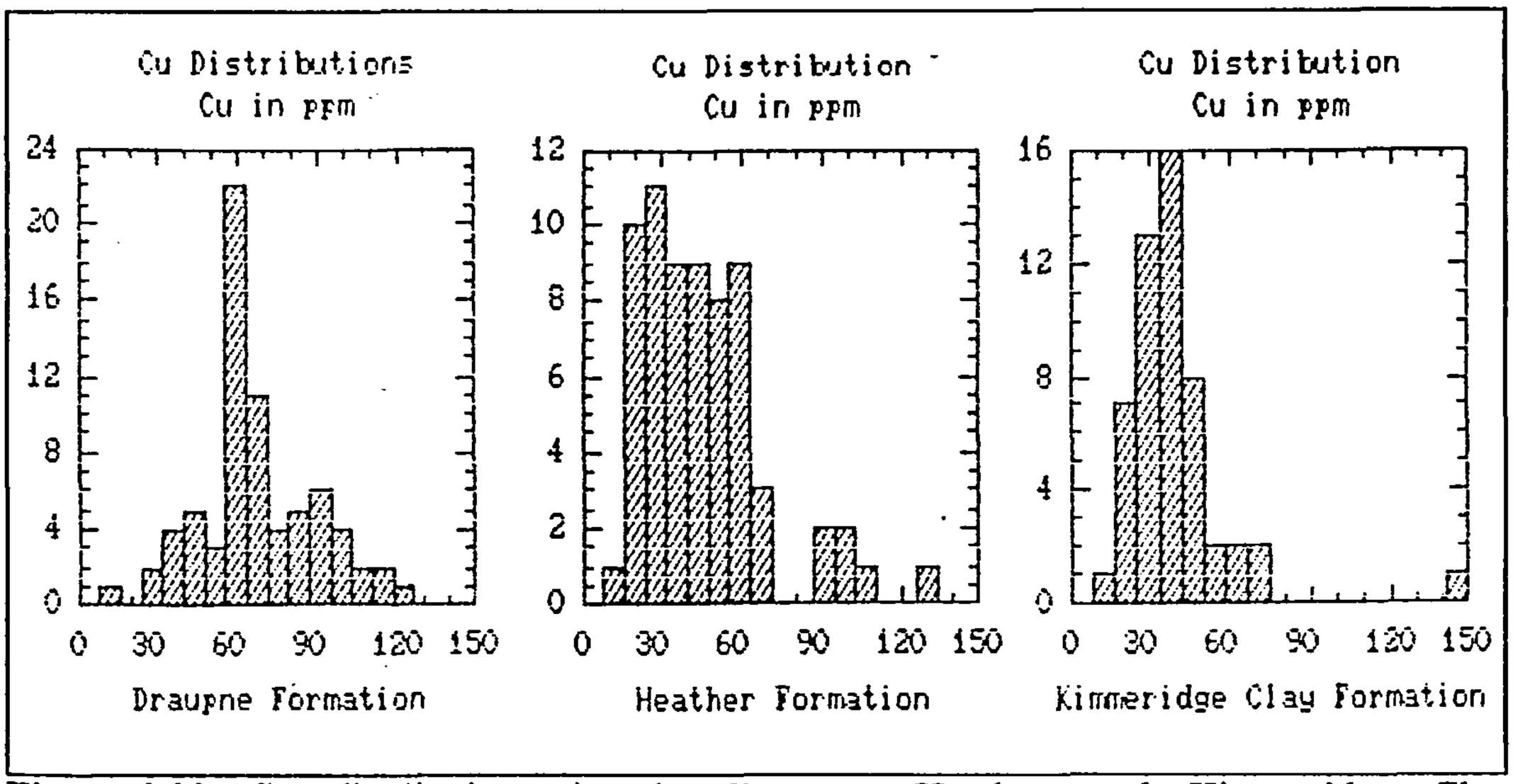

Figure 3.23 Cu distributions in the Draupne, Heather, and Kimmeridge Clay Formations.

Draupne has the highest median Cu content (63ppm), well in excess of published average shale values (45ppm, 50ppm), and only slightly below the average black shale value (70ppm), but the Heather and Kimmeridge Clay Formations (median Cu 44ppm, and 37ppm respectively) are close to the published averages. The Draupne Formation has the highest median Al_2O_3 normalised Cu content (3.78) which is greater than the average shale values (2.98 and 2.87) but less than the average black shale (5.30). The Heather and Kimmeridge Clay Formations are lower (2.36 and 2.26 respectively). The lower Cu content of the Kimmeridge Clay formation is probably due mainly to carbonate dilution as its normalised Cu content is similar to that of the Heather Formation.

3.2.2.6 Li

The distributions of Li (Fig. 3.24) have slight negative skews, the highest recorded Li value being 230ppm for a sample from the Heather Formation. The Heather also has the highest

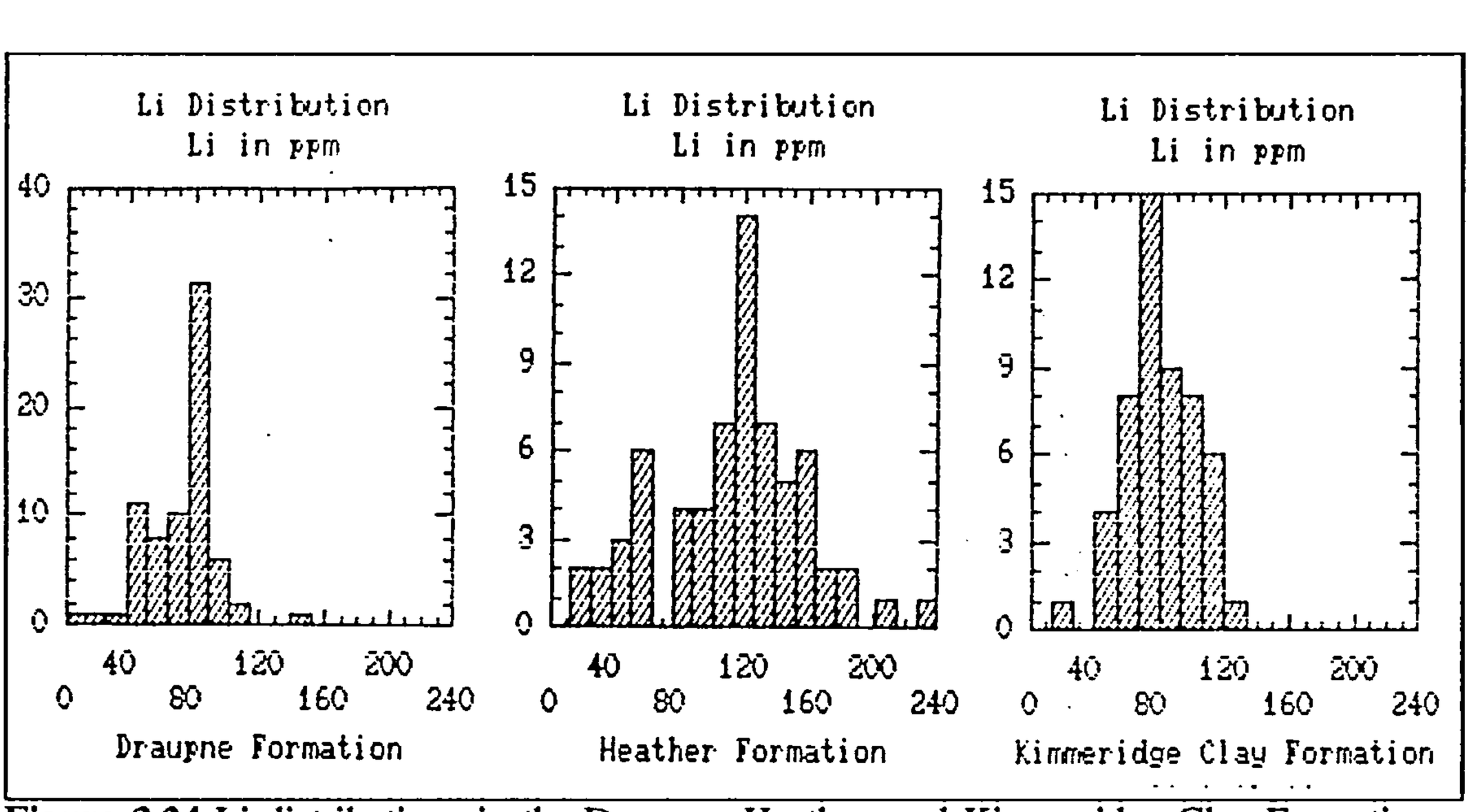

Figure 3.24 Li distributions in the Draupne, Heather, and Kimmeridge Clay Formations.

median Li content (119ppm), the Draupne and Kimmeridge Clay Formations being lower (both 79ppm). When compared with average shale contents (66ppm and 60ppm) the Heather Formation is enriched in Li to a considerable extent, and the Draupne and Kimmeridge Clay Formations are also Li rich. As with the raw contents the Heather Formation has the highest median Al_2O_3 normalised value (6.91). The median normalised Li contents of the Draupne Formation (4.54) and the Kimmeridge Clay Formation (5.37) show that the similarity in gross Li content between these formations is coincidental, with the latter having a larger normalised Li content. The formations analysed in this study have greater Al_2O_3 normalised Li than published average shales (4.37, 3.45).

3.2.2.7 Mo

The distributions of Mo (Fig. 3.25) are positively skewed, the highest Mo content recorded in the study being 609ppm from a pyrite rich sample of the Draupne Formation. The Draupne

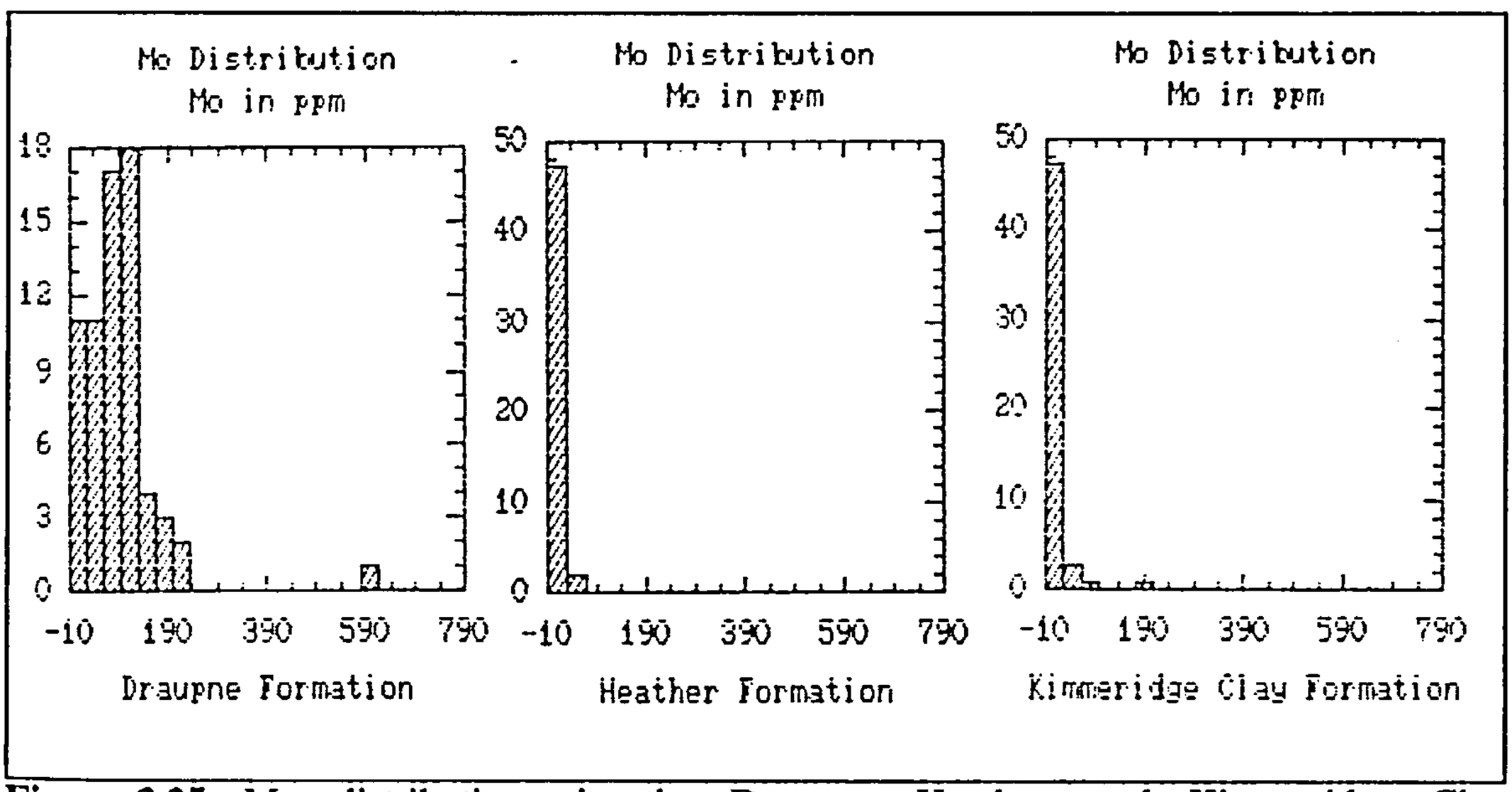

Figure 3.25 Mo distributions in the Draupne, Heather, and Kimmeridge Clay Formations.

(median Mo of 85ppm) is greatly enriched in Mo in comparison with the other formations studied here, and also when compared to published average shales (2.6ppm, 2ppm), and average black shale with 10ppm Mo. The Heather and Kimmeridge Clay Formations (4ppm and 7ppm respectively) also show some Mo enrichment when compared to average shale but have less Mo than average black shale. The Mo enrichment of the Draupne Formation is illustrated by the Al_2O_3 normalised values. The median of this formation (4.83) is more than ten times that of the other formations in the study, and exceeds both average shales (0.17, 0.11) and average black shale (0.76).

3.2.2.8 Nb

All but the Kimmeridge Clay Formation have positive skews for Nb (Fig. 3.26), the Kimmeridge Clay having a negative skew. The maximum recorded Nb content in the study was 50ppm from the Draupne Formation. The median Nb contents are all similar, the Draupne and Heather Formations having the highest Nb content (20ppm), and the Kimmeridge Clay Formation the least (17ppm). All of the medians exceed average shale Nb

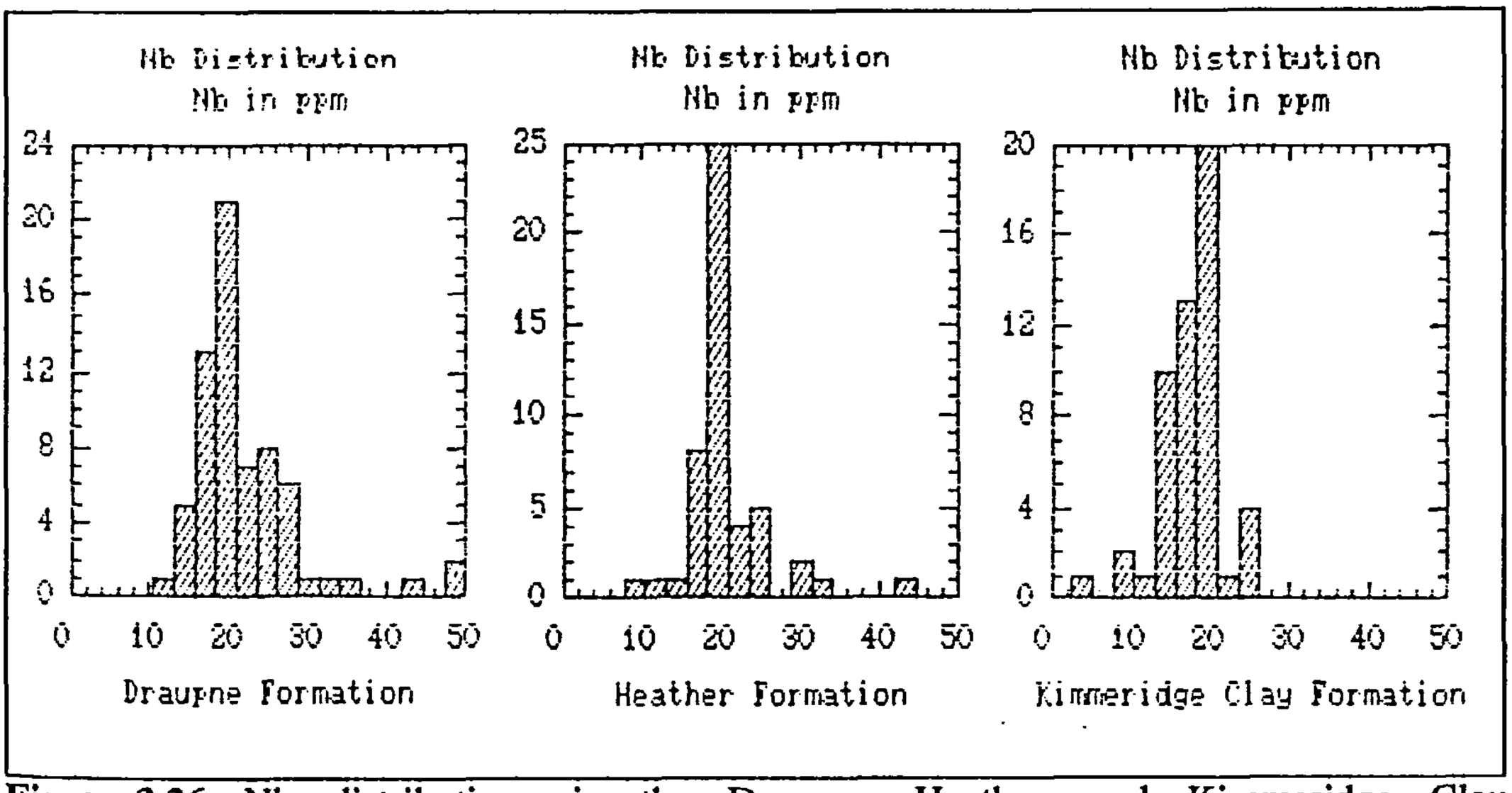

Figure 3.26 Nb distributions in the Draupne, Heather, and Kimmeridge Clay Formations.

contents (11ppm, 15ppm). The Draupne Formation has the highest median Al_2O_3 normalised Nb content (1.21), but the Kimmeridge Clay Formation value (1.14) exceeds that of the Heather Formation (1.10). The lower Nb content of the Kimmeridge Clay Formation is not apparent in the normalised values suggesting that dilution by carbonate minerals is the cause of the lower Nb concentration in this formation. The average shale values of 0.73 and 0.86 are lower than the mudstones studied here (average black shale not determined).

3.2.2.9 Ni

The Ni distributions (Fig.3.27) are positively skewed, the maximum recorded Ni content being 1395ppm in a phosphatic sample from the Heather Formation, while 727ppm was recorded in the Draupne Formation. The median Ni content of the Draupne (162ppm) is considerably higher than the published average shales (68ppm, 80ppm), and the average black shale Ni content (only 50ppm). The Heather Formation (with 78ppm) lies within the range of published shale averages, but the Kimmeridge Clay Formation is slightly depleted (60ppm), lying between the values of average shale and average black shale. The median Al_2O_3 normalised Ni content of the Draupne Formation (9.38) is much larger than the average shale

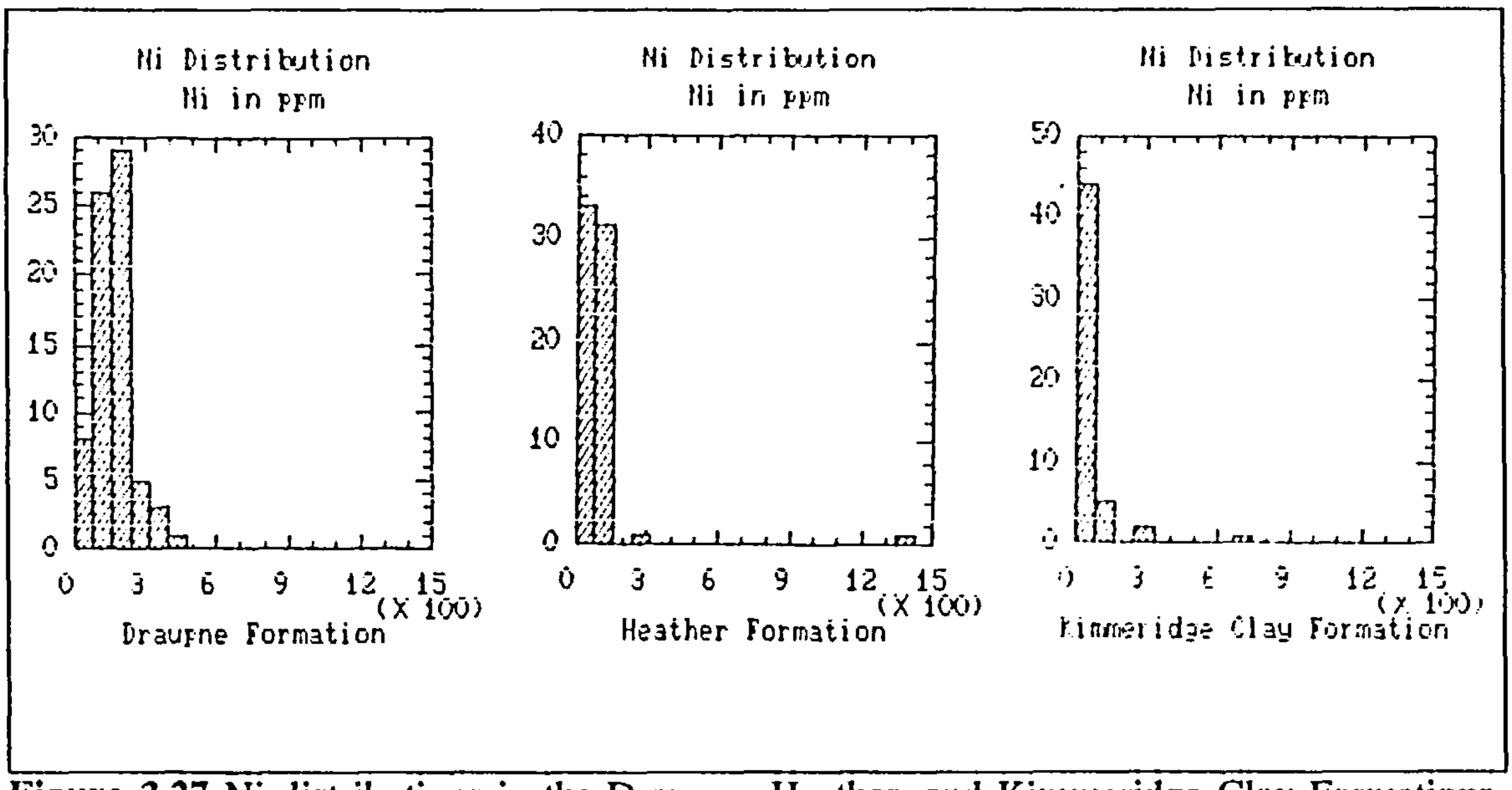

Figure 3.27 Ni distributions in the Draupne, Heather, and Kimmeridge Clay Formations.

values (4.50, 4.60) and the black shale average (3.79) illustrating its enrichment in this formation. The Heather Formation (4.36) remains similar to average shale and the Kimmeridge Clay Formation has the lowest median normalised Ni content (3.48).

3.2.2.10 Pb

The distributions of Pb (Fig. 3.28) are positively skewed, the highest recorded value being 264ppm in a phosphatic sample from the Heather Formation. In comparison with published Pb contents for average shales (both 20ppm) and black shales (also 20ppm) the Heather Formation (25ppm) is enriched in Pb and the Draupne and Kimmeridge Clay Formations (with 22ppm and 20ppm respectively) are similar. The median Al_2O_3 normalised Pb contents of the Draupne and Kimmeridge Clay Formations are similar (1.23 and 1.24) and lie between the range of shale averages (1.32, 1.15) but below average black shale (1.52). The Heather Formation has a higher median normalised Pb content (1.35) but this is still less than that published for average black shale.

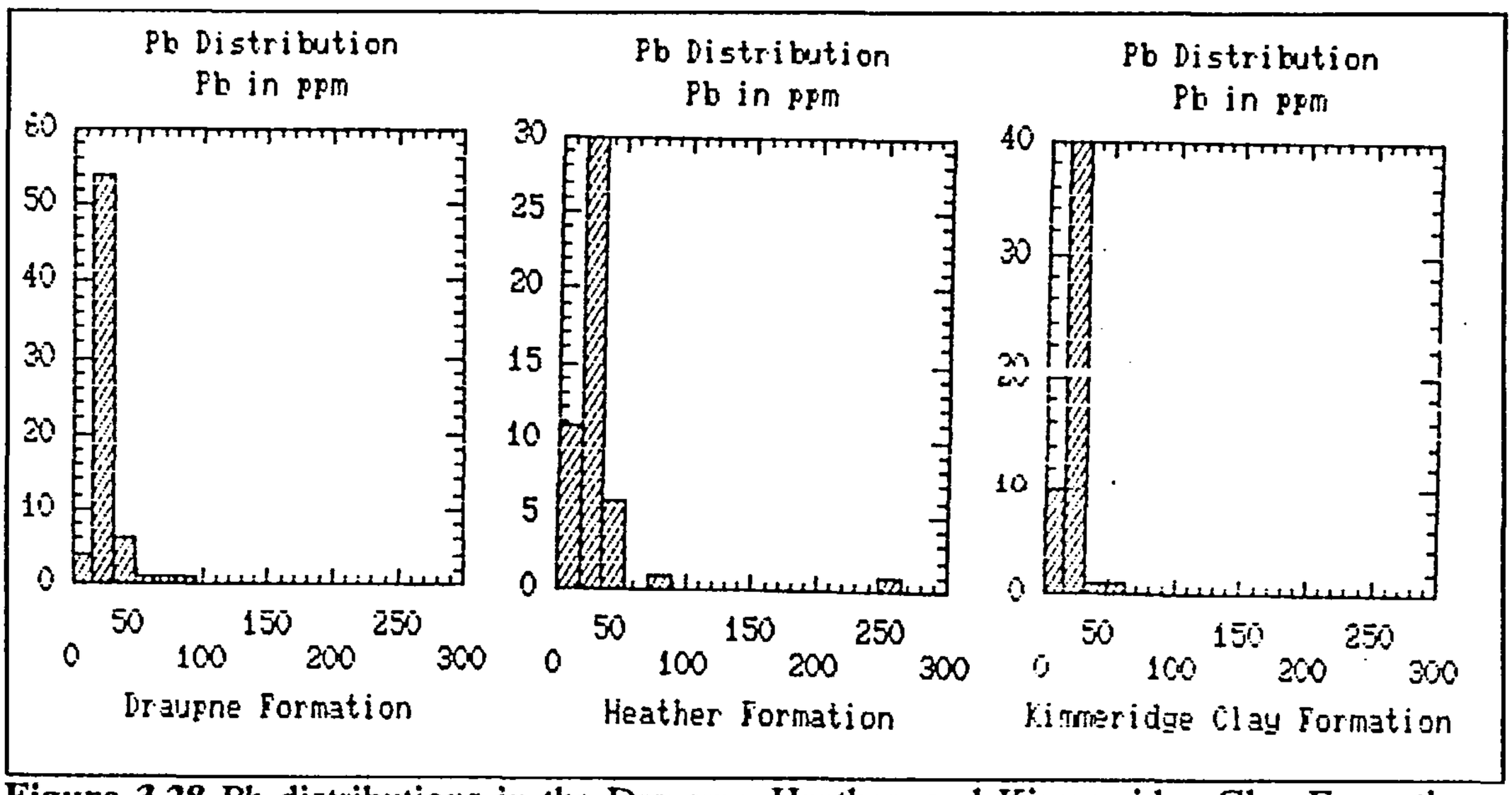

Figure 3.28 Pb distributions in the Draupne, Heather, and Kimmeridge Clay Formations.

3.2.2.11 Rb

Rb distributions (Fig. 3.29) are negatively skewed, although the Kimmeridge Clay is only slightly so. The highest recorded Rb content in the study was 226ppm in the Kimmeridge Clay Formation. The Draupne has the highest median Rb content (160ppm) with the Kimmeridge Clay Formation (140ppm) intermediate and the Heather Formation (113ppm) lowest. Published average shales (140ppm Rb) are similar to the Kimmeridge Clay Formation and suggest that the Heather Formation is depleted in Rb relative to the average, and that the Draupne Formation is slightly enriched. The Kimmeridge Clay Formation has the highest median Al_2O_3 normalised Rb content (9.65) and its similarity with that of the Draupne (9.17) suggests that the detrital fractions of the two sediments are similar in their Rb contents and that the lower overall Rb of the Kimmeridge Clay is due to the greater proportion of carbonates. These two formations are similar to the higher of the average shales (9.27, 8.05). The Heather Formation (6.15) has a much lower average than the average shales.

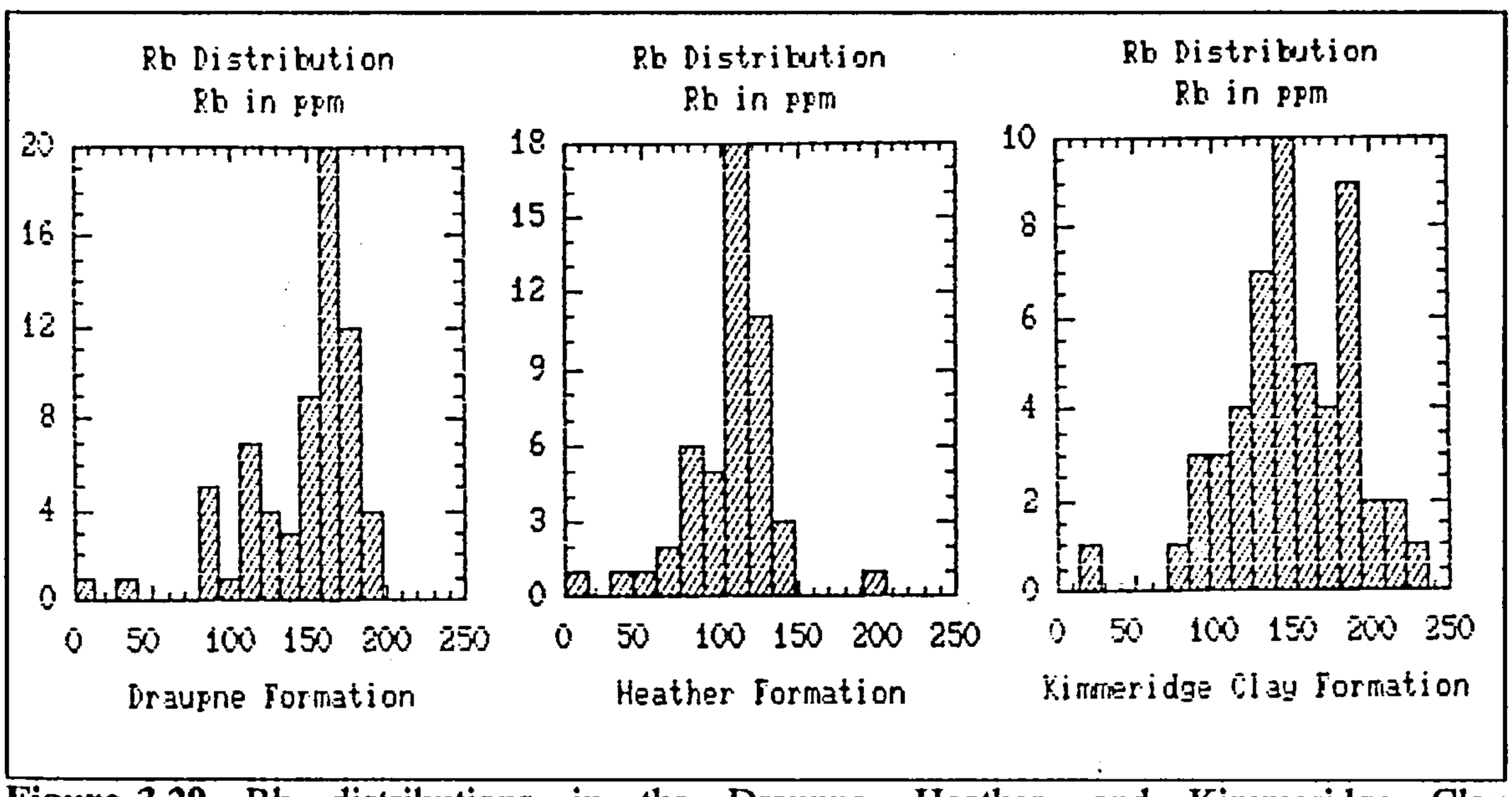

Figure 3.29 Rb distributions in the Draupne, Heather, and Kimmeridge Clay Formations.

3.2.2.12 Sc

Sc distributions (Fig. 3.30) are positively skewed, the Draupne having the greatest median Sc content (13ppm) which is similar to the published average shales (13ppm, 15ppm) but the highest single value recorded, 24ppm was in the Heather Formation. The Heather and Kimmeridge Clay Formation averages (10ppm and 9ppm respectively) are similar to the average black shale (10ppm) and lower than the published shale averages. The Draupne Formation has the highest median Al_2O_3 normalised Sc content (0.77) which is less than the published shales (both 0.86) but similar to average black shale (0.76). The Heather and Kimmeridge Clay Formations are again similar (0.60 and 0.63 respectively).

3.2.2.13 Sr

The distributions of Sr (Fig. 3.31) are positively skewed, the greatest single Sr content recorded in the study being 1293ppm in a phosphate rich sample from the Heather Formation. Only the Kimmeridge Clay (332ppm) has a median Sr content similar to average shale (300ppm, 400ppm). The median of the Draupne Formation (238ppm) is higher than the

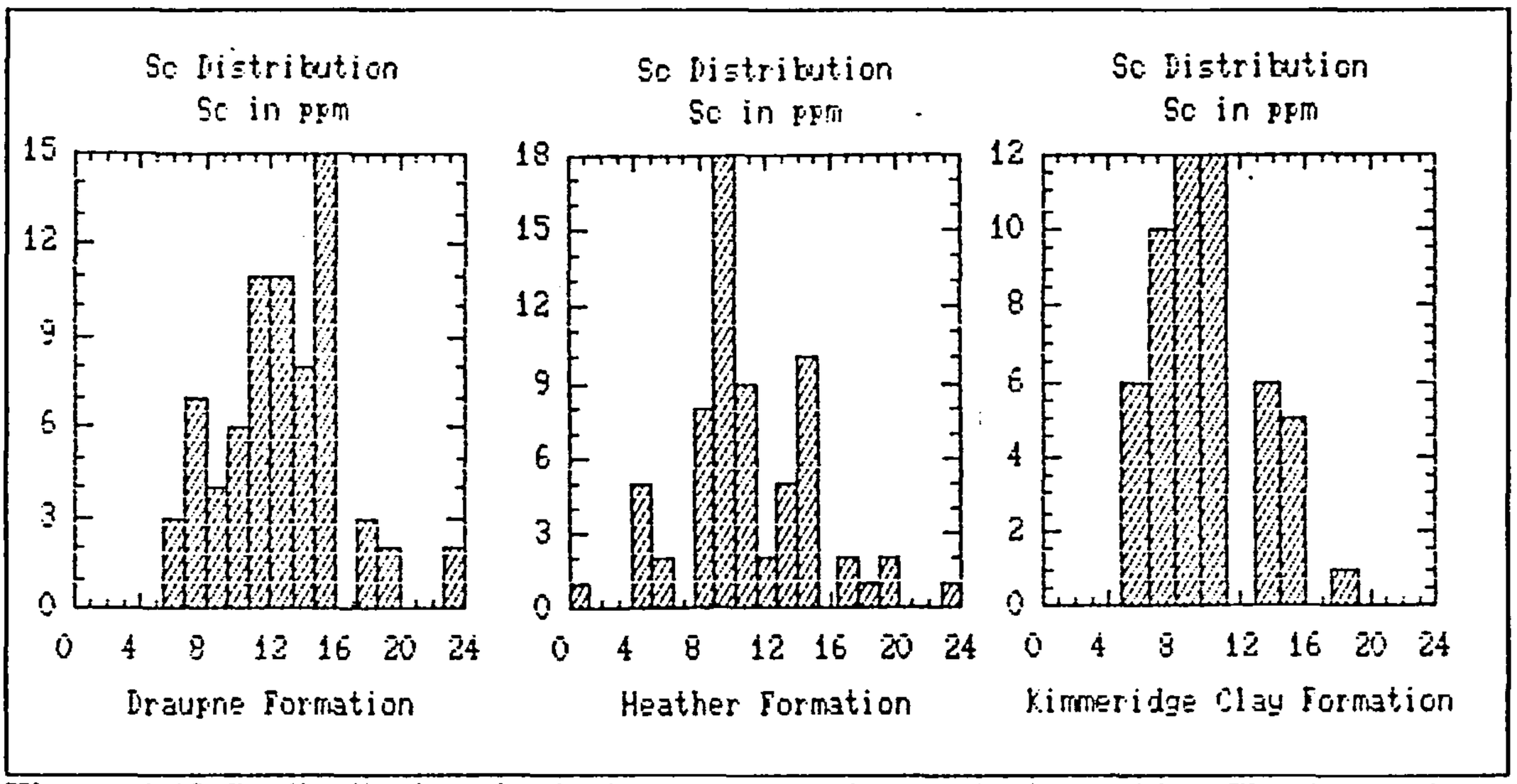

Figure 3.30 Sc distributions in the Draupne, Heather, and Kimmeridge Clay Formations.

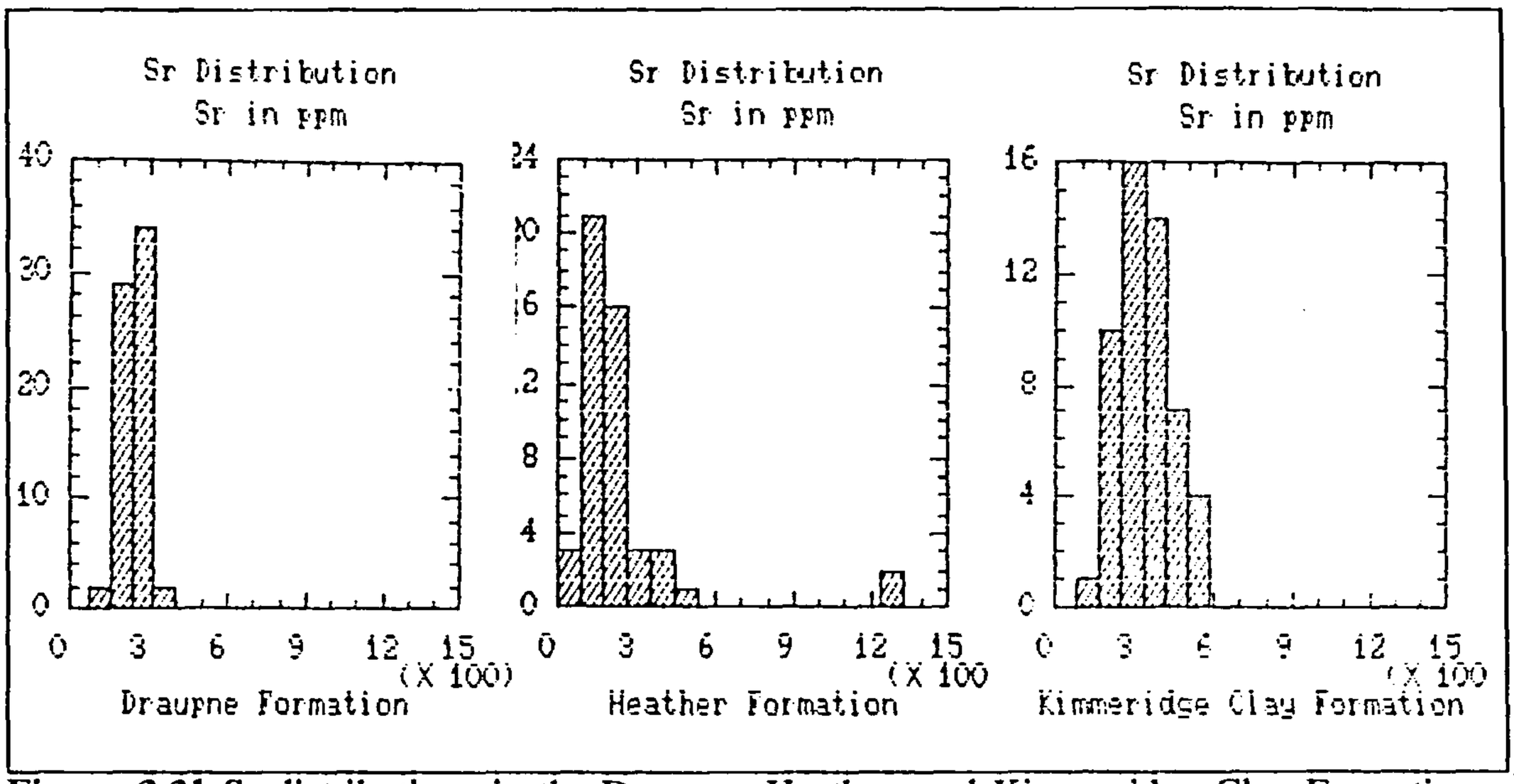

Figure 3.31 Sr distributions in the Draupne, Heather, and Kimmeridge Clay Formations.

average black shale (200ppm) however but the Heather Formation has a median lower than even this (179ppm). The median Al_2O_3 normalised Sr contents show that the Kimmeridge Clay Formation (20.4) has much more Sr in relation to its clay content than do the other sample sets which is probably due to its greater carbonate content. The Draupne and Heather Formations are similar (13.6 and 9.70). The average shales (19.9, 23.0) have normalised Sr contents close to the Kimmeridge Clay Formation and greater than the others. The average of black shales (15.2) is near that of the Draupne Formation but exceeds that of the Heather.

3.2.2.14 Th

Th distributions (Fig. 3.32) of the Draupne and Kimmeridge Clay Formations are negatively skewed and that of the Heather Formation is positively skewed. The highest recorded Th content was 26ppm from a specimen from the Heather Formation. The median Th contents are all are very similar, the Kimmeridge Clay Formation (14ppm) being slightly lower than the Draupne and Heather Formations (both 15ppm). Published average shales have a Th content of 12ppm and the median Th contents of this study are all above this. As with the raw data the Al_2O_3 normalised medians are similar (0.86 for the Kimmeridge Clay Formation, 0.90 for the Draupne, and 0.95 for the Heather Formation) and show these mudstones to be

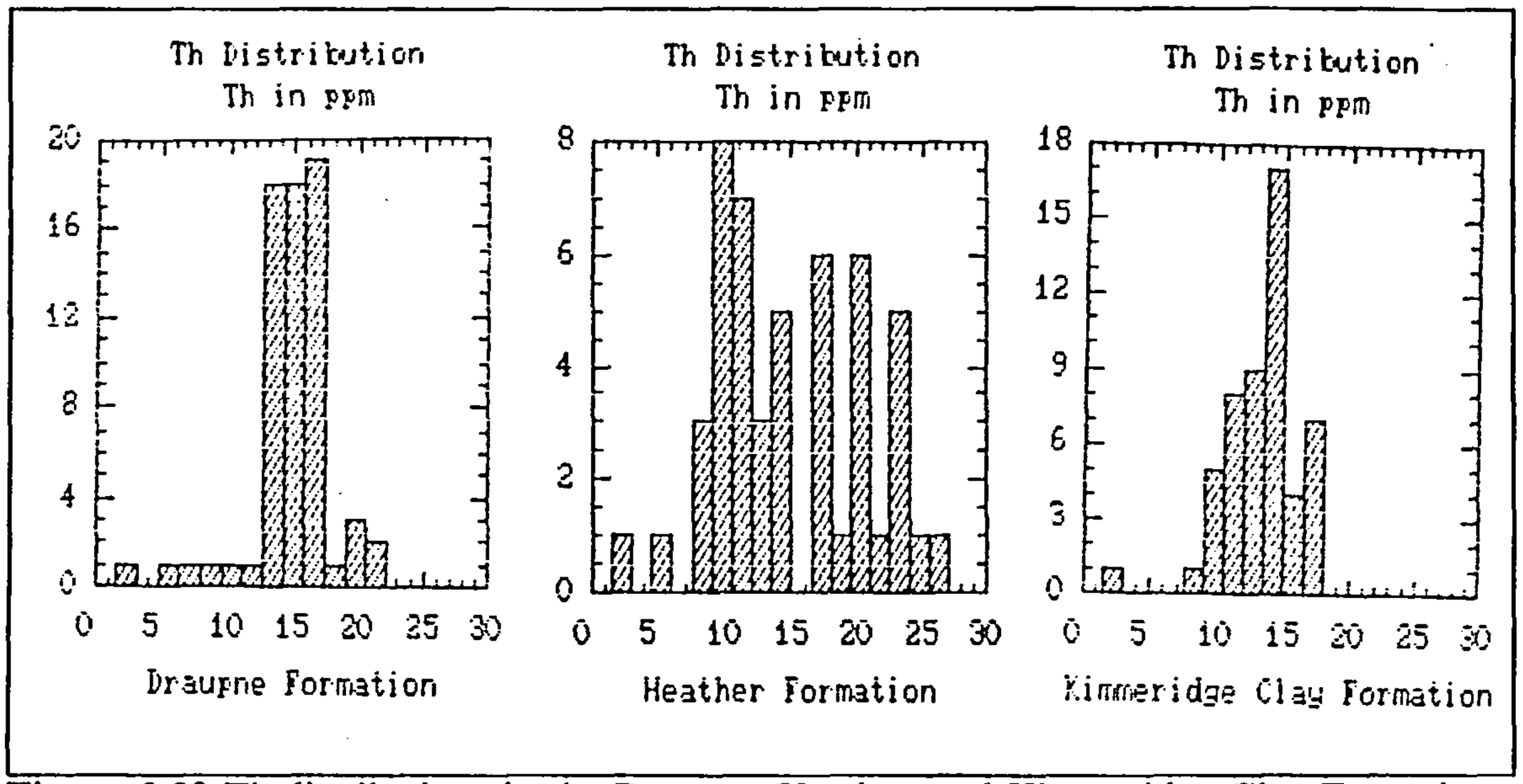

Figure 3.32 Th distributions in the Draupne, Heather, and Kimmeridge Clay Formations.

enriched in Th relative to average shale (0.79 and 0.69).

3.2.2.15 U

U distributions (Fig. 3.33) are positively skewed with the largest recorded U content being 76ppm in the Draupne Formation. The median U content of the Draupne Formation (20ppm)

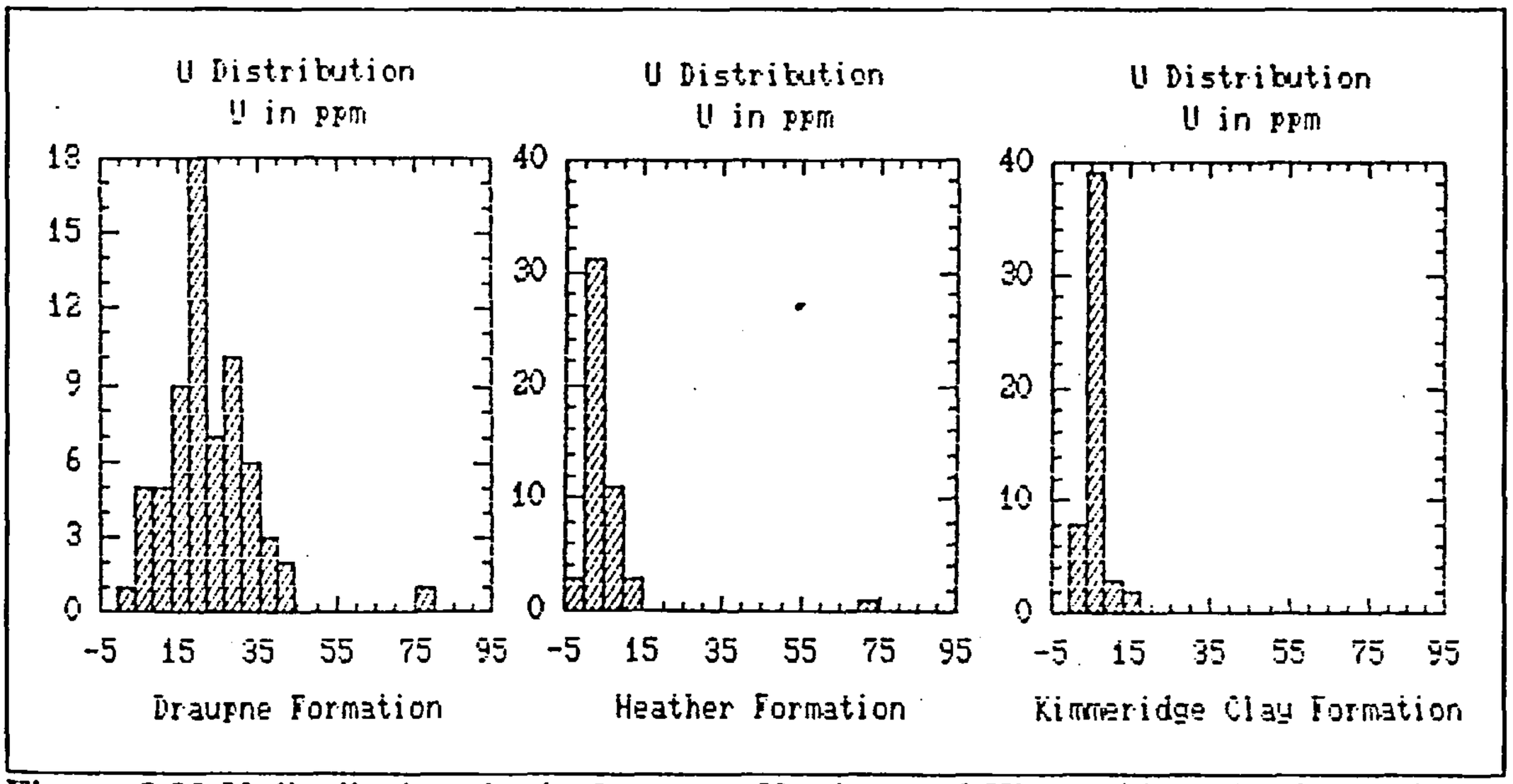

Figure 3.33 U distributions in the Draupne, Heather, and Kimmeridge Clay Formations.

is also very much higher than the other formations in the study, and in comparison with the published average shales (3.7ppm, 3.5ppm). The Heather and Kimmeridge Clay Formations (5ppm each) also exceed these averages. The median Al_2O_3 normalised U content of the Draupne Formation (1.20) is much greater than those of average shales (0.25, 0.20), and that of the Kimmeridge Clay Formation (0.35) is slightly so. The Heather Formation is similar to the average (0.27).

3.2.2.16 V

The V distribution (Fig. 3.34) is negatively skewed in the Draupne Formation whilst for the other formations the distributions are positively skewed. The greatest recorded V content was 1087ppm in the Draupne Formation and this also has by far the highest median V content (592ppm). The Kimmeridge Clay Formation has the lowest (only 140ppm), with the Heather Formation being intermediate (200ppm). Only the Kimmeridge Clay is similar to the published shale averages (both 130ppm) and black shale average (150ppm), the other formations greatly exceeding even the black shale average. The Draupne Formation also has the highest median Al_2O_3 normalised V content (35.7). This is much higher than the

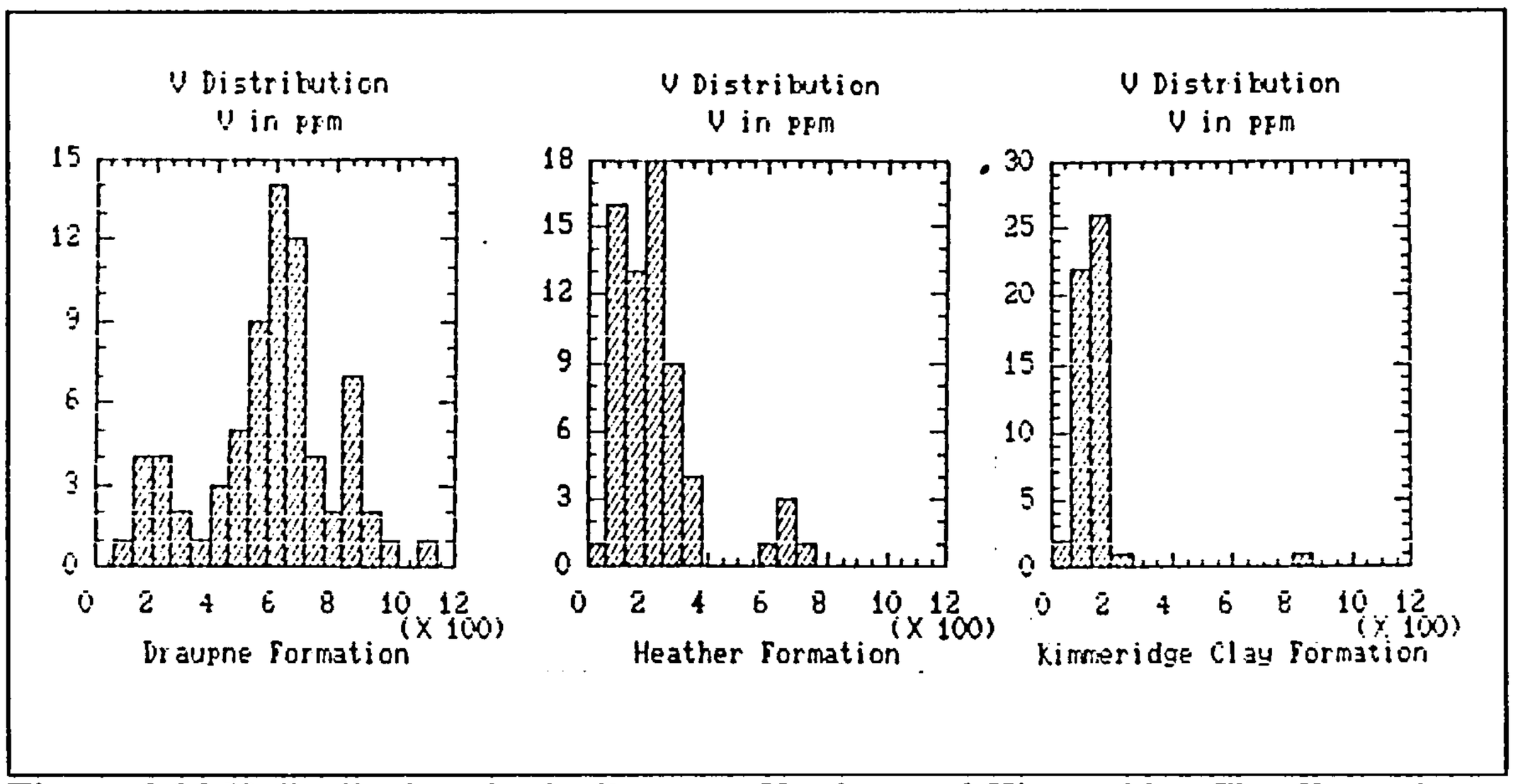

Figure 3.34 V distributions in the Draupne, Heather, and Kimmeridge Clay Formations.

published average shale values (8.61, 7.47) and the average black shale value (11.4) confirming the enrichment of V in this formation. The Heather (10.8) and Kimmeridge Clay (8.59) Formations are similar to average black shale, and average shale respectively.

3.2.2.17 Y

The distributions of Y (Fig. 3.35) are positively skewed with the exception of the Kimmeridge Clay Formation which has a negative skew. The highest recorded Y content is 206ppm in a phosphatic sample of the Heather Formation. The median Y contents of the offshore formations are very similar (34ppm and 31ppm for the Draupne and Heather Formations) but the Kimmeridge Clay Formation has a lower median (27ppm). The published Y contents for average shale (26ppm,35ppm) and black shale (30ppm) are similar to the values found in this study suggesting that the formations have normal Y contents. The medians of the Al_2O_3 normalised Y contents are similar. The Kimmeridge Clay Formation has the lowest value (1.63), the Draupne and Heather Formations being higher (1.97 and 1.79). The offshore formations fall within the range of published average shale values (1.72, 2.01) but the Kimmeridge Clay is lower. None have medians as high as average black shale (2.27).

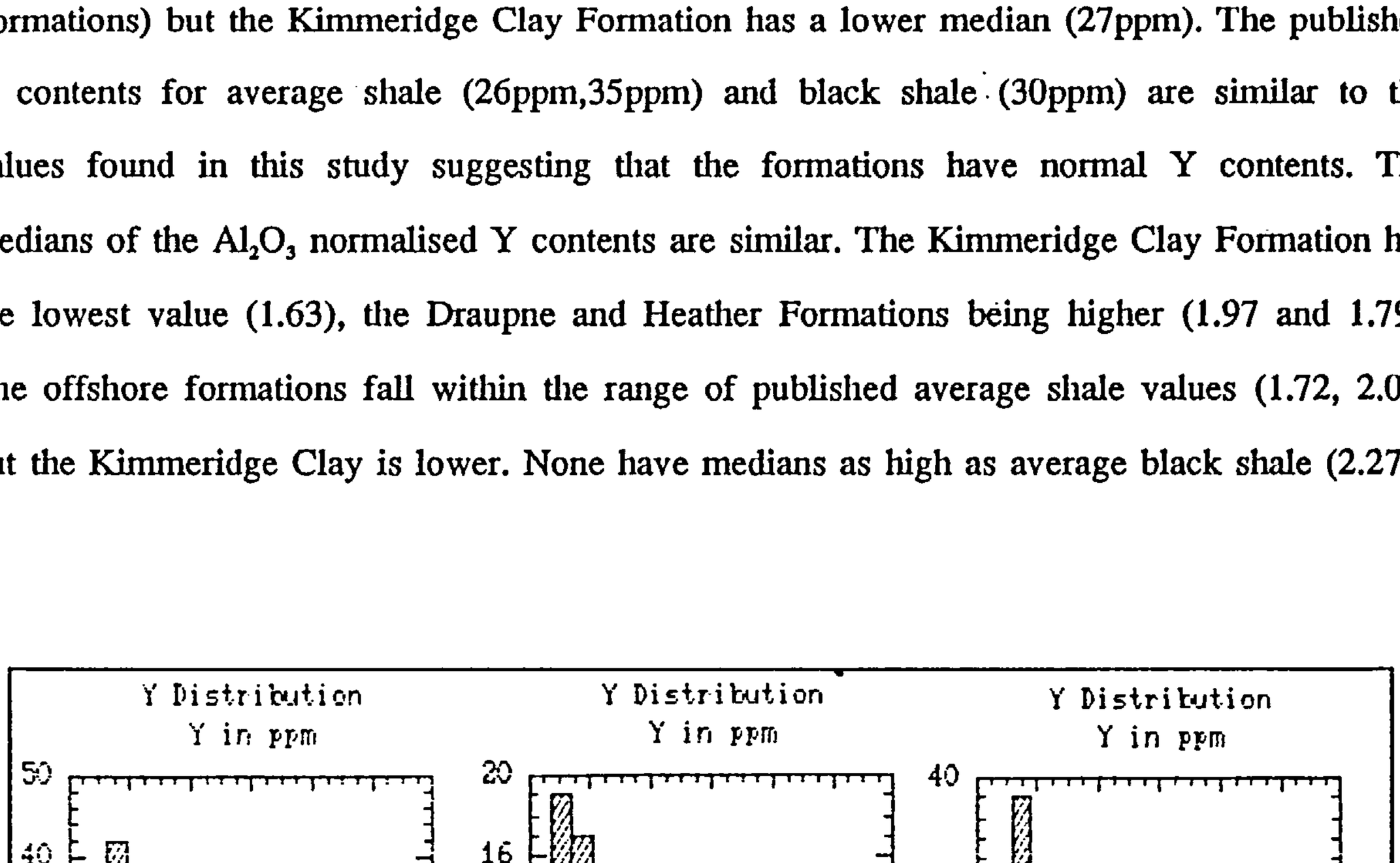

Figure 3.35 Y distributions in the Draupne, Heather, and Kimmeridge Clay Formations.

3.2.2.18 Zn

The distributions of the Zn contents (Fig. 3.36) are positively skewed. The highest Zn content recorded during the study was 6720ppm (0.67%) in a phosphatic sample from the Heather Formation, but up to 1890ppm was also recorded in Draupne Formation samples. The Draupne has by far the greatest average Zn content (328ppm) and the Kimmeridge Clay Formation the smallest (79ppm). The Heather Formation (131ppm) has an intermediate value. The median Zn content of the Draupne Formation exceeds both average shales (95ppm, 90ppm) and average black shale (300ppm), while the Heather Formation falls between. The Kimmeridge Clay Formation is depleted in Zn relative to these averages. The median Al_2O_3 normalised Zn content of the Draupne Formation (21.3) is higher than those of average shales (6.29, 5.17) but slightly lower than average black shale (22.7). The Heather Formation (7.56) exceeds average shale slightly. The Kimmeridge Clay Formation has a lower normalised Zn content than the other shales studied here (only 4.96), so its low Zn content cannot be due to the diluting effect of its high carbonate content.

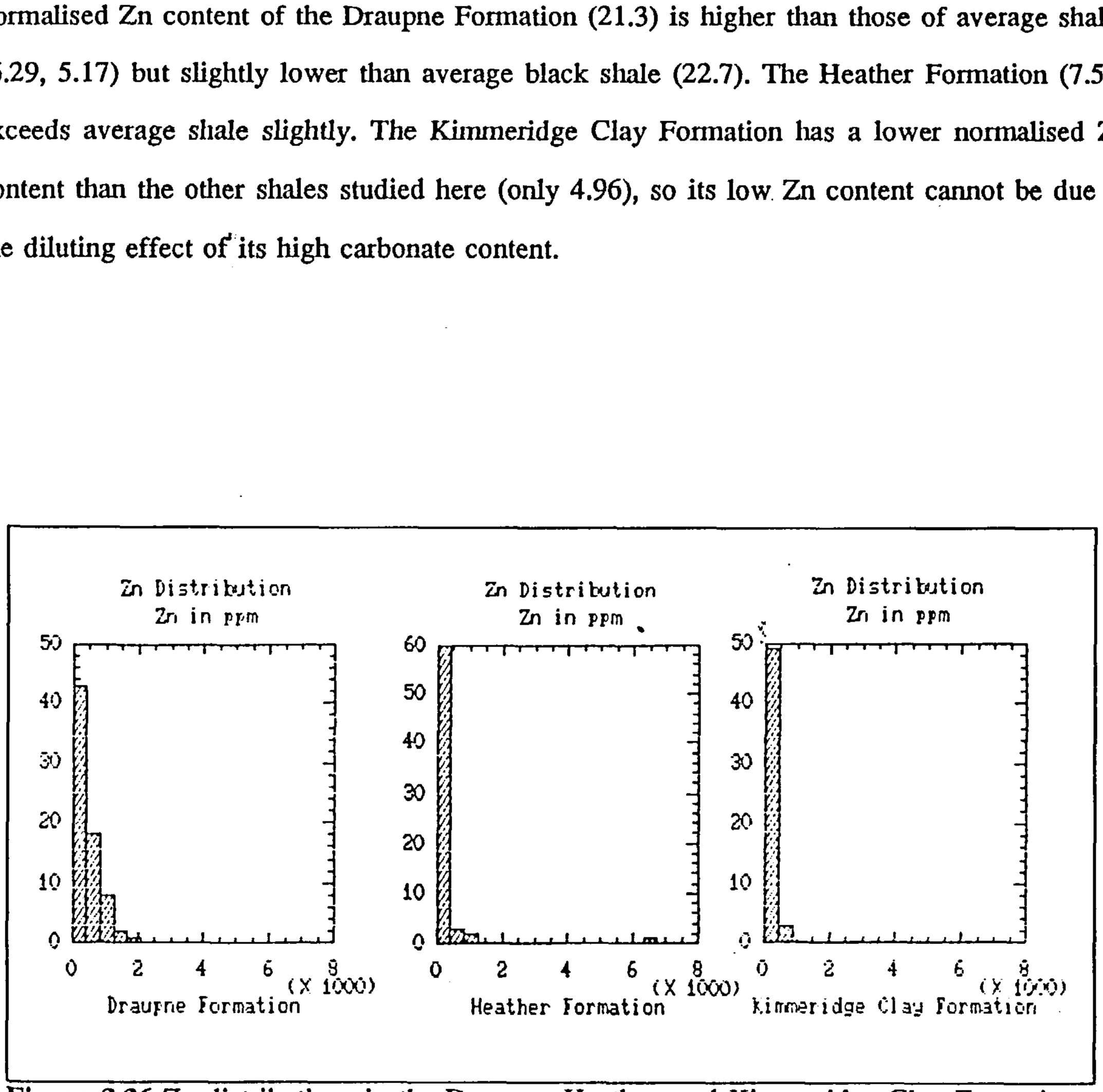

Figure 3.36 Zn distributions in the Draupne, Heather, and Kimmeridge Clay Formations.

3.2.2.19 Zr

Zr distributions (Fig. 3.37) are positively skewed in the Draupne Formation, the Kimmeridge Clay Formation has a slight negative skew but is approximately normal and the Heather Formation has a positive skew but is bimodally distributed with one maximum near to that of the Draupne Formation at about 160ppm and a second peak rather higher at around 330ppm. The highest recorded Zr content in the study was 575ppm in a sample from the Heather Formation. The Draupne and Kimmeridge Clay Formations have similar Zr median contents (136ppm and 135ppm respectively) with the Heather Formation having rather more(187ppm). Published average shale Zr contents (160ppm, 180ppm) are similar to the Heather Formation, the Draupne and Kimmeridge Clay Formations falling below but having more Zr than average black shale (70ppm). The greatest median Al_2O_3 normalised Zr content is that of the Heather Formation (11.5) which is similar to the average shales (10.6, 10.3). The Draupne and Kimmeridge Clay Formations are lower (7.90 and 8.23 respectively) whilst average black shale has a normalised value of only 5.3.

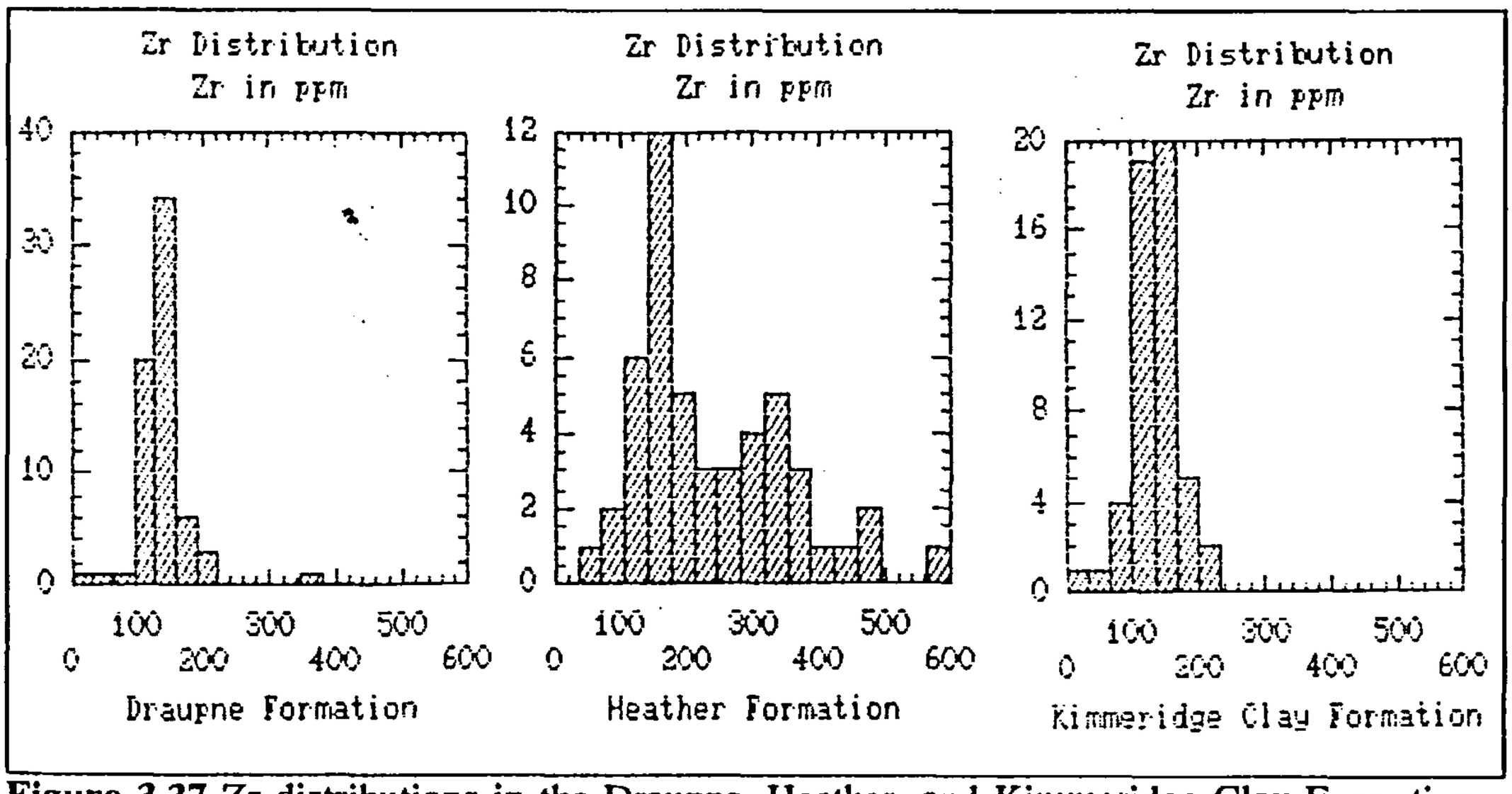

Figure 3.37 Zr distributions in the Draupne, Heather, and Kimmeridge Clay Formations.

3.3 Conclusions

3.3.1 Conclusions drawn from the mineralogy and major element geochemistry

Variation in the major element geochemistry of the shales examined in this work is probably controlled by changes in the mineralogical composition. Examination of the raw and Al_2O_3 normalised chemical compositions of the Draupne, Heather, and Kimmeridge Clay Formations, and comparison with both published 'average' shales and with each other has allowed a number of deductions to be made about the nature of this mineralogy:

The gross composition of the detrital component of the sediment, from SiO_2/Al_2O_3 ratios is similar for the Draupne, Heather, and Kimmeridge Clay Formations. The clay mineralogy of the Draupne Formation is dominated by illite resulting in its high K_2O/Al_2O_3 ratio and a SiO_2/Al_2O_3 ratio which slightly exceeds those of the Heather and Kimmeridge Clay Formations. The clay mineralogy of these latter formations is mainly kaolinite.

The lower overall SiO_2 and Al_2O_3 content of the Kimmeridge Clay Formation is due to dilution of the silicate clastic fraction by large amounts of carbonate minerals, mainly calcite. This is indicated by the high CaO/Al_2O_3, and CO_2/Al_2O_3 ratios. The Draupne, and Heather Formations have very low CaO/Al_2O_3 and CO_2/Al_2O_3 ratios which suggest that these are depleted in carbonate relative to normal shales.

The S contents and S/Al_2O_3 ratios found in this work are very much higher than those of average shales, suggesting that pyrite is much more abundant in the samples of this study. The TOC contents and TOC/Al_2O_3 ratios suggest that organic carbon is similarly enriched.

Curtis (1980) listed the essential qualities of black shale as being: a high organic carbon content; a low carbonate content; a high pyrite content; and fissility. The presence of the last mentioned characteristic may not be determined from the geochemistry but the Draupne,

Heather, and Kimmeridge Clay Formations have been shown to have both high TOC and high pyrite. Apart from the Kimmeridge Clay Formation the carbonate contents are also low.

3.3.2 Conclusions drawn from the trace element geochemistry.

Black shales such as those of this study are often noted for their high trace element contents, and this is the case for a number of elements determined here. In order to illustrate quantitatively the levels of trace element enrichment found, the percentage of the samples in each formation which exceed the average shale value for each trace element determined have been calculated. These are shown in Table 3.9. Where the published average shale contents differ the mid-point has been used in these calculations. A means of comparing the average levels of trace element enrichment between the formations is provided by summing the individual percentages of samples above average shale for each element (similar to the calculation of the minor element enrichment index of Vine and Tourtelot, 1970). The Draupne Formation has the highest sum of these values at 1324. The Heather Formation is second highest at 1020, and the Kimmeridge Clay Formation has the smallest value (829).

An element is defined as being enriched in a given formation if more than 75% of the samples of that formation exceed the average shale value for the element (ie the average shale value < the 25th percentile of the distribution). An element is defined as having a normal abundance if more than 25% of the samples, but not more than 75% exceed the average shale value (ie 25th percentile <= the average shale value < 75th percentile). Similarly a depleted element is defined as one in which 25% or less of the samples exceed the average shale value (ie the 75th percentile <= the average shale value).

Using the definitions above and the data from Table the Draupne Formation is enriched in Cd, Cr, Cu, Mo, Nb, Ni, Th, U, V, Y, and Zn. The formation has approximately average amounts of Co, Li, Pb, Rb, and Sc and is depleted in Sr and Zr only. The Heather Formation is enriched in fewer elements, namely Cr, Li, Mo, Nb, U, and Zn and has average amounts

Table 3.9 Trace element enrichments.

		Percent of Samples Exceeding Average Shale		
Element	Av./ ppm	Draupne	Heather	Kimmeridge Clay
Cd	0.3	88	12	12
Co	19.5	68	41	8
Cr	95	96	89	87
Cu	47.5	83	39	19
Li	63	69	80	79
Mo	2.3	100	94	96
Nb	13	99	96	92
Ni	74	89	53	17
Pb	20	63	61	44
Rb	140	67	2	62
Sc	14	31	12	12
Sr	350	0	12	40
Th	12	91	61	71
U	3.6	99	76	85
V	130	99	74	58
Y	30.5	78	71	10
Zn	92.5	96	86	35
Zr	170	8	61	12
Sum		1324	1020	839

of Co, Cu, Ni, Pb, Th, Y, V, and Zr. It is depleted in Cd, Rb, Sc, and Sr. The Kimmeridge Clay Formation is enriched in Cr, U, Li, Nb, Mo, and U. It has average contents of Pb, Rb, Sr, Th, V, and Zn and is depleted in a large number of elements: Cd, Co, Cu, Ni, Sc, Y, and Zr. The low Zr concentration is to some extent explained by the diluting effect of the high carbonate content. Few elements show the same behaviour in all formations studied. Only Cr, Mo, Nb, and U are enriched in the Draupne, Heather, and Kimmeridge Clay Formations. Pb has an average content in all three formations. None of the elements determined is depleted in all formations.

Chapter Four

Correlation Analysis

4.0 Correlation Analysis

4.1 Methodology of correlation analysis

As described in Chapter 1 the relationships between the elements and minerals determined in the study are first examined by means of correlation analysis. The correlation coefficient is one of the simplest and most widely used multivariate statistics and measures the strength of the linear relationship existing between a pair of variables. It is free to vary between -1 and +1, with a value of 0 usually being taken to indicate the absence of any linear relationship between the two variables (this is discussed further below).

The correlation analysis of compositional data, such as those resulting from geochemical or mineralogical analyses, is problematic and is much misused in geology. The interpretational difficulties arising in such an analysis have been highlighted by Pearson (1897), and more recently in the geosciences by Chayes (1960, 1962) and have come to be known as the problem of constant sums, closed arrays, or often simply as closure (Le Maitre, 1982). The closure problem results from the constraint that the sum of the variables for each observation must equal a constant whole, which in geochemical analyses for example is expressed by the summation of the major rock forming oxides to 100%, so that given a knowledge of the values of all but one of the oxides the magnitude of the remaining one is fixed.

Chayes (1960, 1962) has shown that given such a constraint the sum of the covariances of any variable (any element in the case of geochemical analyses) with all of the remaining variables (other elements) is equal to the negative value of the variance of that variable, ie that:

$VAR_i + ECOV_{ik} = 0$ for k=1-M, k not=i, 1<=i<=M where M=number of variables

A requirement of this relationship is that every row of the covariance matrix must sum to 0, and that therefore each variable must have at least one negative covariance. Furthermore the variable of greatest variance must have at least two covariances with negative values. As the sign of the covariance fixes the sign of the correlation coefficient, so the equivalent correlations must also have negative values, resulting in correlation coefficients being more negative than would be expected if the data were not closed. This negative bias means that significance testing of correlations (which is usually based on the premise that a correlation coefficient of 0 indicates the absence of a relationship) is inappropriate, making the correlation coefficient almost useless as a measure of the relationships existing between the variables of a closed data set such as the elements of a geochemical analysis (Philip and Watson, 1988).

In an attempt to overcome this difficulty, and allow significance testing of correlations between closed data Chayes and Kruskal (1966) proposed a method in which an imaginary open array is constructed with zero covariances between the variables such that on closure it yields a new array whose means and variances are the same as the observed closed array, but in which the covariances are due entirely to closure. This allows the correlation coefficients of the closed data set to be tested against values of null correlations, which indicate no relationship but which are not necessarily zero, to determine their significance.

The approach of Chayes and Kruskal has been criticised for a number of failings which are detailed by Le Maitre (1982). Firstly the conceptual open array has no real meaning as compositional data are naturally closed (for example the amount of a particular oxide in a major element analysis is meaningless until related to the amounts of other oxides). Secondly there is an infinite number of open arrays which will close to give the observed array and no justification for choosing any one in preference to others. Finally for some data the theoretical open array includes negative variances, which by definition are incorrect.

More recently Aitchison (1981, 1982, 1984, 1986) has proposed a logratio transformation for compositional data vectors which makes available the complete range of procedures based on multivariate normality to compositional data analysis, without the interpretational difficulties caused by closure. Another approach has been suggested by Philip and Watson (1988) who argue that the formation of vectors of proportions (such as analyses expressed in percent or ppm), and hence the problem of closure, may be avoided completely if compositional data are viewed as directions rather than points in the sample space. In this thesis the methods of Aitchison (1986) have been followed as these enable standard and familiar techniques of multivariate analysis to be used.

A geochemical or mineralogical analysis normally expresses the amounts of each of the oxides, elements, or minerals determined as a proportion of the whole (ie in units of percent or ppm), and as such is subject to the interpretational difficulties induced by closure outlined above. Geometrically if d+1 components (either oxides, elements, or minerals etc) have been determined the data lie in a d dimensional area of space known as the simplex and not in d+1 dimensional space as might be expected. As an example if three components have been determined then the data do not lie anywhere in 3 dimensional positive real space but are restricted to a 2 dimensional plane: the common triangular diagram.

A compositional data set may be represented by a data vector $X(x_1,..., x_{d+1})$ where d+1 elements, oxides, or minerals have been determined, but because of the constant sum constraint only d components need be known to completely specify the composition as the remaining component can always be found by difference. For example if all the major elements except SiO_2 are given in an analysis, then this may be calculated by subtraction of the others from 100%. Similarly the d ratios $r_i=x_i/x_{d+1}$ i=1-d also completely specify the composition of the sample.

Aitchison (1986) proposes transforming the data vector X consisting of the d+1 raw compositional data (ie the oxides, elements, or minerals determined) to a new vector $Y(y_1,..., y_d)$ by means of the operation $y_i=\log(x_i/x_{d+1})$ i=1-d. The new transformed data vector Y completely describes the composition of the original sample but is no longer restricted to the simplex and is free to lie anywhere in d dimensional real space. The transformed data are therefore free from the effects of closure and may be examined by the techniques of multivariate statistics without interpretational difficulties induced by enforced negative covariances and correlations. In geochemical terms the compositional data are normalised to one oxide or element and the log of the normalised value is taken. Similarly for mineralogical determinations all minerals are normalised to one other mineral prior to taking logs.

Aitchison (1986) has shown that choice of divisor does not effect the results of any of the statistical analyses which may be performed,but from a geological viewpoint the choice of denominator is an important consideration if sensible interpretations are to be made, bearing in mind the aims of the project. In this work Al_2O_3 was chosen to be the common denominator for the geochemical data for two reasons. Firstly many element/Al_2O_3 ratios have relatively simple and useful geochemical or mineralogical interpretations (some of these have been discussed in Chapters 3 and 5). Secondly Al_2O_3 is essentially immobile in the early diagenetic environment, hence changes in an element/Al_2O_3 ratio with increasing organic maturity may be attributed to mobility of the element in question.

For the bulk mineralogical data the chosen denominator was total clay (being the sum of the chlorite, smectite, illite, and kaolinite contents). This was chosen because clays are the essential minerals of shales, and because normalising the mineralogy to the clay content would be consistent with the choice of Al_2O_3 as denominator for the geochemical data. The choice also has the added advantage that while the individual clay mineral analyses by the bulk XRD method may be subject to some error, the total clay content is probably rather more accurately known. Within the clay mineral assemblage the amounts of chlorite, smectite, and illite were normalised to kaolinite as this is the simplest of the clay minerals.

Following the approach of Aitchison (1986) it is thus possible to interpret the relationships existing between the elements in the analyses by means of the logs of the element to Al_2O_3 ratios, and their correlations with others. In a similar manner the mineralogical data may be interpreted. Tests of the significance of these correlations may be made secure in the knowledge of their validity.

An often forgotten, or ignored assumption however of the Pearson product moment coefficient (r), the most widely used of the correlation coefficients, is that the distributions of the variables being analysed are normal. Some geological data approximately satisfy this assumption but many do not (Le Maitre, 1982), and some workers have questioned the validity of assuming any underlying distribution (Philip and Watson, 1987; Hall, 1983). Transformations may be used to give approximately normal distributions (eg Walters et al 1987) but some distributions such as multimodal ones cannot be successfully transformed to approximate normality.

Aitchison's logratio transformation whilst freeing the data from unit sum problems produces new variables with distributions which range from near normal to very skewed and occasionally multimodal. Pearson product moment correlation coefficients may thus be biased by observations with extreme values of two or more variables leading to apparently significant correlations where none exist and vice versa (Hall, 1983). In such cases it is wise to examine non-parametric correlation coefficients which assume no underlying distributions. The Spearman correlation coefficient (p) is one such non-parametric correlation coefficient and is determined by ranking the data and calculating the product moment correlation between the ranked variables, resulting in a coefficient which is less sensitive to extreme values than Pearson's r. This is analogous to the relationship between the mean and the median averages. In this section both Pearson and Spearman correlation coefficients have been calculated for each element-element pair and the resulting correlation matrices are shown

in Tables 4.1-4.6 (at end of volume). In most cases the two coefficients are surprisingly similar but occasionally they are very different.

The minerals and elements determined have been summarised in Chapter 3. In that chapter the total Fe content (EFe_2O_3) was split into two parts namely pyrite Fe and non-pyrite Fe. This distinction is continued into this chapter as it is thought to be more useful than treating Fe solely as EFe_2O_3. A variable included here but not summarised in Chapter 3 is the corrected ignition loss. This is calculated from the measured ignition loss by correcting for TOC, CO2, S, and pyrite Fe, and has been included to complete the summations of the analyses. The corrected ignition loss usually has a value of between 2-10% in the Draupne, and Heather Formations, and up to 6% in the Kimmeridge Clay Formation and probably represents a number of volatile species not otherwise determined in the analyses such as water and the non-carbon component of organic matter.

Acceptance of the logratio transformation procedure does pose a problem with values which are below the detection limits of the analytical methods. For non-zero results which should strictly be reported as <detection limit, the actual recorded values have been retained as these will add only noise to the data but no systematic bias. For analyses which were recorded as zero however a different approach must be followed as this results in a ratio of zero, and the log of zero cannot be taken. These values probably do not mean that absolutely none of the element or mineral in question is present, rather that it is in such small quantities that it cannot be measured. Aitchison (1986) has a number of suggestions in this case, of which the most appropriate is the replacement of the recorded zero by a number which is smaller than the smallest recorded value.

Eight of the minerals determined (quartz, plagioclase feldspar, chlorite, kaolinite, calcite, dolomite, siderite, and pyrite) and seven of the chemical variables (Fe_2O_3, CO_2, Corrected Ignition Loss, Cd, U, and Mo) are troubled by this problem. The zero values for the mineral contents were all replaced by the arbitrary value of 0.01%. Zero or small negative values for

Fe_2O_3 and Corrected Ignition Loss are replaced by the arbitrarily chosen value of 0.05%. The CO_2 contents were calculated from the difference between total and organic carbon analyses (Appendix A), zero or small negative values were treated as zero in the descriptive statistics used above but are replaced here by the value of 0.03% C which is smaller than the smallest consistently measured values and which is equivalent to 0.11% CO_2. For Cd the average shale value of 0.3ppm is below the smallest measured value and is substituted for the zero values. For U and Mo the average shale values of 4 and 3ppm respectively should be detected so recorded zeros are replaced by the value of 0.5ppm chosen arbitrarily as a value less than the minimum recorded non-zero value. The Spearman correlation coefficient is in any case not sensitive to the choice of these values.

4.2 The Draupne Formation

4.2.1 Major element relationships

Significant amounts of SiO_2 are probably present in the Draupne Formation in quartz and feldspar as log(SiO_2/Al_2O_3) is strongly correlated with log(quartz/total clay) (p=0.78, r=0.47), and moderately with log(K-feldspar/total clay) (p=0.49, r=0.37) and log(plagioclase feldspar/total clay) (p=0.46, r=0.41) (Tables 4.1 and 4.2). These relationships are probably due to the mineralogical association of quartz and feldspars in the silt sized detrital fraction of the shales (Pettijohn, 1975).

Log (TiO_2/Al_2O_3) is correlated with both log(SiO_2/Al_2O_3) (p=0.53, r=0.59) and log(quartz/total clay) (p=0.51, r=not sig.), this probably being a result of the concentration of Ti-oxides in the quartz rich, silt sized detritus because of similar hydrodynamic properties. Spears and Kanaris-Sotiriou (1976) noted a positive relationship between quartz and the TiO_2/Al_2O_3 ratio in Carboniferous mudstones and siltstones for this reason and it might reasonably be expected to be reflected in the log ratio transformed SiO_2 and TiO_2 data. Similar correlations are found in the Heather Formation although the magnitudes are greater.

Log(Na_2O/Al_2O_3) has a weak but significant correlation with log(SiO_2/Al_2O_3) (p=0.24, r=0.24) but the Spearman coefficient is not significant between log(K_2O/Al_2O_3) and log(SiO_2/Al_2O_3) and the Pearson coefficient is only barely significant (r=0.24) despite the correlation noted between log(SiO_2/Al_2O_3) and log(K-feldspar/total clay), and the strong correlation between the two in the Heather Formation. The reason for this may be that the expected covariation of log(K_2O/Al_2O_3) and log(SiO_2/Al_2O_3) due to the association of quartz and K-feldspar in the silt fraction of the sediment is being reduced in this formation by an opposing negative relationship between the two variables arising from increasing proportions of K bearing illite and mixed layer clays to kaolinite in the finer sediments (ie those with less quartz and feldspar and a resulting lower SiO_2/Al_2O_3 ratio).

This suggestion is supported by the negative correlation of log(quartz/total clay) with log(smectite/kaolinite) (p=-0.50, r=0.29) and log(illite/kaolinite) (p=-0.45, r=not sig.) which confirms that illite and mixed layer clays increase in relation to kaolinite in samples having the lower quartz/total clay ratios, and hence finer grain size. Furthermore, the positive correlation of log(illite/kaolinite) and log(smectite/kaolinite) with log(K_2O/Al_2O_3) (p=0.55, r=0.53 and p=0.33, r=0.28 respectively), and the negative correlation of log(Na_2O/Al_2O_3) with log(illite/kaolinite) (p=-0.31, r=not sig.) indicate that an overall increase in K_2O/Al_2O_3 occurs as the clay mineralogy becomes more illitic, and that this is associated with a lowering of the Na_2O/Al_2O_3 ratio due to less Na-feldspar. This explains the observed weak negative correlation between log(K_2O/Al_2O_3) and log(Na_2O/Al_2O_3) (p=-0.34, r=-0.28) which occurs despite the very strong correlation between log(K-feldspar/total clay) and log(plagioclase feldspar/total clay) (p=0.81, r=0.62).

A second possible cause may be that the poor correlation between log(SiO_2/Al_2O_3) and log(K_2O/Al_2O_3) is due to a decoupling of the supply of quartz from that of the feldspars, which would also explain the lower correlation between log(SiO_2/Al_2O_3) and log(Na_2O/Al_2O_3) in the Draupne. This is not supported however by the weak but significant positive correlation

of log(quartz/total clay) with log(K-feldspar/total clay) (p=0.29, r=not sig.) and log(plagioclase feldspar/total clay) (p=0.28, r=not sig.), but is consistent with the conclusions drawn from the differentiable sedimentary component treatment given in Chapter 5.

Both $\log(Fe_2O_3/Al_2O_3)$ and $\log(MgO/Al_2O_3)$ have significant correlations with some of variables discussed above. $\text{Log}(Fe_2O_3/Al_2O_3)$ is correlated strongly with $\log(K_2O/Al_2O_3)$ (p=0.63, r=0.56) and negatively but more weakly with $\log(Na_2O/Al_2O_3)$ (p=-0.24, r=not sig.), whilst $\log(MgO/Al_2O_3)$ has a weak negative correlation with $\log(SiO_2/Al_2O_3)$ (p=-0.24, r=not sig.) and is positively correlated with $\log(K_2O/Al_2O_3)$ (p=0.34, r=not sig.). The correlation between $\log(Fe_2O_3/Al_2O_3)$ and $\log(MgO/Al_2O_3)$ is positive and moderately strong (p=0.56, r=0.36). The positive relationships with $\log(K_2O/Al_2O_3)$ and the negative associations with $\log(Na_2O/Al_2O_3)$ and $\log(SiO_2/Al_2O_3)$ suggest that some Fe and Mg may reside in the illite and mixed-layer clays. This is supported by the correlation of $\log(Fe_2O_3/Al_2O_3)$ with log(illite/kaolinite) (p=0.54, r=0.44), and $\log(MgO/Al_2O_3)$ with both log(illite/kaolinite) (p=0.72, r=0.57) and log(smectite/kaolinite) (p=0.71, r=0.64).

Calcite and particularly dolomite would appear to be important hosts for Ca in the Draupne Formation as $\log(CaO/Al_2O_3)$ is correlated with log(calcite/total clay) (p=0.26, r=0.41), log(dolomite/total clay) (p=0.59, r=0.76), $\log(MgO/Al_2O_3)$ (p=0.48, r=0.63), and $\log(CO_2/Al_2O_3)$ (p=0.30, r=0.59). Similarly dolomite is also suggested as a major host for Mg by the correlation of $\log(MgO/Al_2O_3)$ with log(dolomite/total clay) (p=0.52, r=0.68) and $\log(CO_2/Al_2O_3)$ (p=0.32, r=not sig.). In this context the correlation with $\log(Fe_2O_3/Al_2O_3)$ may also partly represent a carbonate mineral association between Mg and Fe. $\text{Log}(MnO/Al_2O_3)$ is correlated with log(dolomite/total clay) (p=0.49, r=0.80) and $\log(CO_2/Al_2O_3)$ (p=0.36, r=0.53) as well as $\log(CaO/Al_2O_3)$ (p=0.50, r=0.81) and $\log(MgO/Al_2O_3)$ (p=0.27, r=0.58) suggesting a carbonate residence for Mn too.

Phosphate minerals of the apatite group would appear to host some Ca and Mn in addition to the carbonate minerals as $\log(P_2O_5/Al_2O_3)$ is correlated with both $\log(CaO/Al_2O_3)$ (p=0.36,

r=0.37) and log(MnO/Al_2O_3) (p=0.52, r=0.52). Log(P_2O_5/Al_2O_3) is also correlated with log(CO_2/Al_2O_3) (p=0.26, r=0.27) which suggests that the dominant apatite mineral present is a carbonate-apatite such as francolite. This was recorded by Pearson (1977) in a phosphatic concretion in Carboniferous mudstones and was thought to be the likely phosphate mineral in other Carboniferous mudstones (Pearson, 1979). Beier and Hayes (1989) have also noted its presence in phosphatic concretions in the New Albany Shale of Devonian to Carboniferous age. Log(P_2O_5/Al_2O_3) is also correlated with a number of other variables. Its association with log($PyFe/Al_2O_3$) (p=0.34, r=0.46) is probably due to the tendency of francolite to precipitate as a result of microbial sulphate reduction during early diagenesis, a process which is also responsible for pyrite formation (Curtis, 1987 and Chapter 5) and a correlation with log(TOC/Al_2O_3) (p=0.32, r=not sig.) may occur for the same reason as that between pyrite and TOC, namely that a constant proportion of the total deposited organic matter is consumed during sulphate reduction (Berner, 1984 and Chapter 5), so that the remaining organic matter buried in the sediment is related to the amount of phosphate released from the fraction which was consumed. The correlation with log (SiO_2/Al_2O_3) (p=0.28, r=0.34), and log(K_2O/Al_2O_3) (p=0.27, r=not sig.) may suggest that a small proportion of the total phosphate is detrital, as proposed by Pearson (1979) for the Carboniferous mudstones, and is associated with quartz and feldspars. Alternatively it may be due to more reducing depositional conditions in those places in which coarser sediment had been deposited.

Log($PyFe/Al_2O_3$) is very strongly correlated with log(pyrite/total clay) (p=0.86, r=0.68) which suggests that the assumptions made regarding the calculation of pyrite Fe are indeed valid. A further moderately strong correlation with log(TOC/Al_2O_3) (p=0.51, r=0.44) illustrates the relationship between C and S often seen in marine shales (Berner, 1984 and Chapter 5). The moderate negative correlation with log(Fe_2O_3/Al_2O_3) (p=-0.46, r=-0.68) reflects the extraction of iron from clay minerals during pyrite formation (Pearson, 1979). The weaker correlation with log(CO_2/Al_2O_3) (p=0.33, r=0.44) may be due to the association of authigenic pyrite and francolite, or may indicate that depositional conditions during sulphate reduction were suitable for carbonate precipitation as there is a weak correlation with log(calcite/total clay) (p=0.30,

r=0.29). The weak correlation between log(MnO/Al_2O_3) and log($PyFe/Al_2O_3$) (p=0.25, r=0.39) possibly reflects the accumulation of Mn in the diagenetic sulphide (Suess, 1979; Curtis, 1987) or may be a result of the correlation with carbonates and phosphates. Weak or moderate positive correlations are observed between log($PyFe/Al_2O_3$) and such variables as log(SiO_2/Al_2O_3) (p=0.38, r=0.28), log(quartz/total clay) (p=0.40, r=not sig.), and log(plagioclase/total clay) (p=0.52, r=0.43), suggesting that pyrite precipitation in the Draupne Formation was greatest in areas of coarser sediment deposition. That this is a result of the nature of the sedimentation and the particular depositional environment of the basin is illustrated in the next chapter. It is not a result of any genetic importance.

Log(TOC/Al_2O_3) in this formation is correlated positively with log(SiO_2/Al_2O_3), (p=0.39, r=0.28) suggesting that greater abundances of organic matter are found in the coarser, more silt rich sediment which is unusual. This conclusion is consistent with those drawn about the distributions of pyrite and phosphate however.

In general the relationships between the logratio transformed major element variables may be related to the mineralogy, both detrital and authigenic, hence it can be seen that the mineralogy is the main control of the major element composition of the formation. By examining the correlation structure of the logratio transformed trace element data an attempt is made to determine the main mineralogical hosts of each of the trace elements.

4.2.2 Trace element relationships

4.2.2.1 Elements associated with the detrital fraction

Log(Rb/Al_2O_3) in the Draupne Formation has weak to moderate negative correlations with log(SiO_2/Al_2O_3) (p=-0.26, r=not sig.), log(quartz/total clay) (p=-0.59, r=0.36), and log(TiO_2/Al_2O_3) (p=-0.25, r=not sig.) which suggest that Rb was not associated with the quartz and feldspar rich silt sized detritus during deposition. In this behaviour it differs from

the Heather and Kimmeridge Clay Formations. A positive correlation with $\log(K_2O/Al_2O_3)$ (p=0.41, r=0.73) (lower than in the Heather and Kimmeridge Clay) suggests that Rb is substituting for K which is normally the case as it forms no minerals of its own (Heier and Billings, 1970). The K mineral host here is probably not K-feldspar because of the evidence above against a relatively coarse sediment residence and is probably illite and mixed-layer clay. Support for this is given by the correlation with $\log(Fe_2O_3/Al_2O_3)$ (p=0.49, r=0.63) and $\log(MgO/Al_2O_3)$ (p=0.60, r=not sig.) which are thought to be clay associated in this formation, and log(smectite/kaolinite) (p=0.71, r=0.45) and log(illite/kaolinite) (p=0.79, r=0.63). A similar detrital mixed-layer clay origin for Rb in the Marl Slate was proposed by Hirst and Dunham (1963), and for Namurian marine black shales by Spears and Amin (1981).

$Log(Li/Al_2O_3)$ too is negatively correlated with $\log(SiO_2/Al_2O_3)$ (p=-0.53, r=-0.49), log(quartz/total clay) (p=-0.49, r=not sig.), log(TiO2/Al2O3) (p=-0.26, r=not sig.) and other variables indicative of silt sized detritus which is strong evidence that it is not associated with the silt size sediment fraction. Its associations with authigenic phases are also negative: eg with $\log(PyFe/Al_2O_3)$ (p=-0.41, r=-0.45), and with $\log(P_2O_5/Al_2O_3)$ (p=-0.26, r=-0.25). A clay mineral host remains probable and the correlation with $\log(Rb/Al_2O_3)$ (p=0.31, r=0.50) suggests an illite or mixed-layer clay residence for Li too, a proposal which is supported by the correlation with log(illite/kaolinite) (p=0.26, r=0.35). This interpretation is consistent with the conclusions of Nicholls and Loring (1962) on Li in Carboniferous shales.

In contrast $\log(Zr/Al_2O_3)$ is correlated with $\log(TiO_2/Al_2O_3)$ most strongly (p=0.61, r=0.63), but also with log(quartz/total clay) (p=0.49, r=not significant), $\log(SiO_2/Al_2O_3)$ (p=0.32, r=0.46) and $\log(K_2O/Al_2O_3)$ (p=0.33, r=0.26) suggesting its occurrence is primarily as zircon associated with the heavy mineral and silt fraction of the original detritus. Such an origin for Zr has often been proposed in studies of mudrock sequences (Gad et al, 1968; Spears and Amin, 1981; Dill et al, 1988). The correlations are lower than in the other formations however and this may reflect a proportion of the Zr being clay bound (illite and smectite may

contain >100ppm Zr; Erlank et al, 1978) although the negative correlation with log(Rb/Al_2O_3) (p=-0.30, r=not sig.) does not support this.

Log(Cr/Al_2O_3) is also moderately correlated with log(TiO_2/Al_2O_3) (p=0.45, r=0.54) and weakly with log(quartz/total clay) (p=0.30, r=not sig.), and log(K_2O/Al_2O_3) (p=0.33, r=0.33) which again suggests that much may be found in a heavy mineral form in the sediment. This is supported by the association with log(Zr/Al_2O_3) (p=0.32, r=not sig.) and log(Th/Al_2O_3) (p=0.24, r=not sig.), although as with log(Zr/Al_2O_3) the corresponding correlations in the Heather Formation are stronger and clay minerals may carry some Cr. Geochemical studies of other mudstone sequences have usually assigned Cr a dominantly clay mineral residence (Gad et al, 1963; Spears and Amin, 1981; Patterson et al, 1986; Dill, 1986), which in the absence of any correlations with clay associated variables does not seem to be applicable here, nor does an organic association seem suitable. Dypvik (1984), noting the correlation between Cr and TiO_2 in Mesozoic clays of Yorkshire, suggested that Cr was present in the non-clay residual sediment (heavy minerals) concentrated by reworking to some extent, whilst Bjorlykke (1974) states that chromite may make an important contribution in high Cr samples. It is concluded here that a heavy mineral, possibly chromite, is the major Cr bearing phase in the Draupne Formation.

Log(Th/Al_2O_3) shows correlations with log(SiO_2/Al_2O_3) (p=0.39, r=not sig.), log(K-feldspar/total clay) (p=0.28, r=not sig.) and log(plagioclase feldspar/total clay) (p=0.28, r=not sig.) in the Draupne Formation. These are very different to the corresponding correlations observed in the Heather Formation which have negative values. The correlations suggest that Th in the Draupne Formation was introduced into the sediment with the detrital silt, and as such it was probably heavy mineral associated. Th in weathering tends to be concentrated in resistant minerals and a number of these heavy minerals have very significant Th contents, eg in zircon up to 10,000ppm Th, and in monazite up to 125,000ppm Th commonly occur (Rogers and Adams, 1969). Patterson et al (1986) suggest however that mixed-layer clays are the main Th host in Australian oil shales. The correlation with log(P_2O_5/Al_2O_3) (p=0.33,

r=0.26) may suggest that apatite is a Th host as it can contain up to 250ppm Th (Rogers and Adams, 1969) but it is more likely to result from the association of phosphates with the coarser sediment in this formation.

Log(Pb/Al_2O_3) is weakly correlated with log(SiO_2/Al_2O_3) (p=0.27, r=0.35), log(quartz/total clay) (p=0.30, r=not sig.) and log(TiO_2/Al_2O_3) (p=0.35, r=0.44) which is the opposite of its behaviour in the Heather and Kimmeridge Clay Formations and which suggests that Pb is found in the siltier sediment fraction where it may replace K in feldspars. Notable are the negative correlations with a number of the trace elements enriched in the Draupne and in other black shales such as Mo, Ni, and U (correlations with: log(Mo/Al_2O_3) p=-0.26, r=-0.44; log(Ni/Al_2O_3) p=-0.28, r=not sig.; and log(U/Al_2O_3) p=-0.32, r=-0.50) which suggest that Pb, which is not enriched here is not associated with the organic or sulphide fraction in the Draupne. Other workers have also assigned Pb a detrital origin in shales, eg Gad et al (1968), but Patterson et al (1986) proposed that galena was the main host in the oil shales of their study, although these did have a low detrital content.

The location of Nb in the Draupne Formation is difficult to determine unequivocally. Log(Nb/Al_2O_3) is correlated negatively with log(SiO_2/Al_2O_3) (p=-0.41, r=-0.36) and log(plagioclase feldspar/total clay) (p=-0.30, r=not sig.) suggesting that Nb may reside in the finer, more clay rich sediment, but the positive association with log(Zr/Al_2O_3) (p=0.32, r=not sig.) may support a heavy mineral host. Correlations have previously been noted in mudstones between Nb and Zr, and Nb and Ti (Erlank et al, 1978), whilst the similarity in ionic size allows substitution of Nb^{5+} for Ti^{4+} in Ti minerals (Deer et al, 1983), which supports the possibility of a heavy mineral host in the Draupne Formation. In coals however it has been suggested that Nb may be partly clay bound and partly associated with organic matter (Asuen, 1988). Patterson et al (1986) in a study of oil shales found Nb to be associated with the alumino-silicate detritus and the same conclusion may be drawn here; from the correlation evidence it is not possible be more specific.

4.2.2.2 Carbonate and phosphate associated elements

Log(Sr/Al_2O_3) is correlated significantly with log(CaO/Al_2O_3) (p=0.44, r=0.81), log(calcite/total clay) (p=0.38, r=0.46), log(dolomite/total clay) (p=0.38, r=0.63), log(P_2O_5/Al_2O_3) (p=0.33, r=0.31), and log(CO_2/Al_2O_3) (p=0.37, r=0.55). On this evidence Sr may also confidently be assigned a dominantly carbonate host, with phosphate playing a secondary role. Such a suggestion is in good agreement with the conclusions of other studies: eg Bjorlykke (1974), Spears and Amin (1981), Patterson et al (1986). These latter authors found 95% of the Sr in oil shales to be associated with carbonate or phosphate minerals. The work of Hirst and Dunham (1963), and Gad et al (1968) however both suggest that about 120ppm Sr may be bound in minerals other than carbonates and phosphates, mainly clays but also feldspars. This would suggest that about 50% of the Sr in the Draupne Formation occurred in carbonate minerals and 50% in the detrital silicates. This is considered to be more reasonable than the figure of 95% determined by Patterson et al (1986) which was obtained for a sequence with a low detrital content and a high carbonate content.

Log(Y/Al_2O_3) has a very strong correlation with log(P_2O_5/Al_2O_3) (p=0.78, r=0.86) indicating that apatite (probably francolite) is the dominant host for Y in the Draupne Formation (and for the other shales in the study). Y is probably substituting for Ca in the crystal structure as the ionic radii are similar. Y is only rarely determined in shale studies, but Patterson et al (1986), by microprobe work found high Y contents in fish debris composed dominantly of apatite and concluded that this supplied much of the total Y content in some Australian oil shales. The other correlations of log(Y/Al_2O_3) are much lower and are probably due to the association of apatite with other minerals.

Log(Sc/Al_2O_3) is generally correlated with the carbonate variables; with log(CaO/Al_2O_3) (p=0.34, r=0.65), log(MgO/Al_2O_3) (p=0.25, r=0.45), and with log(dolomite/total clay) (p=0.28, r=0.47). This supports a carbonate (probably dolomite) host for much of the Sc present. A correlation with log(Y/Al_2O_3) (p=0.24, r=not sig.) could be indicative of a phosphate residence

for some Sc or may represent some Y being carbonate bound. Sc and Y are commonly found together in minerals. The conclusion reached here for the mineralogical residence of Sc is different to that summarised by Frondel (1970) who suggests clay minerals and heavy residual minerals are the main carriers of Sc. Patterson et al (1986) also find clays to be responsible for the Sc in the oil shales of their study. Phosphorites and phosphatic shales are rich in Sc but the correlations between $\log(Sc/Al_2O_3)$ and $\log(P_2O_5/Al_2O_3)$ found for the Draupne Formation, though positive are not significant at the 95% level.

4.2.2.3 Elements associated with the sulphide or organic fractions

$Log(Mo/Al_2O_3)$ is very strongly correlated with $\log(PyFe/Al_2O_3)$ (p=0.80, r=0.86), and log(pyrite/total clay) (p=0.86, r=0.83) which strongly supports the abundance of pyrite as the major control of Mo content. The correlation with $\log(TOC/Al_2O_3)$ is strong (p=0.62, r=0.68), though weaker than the relationship with the pyrite variables and is probably a consequence of the association of pyrite with organic matter, whilst the weak correlations with $\log(P_2O_5/Al_2O_3)$ (p=0.32, r=0.36) and $\log(Y/Al_2O_3)$ (p=0.37, r=0.40) occur because of the genetic association of pyrite with phosphate. Mo is often associated with organic matter in shales (Holland, 1984), but the Mo content of pyrite has also been noted as significant in previous work (Gad et al, 1968; Manheim and Landergren, 1974; Raiswell and Plant, 1980; Patterson et al, 1986). The remaining correlations of $\log(Mo/Al_2O_3)$ with major elements and minerals are weak but $\log(Mo/Al_2O_3)$ has very strong correlations with other enriched trace elements particularly $\log(Ni/Al_2O_3)$ (p=0.91, r=0.90), but also $\log(U/Al_2O_3)$ (p=0.77, r=0.73) and $\log(Co/Al_2O_3)$ (p=0.77, r=0.71).

$Log(Ni/Al_2O_3)$ too, is very strongly correlated with $\log(PyFe/Al_2O_3)$ (p=0.80, r=0.83) and log(pyrite/total clay) (p=0.81, r=0.78) and as with Mo this suggests a primarily pyrite residence for Ni in the Draupne Formation. The correlation with $\log(TOC/Al_2O_3)$ (p=0.63, r=0.65) is lower than with the pyrite variables. Gad et al (1968) found little Ni present in

pyrite nodules, but Raiswell and Plant (1980) suggest that framboidal pyrite may contain significant Ni, and Patterson et al (1986) found Ni to be abundant in pyrite framboids. Of the other variables $\log(Ni/Al_2O_3)$ shows very strong correlations with $\log(Mo/Al_2O_3)$ ($p=0.91$, $r=0.90$), as might be expected if both are pyrite associated, and $\log(Co/Al_2O_3)$ ($p=0.89$, $r=0.87$) and to a lesser extent $\log(U/Al_2O_3)$ ($p=0.72$, $r=0.71$).

$\text{Log}(Co/Al_2O_3)$ also has strong correlations with $\log(PyFe/Al_2O_3)$ ($p=0.66$, $r=0.71$) and log(pyrite/total clay) ($p=0.63$, $r=0.67$) but these are lower than the corresponding correlations of $\log(Mo/Al_2O_3)$ and $\log(Ni/Al_2O_3)$. They do still exceed that with $\log(TOC/Al_2O_3)$ ($p=0.46$, $r=0.38$) however, again suggesting pyrite rather than organic matter as a host, although perhaps with a reduced dominance. As with $\log(Mo/Al_2O_3)$ and $\log(Ni/Al_2O_3)$ a weaker correlation exists with $\log(P_2O_5/Al_2O_3)$ ($p=0.42$, $r=0.62$) demonstrating a relationship with phosphate, but the greater relative strength of the relationship may indicate some phosphate hosted Co rather than a mere association between pyrite and phosphate. Clay minerals were proposed as the main Co bearing phase by Spears and Amin (1981), Gad et al (1968) believed organic matter to be important, and Patterson et al (1986) found sphalerite to be the dominant host (correlation here between $\log(Co/Al_2O_3)$ and $\log(Zn/Al_2O_3)$: $p=0.37$, $r=0.39$). The pyrite contribution to the Co content was thought to be small by Gad et al (1968) but Raiswell and Plant (1980) suggest that framboidal pyrite may carry significant Co. Strong correlations are found with other enriched trace elements particularly $\log(Ni/Al_2O_3)$ ($p=0.89$, $r=0.87$) and $\log(Mo/Al_2O_3)$ ($p=0.77$, $r=0.71$), which are both also thought to be pyrite bound.

$\text{Log}(U/Al_2O_3)$ shows a number of strong correlations with other variables. Strongest are with $\log(PyFe/Al_2O_3)$ ($p=0.62$, $r=0.59$), log(pyrite/total clay) ($p=0.62$, $r=0.39$), and $\log(TOC/Al_2O_3)$ ($p=0.53$, $r=0.65$). This would suggest that organic matter or pyrite are important as a host for U. Patterson et al (1986) found 25% of U to be sulphide associated. A weaker but still significant correlation is found with $\log(P_2O_5/Al_2O_3)$ ($p=0.39$, $r=0.41$) which indicates that phosphate is also a likely site for U in the Draupne Formation. Dill (1986) found about 60% of the total U to be within phosphates, while Patterson et al (1986) obtained a value of 55%

for the phosphate U in their study. A correlation with log(Th/Al_2O_3) (p=0.47, r=0.62) may indicate some detrital heavy mineral component to the U content of the formation, many heavy minerals having abundant U (Rogers and Adams, 1969). Log(U/Al_2O_3) is strongly correlated with a number of other elements particularly log(Mo/Al_2O_3) (p=0.77, r=0.73) and log(Ni/Al_2O_3) (p=0.72, r=0.71).

Unlike the elements discussed above log(V/Al_2O_3) is most strongly correlated with log(TOC/Al_2O_3) (p=0.68, r=0.85), and secondarily with log($PyFe/Al_2O_3$) (p=0.54, r=0.59) and log(pyrite/total clay) (p=0.57, r=0.52). This suggests that for V the major host is organic matter. Strong relationships between TOC and V have often been observed in other studies (Gad et al, 1968; Spears and Amin, 1981; Leventhal and Hostermanm, 1982). V has also frequently been demonstrated to reside in clay minerals (Glikson et al, 1985; Patterson et al, 1986; Stow and Atkin, 1987) but correlations of log(V/Al_2O_3) with for example log(SiO_2/Al_2O_3) (p=0.32, r=0.25) or log(plagioclase feldspar/total clay) (p=0.35, r=0.36) support a coarse sediment preference for V in the Draupne Formation, which is a consequence of the positive relationship between organic matter and the siltier sediment. Log(V/Al_2O_3) is associated strongly with other trace elements especially with log(Cu/Al_2O_3) (p=0.81, r=0.82), log(Zn/Al_2O_3) (p=0.82, r=0.76), and log(Cd/Al_2O_3) (p=0.80, r=0.85).

Log(Cu/Al_2O_3) like V is also strongly correlated with log(TOC/Al_2O_3) (p=0.66, r=0.73), log($PyFe/Al_2O_3$) (p=0.67, r=0.60), and log(pyrite/total clay) (p=0.63, r=0.48), but unlike Ni, Co, and Mo these correlations are all of the same magnitude. It is therefore difficult to determine the exact relationship of Cu with organic matter and pyrite. Gad et al (1968) suggested organic matter was the main concentrating agent for Cu and that pyrite was unimportant but Spears and Amin (1981) found a strong correlation between Cu and pyrite. Patterson et al (1986) found sulphide to be the main Cu host probably as chalcopyrite associated with the pyrite framboids. Of the other abundant trace elements log(Cu/Al_2O_3) is correlated almost equally with log(V/Al_2O_3) (p=0.81, r=0.82), log(Zn/Al_2O_3) (p=0.86, r=0.85) and log(Cd/Al_2O_3) (p=0.79, r=0.80).

As with V and Cu log(Zn/Al_2O_3) is correlated at a similar level with log(TOC/Al_2O_3) (p=0.56, r=0.60), log($PyFe/Al_2O_3$) (p=0.59, r=0.58) and log(pyrite/total clay) (p=0.64, r=0.55) and thus it is difficult to be specific as to the main mineralogical residence of Zn on this evidence alone. Gad et al (1968) found Zn to be correlated with both organic matter and carbonates, in addition to a detrital component. Bjorlykke (1974) also found Zn to be correlated with the detrital and carbonate fraction of the sediment with some sphalerite also probable. Sphalerite was considered by Patterson et al (1986) to be abundant enough to contribute the majority of the Zn present in their samples. Correlations are greatest with the other elements of this group namely: log(Cu/Al_2O_3) (p=0.86, r=0.85), log(Cd/Al_2O_3) (p=0.95, r=0.91), and log(V/Al_2O_3) (p=0.82, r=0.76).

Cd behaves in a manner similar to that of Zn as might be expected from the very high correlation observed between log(Cd/Al_2O_3) and log(Zn/Al_2O_3) (p=0.95, r=0.91). It is an element not often determined in studies of sedimentary geochemistry probably because of the low levels in which it is usually present. Gong et al (1977) state that Cd in organic rich sediments is concentrated primarily by organic matter, a suggestion in accordance with the evidence here, whilst Patterson et al (1986) found sphalerite to be the main mineralogical host and calculated the product moment correlation coefficient (r) between Cd and Zn to be 0.86. This does not preclude an initial concentration by organic matter however. Of the other variables the best correlations are with log(Cu/Al_2O_3) (p=0.79, r=0.80), and log(V/Al_2O_3) (p=0.80, r=0.85).

The trace elements in the Draupne Formation may be divided into three broad groups on the basis of their logratio transformed correlation structure. Firstly the elements Rb, Li, Zr, Cr, Th, Pb and Nb appear to be associated with the detrital silicate fraction. Secondly Sr, Y, and Sc, are mainly associated with the carbonate or phosphate mineral fraction of the formation, whilst finally Mo, Ni, Co, Cu, V, Zn, Cd, and U are related to the organic matter or sulphide content.

4.3 The Heather Formation

The inter-element relationships found in the Heather Formation are simpler than those discussed in the preceding section on the Draupne Formation as the Heather has a simpler clay mineralogy which shows much less variation than the Draupne, and because it lacks the large amounts of organic matter and the resulting authigenic minerals found in that formation. The aim of the following discussion is to summarise the correlation structure of the Heather Formation, as illustrated by the logratio transformed variables and to highlight the differences between the Heather Formation and the Draupne discussed above. Pearson and Spearman correlation coefficients are shown in Tables 4.3 and 4.4.

4.3.1 Major element relationships

$Log(SiO_2/Al_2O_3)$ is correlated most highly with $log(TiO_2/Al_2O_3)$ (p=0.76, r=0.78), a relationship which is stronger than the corresponding one found in the Draupne Formation, and which is probably due to the association between the quartz content of a shale and the TiO_2/Al_2O_3 ratio (Spears and Kanaris-Sotiriou, 1976; discussed above). The increased magnitude of this correlation coefficient probably reflects a greater proportion of the total SiO_2 being present as quartz and a greater dominance by Ti-oxides of the total TiO_2 content. Despite this however the correlation with log(quartz/total clay) (p=0.59, r=not sig.) is lower than in the Draupne, and the relationship between log(quartz/total clay) and $log(TiO_2/Al_2O_3)$ (p=0.44, r=not sig.) is also lower.

$Log(SiO_2/Al_2O_3)$ is also highly correlated (p=0.71, r=0.71) with $log(K_2O/Al_2O_3)$ and moderately with log(K-feldspar/total clay) (p=0.53, r=0.51), while log(quartz/total clay) is also associated with $log(K_2O/Al_2O_3)$ (p=0.71, r=0.33) and log(K-feldspar/total clay) (p=0.34, r=not significant) probably because of the physical association of quartz with K-feldspar in the coarse detrital fraction of the sediment, although a small amount of the potassium present is

undoubtedly in mixed layer or illitic clay. These correlations, particularly the chemical ones are higher in the Heather Formation than the Draupne (where the correlation between $\log(K_2O/Al_2O_3)$ and $\log(SiO_2/Al_2O_3)$ was not significant for p, and only barely significant by r) and reflect the much diminished importance of K bearing clays in the former. A mainly feldspar location for the potassium in the Heather is also supported by the strong correlation found between $\log(K_2O/Al_2O_3)$ and $\log(TiO_2/Al_2O_3)$ (p=0.61, r=0.57), and log(K-feldspar/total clays) and $\log(TiO_2/Al_2O_3)$ (p=0.69, r=0.71) which are both increased in magnitude relative to the Draupne.

Similarly the association found between $\log(SiO_2/Al_2O_3)$ and $\log(Na_2O/Al_2O_3)$ (p=0.47, r=0.53), $\log(TiO_2/Al_2O_3)$ and $\log(Na_2O/Al_2O_3)$ (p=0.49, r=0.59) and log(plagioclase feldspar/total clay) and $\log(Na_2O/Al_2O_3)$ (p=0.43, r=not sig.) is thought to be due to the presence of plagioclase feldspar in the coarse sediment fraction of the Heather although this is not supported by the weak negative correlation existing between log(quartz/total clay) and log(plagioclase feldspar/total clay) (p=-0.27, r=-0.22).

$Log(Fe_2O_3/Al_2O_3)$ is correlated with $\log(SiO_2/Al_2O_3)$ (p=0.42, r=0.39), log(K-feldspar/total clay) (p=0.52, r=0.46) and log(plagioclase feldspar/total clay) (p=0.39, r=not sig.) which suggests that a greater amount of non-pyrite Fe is present in the coarser sediment. This is the reverse of the situation in the Draupne Formation where pyrite was more abundant in the siltier mudstones. The very high correlation between $\log(Fe_2O_3/Al_2O_3)$ and $\log(MgO/Al_2O_3)$ (p=0.87, r=0.85) indicates that Fe and Mg occur in the same minerals. Log(smectite/kaolinite) is correlated with both $\log(Fe_2O_3/Al_2O_3)$ (p=0.50, r=0.73) and $\log(MgO/Al_2O_3)$ (p=0.56, r=0.79) as is log(illite/kaolinite) (p=0.51, r=0.70; p=0.61, r=0.77 respectively) which suggests that mixed layer clay and illite are of importance in this respect.

Carbonates may also contain some Fe and Mg as both are also associated with $\log(CO_2/Al_2O_3)$: p=0.39, r=0.53 for $\log(Fe_2O_3/Al_2O_3)$; p=0.52, r=0.73 for $\log(MgO/Al_2O_3)$. That $\log(MgO/Al_2O_3)$ is more strongly correlated with $\log(CO_2/Al_2O_3)$ and less well correlated with

log(SiO_2/Al_2O_3) (p=0.33, r=0.33) than is log(Fe_2O_3/Al_2O_3) suggests that proportionally more of the Mg is carbonate bound although this is not reflected by a significant correlation with dolomite in this formation whereas log(Fe_2O_3/Al_2O_3) is correlated with log(siderite/total clay) (p=0.34, r=0.51)

Log(CaO/Al_2O_3) is correlated very strongly with log(MgO/Al_2O_3) (p=0.80, r=0.82), strongly with both log(Fe_2O_3/Al_2O_3) (p=0.69, r=0.73), and log(CO_2/Al_2O_3) (p=0.62, r=0.83), and weakly with log(calcite/total clay) (p=0.29, r=0.45). The correlation with log(dolomite/total clay is significant only by means of the product moment coefficient (r=0.45). These correlations, particularly those between the chemical variables suggest that carbonates are probably an important host for Ca in addition to Mg. There are other correlations of log(CaO/Al_2O_3) with mineralogical variables, namely with log(smectite/kaolinite) (p=0.62, r=0.76) and log(illite/kaolinite) (p=0.59, r=0.74) which seem to indicate either a significant Ca content of the mixed layer clays, or else a greater calcite content of illite and smectite bearing samples, and with log(plagioclase feldspar/total clay) (p=0.35, r=not sig.) and log(Na_2O/Al_2O_3) (p=0.52, r=0.72) suggesting that a significant amount of Ca may be present in plagioclase.

Log(MnO/Al_2O_3) is correlated strongly with log(CaO/Al_2O_3) (p=0.66, r=0.82), log(MgO/Al_2O_3) (p=0.60, r=0.79), and log(CO_2/Al_2O_3) (p=0.61, r=0.83), moderately well with log(Fe_2O_3/Al_2O_3) (p=0.46, r=0.62), and log(dolomite/total clay) (p=0.49, r=0.50), and weakly with log(siderite/total clay) (p=0.31, r=0.41) suggesting that Mn is also probably present to a large extent in carbonate minerals in the Heather Formation.

Log(CaO/Al_2O_3) is weakly correlated with log(P_2O_5/Al_2O_3) (p=0.35, r=0.75) suggesting that some of the calcium of the Heather formation is phosphate bound, probably as apatite. The large difference in the correlation coefficients here is an example of the Pearson coefficient being misled by a single sample high in apatite, leading to an over-emphasised importance being attached to the relationship between the two variables for the formation as a whole. The moderate correlation found between log(P_2O_5/Al_2O_3) and log(CO_2/Al_2O_3) (p=0.42, r=0.65)

suggests that the phosphate may be a carbonate apatite such as the francolite found by Pearson (1977). This conclusion is similar to that made for the Draupne Formation. Log(MnO/Al_2O_3) is also weakly correlated with log(P_2O_3/Al_2O_3) (p=0.29, r=0.58), and Suess (1979) has shown Mn phosphate to form authigenically during early diagenesis.

Log($PyFe/Al_2O_3$) and log(S/Al_2O_3) are of course perfectly related because of the manner in which PyFe was calculated, and are negatively correlated with log(Fe_2O_3/Al_2O_3) (p=-0.28, r=not sig.) in the same manner as the Draupne Formation. The correlation with log(pyrite/total clay) is moderate (p=0.51, r=0.41) but is not as high as in the Draupne Formation possibly because of the lower overall pyrite content increasing the importance of noise. Log(S/Al_2O_3), and hence log($PyFe/Al_2O_3$) are also correlated with log(TOC/Al_2O_3) (p=0.58, r=0.67) as is log(pyrite/total clay) (p=0.44, r=0.37) which reflects the often reported relationship between S and TOC in normal marine shales (Berner, 1984), the correlation being stronger than in the Draupne Formation (Chapter 5). The weak correlation between log(MnO/Al_2O_3) and log($PyFe/Al_2O_3$) (p=0.26, r=0.26) and that of log(P_2O_3/Al_2O_3) with log($PyFe/Al_2O_3$) (p=0.38, r=0.47) are similar to those noted in the Draupne Formation and probably occur for the same reason.

Log(TOC/Al_2O_3) is negatively correlated with log(quartz/total clay) (p=-0.28, r=-0.29), log(K_2O/Al_2O_3) (p=-0.26, r=not sig.) and log(TiO_2/Al_2O_3) (p=-0.25, r=not sig.) which indicates that greater amounts of organic matter are preserved in the finer, more clay rich sediments in contrast to the previously discussed Draupne in which both organic matter and pyrite were more abundant in the siltier sediment.

In summary the correlation structure of the logratio transformed major element chemical and mineralogical variables suggest that the Heather Formation differs from the Draupne Formation in two main ways. Firstly in its lower proportion of mixed layer and illite clays in the silicate detritus arriving in the basin, and secondly in the association of organic matter

and its degradation product pyrite with the fine grained sediment rather than the coarser sediment of the Draupne Formation.

4.3.2 Trace element relationships

4.3.2.1 Elements associated with the detrital silicates

In contrast to the Draupne Formation, $\log(Th/Al_2O_3)$ here is negatively correlated with the coarse detrital variables such as $\log(SiO_2/Al_2O_3)$ (p=-0.41, r=-0.33), log(quartz/total clay) (p=-0.55, r=-0.51), $\log(TiO_2/Al_2O_3)$ (p=-0.46, r=-0.39), and others, suggesting that Th is present mainly in the clay mineral fraction; Th being concentrated particularly in kaolinitic weathering resistates (Rogers and Adams, 1969). There is also a strong correlation with $\log(P_2O_5/Al_2O_3)$ (p=0.60, r=0.40) and $\log(CO_2/Al_2O_3)$ (p=0.38, r=0.51); apatite containing up to 250ppm Th. $\text{Log}(Li/Al_2O_3)$, like Th is negatively correlated with $\log(SiO_2/Al_2O_3)$ (p=-0.44, r=-0.31), log(quartz/total clay) (p=-0.56, r=-0.47), and $\log(K_2O/Al_2O_3)$ (p=-0.47, r=-0.26),) suggesting the same clay mineral residence as was interpreted for the Draupne Formation

Unlike Th and Li $\log(Zr/Al_2O_3)$ is most highly correlated with $\log(TiO_2/Al_2O_3)$ (p=0.92, r=0.92), a very close relationship, is very strongly correlated with $\log(SiO_2/Al_2O_3)$ (p=0.83, r=0.87) and $\log(K_2O/Al_2O_3)$ (p=0.83, r=0.85), and strongly with log(quartz/total clay) (p=0.61, r=0.49) and $\log(Na_2O/Al_2O_3)$ (p=0.55, r=0.71). These are higher coefficients than are observed in the Draupne Formation, but are with essentially the same variables suggesting that the Zr is present in the same mineralogical form. There is little doubt that Zr is almost entirely present as the heavy mineral zircon in the coarse detrital fraction of the sediment where it is physically associated with quartz, feldspars and Ti-oxides.

Cr and Nb too are probably resident in the heavy mineral fraction in the Heather Formation. $\text{Log}(Cr/Al_2O_3)$ is correlated strongly with $\log(SiO_2/Al_2O_3)$ (p=0.64, r=0.61), $\log(K_2O/Al_2O_3)$ (p=0.60, r=0.75), and $\log(TiO_2/Al_2O_3)$ (p=0.59, r=0.60), and as for Zr these correlations are

considerably higher than in the Draupne. Similarly log(Nb/Al_2O_3) is most highly correlated with log(SiO_2/Al_2O_3) (p=0.64, r=0.55), and moderately so with log(K_2O/Al_2O_3) (p=0.50, r=0.64) and other variables indicative of the silt fraction. It is probably present in Ti-oxides although the correlation with log(TiO_2/Al_2O_3) is not its strongest (p=0.42, r=0.49), and it has only a moderate correlation with log(Zr/Al_2O_3) (p=0.44, r=0.57).

Rb was believed to reside in clay minerals in the Draupne Formation but in the Heather log(Rb/Al_2O_3) is strongly correlated with a number of variables characteristic of the silt fraction. The correlations with log(K_2O/Al_2O_3) (p=0.68, r=0.67), log(K-feldspar/total clay) (p=0.39, r=not sig.), log(SiO_2/Al_2O_3) (p=0.66, r=0.70), log(quartz/total clay) (p=0.39, r=not sig.), and others suggests that Rb too is hosted by the coarse detrital fraction in this formation, where it probably substitutes for K in K-feldspar. However the correlations with log(Fe_2O_3/Al_2O_3) (p=0.71, r=0.51), log(MgO/Al_2O_3) (p=0.70, r=0.50), and log(illite/kaolinite) (p=0.38, r=0.43) indicate that some Rb may also reside in the mixed layer and illitic clay.

4.3.2.2 Elements associated with carbonate and phosphate minerals

Log(Sr/Al_2O_3) is correlated most strongly with log(CaO/Al_2O_3) in the Heather Formation (p=0.56, r=0.78) and is also correlated with log(MgO/Al_2O_3) (p=0.37, r=0.65), and log(CO_2/Al_2O_3) (p=0.36, r=0.53) which suggests that Sr is to a large extent borne in carbonate minerals where it substitutes for Ca, although there is no significant correlation with either log(calcite/total clay) or log(dolomite/total clay). The Pearson correlation coefficient is very high (r=0.74) between log(Sr/Al_2O_3) and log(P_2O_5/Al_2O_3) but the Spearman correlation is not significant illustrating the effect of a single observation with high P_2O_5 and high Sr on the Pearson coefficient, although some Sr probably is found in phosphate.

Log(Y/Al_2O_3) is very strongly correlated with log(P_2O_5/Al_2O_3) indeed (p=0.88, r=0.97), and a phosphatic host for Y is beyond doubt. Presumably it substitutes for Ca in apatite but it is not significantly correlated with log(CaO/Al_2O_3), possibly because this also varies with the

carbonate content while Y shows a preference for phosphate rather than carbonate. The correlation with log(CO_2/Al_2O_3) (p=0.29, r=0.56) suggests again that the phosphatic phase has some CO_2 content. Sc is also probably phosphate associated, log(Sc/Al_2O_3) having correlations with log(P_2O_5/Al_2O_3) (p=0.45, r=0.74) and log(CaO/Al_2O_3) (p=0.31, r=0.61) although some may be carbonate hosted. The slightly weaker correlations with log (SiO_2/Al_2O_3) (p=0.30, r=0.50) and log(TiO_2/Al_2O_3) (p=0.33, r=0.61) may indicate that some is also associated with the coarse detrital fraction of the sediment.

4.3.2.3 Elements associated with the sulphide and organic fractions

In the Draupne Formation the elements Mo, Ni, Co, Cu, V, Zn, Cd, and U were strongly associated with either S (and hence pyrite) or TOC. These elements were generally enriched in the Draupne relative to average shales and to the Heather Formation. Pb was not enriched in the Draupne and was associated with the coarse detritus. In the Heather Formation the relationships observed in the Draupne are still generally apparent, but are often weaker suggesting the greater relative importance of the silicates as hosts for these elements.

In the Heather Formation log(Mo/Al_2O_3) is moderately correlated with log($PyFe/Al_2O_3$) (p=0.41, r=0.66) and log(pyrite/total clay) (p=0.48, r=0.61) suggesting that pyrite is again an important host, although these relationships are weaker than those observed for the Draupne. The correlation with log(TOC/Al_2O_3) (p=0.32, r=0.60) may be due to the association of pyrite and TOC, or to Mo being adsorbed onto the organic material. There also exists some association of Mo with the silt sediment fraction, illustrated by positive correlations with log(SiO_2/Al_2O_3) (p=0.35, r=0.31), log(K_2O/Al_2O_3) (p=0.38, r=0.41) and others although the nature of this relationship is unclear.

Log(Ni/Al_2O_3), log(Co/Al_2O_3), log(Cu/Al_2O_3), log(V/Al_2O_3) and log(Pb/Al_2O_3) are all highly inter-correlated in the Heather Formation. Within themselves these variables generally have correlation coefficients (p) of between 0.7 and 0.8, and are here considered together. All show

negative correlations with the variables typical of the coarse sediment fraction such as log(quartz/total clay), log(K_2O/Al_2O_3), and log(TiO_2/Al_2O_3), the coefficients for log(Cu/Al_2O_3) for example being p=-0.64, r=-0.51; p=-0.53, r=not sig.; and p=-0.35, r=not sig. respectively. This suggests that these elements are preferentially concentrated in the finer, more clay rich sediment fraction which contrasts with the situation observed in the Draupne Formation where they were more abundant in the coarser fraction. Most are positively correlated with log(smectite/kaolinite) and log(illite/kaolinite) probably because of the greater suitability of the mixed layer and illitic clays as hosts.

Moderate to strong positive correlations are found with log($PyFe/Al_2O_3$), log(TOC/Al_2O_3), and log(P_2O_5/Al_2O_3) suggesting that either pyrite, organic matter or phosphatic materials may play a host role for these elements to some extent. The relative importance of these different phases varies within the group, as it did in the Draupne. Log(Cu/Al_2O_3 is correlated almost equally with log(TOC/Al_2O_3) (p=0.56, r=0.71) and log($PyFe/Al_2O_3$) (p=0.58, r=0.68) for example, as is log(V/Al_2O_3) (p=0.51, r=0.62; and p=0.53, r=0.55 respectively). Log(Ni/Al_2O_3) is again more strongly associated with log($PyFe/Al_2O_3$) (p=0.68, r=0.67) than log(TOC/Al_2O_3) (p=0.54, r=0.64) although this is not so pronounced as in the Draupne, whilst log(Co/Al_2O_3) is correlated with log(P_2O_5/Al_2O_3) (p=0.60, r=0.78), and log($PyFe/Al_2O_3$) (p=0.50, r=0.55) much more strongly than with log(TOC/Al_2O_3) (p=0.25, r=0.47), a trend noted in the Draupne. Log(Pb/Al_2O_3) too is correlated best with log($PyFe/Al_2O_3$) (p=0.50, r=0.46) and log(P_2O_5/Al_2O_3) (p=0.44, r=0.72).

Zn is not included in the above group because although log(Zn/Al_2O_3) is correlated with these other elements the magnitudes of the coefficients are markedly lower (p lies in the range 0.6-0.7). Log(Zn/Al_2O_3) also has no significant negative correlations with the coarse sediment variables as do the other elements of the group suggesting that Zn shows less affinity for the more clay rich sediment. Zn is most similar to Co in the Heather Formation (correlation with log(Co/Al_2O_3) p=0.70, r=0.85) in that log(Zn/Al_2O_3) is correlated with log(P_2O_5/Al_2O_3) (p=0.50, 0.73), with log($PyFe/Al_2O_3$) (p=0.45, r=0.55), and to a lesser extent with

log(TOC/Al_2O_3) (p=0.32, r=0.59) which makes it hard to specify a definite host in the Heather Formation which is not greatly enriched in Zn. Wedepohl however does confirm that Zn may be present in black shales in phosphate and quotes a maximum Zn content of 6800ppm for phosphatic rocks. This is very close to the 6750ppm recorded in a phosphatic Heather sample.

The behaviour of log(Cd/Al_2O_3) in the Heather is unusual and is probably due to the small number of non-zero analyses. Log(Cd/Al_2O_3) is correlated with log(SiO_2/Al_2O_3) (p=0.72, r=0.34), log(Na_2O/Al_2O_3) (p=0.40, r=0.33), log(K_2O/Al_2O_3) (p=0.40, r=not sig.), and other variables suggestive of coarse sediment association. The correlation with log(Zn/Al_2O_3) is much lower than in the Draupne (p=0.42, r=0.76) and weak correlations occur with log(PyFe/Al_2O_3) (p=0.30, r=0.58), log(P_2O_5/Al_2O_3) (p=0.26, r=0.48) and log(CO_2/Al_2O_3) (p=0.38, r=0.35) suggesting some association with pyrite or phosphate.

Log(U/Al_2O_3) is correlated with only log(TOC/Al_2O_3) (p=0.32, r=0.59) of all the major elements suggesting some association with organic matter as discussed above with regard to the Draupne Formation. It is also correlated with log(Cr/Al_2O_3) (p=0.30, r=0.30), and log(Nb/Al_2O_3) which may indicate that a proportion of the total U is present in detrital heavy minerals.

As in the Draupne Formation a three fold division of the trace elements may be made on the basis of the logratio correlation structure. The elements Zr, Cr, Rb, Nb, Th, and Li are associated with the silicate detritus and once more may be subdivided into those elements associated with the clays (Th and Li), and those which are partitioned into the siltier fraction (Zr, Cr, Rb, and Nb). A second group consisting of Sr, Y, and Sc is recognised and is composed of elements found mainly within carbonate or phosphate minerals. Finally the elements Mo, Ni, Co, Cu, V, Zn, Cd, and U are concentrated in the finer sediment and are probably associated with pyrite and organic matter.

4.4 The Kimmeridge Clay Formation

4.4.1 Major element relationships

In the Kimmeridge Clay Formation $\log(SiO_2/Al_2O_3)$ is correlated strongly with $\log(Na_2O/Al_2O_3)$ ($p=0.65$, $r=0.64$) and moderately with both $\log(K_2O/Al_2O_3)$ ($p=0.40$, $r=0.45$) and $\log(TiO_2/Al_2O_3)$ ($p=0.37$, $r=0.45$) (Tables 4.5 and 4.6). This is similar to the Heather Formation although the correlation with $\log(Na_2O/Al_2O_3)$ is considerably stronger, and those with $\log(K_2O/Al_2O_3)$ and $\log(TiO_2/Al_2O_3)$ weaker than in that formation. Si is probably present in quartz and Na in feldspar, both of which are associated in the silt fraction of shales but K may be present in both feldspar and illitic and mixed layer clays as is suggested here by the lower correlation between $\log(K_2O/Al_2O_3)$ and $\log(SiO_2/Al_2O_3)$ and by the correlation of $\log(K_2O/Al_2O_3)$ with $\log(Fe_2O_3/Al_2O_3)$ ($p=0.36$, r=not sig.) and $\log(MgO/Al_2O_3)$ ($p=0.63$, $r=0.41$). As such the Kimmeridge Clay appears to be intermediate between the Heather Formation where K was primarily within feldspar, and the Draupne Formation where K resided dominantly in the clays.

No significant correlation exists between $\log(K_2O/Al_2O_3)$ and $\log(Na_2O/Al_2O_3)$ here, which is again intermediate between the negative correlation of the Draupne and the incipient positive relationship observed in the Heather Formation. This is probably a result of Na being mainly feldspar hosted and hence concentrated in the detrital silt, and K being found in both feldspars and clay.

As in the Heather Formation $\log(Fe_2O_3/Al_2O_3)$ is correlated with many of the variables characteristic of the detrital silt fraction such as $\log(SiO_2/Al_2O_3)$ ($p=0.28$, r=not sig.), $\log(TiO_2/Al_2O_3)$ ($p=0.56$, $r=0.42$), and others which suggests that pyritisation has been less complete in the coarser sediment. The correlation with $\log(MgO/Al_2O_3)$ is strong ($p=0.61$, $r=0.54$), and illitic clays may be a host for both elements as $\log(Fe_2O_3/Al_2O_3)$ and particularly

log(MgO/Al_2O_3) are correlated with log(K_2O/Al_2O_3) (p=0.36, r=not sig.; p=0.63, r=0.41 respectively).

The other important Fe and Mg bearing mineral phases present are carbonates, and both log(Fe_2O_3/Al_2O_3) and log(MgO/Al_2O_3) are correlated with log(CO_2/Al_2O_3) (p=0.54, r=0.38; p=0.50, r=0.60 respectively), and other carbonate hosted elements such as log(CaO/Al_2O_3) (p=0.54, r=0.35; p=0.43, r=0.58 respectively). Log(CaO/Al_2O_3) is very strongly associated with log(CO_2/Al_2O_3) in this formation (p=0.94, r=0.94), and the correlations with both log(Fe_2O_3/Al_2O_3) and log(MgO/Al_2O_3) have been noted above. Calcite probably contains most of the Ca in the Kimmeridge Clay, and is much more abundant in this formation than in the others studied here, as was described in Chapter 3. All of the carbonate associated elements are correlated weakly or moderately with log(TiO_2/Al_2O_3), the coefficients for log(CO_2/Al_2O_3) for example being p=0.52, r=0.49 which may suggest that the carbonate minerals are more abundant in coarser sediment.

Log(TOC/Al_2O_3) is negatively correlated with all of the carbonate elements (eg with log(CaO/Al_2O_3) p=-0.32, r=not sig.) and strongly negatively with log(TiO_2/Al_2O_3) (p=-0.74, r=-0.64) which is consistent with organic matter being most abundant in relatively fine grained, carbonate free sediment, as in the Heather Formation and unlike the situation observed in the Draupne. A positive relationship exists with log($PyFe/Al_2O_3$) (p=0.53, r=0.48), a feature which is common to all of the shales studied here, and the strength of this relationship is similar to that of the Draupne Formation, and rather weaker than that observed in the Heather. Log($PyFe/Al_2O_3$) is itself negatively associated with log(TiO_2/Al_2O_3) suggesting greater pyrite abundance in the finer sediments of this formation, and is correlated with log(P_2O_5/Al_2O_3) (p=0.39, r=0.37) as in the other formations.

Log(P_2O_5/Al_2O_3) is correlated with both log(CaO/Al_2O_3) (p=0.50, r=0.61) and log(CO_2/Al_2O_3) (p=0.46, r=0.57) suggesting a carbonate apatite as in the other formations, but is unusual here in having a moderate correlation with log(SiO_2/Al_2O_3) (p=0.41, r=0.34). No such correlation

was found for the Heather Formation, and although one was observed for the Draupne, this was in the context of both log(TOC/Al_2O_3) and log($PyFe/Al_2O_3$) having positive correlations with log(SiO_2/Al_2O_3) which is not the case in the Kimmeridge Clay Formation. An explanation for this may be the occurrence of reworked detrital phosphatic pebbles which have been recorded by Richardson (1979).

In general the Kimmeridge Clay Formation occupies a position intermediate between those of the Draupne and Heather Formations. Its clay mineralogy is more illitic than the Heather Formation but it has more kaolinite than the Draupne. Pyrite and organic matter are concentrated in the finer sediment which is similar to the Heather Formation and is in contrast to the relationship observed in the Draupne.

4.4.2 Trace element relationships

4.4.2.1 Elements associated with the detrital silicates

Rb is seen to follow K in the Kimmeridge Clay, as in the other formations, the correlation between log(Rb/Al_2O_3) and log(K_2O/Al_2O_3) being p=0.60, r=0.82. K in the Kimmeridge Clay is probably present both in feldspar and clay and it is likely that Rb too is found in both the detrital silt and clay fractions. Li is again difficult to assign to a particular mineral but a weak correlation with log(Rb/Al_2O_3) (p=0.35, r=0.47) is most likely to arise from a clay host for Li although there is little other evidence to support this. V too, is probably bound to clay minerals as log(V/Al_2O_3) is negatively correlated with log(SiO_2/Al_2O_3) (p=-0.48, r=not sig.) and log(Na_2O/Al_2O_3) (p=-0.30, r=not sig.). Unlike the Draupne and Heather Formations there are no strong correlations with other trace element variables.

Zr is present in the Kimmeridge Clay Formation mainly in the mineral zircon associated with the silt sized detrital fraction, the same interpretation as in the other formations studied. This is supported by the correlation of log(Zr/Al_2O_3) with log(SiO_2/Al_2O_3) (p=0.80, r=0.87),

$\log(TiO_2/Al_2O_3)$ (p=0.48, r=0.51), and other variables characteristic of the siltier sediment. Cr also follows the pattern seen in the Draupne and Heather Formations and resides in a heavy mineral, $\log(Cr/Al_2O_3)$ being correlated with $\log(SiO_2/Al_2O_3)$ (p=0.47, r=0.35), $\log(Zr/Al_2O_3)$ (p=0.45, r=0.36) and others.

$Log(Th/Al_2O_3)$ has a limited number of significant correlations in this formation, but those with $\log(SiO_2/Al_2O_3)$ (p=0.49, r=0.52) and $\log(Na_2O/Al_2O_3)$ (p=0.31, r=0.30) point to a coarse sediment location similar to that suggested for the Draupne, and in contrast with the interpretation for the Heather Formation. $Log(Nb/Al_2O_3)$ too, correlates with $\log(SiO_2/Al_2O_3)$ (p=0.55, r=0.45) and with other variables characteristic of the silt fraction and is likely to have a heavy mineral residence in the Kimmeridge Clay as in the Heather.

4.4.2.2 Elements associated with carbonate or phosphate minerals

Sr, Y, and Sc follow the same pattern as in the Draupne and Heather Formations. $Log(Sr/Al_2O_3)$ is extremely well correlated with $\log(CaO/Al_2O_3)$ (p=0.85, r=0.88), and strongly with $\log(CO_2/Al_2O_3)$ (p=0.77, r=0.82) and probably replaces Ca in carbonates. $Log(Y/Al_2O_3)$ is strongly correlated with $\log(P_2O_5/Al_2O_3)$ (p=0.78, r=0.80), and moderately with $\log(CaO/Al_2O_3)$ (p=0.50, r=0.63) and $\log(CO_2/Al_2O_3)$ (p=0.50, r=0.62) and probably resides mainly within phosphate. $Log(Sc/Al_2O_3)$ is correlated with $\log(CaO/Al_2O_3)$ (p=0.61, r=0.64), $\log(CO_2/Al_2O_3)$ (p=0.62, r=0.63) and $\log(P_2O_5/Al_2O_3)$ (p=0.40, r=0.53) and is located in either, or both carbonates and phosphates.

4.4.2.3 Elements associated with the sulphide or organic fraction

The elements noted in the Draupne and Heather Formations as being highly intercorrelated and associated with organic matter or pyrite are with some exceptions much less highly intercorrelated in this formation. As in the Heather Formation few of these elements are present in excessive concentrations. $Log(Cu/Al_2O_3)$ is very strongly correlated with

log(TOC/Al_2O_3) (p=0.83, r=0.78), and organic matter is probably an important host for this element here, the magnitude of this correlation being considerably greater than in either the Draupne or Heather Formations. With log(PyFe/Al_2O_3) the correlation is lower (p=0.49, r=0.58) and is probably a result of the association between pyrite and organic matter. Strong or very strong correlations are noted only with log(Ni/Al_2O_3) (p=0.80, r=0.58) and log(Mo/Al_2O_3) (p=0.73, r=0.81). Log(Mo/Al_2O_3) is itself also highly correlated with log(TOC/Al_2O_3) (p=0.80, r=0.75) and less so with log(PyFe/Al_2O_3) (p=0.64, r=0.71) which is in contrast to the observations in the Draupne Formation where Mo was thought to reside in pyrite. Here as with Cu, organic matter must be considered as the main Mo host. Log(Mo/Al_2O_3) too is strongly associated with log(Ni/Al_2O_3) (p=0.67, r=0.72), but only moderately with the other elements that it was so closely related to in the Draupne.

Log(Ni/Al_2O_3), despite strong correlations with log(Cu/Al_2O_3) and log(Mo/Al_2O_3) is not so highly correlated with log(TOC/Al_2O_3) as are these two elements (p=0.65, r=0.43) and the correlation with log(PyFe/Al_2O_3) is of equal magnitude (p=0.65, r=0.74) whereas in the previous formations it was greater. In the Draupne Formation, and to a lesser extent in the Heather Formation pyrite was thought to be an important Ni host but here this is not clear. Co was also thought to be pyrite associated in other formations, a suggestion which is supported by the correlation of log(Co/Al_2O_3) with log(PyFe/Al_2O_3) (p=0.52, r=0.66). The correlation with log(Ni/Al_2O_3) is stronger than with most other trace elements and may support a pyrite residence for a proportion of the Ni also. Log(Pb/Al_2O_3) is correlated moderately with both log(Ni/Al_2O_3) (p=0.58, r=0.56) and log(Co/Al_2O_3) (p=0.64, r=0.63) and its correlation with log(PyFe/Al_2O_3) is similar (p=0.65, r=0.61). With log(TOC/Al_2O_3) the strength of the relationship is lower, but the correlation is still significant (p=0.36, r=not sig.). Thus for Pb also pyrite or sulphides are a probable host.

Log(Zn/Al_2O_3) is not strongly correlated with any other variable. With log(PyFe/Al_2O_3) the correlation is weak (p=0.28, r=0.57), as it is with log(P_2O_5/Al_2O_3) (p=0.30, r=0.35). Where Zn contents are low such as in this formation the importance of detrital, probably clay mineral

bound Zn will increase. With other trace elements log(Zn/Al_2O_3) is best correlated with log(Ni/Al_2O_3) (p=0.51, r=0.51). The correlation with log(Cd/Al_2O_3) (p=0.42, r=0.64) is of the same strength as in the Heather Formation and is much lower than that of the Draupne where both Zn and Cd were present in considerable abundance. Log(Cd/Al_2O_3) here is correlated noticeably with phosphatic variables such as log(P_2O_5/Al_2O_3) (p=0.65, r=0.40), log(CaO/Al_2O_3) (p=0.74, r=0.28), and log(CO_2/Al_2O_3) (p=0.73, r=0.30) suggesting the importance of phosphatic minerals.

A host for the U content of the Kimmeridge Clay is difficult to determine. Log(U/Al_2O_3) is correlated with log($PyFe/Al_2O_3$) (p=0.28, r=0.40) and with elements of the carbonate group such as log(CaO/Al_2O_3) (p=0.30, r=not sig.) and log(CO_2/Al_2O_3) (p=0.30, r=not sig.) suggesting some association with carbonates, although these correlations are weak. Possibly some U is within the carbonate lattice.

The trace element relationships in the Kimmeridge Clay Formation are generally similar to those seen in the two formations discussed above. Rb is thought to be found in the clays and feldspars, a position intermediate between the previous two formations, but Li is once more interpreted as having a clay mineral residence as is V in this formation where it is not greatly enriched. Zr, Cr, Th, and Nb are all interpreted as having a primarily heavy mineral location. Sr, Y, and Sc show behaviour similar to that in the Draupne and Heather Formations and carbonate and phosphate minerals are their main hosts. Cu, Mo, Ni, Co, Pb, Zn, Cd, and U all show varying degrees of association with pyrite and organic matter but where their abundances are low the importance of the silicate detritus increases.

4.5 Summary

The raw compositional data resulting from the study of major and trace elements and minerals have been transformed to new Al_2O_3 normalised logratios whose correlations are examined. This process avoids the interpretational difficulties arising from the effects of

closure. The major element compositions of the three formations of Upper Jurassic mudstones considered are related to, and controlled by their mineralogy, both detrital and authigenic.

The mineralogical residences of the trace elements determined have also been investigated by analysis of the correlation matrices. For each formation studied three broad groups of trace elements have been identified. The elements Zr, Cr, Nb, Th, Rb, and Li were found to be consistently associated with the detrital silicate fractions. Of these Zr, Cr, and Nb were recognised as being present in the silt sized fraction of the detritus, heavy mineral residences being likely. This is also true for Th in the Draupne and Kimmeridge Clay Formations but in the Heather Formation the Th distribution is controlled by the clay mineral content. Li is also clay mineral bound whilst Rb substitutes for K in whichever are the dominant K bearing minerals.

Sr, Y, and Sc were associated with carbonate or phosphate minerals, Sr being mainly carbonate hosted, and Y content being related to the abundance of phosphate. Sc generally falls between these two.

Of the remaining elements Mo, Ni, Co, Cu, V, Zn, Cd, and U are mainly associated with either organic matter or pyrite, a product of its bacterial degradation. Where they are enriched pyrite appears to be the main host for Mo, Ni, and Co, with organic matter being strongly associated with Cu, V, Zn, Cd, and U. Pb is correlated with the detrital fraction in the Draupne Formation but with organic matter and pyrite in the Heather and Kimmeridge Clay Formations.

Chapter Five

Sedimentological and Diagenetic Variation

5.0 Sedimentological and Diagenetic Variation

Chapters 3 and 4 have been largely descriptive in content and have summarised the composition of the sample suite studied (Chapter 3), and the relationships between the different variables (Chapter 4). The ultimate aim of the current research is to examine the extent of the dependence of the geochemistry of a shale on its organic maturity and hence burial history. Before this may be accomplished however the effects of depositional and diagenetic processes must be considered, as these processes are important controls on sedimentary geochemistry. The extent of the variation in the grain size, sedimentological maturity, and depositional environment of the sample set is described below. Finally in this chapter the organic maturity parameters employed are discussed and the organic maturity of the suite is illustrated.

5.1 Sedimentological variation

5.1.1 Grain size parameters

The mineralogy and major element geochemistry of fine grained clastic sediments to a large extent depends on the grain size of the detritus and its petrographic maturity (Pettijohn, 1975; Paropkari, 1990). The coarser siltier fractions of the sediment are enriched in quartz and feldspars relative to the finer fractions which are composed mainly of clays, and this results in the coarser fractions having the greater SiO_2 content, and the finer fraction more Al_2O_3 (Pettijohn, 1975; Paropkari, 1990). Similarly more mature sediments are also generally richer in Al_2O_3, but are depleted for example in Na_2O. The dependence of the geochemistry and mineralogy on such textural and sedimentological properties of rocks allows us to use some geochemical parameters as indices of sedimentological properties.

A number of geochemical and mineralogical parameters have been used in the geological literature to discern grain size information from fine-grained sediments. The parameters

employed in this study are the SiO_2/Al_2O_3 ratio, the TiO_2/Al_2O_3 ratio, and the ratio of quartz+feldspar/total clay. The SiO_2/Al_2O_3 ratio has been used by Bjorlykke (1974), Dypvik (1984), and Dill et al (1988) as a grain size index for sediments. From the data of Grout (1925) in Pettijohn (1975) this ratio has a value of 7.00 in the fine sand fraction separated from shales, 4.64 in the silt fraction, and only 2.1 in the fine clay from the same suite, the latter value approaching that of pure kaolinite (1.2) which is probably the lowest value likely to be found in normal shales. Dill et al (1988) found the response to changes between conglomeratic and arenaceous sediments to be poor, but this is not anticipated to be a problem in this study where the grain sizes are much finer.

Spears and Kanaris-Sotiriou (1976) have noted that the TiO_2/Al_2O_3 ratio increases in Carboniferous mudstones with increasing grain size as Ti-oxides become more important relative to clay bound Ti, the hydrodynamic properties of the oxides and the siltier fraction of the mudstones being similar. The ratio has a lowest value of about 0.025 for pure clay sized sediment, increasing to about 0.060 for the siltstones in their study and to about 0.13 for sandstones. This relationship has allowed the ratio to be used as a grain size index (eg Spears and Amin, 1981).

As the effects of sorting enrich the coarser detritus in quartz and feldspars relative to the finer sediment, the ratio of quartz+feldspar/total clay may also be used as a grain size index (eg Bjorlykke, 1974; Dypvik, 1984). Grout (1925) indicates that the silt fraction of a shale will have a value for this ratio of about 1.5 whereas for the fine clay of the same samples the value will be about 0.4.

5.1.2 Petrological maturity parameters

A variety of chemical and mineralogical parameters have also been used to ascertain the petrographic maturity of sediments. The quartz/feldspar ratio is one such (Bjorlykke, 1974; Dypvik, 1984). The value of this ratio increases as the detritus becomes more

sedimentologically mature. This occurs because quartz is more resistant to weathering and erosion than are feldspars and hence comes to dominate the siltier sediment. That both quartz and feldspars are concentrated into the silty fraction of shales should minimise the effects of grain size variation on the magnitude of this parameter.

The Chemical maturity index $M=(K_2O+Al_2O_3)/(Na_2O+MgO)$ has often been used for the evaluation of sedimentological maturity as both K and Al are concentrated in weathering profiles relative to Na and Mg. As Dill et al (1988) point out however this ratio is susceptible to variation in the MgO content due to authigenic dolomite formation and as such is not a reliable index of maturity where authigenic dolomite cannot be ruled out. In preference to the parameter M, the chemical index of alteration (CIA) proposed by Nesbitt and Young (1982) has been used as a geochemical index of maturity in this study where authigenic dolomite is likely. This concentrates on the extent of feldspar dissolution and clay mineral formation as a measure of maturity. During such alteration the elements Ca, Na, and K are lost relative to Al so the CIA is defined as: $CIA=[(Al_2O_3)/(Al_2O_3+CaO^*+Na_2O+K_2O)]*100$ using the molecular proportions. In this case, unlike the definition of M the value CaO^* is the Ca content of the silicate fraction only and is calculated from the total CaO by correction for apatite and calcite (for this purpose it is assumed that all CO_2 is as calcite). Values of the CIA are about 50 for undegraded feldspars. The clay products of feldspar degradation have higher values: illite having a CIA of 70-75, and kaolinite of about 100. This results in typical shales having CIA values of around 70 to 75.

The effects of sorting inherent in the sedimentological process, and the resulting mineralogical differentiation were noted by Nesbitt and Young (1982) as possible sources of error in the interpretation of CIA values. To counter this they studied only rocks of mud grade where the effects of sorting were minimal. A similar restriction is employed here although the possibility of some grain size influence even within a mudstone suite is not ruled out.

5.1.3 The Draupne Formation

For the Draupne Formation the median SiO_2/Al_2O_3 ratio of each well examined is shown in Fig. 5.1. It can be seen that there is a distinct increase in the median value from about 3 for the wells from the Horda Platform and the Bergen High areas to about 3.5 for wells from the western margins of the Viking Graben which suggests an increase in grain size from east to west across the area studied. The median TiO_2/Al_2O_3 ratios (see Fig. 5.2) are not entirely

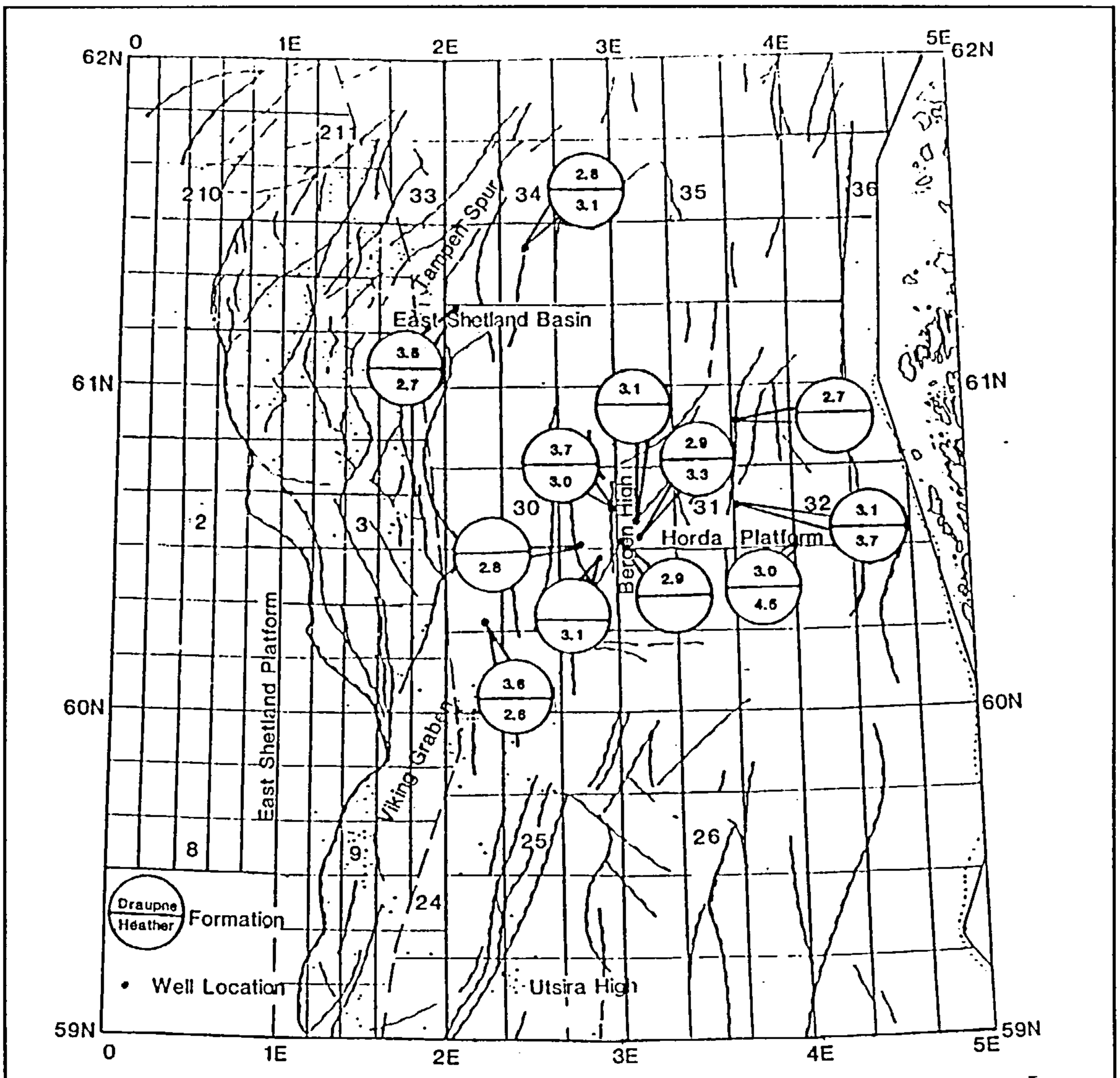

Figure 5.1 Median SiO_2/Al_2O_3 ratios by well for the Draupne and Heather Formations.

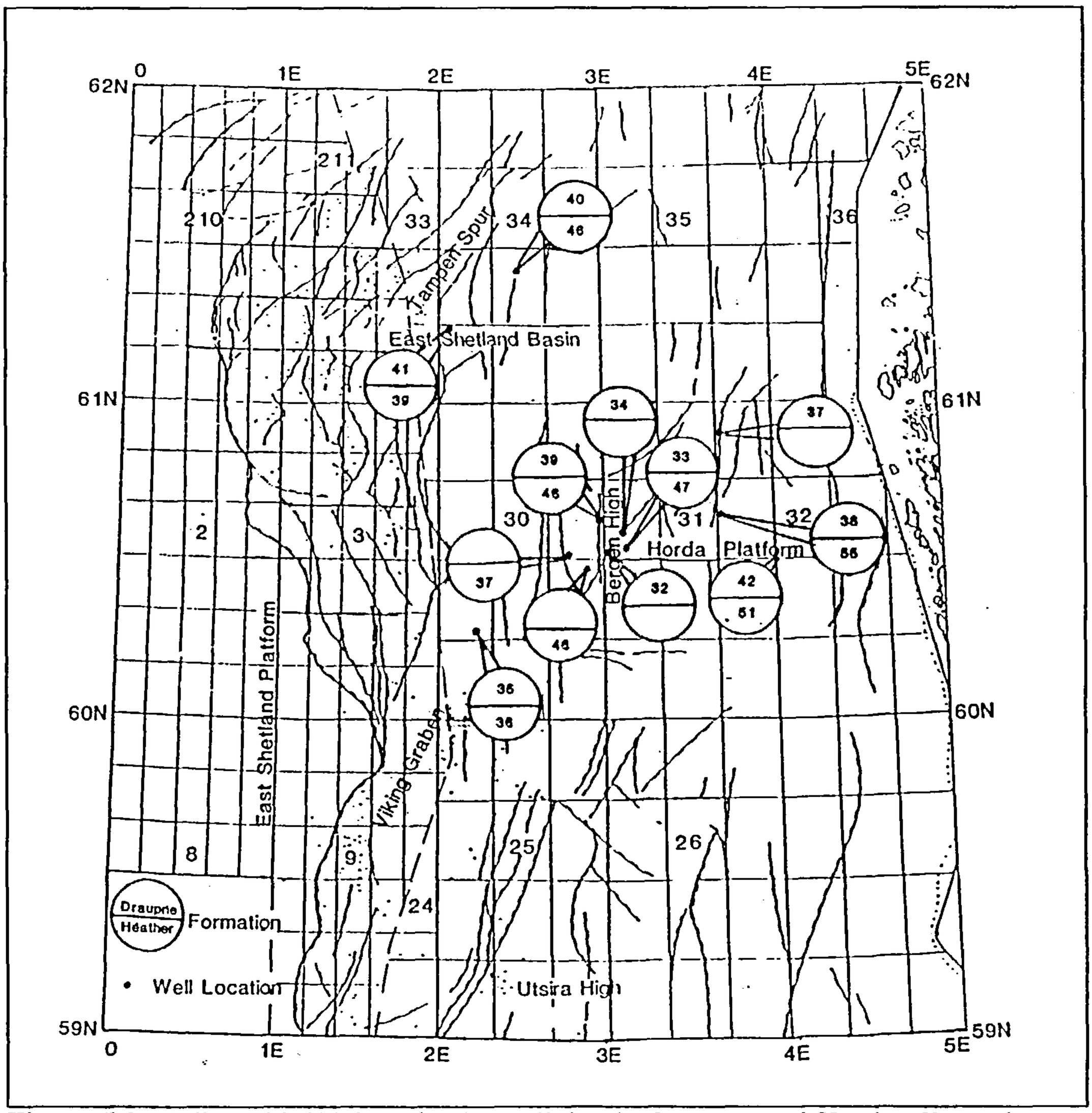

Figure 5.2 Median TiO_2/Al_2O_3 ratios by well for the Draupne and Heather Formations.

consistent with this and suggest that the westernmost and easternmost samples are relatively coarse (TiO_2/Al_2O_3 of about 0.040) with a grain size minimum in the vicinity of the Bergen High (TiO_2/Al_2O_3 of about 0.033). The median values of the (quartz+feldspar/clay) parameter are shown in Fig. 5.3 and are consistent with the SiO_2/Al_2O_3 data in showing that the Draupne is coarsest in the western Viking Graben (with a median (quartz+feldspar/clay) ratio of about 0.55). Whether or not the grain size is finer near the Bergen High than to the east on the Horda Platform is unclear, both areas having a scatter of values in the range 0.30-0.40.

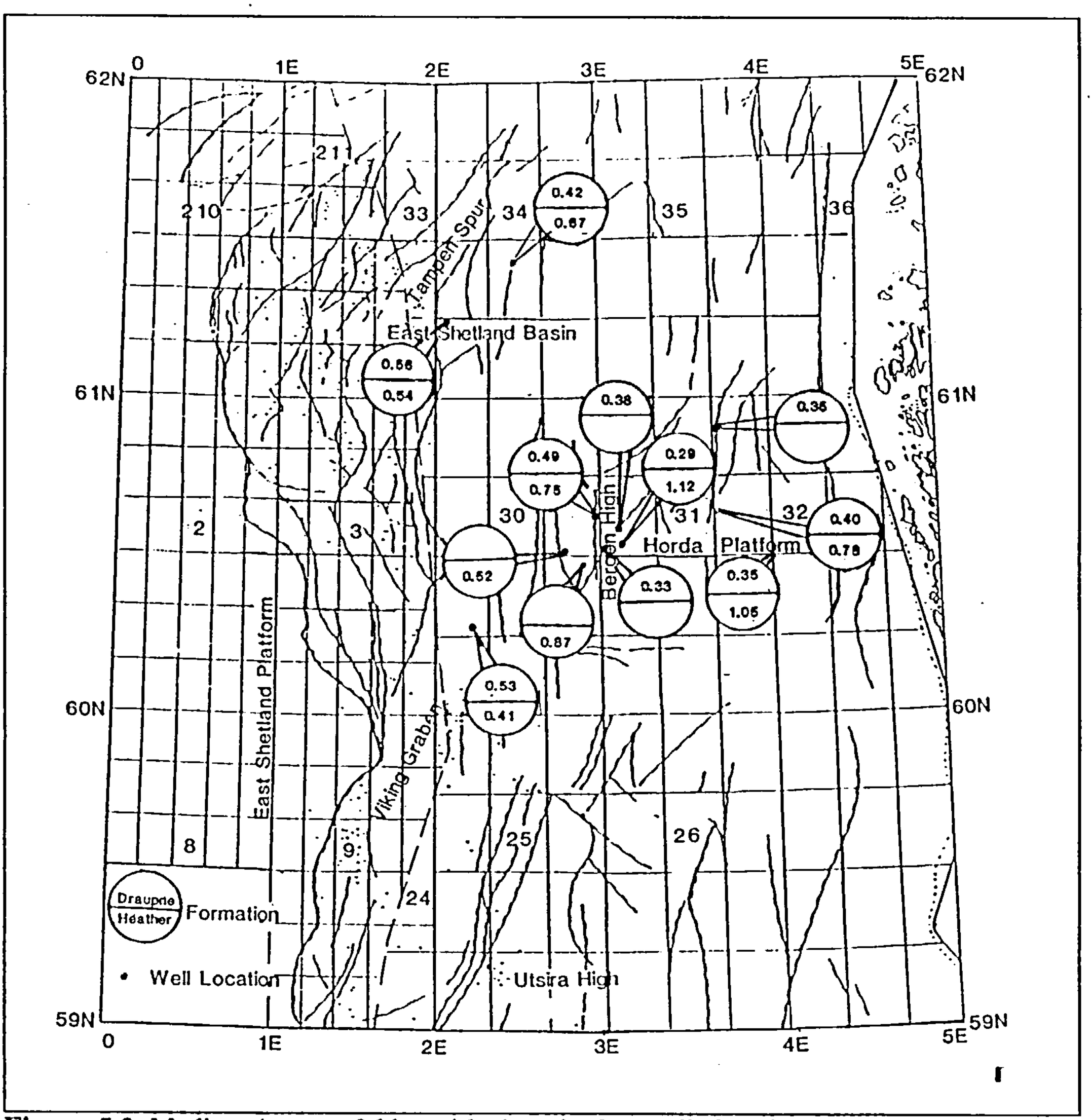

Figure 5.3 Median (quartz+feldspar/clay) ratio by well for the Draupne and Heather Formations.

Overall the grain size parameters suggest that the Draupne Formation in the area studied is coarsest in the vicinity of the western flank of the Viking Graben. To the east the grain size would appear to be generally finer, but there is some evidence that in the Bergen High and adjacent areas the grain size may decrease relative to that found on the Horda Platform.

The grain size evidence points to a western derivation for some of the sediment of the Draupne Formation and appears to be consistent with the suggestions of Ziegler (1981) that during the Upper Jurassic uplifted fault blocks were undergoing erosion and shedding detritus eastwards into the Viking Graben. Badley et al (1988) state that even in the Ryazanian, at the close of Draupne Formation deposition the major fault blocks of the Brent and Gullfaks fields were still above sea level and hence were available as local sources of sediment. Further south in the Brae Field the reservoir is in Upper Jurassic coarse clastics which have been variously interpreted as fan deltas (Harms et al, 1981) or submarine fans (Stow et al, 1982), and in the East Shetland Basin the Magnus Field also has a submarine fan reservoir of upper Jurassic age. Glasman et al (1989c) have measured K/Ar ages for detrital illites in Mesozoic shales of the Bergen High area and found them to be older than the depositional ages of the sediment but similar to, and slightly younger than the muscovites and biotites of the Brent Group sands (Glasman et al 1989a) which gave Caledonian ages of around 400Ma. Thus erosion of the Brent sands on exposed uplifted fault blocks may have provided some of the material for the Draupne Formation, the reworking being responsible for some loss of Ar and resulting in the slightly younger measured ages.

Median (quartz/feldspar) ratios show no clear trends in petrographic maturity over the region studied (Fig 5.4), but the CIA shows a distinct increase in median values from east to west (Fig 5.5). The most westerly parts of the formation might reasonably have be expected to be most mature if as is suggested above much of the material for the Draupne Formation in the west of the area studied was supplied by re-erosion and deposition of previously deposited sediment. If the variation in CIA values were due to sorting one would expect the trend to be the reverse of that observed.

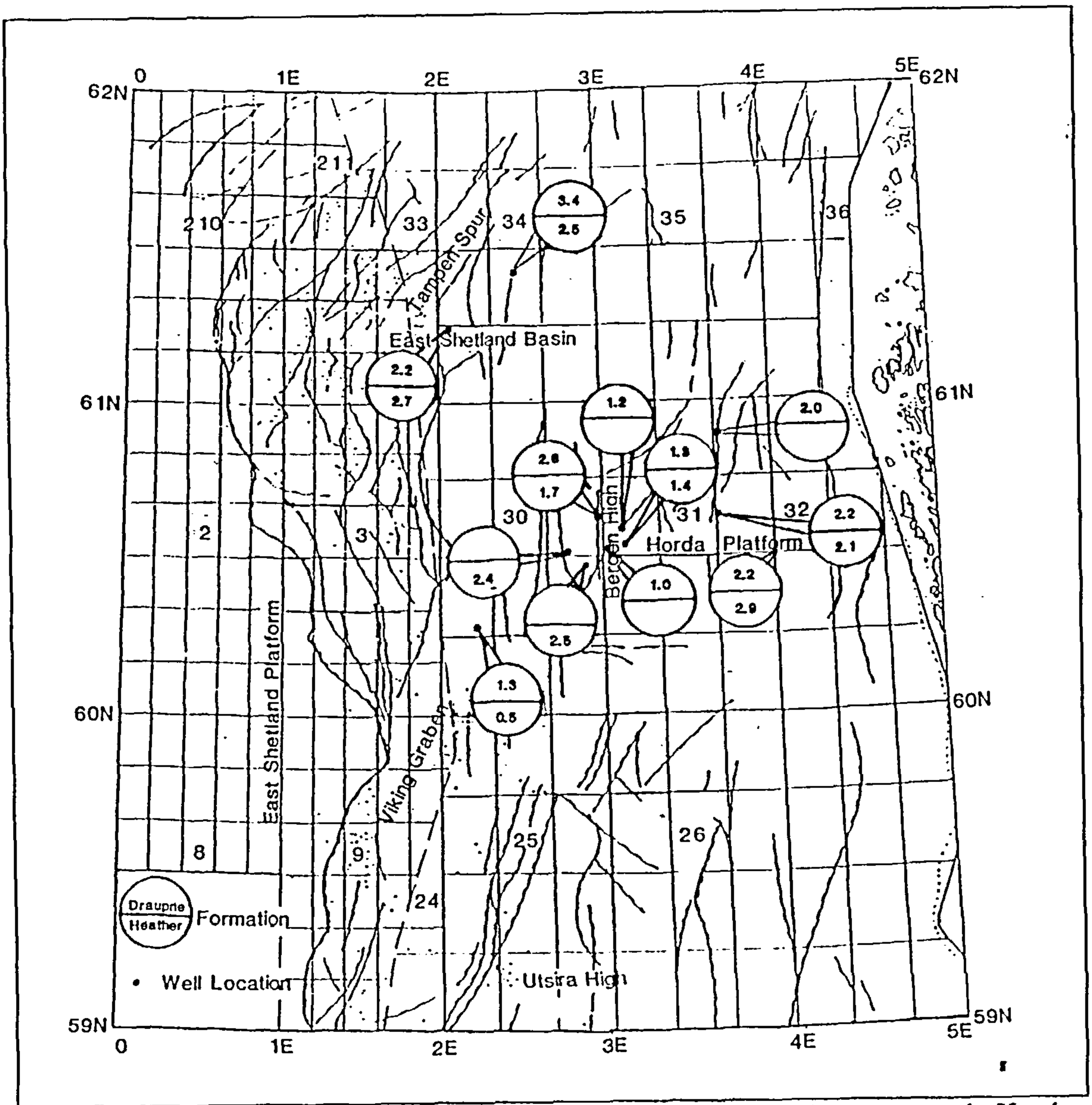

Figure 5.4 Median quartz/feldspar ratios by well for the Draupne and Heather Formations.

5.1.4 The Heather Formation

In the Heather Formation there is a clearly defined decrease in the values of the median SiO_2/Al_2O_3 ratios from a maximum of 4.49 on the Horda Platform to a minimum of only 2.64 on the western margin of the Viking Graben (Fig. 5.1). This is clear evidence for a grain size decrease from east to west, a trend opposite to that observed in the overlying Draupne Formation, and suggesting a sediment transport direction from the east. Similar conclusions

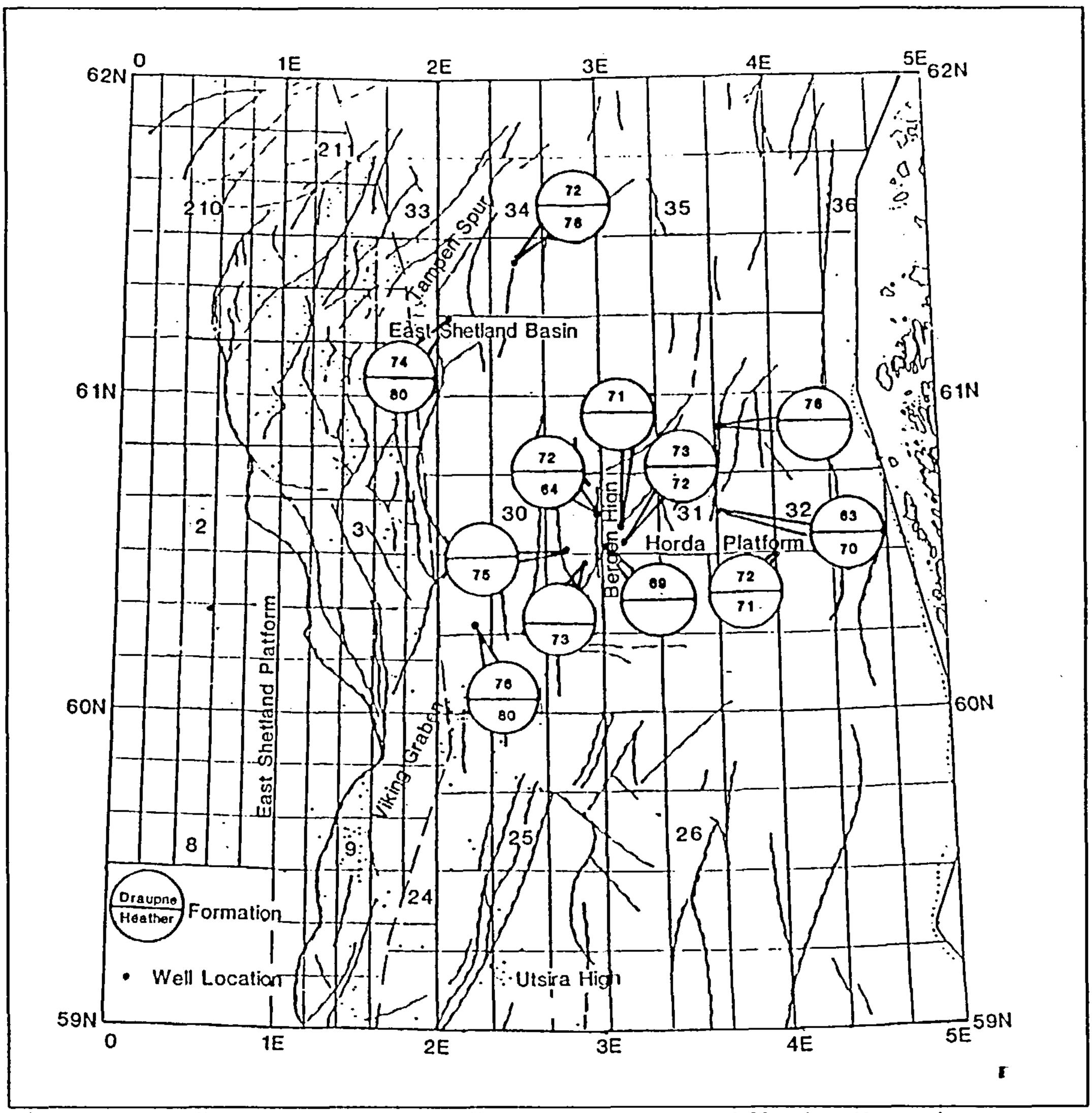

Figure 5.5 Median CIA values by well for the Draupne and Heather Formations.

may be drawn from the values of the median TiO_2/Al_2O_3 ratios for each well sampling the Heather (Fig. 5.2) and from the (quartz+feldspar/clay) ratio distributions (Fig 5.3). In general the Heather Formation shows much greater variation in all of the grain size parameters studied than does the Draupne which indicates that at its coarsest the Heather is considerably coarser than the Draupne, and likewise at its finest it is finer. The quartz/feldspar ratio shows no significant trend but as in the Draupne Formation the CIA values increase from a low in the east to a maximum in the west (Figs. 5.4 and 5.5), both of these figures being higher than the corresponding Draupne Formation values. This observed trend in maturity could however be interpreted as a sorting effect.

The sedimentological parameters suggest that for the Heather Formation the main source of detritus was to the east, most probably the Scandinavian massif, and that any local sources supplying sediment from the west were insignificant. The very coarse nature of some of the Heather sediments of the Horda Platform is probably a result of the same prograding shallow marine coarse clastic influx responsible for the coarse grained formations of the lower Viking Group (eg the Sognefjord Formation) which form the reservoir in the Troll Field.

5.1.5 The Kimmeridge Clay Formation

The four beds analysed from the Kimmeridge Clay Formation (44, 32, 24, and 18, Cox and Gallois, 1981) are here considered separately. These beds have been described as primarily calcareous (beds 44 and 18), organic rich (bed 32), and silty (bed 24) by Scotchman (1989) who has sampled these beds in much greater detail than in this work. The values of the SiO_2/Al_2O_3 ratios usually fall between 2.5 and 3.5 with few exceptions, the median values being (3.2, bed 24), (3.0, bed 44), (2.9 bed 32), and (2.8 bed 18) which confirms the siltier nature of bed 24. TiO_2/Al_2O_3 ratios show more variation with medians being (0.043, bed 24), (0.043, bed 44), (0.039, bed 18) and 0.033, bed 32) suggesting again that bed 24 is relatively coarse but also that bed 32 is slightly finer than the others.

Scotchman (1989) also noted lateral changes in the nature of these beds along the length of the outcrop. Changes in the SiO_2/Al_2O_3, and TiO_2/Al_2O_3 ratios are shown in Figs. 5.6 and 5.7. Values represent single analyses from each bed at each location with the exception of bed 32 were the values are averages of two analyses (3 at Marton). Both of the calcareous beds (44 and 18) are by far the coarsest at Warlingham, an interpretation supported by both the SiO_2/Al_2O_3 and TiO_2/Al_2O_3 ratios, and show no great variation elsewhere. Bed 24 appears to be coarsest in the south at Portesham and Tisbury, and again shows a good agreement

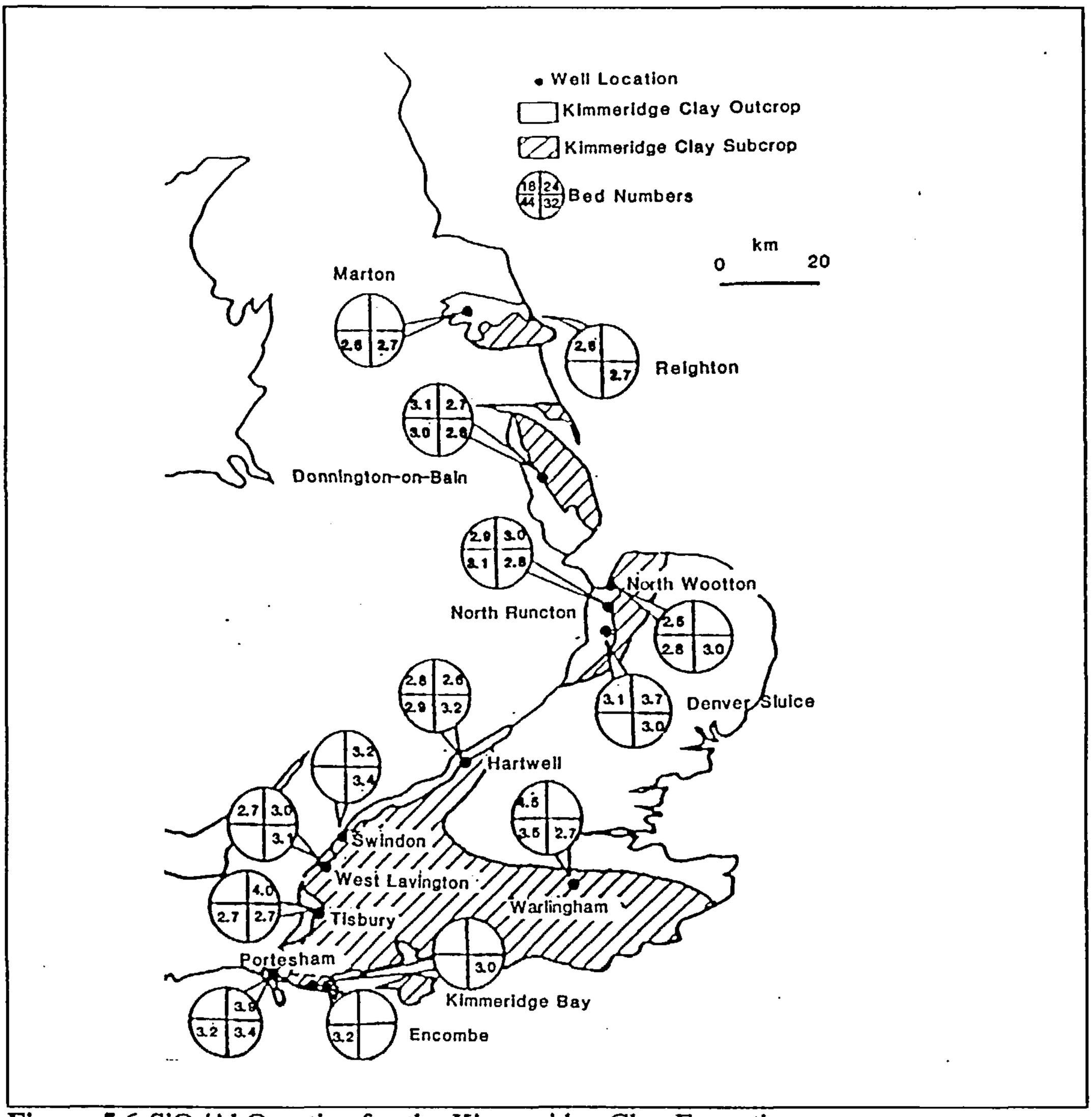

Figure 5.6 SiO_2/Al_2O_3 ratios for the Kimmeridge Clay Formation.

between the SiO_2/Al_2O_3 and TiO_2/Al_2O_3 indices. The organic rich bed 32 which has been most thoroughly sampled of the beds in this study shows a gradation in SiO_2/Al_2O_3 ratios, suggesting that in Dorset it is relatively fine, but becomes coarser northwards, peaking in the Swindon area and becoming finer to the north of there into the Wash and Yorkshire. Agreement between the two grain size parameters is not as striking in this bed as in the others but the TiO_2/Al_2O_3 ratios in the Swindon and Hartwell samples are higher than those to the north in the Wash and to the South in Dorset.

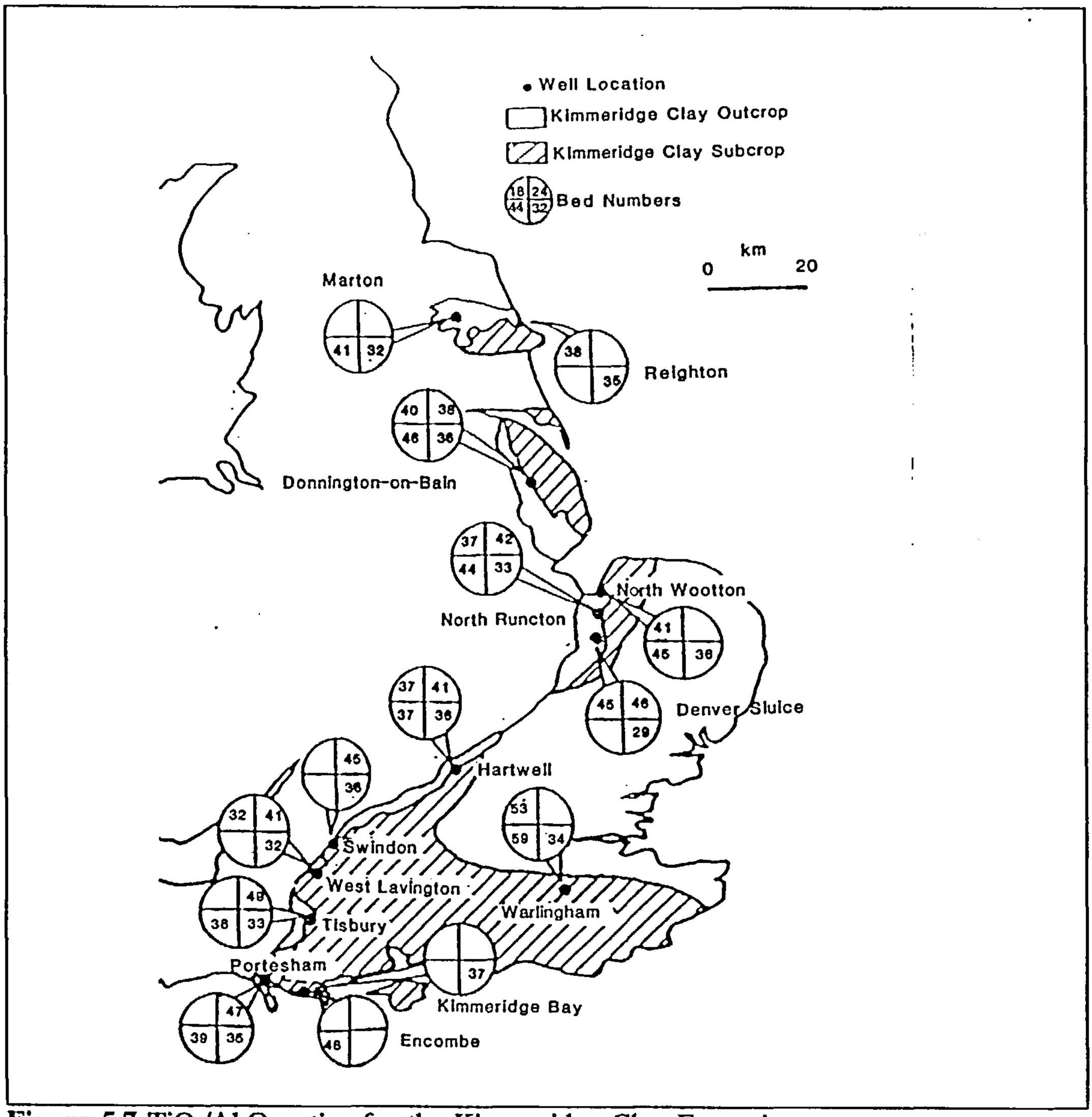

Figure 5.7 TiO_2/Al_2O_3 ratios for the Kimmeridge Clay Formation.

Median values of the CIA are lower in beds 24 and 44 than in bed 18 and 32 suggesting that bed 32 is most sedimentologically mature, but there is a large amount of scatter in these values. Lateral changes in CIA are illustrated in Fig. 5.8. Bed 32 in particular shows a decrease in maturity over the swell area of the south midlands suggestive of a local supply of less weathered material in this area.

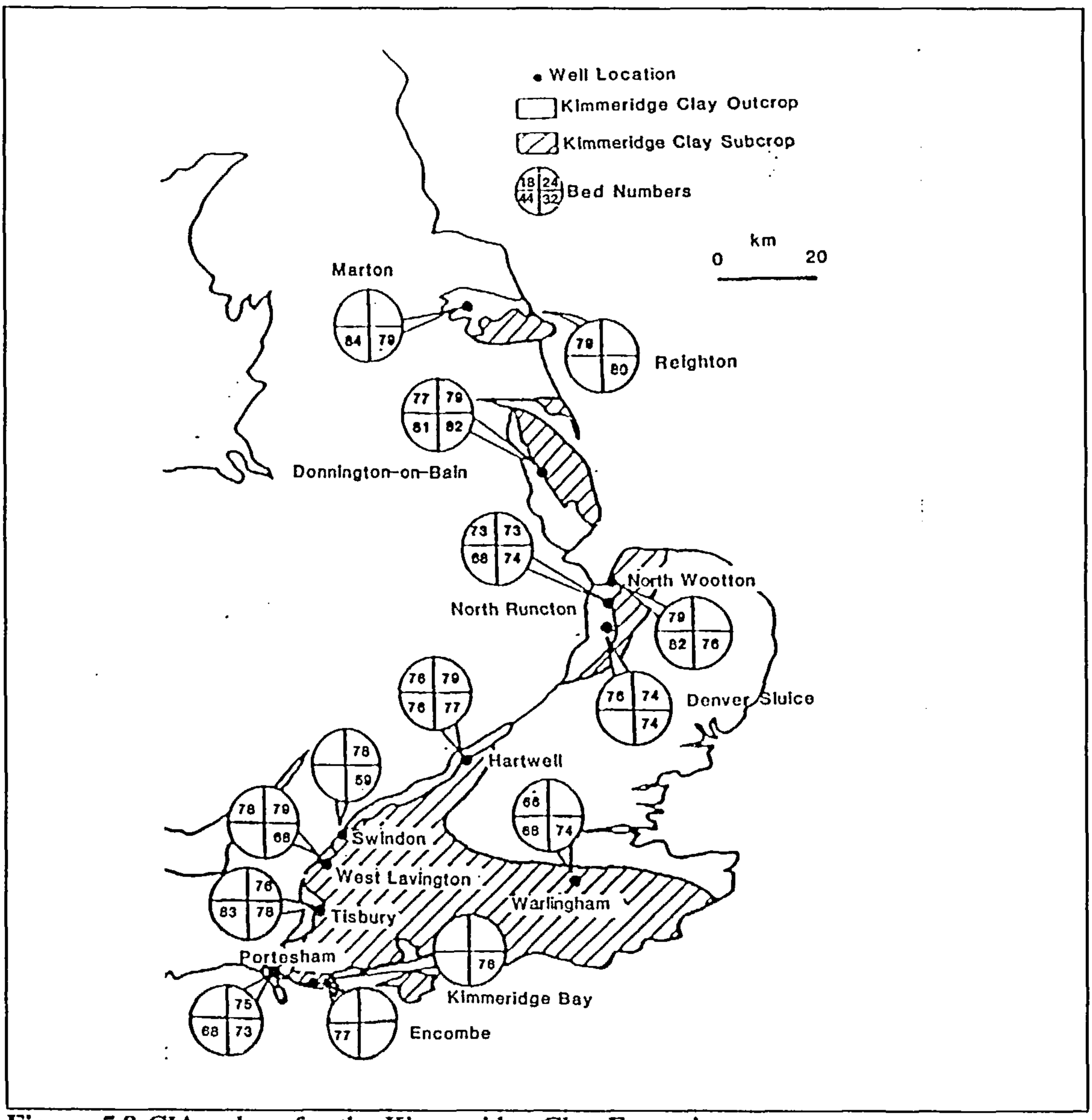

Figure 5.8 CIA values for the Kimmeridge Clay Formation.

5.2 Differentiable sedimentary component study

5.2.1 Differentiable sedimentary components

Further sedimentological information may be gained by following an approach modified from that of Argast and Donnelly (1986) who were interested in determining the original mineralogy of sedimentary rocks from their chemical compositions. By examination of bivariate variation diagrams these authors were able to determine the compositions of two or more "differentiable sedimentary components", variations in the proportions of which would explain the chemical variation observed in the suites investigated. A differentiable sedimentary component is defined as a mineral or group of minerals which is sorted independently of other components. Due to the differing hydrodynamic properties of the particles phyllosilicates often form a fine grained differentiable component, and quartz or quartz and feldspars a coarse grained differentiable component. This was inferred from the interpretation of the correlation structure in Chapter 4 where coarse sediment and fine sediment groupings of variables was observed for each formation.

This method of course relies on the bulk chemical composition of a sediment being unaltered by diagenesis or metamorphism. This was shown to be the case by Argast and Donnelly (1986) and is supported by the evidence of Hower et al (1976) which shows little bulk chemical change in a sedimentary sequence during burial diagenesis despite considerable mineralogical transformation. Only Ca was seen to decrease with a concomitant decrease in calcite.

The work published by Argast and Donnelly (1986) made use of bivariate plots such as K_2O against Al_2O_3, SiO_2 versus Al_2O_3, or other plots of the raw data. In such cases samples consisting solely of silicate detrital minerals tend to lie on straight lines joining the points representing the compositions of end member differential components. When more than two differentiable components were present for example if calcite were added to the coarse and

fine silicate components discussed already more complex patterns were observed, with samples occupying fields rather than lines on the plots.

For this work the Al_2O_3 normalised data were used as it was desired to infer conclusions about the detrital silicates only and it was therefore advantageous to remove the complicating effects due to variable dilution by carbonate minerals, TOC, or pyrite (ie the problem of closure once more). The data thus plotted could then be compared with the Al_2O_3 normalised compositions of the detrital minerals identified by XRD and the likely compositions of the differentiable components could be examined.

5.2.2 The Draupne Formation

Plots of SiO_2/Al_2O_3 versus K_2O/Al_2O_3, and to a lesser extent SiO_2/Al_2O_3 versus Na_2O/Al_2O_3 were found to be most useful here. Fig. 5.9 shows the SiO_2/Al_2O_3 versus K_2O/Al_2O_3 plot for the Draupne Formation. Marked are the locations of the minerals quartz, orthoclase, albite, kaolinite, and the end member illite and smectite of North Sea mixed-layer clays from Pearson and Small (1986). These minerals have been identified by XRD as the dominant detrital silicate phases in the Draupne Formation (Chapter 3). The correlation between the two variables is significant but is not so good as in the Heather Formation (Chapter 4). It can still be seen however that much of the variation in the SiO_2/Al_2O_3 and K_2O/Al_2O_3 ratios could be explained by the mixing of two differentiable sedimentary components; a fine grained component consisting of a mixture of kaolinite, end member illite, and end member smectite clays, and a coarser component comprised of quartz, orthoclase and albite silt. It can also be observed in Fig. 5.9 that very few points lie on the kaolinite side of the line joining the compositions of end member illite and smectite which represents the composition of mixed-layer clays. This means that the variation in the SiO_2/Al_2O_3 and K_2O/Al_2O_3 ratios of the Draupne Formation may be explained by the mixing of a fine grained component consisting solely of illite and smectite with a quartz and feldspar bearing coarse grained component. This does not of course prove that kaolinite is not present in this formation but that it is not

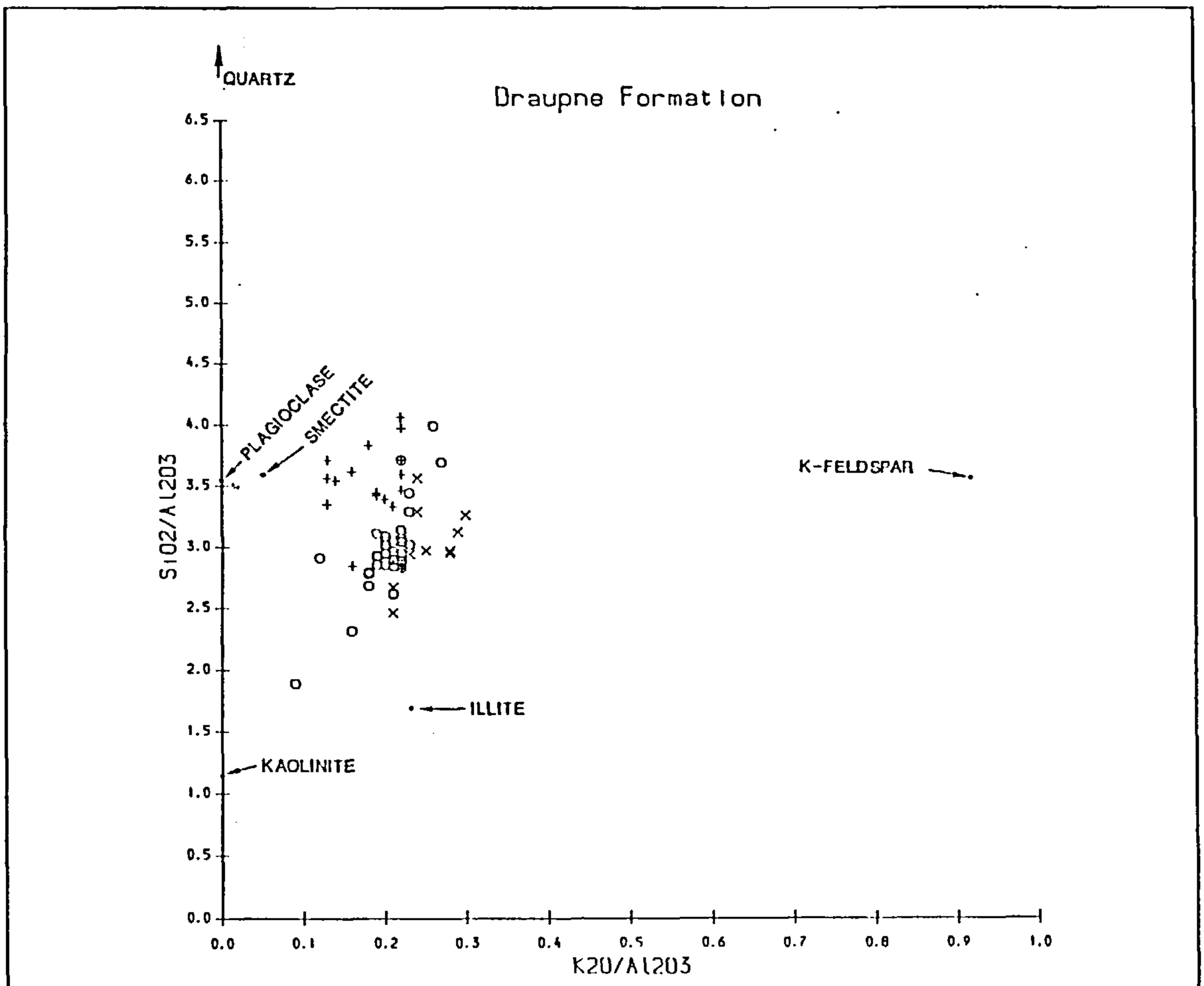

Figure 5.9 SiO_2/Al_2O_3 versus K_2O/Al_2O_3 Draupne Formation. Western wells denoted by vertical crosses, Bergen High wells by open circles, Horda Platform wells by diagonal crosses.

required by the chemical composition. This contrasts with the observations of the Heather Formation and to a lesser extent with the Kimmeridge Clay Formation described below.

The increase in grain size from wells on the Horda Platform to those in the Viking Graben and Tampen Spur, previously interpreted from the SiO_2/Al_2O_3 ratios and the TiO_2/Al_2O_3 ratios can also be observed in Fig. 5.9 as those samples from the western part of the area studied lie relatively closer to the coarse grained differentiable component than do those from intermediate and easterly positions.

A further observation of note is that the position of the coarse grained differentiable component required to account for the patterns of variation seen moves from being relatively orthoclase rich in the wells on the Horda Platform to being depleted in wells from the Viking Graben and Tampen Spur with wells in intermediate positions having intermediate compositions. Such a trend is not observed in the plot of SiO_2/Al_2O_3 versus Na_2O/Al_2O_3 (Fig 5.10) suggesting that the coarse grained differentiable component consisted of a small but relatively constant proportion of albite, but that the proportion of orthoclase decreased towards the centre of the basin whilst the relative quartz content increased. This is consistent with uplift and reworking of older sediments providing a local sediment source for the western parts of the Draupne Formation.

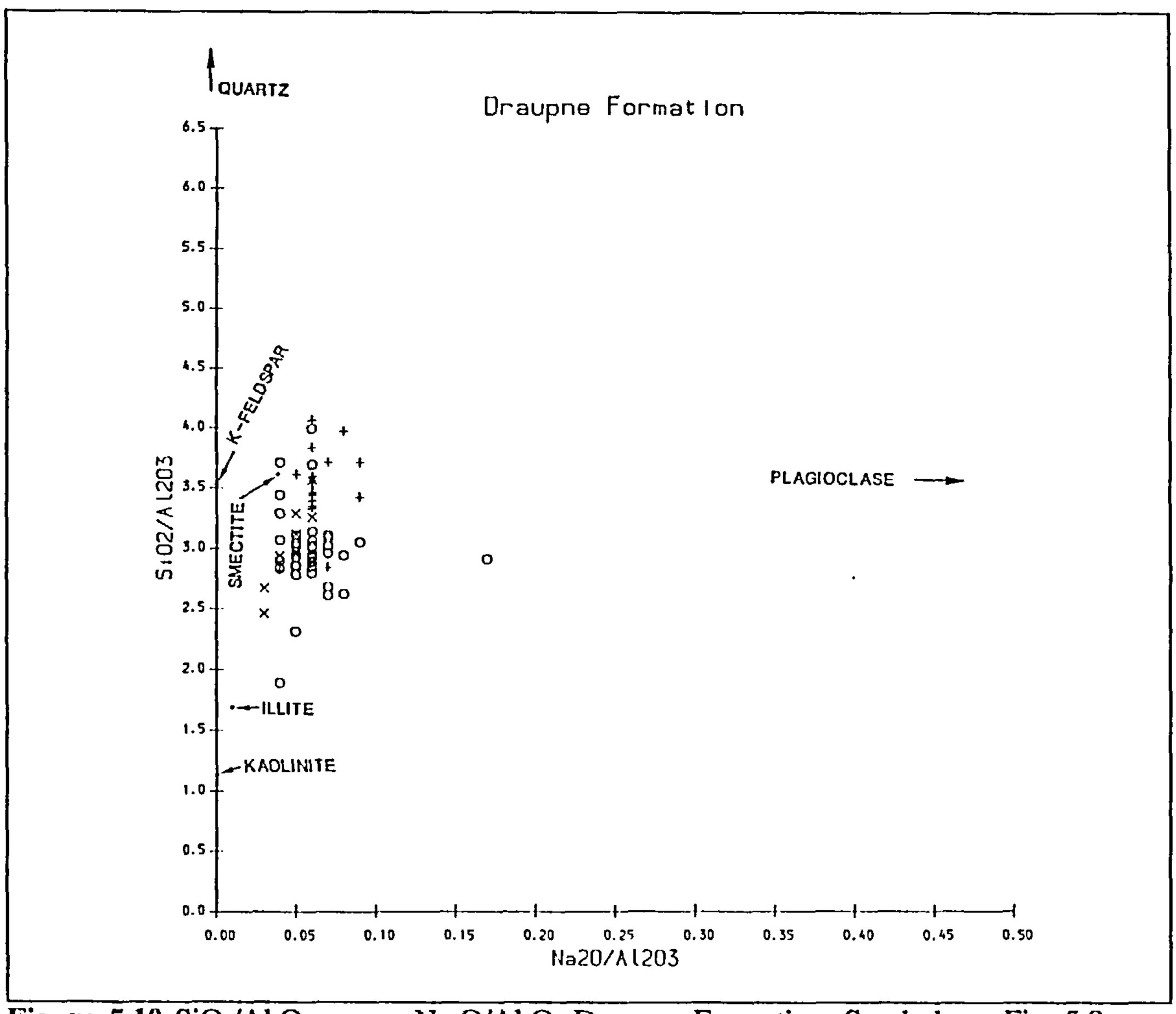

Figure 5.10 SiO_2/Al_2O_3 versus Na_2O/Al_2O_3 Draupne Formation. Symbols as Fig. 5.9.

5.2.3 The Heather Formation

Plots of SiO_2/Al_2O_3 versus K_2O/Al_2O_3 and Na_2O/Al_2O_3 for the Heather Formation are shown in Figs. 5.11 and 5.12 respectively. There is noticeably less scatter than in the Draupne Formation which is reflected in the greater magnitudes of the correlation coefficients (Chapter 4), but the range of values is considerably greater, supporting the suggestion of a wider range in grain sizes for this formation made above. Earlier interpretations of grain size trends are also supported by the data in Figs. 5.11 and 5.12 which show that the Horda Platform is the site of the coarsest Heather Formation samples with finer sediment being deposited westwards.

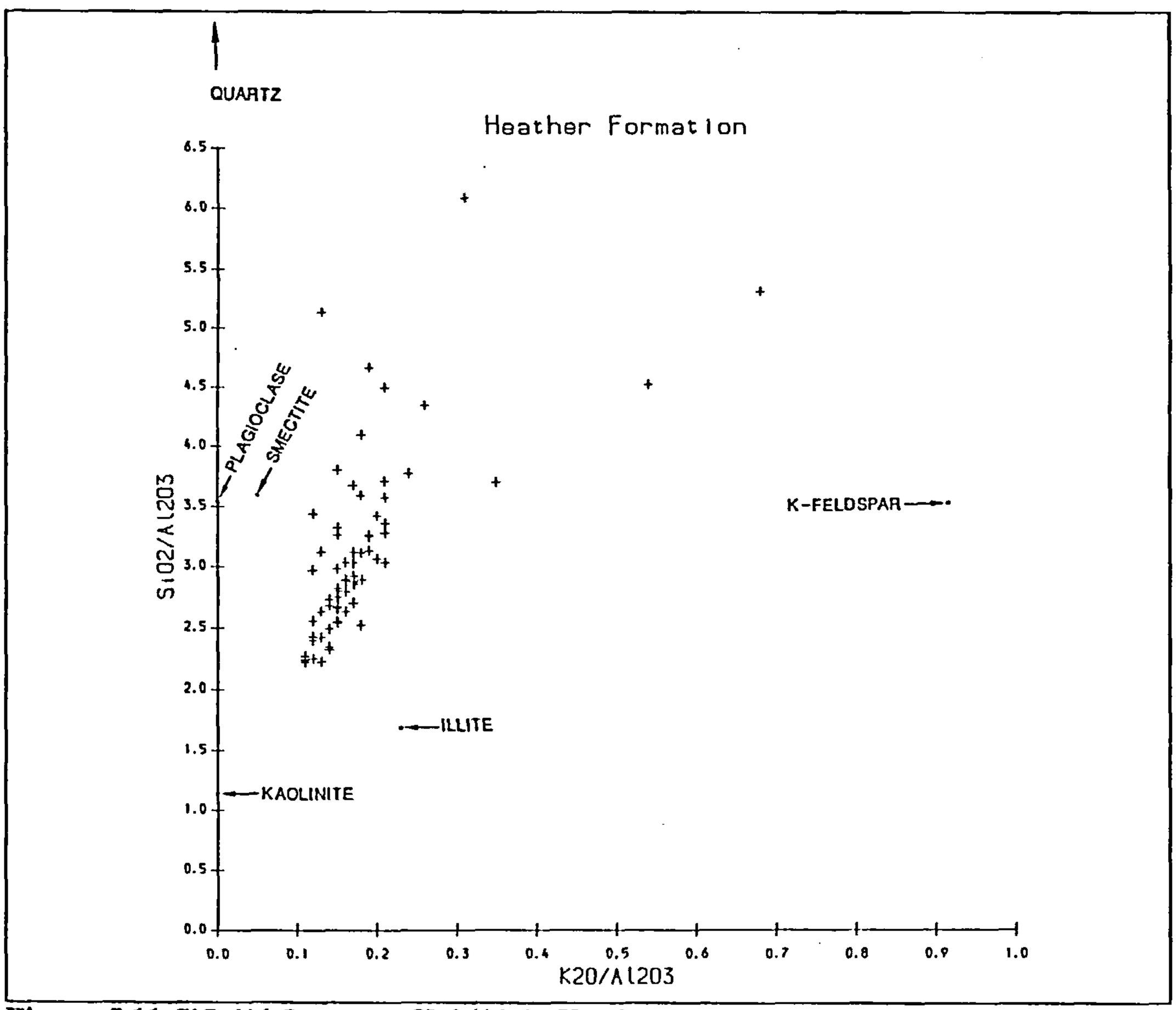

Figure 5.11 SiO_2/Al_2O_3 versus K_2O/Al_2O_3 Heather Formation.

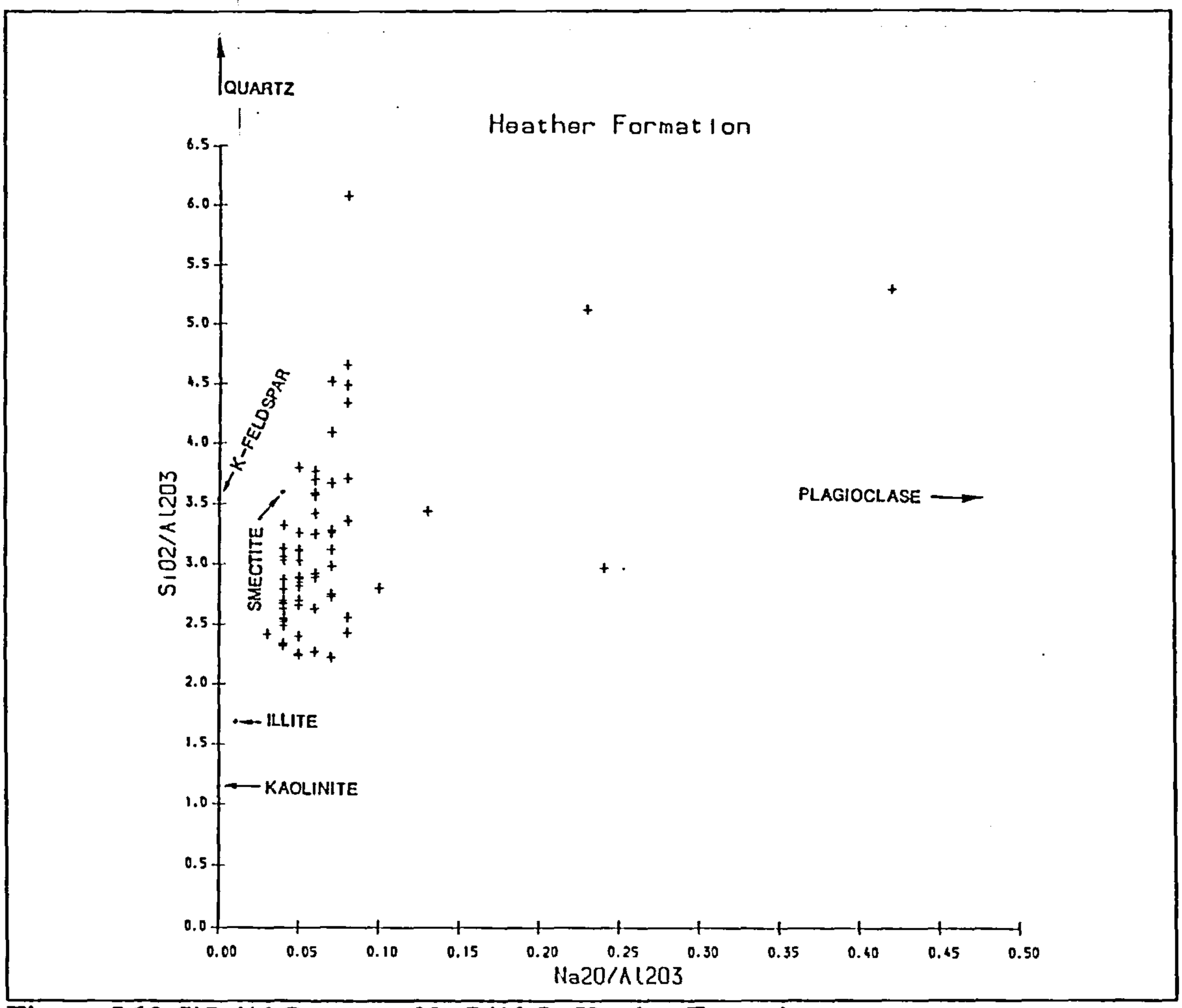

Figure 5.12 SiO_2/Al_2O_3 versus Na_2O/Al_2O_3 Heather Formation.

Contrasting with the Draupne Formation there is no great shift in the composition of either of the differentiable components of the Heather Formation with the samples from most wells tending to lie along a single mixing line. As many of the Heather Formation samples however lie on the kaolinite side of the line joining the locations of smectite and illite the clay differentiable component of the Heather Formation must include some kaolinite. Indeed the mixing lines for the Heather Formation appear to pass directly through the location of kaolinite removing the need for the presence of smectite or illite. From XRD evidence however it is known that some illite and mixed-layer clays are found in the Heather Formation, and some kaolinite is found in the Draupne though it is not required by the geochemical mixing model.

5.2.4 The Kimmeridge Clay Formation

The Kimmeridge Clay Formation is in many ways intermediate between the Draupne and Heather Formations. The plots of SiO_2/Al_2O_3 versus K_2O/Al_2O_3 and Na_2O/Al_2O_3 are shown in Figs. 5.13 and 5.14 respectively. As with the Draupne few of the Kimmeridge Clay samples lie to the kaolinite side of the illite smectite composition line so that the presence of kaolinite is not necessary. The SiO_2/Al_2O_3 and K_2O/Al_2O_3 mixing line does pass close to the composition of kaolinite however, as in the Heather but the mixing line for SiO_2/Al_2O_3 and Na_2O/Al_2O_3 does not. The grain size variation is less than that of the Heather Formation and similar to the Draupne.

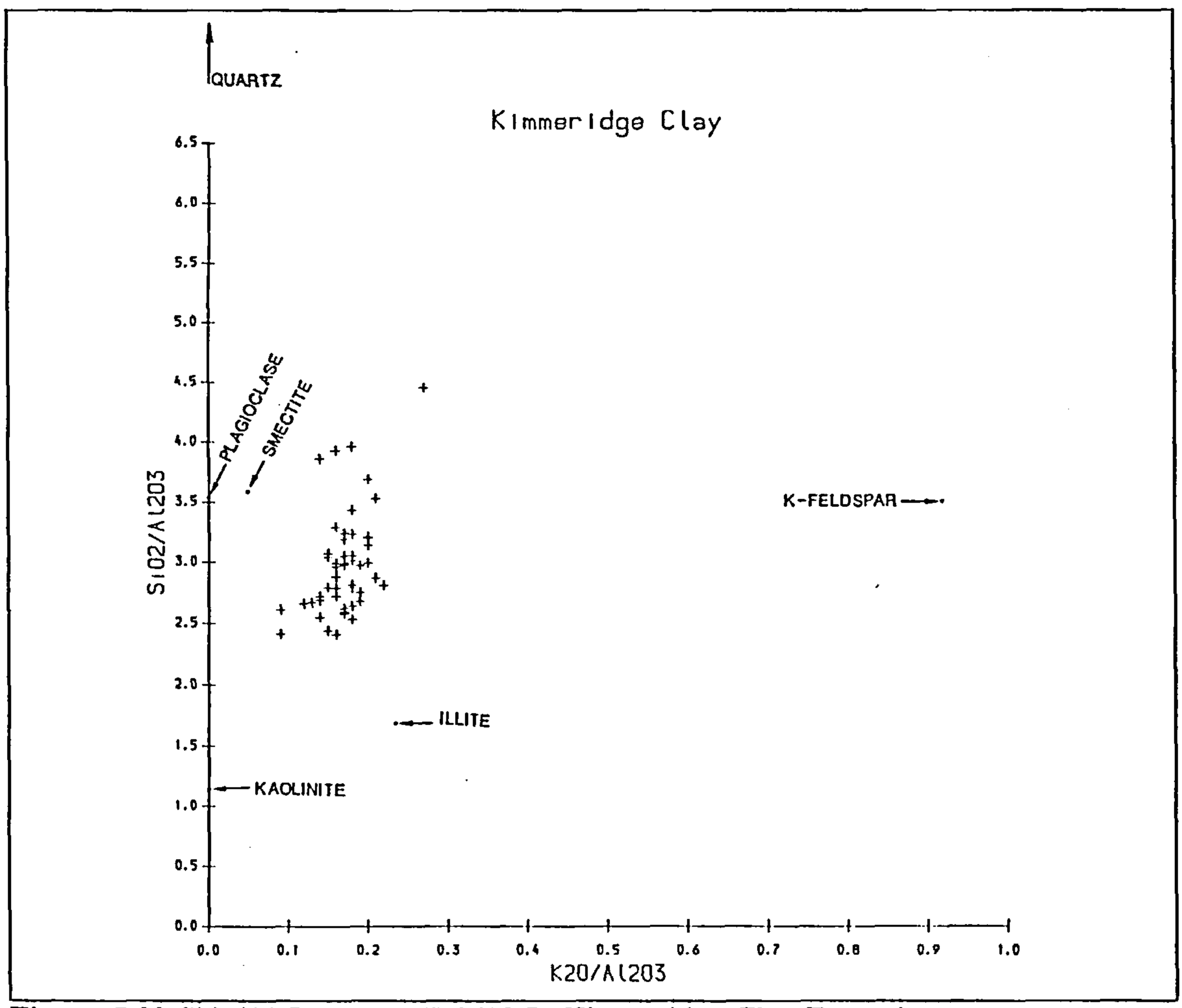

Figure 5.13 SiO_2/Al_2O_3 versus K_2O/Al_2O_3 Kimmeridge Clay Formation.

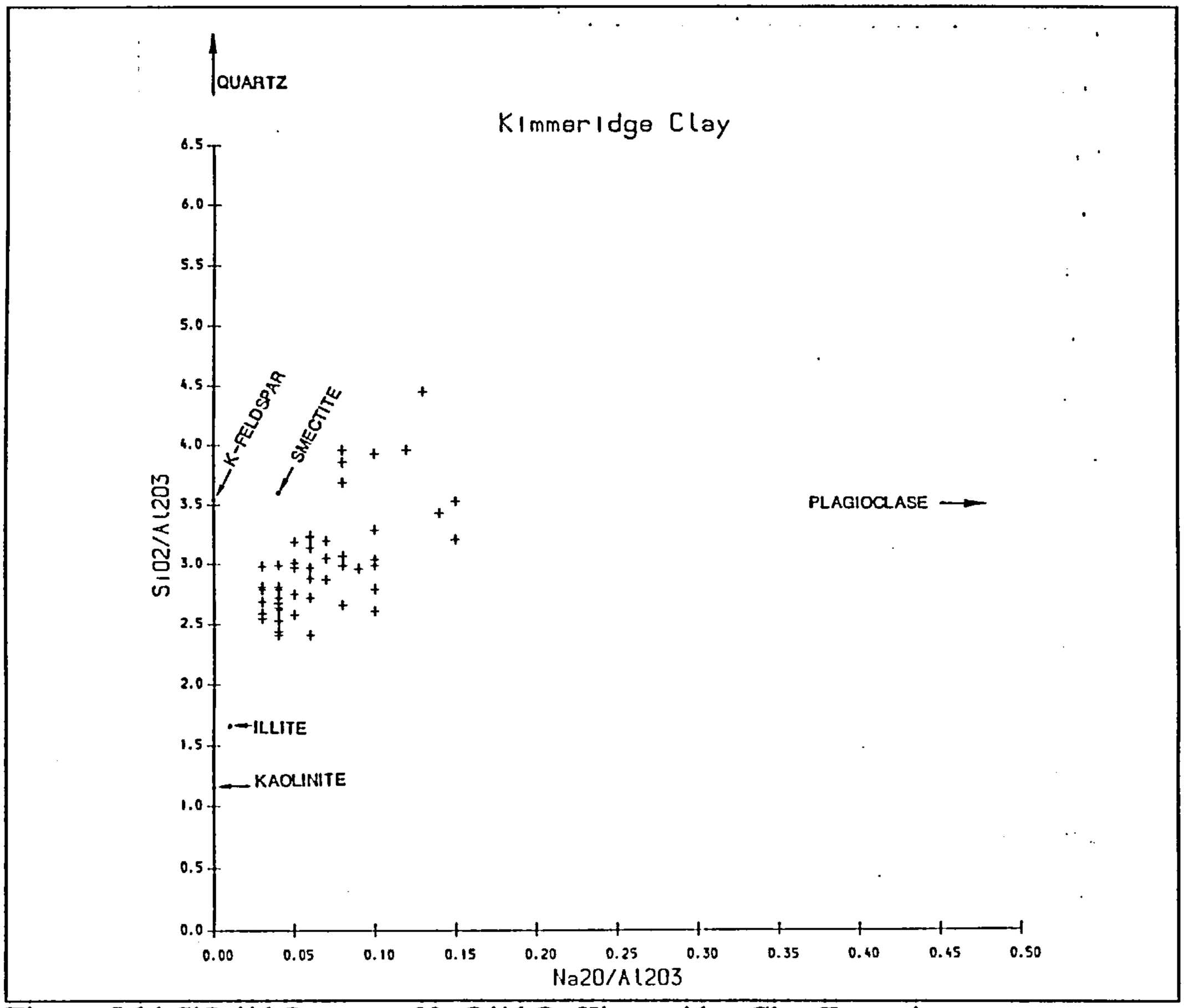

Figure 5.14 SiO_2/Al_2O_3 versus Na_2O/Al_2O_3 Kimmeridge Clay Formation.

5.3 Diagenetic variation

5.3.1 Diagenetic reaction zones

On deposition modern organic rich muds comprise an unstable mineralogical assemblage rich in both reduced compounds (organic matter) and oxidised phases (soil oxides). Their mineralogy also differs from their lithified counterparts-mudstones as the processes of diagenesis act to destroy the original unstable components, and precipitate new stable phases (Curtis 1977, 1978, 1980, 1983a and b, 1987). These processes involving organic matter and Fe and Mn oxides and causing the precipitation of pyrite, and carbonate and phosphate

have a profound effect on the trace element content of a sediment as it has been shown in Chapter 4 that these are important trace element hosts.

Based on studies of modern sediments, diagenesis is believed to occur in a series of depth related, generally bacterially mediated redox reactions involving the oxidation of the deposited organic matter and the reduction of various inorganic species (Claypool and Kaplan, 1974; Bender et al, 1977; Froelich et al, 1979). A sequence of diagenetic zones may be constructed each of which is characterised by single dominant redox reaction, the order of occurrence of these reaction zones being governed by the decreasing magnitude of the Gibbs free energy of their characteristic reactions. These diagenetic zones have also been recognised in ancient sediments (Irwin et al, 1977; Maynard, 1982; Curtis et al, 1986), and Curtis (1987) has summarised the zonal sequence occurring, and the likely effects on authigenic mineral precipitation (Fig. 5.15). In general the diagenetic reactions acidify the pore water and promote carbonate dissolution. Only iron reduction (FeR) is capable of reducing the pore water acidity to any extent and causing carbonate precipitation. Irwin et al (1977) have shown that the carbonates precipitated in the various diagenetic zones may be distinguished by their C isotope compositions.

In sediments deposited below an oxic water column the first zone is that of aerobic oxidation (Ox). This is usually very thin (only a few mm) due to the limited ability of diffusion to supply the oxygen required for the intense oxidative degradation of organic matter which occurs, although biorturbation may increase this ability somewhat. Due to the proximity of the sediment surface conditions are effectively open and most solubilised species will be lost by diffusion to sea water. When the oxygen supply becomes insufficient to meet the demands of aerobic oxidation, or in sediments deposited beneath an anoxic water column, oxygen is absent from the interstitial waters and in marine conditions where sulphate is abundant the bacterial reduction of sulphate to sulphide becomes the dominant reaction oxidising organic matter (SR). Carbonates may tend to either dissolve or precipitate (but precipitated carbonates will be iron poor) depending on the relative rates of the FeR and SR reactions, and pyrite or

Diagenetic zone	Probable mineral precipitates
Zone Ox Oxidation by molecular oxygen	Organic matter is degraded by respirative bacteria and benthic fauna. The lower limit of the zone is probably determined by the water circulating activity of burrowers (usually a few cm). This mixing will prevent high solute concentrations building up hence significant mineral authigenesis is unlikely. Fe(III) should be the stable valence state and reduction will not occur except in transient (?) *microenvironments.*
Zone SR Oxidation by sulphate and Fe(III)	The following equation represents the sum of SR and FeR when the amount of iron reduced is exactly balanced by sulphide produced. $15CH_2O + 2Fe_2O_3 + 8SO_4^{2-}$ $= 4FeS_2 + 7H_2O + 15HCO_3^- + OH^-$ Pyrite precipitation is thus accompanied by a very large increase in porewater bicarbonate activity without lowering pH. Fe-poor carbonates (iron sulphide is highly insoluble) are very likely to form alongside pyrite (calcite, dolomite). Phosphate released by organic degradation should also precipitate (*francolite*; a complex calcium phosphate mineral). Manganese reduction (MnR) will also occur in the SR Zone with Mn incorporated into both carbonates and sulphides.
Zone Me Methanogenesis and oxidation by Fe(III)	The combination of microbial methanogenesis with Fe(III) reduction is extremely conducive to carbonate precipitation; but this time of iron-rich carbonates (siderite, ankerite, ferroan dolomite). $7CH_2O + 2Fe_2O_3 = 3CH_4 + 4FeCO_3 + H_2O$ In this combination of Me and FeR, the two contributions are just sufficient to precipitate HCO_3^- and Fe^{2+} quantitatively. An excess of iron reduction would lead to alkaline pore waters and, perhaps, precipitation of Fe(II)-silicates such as berthierine. Conversely, depletion of the iron supply would create less alkaline (even acid) environments wherein phosphate minerals stabilized relative to carbonates

Figure 5.15 Early diagenetic reaction zones (Curtis, 1987).

its precursors will also be precipitated (see below). The depth of the base of the SR zone is controlled by the ability of diffusion to supply sulphate and is usually of the order of a few metres.

Succeeding the sulphate reduction zone is the fermentation or methanogenesis zone (Me). This requires no diffusional supply of species from the water column as do the Ox and SR reactions and can continue to considerable depth (about 1km, or 75°C Gautier and Claypool, 1984), probably being limited by the temperature resistance of the bacteria themselves. In this zone Fe carbonates are likely to precipitate as long as significant Fe reduction is continuing.

5.3.2 Environmental parameters

Whilst the mineralogy and hence the major element geochemistry are to a large extent dependent on the physical properties of a sediment such as the grain size the trace element composition is particularly sensitive to the depositional environment (Krecji-Graf, 1975), although the physical properties may remain important for some elements. The interpretation of ancient depositional and diagenetic environments is of great value, and is of importance here because the influence that differing environments may have had on the geochemistry must be evaluated prior to examining the relationship between the geochemistry and the organic maturity. A number of parameters have been proposed that may be useful indices of the depositional environment; those considered here are discussed below.

The V/Cr ratio has been employed as an indicator of palaeo-oxygenation in a number of previous studies (Krecji-Graf, 1975; Ernst, 1970; Bjorlykke, 1974; Dill, 1986; and Dill et al, 1988). Cr is usually associated with the clastic fraction of a sediment where it is either adsorbed on clays, substituting for Al within clays, or present as chromite (this has been demonstrated for this study in Chapter 4). V by comparison is usually bound to organic matter (eg in porphyrins) and as such is concentrated in reducing conditions. Values of V/Cr above about 2 are considered to represent anoxic depositional conditions (Krecji-Graf, 1975) whereas values much below 2 result from deposition in oxygenated waters.

The Ni/Co ratio has also been used as a redox index by Dypvik (1984) and Dill (1986) with high values again representing deposition in reducing conditions. Ni and Co are found to some extent in pyrite in sediments (demonstrated for this study in Chapter 4) and pyrite formed in diagenetic environments usually has Ni/Co > 1.

It has been noted for some time that the U/Th ratio may be used as a redox index (Adams and Weaver, 1958; Rogers and Adams, 1969) with the U/Th ratio being higher in organic rich shales. This comes about because Th is relatively immobile in the low temperature

surface environment and so is concentrated in resistate minerals such as zircon and monazite. In sediments such as shales it is usually found therefore in the detrital fraction (Chapter 4) associated with heavy minerals or clays. U by contrast is soluble in its 6^+ valence state and is usually lost in solution during weathering. In valence state 4^+ it is insoluble and is concentrated relative to Th in the reducing conditions favouring the preservation of large amounts of organic matter, raising the U/Th ratio. The concentration mechanism is not entirely clear but probably involves adsorption and reduction by organic matter.

Myers and Wignall (1987) and Wignall and Myers (1988) have suggested "authigenic U" as an index of the palaeo-redox conditions in the sediment and have compared it to palaeo-ecological data for the Jurassic mudstones of Dorset and Yorkshire. Adams and Weaver (1958) found the average U/Th ratio of normal shales to be 0.26 and in the calculation of authigenic U this is assumed to represent the ratio of U to Th in the detrital sediment. Any increase in this value is interpreted as representing the addition of U to the sediment by concentration by organic matter. This is consistent with the data and interpretations of Chapters 3 and 4 of this study that the Th content is relatively constant and has a detrital origin. For the calculation of authigenic U a U/Th ratio of 0.33 is suggested by Myers and Wignall (1987) to ensure that the calculated U is significant. The calculation is then trivial: (authigenic U)=(total U)-(detrital U) where (detrital U)=Th/3.

These authors warn that small authigenic U contents of about 2ppm may be a result of U in carbonates but this is unlikely in the low carbonate samples from the North Sea. In the much more carbonate rich Kimmeridge Clay this may be significant however. Sediments deposited under anoxic conditions have appreciable authigenic U, the maximum recorded being 10ppm in a coccolith limestone of the Kimmeridge Clay, and 8.2ppm in the Jet Rock. The correlation between authigenic U and organic matter content is poor in the Kimmeridge Clay however.

In addition to the inorganic geochemical parameters considered above the pristane/phytane ratio is an organic geochemical palaeo-environmental indicator (Didyk et al, 1978) suggested from studies on ancient and modern sediments. Both pristane (pr) and phytane (ph) are derivatives of the phytol side chain of chlorophyll. It is believed that degradation of the original biochemical molecule in anoxic reducing conditions favours production of the C_{20} skeleton (ph) but that in oxidative conditions pristane (C_{19}) is favoured. As a result sediments deposited in anoxic conditions have a lower pr/ph than those deposited under oxic conditions. It is thought that values <1 indicate anoxic deposition below an anoxic water column, that an alternating oxic/anoxic interface results in a value of about 1, and that wholly oxic conditions produce a pr/ph ratio >1. Didyk et al (1978) do introduce a note of caution however as the ratio will tend to increase with increasing maturity. Pr/ph data were available in this study for the Draupne and Heather Formations only.

5.3.3 The Draupne Formation

Median values by well of the environmental parameters discussed above (V/Cr, Ni/Co, authigenic U, and Pr/Ph) are shown in Figs. 5.16-5.19 for the Draupne Formation. These all clearly show the increase in the reducing nature of the depositional environment from the eastern Horda Platform where oxygenation was probably normal (only in the south eastern Horda Platform are V/Cr values of <2 observed) to the Viking Graben and surroundings where conditions were strongly reducing (V/Cr ratios >>2) and probably euxinic (see also below). This is consistent with the conclusions of previous studies on the depositional environments of the Draupne Formation which have been based mainly on organic geochemistry (eg Thomas et al, 1985), and the correlation between various organic geochemical parameters with some of the inorganic environmental indices has been noted by Telnaes et al (1990).

5.3.4 The Heather Formation

During Heather Formation deposition oxygen levels is the water column were nearer normal than those found during the subsequent deposition of the Draupne Formation. This is suggested by the generally lower values of the inorganic redox parameters and the higher pr/ph ratios (Figs 5.16-5.19). Most of the parameters also show a trend of increasing anoxicity towards the west with the Viking Graben again having the most reducing conditions. The V/Cr ratios are much lower than in the Draupne Formation with a median value exceeding 2 being found in one well only. This would suggest that anoxic and euxinic conditions were restricted to parts of the Viking Graben that and even here that they were the exception rather than the rule.

Vertical variation of these environmental parameters is also apparent within single wells. Clearly visible is the much more reducing depositional environment of the Draupne Formation of the Viking Graben, but also noted is the occurrence of anoxic conditions at the base of the Heather Formation in this area (Thomas et al, 1985: Telnaes et al, 1990).

5.3.5 The Kimmeridge Clay Formation

The distribution of the environmental parameters for the Kimmeridge Clay Formation is shown in Figs 5.20-5.22. In general they do not indicate conditions as reducing as the Draupne Formation. V/Cr ratios are consistently below 2, only the organic rich bed 32 having higher values (up to 8.60 at Marton in the Cleveland Basin). Ni/Co ratios are similar in value to those of the Heather Formation, again with the exception of bed 32 whose median is higher than that of most Heather Formation wells. Similarly authigenic U parameter suggests conditions similar to those of the Heather Formation.

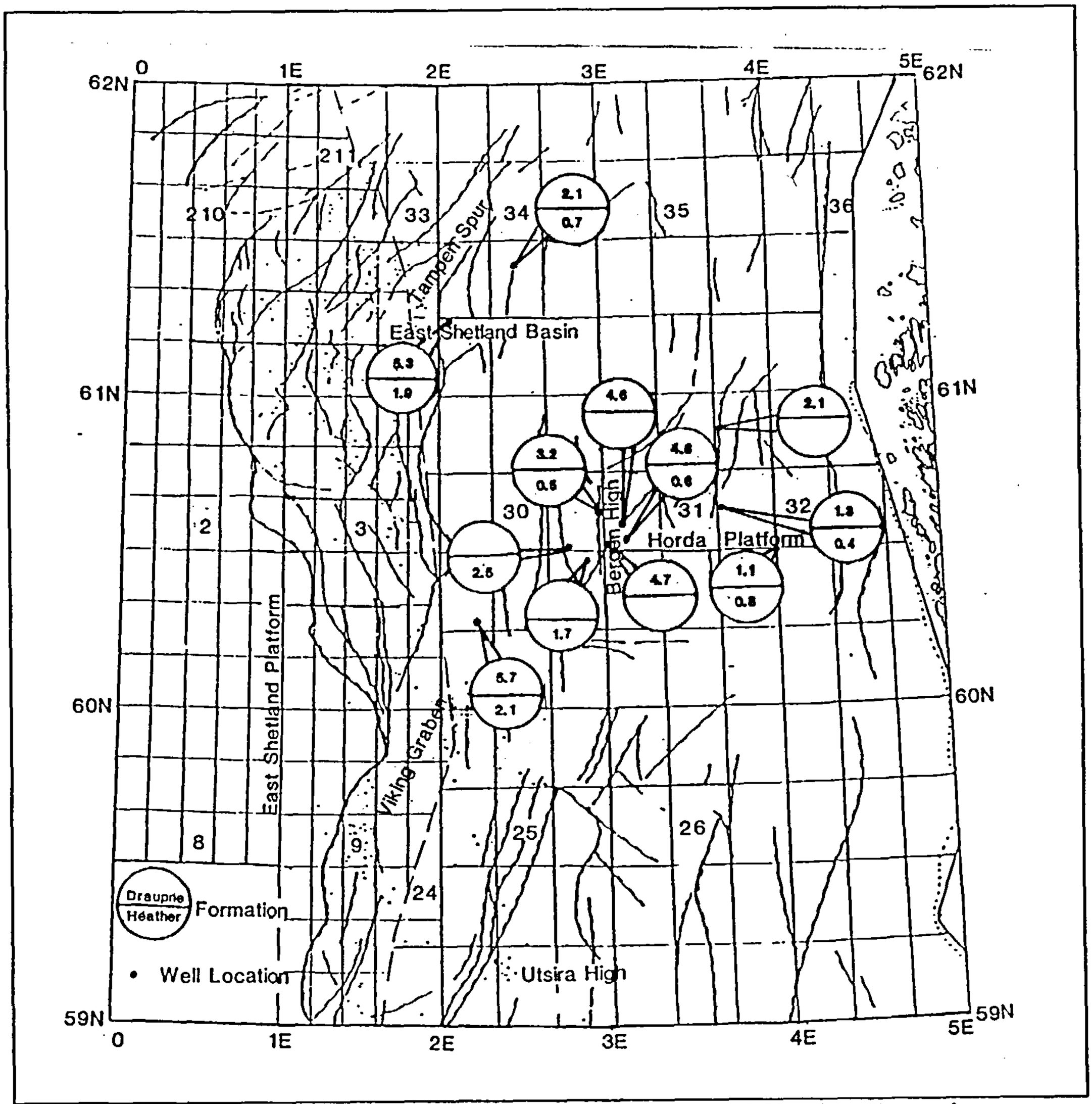

Figure 5.16 Median V/Cr ratios by well for the Draupne and Heather Formations.

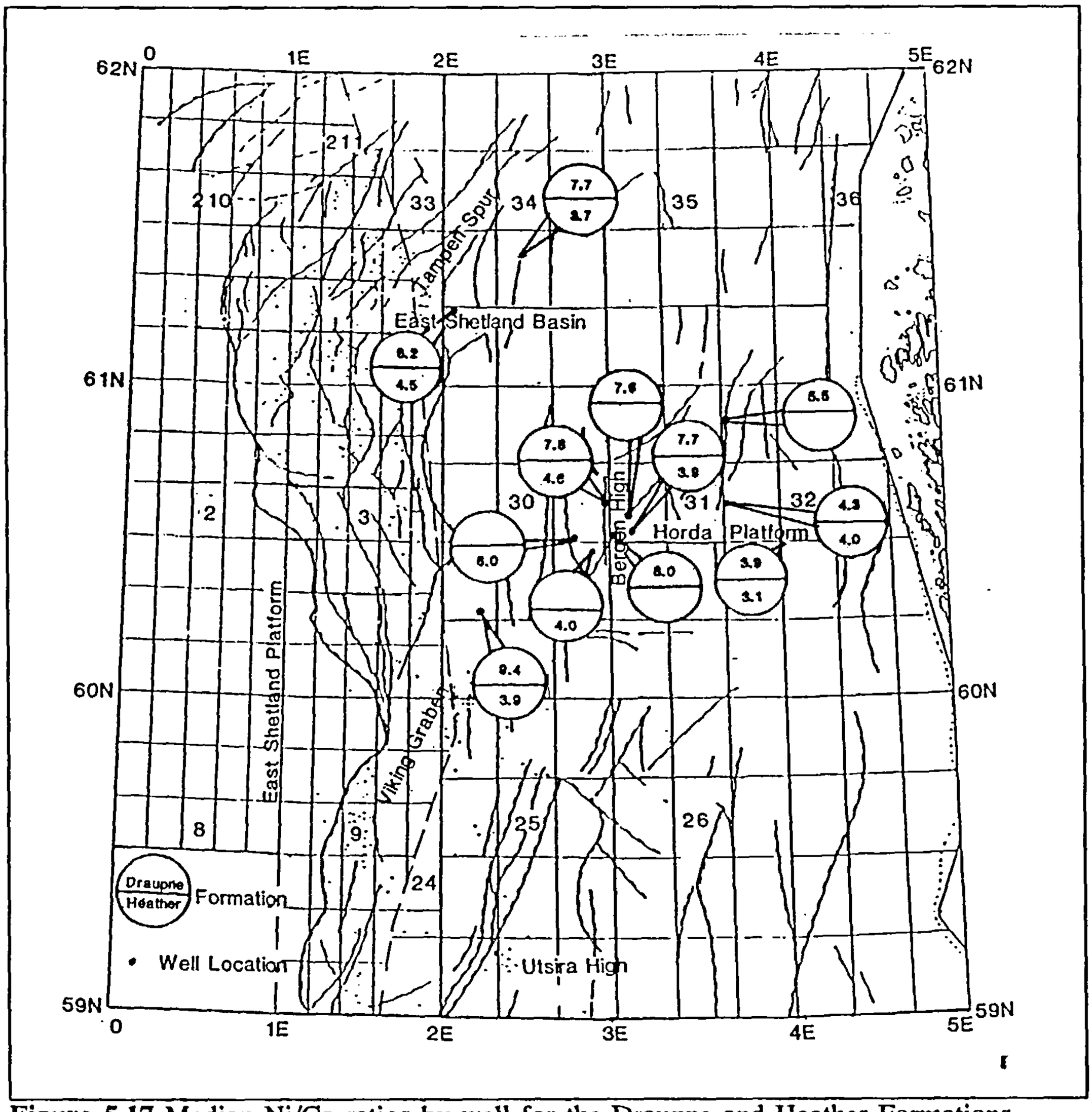

Figure 5.17 Median Ni/Co ratios by well for the Draupne and Heather Formations.

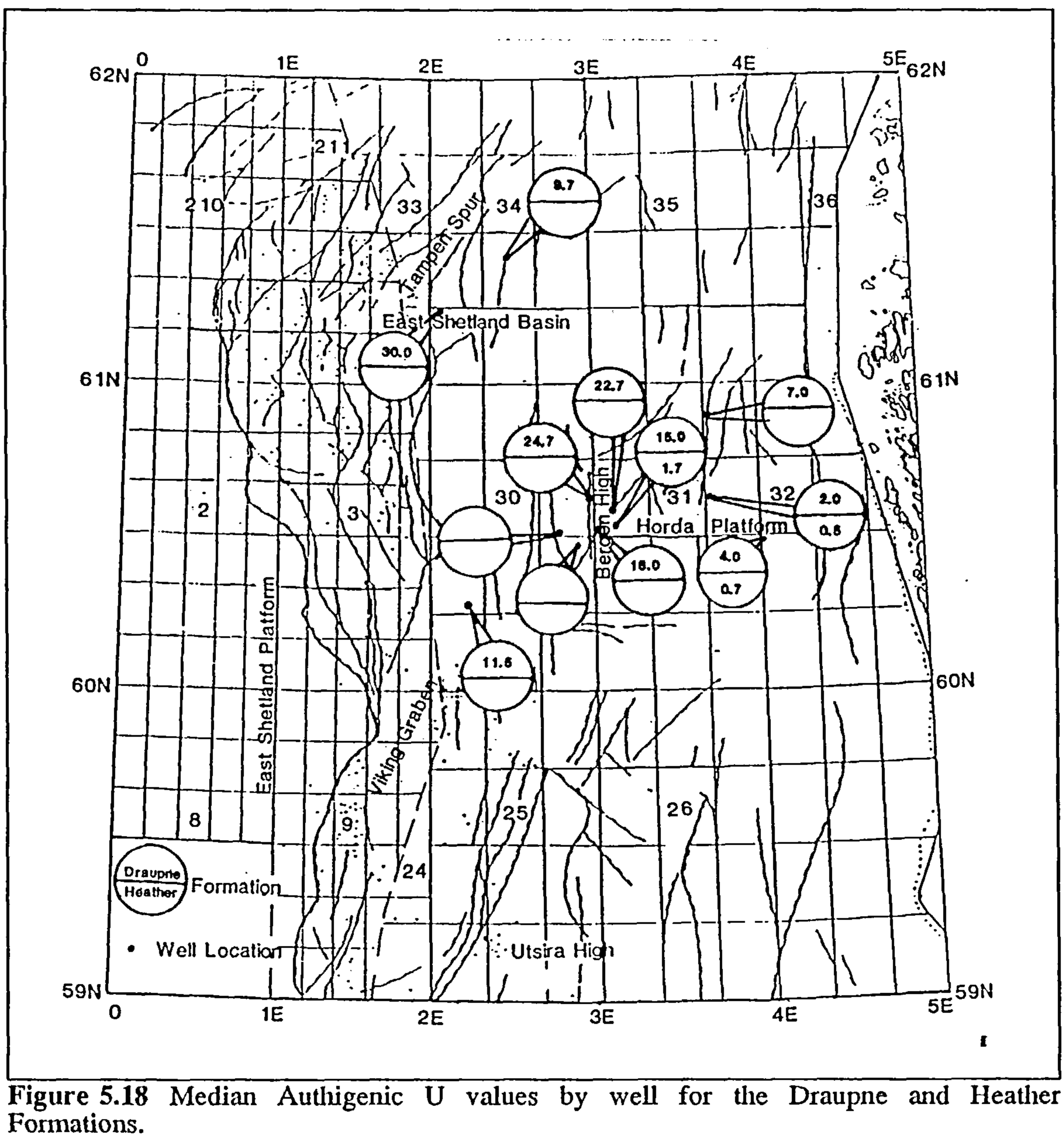

Figure 5.18 Median Authigenic U values by well for the Draupne and Heather Formations.

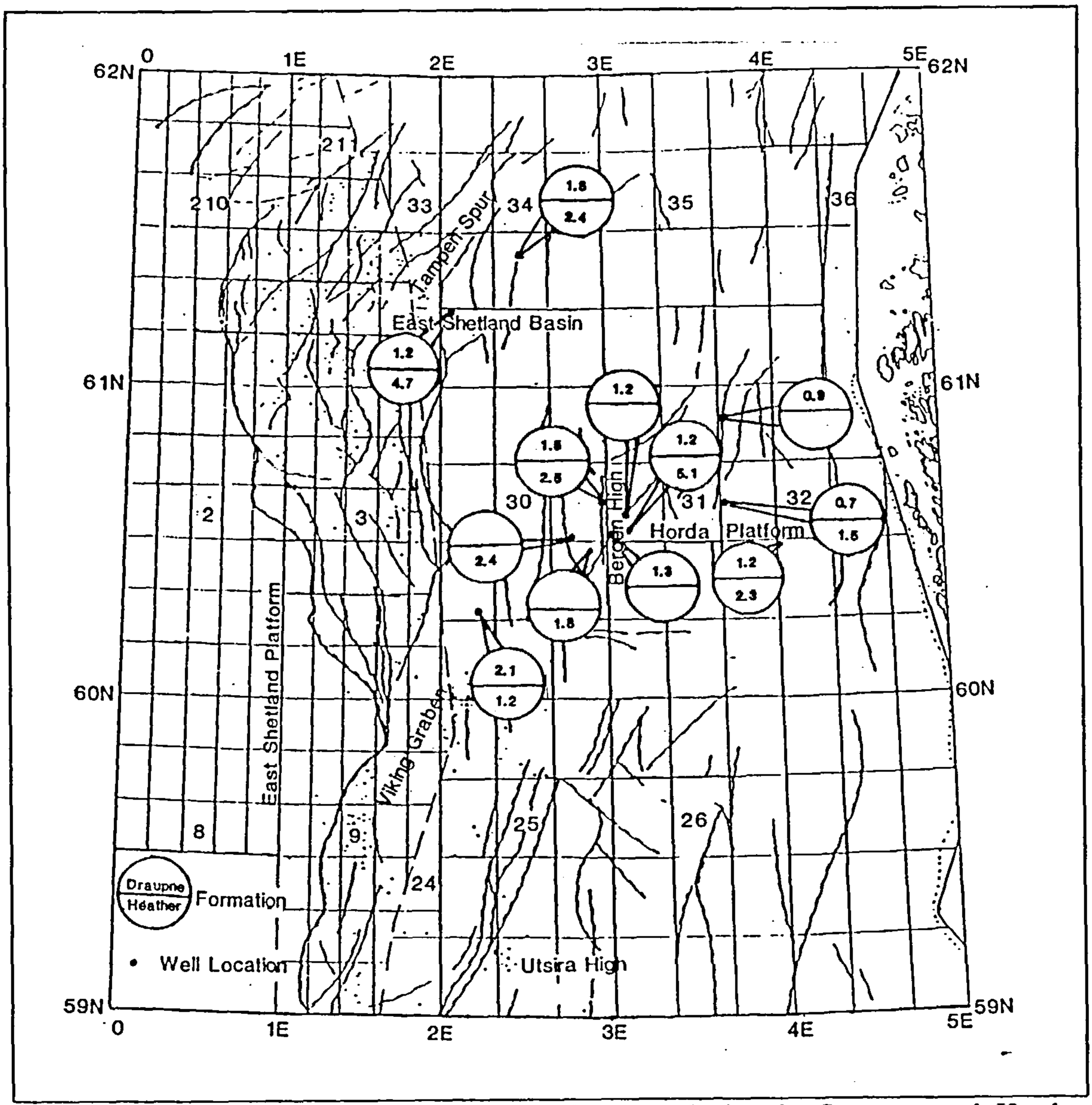

Figure 5.19 Median values of the Pr/Ph ratio by well for the Draupne and Heather Formations.

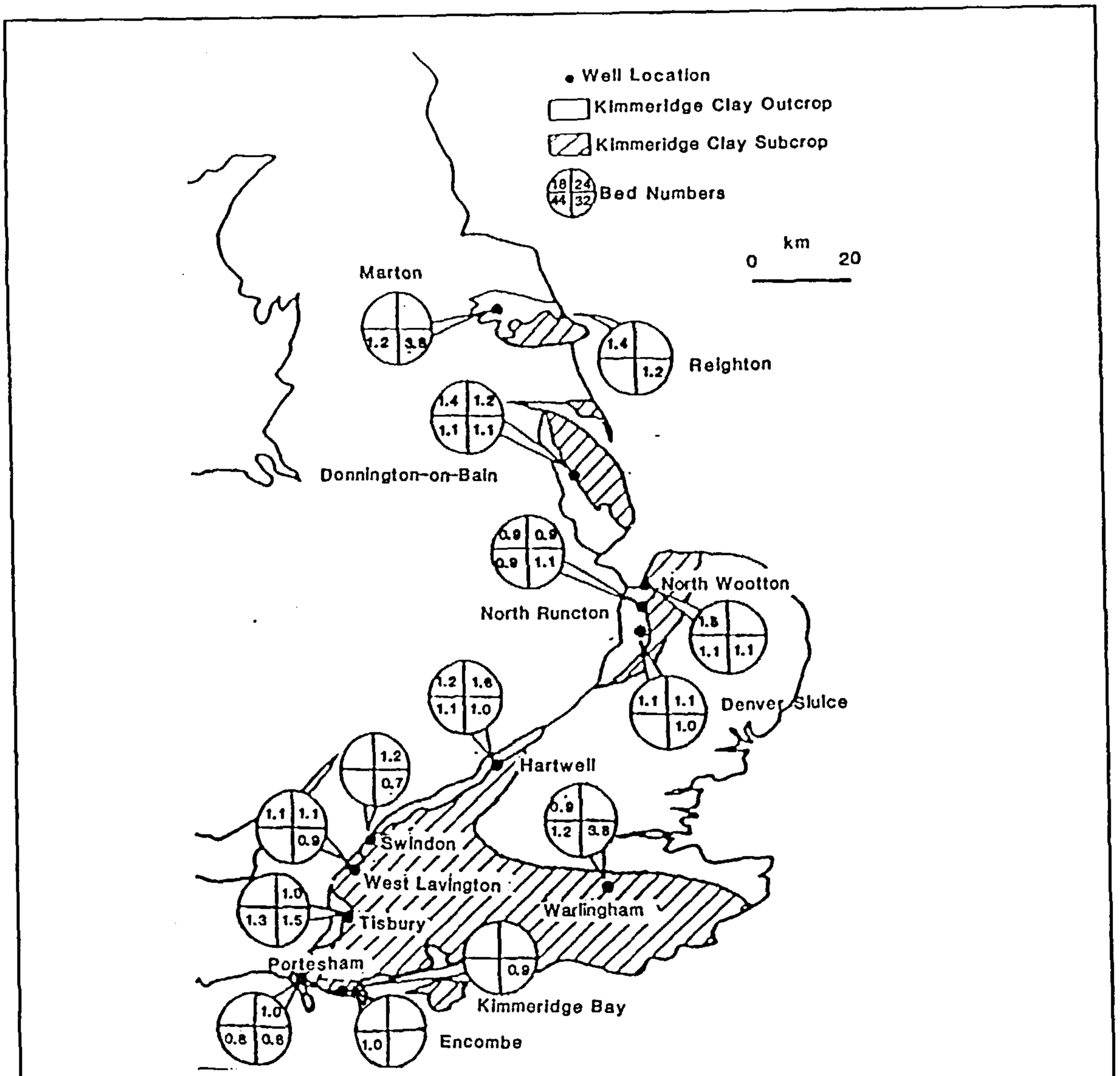

Figure 5.20 V/Cr ratios Kimmeridge Clay Formation.

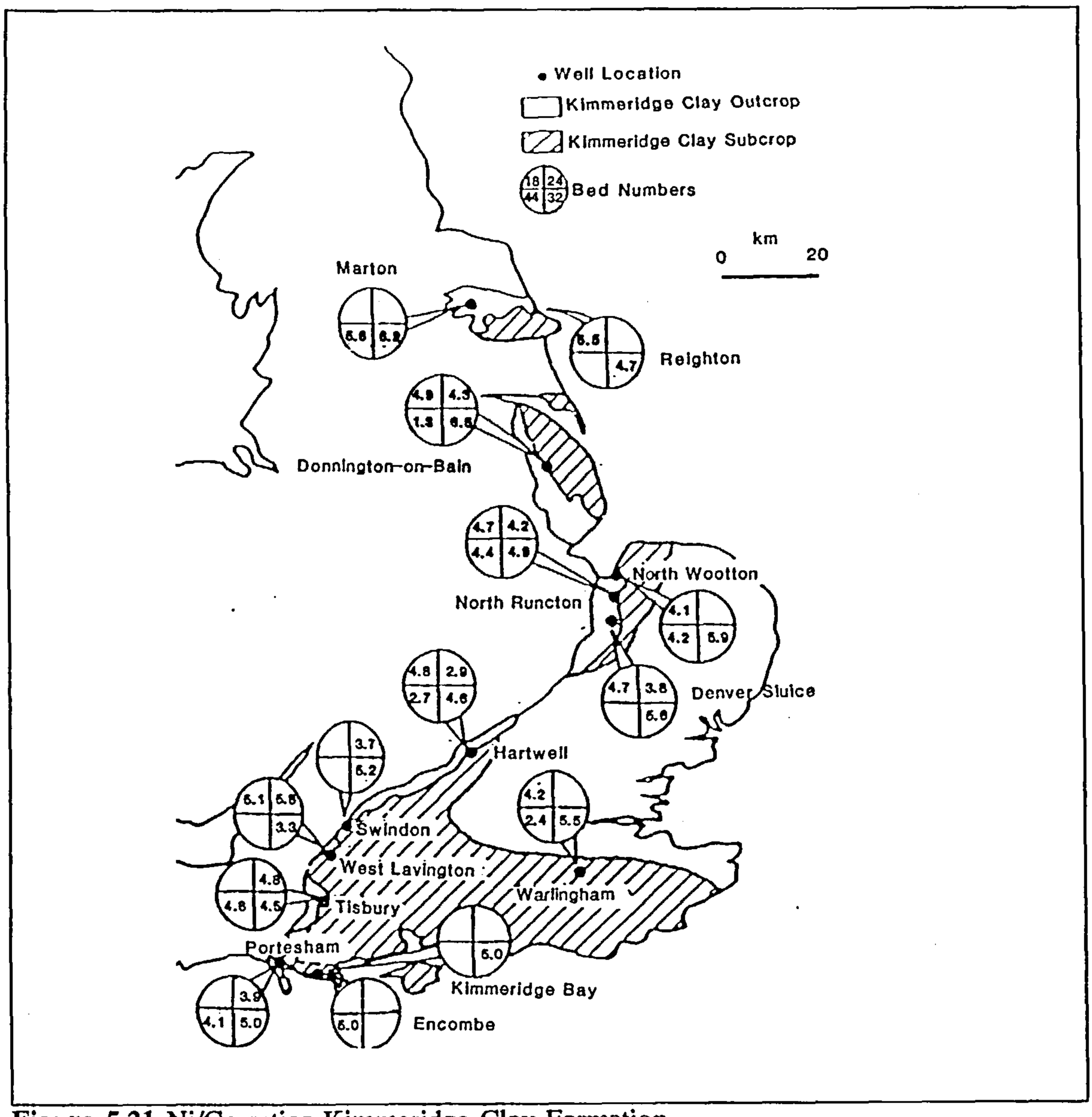

Figure 5.21 Ni/Co ratios Kimmeridge Clay Formation.

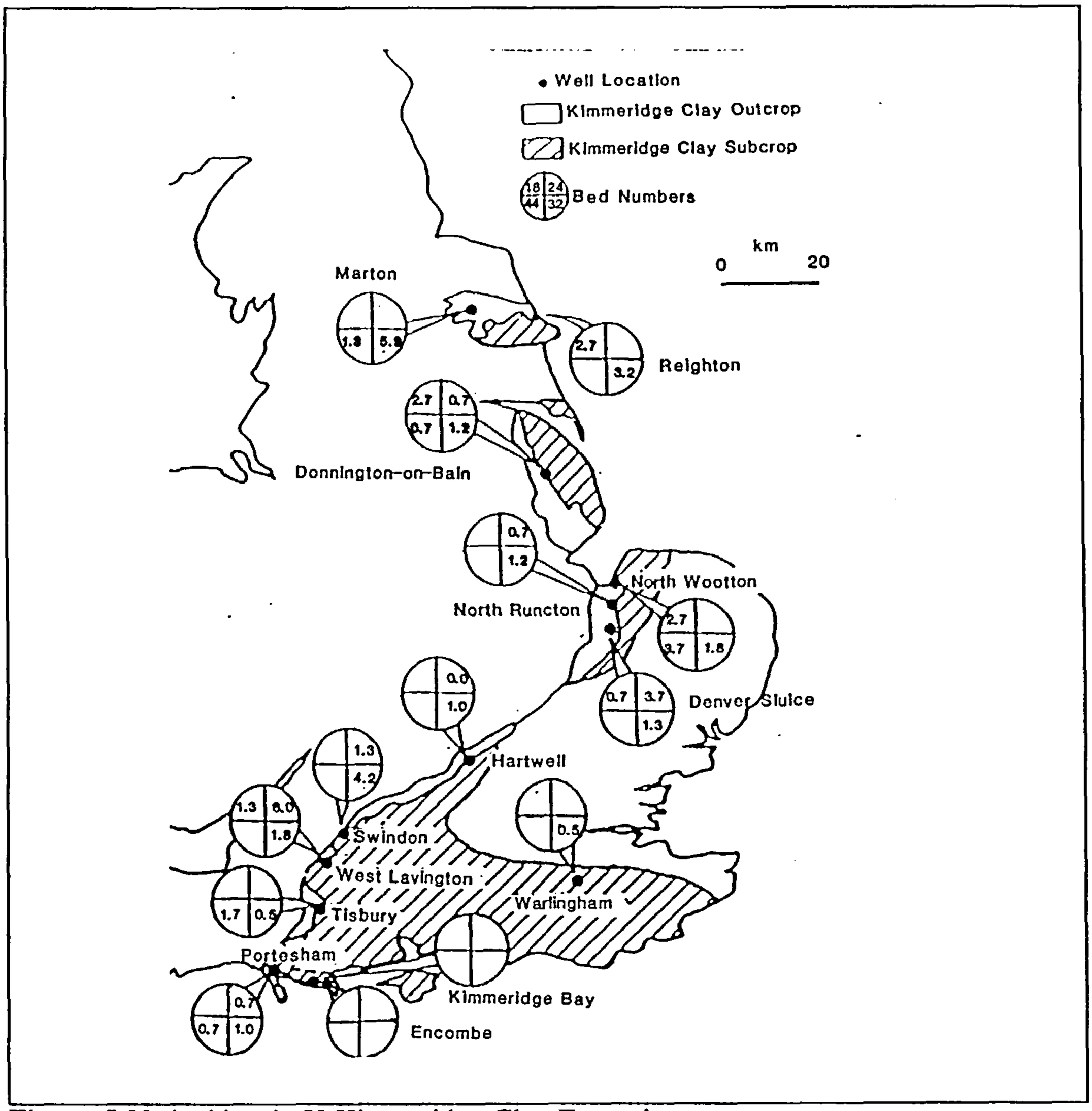

Figure 5.22 Authigenic U Kimmeridge Clay Formation.

5.4 Pyrite formation

5.4.1 A summary

Pyrite formation and the nature of the relationships between Fe, S, and C in sediments have been the subject of a considerable volume of geological literature in recent years. Here after summarising the nature of pyrite formation, and its relationship with the depositional environment, the data collected in this study are examined to further illustrate the nature of the depositional environments of the studied sequences.

The mechanism by which pyrite forms in sediments, and the controls on pyrite formation, are now relatively well understood (Berner, 1970, 1984). In brief pyrite forms during early diagenesis by the reaction of H_2S in the pore water (or in some cases in the water column above the sediment) with detrital Fe minerals. This initially results in the formation of Fe monosulphides, greigite and mackinawite, which are subsequently altered to pyrite by further reaction. The major source of the required H_2S is the bacterially mediated reduction of sulphate whose overall stoichiometry may be represented by the equation: $2CH_2O+SO_4^{2-} =H_2S+2HCO_3^-$. This occurs only in the absence of oxygen and is thus limited to either anoxic depositional waters or more commonly to pore waters which have become depleted in oxygen as a result of other bacterial activity, a process which is usually complete in the top few cm of normal marine sediment. The supply of sulphate and hence the ultimate source of the pyrite sulphide is sea water in marine sediments. In freshwater sediments where the SO_4^{2-} concentration is low pyrite formation is limited and the main authigenic Fe mineral is usually siderite (Curtis and Spears, 1968).

The nature of the sulphate reduction reaction is more complex than the equation given above suggests and first involves fermentative bacteria to produce the small organic molecules required for metabolism by the sulphate reducing bacteria themselves. The rate of the reaction is controlled by the amount of reactive (that is metabolisable) organic matter supplied to the

sediment rather than the total amount. This is rapidly consumed near the sediment water interface and as a result the sulphate reduction rate decreases rapidly with depth below the sediment water interface. The amount of metabolisable organic matter reaching the sulphate reducing bacteria is increased if burial is sufficiently rapid to prevent destruction of such matter by aerobic bacteria and hence a relationship has been noted between the sulphate reduction rate and the rate of sedimentation (Goldhaber and Kaplan, 1975; Berner, 1978). Studies of biorturbation show that this too affects the sulphate reduction reaction by adding organic matter at depth and allowing increased oxidation of reduced S back to sulphate (Berner and Westrich, 1985).

The usually good correlation between C and S (see below) in normal marine sediments occurs because a near constant proportion of the original organic matter is consumed and therefore pyrite correlates with the remaining organic matter. This is illustrated by sulphate reduction equation of Leventhal (1983): $2[R\text{-}CH_2O]+SO_4^{2-}=H_2S+2HCO_3^-+2R$ where R=an unmetaboliseable organic molecule. In most normal marine sediments it is the amount of reactive organic matter which limits the extent of pyrite formation as is indicated by the correlation of C with S. In some cases, particularly in calcareous and very anoxic sediments the amount of reactive Fe may limit the formation of pyrite. Deposition under euxinic conditions differs from the situation for normal marine sediments in that the presence of abundant H_2S means that slow rates of sedimentation favour the greatest pyrite formation, and also there is no need at all for a local organic carbon supply. In addition the organic matter reaching the sediment is usually more reactive resulting in even higher rates of sulphate reduction.

Much of the pyrite found in sediments has a distinctive framboidal texture (eg Love and Amstutz, 1966) and this has been related to the nature of pyrite formation by Raiswell (1982). The initial product of the reaction between H_2S and the detrital Fe minerals is not usually pyrite but a metastable monosulphide-mackinawite or greigite and these are subsequently transformed to pyrite by reaction with elemental S (Berner, 1970) or

polysulphides, by a mechanism which is not entirely clear. Pyrite which is precipitated directly lacks the framboidal texture.

5.4.2 Pyrite formation in relation to depositional environment

Pyrite formation and Fe-C-S relationships in shales have been related to the depositional environment in a number of recent papers (eg Leventhal, 1983; Berner and Raiswell, 1983; Berner, 1984; Gibson, 1985; Raiswell and Berner, 1985; Gautier, 1986; Raiswell and Berner, 1986; Leventhal, 1987; Anderson et al, 1987; and Raiswell et al, 1988). In modern normal marine sediments (defined by Berner and Raiswell (1983) as being deposited from oxygenated waters) the organic C and pyrite S contents tend to have a high correlation and lie on or close to a regression line which passes through the origin (Berner, 1984). The slope of this line and hence the S/C ratio of normal marine sediments is 0.36 (Sweeney and Kaplan, 1980a+b). This results from the dependence of the sulphate reduction rate and hence the pyrite content of a sediment on the abundance of reactive (and therefore total) organic matter. Ancient normal marine sedimentary rocks also show a good correlation between C and S but the S/C ratio tends to be higher (Raiswell and Berner, 1986). In freshwater sediments where the sulphate concentration is minimal the S/C ratio is much lower (Fig. 5.23) and so the S/C ratio may be used to distinguish between marine and non-marine depositional conditions (strictly between sulphate bearing and sulphate free conditions).

Leventhal (1983) and Raiswell and Berner (1985) have shown that S vs C plots may also be used to distinguish between normal marine sediments (defined above) and those in which the bottom waters were anoxic (containing no oxygen) and euxinic (H_2S bearing, definition from Raiswell and Berner, 1985). In these cases plots of S versus C are characterised by high concentrations of S at low C levels and a generally poorer correlation between the two variables. The data usually lie above the regression line of normal marine sediments though overlap may occur where samples have high C and S contents, and their regression line has a positive intercept on the S axis (Fig. 5.24). In some cases no correlation may be apparent at

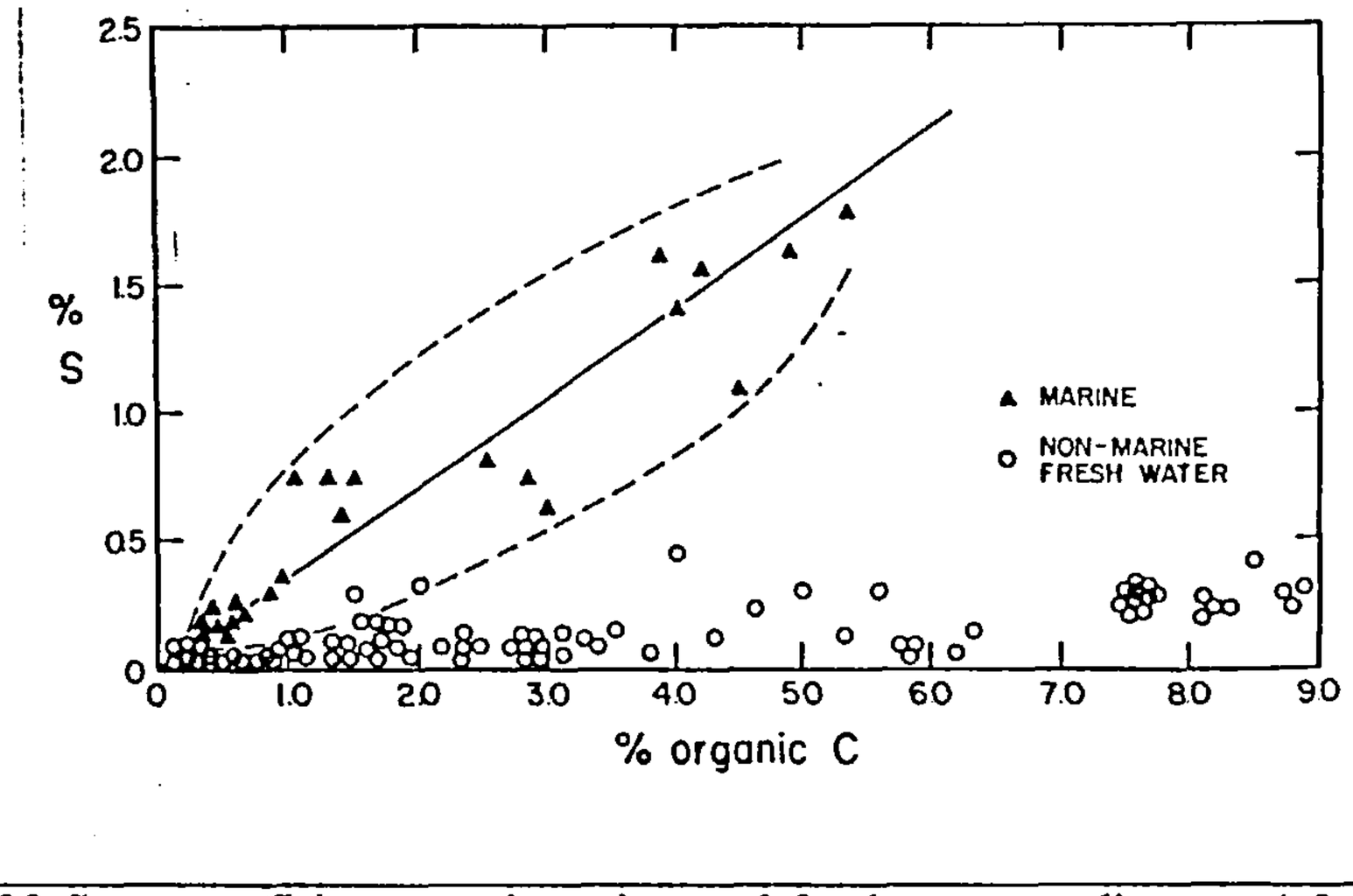

Figure 5.23 S versus C in normal marine and fresh water sediments (after Berner, 1984)

all between S and C.

This difference in the type of S vs C plot between normal and euxinic conditions is due to the occurrence of sulphate reduction and hence H_2S in the water column above the sediments allowing pyrite formation both in the water column and on the sediment surface. The positive intercept on the S axis of S/C plots of data from euxinic sediments such as those from the Black Sea may be interpreted as representing the amount of S fixed in the water column ie with no associated C input to the sediment (Leventhal, 1983; Raiswell and Berner, 1985). As organic matter is being reacted in the water column a local source of organic matter is not required for pyrite formation to continue and thus the lower correlation between S and C arises. Furthermore the high levels of H_2S which may arise in such conditions may result in Fe not organic matter becoming the limiting factor in pyrite formation. As with organic C some Fe may never react to form pyrite and it is usually reactive rather than total Fe which is limiting.

S vs C plots as used by Leventhal (1983) may be insufficient to distinguish between situations where water column pyrite formation is followed by C limited pyrite formation in the sediment, and those in which pyrite formation was limited by reactive Fe, but where

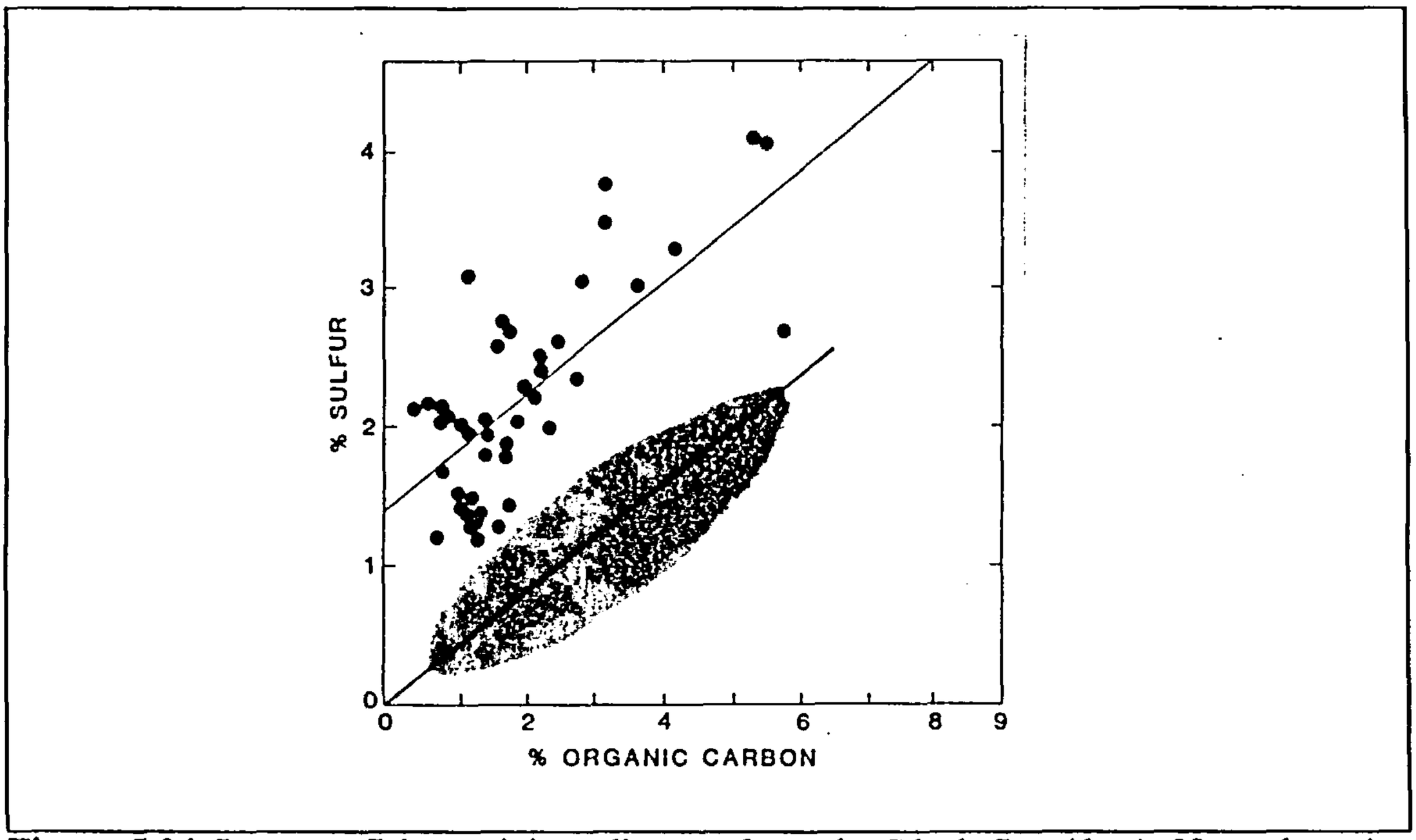

Figure 5.24 S versus C in euxinic sediments from the Black Sea (dots). Normal marine field shaded. After Leventhal (1983).

reactive Fe is correlated with C because of the association of fine grained organic matter and Fe particles on clays, as both will show a positive intercept and generally increasing Fe content with C (Raiswell and Berner, 1985). In this respect the Degree of Pyritisation (DOP) (Berner, 1970) is a useful parameter to consider. This may be defined as DOP=(pyrite Fe)/(total Fe) (Raiswell and Berner, 1985) and indicates the proportion of Fe in the sediment which has been converted to pyrite and hence removes the effects of variation in absolute Fe content. The higher the value of the DOP then the higher must have been the reactivity of the detrital Fe minerals, or the longer the reaction time, or the more concentrated the H_2S in the water. In the first of the cases postulated above the DOP would increase with increasing C as more Fe was pyritised in the sediment. In the second case however DOP would be independent of C as all of the reactive Fe was pyritised in the water column.

Raiswell and Berner (1985) have applied plots of DOP versus C to ancient sediments and have compared their interpretations with palaeo-ecological data. The palaeo-ecological classification of Morris (1979) recognises three groups: aerobic sediments which were deposited in fully oxygenated waters; restricted sediments which were deposited under low

but non-zero oxygen levels (these two classes correspond to the normal marine group as defined above); and inhospitable bottom conditions where oxygen is absent or in very low concentration, and where H_2S may occur.

More recent work (Raiswell et al, 1987) suggests that the DOP alone may be used to distinguish between sediments deposited in differing environments. The method is calibrated against the faunal classes of Morris (1979) using a suite of samples from a variety of areas and of differing ages. It was found that sediments classified as having normal depositional conditions always had DOP values <0.42. Samples from a restricted environment had DOP values falling within the range 0.46-0.80 and these overlapped somewhat with samples from the inhospitable bottom conditions which had DOP values of 0.55-0.93. A boundary of 0.75 correctly distinguishes more than 90% of the data however. The DOP data thus used were found to be a better method for environmental interpretation than either C contents or S/C ratios. S/C ratios are better than using C content alone, but at high C levels there is overlap between normal and anoxic samples because of Fe limitations.

The use of DOP and plots of C and S to determine depositional environments is subject to a number of constraints which have been summarised by Raiswell et al (1987) and Raiswell and Berner (1987). Firstly there must be a reasonable amount of organic C present (eg >0.15%) else the non-pyrite S may be relatively important in comparison with that produced during diagenesis. To prevent the oxidative loss of S fresh outcrop material or core should be used where possible and there should be sufficient Fe for accurate measurement of the DOP which may be a problem in carbonate rich sediments; a maximum non-clastic component of 65-75% is suggested. No changes in S content should occur because of processes other than early diagenetic pyrite formation and samples containing late diagenetic carbonates should be avoided as these may introduce authigenic Fe from elsewhere. Furthermore Devonian or older sediments may be suspect as a lack of terrestrial plant debris in rocks of this age means that more reactive organic matter may have been supplied to the sediment although more recent

work by Raiswell and Al Biatty (1989) suggests that this last limitation may not be important however.

As might be expected the relationship between C and S is affected by the changes that kerogen undergoes with increasing burial temperature (increasing maturity). The effects of methanogenesis (Claypool and Kaplan, 1974) and decarboxylation (Carothers and Kharaka, 1978) can result in an increase in the S/C ratio due to preferential C loss from about 0.36 in normal marine sediments today to about 0.56 in normal marine sediments of Tertiary, Cretaceous or Jurassic age (Raiswell and Berner, 1986), a maximum loss of about 35% (Fig. 5.25). Further loss of C may be expected as the sediment reaches maturity for oil generation and migration. This has been studied by Raiswell and Berner (1987) whose results are shown in Fig. 5.26, and who found an increasing S/C ratio with increasing organic maturity for normal marine sedimentary rocks. This interpretation assumes that the sedimentary organic matter is of constant composition and is justified only for large samples. Similar effects will also occur when euxinic sediments are buried but these are more difficult to quantify as the initial S/C ratios are unknown. The data of this study can still be compared with those for the normal marine shales of similar age in Figs 5.25 and 5.26 however.

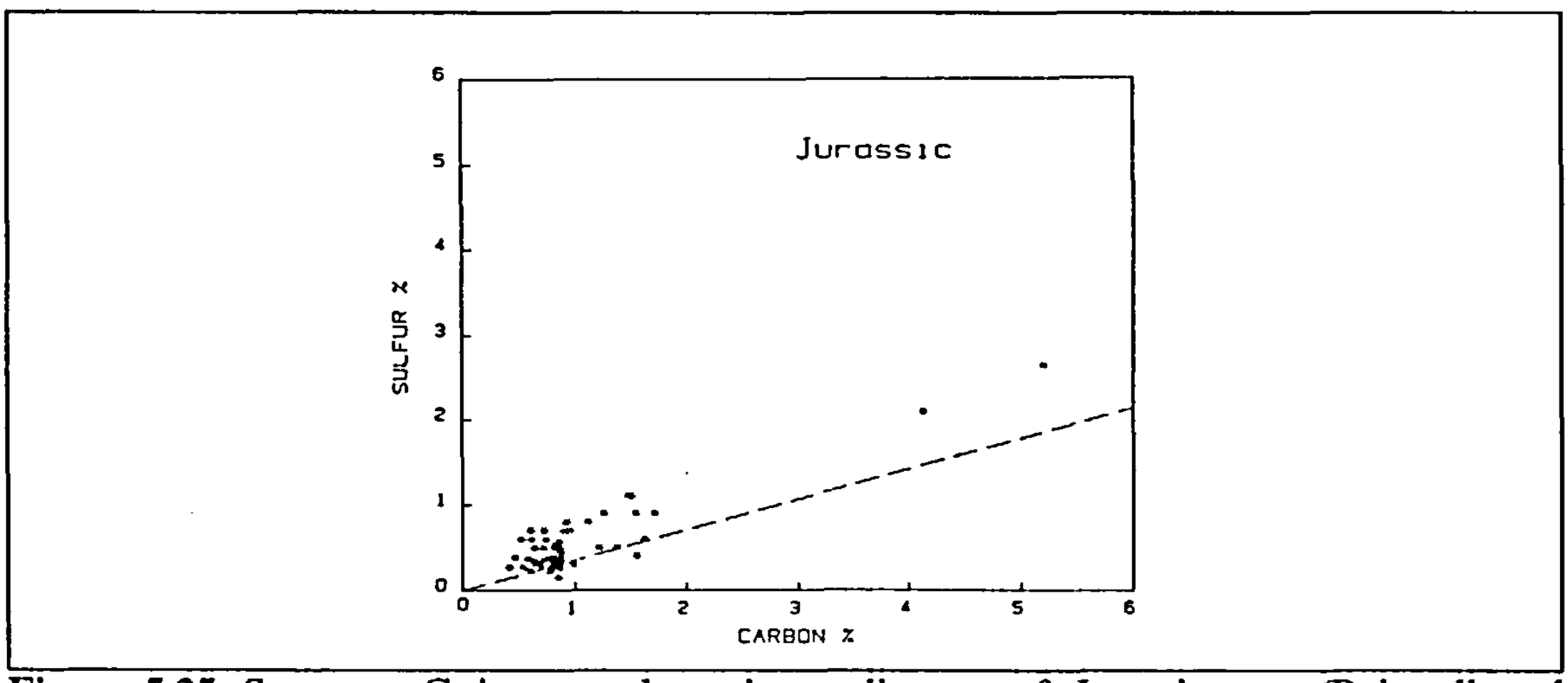

Figure 5.25 S versus C in normal marine sediments of Jurassic age (Raiswell and Berner, 1986).

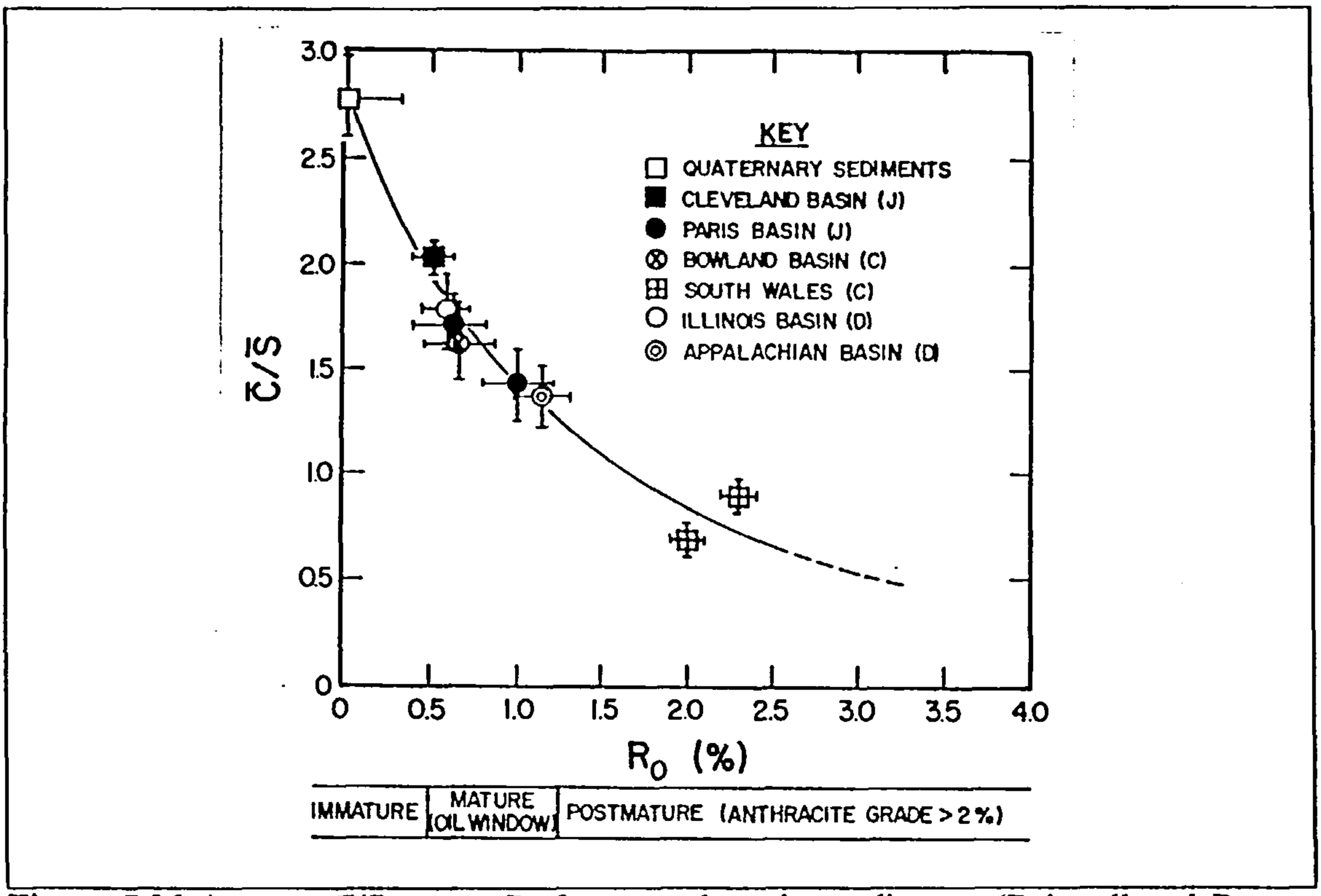

Figure 5.26 Average C/S versus R_o for normal marine sediments (Raiswell and Berner, 1987).

DOP as defined above is the proportion of total Fe present as pyrite. In practice total Fe is often replaced by the amount of Fe which is soluble in hot concentrated HCl plus that in the pyrite, as this is all that is likely to have been reactive towards H_2S. In this study the use of total Fe has been retained because it had been determined as a part of the major element analyses, and because the (%Fe soluble in HCl)/(%total Fe) may change as non-pyrite Fe is involved in diagenetic reactions. Pyrite Fe once fixed is effectively removed from further diagenetic reaction. The DOP values of this study might therefore be expected to be a little lower than those using HCl reactive Fe. Pyrite Fe as in previous chapters has been calculated from the total S content, assuming that all S is present as pyrite.

5.4.3 C-S-Fe Relations in the Jurassic mudstones of this study and their environmental interpretation

In order to use C-S-Fe data for environmental interpretations a number of criteria must be met (Raiswell et al, 1987), these being summarised above. Meeting these constraints results in a reduction in the number of samples used for this portion of the study. For the Draupne Formation 2 samples have been omitted with 70 remaining. For the Heather Formation 19 samples were removed from the data set, this including 10 samples for which data were missing, leaving 55 samples remaining. The Kimmeridge Clay Formation has had 3 samples removed leaving 49. In total therefore 174 samples are included for the C-S-Fe study.

There are strong theoretical grounds for assuming that the S content of a sediment is dependent on the organic carbon content (see above) hence least squares regression lines have been drawn on S versus C plots, with S being taken as the dependent variable. As both C and S are subject to normal analytical error other regression techniques such as that of reduced major axis regression may provide a better description of the relationship between the two variables.

5.4.3.1 The Draupne Formation

Scatter plots of S vs C, DOP vs C, and Fe_2O_3 vs C for the Draupne Formation are illustrated in Figs. 5.27-5.29. Initial examination of the DOP values suggests that only a small proportion of these samples were deposited under normally oxygenated conditions and that the majority were deposited in either restricted or inhospitable bottom conditions (terminology of Raiswell et al, 1987); the DOP values being generally high. When the median DOP values are plotted by well (Fig. 5.30) it can be seen that these data are in agreement with the earlier interpretations of depositional environments made above. Examining the S vs C diagram it is obvious that there is much more scatter in these Draupne Formation data than in the corresponding Heather or Kimmeridge Clay plots, this being reflected in the relatively low

correlation coefficients between S and C of p=0.32, r=0.30 in the Draupne Formation. Furthermore the least squares regression line calculated for this formation has a positive intercept on the S axis of 2.03%, both of these features being characteristic of deposition beneath a euxinic or semi-euxinic water column (Leventhal, 1983; Raiswell and Berner, 1985).

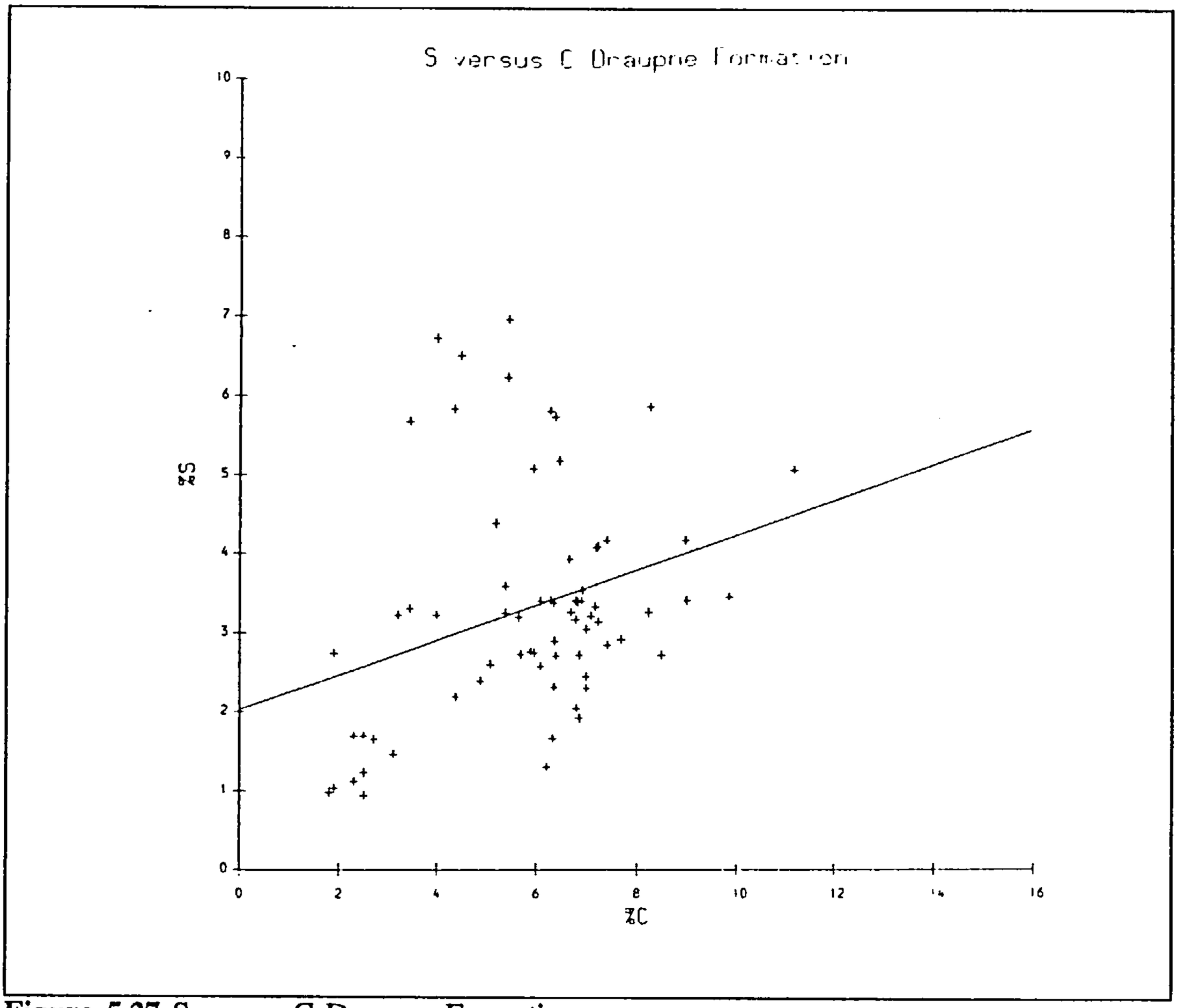

Figure 5.27 S versus C Draupne Formation

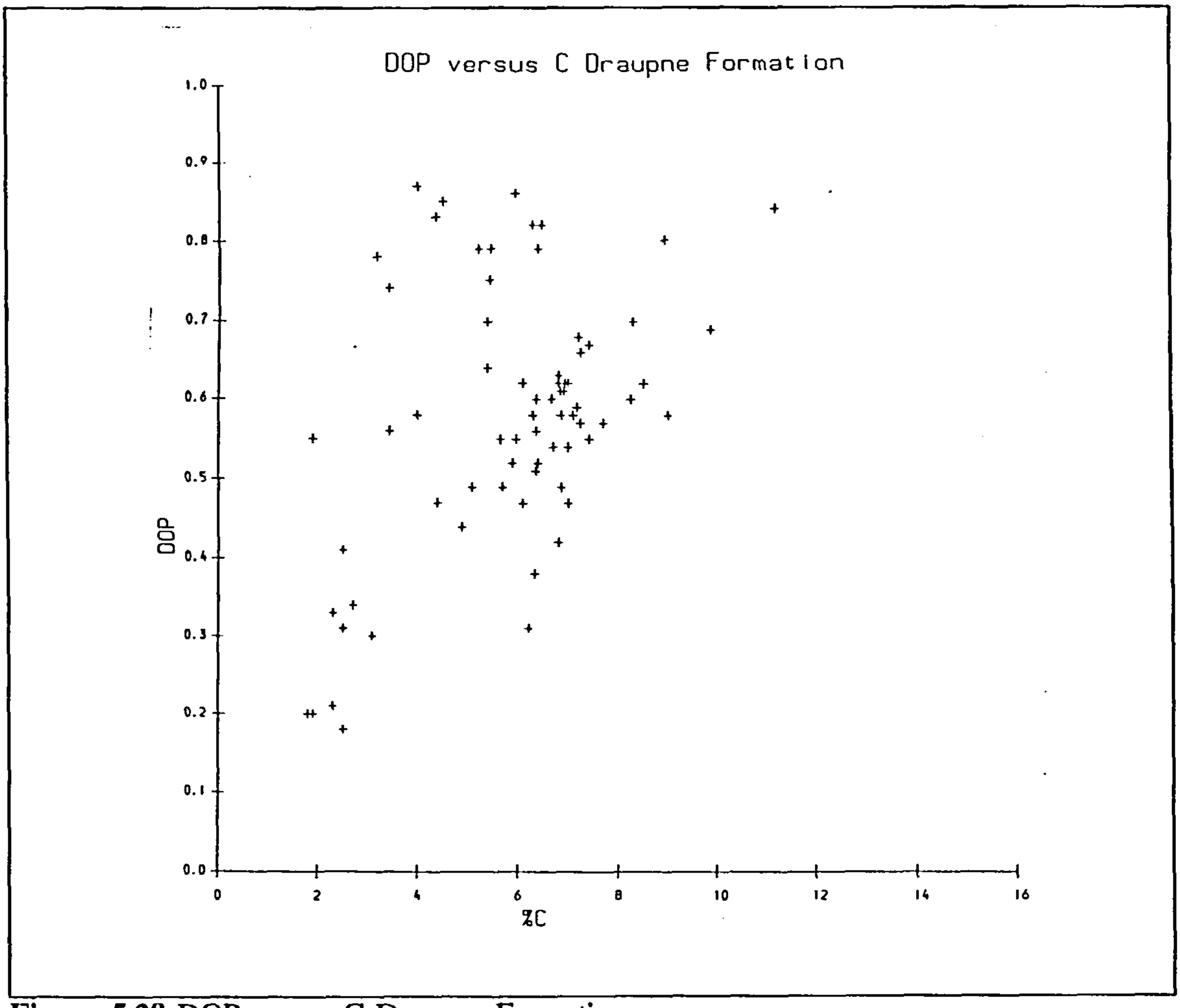

Figure 5.28 DOP versus C Draupne Formation.

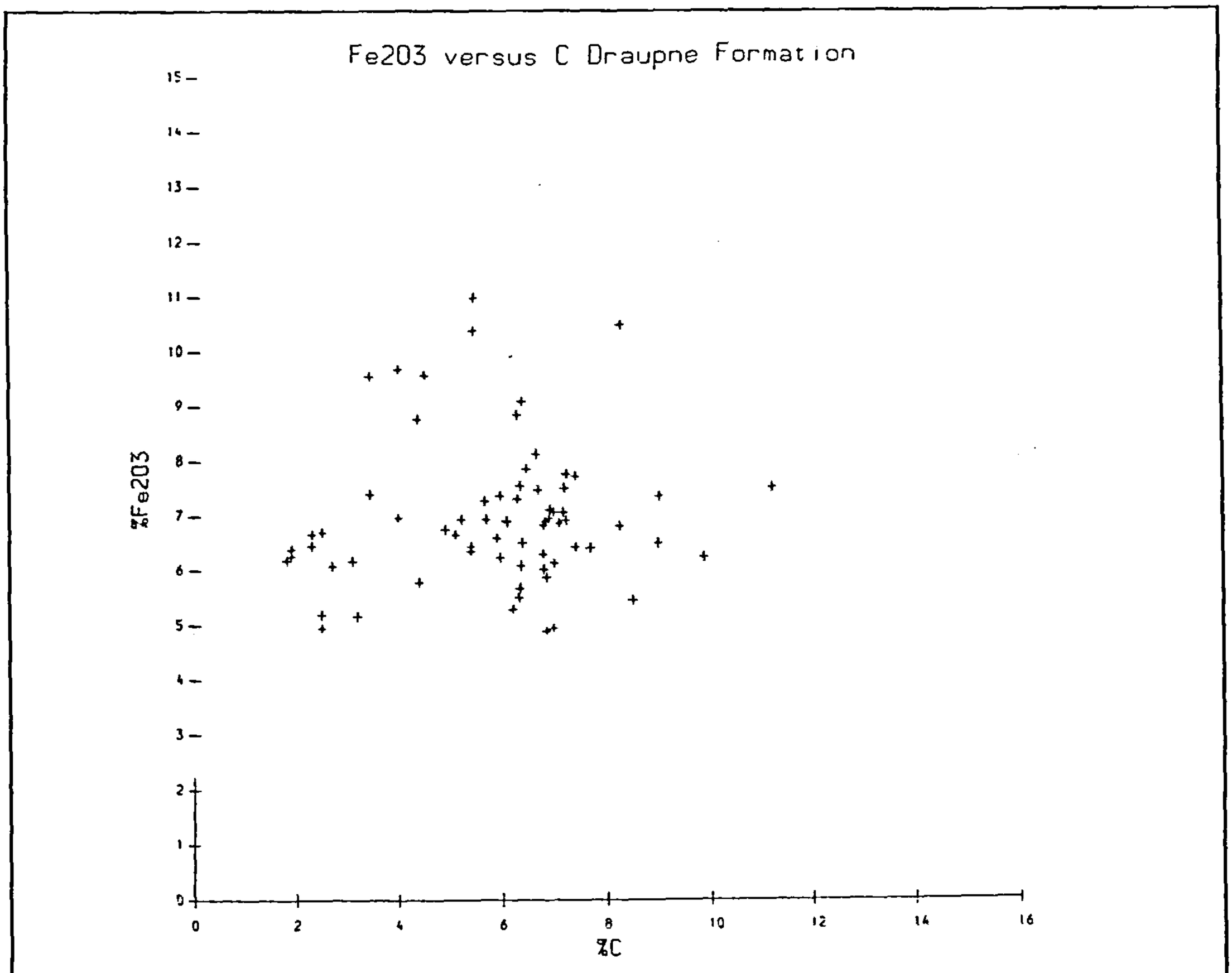

Figure 5.29 Fe_2O_3 versus C Draupne Formation.

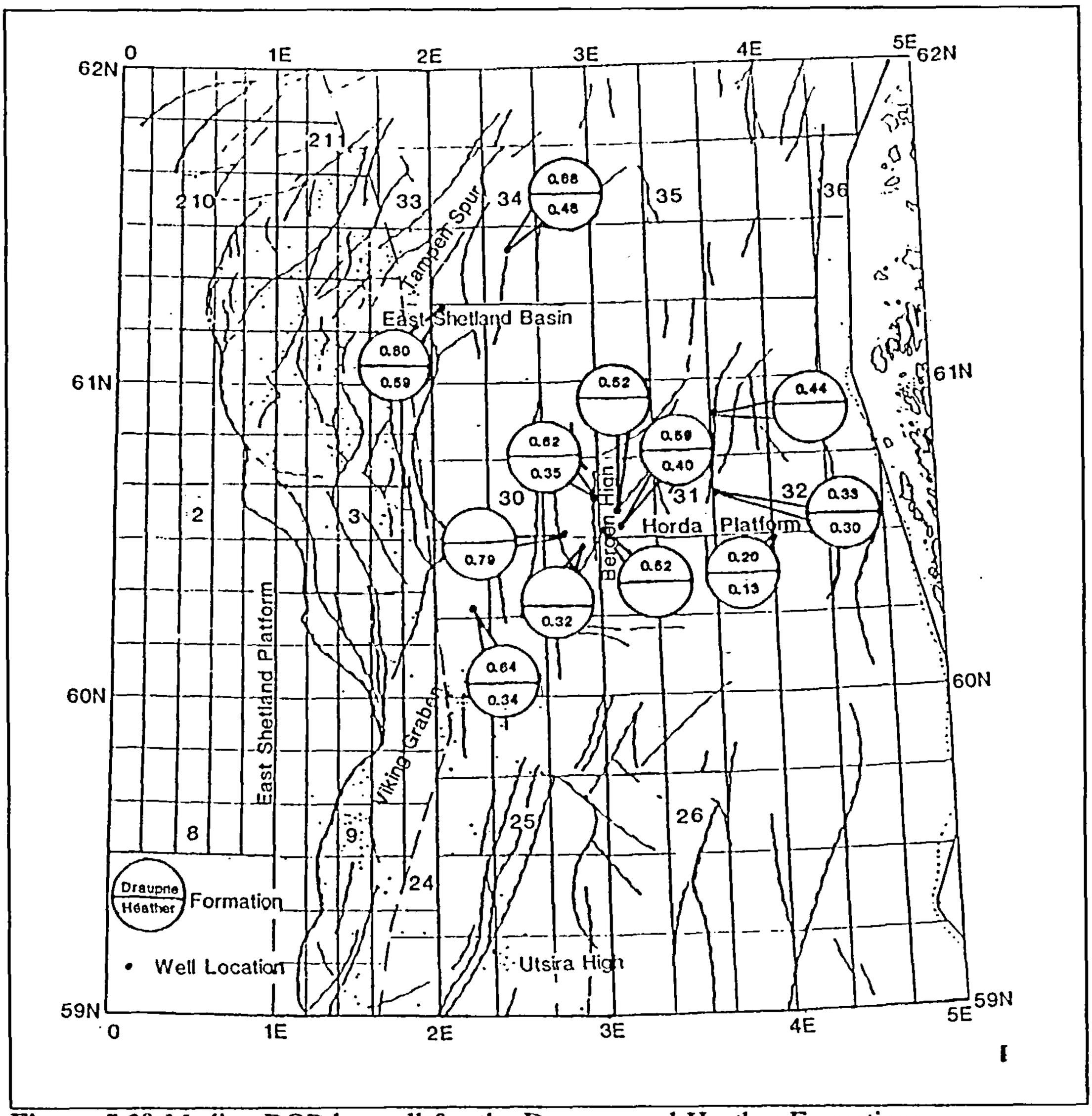

Figure 5.30 Median DOP by well for the Draupne and Heather Formations.

A more detailed study of the S vs C and DOP vs C plots for the Draupne Formation allows the data to be subdivided into 2 groups. In the 56 samples with DOP values below 0.7 (Figs 5.31 and 5.32) not only are S and C much better correlated (p=0.58, r=0.66) than for the formation as a whole, but the S intercept is very much reduced though still significant, being only 0.93%. This group also shows a correlation between DOP and C of p=0.66, r=0.74 suggesting that pyrite formation in these samples was limited by organic C content only, and that Fe did not play a limiting role. As these 56 samples are interpreted to have been deposited in either aerobic or restricted bottom waters (and are thus normal marine under the definition of Berner and Raiswell, 1983) a significant positive S intercept is not anticipated. One reason for its occurrence may be the inclusion of some samples in this group which were deposited under anoxic or euxinic conditions but which were not excluded by the DOP

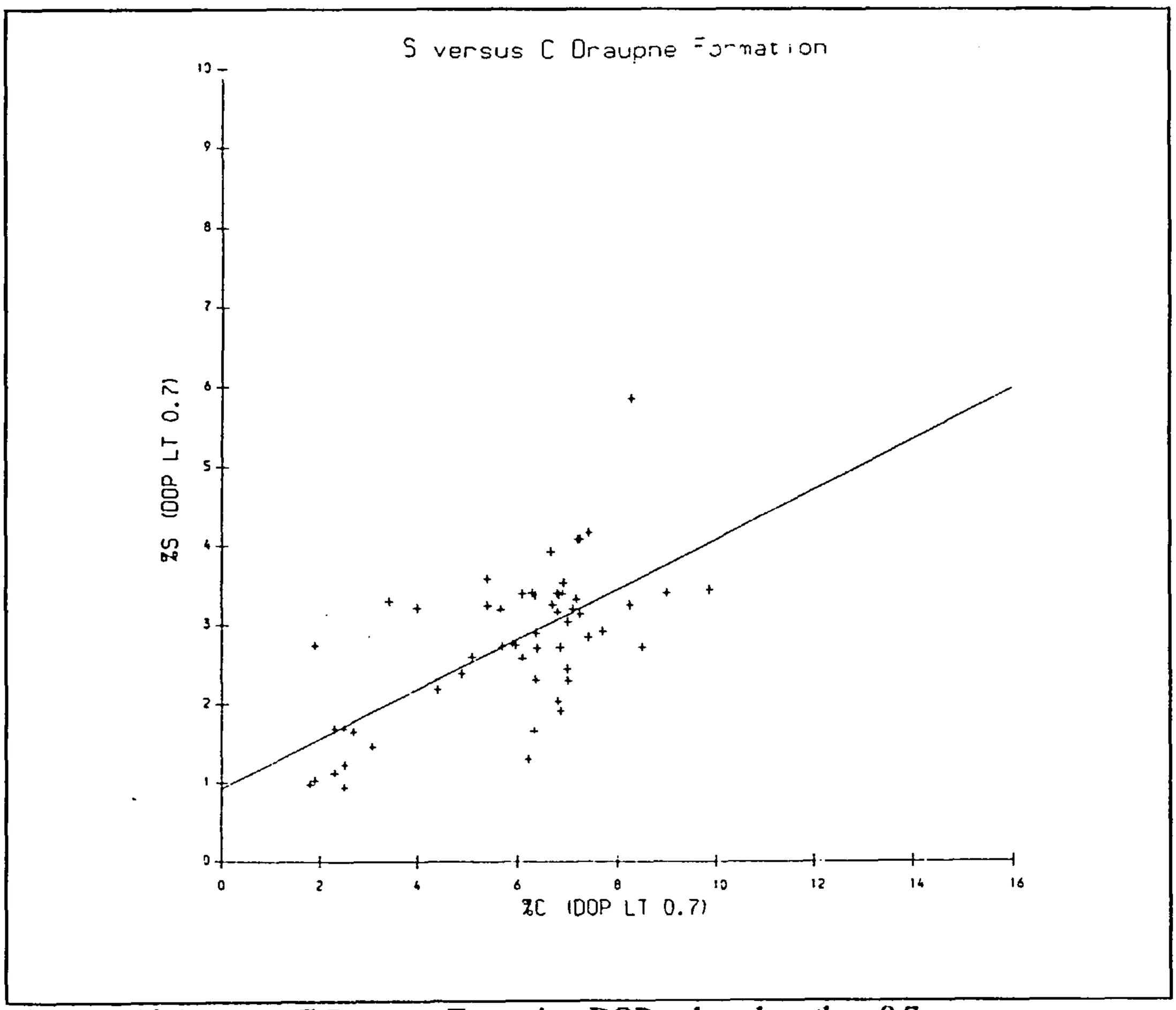

Figure 5.31 S versus C Draupne Formation DOP values less than 0.7.

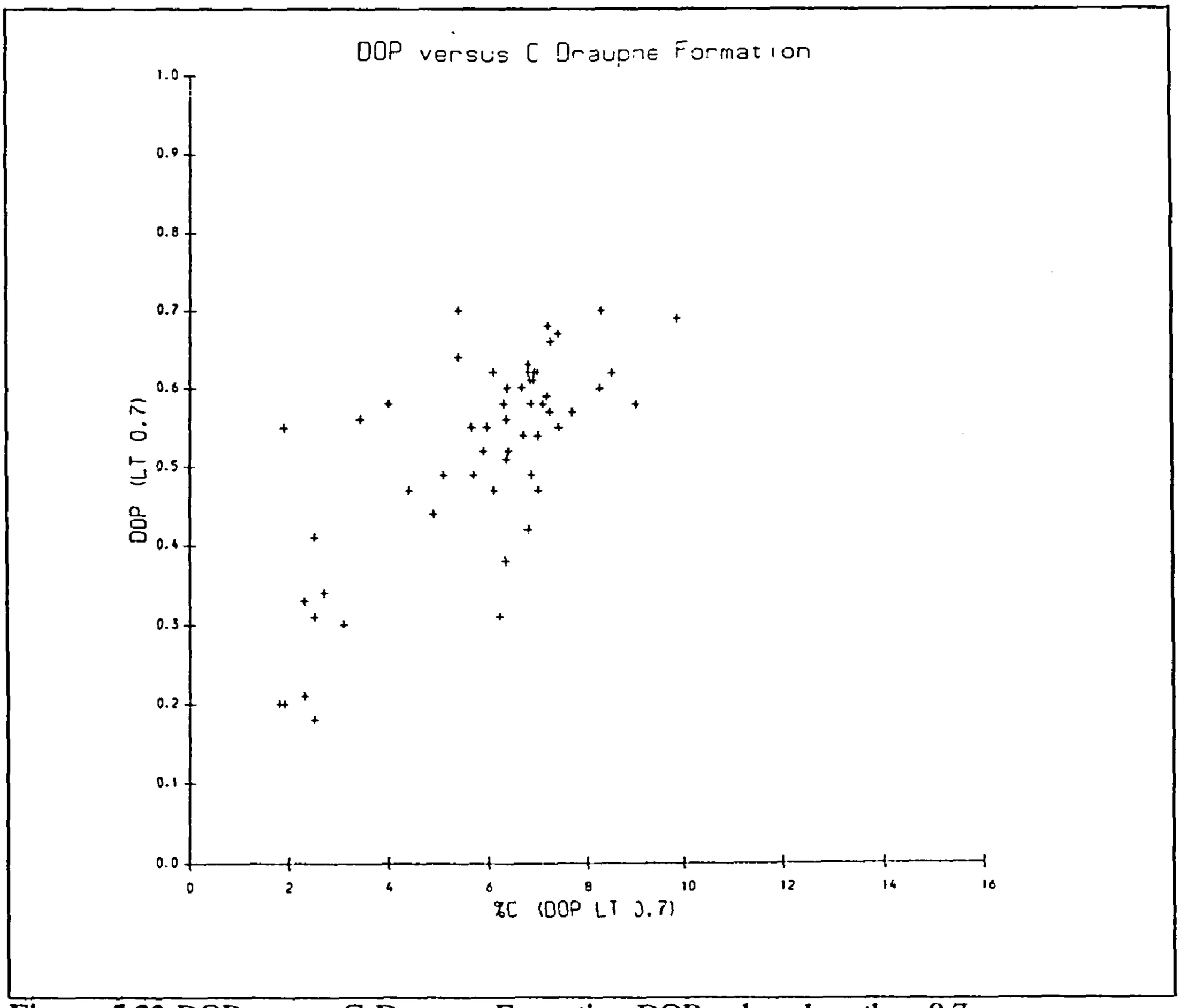

Figure 5.32 DOP versus C Draupne Formation DOP values less than 0.7.

selection criterion. These samples may be recognised as they fall away from the regression line and have unusually large S contents and DOP values but only low to moderate organic C contents.

For the 14 samples with DOP contents in excess of 0.7 (Figs. 5.33 and 5.34) the slope of the S vs C regression line is not significantly different from zero at the 95% significance level and hence S is independent of the C content, with very high S contents being associated with low or moderate C contents. The S intercept for this group of samples is about 6%. The DOP is also independent of the C content of the sediment at the 95% significance level. C-S-DOP relationships such as these are similar to those of the Posidonia Shales and other formations in Berner and Raiswell (1985) thought to have been deposited in euxinic conditions, and are

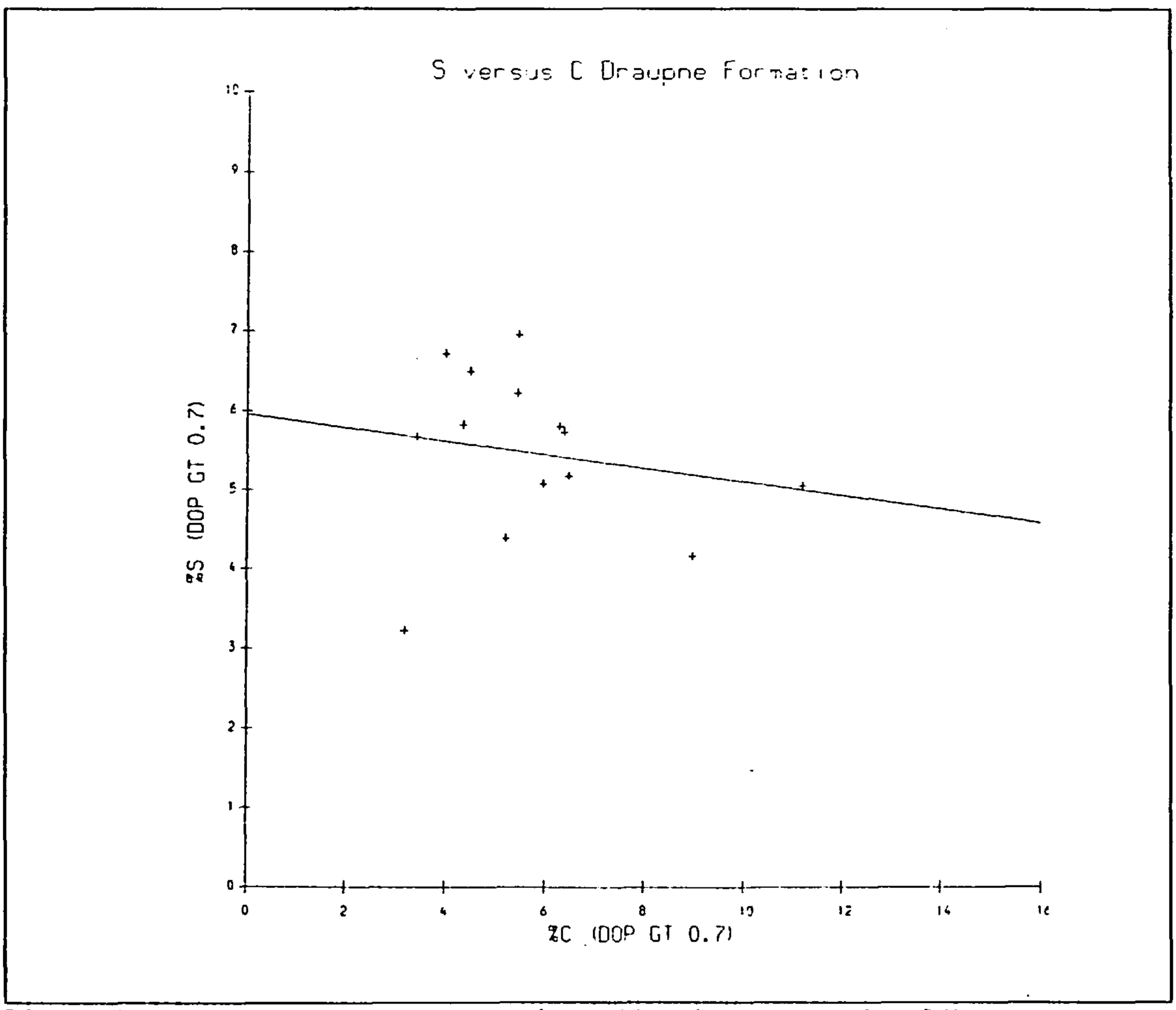

Figure 5.33 S versus C Draupne Formation DOP values greater than 0.7.

indicative of Fe limited pyrite formation. In such cases all of the reactive Fe in the sediments had been pyritised prior to deposition and there was no opportunity for carbon limited pyrite formation within the sediment. Interpretation of the DOP data alone confirms the generally euxinic depositional environment of these samples.

The plot of Fe_2O_3 vs C (Fig. 5.29) illustrates that Fe_2O_3 is independent of C in the Draupne Formation at the 95% significance level, and that the input of organic matter and Fe was not coupled. This differs from the other mudstones studied here and may reflect the more important contribution of marine organic matter in the Draupne which might not be expected to be correlated with the detrital input in contrast to the terrestrial organic matter found to be more common in the other formations.

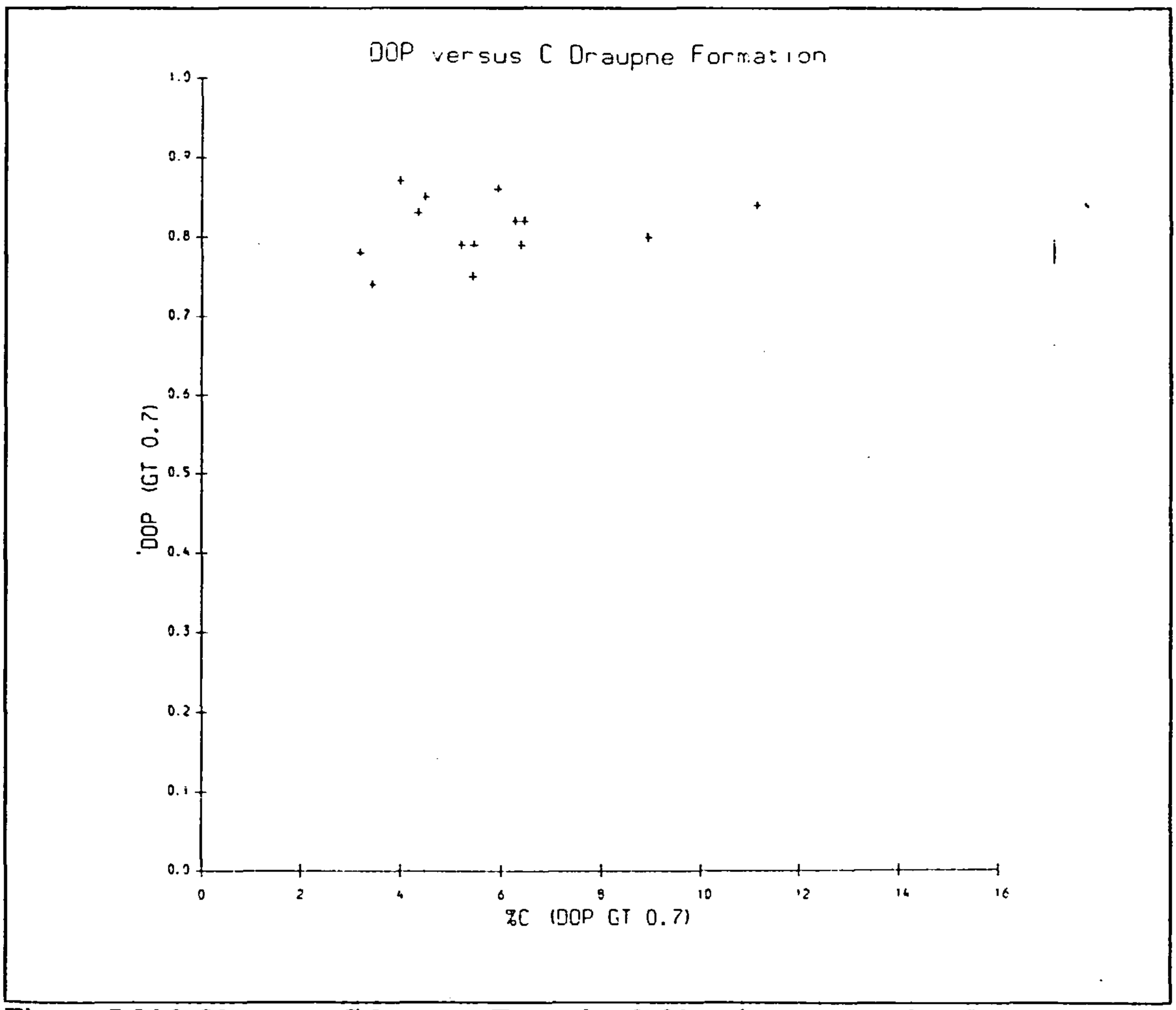

Figure 5.34 DOP versus C Draupne Formation DOP values greater than 0.7.

5.4.3.2 The Heather Formation

In contrast to the Draupne Formation examination of the DOP vs C diagram (Fig. 5.35) for the Heather shows that a large number of samples were apparently deposited beneath aerobic water, and most of the remainder beneath restricted conditions. The number of samples for which inhospitable bottom conditions are suggested are very small. In such a case one would expect to find a good correlation between S and C and a zero S intercept. This is so; the correlation coefficients are p=0.60, r=0.75 and the small intercept of 0.58% on the S axis is not significantly different from zero at a 95% significance level. Again the median DOP values plotted by well are in good agreement with the interpretations of the environmental parameters discussed above and clearly illustrate the generally better oxidised depositional environment of this formation.

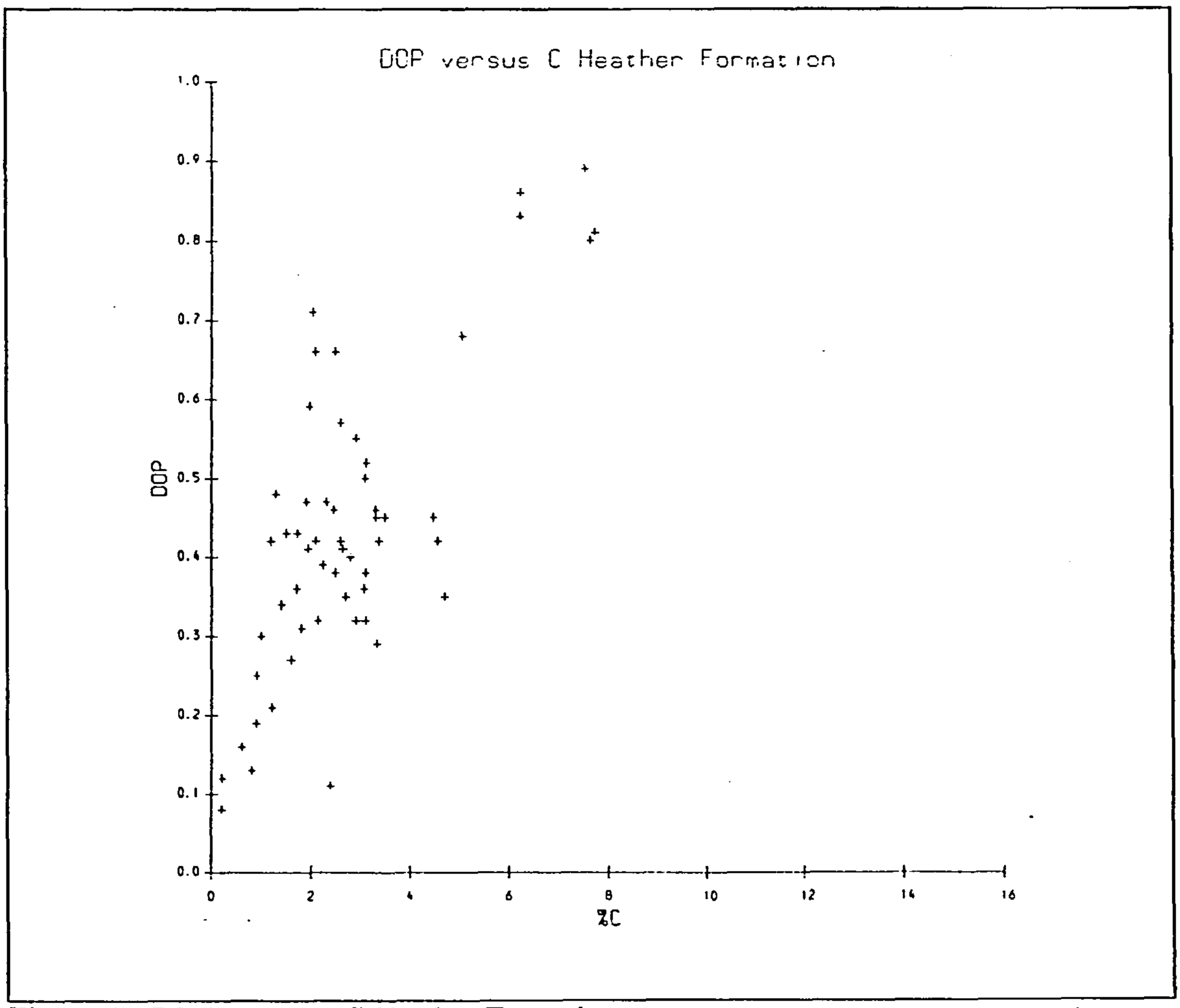

Figure 5.35 DOP versus C Heather Formation.

The slope of the S vs C regression line (Fig 5.36) for the Heather Formation (0.76) is considerably steeper than that found in modern normal marine sediments (0.36), and is also steeper than that of normal marine Jurassic shales (0.53) from the onshore UK (Raiswell and Berner, 1986). Loss of C during diagenesis and catagenesis is unlikely to be responsible for this as the Heather Formation sampled here is mainly immature to mature for oil generation, and is broadly similar in maturity to the Jurassic sediments in Raiswell and Berner (1986). The steepness is however partly due to the influence of the few high S and high DOP samples which were probably deposited under euxinic conditions. Omission of 9 samples with high S contents and high DOP values results in a slope of only 0.38 albeit with the development of a positive S intercept.

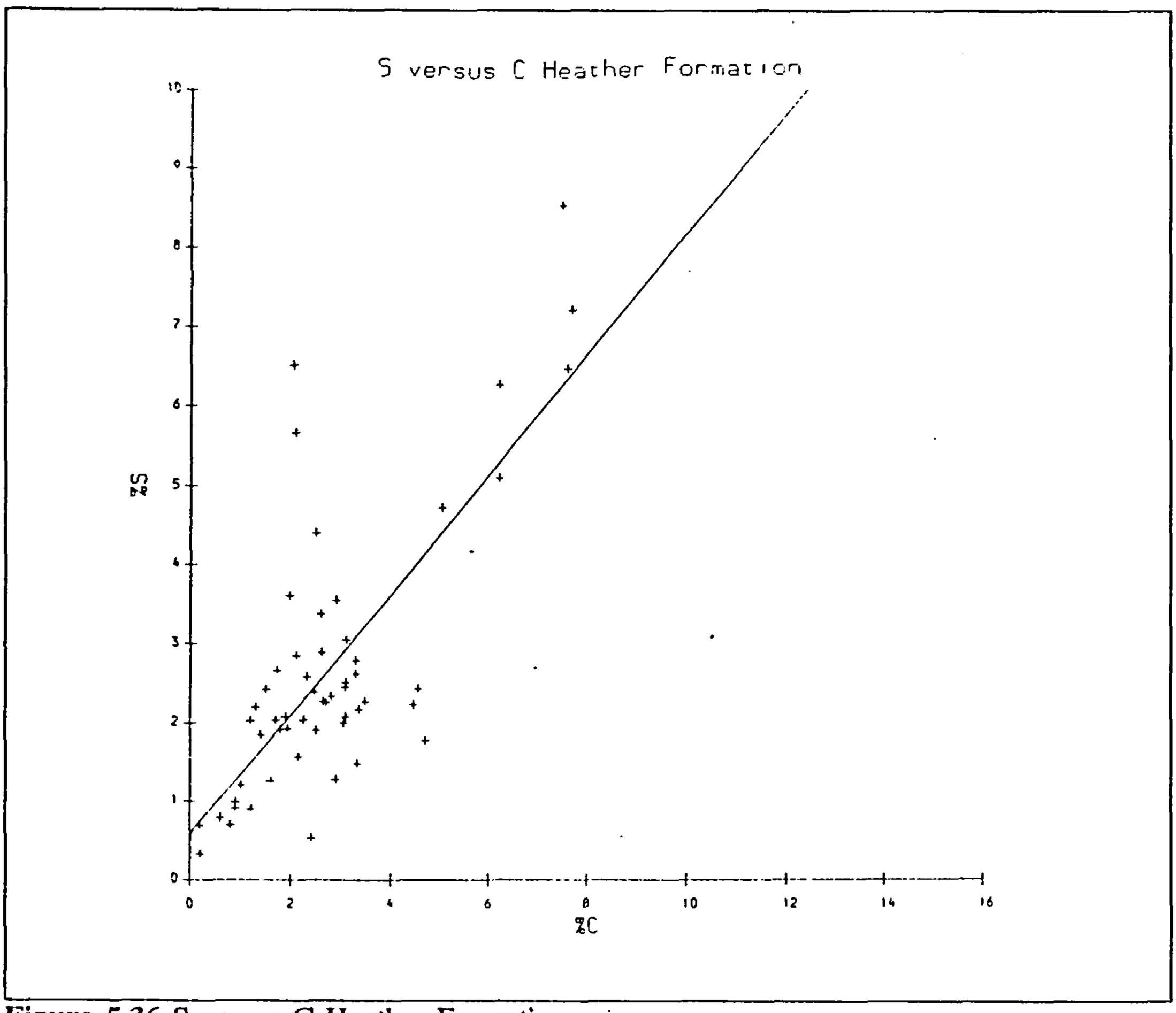

Figure 5.36 S versus C Heather Formation.

The DOP is significantly correlated with the C content p=0.56, r=0.75, as is the total Fe_2O_3 content p=0.46, r=0.56 (Fig. 5.37) again suggesting that C not Fe was the limiting control on pyrite formation. Unlike the Draupne the correlation between Fe_2O_3 and C suggests that deposition of these two components was coupled, with both probably being transported together in association with fine grained sediment.

5.4.3.3 The Kimmeridge Clay Formation

The C-S-DOP data for the Kimmeridge Clay Formation (Fig. 5.38-5.40) are similar to those of the Heather in that the majority of samples fall into the aerobic field, with most of the remainder having been deposited in a restricted environment. Only a few samples were

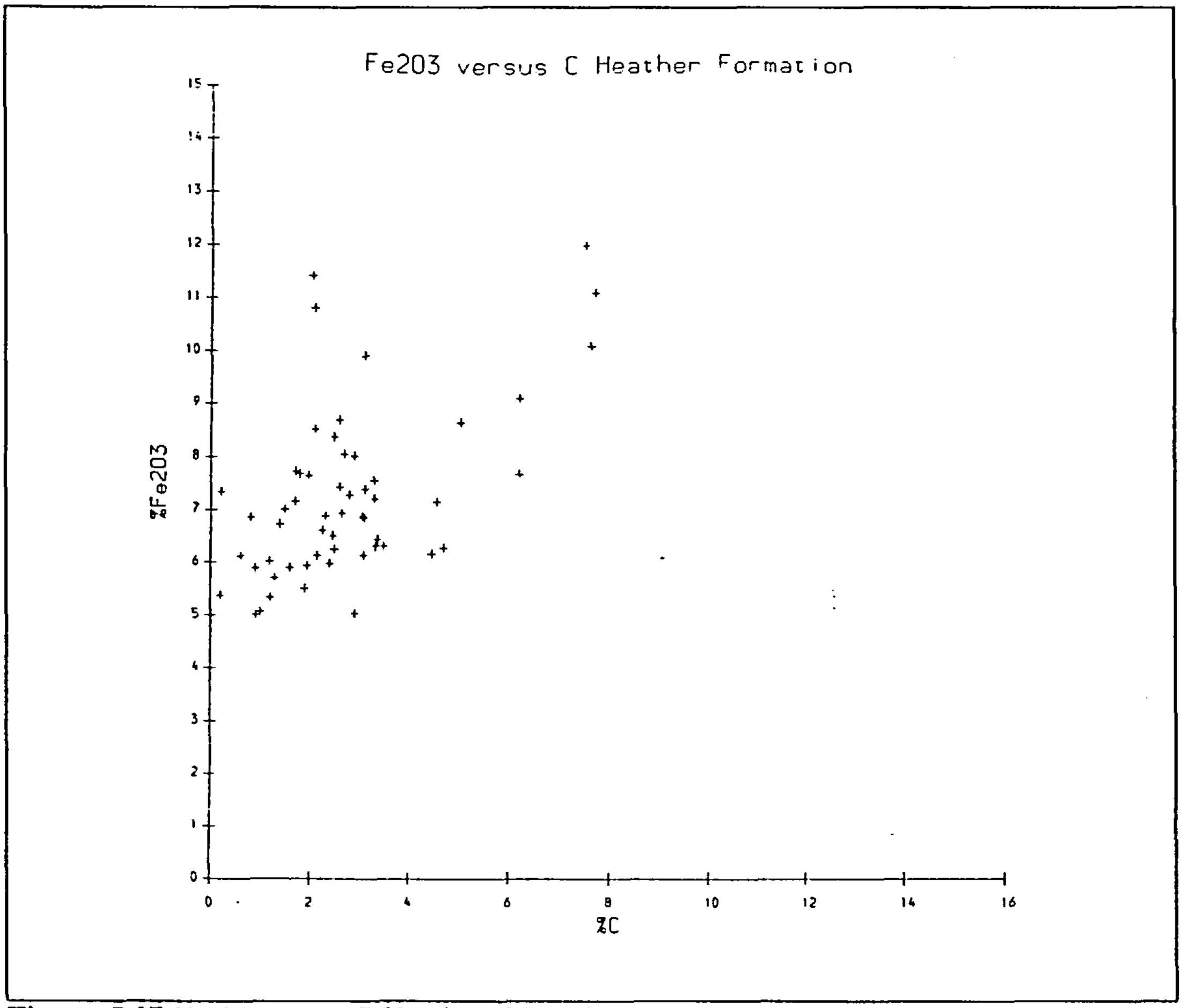

Figure 5.37 Fe_2O_3 versus C Heather Formation.

deposited under inhospitable bottom water conditions. With the exception of one sample from Bed 44 with a DOP of 0.44 the organic rich Bed 32 was the only bed studied where DOP values in excess of 0.42 were measured. As in the Draupne Formation the data may be divided into samples having a DOP less than 0.7, and a minority of samples with DOP values in excess of 0.7 (all from Bed 32). For the former group the S-C correlation is good (p=0.73, r=0.73) (Fig. 5.41) but the S intercept although small (0.68%) is significant at the 95% level. The 3 samples with a DOP greater than 0.7 have no S correlation with organic C (Fig. 5.42). Overall Fe_2O_3 is correlated with organic C (p=0.46, r=0.47) (Fig. 5.43) suggesting that deposition of organic matter was coupled in some way with that of Fe.

5.5 Organic maturity parameters

Three indices of organic maturity have been employed in this study, these being the reflectance of the vitrinite maceral in oil (R_o), the Rock-Eval T_{max} temperature, and the Spore Colour Index (SCI). R_o has long been in widespread use for the determination of the rank of coals. Its value increases with increasing burial and is related to the C content of the coal. Further work on the reflectance of vitrinite particles amongst the dispersed organic matter found in sediments has established its usefulness as an organic maturity parameter for sedimentary rocks also. Despite some drawbacks such as the difficulties in distinguishing between vitrinite and other phytoclasts in fine grained sediment, and between true vitrinite and reworked material R_o has become the most widely used of organic maturity parameters and is the one to which most others are correlated (eg Heroux et al, 1979; Espitalie, 1986). An R_o value of about 0.5-0.7% may be taken to indicate that a sediment is mature for oil generation, a process which is usually complete when R_o=1.0%. Vitrinite reflectances of 1.2-1.35% represent the onset of thermal degradation of hydrocarbons-the oil floor. Thomas et al (1985) have shown that for the Draupne Formation in the North Sea most oil generation occurs in the R_o range 0.75-1.0% peaking at about 0.8%.

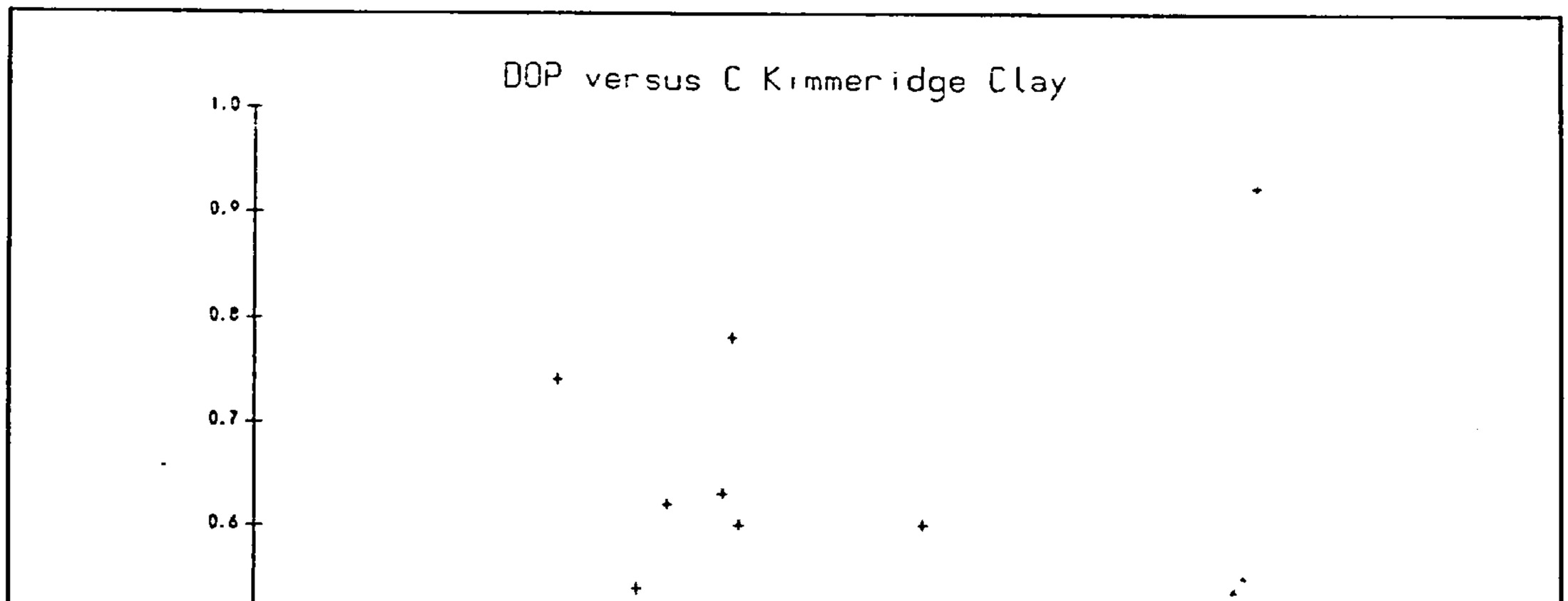

Figure 5.38 DOP versus C Kimmeridge Clay Formation.

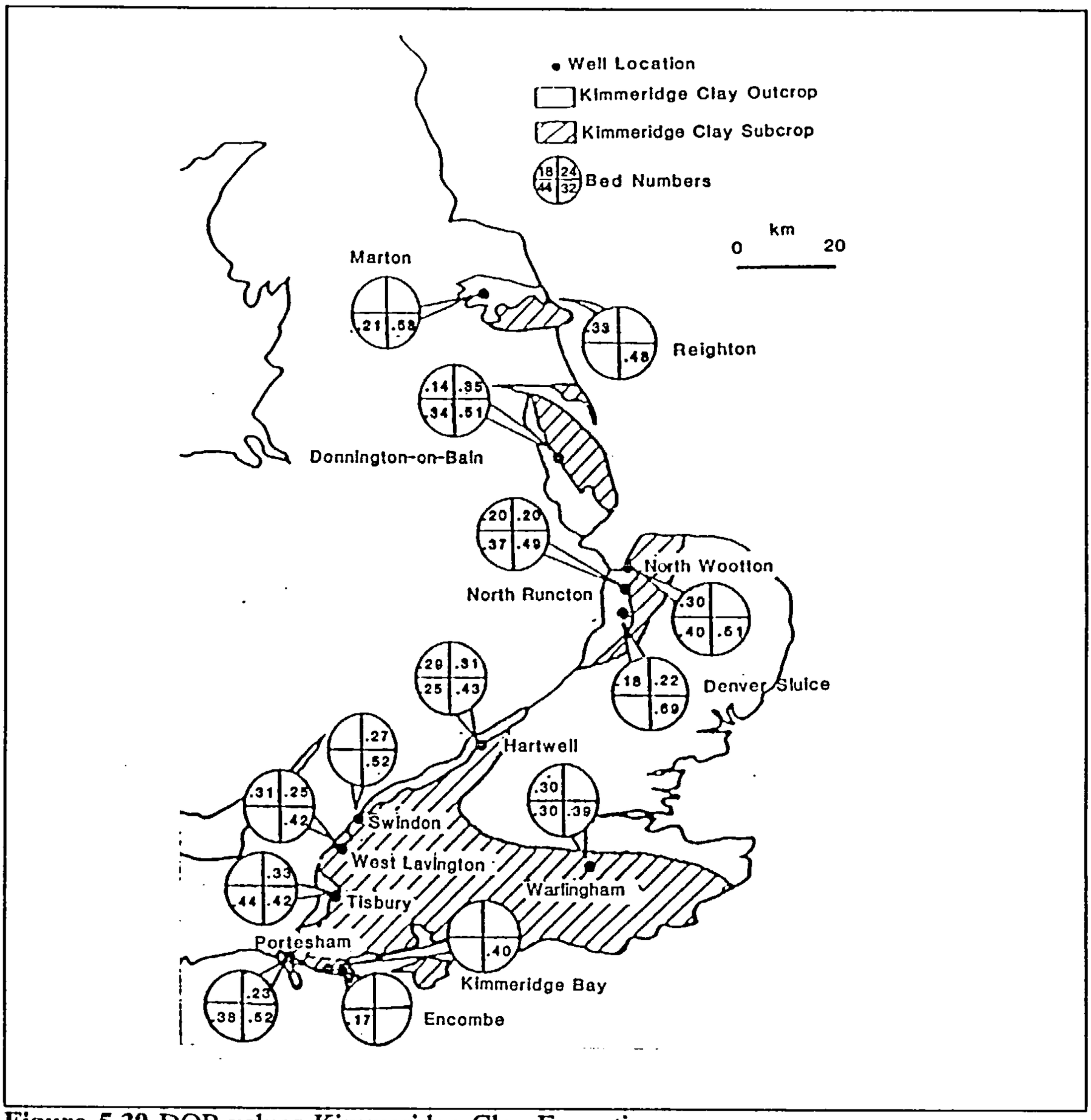

Figure 5.39 DOP values Kimmeridge Clay Formation.

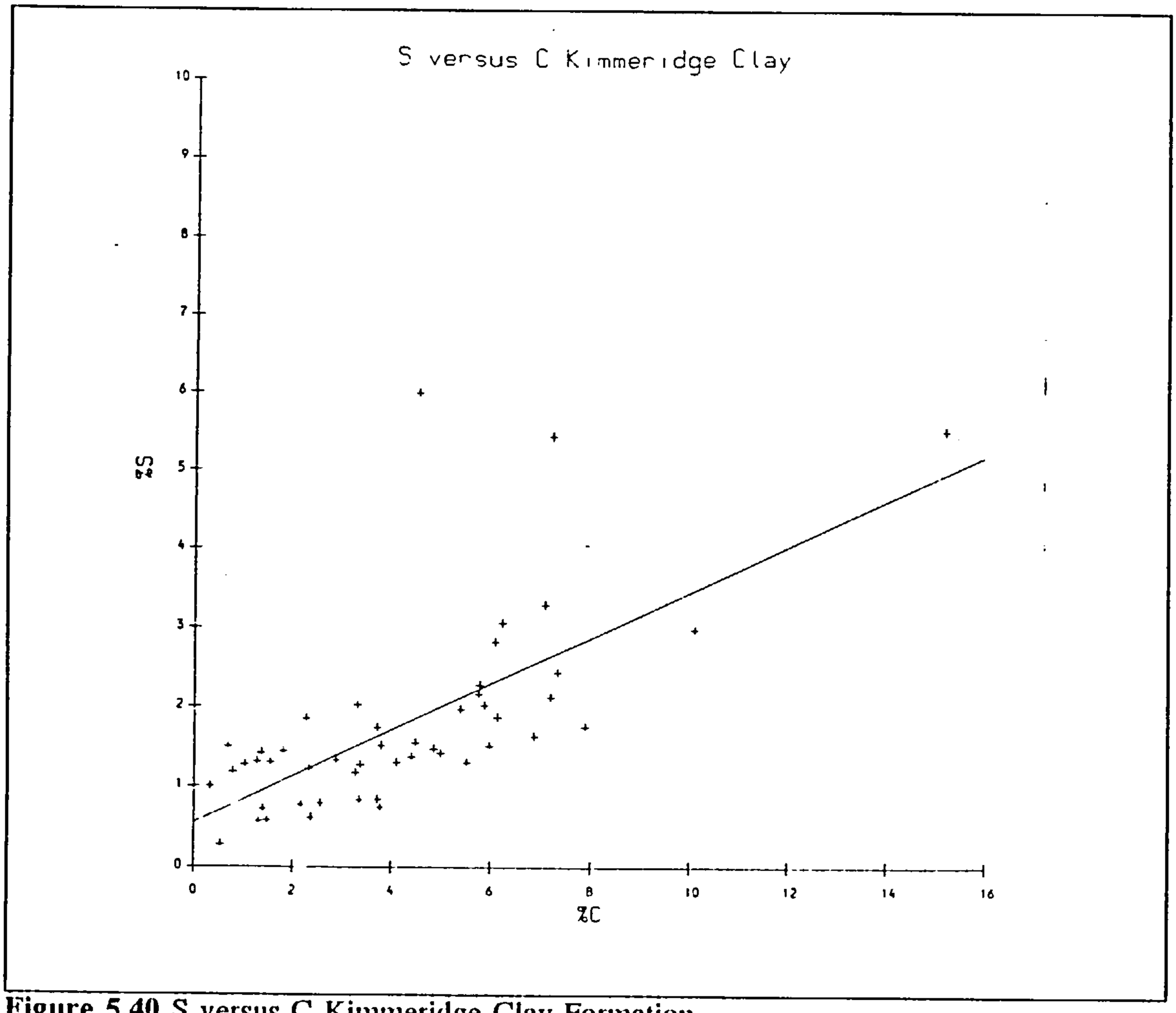

Figure 5.40 S versus C Kimmeridge Clay Formation.

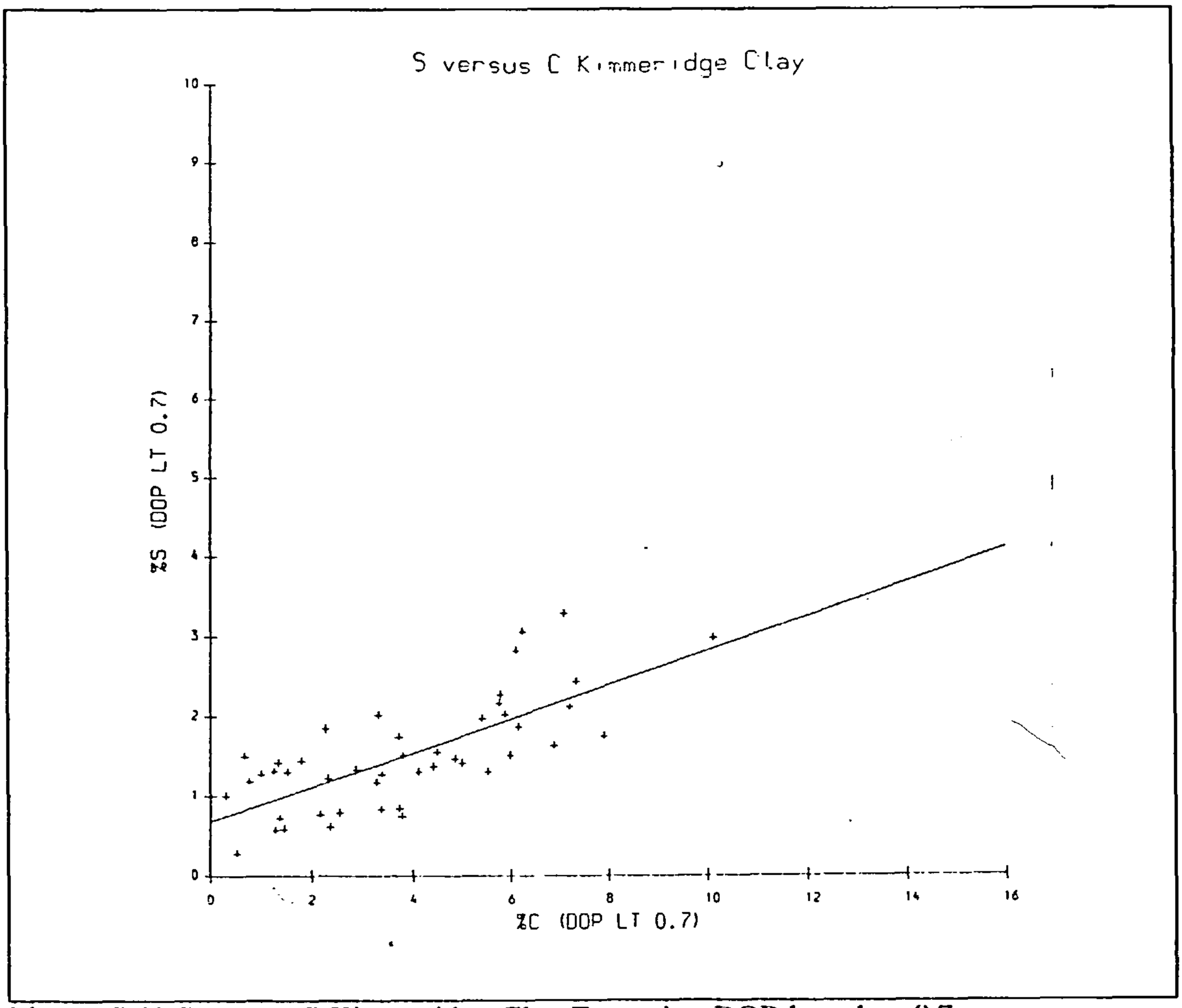

Figure 5.41 S versus C Kimmeridge Clay Formation DOP less than 0.7.

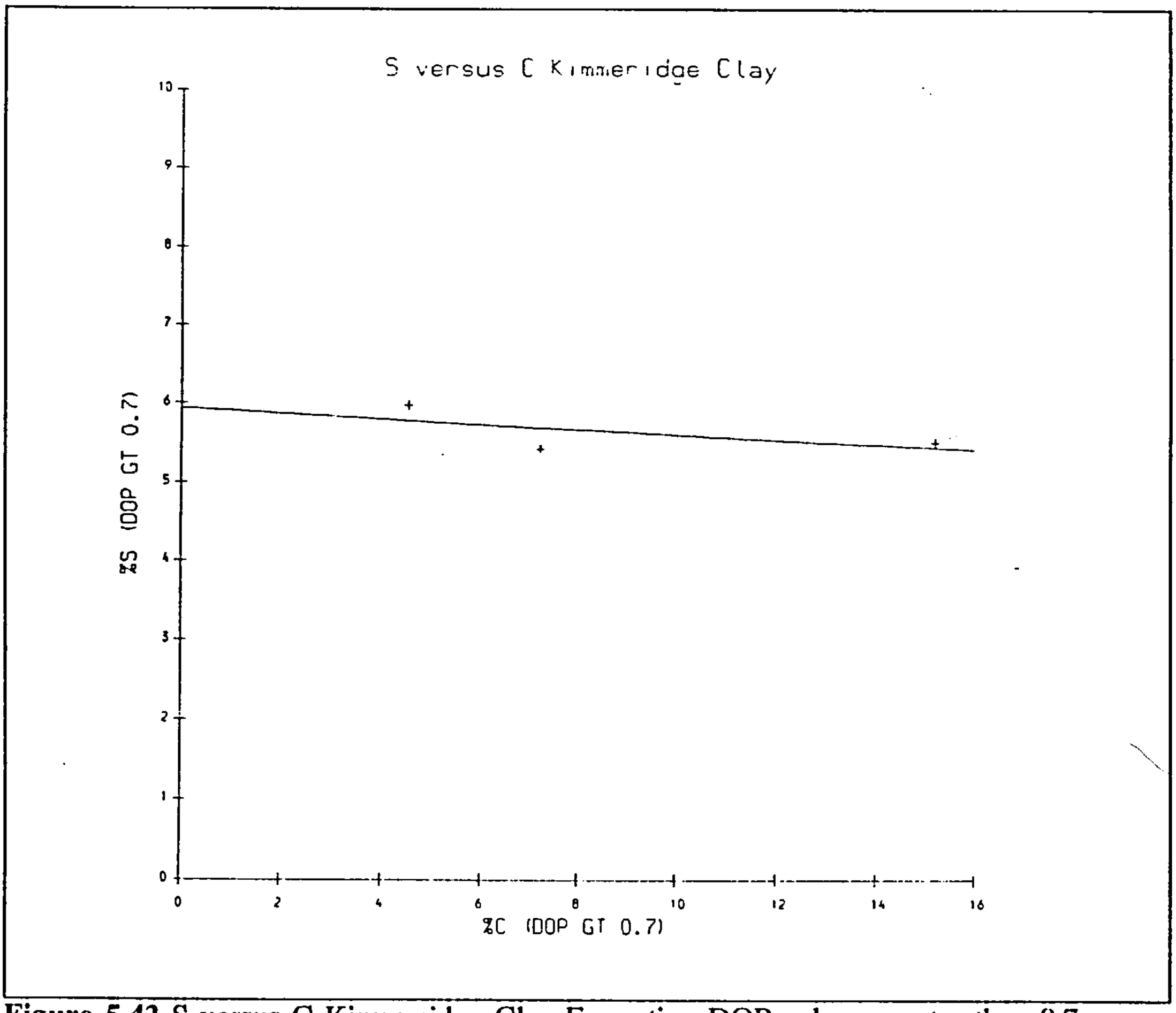

Figure 5.42 S versus C Kimmeridge Clay Formation DOP values greater than 0.7.

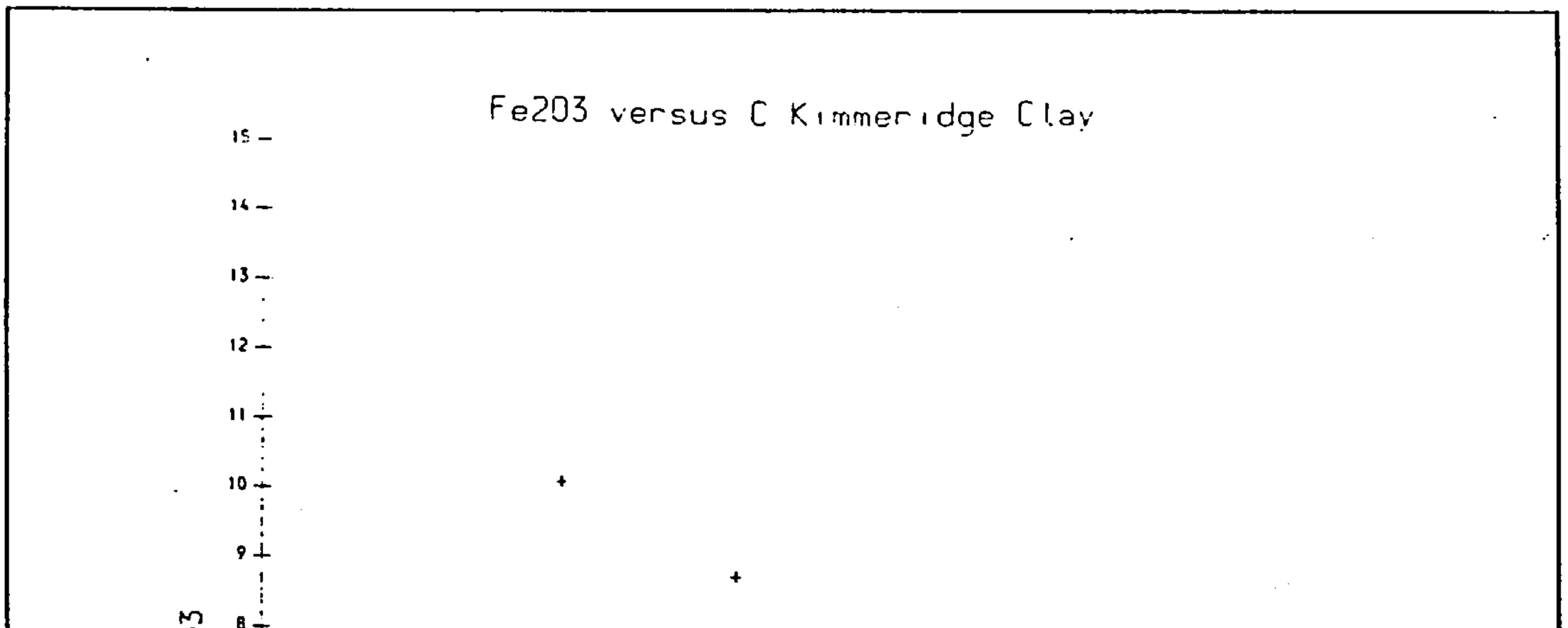

Figure 5.43 Fe_2O_3 versus C Kimmeridge Clay Formation.

R_o data for the Draupne and Heather Formations were supplied with the samples by Norsk Hydro. Those for the Kimmeridge Clay were taken from Scotchman (1987). It was necessary for the analyses presented in the Chapter 6 that each sample have an R_o value but in general only one measurement was available per well. As the depth intervals over which sampling occurred in each well were small, in most cases it was sufficient to assign to each sample in a well the same value of R_o. In cases where two or more measurements were available for a single well the missing data were estimated by linear regression. In the few cases a well had no R_o data these were estimated from the other maturity parameters (see below).

The second organic maturity parameter employed in the study is the Rock-Eval T_{max} temperature. This is the temperature of maximum kerogen cracking during Rock-Eval pyrolysis, and is a more recent technique for the determination of organic maturity (Espitalie, 1986). It is a particularly useful technique where vitrinite particles are absent or difficult to identify. T_{max} varies with lithology and organic matter type but for type II kerogen such as that found in much of the Draupne Formation oil generation is to be expected at around a T_{max} of 430-435°C with oil generation being complete at about 450°C. For the type III kerogen such as that common in the Heather Formation oil generation begins at a similar temperature and is essentially finished at about 460°C. Rock-Eval data were supplied with the majority of North Sea samples and were determined for the Kimmeridge Clay data as a part of this study.

Finally, for the Draupne and Heather Formations SCI data were also available. As with vitrinite reflectance this is an optical technique of maturity determination. During burial diagenesis and thermal maturation spore colours viewed in transmitted light change from colourless through yellow and brown to black with increasing maturity. The SCI is a commonly used 10 point scale quantifying this colour change. Oil generation begins at about 3 with the oil floor around 8. SCI data were more abundant than R_o data points but it was still necessary for some wells to estimate missing values. In these cases a similar strategy to that employed for the R_o data was adopted.

Median values for each of these parameters in the wells studied are illustrated in Figs. 5.44-5.48.

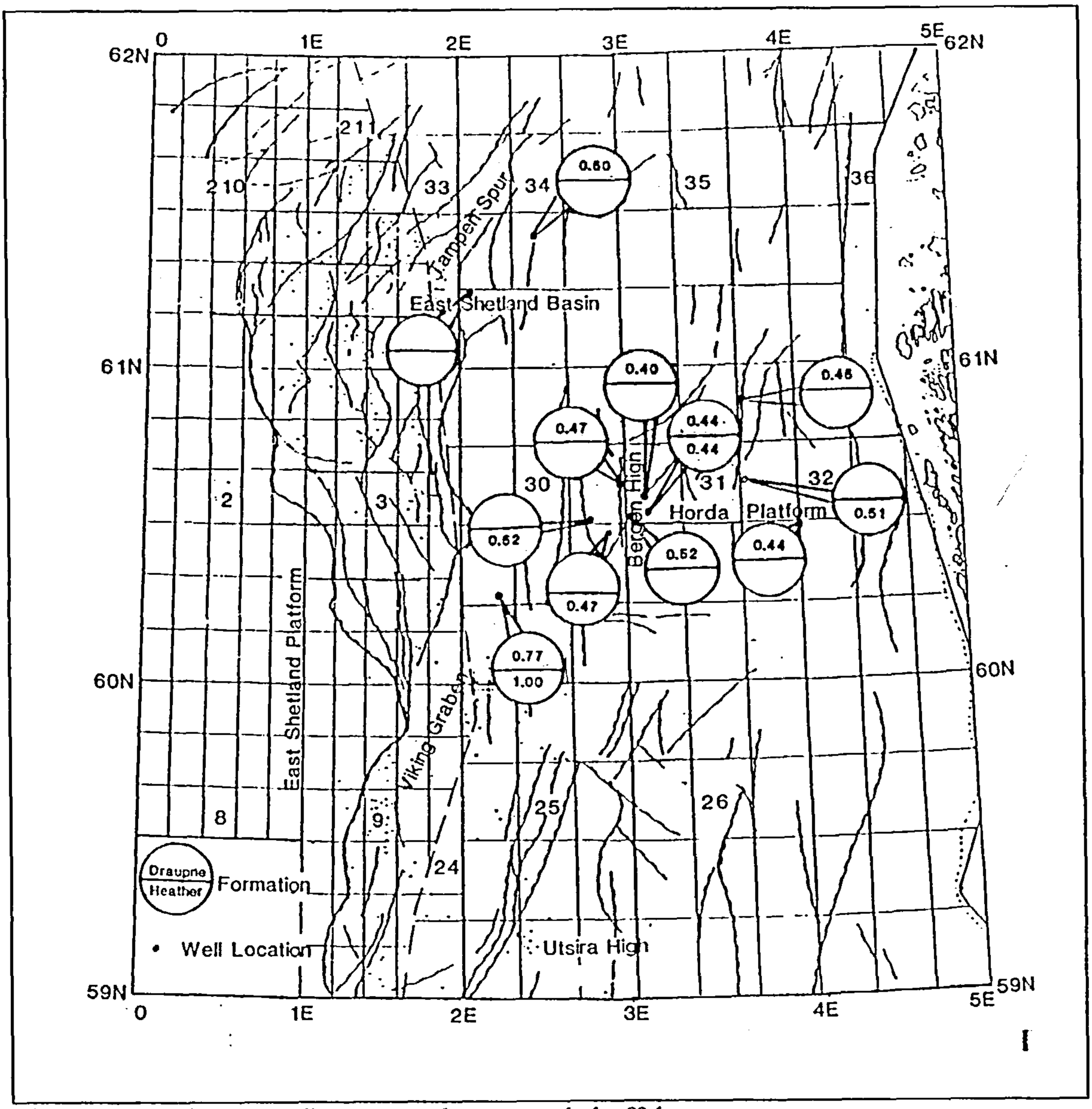

Figure 5.44 Vitrinite reflectance values recorded offshore.

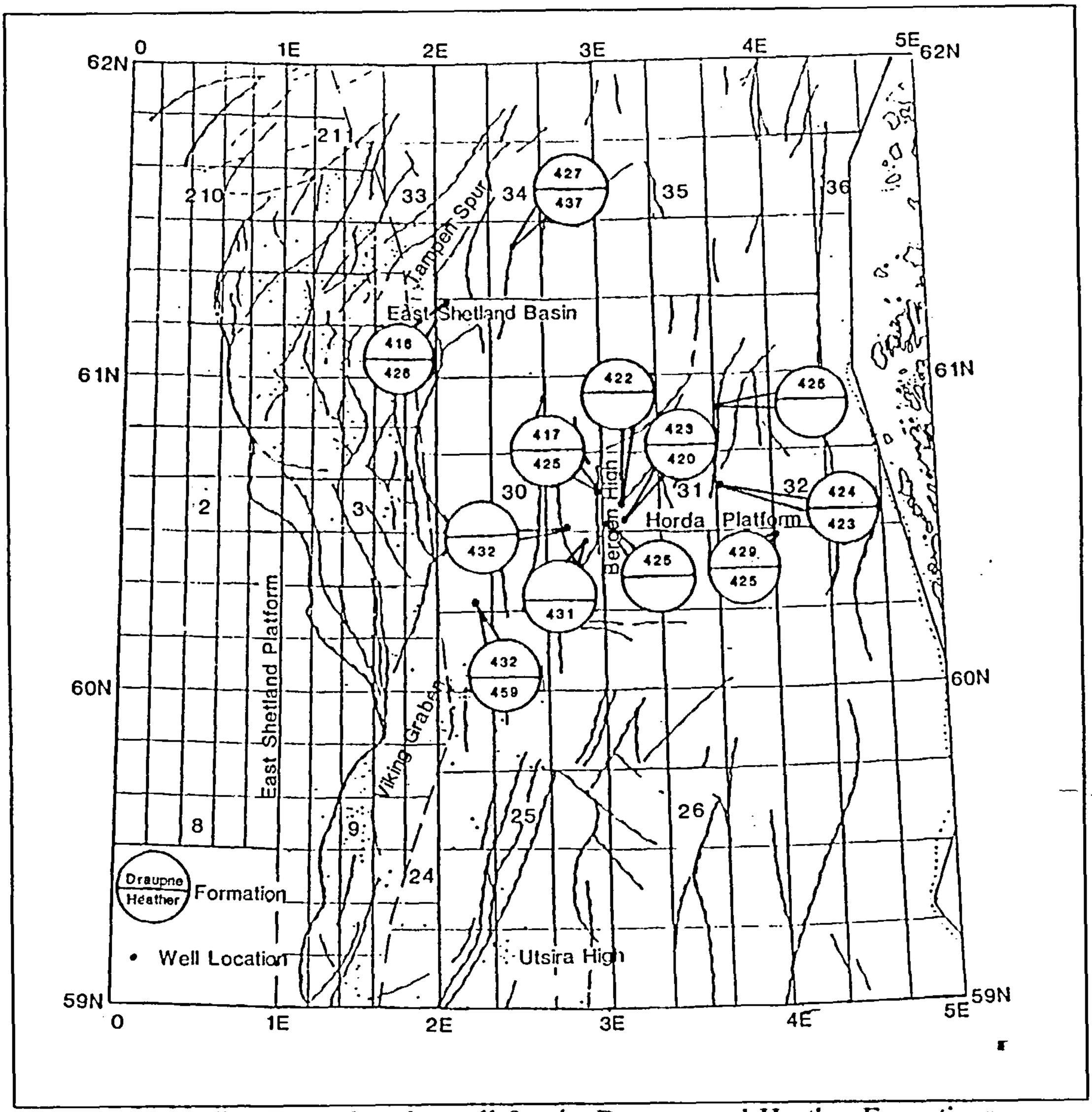

Figure 5.45 Median T_{max} values by well for the Draupne and Heather Formations.

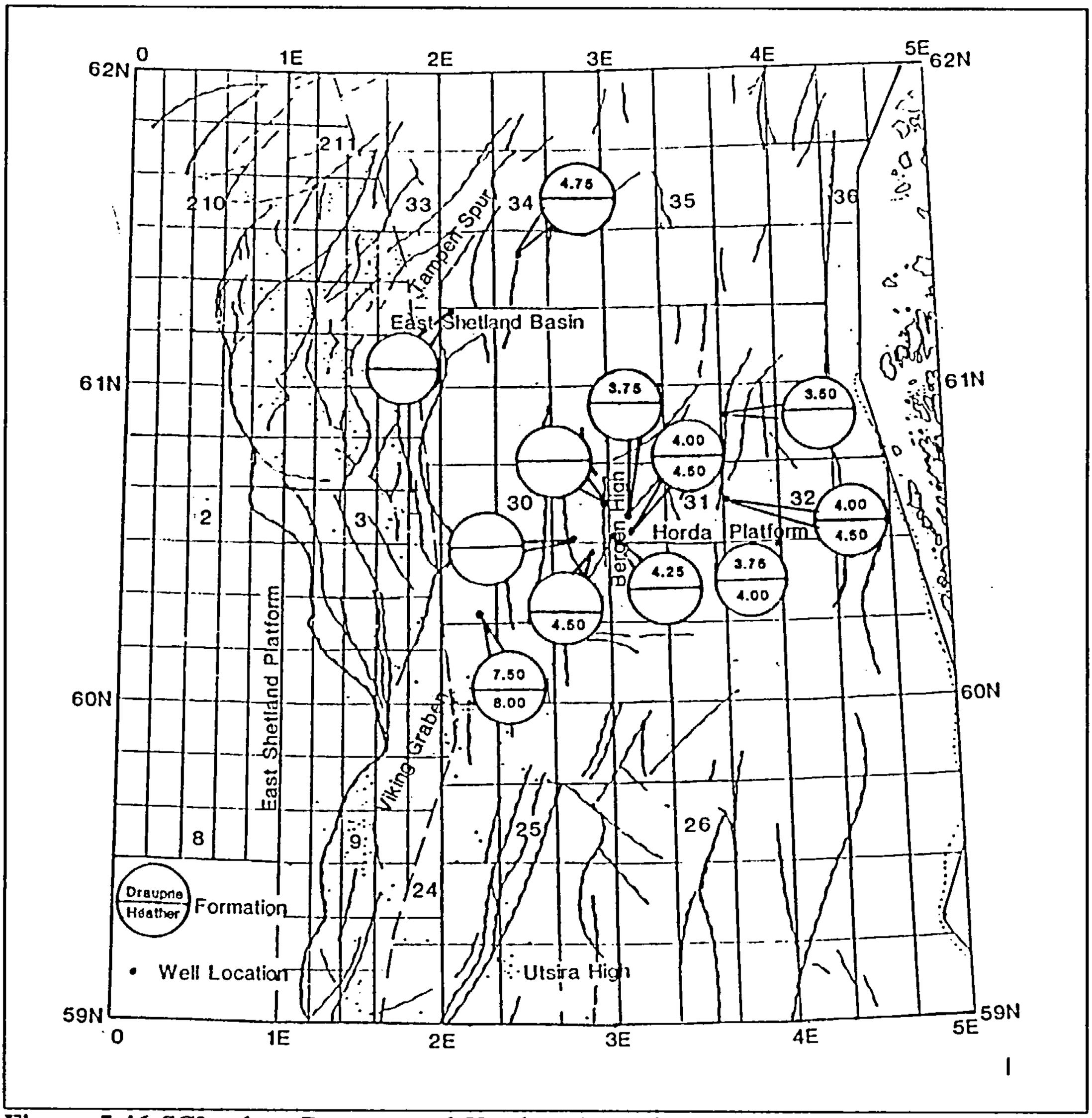

Figure 5.46 SCI values Draupne and Heather Formations (medians where more than one value per well).

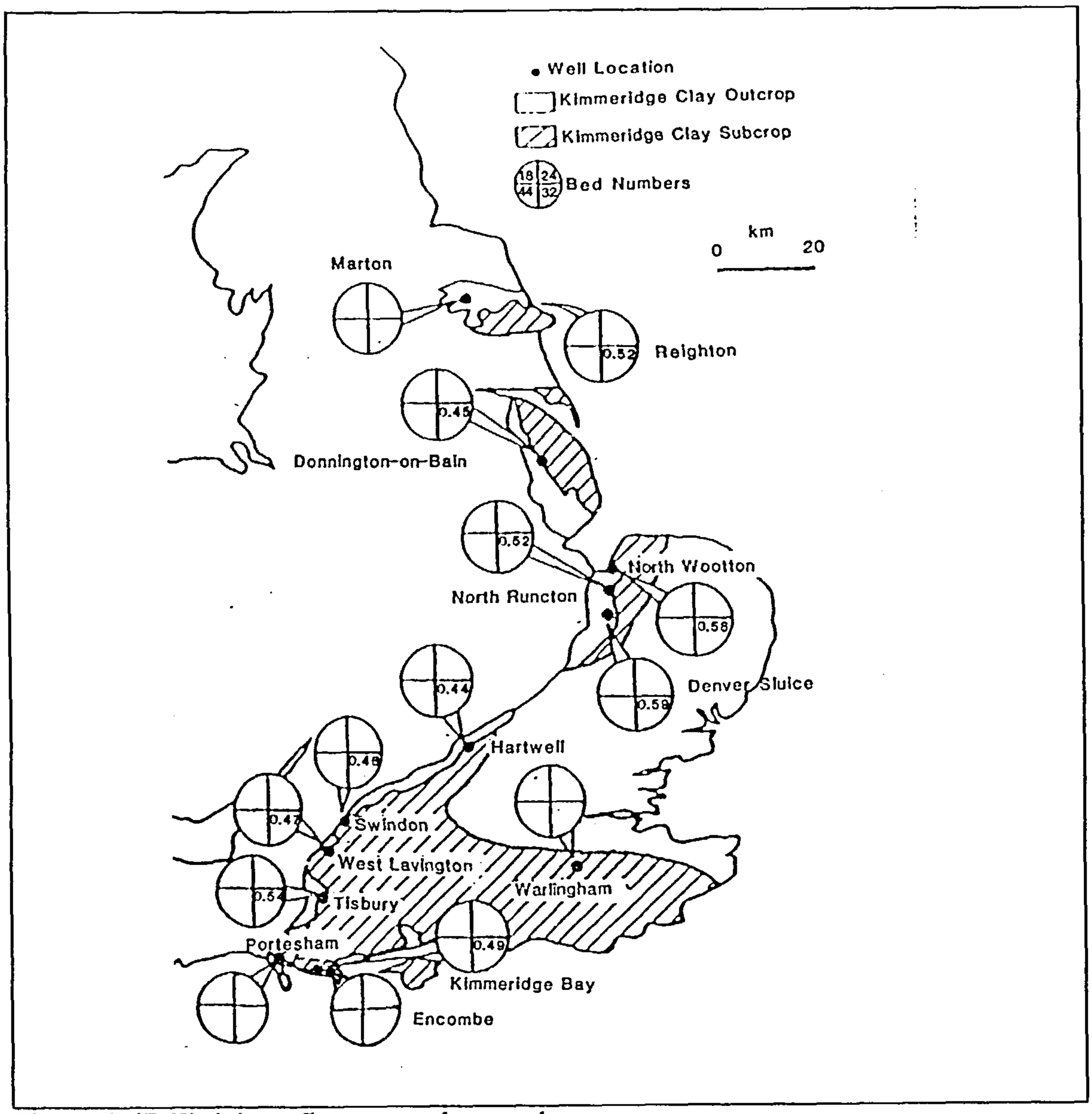

Figure 5.47 Vitrinite reflectance values onshore.

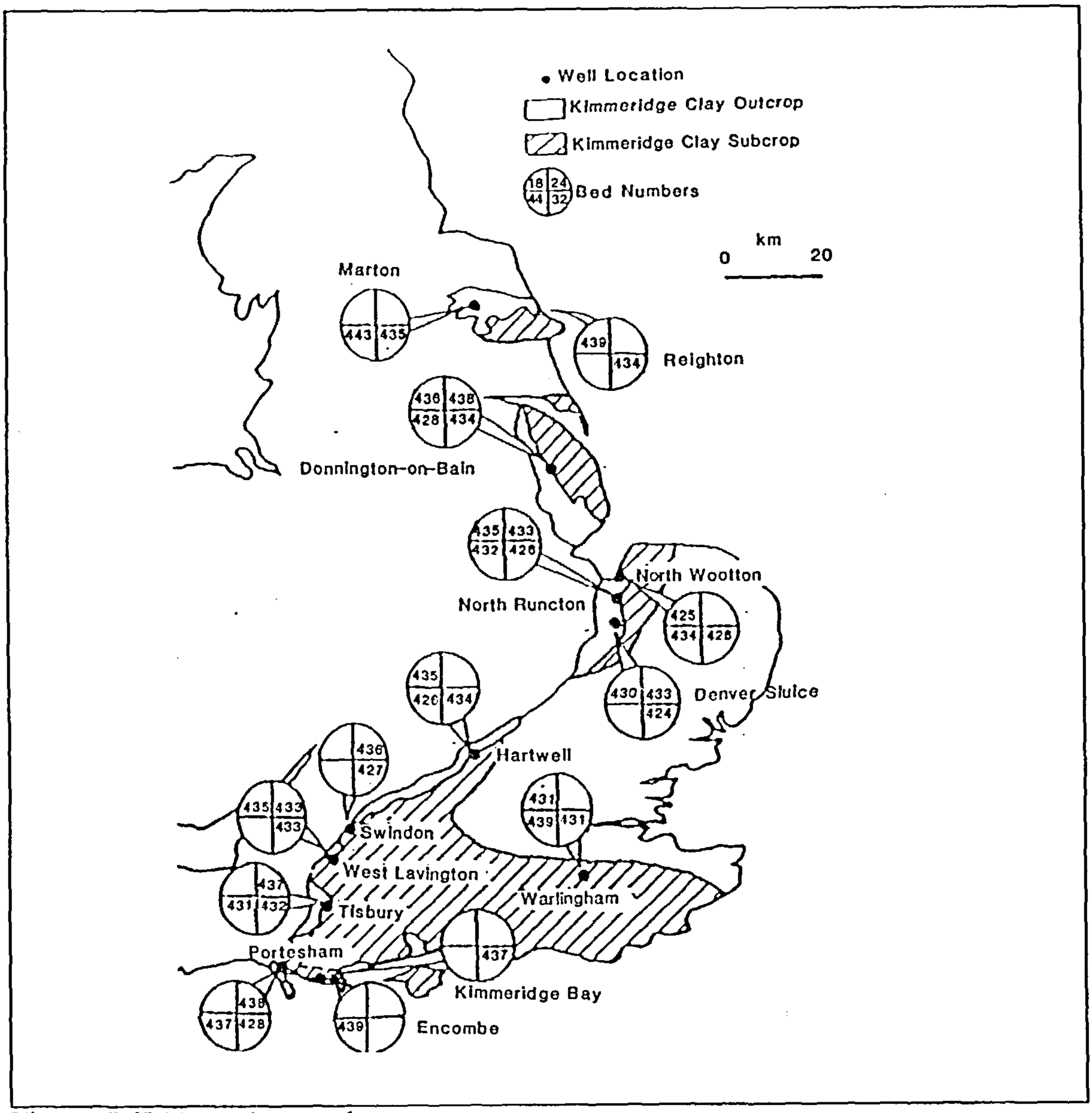

Figure 5.48 T_{max} values onshore.

5.6 Conclusions

It has been demonstrated in this chapter that variations in the grain size, sedimentological maturity, and depositional environment of the suite studied are not negligible. The geochemical effects of these variations must be considered prior to examination of the relationship between the organic maturity and the geochemistry.

In brief, the Draupne Formation is coarsest and probably most sedimentologically mature in the west of the area studied. The depositional environment of the formation varied from being normal marine over much of the Horda Platform, through more oxygen deficient conditions in intermediate areas, to anoxic and probably euxinic conditions in the Viking Graben. The Heather Formation displayed a wider range of grain sizes than the Draupne and was coarsest in the east of the area studied, fining westwards. The sedimentological maturity trend still increased westwards as in the Draupne Formation. Anoxic euxinic conditions were limited in the Heather Formation, the majority of samples having been deposited in either normally oxygenated or restricted conditions, but as in the Draupne palaeo-oxygen levels generally decreased from east to west. The Kimmeridge Clay Formation displays lateral variation in grain size and maturity along the length of the onshore outcrop studied, and also differs between beds. With the exception of Bed 32 an aerobic depositional environment seems to have been dominant for the Kimmeridge Clay as sampled. The organic rich Bed 32 appears to have been associated mainly with a restricted environment which locally gave way to anoxic or euxinic conditions.

Chapter 6

Investigation of the Factors Controlling Trace Element Geochemistry

6.0 Investigation of the Factors Controlling Trace Element Geochemistry

6.1 Introduction

In Chapter 5 variation in the physical properties and composition of the sediment suite (grain size and petrographic maturity), its depositional environment (particularly palaeo-oxygen levels), and subsequent burial history, as reflected by the extent of thermal metamorphism of the organic component have been illustrated by examining a number of parameters derived from the mineralogy and geochemistry. The aim of this chapter is to examine the importance, if any, of organic maturity as a factor influencing the trace element geochemistry of these shales. The former factors (ie sediment grain size, sediment maturity, and depositional environment) are already widely accepted as being of importance in this respect (eg Bjorlykke, 1974; Doyle and Feldhausen, 1981; Paropkari, 1990).

Ideally for such a study a sample suite should be selected which varies only in the property of interest (ie organic maturity), and which has constant grain size, composition, and depositional history. Such a sample suite may be impossible to obtain and as Chapter 5 illustrates considerable variation exists in the Upper Jurassic suite studied. A means of disentangling the effects of such variation is thus required in order that the true importance of organic maturity be assessed. The methodology employed to this aim is described below.

6.2 Statistical methodology

To simply investigate the existence of a linear relationship between two variables the correlation coefficient is the most suitable statistic (Chapter 4). The requirements of this chapter are more complex however and this elementary approach is not sufficient to elucidate the nature of the relationships studied. Multivariate regression analysis may be employed in a descriptive manner to illustrate the relationship between a single dependent variable and one

or more independent variables in addition to its widely employed predictive uses, and it is this technique which has been chosen to examine the relationships here.

6.2.1 Multivariate linear regression

The basic mathematical model of linear regression analysis is that the dependent variable (Y) is a linear function of the independent variables (the X variables):

$$Y=A+B_1X_1+B_2X_2+.....B_pX_p$$

where A is a constant and X_1-X_p are the p independent variables in the model. Estimates of B_1-B_p and A are obtained by the method of least squares (a detailed discussion of which may be found in many statistical text books).

The significance of the regression plane (whether or not it is better at predicting the dependent variable than is the mean) is usually tested by means of an analysis of variance table. Another useful way of examining the goodness of fit of a regression model is by examining the multiple correlation coefficient R and its square R^2. R measures the strength of the linear relationship between the dependent variable and the set of independent variables used in the regression model. It is calculated as the simple Pearson correlation between each Y point and the corresponding value predicted from the regression equation. The value of R varies between 0 for no linear relationship and +1 for a perfect model.

The value of R^2 (alternatively known as the coefficient of determination) is also useful as it indicates the proportion of the total variance of Y which is explained by the regression model. Again values approaching +1 suggest that the model is very successful in predicting Y whereas near zero magnitudes indicate a poor fit. As regression models usually fit the data rather better than the populations from which they are selected R^2 is often an over optimistic measure of the fit to the population as a whole. To reflect this R^2 may be adjusted to give a

more realistic measure of the success of the model. The adjusted R^2 parameter is calculated as:

$$AdjR^2=R^2-(P(1-R^2)/(N-P-1))$$

where N=the number of observations and P=the number of independent variables. Increasing the number of independent variables will always increase R^2 but the adjusted value will often reach a peak and then decrease as superfluous variables are added to the model.

The parameter directly of interest in this study is the partial correlation coefficient. This is used to measure the degree of association existing between two variables after removing the linear effect of one or more further variables. A significant partial correlation between two variables indicates that there exists a relationship between them after the linear effects of the further variables have been removed. In geological terms we can use the partial correlation coefficient to examine the strength of the relationship between organic maturity and trace element content after adjusting for the complicating effects of variation in other influential variables such as grain size and depositional environment. The partial correlation between two variables can be envisaged in a number of ways. Firstly it is the simple correlation existing between the residuals when both variables of interest are regressed against the variable or variables it is wished to partial out of the analysis. It is also the proportion by which the unexplained variance remaining in a regression model prior to entry of a variable is reduced on entry of that variable.

The magnitudes of the partial regression coefficients, the B values in the regression equation, represent the rate of change of the dependent variable as a function of the particular independent variable after adjusting for the other independent variables in the model. The magnitude of these coefficients depends entirely on the units in which the independent variables are measured and therefore in no way represents the relative importance of the

different independent variables in determining the value of the dependent variable unless all are measured in the same units.

A better way to analyse the partial regression coefficients is to standardise them, giving the values which would result if all of the variables were in standard form prior to the analysis. These standardised coefficients may then be directly compared so that the relative importance of the independent variables may be determined. Variables with very large standardised partial regression coefficients are important contributors to the predicted value and those with small coefficients have only minor importance. Even the standardised partial regression coefficients do not indicate the importance of variables in any absolute sense as all depend on the other variables present in the model.

6.2.2 Variable selection

Regression analysis requires that the variables be split into dependent and independent variables. The independent variables chosen for the model are discussed in greater detail below but are based on the parameters discussed in Chapter 5 which represent in a quantitative manner the physical and compositional properties of the sediment, its depositional environment, and its burial history. The dependent variables used in the models are the Al_2O_3 normalised trace element contents described in Chapter 3 and in log transformed form in Chapter 4. The choice of which variables to assign to a dependent or independent status is not one which can be made on statistical grounds but is based on an *a priori* knowledge of trace element geochemistry. The properties represented by the independent variables are widely accepted as being of importance in controlling trace element geochemistry whilst the converse, that the trace element content of a sediment is in some way a controlling factor on (for example) its grain size or burial history is patently absurd.

In Chapter 5 a large number of parameters were examined, many of which purported to measure the same property of a sediment. There were for example 3 measures of grain size

and 5 of depositional environment. This was desirable because of the averaging effect inherent in considering a number of independent measures of the same property, all of the parameters probably being imperfect measures. Many of the parameters were highly intercorrelated and indeed it would be disconcerting were they not. Highly correlated independent variables may cause problems in regression analysis however because multicolinearity results in the estimates of the regression coefficients being unstable. This factor, and the large number of possible X variables to be included in the model could make interpretation difficult and it was thought to be advantageous at this stage to reduce the number of independent variables to one for each of the properties of the sediment under investigation. One variable would then represent grain size, one sedimentological maturity, one depositional environment, and one organic maturity.

This variable reduction could have been achieved simply by selecting one parameter from each group in an arbitrary fashion but this would lose the benefit of the averaging effect discussed above. The preferred solution was to calculate new variables which retained the maximum of the information conveyed by the original parameters. This was performed by means of principle components analyses (eg Till and Colley, 1973; Le Maitre, 1982). Principle components analysis involves transforming the original variables into a new set, the principle components, which are linear combinations of the original variables and which are uncorrelated with each other. The principle components are conventionally listed in order of decreasing variance hence the first component displays the greatest variance and conveys more of the original information than any other of the components. Usually a small number of principle components convey nearly all of the original variance and may thus be used in the place of a larger number of original variables without losing much of the original information thereby simplifying interpretation. It is this variable reducing property which is of use here.

Principle components analysis may be performed using either the correlation or covariance matrices, the latter being preferred when all variables are measured in the same units. For this

study the correlation matrix has been used (the variables have effectively been standardised) giving the same weight to each of the original variables as there is no evidence that any of the parameters are more reliable than any of the others.

For each formation studied a principle components analysis has been performed for each group of parameters summarised in the previous chapter (ie for the grain size indices, the sedimentological maturity indices, the depositional environment indices and the organic maturity indices), and the first principle component resulting from each analysis has been selected to represent the original group of variables in the regression analysis. The new variables have been named Gnsize1, Sedmat1, Depenv1, and Orgmat1 respectively. In addition a principle components analysis has been performed on the CaO/Al_2O_3 and CO_2/Al_2O_3 ratios to give a measure of the carbonate content, the subsequent new variable being named Carbs1. Principal component loadings are given in Table 6.1

High scores on Gnsize1 result from a coarse grain size, Sedmat1 is highest in those observations thought to be most sedimentologically mature, Depenv1 is highest for observations which had the most reducing depositional environment, and Orgmat1 is greatest for those samples with the highest organic maturity. Carbonate rich samples are represented by high scores on Carbs1.

The pristane/phytane and authigenic U variables were omitted from the principle components analyses for all formations because their inclusion would have resulted in too great a number of missing values. Lack of mineralogical data for the Kimmeridge Clay Formation also resulted in the (quartz+feldspar/clay) ratio being omitted from the grain size analysis for this formation, the CIA value being the only sedimentological maturity parameter used. The organic maturity analysis was performed using only R_0 and T_{max} as no SCI data were available for this formation.

Table 6.1 Principal Components Loadings

Draupne Formation:

$$Gnsize1=0.61(SiO_2/Al_2O_3)+0.51(TiO_2/Al_2O_3)+0.61(quartz+feldspar/clay)$$

$$Sedmat1=0.71CIA+0.71(quartz/feldspar)$$

$$Depenv1=0.61(V/Cr)+0.54(Ni/Co)+0.59DOP$$

$$Orgmat1=0.63R_o+0.64SCI+0.45T_{max}$$

$$Carbs1=0.71(CaO/Al_2O_3)+0.71(Mineral\ C/Al_2O_3)$$

Heather Formation:

$$Gnsize1=0.62(SiO_2/Al_2O_3)+0.60(TiO_2/Al_2O_3)+0.51(quartz+feldspar/clay)$$

$$Sedmat1=0.71CIA+0.71(quartz/feldspar)$$

$$Depenv1=0.56(V/Cr)+0.62(Ni/Co)+0.55DOP$$

$$Orgmat1=0.59R_o+0.58SCI+0.56T_{max}$$

$$Carbs1=0.71(CaO/Al_2O_3)+0.71(Mineral\ C/Al_2O_3)$$

Kimmeridge Clay Formation:

$$Gnsize1=0.71(SiO_2/Al_2O_3)+0.71(TiO_2/Al_2O_3)$$

$$Depenv1=0.43(V/Cr)+0.56(Ni/Co)+0.70DOP$$

$$Orgmat1=0.71R_o-0.71T_{max}$$

$$Carbs1=0.71(CaO/Al_2O_3)+0.71(Mineral\ C/Al_2O_3)$$

As all of the variables in each group are claimed to measure the same property the first principle component should account for all of the original variance. In practice this ideal is not reached and the first component usually accounts for not the theoretical 100%, but 60-80% of the variance of the original variables. The new variables resulting from the principle components analyses are still intercorrelated to some extent but the magnitudes of the correlation coefficients are much lower than previously.

6.2.3 Running the analyses

In using linear regression analysis a number of assumptions are made about the data (strictly about the population from which the data were selected). The technique is robust as is illustrated by its widespread use and deviations from these assumptions are not usually critical. Firstly we assume that the variance of the dependent variable (Y) is constant over the range of the independent (X) variables studied. This assumption is not very important as it does not produce a biased estimate of either A or the B coefficients even if violated hence no effort has been made to ensure compliance.

Secondly we assume that the Y variable is normally distributed when we make tests of hypotheses concerning the model. Small deviations from this assumption are not thought to seriously alter inferences from the model if the sample set is sufficiently large. The Y values in this study have been transformed to approximate normality in most cases by a log transformation to meet this requirement. No formal tests of normality have been made because of the uncertainty over suitable probability levels to be used in such tests. The data have been also been screened for outliers, and observations which are unusual or unduly influential have been examined and removed if necessary so that their effect on the parameter estimates may be judged. In most cases these were not seriously perturbed. Outliers were detected by means of examining the distributions of the residuals, unusual values by observing the Mahalanobis Distance statistic, and influential points by examining the Cooks Distance statistic.

Thirdly and possibly of greatest importance is the assumption of linearity in the relationships under study. This is checked for in residual and partial regression plots and in the few cases where non-linearity is apparent further transformations have been applied in attempts to coax the relationship to linearity.

The principle components and linear regression analyses were run using the SPSSX statistical package. Rather than include all of the independent variables in each model the important variables were selected from amongst those thought to be possible influences (gnsize1, sedmat1, depenv1, orgmat1, and carbs1) by means of stepwise selection. In this process the first variable to be selected is that with the highest magnitude correlation coefficient with the dependent variable. This is selected provided that it produces a significant regression at the 95% significance level. A second variable, having the highest partial correlation with the dependent variable is then chosen from among those remaining, on the condition that its selection significantly improves the model (95% level). Following selection of a second variable the first is re-examined, and if its deletion would significantly improve the model (90% significance level for removal) it is removed, and so the process continues. For each step the variables not in the model are examined and the best is selected subject to the entry requirements, following this those variables already in the model are examined and removed subject to satisfying the removal criterion. The process continues until no more variables can be entered or removed.

Missing values were dealt with on a pairwise basis, that is all observations were included if they had a value for a particular trace element and values for each of the independent variables whether or not the observation had a complete set of measurements for other trace elements. A consequence of this is that differing numbers of observations were used for different variables even within the same formation with the result that significance levels may vary slightly for equal correlation coefficients.

6.2.4 Path analysis

The raw output supplied by the SPSSX package contains all of the necessary information concerning the regression models, but the form in which it is produced is not ideal for easy comparison. In order to better display the relationships present between the trace element contents and the independent variables in the formations studied the technique of path analysis has been used. To the author's knowledge this is the first application of this technique to a geological data set. Path analysis is briefly explained by Afifi and Clark (1984), and in greater detail by Dudley Duncan (1966), and is a way of clearly representing the structure of a (possibly) complex set of causal relationships. To paraphrase the latter author path analysis as a statistical technique adds nothing to conventional regression analysis, but as a pattern of interpretation it is invaluable in making explicit the rationale for a set of regression equations.

It should be noted at this point that the presence of a correlation between two variables is no proof of causality; it indicates only that a linear relationship exists between the two variables. The causal structure of the model must be supplied by the investigator and as in the choice of dependent and independent variables for the regression analyses it must in this case be based on a knowledge of sedimentary geochemistry and the factors likely to control the abundance of trace elements.

Path analysis is based on the assumption that certain variables in a set, the dependent variables, may be completely determined as linear functions of other variables in the set, the independent variables. The independent variables may be intercorrelated as in regression analysis but this is not considered for explanation. To ensure complete determination of the dependent variable it is permissible and indeed usually necessary to include a residual variable which is uncorrelated with the other independent variables of the set and which represents the effect of relevant factors not included specifically in the model.

Path analysis is best suited to graphical illustration in path diagrams. In these representations of the model straight, one way, arrows are used to link the independent variables to those dependent variables over which they have influence. Correlations between independent variables not themselves influenced by other variables in the system are illustrated with curved, two headed arrows linking the two correlated variables. In order to illustrate the influence of the various independent variables on the dependent ones the straight arrows indicating causality are labelled with path coefficients which are in fact the standardised partial regression coefficients discussed earlier. Positive coefficients occur when the dependent variable increases with increasing values of the independent variable. A negative path coefficient is used when the dependent variable decreases with increasing magnitudes of the independent variable. The curved arrows between independent variables are labelled with the Pearson correlation coefficients between the two variables. To complete the diagram the residual variable is included and the arrow between it and the dependent variable is labelled with the proportion of the standard deviation of the dependent variable not explained by the other variables in the model. This is calculated as the square root of $1-R^2$.

Only variables which significantly contributed to the models were included in the path diagrams, these being chosen by the stepwise procedure. The diagrams have also been labelled with the average values of the dependent variables (trace element contents) in each of the formations allowing easier comparison to be made.

6.3 Commentary on the path diagrams

In the discussion accompanying the path diagrams a number of points need be noted. Firstly there are no perfect regression models, all of the path diagrams being subject to variation as particular observations are included or excluded from the models. Examination suggests that they are relatively stable and not overly sensitive to the inclusion or exclusion of individual points except where noted.

Greater weight has been attached to models which explain a large proportion of the original variance (ie those having a high value for R^2) as in these cases the models fit the data well and it is likely that all of the important factors controlling an element's behaviour have been included. Conversely where the fit is poor it seems likely that one or more important variables have not been considered and are represented in the analysis by the residual variable 'other'. In such cases it might be unwise to base any interpretations on the model alone.

Finally particular attention has been applied to finding consistent patterns of behaviour for each element in all three formations studied as these may be applicable to all organic rich mudrocks, or even mudrocks in general. The presence of a statistically significant relationship in one of the formations need not mean that any geologically significant relationship exists, but if the same relationship is found in all three formations it is much more likely to be of geological importance.

6.3.1 Group 1: Elements influenced by Depenv1

On the basis of their path diagrams the elements Cu, Ni, V, U, Mo, Zn, and Cd may be grouped together. In general these elements produce well fitting regression models in which Depenv1 is the dominant variable. The path diagram illustrated immediately below, for Cu in the Draupne Formation shows that the Depenv1 variable has roughly twice the influence over the Al_2O_3 normalised Cu content than does Gnsize1. The two independent variables here are to all extents uncorrelated. The Other variable represents the extent to which the model fails to predict the Cu content successfully due to the effect of controls not included in the model; these other factors may only be speculated upon.

Draupne Formation

Median Cu=63ppm

n=58, R^2=0.76

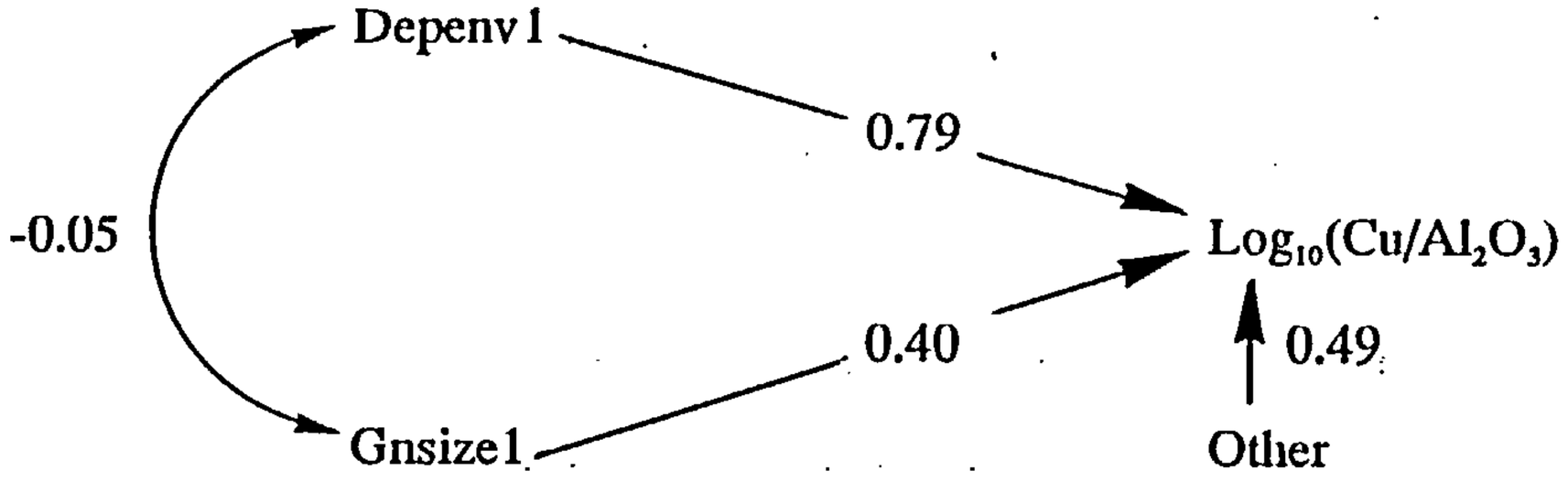

Heather Formation

Median Cu=44ppm

n=61, R^2=0.78

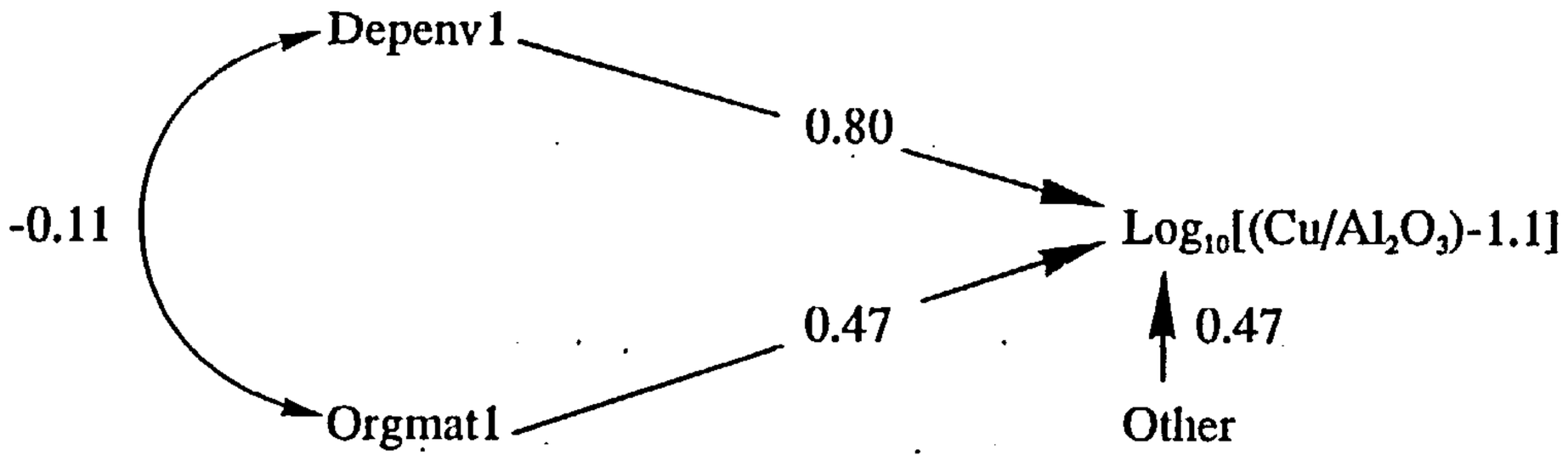

Kimmeridge Clay Formation

Median Cu=37ppm

n=49, R^2=0.53

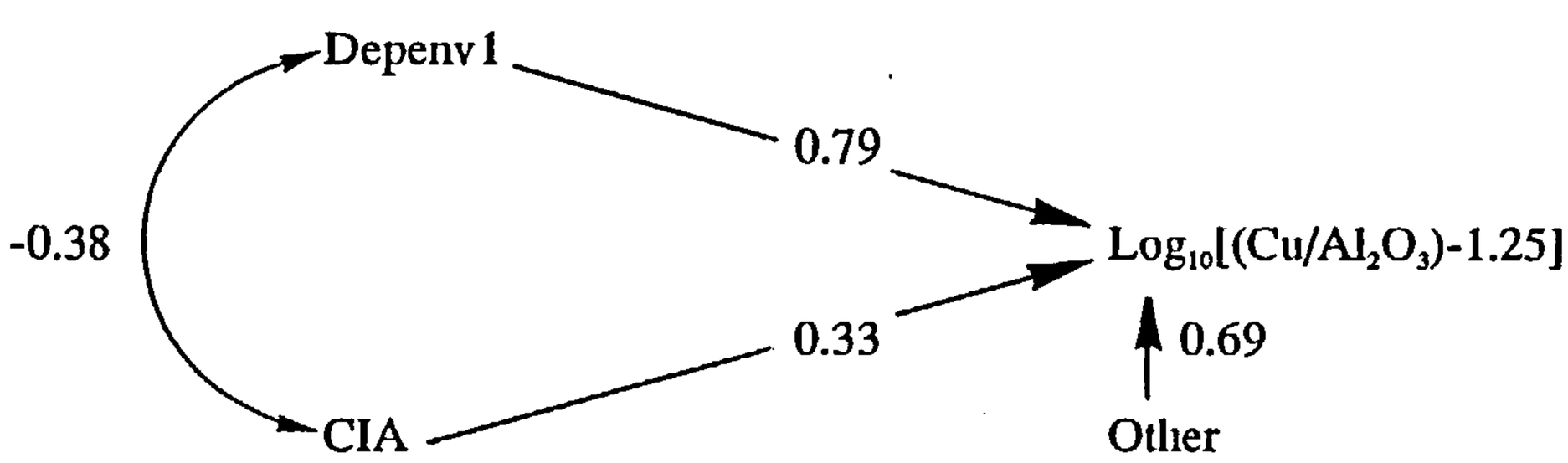

For Cu the model fit is best for the Draupne and Heather Formations while that for the Kimmeridge Clay Formation is a little poorer. Despite this, and the variation in median Cu contents all of the formations have similar path diagrams in which the Depenv1 variable is the most influential of the independent variables, having large, positive path coefficients. The next most influential variable differs between the formations but in each case it has only approximately half of the influence of Depenv1.

The Ni path diagrams are very similar to those of Cu in both goodness of fit and variable selection, and as before the fit for the Kimmeridge Clay Formation is worse than for the two North Sea formations. The selection of variables and their relative importance differs only in the inclusion of Orgmat1 in the Draupne Formation where it has a negative path coefficient.

Draupne Formation

Median Ni=162ppm

$n=57$, $R^2=0.79$

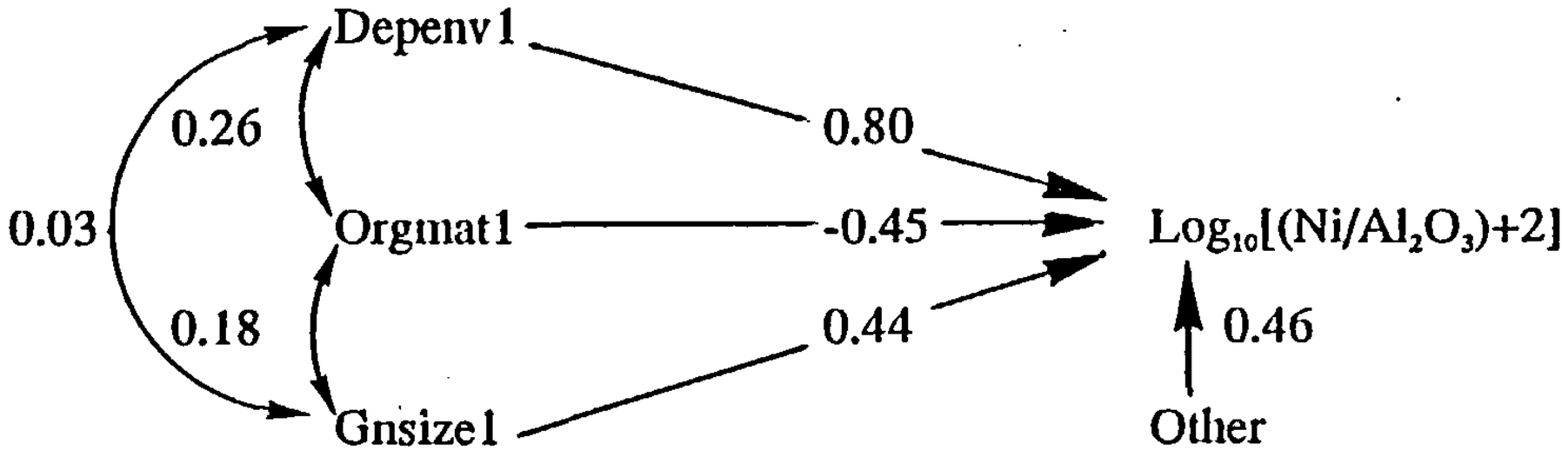

Heather Formation

Median Ni=78ppm

n=57, R^2=0.75

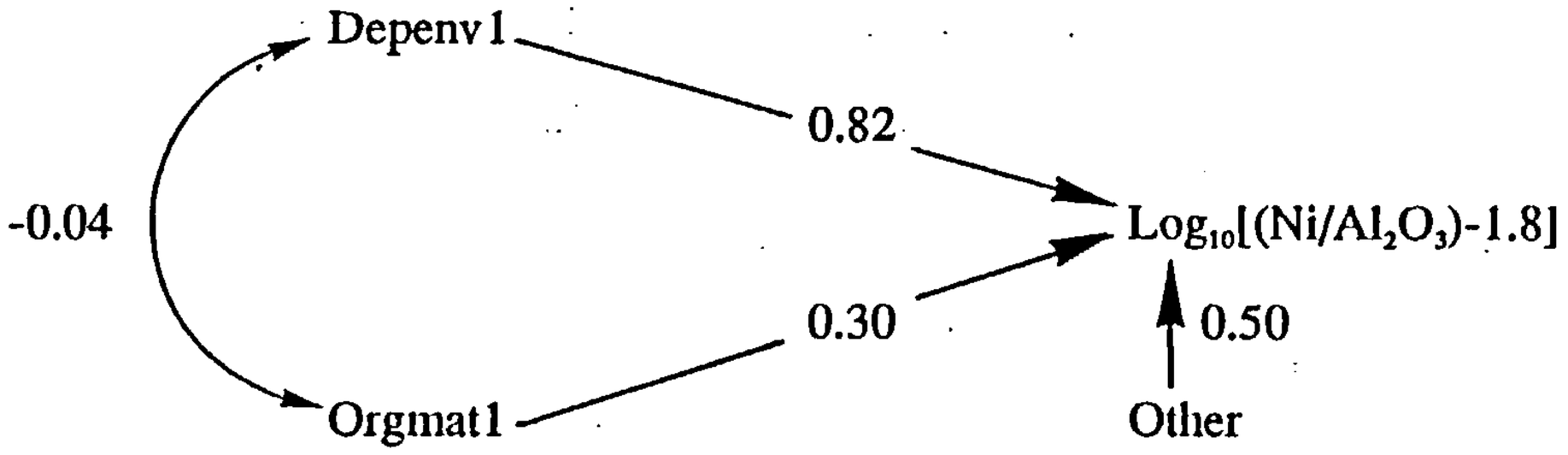

Kimmeridge Clay Formation

Median Ni=60ppm

n=44, R^2=0.58

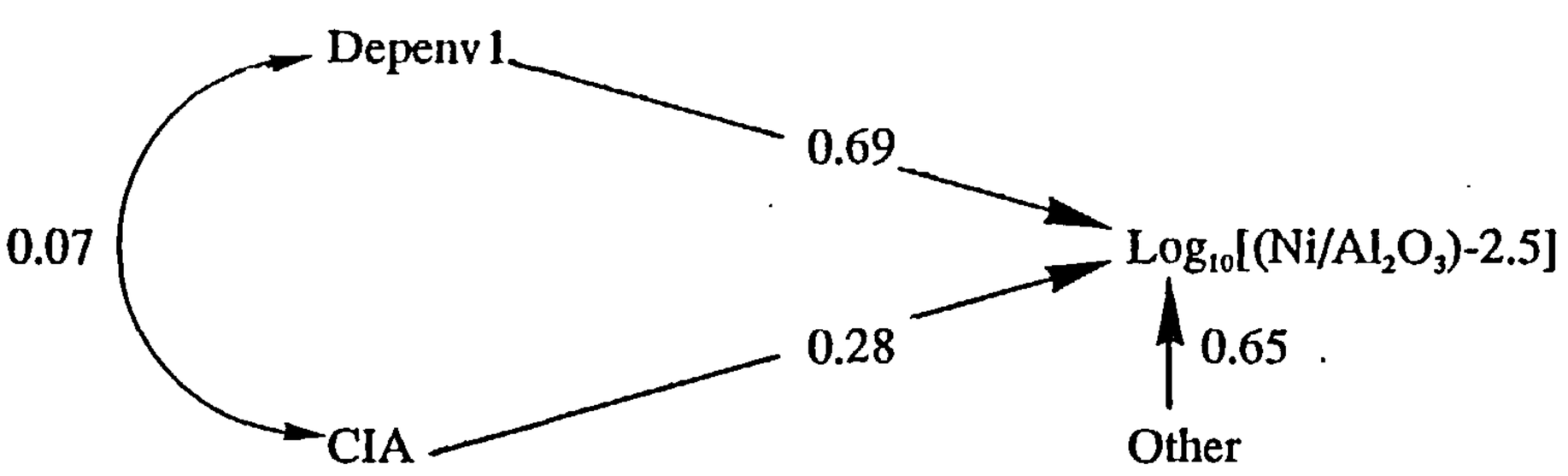

V also has path diagrams of similar structure to those of both Cu and Ni. The variables selected match those for Ni except in the Kimmeridge Clay Formation where the fit is poor. For the Draupne and Heather Formations the path coefficients related to Depenv1 are some four times as great as the next most influential variables. In the Kimmeridge Clay Formation the only selected variable is the CIA. This model is however sensitive to the presence of one observation with a high V content and having a high score for Depenv1. Inclusion of this very influential point will cause the selection of Depenv1 as the variable of most influence, with CIA subordinate to this, and will raise the value of R^2.

Draupne Formation

Median V=592ppm

n=58, R^2=0.74

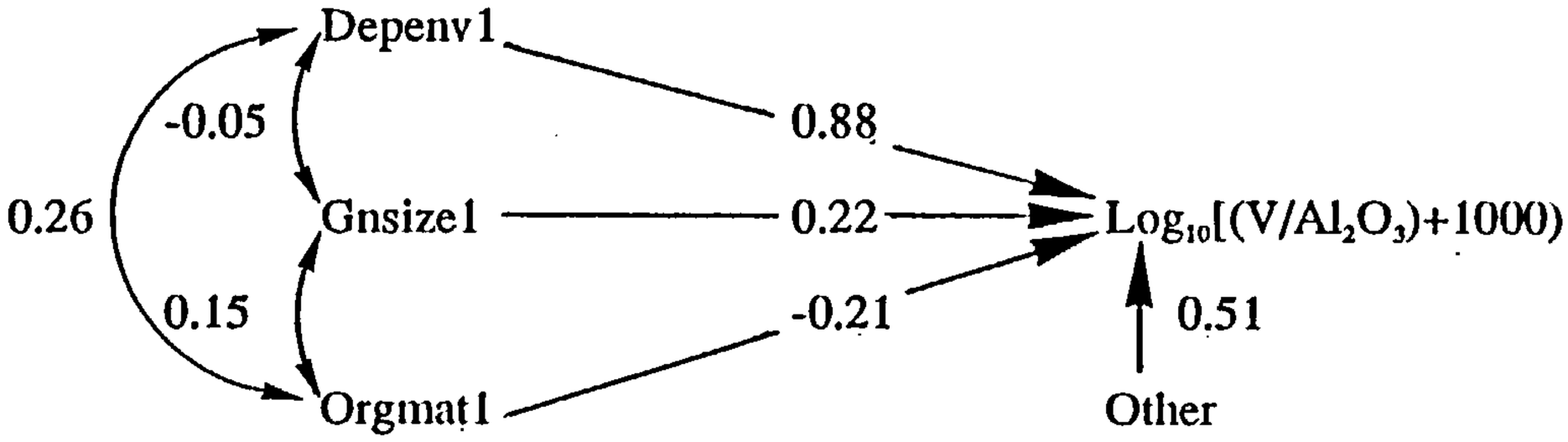

Heather Formation

Median V=200ppm

n=56, R^2=0.75

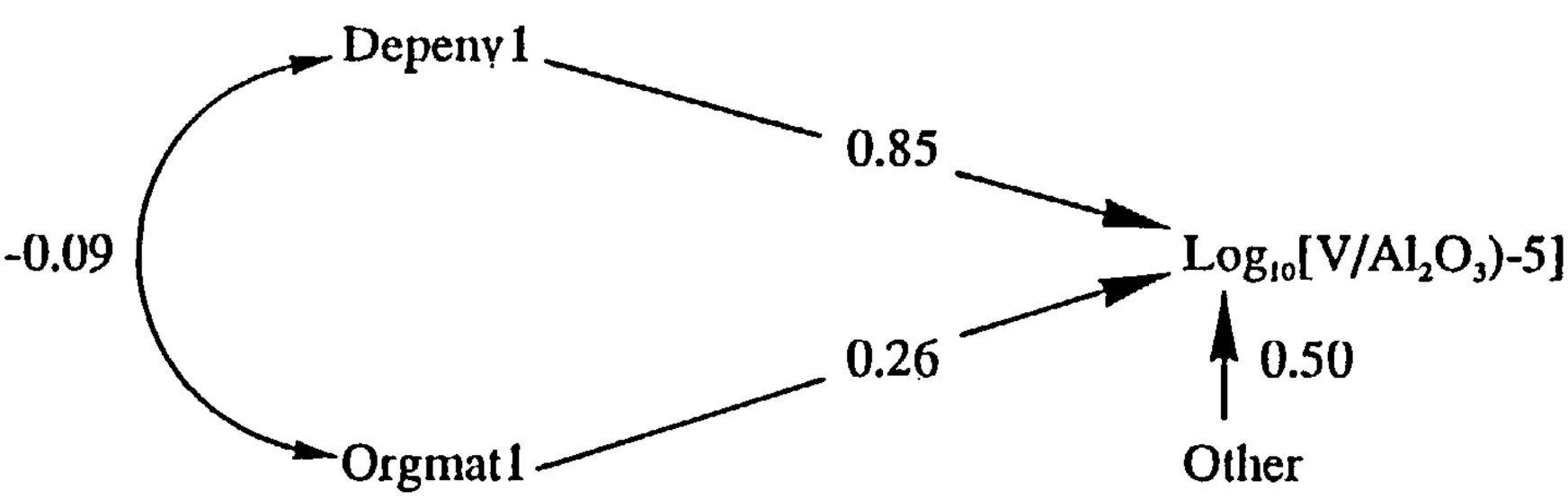

Kimmeridge Clay Formation

Median V=140ppm

n=46, R^2=0.28

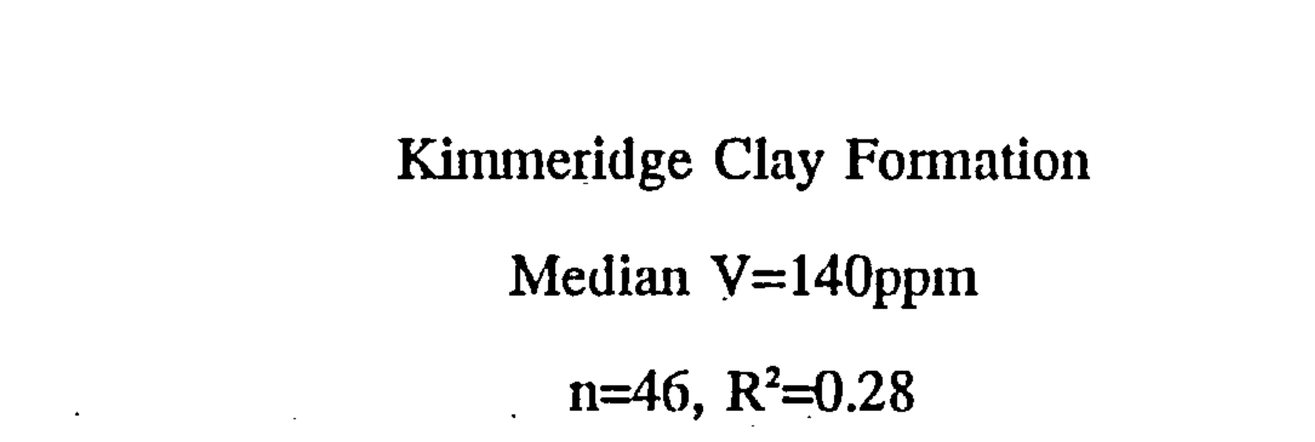

The Mo path diagrams are similar to those of Cu, Ni, and V in that Depenv1 is selected in all three models, but the similarities are not as great as those existing within those three elements. The Mo path diagrams are notable because of the very wide range in average Mo contents that they cover. In the Draupne Formation where the Mo content is very high the pattern is similar to those seen before, with Depenv1 being roughly twice as influential as the next most important variable.

In the Heather Formation which has the lowest Mo content the maturity parameter has been transformed to increase linearity and has displaced Depenv1 from the position of greatest importance. The fit for this formation is also poorer than for the preceding elements although it is still reasonable, the model having accounted for about 50% of the original variance of the dependent variable.

Conversely the fit for Mo in the Kimmeridge Clay is slightly better than in the previous models and Depenv1 is the only variable of significance. The Kimmeridge Clay Formation model is once more subject to variation depending on the inclusion or exclusion of one influential observation. If it is included then Orgmat1 is selected alongside Depenv1 with a small negative path coefficient. As the model is illustrated, with the sample omitted Orgmat1 is not quite significant.

Draupne Formation

Median Mo=85ppm

n=53, R^2=0.76

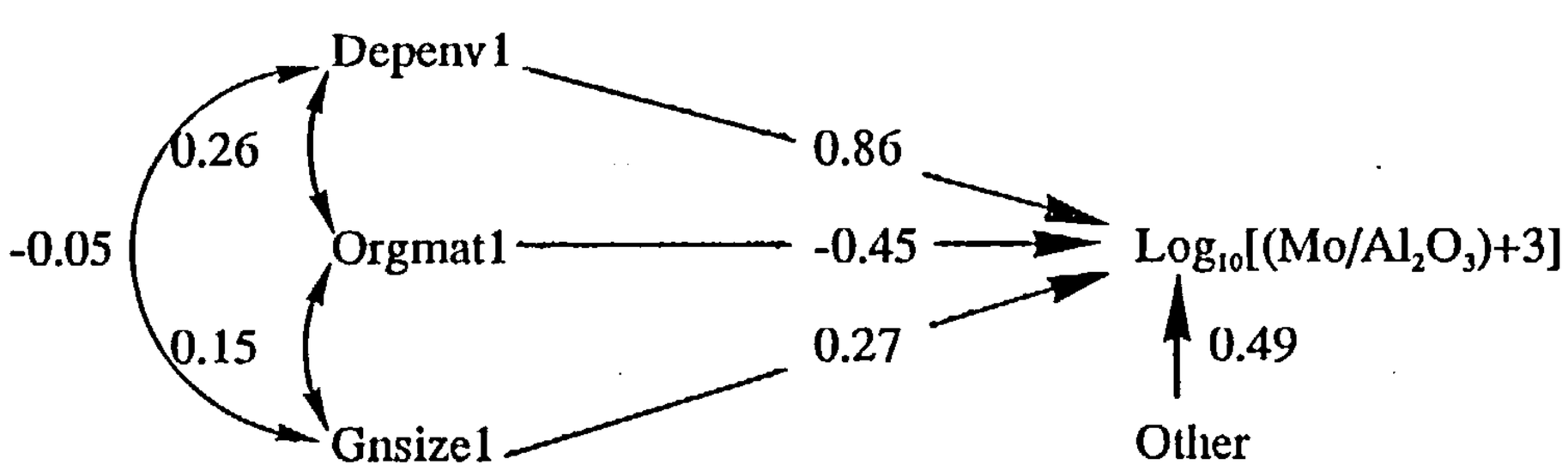

Heather Formation

Median Mo=4ppm

n=44, R^2=0.46

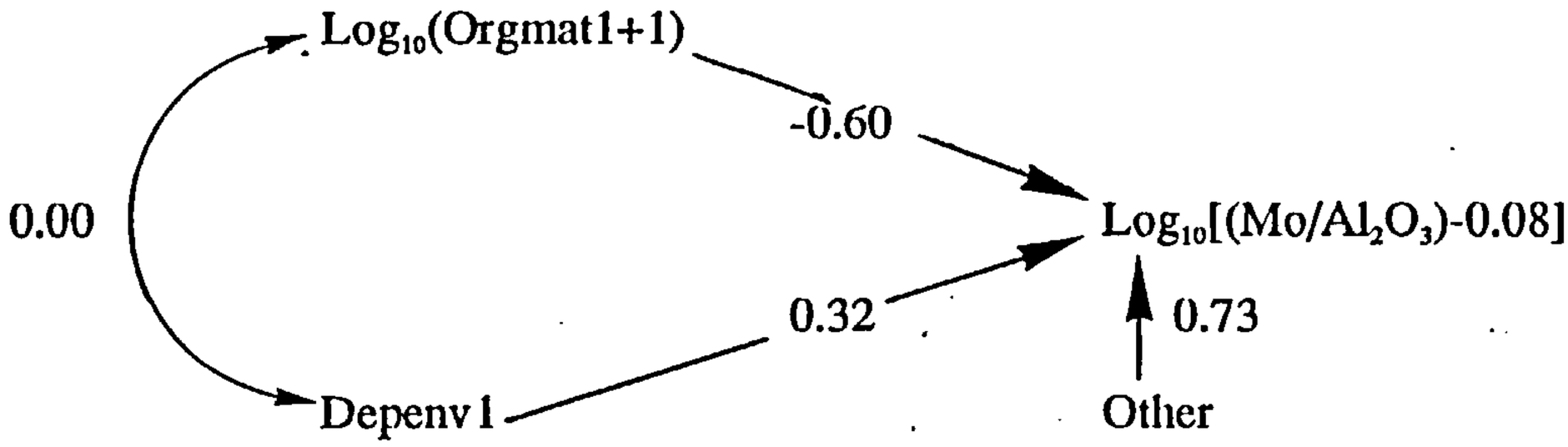

Kimmeridge Clay Formation

Median Mo=7ppm

n=49, R^2=0.60

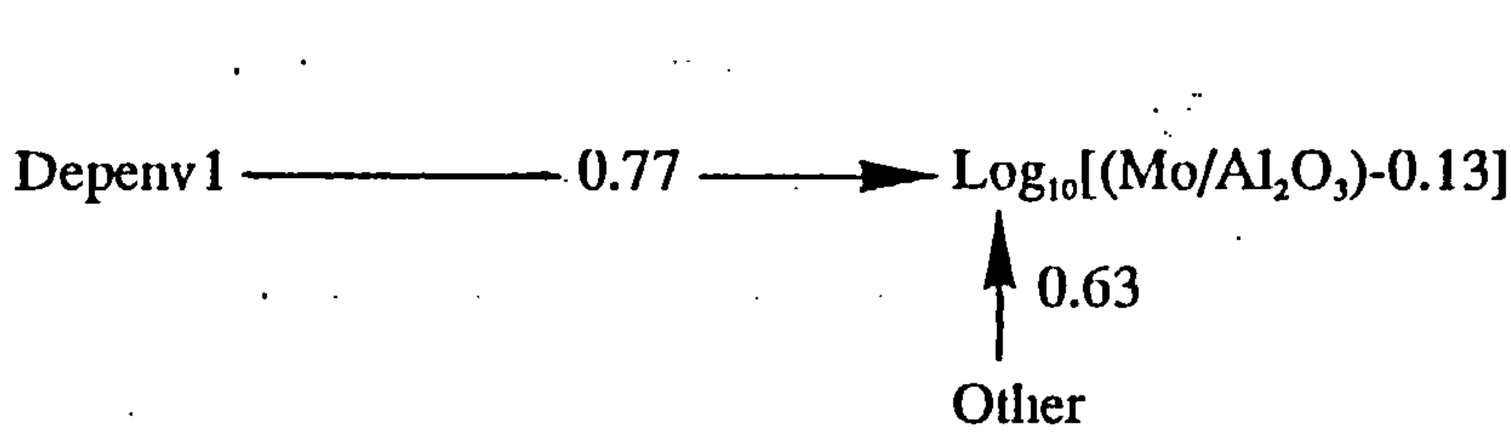

U, like Mo is not so closely related to Cu, Ni, and V. For U the fit is again good for the Draupne Formation in which it is enriched to a great extent, and Depenv1 is by far the most important variable. For the Heather Formation which has a much lower U content the fit is barely significant although the Depenv1 variable is still selected. The fit is slightly better for the Kimmeridge Clay Formation despite a similar U content. Two variables of roughly equal importance have been identified here, these being Carbs1 (selected for the first time) and Depenv1.

Draupne Formation

Median U=20ppm

n=50, R^2=0.76

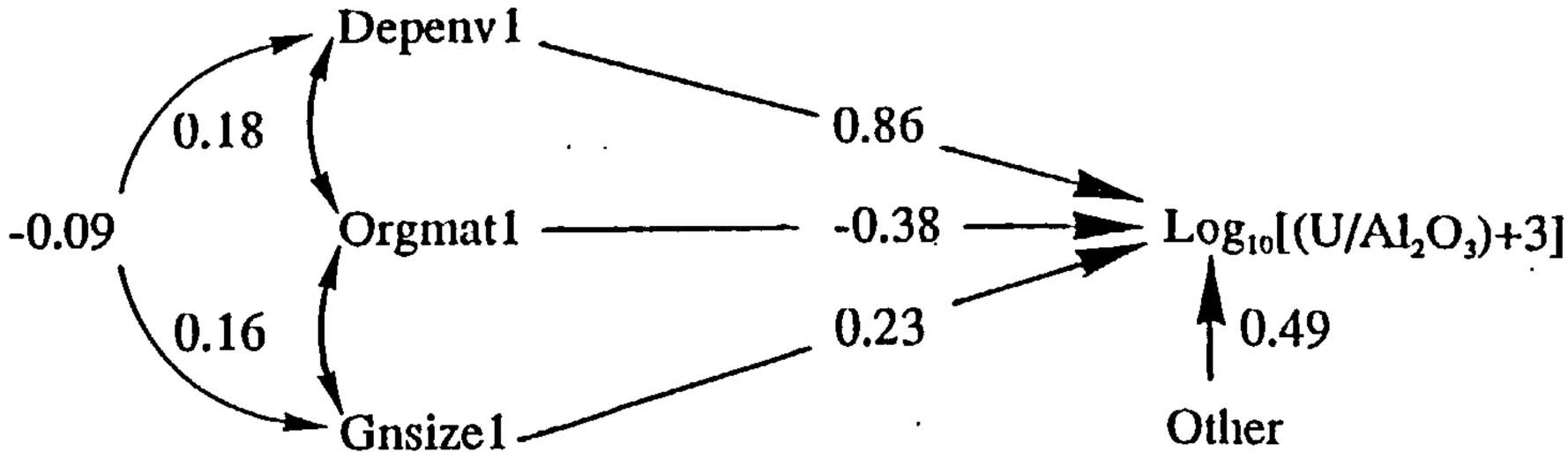

Heather Formation

Median U=5ppm

n=47, R^2=0.15

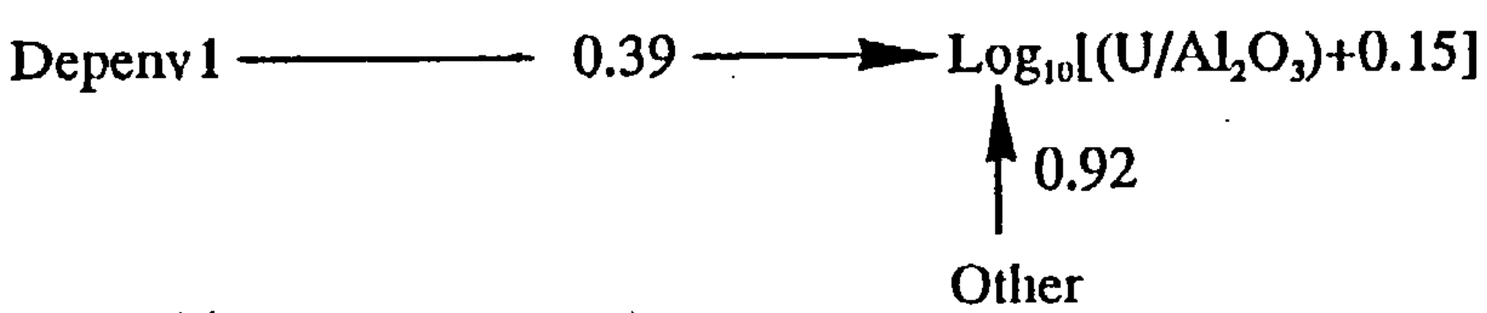

Kimmeridge Clay Formation

Median U=5ppm

n=49, R^2=0.35

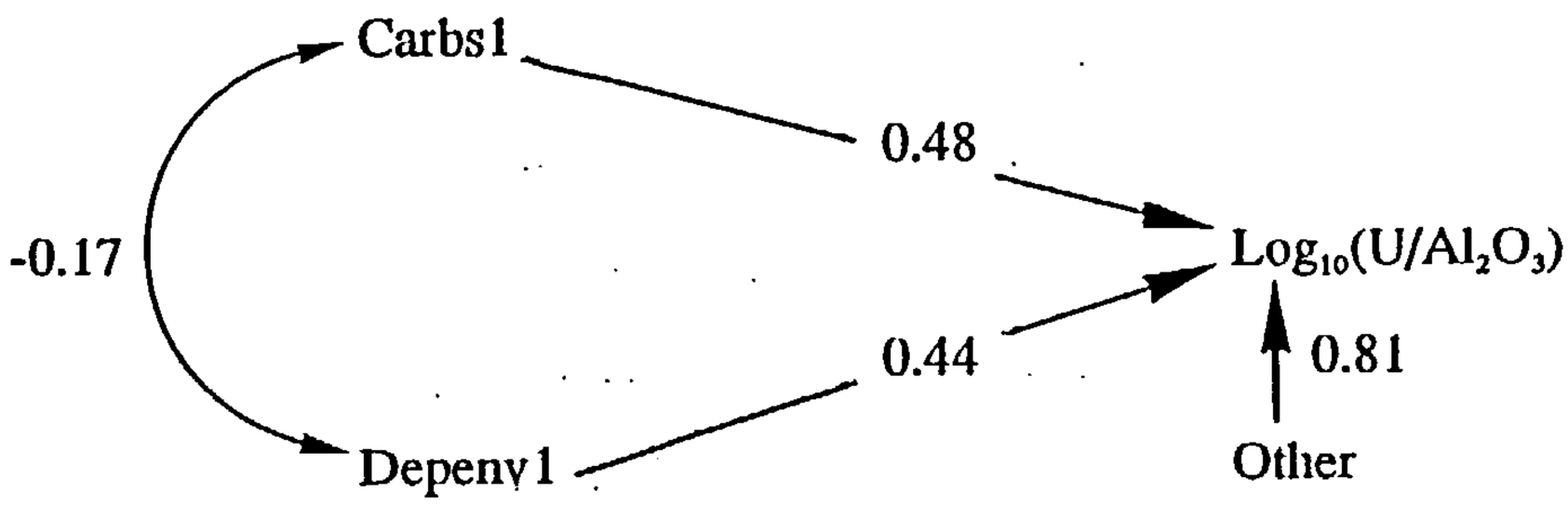

The path diagrams for Zn show that the regression models do not generally fit as well as for Cu, Ni and V except in the Draupne Formation where Zn is most enriched. Zn is included however on the grounds of the consistent selection of Depenv1. For the Draupne Formation the maturity variable was transformed somewhat in an attempt to induce linearity in a relationship which appeared non-linear.

Draupne Formation

Median Zn=328ppm

n=56, R^2=0.73

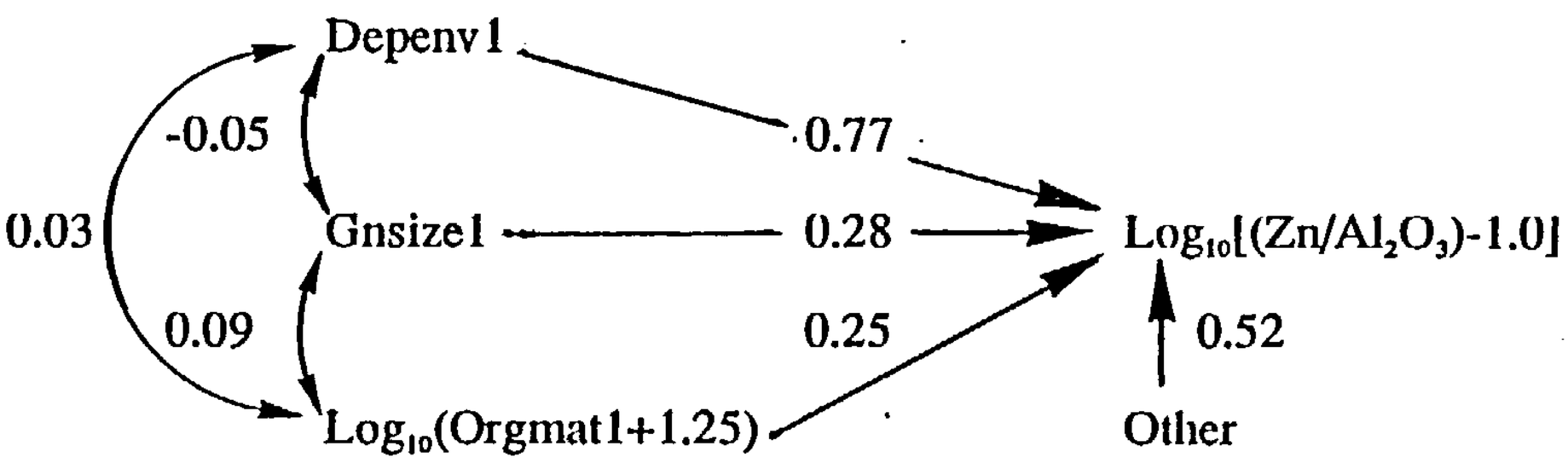

Heather Formation

Median Zn=131ppm

n=58, R^2=0.44

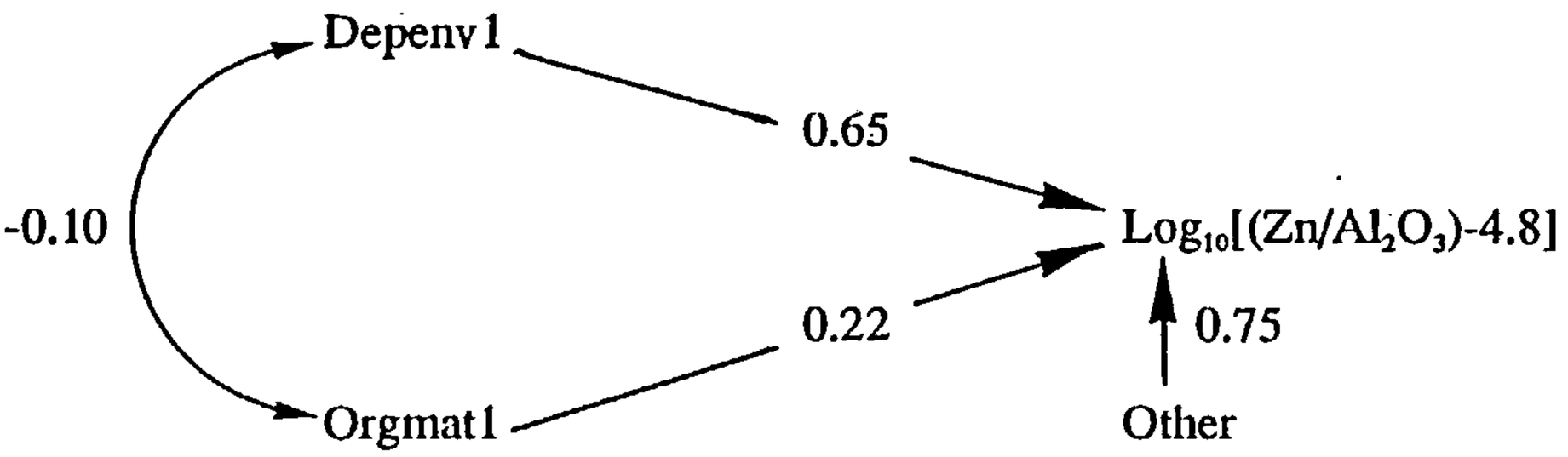

Kimmeridge Clay Formation

Median Zn=79ppm

n=47, R^2=0.26

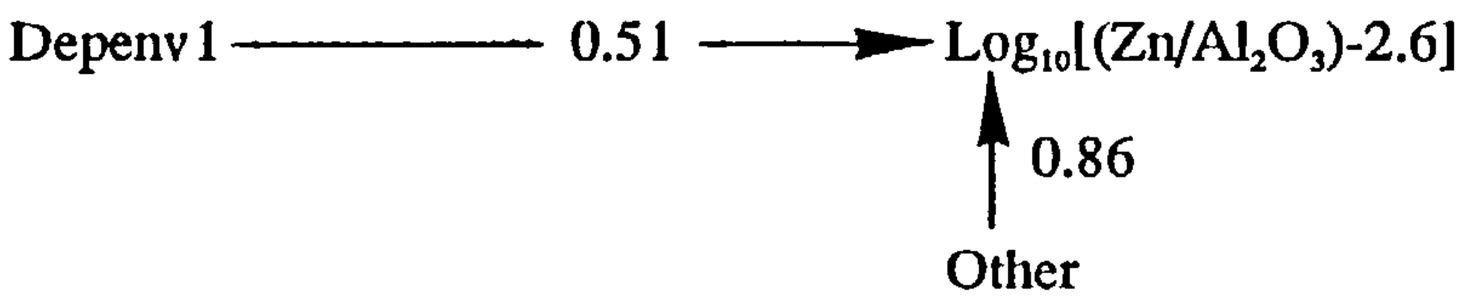

The goodness of fit of the models is ranked in the same order as the Zn contents suggesting that the models fit best at high Zn contents where the depositional environment is by far the most important factor. At lower Zn contents the depositional environment remains the most influential of the independent variables considered, but as the models explain less of the variation in Zn content other variables not included in the current models may also exert important controls.

A Cd path diagram has been included only for the Draupne Formation as the small number of non-zero values for the other formations makes any interpretation tenuous.

Draupne Formation

Median Cd=4ppm

n=55, R^2=0.65

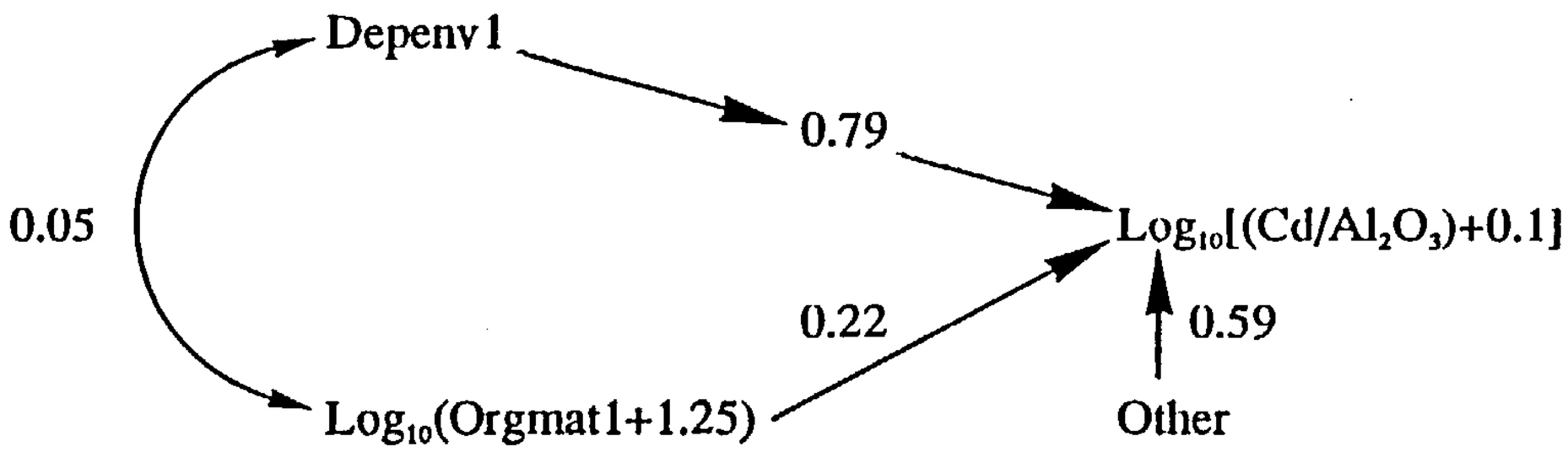

It is generally similar to Zn in the same formation which is unsurprising considering the similarity of the chemistry of these two elements.

6.3.2 Group 2: Elements influenced by Gnsize1

A second group may also be identified through the path diagrams, consisting of Zr, Th, Cr, and Nb whose path diagrams are illustrated below. The goodness of fit of the models in this group varies from excellent to poor but is not generally as good as for the preceding elements. The common characteristic is the selection of Gnsize1 as the variable of greatest importance.

The best fits of the group are demonstrated by Zr. The path diagrams for Zr in the Draupne and Kimmeridge Clay Formations are straightforward with Gnsize1 being in both cases the most influential variable by a wide margin. The fits for these two formations are similar but are lower than for the Heather Formation. This has an extremely high value for R^2, namely 0.99 suggesting a very good fit indeed. Unfortunately it would appear that some of the assumptions made regarding this formation during the regression analysis may have been invalid. This is revealed in a number of ways.

Firstly the distribution of the residuals is unlike the normal distribution expected where the assumptions are valid, and which is found for most of the other analyses performed for this study. Instead of many small residuals and progressively fewer large ones there are many observations with large residuals and few with small ones. This could be a result of the markedly bimodal distribution of the Zr/Al_2O_3 ratio which no transformation can remove. A second indication that there is deviation from the assumptions of the analysis is given by the values of the Cooks Distance statistic. This is a measure of the influence of individual points and is usually small; the average values for the Zr analyses of the Draupne and Kimmeridge Clay Formations being 0.0179 and 0.0268 respectively for the models presented. For the

Heather Formation the average value is 0.5090 again illustrating the number of points with large residuals and undue influence.

Draupne Formation

Median Zr=136ppm

n=52, R^2=0.71

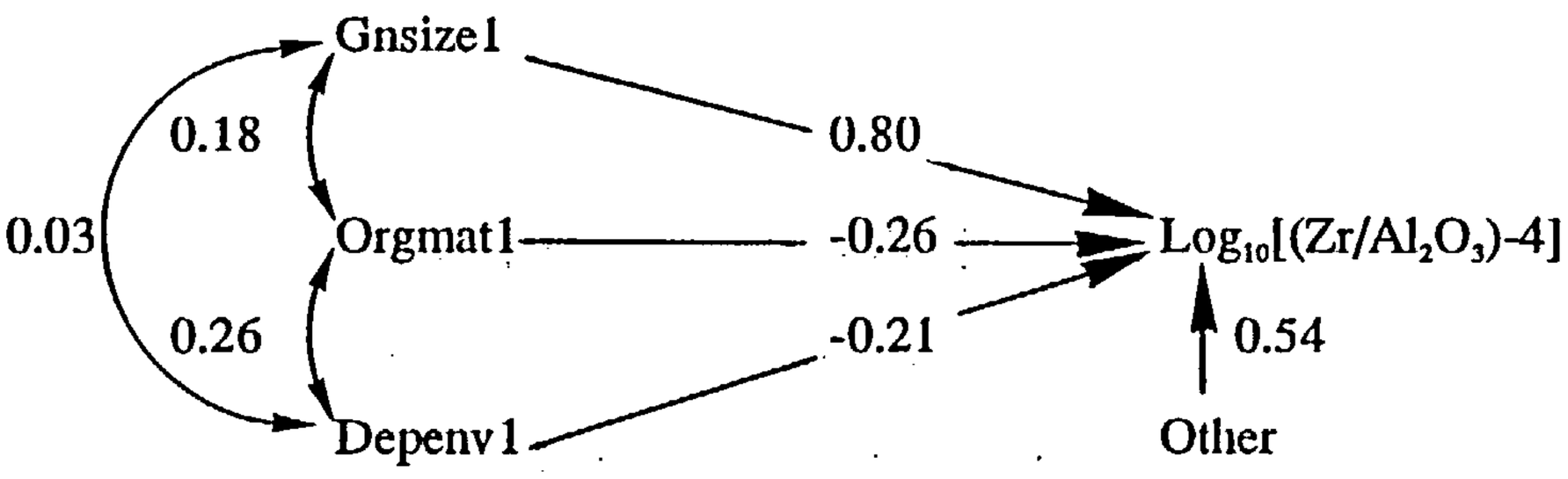

Heather Formation

Median Zr=187ppm

n=46, R^2=0.99

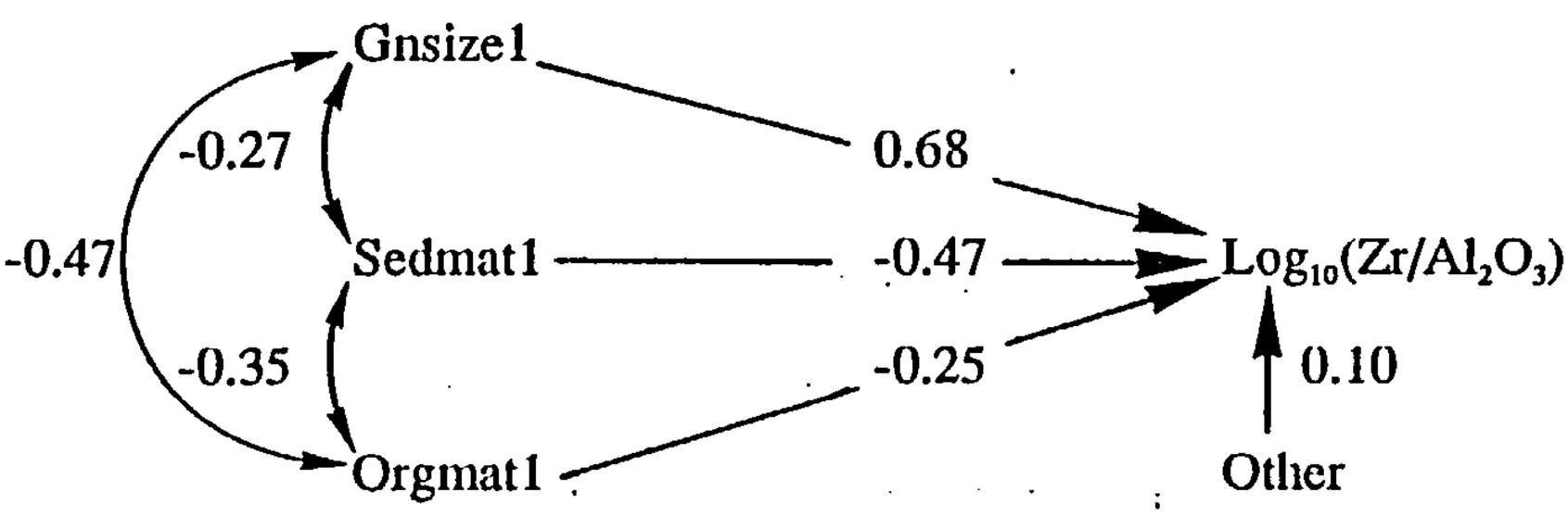

Kimmeridge Clay Formation

Median Zr=135ppm

n=46, R^2=0.76

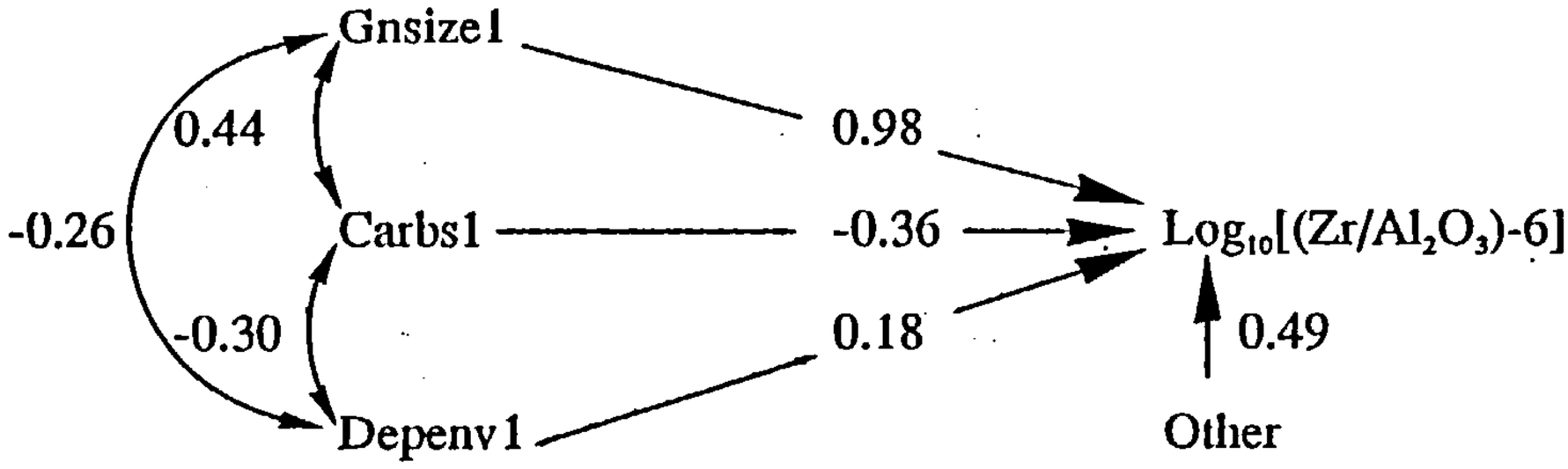

The path diagrams for Th demonstrate fits which while not as good as Zr are generally better than for Cr. Gnsize1 is selected for all of the formations studied, and is the most influential variable for the Heather and Kimmeridge Clay Formations, being particularly important in the latter. Notable is the negative path coefficient for Gnsize1 in the Heather Formation which contrasts with the positive coefficients found for the rest of this group.

Draupne Formation

Median Th=15ppm

n=52, R^2=0.24

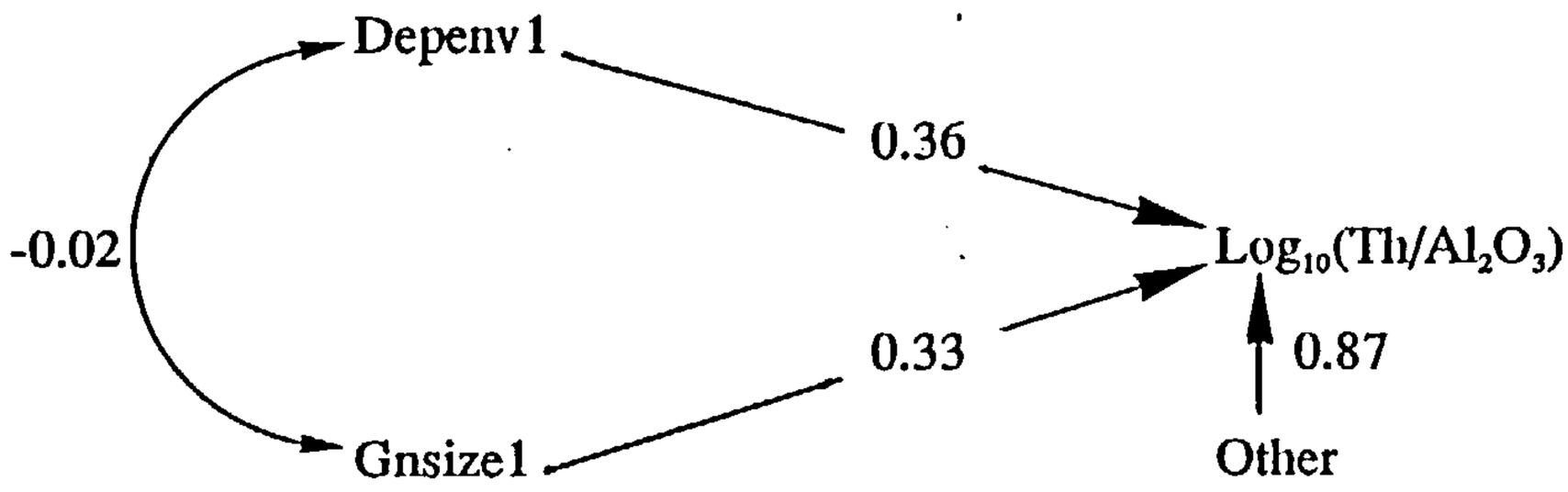

Heather Formation

Median Th=15ppm

n=0.45, R^2=0.82

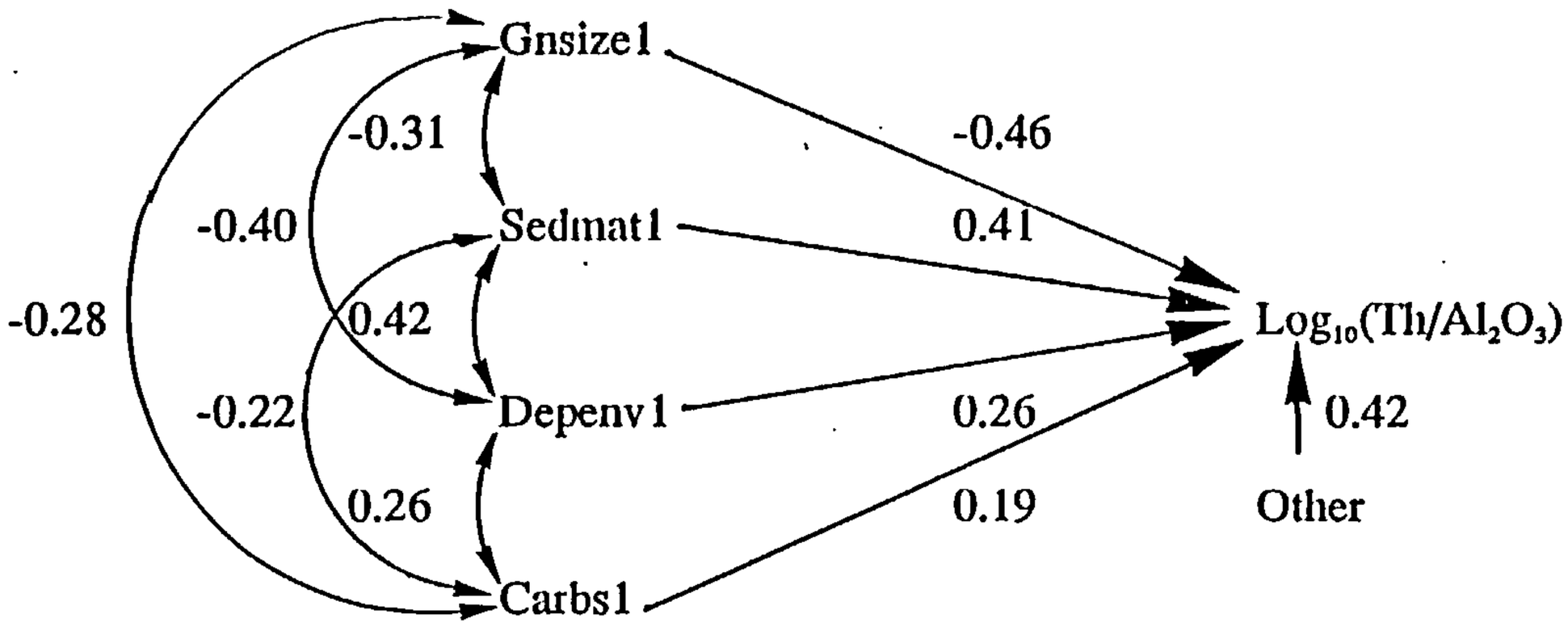

Kimmeridge Clay Formation

Median Th=14ppm

n=46, R^2=0.56

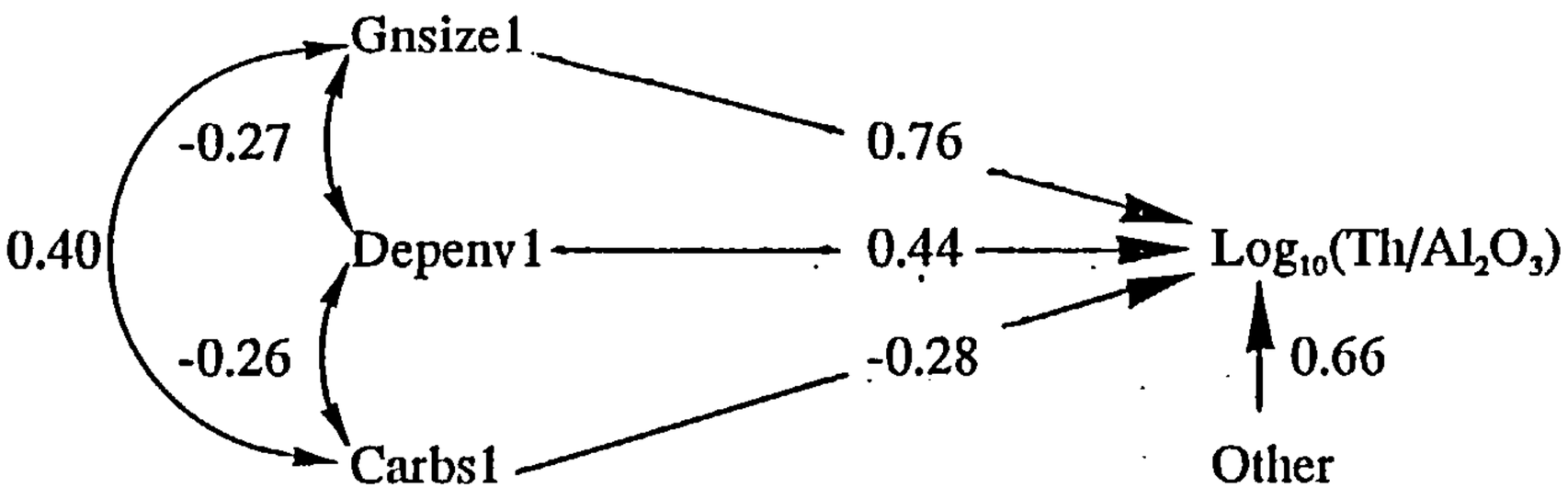

The fit of the Cr models is much lower than for Zr but Gnsize1 is selected as the most important variable for both the Draupne and Heather Formations. It has not been selected for the Kimmeridge Clay Formation where Carbs1 is the only significant variable. The path diagram in this case is only barely significant and the selection of Carbs1 is dependent on the inclusion of single observation. If this is omitted the model itself is not significant and no variables are selected.

Draupne Formation

Median Cr=138ppm

n=56, R^2=0.33

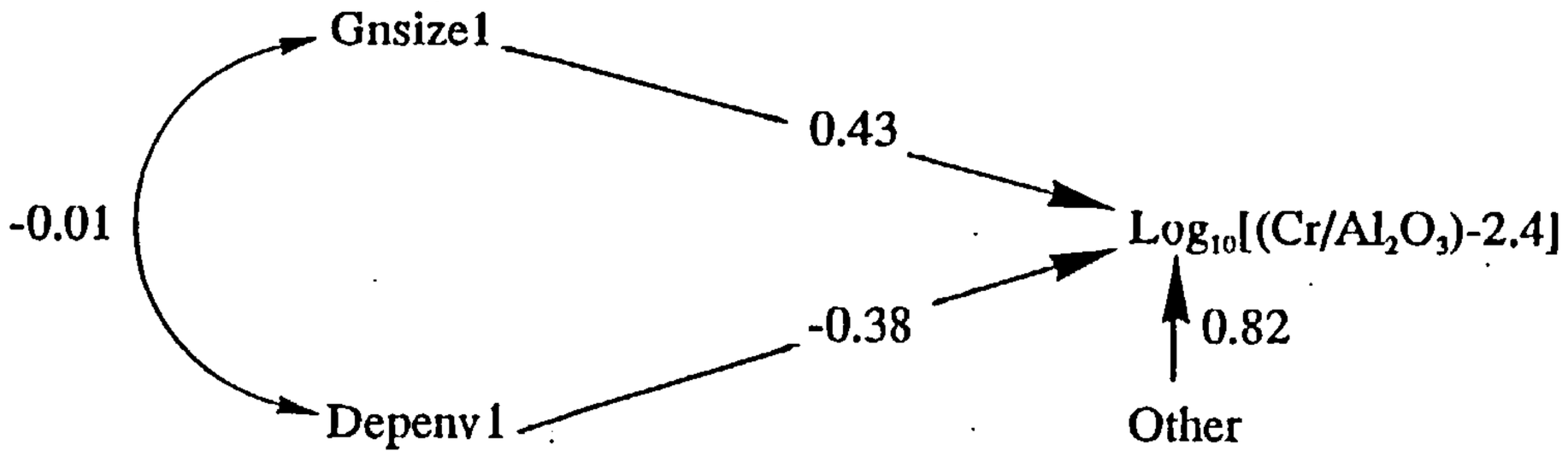

Heather Formation

Median Cr=135ppm

n=58, R^2=0.45

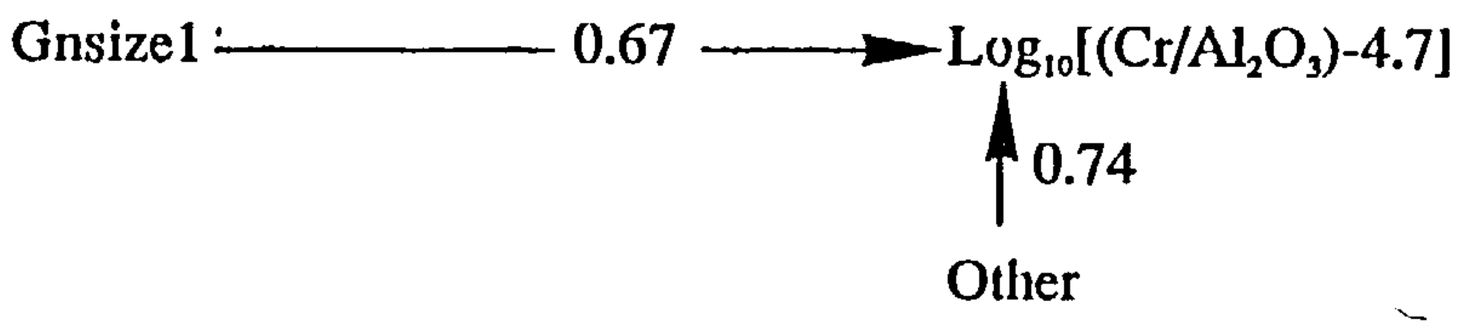

Kimmeridge Clay Formation

Median Cr=118ppm

n=47, R^2=0.11

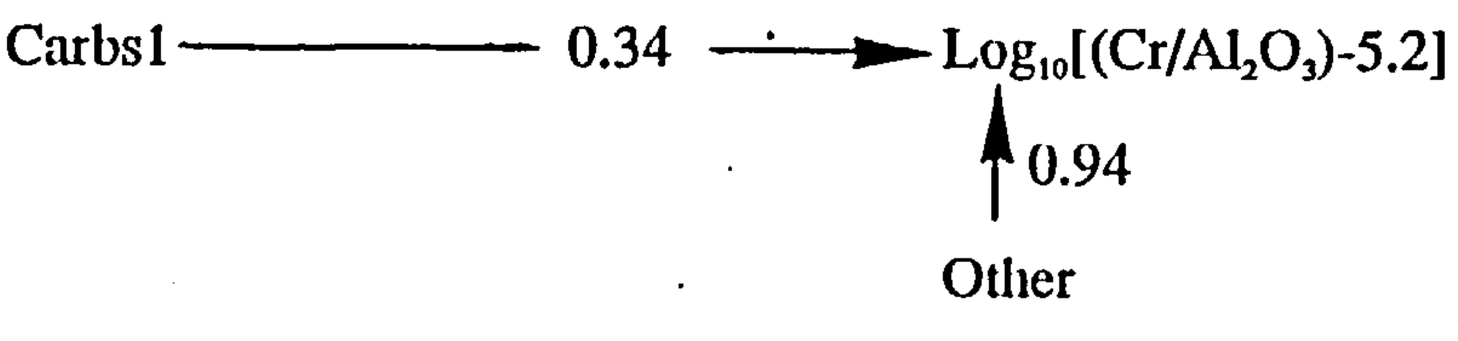

Nb is the final member of the group. Gnsize1 is not selected for the Draupne Formation whose model is barely significant. In both the Heather and Kimmeridge Clay Formations

however it is the most important variable, and reasonable fits are obtained in these two formations.

Draupne Formation

Median Nb=20ppm

n=51, R^2=0.12

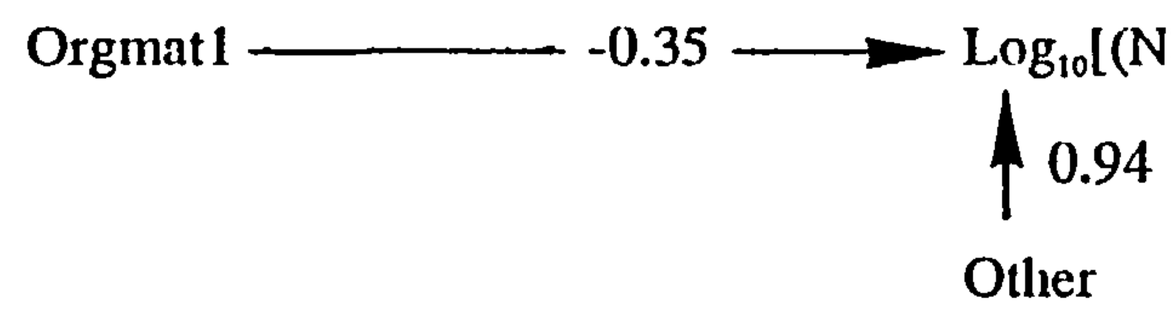

Heather Formation

Median Nb=20ppm

n=46, R^2=0.50

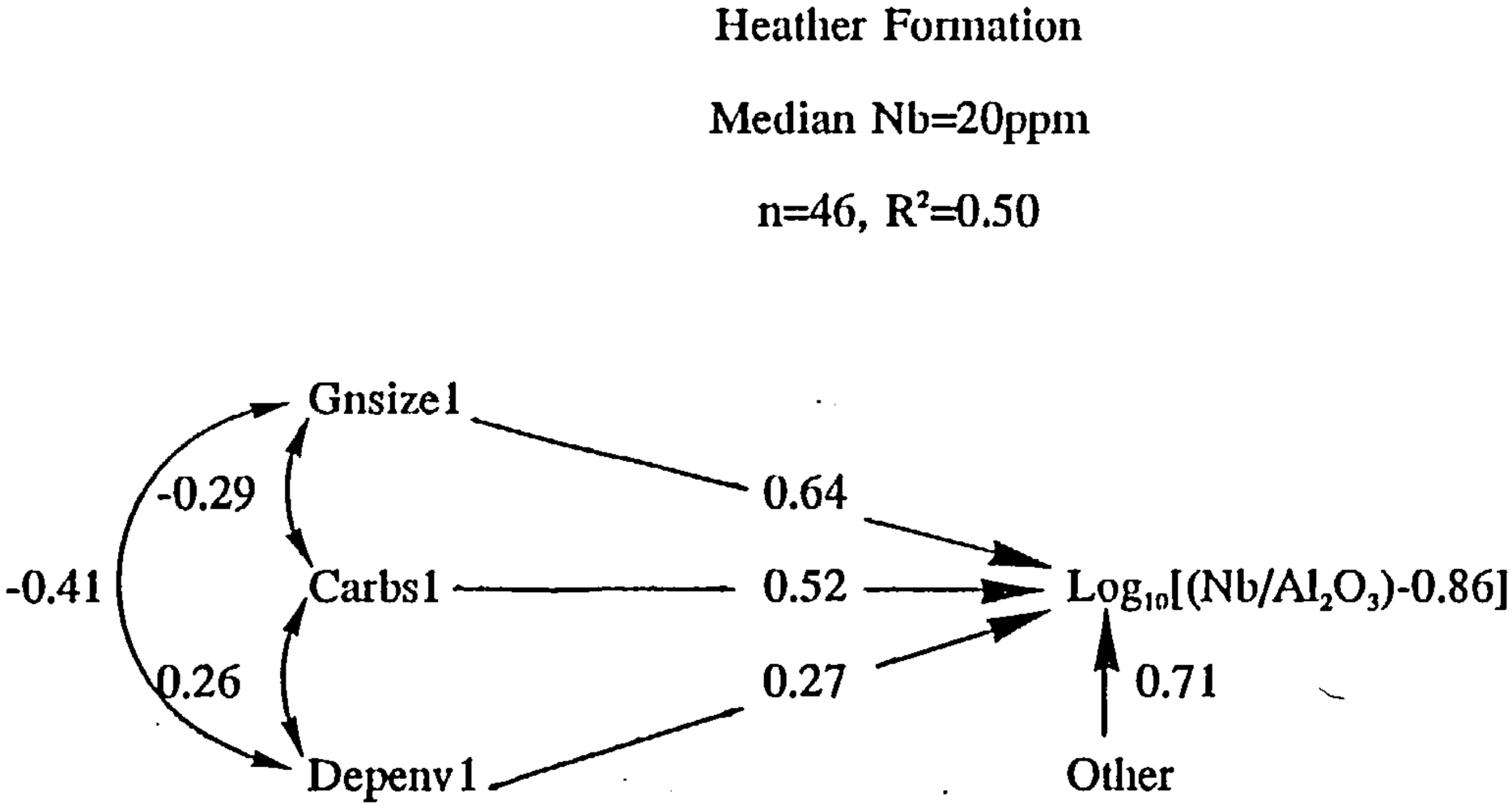

Kimmeridge Clay Formation

Median Nb=17ppm

n=45, R^2=0.61

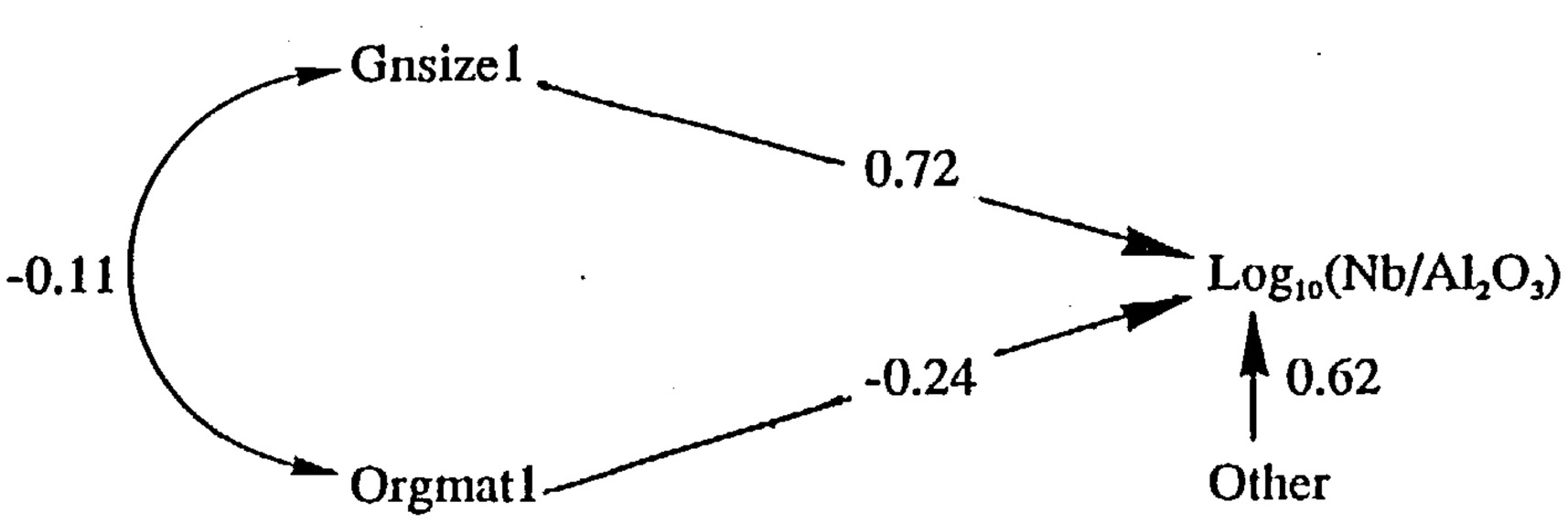

6.3.3 Group 3: Elements influenced by Carbs1

A third grouping which may be recognised on examination of the path diagrams is that of Sr, and Sc although this is somewhat more tenuous than the previous two groups. The characteristic common to this pair is the general pre-eminence of the Carbs1 variable in their models, particularly in those which display a better fit. It should be borne in mind here that observations having high carbonate contents and hence high scores for Carbs1 usually have low Al_2O_3 and trace element contents resulting in a larger relative error in the trace element/Al_2O_3 ratio than is otherwise usually the case. For this reason it is often the high carbonate samples which are omitted as outliers. As the study is concentrating on the mudstones which are generally low in carbonate with the exception of the Kimmeridge Clay; the loss of the carbonate rich samples is not considered to be a problem.

The fit of the Sr regression models illustrated by the path diagrams varies from poor to reasonable, the Heather Formation having the lowest median Sr content and the worst fit. The fit of the Kimmeridge Clay Formation is by far the best, this formation having the greatest median Sr content. The Carbs1 variable is not selected for the Draupne Formation where the only significant variable is Orgmat1, but it is the most significant variable for both the Heather and Kimmeridge Clay Formations, both having a positive path coefficient.

Draupne Formation

Median Sr=238ppm

n=53, R^2=0.29

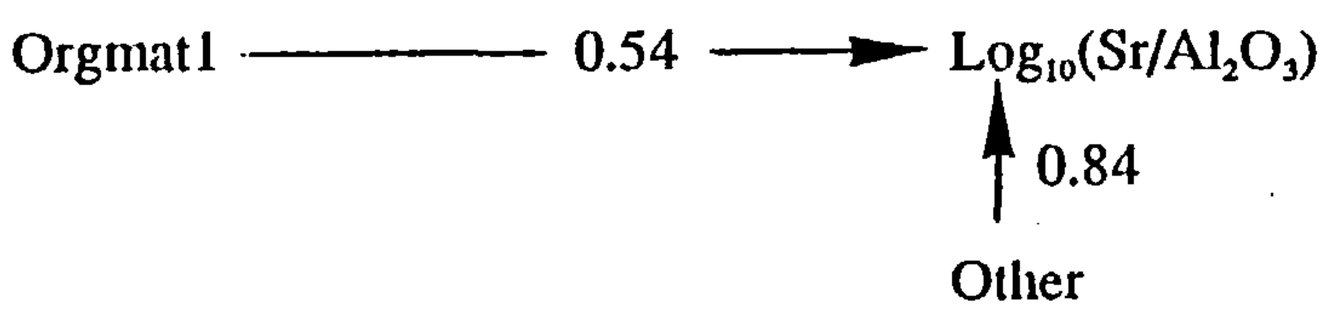

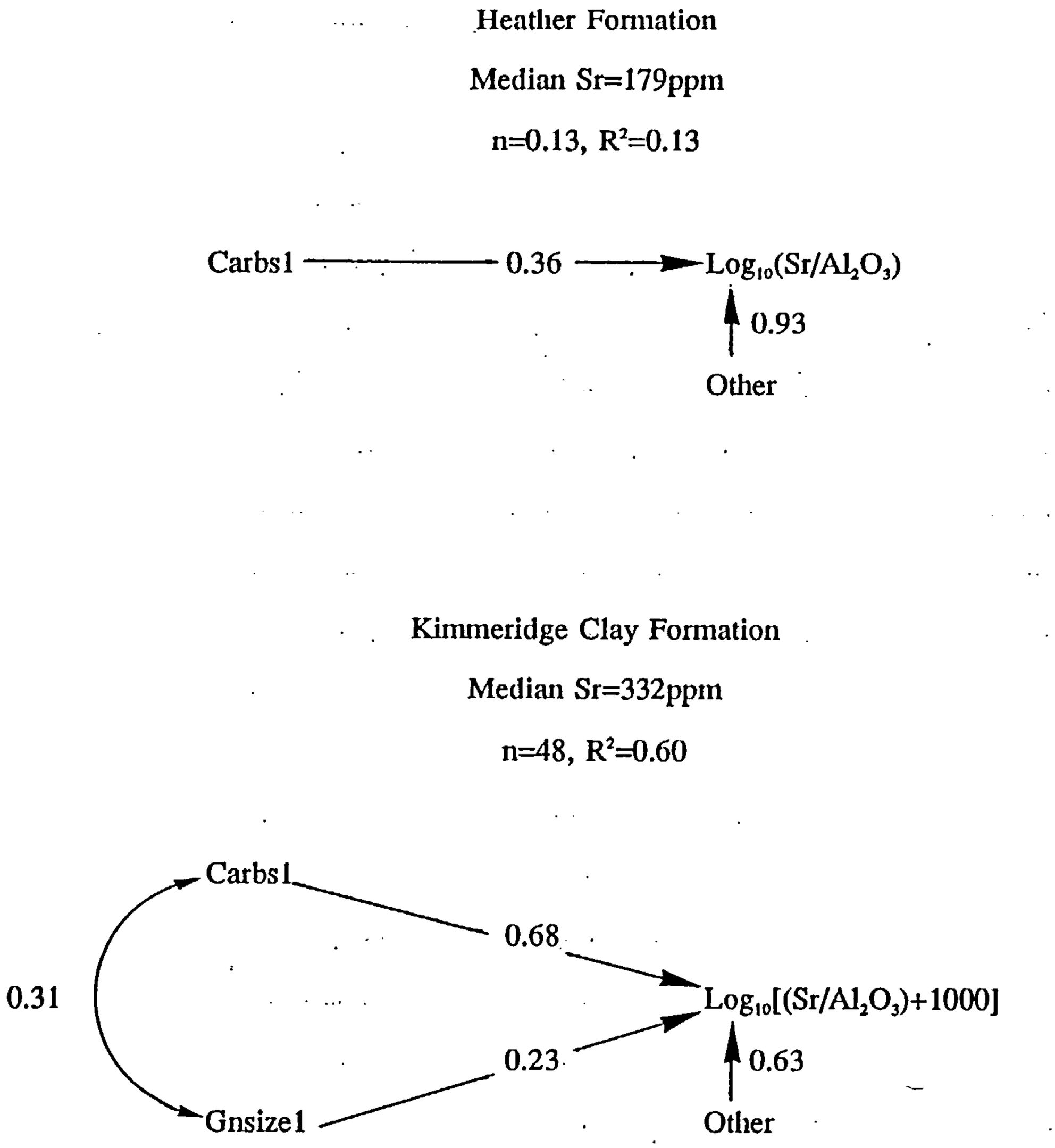

The path diagrams for Sc are generally poorly fitting with that of the Kimmeridge Clay Formation being best. For the Draupne Formation only Sedmat1 is selected as a significant variable, while the Heather Formation which is little better in terms of goodness of fit shows Orgmat1 and Carbs1 to be of roughly equal influence. In the Kimmeridge Clay Formation however Carbs1 is clearly more influential than the next most important variable which is Orgmat1.

Draupne Formation

Median Sc=13ppm

n=58, R^2=0.13

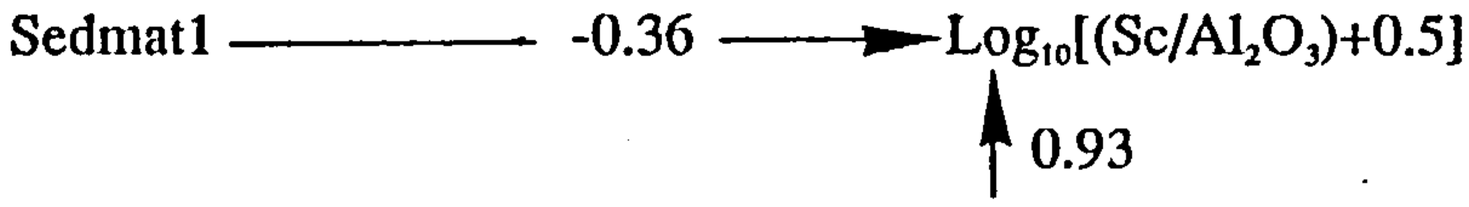

Heather Formation

Median Sc=10ppm

n=58, R^2=0.19

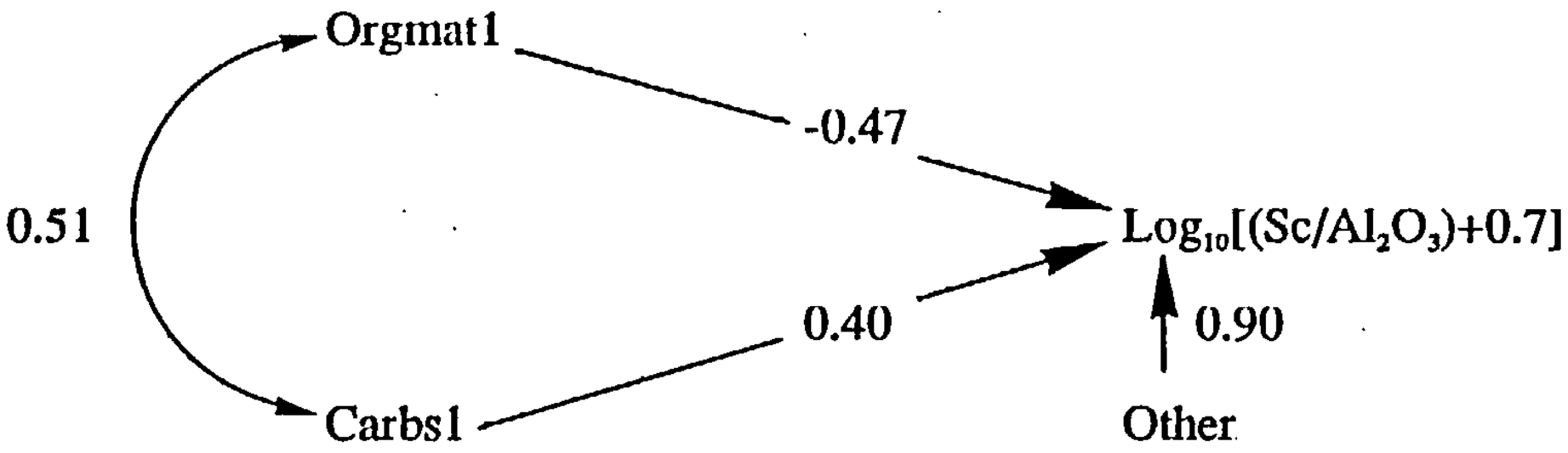

Kimmeridge Clay Formation

Median Sc=9ppm

n=47, R^2=0.45

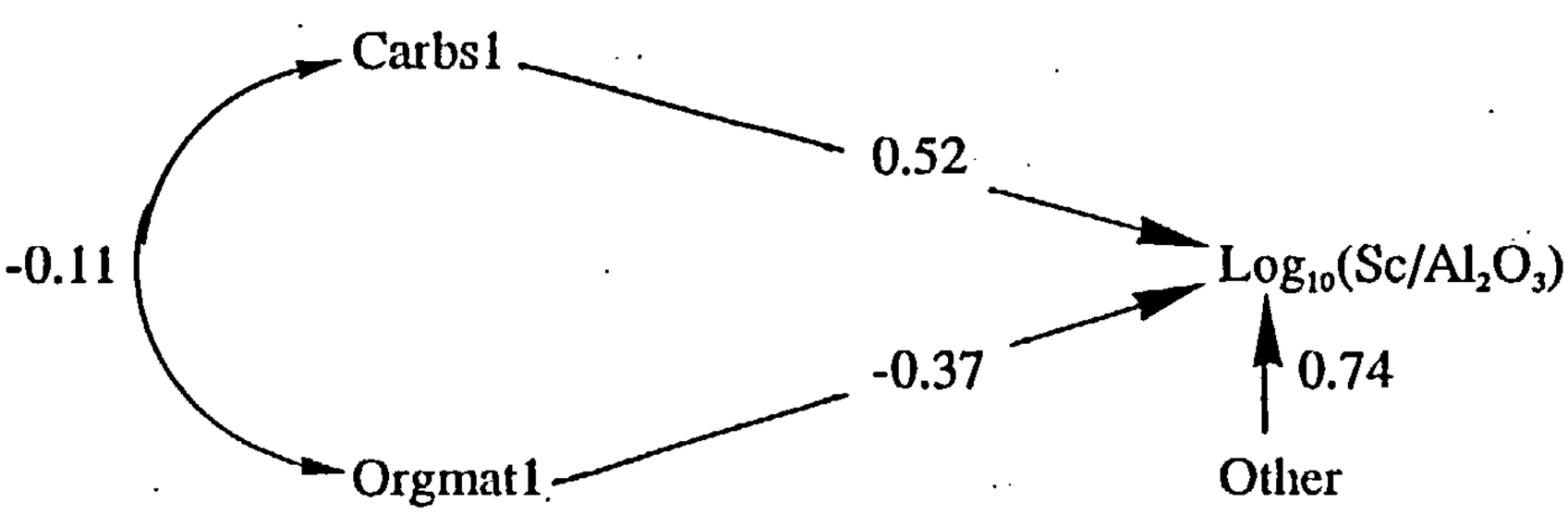

6.3.4 Group 4: Unaligned Elements

The remaining elements studied (Co, Li, Pb, Rb, and Y) cannot be assigned to any of the groups and are described individually.

No conclusions are drawn from the Co path diagrams as despite the reasonable fits obtained for the Draupne and Heather Formations no variable or variables are consistently selected as being important.

Draupne Formation

Median Co=22ppm

n=57, R^2=0.61

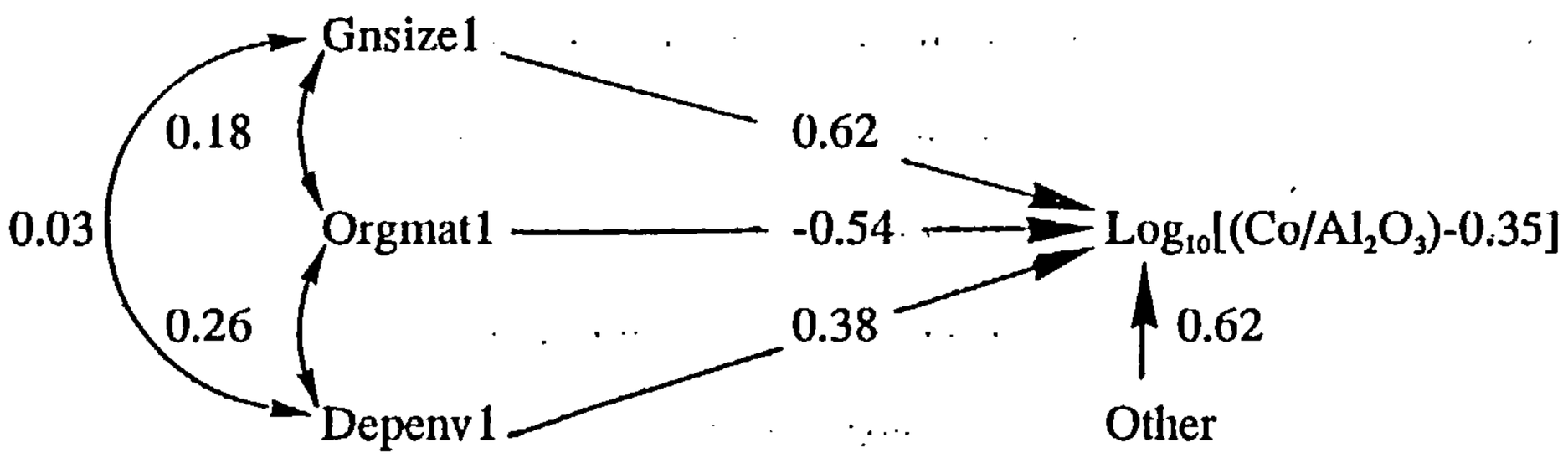

Heather Formation

Median Co=17ppm

n=56, R^2=0.53

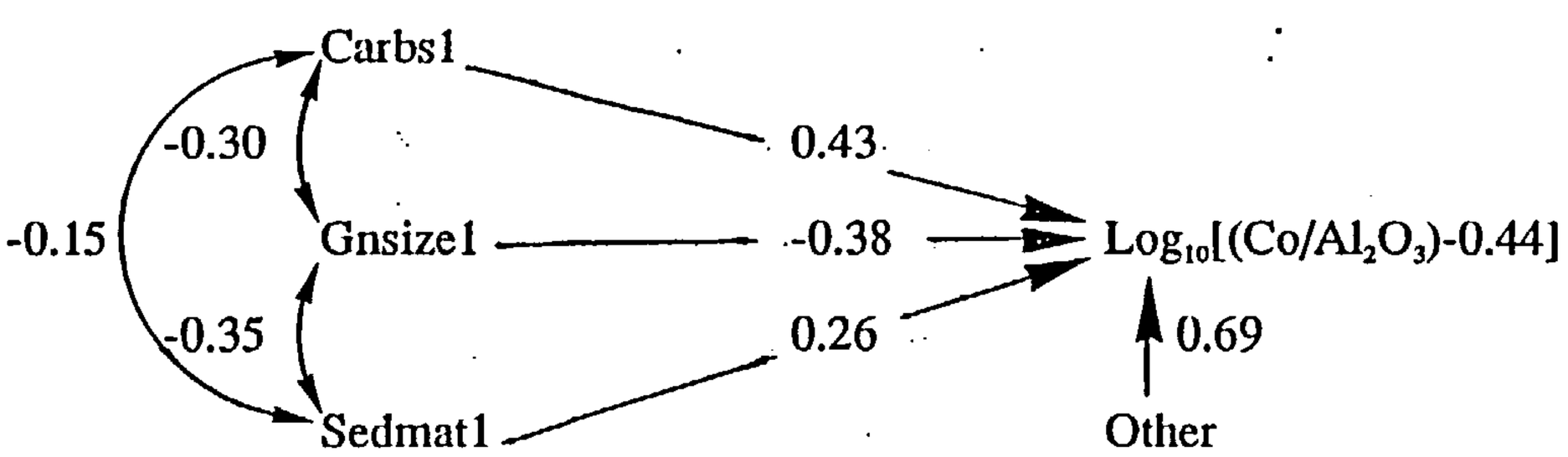

Kimmeridge Clay Formation

Median Co=12ppm

n=46, R^2=0.17

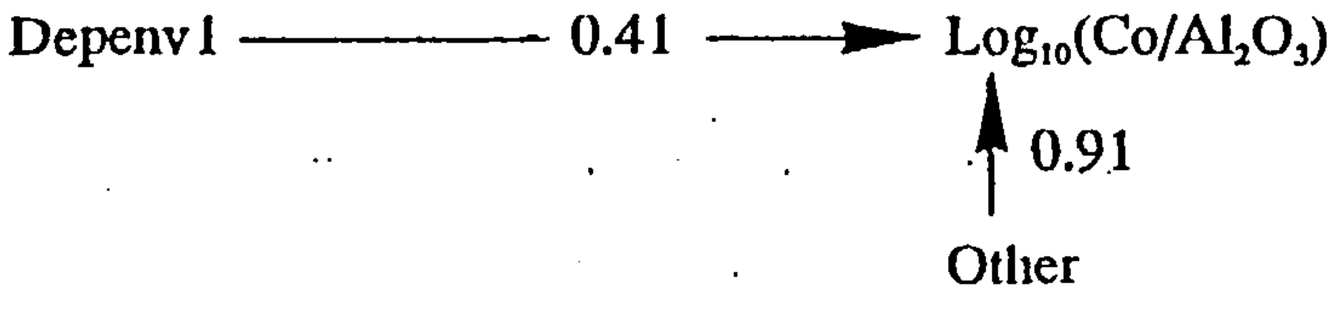

The Li path diagrams display a poor to reasonable fit but allow some generalisation to be made. Gnsize1 is selected for both the Draupne (where it is the most important variable) and Heather Formations with negative path coefficients. Depenv1 is selected as a minor influence in each model, again with a negative coefficient. Orgmat1 is also selected for each model, being the most influential variable in the Heather and Kimmeridge Clay Formations but the path coefficients here are opposed to those in the Draupne Formation.

Draupne Formation

Median Li=71ppm

n=58, R^2=0.42

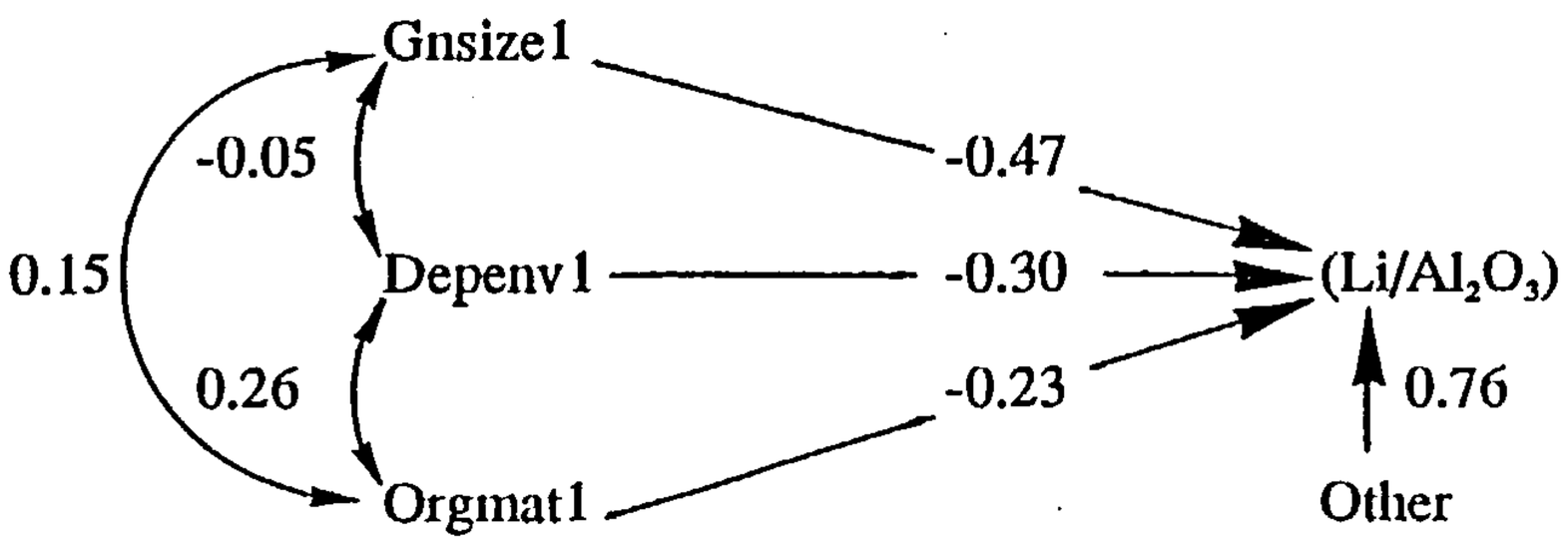

Heather Formation

Median Li=119ppm

n=59, R^2=0.50

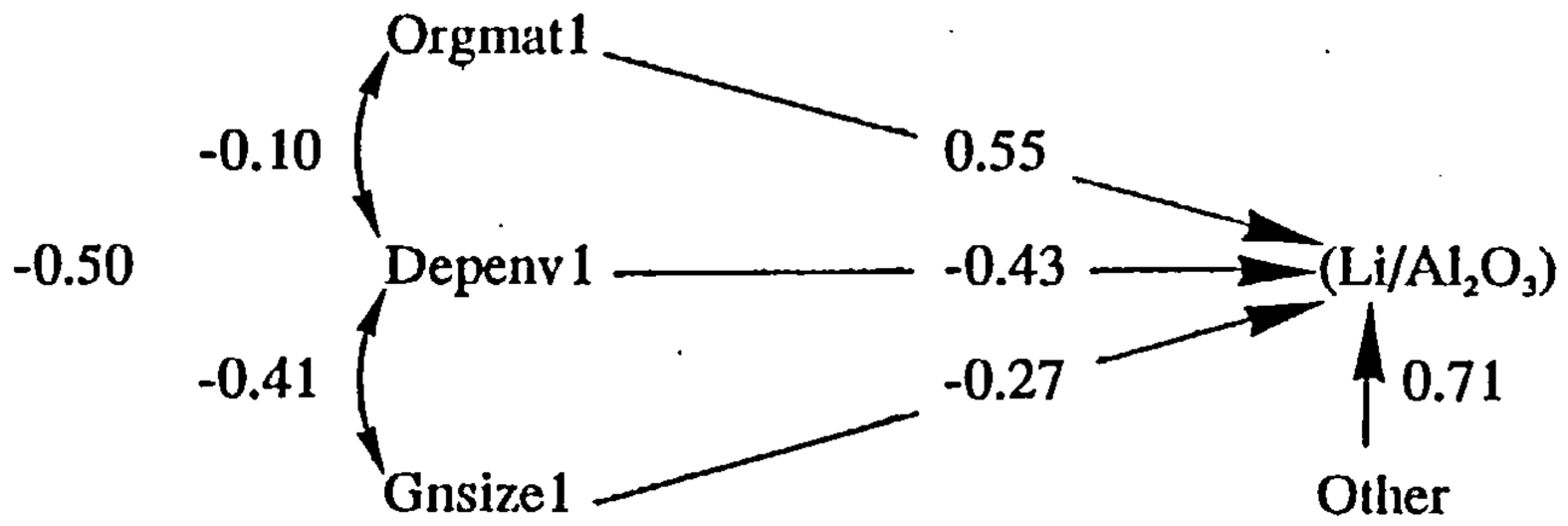

Kimmeridge Clay Formation

Median Li=79ppm

n=47, R^2=0.28

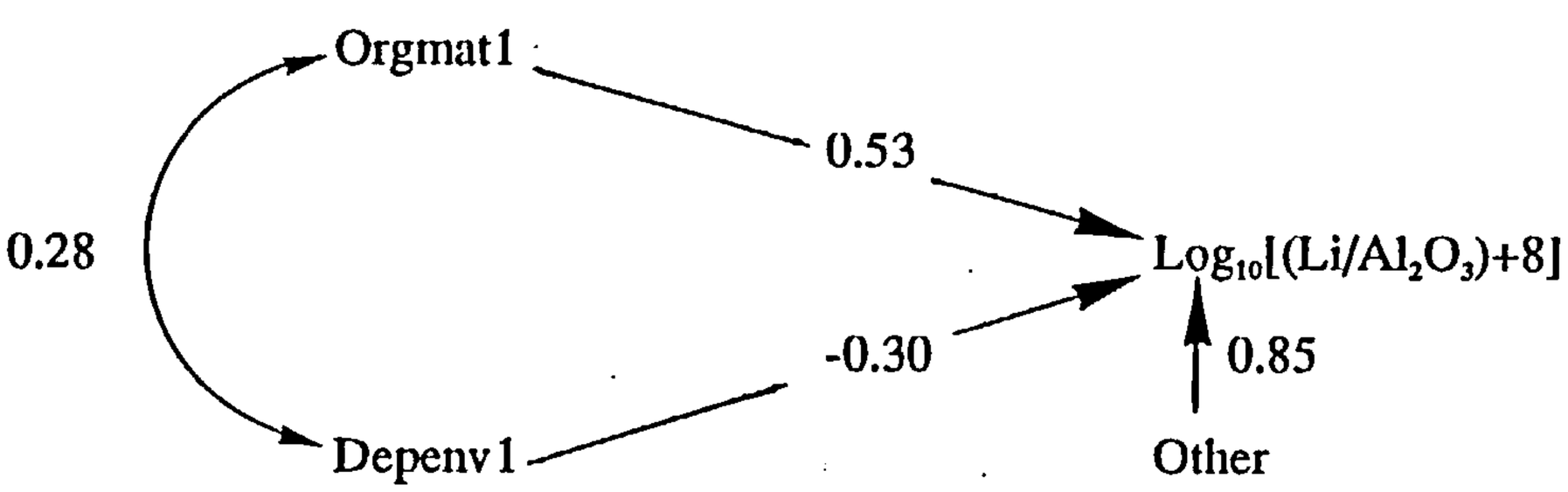

Interpretation of the Pb path diagrams is also hampered by their inconsistency. The fit is extremely good for the Heather Formation but poor for the Draupne and Kimmeridge Clay despite the similarity in their Pb contents. The Draupne model is troubled by the skewness of the Pb/Al_2O_3 ratio which it was not found possible to correct, and which is possibly the cause of its skewed residuals. The Heather Formation diagram is straightforward with Sedmat1 being marginally the most important of the four variables selected. In the Kimmeridge Clay the model selects only Depenv1.

Draupne Formation

Median Pb=22ppm

n=51, R^2=0.29

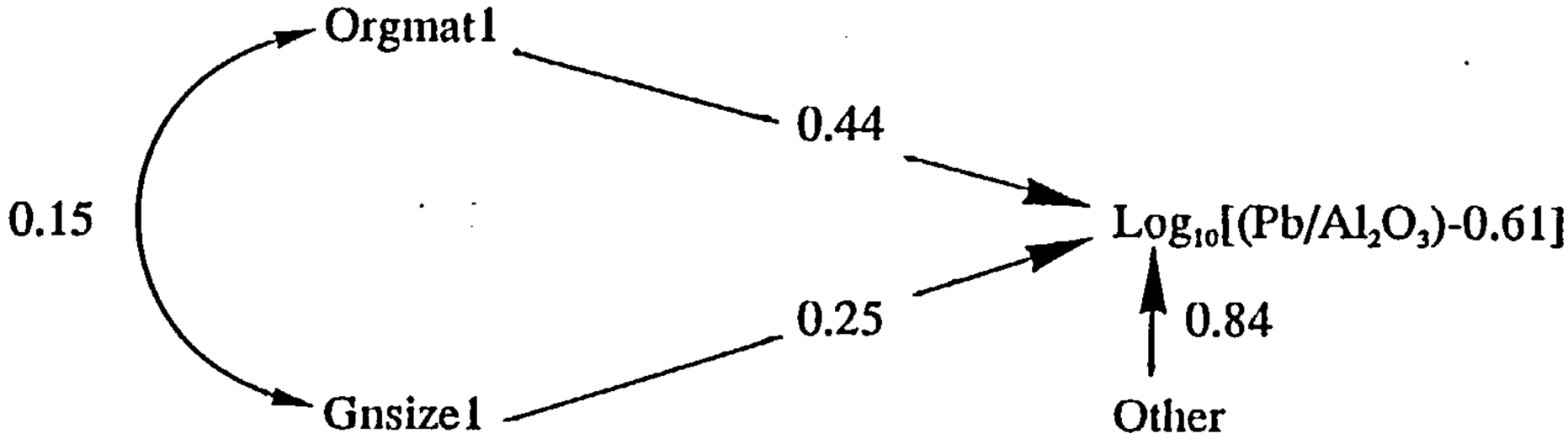

Heather Formation

Median Pb=25ppm

n=45, R^2=0.79

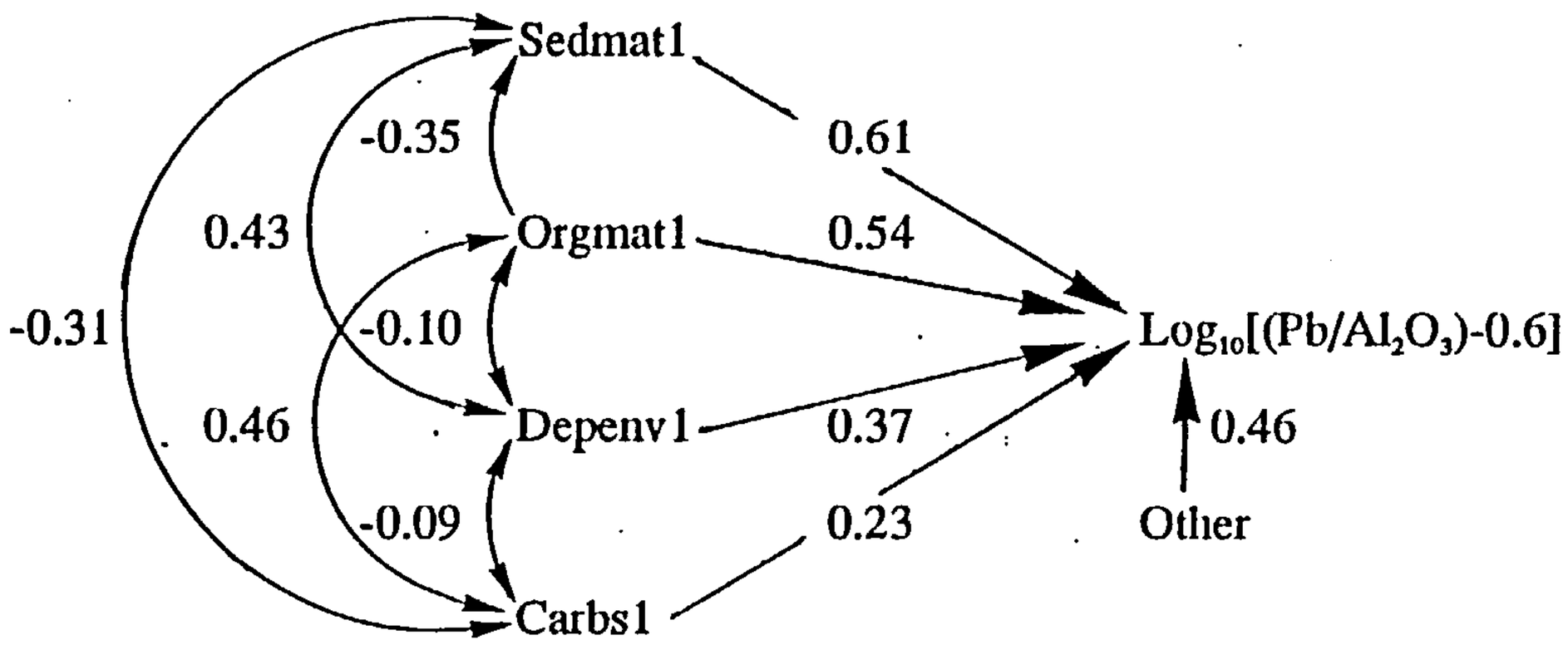

Kimmeridge Clay Formation

Median Pb=20ppm

n=47, R^2=0.20

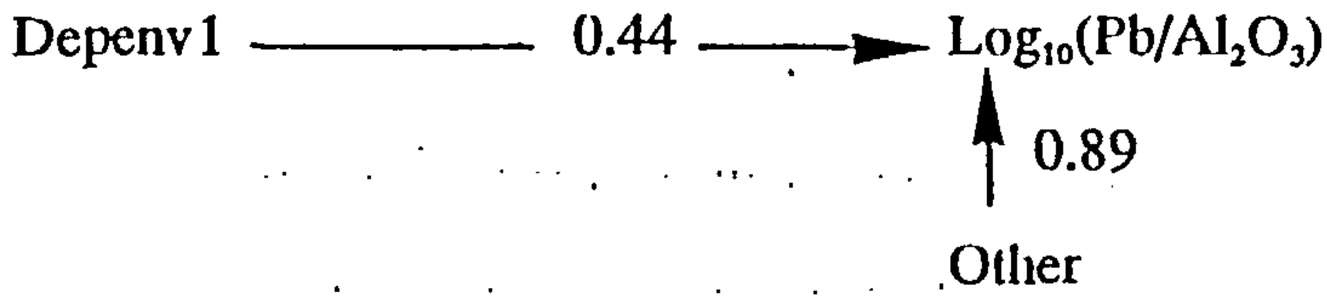

The fit of the Rb models is reasonable for the Draupne and Heather, but poorer for the Kimmeridge Clay. It should be noted that the transformation applied to the Rb variable in the Draupne Formation model is such that the sign of the variable has been altered ie when the Rb/Al_2O_3 ratio increases the value of the transformed variable decreases. The result of this is that the signs of path coefficients of the selected variables are opposed to the true relationship. No clear interpretations may be made though Gnsize1 is selected for both the Heather (where it is most important) and the Draupne, where Orgmat1 is most influential. Depenv1 is common to both the Heather and Kimmeridge Clay Formations where the magnitudes of the path coefficients are similar.

Draupne Formation

Median Rb=160ppm

n=53, R^2=0.48

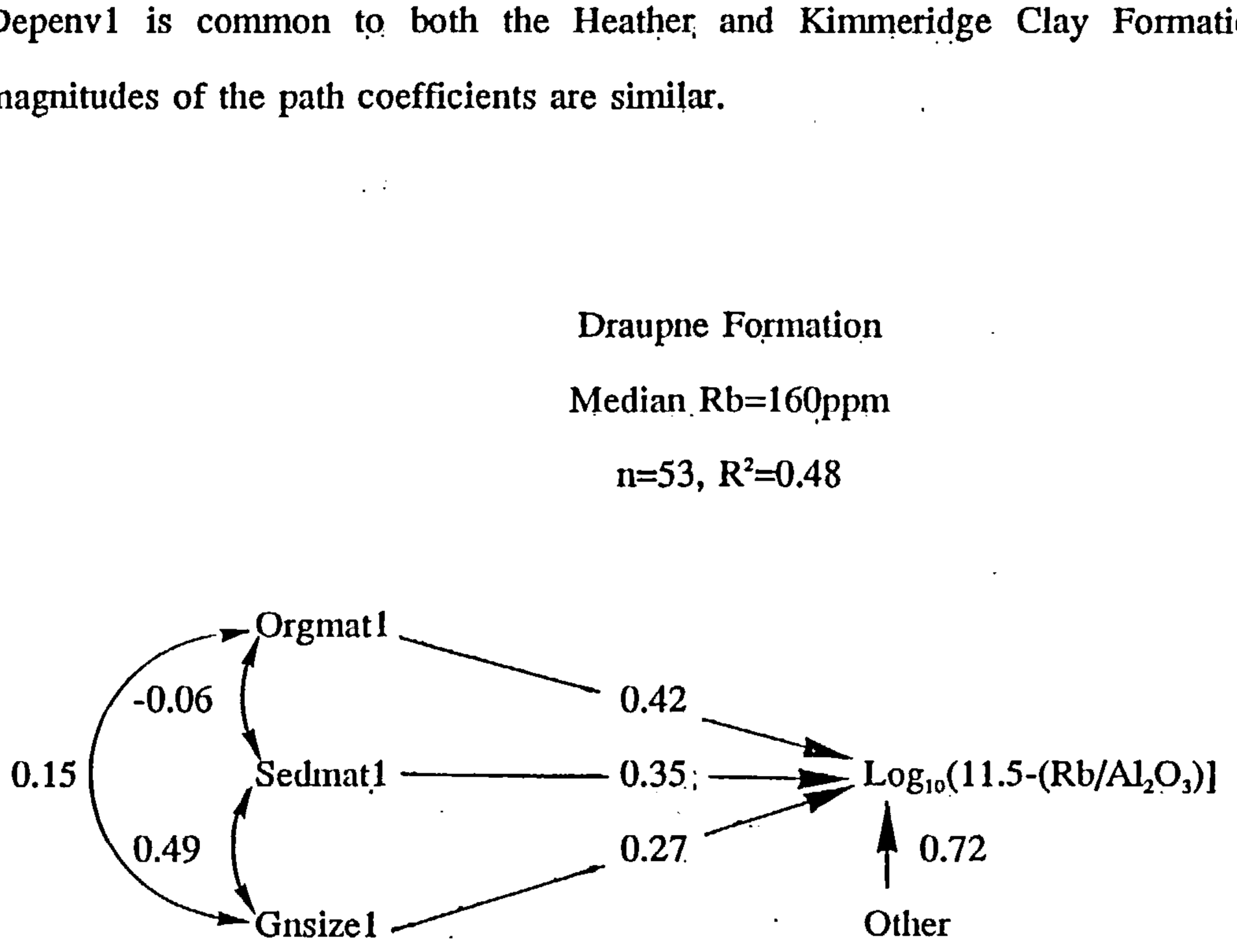

Heather Formation

Median Rb=113ppm

n=45, R^2=0.53

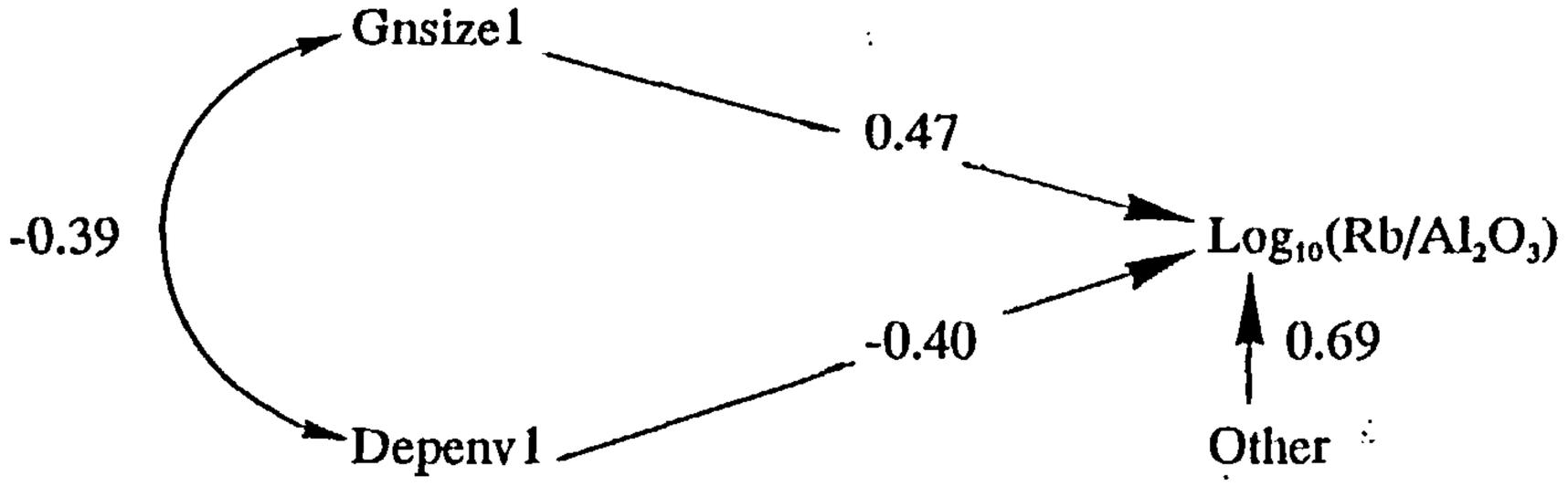

Kimmeridge Clay Formation

Median Rb=146ppm

n=47, R^2=0.15

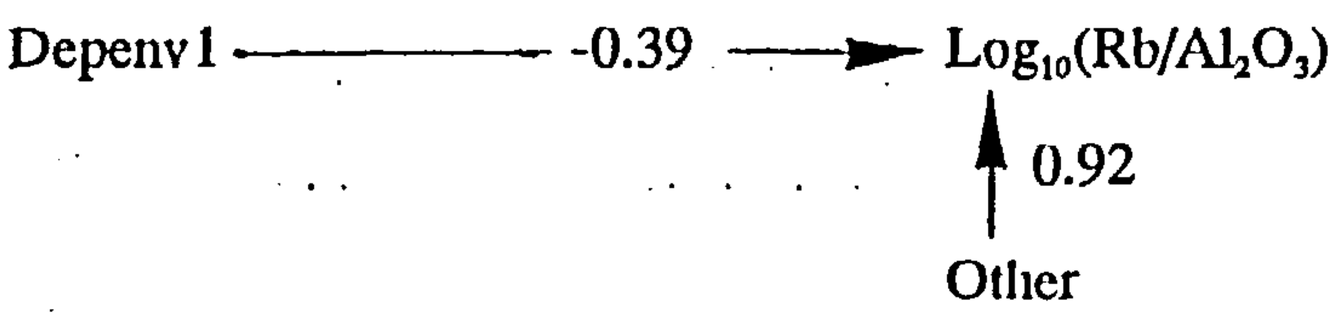

Y is in some ways similar to the first group identified (Cu, Ni, V etc), but has not been included here with those elements because of the much poorer goodness of fit of the Y models which suggests that other factors may be important in addition to those included in the models. For the Draupne Formation the path diagram is barely significant and the selection of Gnsize1 is dependent on the omission of one highly influential point whose inclusion would cause the selection of Sedmat1 as the single most important variable. In both cases Depenv1 is only not selected as a second variable by a narrow margin. For the Heather Formation the model is better fitting and Depenv1 is the only variable of significant importance. The best fitting model is that of the Kimmeridge Clay Formation however where Depenv1 is again the most influential variable, although its path coefficient here is not much greater than those of Carbs1 or Gnsize1.

Draupne Formation

Median Y=34ppm

n=52, R^2=0.09

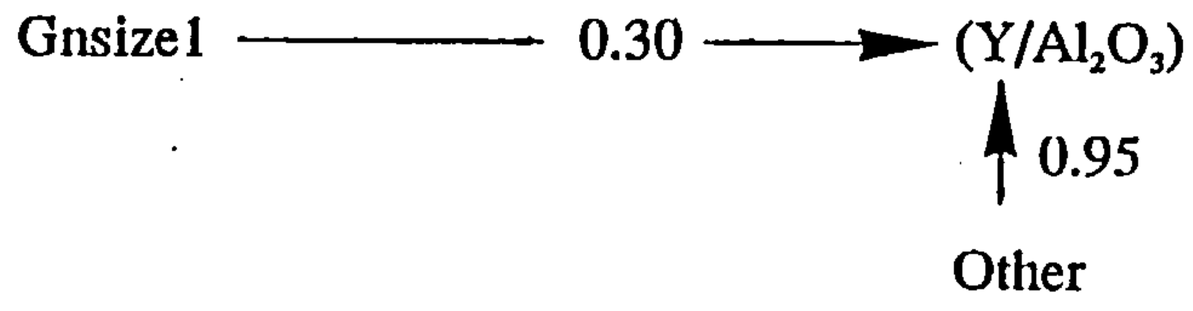

Heather Formation

Median Y=31ppm

n=44, R^2=0.30

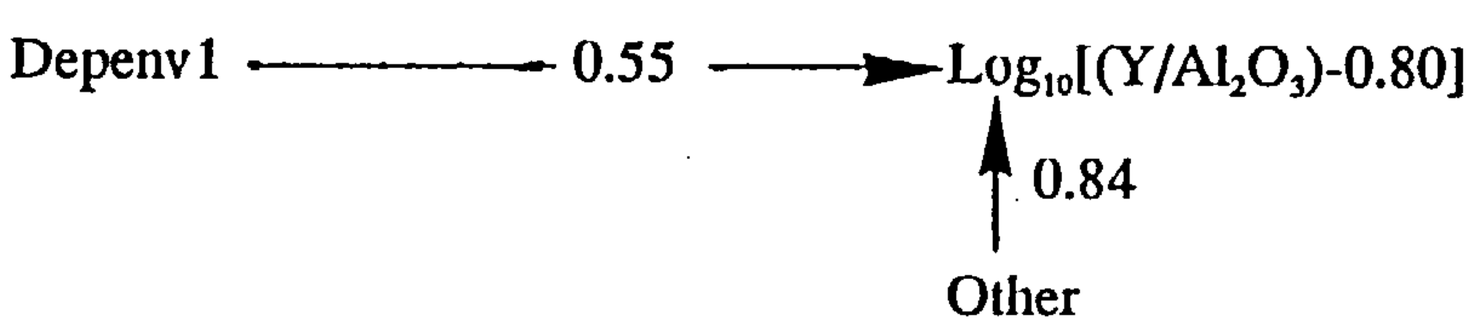

Kimmeridge Clay Formation

Median Y=27ppm

n=47, R^2=0.51

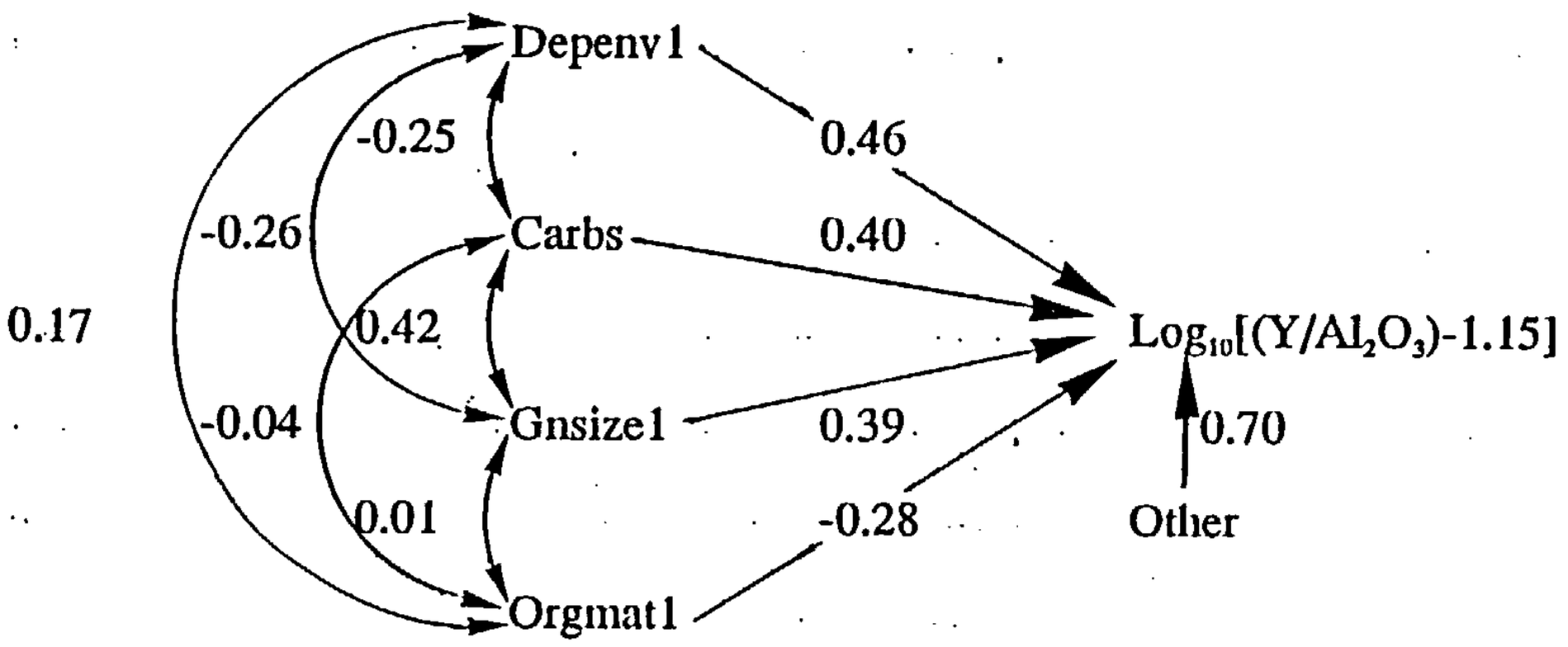

6.4 The role of organic metamorphism

Particular attention has been paid to examining the role of organic maturity (and hence burial history) in controlling the trace element geochemistry of these sediments. The Draupne and Heather Formations both cover wide ranges in maturity whereas the Kimmeridge Clay is more restricted in its coverage but Orgmat1 has been selected for path diagrams from each formation a number of times. Only for Li has Orgmat1 been identified as influential in all of the formations studied but for this element the signs of the three path coefficients are inconsistent making it difficult to draw any conclusions about the behaviour of this element in mudrocks as a whole.

The Orgmat1 variable has been selected in two of the three formations for eight elements (Ni, V, Mo, Zn, Zr, Nb, Sc, and Pb). For two of the eight elements (Ni and V) the signs of the path coefficients are opposed and no conclusions may be drawn. For Zr one of the regression models appears to break some of the assumptions inherent in the analysis again making interpretations tenuous, while for Nb and Sc the fit of some of the relevant models is poor. This leaves Mo, Zn and Pb remaining with the best evidence for the existence of a relationship between element concentration and organic maturity. Of these Mo would appear to be mobilised during burial whilst Pb and Zn are fixed. Mo is a particularly strong candidate for the existence of a general relationship as even in the Kimmeridge Clay where Orgmat1 was not significantly influential for inclusion the margin was extremely narrow and the coefficient if it had been included was similar in sign to those of the Draupne and Heather Formations.

Of the elements for which Orgmat1 was selected only once (Cu, U, Cd, Sr, Co, Rb, and Y) U remains interesting as a relationship was found in the Draupne Formation where this element would appear to have been particularly concentrated. It is possible that where concentration has occurred above background levels during early diagenesis loss of some of the excess U may occur during later burial. Cd too is greatly enriched in the Draupne

Formation and here its path diagram suggests that some has been fixed during later burial. Cd generally follows Zn in its geochemical behaviour so this observation is as expected.

6.5 Conclusions

In this chapter a statistical procedure has been described by which the extent of the relationship existing between organic maturity and trace element geochemistry may be determined in a suite of mudrocks in the presence of variation caused by the heterogeneity of other factors such as grain size and depositional environment. The results of the analyses have been summarised in a number of path diagrams for convenient visual interpretation. Study of these diagrams allows the recognition of three groups of elements displaying similar behaviour.

Group one consists of the elements Cu, Ni, V, U, Mo, Zn, and Cd. The modelling of these elements by the procedures above has been uniformly successful allowing the major influence on them to be determined with confidence. The most important variable, which represents the factor exerting the greatest control over their contents in these organic rich mudrocks is Depenv1. The path coefficients for this variable are all positive and hence their concentrations increase as the depositional environment becomes more reducing in nature. The importance of Depenv1 suggests that a major proportion of these elements is authigenic and was fixed in the sediment after deposition.

The second group consists of Zr, Th, Cr, and Nb and was identified by the importance of the Gnsize1 variable. The dependence on the grain size of the concentration of these elements suggests that they were associated mainly with the silicate detritus and that their concentrations were effectively fixed on deposition. The path coefficients (with the acceptance of Th in the Heather Formation) are all positive indicating that the concentration of these elements increases with increasing grain size in the mudrocks studied. The situation is

reversed for Th in the Heather Formation where the greatest concentrations are found in the finer sediment.

A third association, namely that of Sr and Sc was also identified by the importance of the Carbs1 variable. The modelling of these two elements is not as successful as in the previous two groups but the Carbs1 variable is selected twice for each element. The Kimmeridge Clay Formation is best fitting by far of the formations studied and Carbs1 is the preferred variable for both of these elements in this formation. This would suggest that the carbonate content is an important control on the concentrations of these two elements especially in the Kimmeridge Clay Formation where the carbonate content is appreciably higher than in the Draupne and Heather.

The elements Co, Li, Pb, Rb, and Y could not be assigned to any of the above groups and were described individually. The modelling of these elements meets with mixed results but consistent conclusions could sometimes be drawn.

Organic maturity was thought to be of probable influence over the concentrations of Mo, Pb, and Zn, and possibly also U and Cd where these are present above background concentrations. Pb, Zn and Cd increase in concentration with increasing organic maturity whereas Mo and U would appear to be mobilised during burial. In the last chapter these results are combined with earlier evidence and interpretations in a discussion of the influences controlling trace element concentrations in these mudrocks with special reference to the role of organic maturity.

Chapter Seven

Applications

7.0 Applications

7.1 Introduction

The depositional environment of the mudstones studied was shown in Chapter 6 to be of great importance in controlling the concentrations of several trace metals (Cd, Cu, Mo, Ni, U, V, Zn). Strong correlations were observed between many of the logratio transformed forms of these elements and $\log(TOC/Al_2O_3)$ (Chapter 4), suggesting that the TOC content of the mudstones might also be controlled to a great extent by the depositional environment. The possibility of predicting the TOC content and also the HI (and hence organic matter type) of mudstones from their inorganic geochemistry has been investigated here. As a number of elements may currently be measured directly downhole by geochemical logging tools it may be possible to log both TOC and HI using models developed here.

7.2 Path analysis of TOC and HI

Path diagrams have been calculated for $\log(TOC/Al_2O_3)$, using the method described in Chapter 6, for the Draupne, Heather, and Kimmeridge Clay Formations. In each formation Depenv1 was found to be the most influential variable indicating that, as anticipated above, the depositional environment was the most important control on the organic carbon content of these mudstones. The path diagrams are presented below:

Draupne Formation R^2 0.83

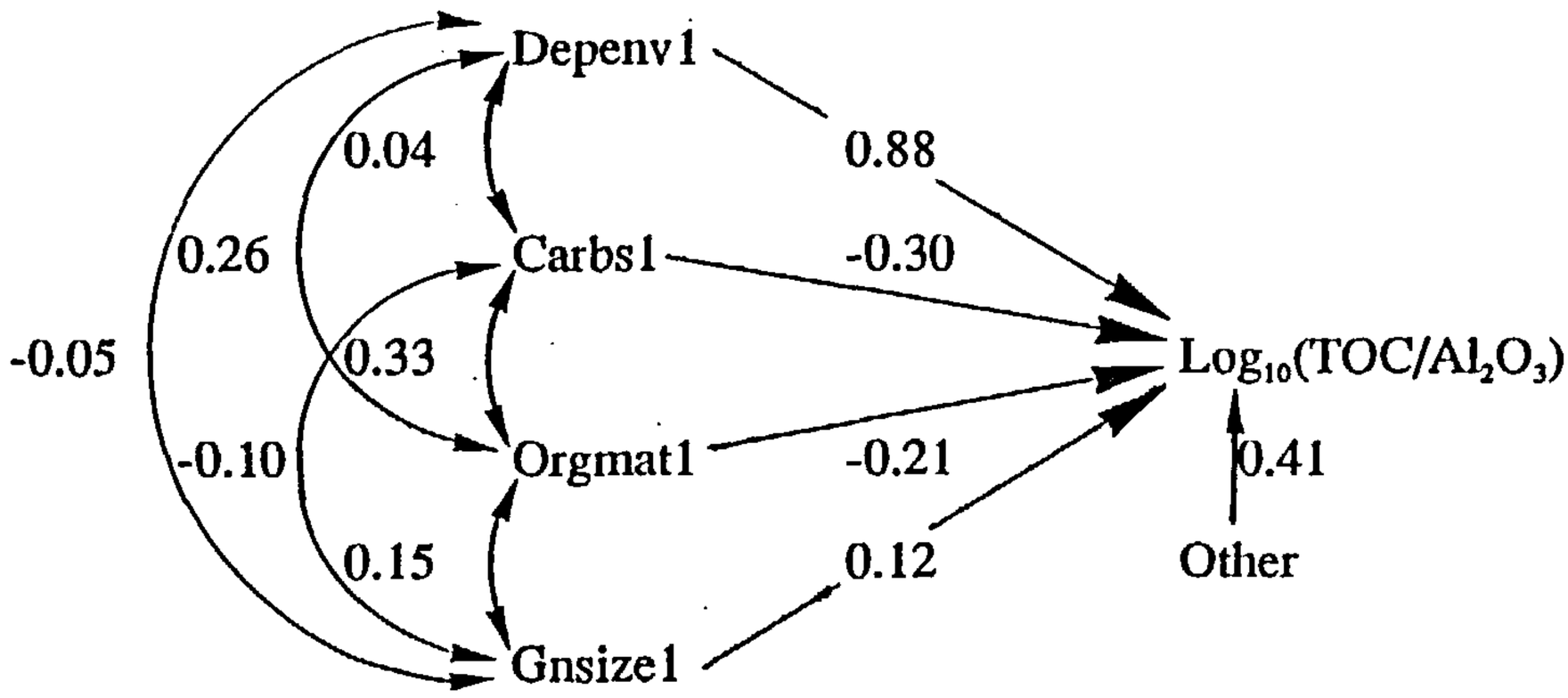

Heather Formation R^2 0.69

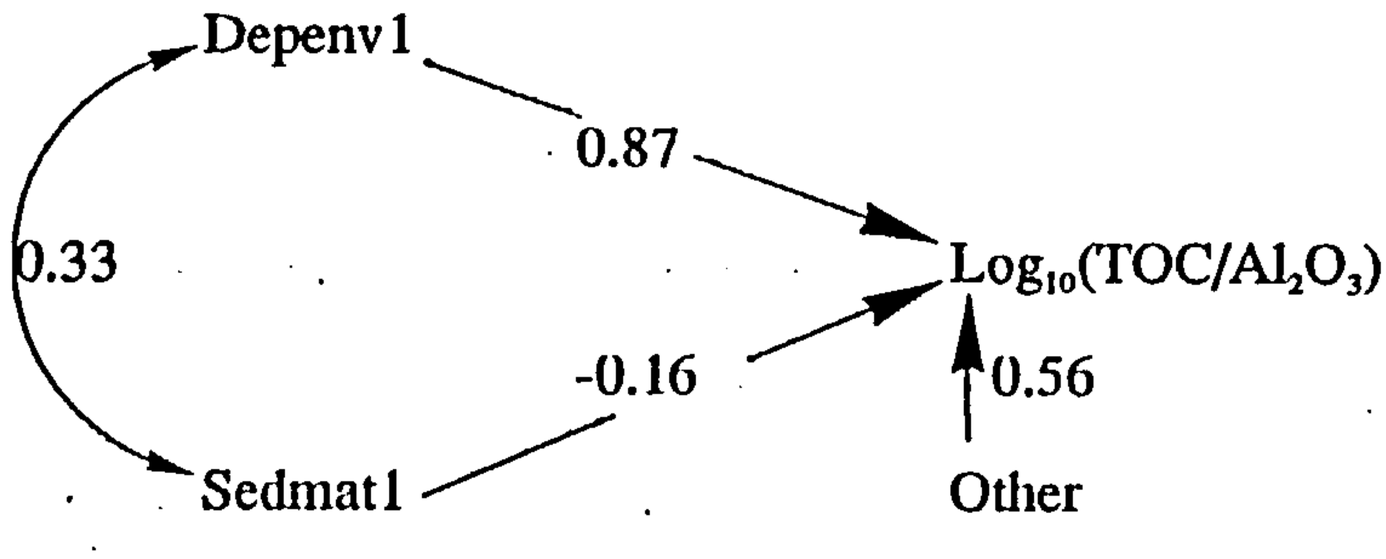

Kimmeridge Clay Formation R^2 0.47

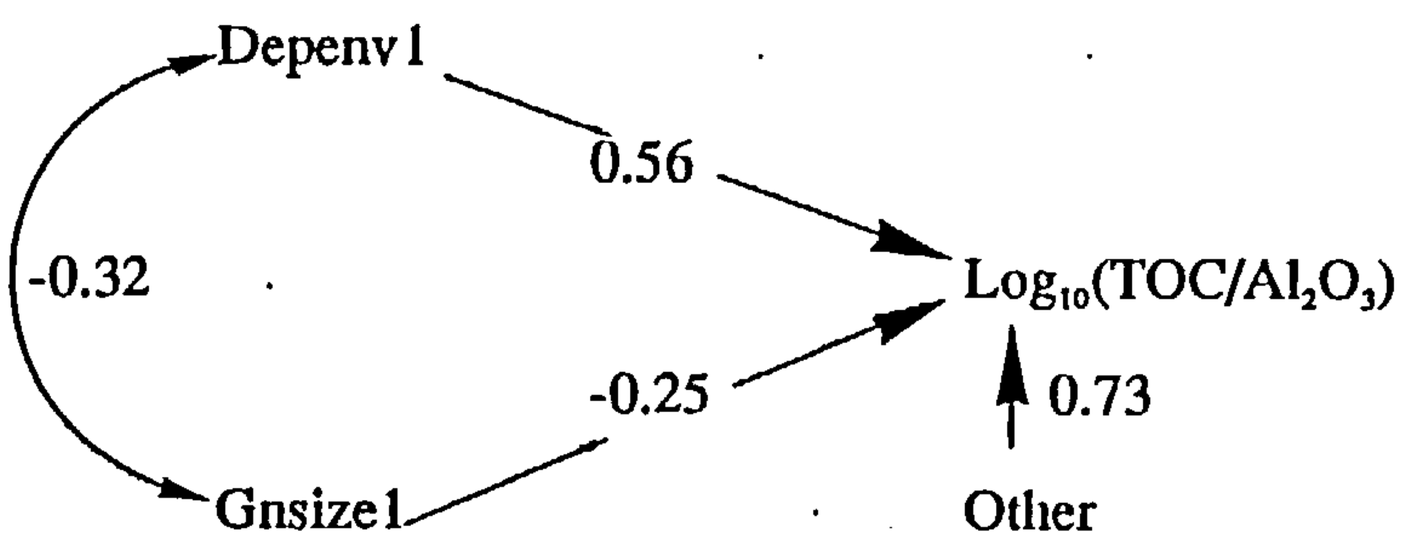

For the Draupne Formation the high R^2 value of 0.83 indicates that the logratio TOC concentration can be predicted very well indeed from the model summarised by the path diagram above (R^2 indicates the proportion of the total variance of the dependent variable which is attributed to the regression model). The corresponding values for R^2 in the Heather and Kimmeridge Clay Formations are 0.69 and 0.47 respectively suggesting that the ability of the models to predict the TOC content of the Kimmeridge Clay Formation is lower than for the two North Sea formations of the Viking Group.

In the Draupne Formation path diagram organic maturity and carbonate content are selected as subsiduary influences. Their negative path coefficients illustrate the decrease in TOC as hydrocarbons are generated, and probably the precipitation of organic-carbon derived

carbonate minerals respectively. A small positive grain size term suggests that in the Draupne Formation high log(TOC/Al_2O_3) ratios are favoured by coarser grain size. In the Heather Formation the negative path coefficient associated with the sedimentological maturity variable may be a result of a predominantly terrestrial supply of organic matter, the log(TOC/Al_2O_3) ratio falling with increasing transportation as the organic matter becomes more degraded. The negative coefficient with grain size in the Kimmeridge Clay suggests the converse, that where grain size increases the log(TOC/Al_2O_3) ratio falls.

Path diagrams for the HI are shown below.

Draupne Formation R^2 0.72

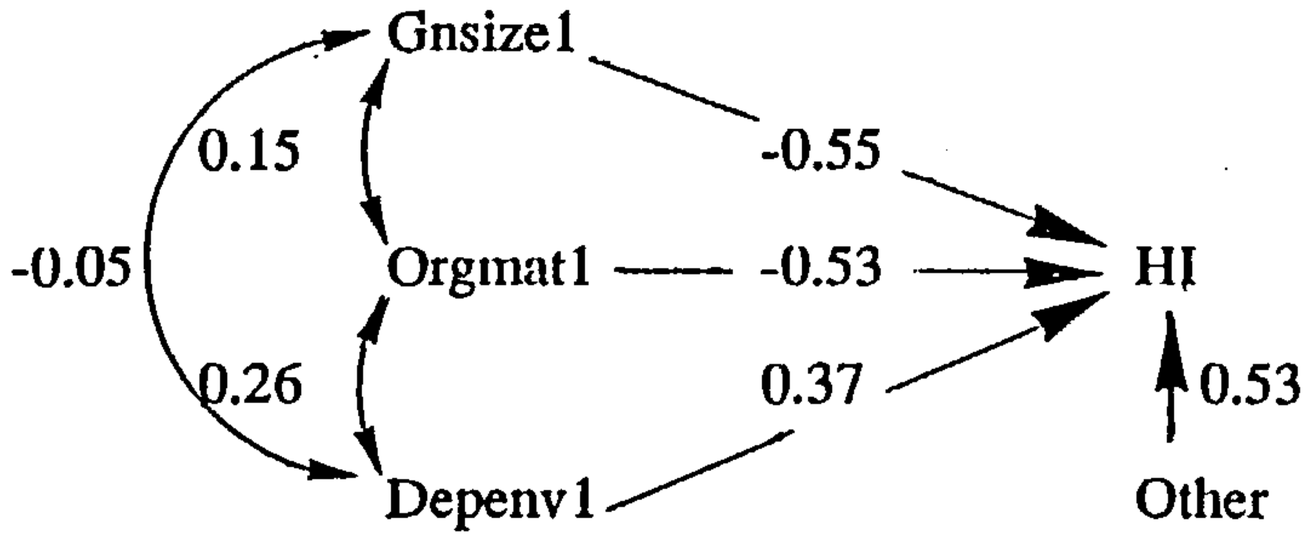

Heather Formation R^2 0.21

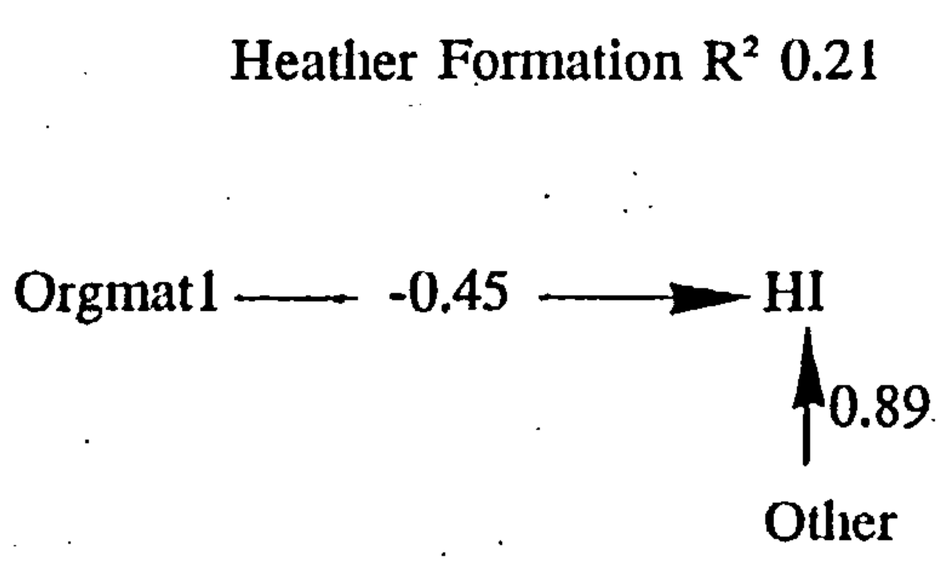

Kimmeridge Clay Formation R^2 0.12

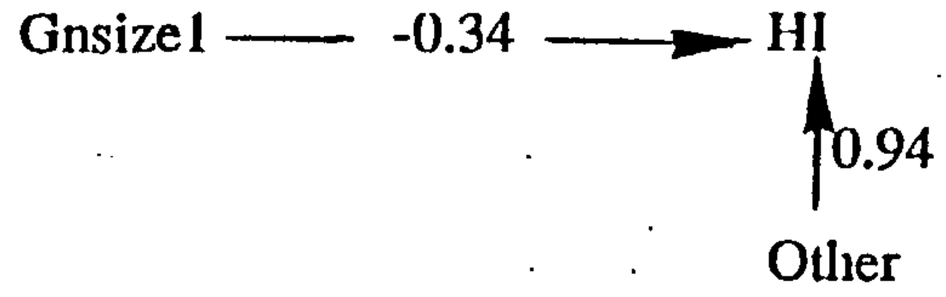

In general the fit of the models predicting HI are lower than those predicting TOC in the corresponding formations. Only in the Draupne Formation is the HI model a good fit, the Heather and Kimmeridge Clay Formation models being poor. Negative path coefficients with organic maturity are noted in both the Draupne and Heather Formations, in accordance with the rapid decrease in HI known to occur over the maturity range studied (R_o range of about 0.4-1.1 in the Draupne and Heather Formations). The maturity variable is not selected in the Kimmeridge Clay Formation model where the maturity range is much more restricted. Negative path coefficients are observed with the grain size variable in both the Draupne and Kimmeridge Clay Formations, suggesting that the HI decreases in coarser samples of these formations, and probably represents the increasing input of marine algal organic material relative to that of terrestrial organic matter away from sources of clastic sediment. Depositional environment is also influential in the Draupne Formation where more hydrogenous material has been preserved in the more anoxic conditions.

From an examination of the path diagrams it would appear that TOC may be determined from the inorganic geochemistry with great success in the North Sea mudstone formations studied, and with rather lower accuracy in the Kimmeridge Clay Formation onshore. The ability of the inorganic geochemistry to predict the HI and hence the organic matter type is more limited but is successful in the Draupne Formation in the North Sea. The practical use of the models described above is limited however because the work involved in measuring the variables required is greater than that necessary to obtain direct measurements of both

TOC and HI once samples of the mudstone are available. The models presented above are of academic interest but would have little practical or commercial use.

7.3 Geochemical well logging

Geochemical well logs, that is logging tools capable of continuous downhole measurement of chemical elements are now commercially available, eg the Schlumberger Geochemical Logging Tool (GLT). The elements which such tools can determine downhole include Si, Al, Fe, Ca, K, Ti, S, Gd, Th, and U (Hertzog et al, 1987; Herron, 1988; Wendlandt and Bhuyan, 1990). Simpler gamma-ray spectroscopy tools such as the Natural Gamma-Ray Spectroscopy Tool (NGT) can determine the concentrations of K, Th, and U only, but are available in portable form (Myers and Wignall, 1987; Wignall and Myers, 1988). Given that tools such as these measure the concentrations of elements in rock volumes very much larger than those normally used in routine laboratory analyses, and hence result in a degree of sample averaging, the correspondence between geochemical log analysis of a sequence and analysis of conventional core from the same interval is usually good (Herron, 1986; Wendlandt and Bhuyan, 1990).

Data collected by such logs have previously been used to determine the mineralogy and lithology of sedimentary sequences downhole (Herron, 1986; Herron and Grau, 1987; Wendlandt and Bhuyan, 1990), and for the geochemical classification of sands and shales (Herron, 1988) although in the words of Wendlandt and Bhuyan (1990) 'the measurement technology appears to be ahead of the applications'. Suites of various logs have been used in order to predict organic geochemical parameters of interest in source rock studies namely TOC and organic matter type and maturity (Schmoker, 1979, 1980, 1981; Meyer and Nederlof, 1984; Mann et al, 1986; Mann and Muller, 1988). The ability to determine such important source rock characteristics by logging would have several benefits including cheap and rapid data output favouring the method for quick reconnaisance studies of sequences, perhaps to indicate horizons of good source potential for further investigation. There would

be no danger of error resulting from cavings and cutting contamination, and there would be continuous output of results in the place of a small number of often widely spaced core analyses. In all probablity greater amounts of such data would be collected and might also be used for correlation purposes.

7.4 Regression models for TOC and HI

7.4.1 Prediction of TOC

In order to produce a valid regression model having the widest possible application the calibration data set used was not based on a single formation but on merged data. The possible cost of a more broadly based model however is a poorer result for any particular formation studied. The data from the Kimmeridge Clay Formation was not included in the merged data set for two reasons. Firstly the fit of the path diagrams for TOC and HI listed above were much poorer in this formation than in the Draupne and Heather Formations and secondly because the Kimmeridge Clay which was deposited in a sub-basinal setting has a rather different lithology to the petroleum source rocks of the North Sea basins proper. Thus the data used for the calibration of the model, the 'training set' were taken from the Draupne and Heather Formations only.

As described above tools such as the GLT cannot currently measure Na or Mg. The log output can be corrected for (water filled) porosity to allow the dry weight percent as oxides to be calculated assuming that these sum to 100% as is normal practice. Obviously this results in some error, so that in samples with unusually large amounts of Na_2O or MgO the proportions of the other oxides are overestimated. In the mudstones studied here these oxides rarely contribute more than two or three percent (in the Draupne Formation for example the median averages of Na_2O and MgO are 0.91% and 2.16% respectively) so that this assumption is not a serious problem, although it will introduce noise to the measurements due to small variations in Na_2O and MgO. More important is the presence of several weight

percent of organic matter in these samples (eg a median average of 6.30% organic C in the Draupne) which might result in a more serious overestimate of most elements. For this reason, and for consistency within this work, it is suggested that Al_2O_3 normalised results are taken from the geochemical logs as these will be unaffected by variation in the compositional components of the rock which can not be measured.

Stepwise regression (see Chapter 6 for an explanation) was once more used to select variables for inclusion in the predictive models presented below. As the elements output from the geochemical logs have been Al_2O_3 normalised the following variables were available for selection by the stepwise procedure: SiO_2/Al_2O_3, Fe_2O_3/Al_2O_3, CaO/Al_2O_3, K_2O/Al_2O_3, TiO_2/Al_2O_3, S/Al_2O_3, Th/Al_2O_3, and U/Al_2O_3. Gd/Al_2O_3 can also be measured by logging tools but was not determined in this study and so could not be included as an independent variable in the regression. Allowing any of these variables to be included in the predictive model resulted in the equation:

$$(TOC/Al_2O_3)=0.153544(U/Al_2O_3)-5.272636(TiO_2/Al_2O_3)+0.334671$$

The value of R^2 for this model is 0.72. The model can be further improved upon however by noting that two of the environmental indices discussed and employed in Chapter 5 may be calculated from the geochemical log output. Both U and Th are given by the GLT and also by simpler gamma ray spectroscopy allowing the authigenic U content of the mudstones to be calculated as (Authigenic U)=(Total U)-(Th/3) (Myers and Wignall 1987; Wignall and Myers, 1988). Furthermore if it is assumed (as it has been in this work) that all S is present as pyrite (ie that organic and sulphate sources are negligible) then the DOP (Raiswell et al, 1988) may be calculated as $DOP=(S*1.25)/Fe_2O_3$.

The DOP alone is only a moderate estimator of the TOC content in the combined Viking Group data set. The model:

$$(TOC/Al_2O_3)=0.519718(DOP)+2.98689*10^{-4}.$$

having an R^2 value of 0.44. Authigenic U is rather better having an R^2 value of 0.65 resulting from the model:

$$(TOC/Al_2O_3)=0.011655(AuthU)+0.155509$$

but is still not as good a predictor as the initial model taken from the entire suite of Al_2O_3 normalised elements avalable.

The difference in the predictive abilities of the two environmental indices may result from the DOP being essentially fixed shortly after deposition (as one might expect for a depositional environment index) and hence relating to the depositional environment only, whereas authigenic U may be sensitive to organic maturity in addition to its behaviour as an environmental index (Chapter 6). Thus the DOP estimate may in some way relate more to the original (immediate post burial) organic matter content of the sediment whereas the authigenic U estimate may reflect C loss during burial and hence provides a better prediction of the current organic C content in the calibration set.

Combining both the DOP and authigenic U parameters results in a single model which is significantly better that these two used singly, and is also better than that selected directly from the Al_2O_3 normalised geochemical log output. The value of R^2 for the combined model is 0.76 indicating that TOC/Al_2O_3 can be modelled succesfully in the Viking Group mudstones. The combined model takes the form:

$$(TOC/Al_2O_3)=0.009156(AuthU)+0.287598(DOP)+0.032101.$$

It is this model which is thought to be of most use in predicting the TOC/Al_2O_3 contents of mudstones as it is based on two recognised indices, is simple, and gives the best fitting model observed for the training data set.

7.4.2 Prediction of the HI

Prediction of the HI is generally less successful in terms of model fit. Selecting by stepwise regression from the Al_2O_3 normalised variables resulting from downhole geochemical logs gives a complex model with an R^2 value of 0.64, the model being:

$$HI=101.6(U/Al_2O_3)-231.8(Th/Al_2O_3)-11402.9(TiO_2/Al_2O_3)+1126.1(K_2O/Al_2O_3)+594.87$$

The DOP alone is of limited use in the Viking Group data set as a predictor of the HI, the model:

$$HI=188.244738(DOP)+157.376041$$

having an R^2 of only 0.05. As for TOC above the authigenic U content is a better predictor of HI than is the DOP. This is again probably because the authigenic U content appears to be sensitive to the level of organic maturity, which is an important control on the HI over the maturity range studied, in addition to the depositional environment which it is conventionally believed to describe. R^2=0.54 for the model:

$$HI=11.687912(AuthU)+143.685908$$

Combining both the DOP and the authigenic U content in a single model results in significantly better predictive abilities than from either model alone (R^2=0.57), but the resulting model is still not as good as that employing Al_2O_3 normalised variables selected directly from the log variables. The combined model has the form:

$$HI=13.142926(AuthU)-161.881920(DOP)+209.868353.$$

The model with the greatest success in predicting the HI of the combined Viking Group data was selected from the set of Al_2O_3 normalised variables from the geochemical logs, plus the DOP and authigenic U parameters, and resulted in a model having an R^2 of 0.78 and being of the form:

$$HI=40.347052(AuthU)-498.518892(U/Al_2O_3)-$$
$$7077.502860(TIO_2/Al_2O_3)+765.915722(K_2O/Al_2O_3)-47.230831(Fe_2O_3/Al_2O_3)+461.047951$$

Whilst being the best fitting model applicable to the training set this model might not be as widely applicable as that based on the DOP and authigenic U contents alone as the latter is simpler and the former displays strong correlations between the independent variables which may lead to instability in the model.

7.5 Applicability

Some questions to be answered about models such as those presented above are how applicable are they? To what extent may they be used in predicting the TOC and HI of samples other than those taken from the Viking Group in the Norwegian North Sea? Some recalibration of the models may be required for accurate prediction of these properties in mudstones from other locations and of differing ages. To test the models described above an attempt has been made to predict the TOC content of Jurassic mustones from the Haltenbank area of the Mid-Norwegian Continental shelf. Analytical methods used for the determination of the TOC content, and the inorganic variables are the same as for the calibration data set and are described in Appendix A.

The measured TOC concentrations in the wells sampled in this area ranged between 0.60 and 6.68%. The model used for the prediction of TOC here is that derived from the Authigenic U and DOP parameters in above:

$$(TOC/Al_2O_3)=0.009156(AuthU)+0.287598(DOP)+0.032101$$

The results of the predictive model are presented in Table 7.1 together with the TOC contents measured directly on the samples. The correspondence between predicted and measured values is generally good with an average absolute discrepency of 1.1% between predicted and measured values. The residuals (ie the difference between measured and predicted TOC contents) average -0.38% for these samples indicating that overall the model taken from the Viking Group data underestimates TOC contents slightly in the Haltenbank mudstones. A more detailed examination of Table 7.1 shows that in samples with little organic C the estimated value is higher than that measured, and that where measured TOC is high the estimate is usually lower than the measured value. The residuals have a standard deviation of 1.28% for these data.

These results are comparable to those obtained by Schmoker (1981) (residual average of about 0.18% and std dev of about 0.80% in weight percent terms; Schmoker worked in terms

Table 7.1 Predicted and measured TOC contents of Haltenbanken data.

Measured TOC	Predicted TOC	Residual
0.82	1.15	-0.33
1.13	3.88	-2.75
0.61	1.30	-0.69
1.09	2.05	-0.96
0.60	1.53	-0.93
6.68	5.40	1.28
4.04	2.40	1.64
2.27	2.54	-0.27

of volume percent) for estimates of the organic matter content of mudstones of Devonian age from the Appalachians made from gamma ray logs. These predictive results are considered to be very satisfactory especially as these data are drawn from out of the geographical area of the calibration set, and as studies of the geochemistry suggest that they may in places be considerably different lithologically, so that estimates of Viking Group shales from within the North Sea area may be even better. As the data stand the results are certainly accurate enough to locate rich potential source rock horizons which may be sampled directly for more detailed analysis. For more detailed work the models could be recalibrated against locally sampled material.

7.6 Conclusions

Strong correlations exist between the inorganic geochemistry of the mustones studied and their organic geochemistry. Log(TOC/Al_2O_3) can be modelled succesfully in the Draupne and Heather Formations, and moderately well in the Kimmeridge Clay Formation using the path diagram approach described in the previous chapter. The HI can also be successfully modelled in the Draupne Formation by this process, but not so well in the Heather and Kimmeridge Clay Formations. Using such models to predict TOC and HI in mudstones whilst possible, is of limited use as both TOC and HI can be determined directly from sampled material more easily than can the variables required to predict them from the path analysis approach.

Some elements can however be measured directly, downhole, from geochemical logging tools and use of these elements alone still allows good estimates of both TOC and HI to be made in a data set drawn from the Viking Group mudstones. These estimates may be improved further if the DOP and authigenic U contents are calculated from the log output and used as further independent variables in the predictive models. This method offers prospects of a logging system capable of continuous TOC and HI measurement. Application of these models to other data sets allows their applicability to be tested.

Chapter Eight

Discussion and Conclusions

8.0 Discussion and Conclusions

8.1 Discussion

8.1.1 Mechanisms of metal enrichment in black shales

In Chapter 6 it was demonstrated by means of path analysis that depositional environment (particularly the palaeooxygen concentration of the bottom water) was the most influential control over the concentration of the elements Cu, Cd, Mo, Ni, U, V, and Zn in the three Upper Jurassic mudstones studied. These elements are amongst a group commonly found to be enriched in black shales (Vine and Tourtelot, 1970). In this study Mo and U are enriched in all three of the formations relative to average shale, Zn is enriched in the Draupne and Heather Formations, and Cu, Cd, Ni, and V in the Draupne Formation only (Chapter 3). Co, another element often abundant in black shales is enriched in the Draupne Formation. The ultimate source for these increased metal contents is probably sea water itself (Holland, 1979; Brumsack, 1980; Holland, 1984) as the order of increased concentration in black shales usually follows the concentration of the elements in sea water.

Most of these elements display nutrient-like water column profiles in the oceans (Boyle et al, 1976; Bruland, 1980; Collier, 1984; Johnson et al, 1988; Fig 8.1) with near surface depletion and enhancement at depth resulting in variable concentrations. This variation may be accentuated in regimes where water column stratification hinders mixing (Brongersma-Sanders, 1966). The main mechanism by which elements are transported to the sediment surface is by adsorption on sinking particulate matter either of organic origin (Balistieri et al, 1981; Fischer et al, 1986) or composed of metal oxides (Knauer et al, 1982). On deposition diagenesis radically affects these transporting phases (Klinkhammer, 1980; Heggie et al, 1986; Pedersen et al, 1986; Johnson et al, 1988; Shaw et al, 1990) so that the final mineralogical form in which the elements are fixed may be different from the form in which they were introduced to the sediment. Elements are transferred from their initial host to their final

residence via the sediment pore water, and studies of modern pore water systems are considered as evidence below in the discussion of the mechanisms of metal fixation likely to have caused the elevated metal contents observed in these sediments. These studies are often performed on sediments of relatively low C content however as the resolution of the different diagenetic reaction zones is increased under such circumstances. A second line of evidence may be obtained from studies of other ancient mudstones.

A starting point in the consideration of the mechanisms of metal fixation in these mudstones may be the correlation data presented and discussed in Chapter 4. For the Draupne Formation (which is most metal rich) the log transformed variables of Ni, Co, and Mo were found to be correlated most highly with the pyrite and S variables. These correlations remained generally strong in the other formations studied despite the lower contents of these elements and hence the greater relative importance of the non-authigenic fraction and suggested that these three elements are associated with pyrite in the sediment.

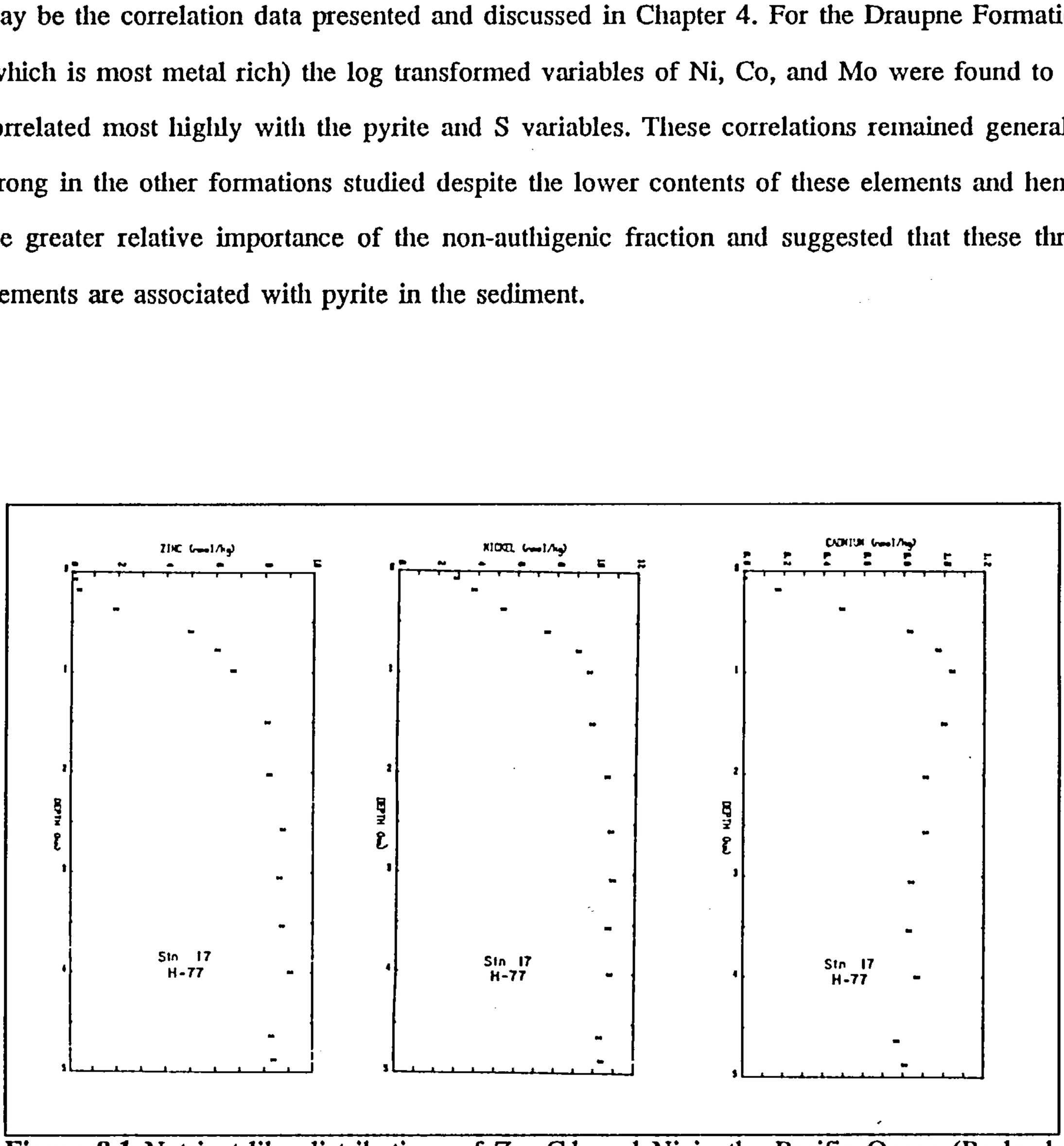

Figure 8.1 Nutrient-like distributions of Zn, Cd, and Ni in the Pacific Ocean (Bruland, 1980)

Co has been demonstrated by Knauer et al (1982) to be scavenged in the water column by Mn oxides resulting in a profile different to most other elements. It is in this adsorbed form that it is probably initially deposited in the sediment. Reduction of these oxides during diagenesis releases Co to the sediment pore waters (Johnson et al, 1988; Shaw et al, 1990). Ni is mobilised by the reduction of Mn oxides, and by Fe oxide reduction (Klinkhammer, 1980; Heggie et al, 1986; Shaw et al, 1990), although other studies suggest that it is deposited adsorbed on particulate organic matter and opal (Bruland, 1980; Balistieri et al, 1980; Heggie et al, 1986). Anoxic conditions promote rapid Co and Ni mobilisation (Johnson et al, 1988; Shaw et al, 1990), and may result in water column dissolution of Mn and Fe oxides with associated release of Co and Ni (Brewer and Spencer, 1974). In sediments deposited beneath a normally oxygenated water column and containing little organic matter the mobilised Co and Ni diffusing upwards is fixed on Mn oxides which precipitate above the zone of diagenetic Mn reduction (Klinkhammer, 1980, Heggie et al, 1986; Johnson et al, 1988; Shaw et al, 1990). Under more reducing conditions Co and Ni may be lost to the overlying sea water as Mn oxides no longer precipitate and scavenge these elements (Johnson et al, 1988; Shaw et al, 1990).

In very C rich sediments such as those of this study the diagenetic reaction zones become telescoped and Mn and Fe reduction may be occurring almost simultaneously with the reduction of sulphate to sulphide, which minimises Fe activity (Curtis, 1987; Shaw et al, 1990). The Co and Ni released from the reduced oxide phases is also likely to be precipitated as sulphide (Elderfield et al, 1981). Raiswell and Plant (1980) have studied the trace element content of pyrite separated from concretions and concluded that the local oxide sources of Fe used to form an early generation of framboidal pyrite were sufficient to account for the observed content of Co and Ni. If the pyrite of these mudstones is 100% early diagenetic framboidal pyrite it might contain 200-700ppm Co and 600-3100ppm Ni (Raiswell and Plant, 1980) which even though these were to be regarded as maximum concentrations is well in excess of the concentration required for the pyrite to contribute a large proportion of the total Co and Ni contents.

Further support is given by the work of Nissenbaum and Swaine (1976), who in a study of recent sediments found Co and Ni to be predominantly present in sulphides even in the early stages of diagenesis. Patterson (1988) detected up to 1000ppm Ni in the framboidal pyrite of Australian oil shales with the average being 300ppm, and Co was at least partly pyrite associated. Patterson et al (1986) found variable but high Ni contents in pyrite framboids (2200ppm) which accounted for 30-100% of the whole rock Ni. About 50% of Co was also associated with sulphides, possibly sphalerite. Patterson et al (1988) found 300ppm Ni and 800ppm Co in framboids and also had some evidence that these concentrations were higher than in later euhedral pyrite. Evidence from other shale studies and from modern pore water compositions would seem to be consistent with the observations made in Chapter 4 that the bulk of the Co and Ni in these sediments is held in pyrite. Organic matter, silicates, and sphalerite (in the case of Co) may also contain smaller amounts of these elements.

The log ratio transformed Mo variable was also found to be highly correlated with the pyrite variables in the Draupne Formation (Chapter 4) suggesting that pyrite was also a major host where this element is greatly enriched. As with both Co and Ni, Mo appears to be concentrated in very oxidising sediments and also under very reducing conditions (Turekian and Bertine, 1971; Bertine and Turekian, 1973; Pilipchuk and Volkov, 1974; Contreras et al, 1978; Shimmield and Price, 1986). In sea water the concentration of Mo is both high and uniform (Bruland, 1983) unlike the nutrient like profiles of other elements (Bruland, 1980), and Mo in its oxidised form displays a strong affinity for Mn oxides (Shimmield and Price, 1986). Release of Mo as with Ni and Co occurs in the early diagenetic Mn reduction zone (Contreras et al, 1978; Shimmield and Price, 1986; Shaw et al, 1990) and depending on conditions may involve reduction from the strongly adsorbed Mo(VI) form to Mo(III) in solution (Shimmield and Price, 1986), and further release from degrading organic matter (Contreras et al, 1978, Brumsack and Geiskes, 1983). The resulting pore water Mo is then fixed in the sediment either as sulphide (Bertine, 1972; Bertine and Turekian, 1973) as would appear to be the case in the Draupne and Heather Formations, or associated with organic

matter as is apparent in the Kimmeridge Clay Formation (Nissenbaum and Swaine, 1976; Brumsack and Geiskes, 1983; Shimmield and Price, 1986). In sediments deposited under very reducing conditions Mo may also be fixed directly by the reduction of Mo in sea water (Shaw et al, 1990) leading to very high concentrations, a process which may have been of importance in the Draupne Formation.

There is also evidence of a later episode of mobilisation to the pore water (Brumsack and Geiskes, 1983; Shaw et al, 1990) attributed to complexation by dissolved organic matter although that analysed by Nissenbaum and Swaine (1976) was low in Mo. The recrystallisation of Fe monosulphides to pyrite may also be responsible for Mo mobilisation. In their study of concretionary pyrite Raiswell and Plant (1980) found that unlike Co and Ni large amounts of Mo are not fixed in early framboidal pyrite (<60ppm in pyrite if all is framboidal) which is insufficient to account for the Mo content of the Draupne Formation although it may be significant in the Heather. It was postulated that more Mo was incorporated in the later generation of euhedral pyrite which was precipitated directly from the pore water without passing through a monosulphide precursor. The presence of Mo in this later pyrite generation supports its continued availability in the pore waters to some depth. It is interesting to note in this context that one Draupne Formation sample containing 24.9% S, and hence approximately 50% pyrite most of which is probably a later euhedral pyrite concretion, has a Mo content of 609ppm. In the Heather Formation a similar pyrite concretion sample has only 10ppm Mo; this possibly reflects the much lower concentration of Mo in the pore waters of this formation relative to the Draupne. In the case of the Draupne Formation unless the pyrite has an unusually high concentration of Mo other hosts must also be present, organic matter being most likely although this is hard to discern as the organic C content is correlated with the pyrite variables.

In the pyrite studied by microprobe by Patterson et al (1986) the Mo contents were variable and other sources were needed to account for all Mo observed.

In contrast to Co, Ni, and Mo the log transformed variables of the elements V, Cu, Zn, and Cd were usually correlated with the organic C variable more strongly than, or equally with, the pyrite variables, where their concentrations were abundant, making the determination of their host difficult in Chapter 4. As concentrations decreased towards the average these correlations were reduced and became more erratic as a result of the greater relative importance of silicate hosts. The distributions of these elements in sea water are all nutrient-like (Boyle et al, 1976; Bruland, 1980, 1983; Collier, 1984). V and Cd appear to show rapid near surface cycling (Boyle et al, 1976; Collier, 1984), whereas Zn is regenerated at greater depths associated with carbonate or opal dissolution (Bruland, 1980). Cu displays a depth distribution which is almost linear and which has been interpreted as a result of surface removal and deep water replenishment from sediments complicated by the effects of scavenging by particulates (Bruland, 1980). The main supply of these elements to the sediments is due to adsorption on sinking particulate matter such as organics or metal oxide grain coatings (Balistieri et al, 1981).

Cu, which is only enriched relative to average shale in the Draupne Formation, is mobilised from the sediment to the overlying waters under oxic conditions although some is retained by adsorption (Fischer et al, 1986; Heggie et al, 1986; Shaw et al, 1990). As conditions become more reducing this flux decreases and may be reversed, probably because of enhanced preservation of the organic matter carrier phase (Johnson et al, 1988; Shaw et al, 1990). The Cu content preserved in a sediment is probably mainly adsorbed on organic matter and other suitable sites, Nissenbaum and Swaine (1976) having shown that humic substances may contain a large proportion of the Cu content of marine sediments. Where pore waters are sulphidic some Cu may also be precipitated as chalcopyrite.

V too is concentrated relative to average shales only in the Draupne Formation (Chapter 3), where it displays a good correlation with the log transformed organic C variable. As with Cu it is probably initially associated with particulate organic matter probably as the reduced vanadyl form which is relatively insoluble and strongly adsorbed on particulates. In oxic

conditions V is freed to the pore waters by degradation of the host organic matter (Heggie et al, 1986; Shaw et al, 1990), and in the Mn reduction zone where adsorption on Mn oxides may aid oxidation to the more soluble higher oxidation states (Wehrli and Stumm, 1989), and some may be lost from the sediment. In more reducing sediments the potential for retention of V in its reduced form is increased and V concentrations may be further increased by in situ reduction of V from overlying sea water (Lewan and Maynard, 1982; Shaw et al, 1990). V is noted for its concentration in organic matter, particularly tetrapyrrole complexes (Lewan and Maynard, 1982; Premovic et al, 1986) which may be found in both the bitumen and kerogen. Maximum concentrations of such complexes are found when the organic matter concerned has the shortest possible exposure to aerobic oxidation, with algal matter being most suitable (Lewan and Maynard, 1982). These factors explain why the Draupne Formation of those examined is enriched in V.

Zn is enriched in both the Draupne and Heather Formations relative to the average (Chapter 3). It is introduced into the sediment adsorbed on particulate organic matter as with other elements (Balistieri et al, 1981) and is released to the pore waters as this is decomposed, and also in the Mn reduction zone. Fischer et al (1986) show that about 75% of the Zn deposited in oxic sediments is returned to the overlying water. In organic rich sediments such as those of this study organic matter is able to fix Zn (Nissenbaum and Swaine, 1976), and may account for some of the Zn present. The occurrence of reduced S in the pore water resulting from sulphate reduction will also cause Zn fixation as the sulphide, and this will be of greater importance where the diagenetic zones have been telescoped allowing overlap of the reactions. Brumsack (1980) suggests that Zn precipitation as sphalerite may occur in an anoxic water column prior to pyrite formation in the sediment, and in the Black Sea dissolved Zn concentrations decrease rapidly below the O_2/H_2S interface (Brewer and Spencer, 1974). Sweeney et al (1987) propose the reverse process however with framboidal pyrite formation occurring in the water column followed by base metal sulphide precipitation in the sediment. This would be consistent with the implication of Wedepohl (1972) that Zn sulphide precipitation is favoured by low Fe concentrations and is in agreement with the limited

amount of SEM investigation undertaken in this study. This shows that for the Draupne Formation Zn is present as sphalerite which overgrows early formed framboidal pyrite, which may have a water column origin in the often anoxic and euxinic depositional conditions of the Draupne (Chapter 5). In this context it is significant that the log ratio transformed Zn content has a greater correlation with the DOP (p=0.65) than with either the S (p=0.59) or organic C (p=0.56) variables suggesting that the bulk of sphalerite precipitation occurred after pyrite formation had all but ceased because of the consumption of all of the available reactive Fe, and that the resulting increase in reduced S activity and decrease in Fe may have contributed to sphalerite precipitation.

Cd is also enriched in the Draupne Formation and in oxic sediments is usually rapidly cycled at the sediment surface (Fischer et al, 1986) most probably because of the near surface degradation of organic matter (Heggie et al, 1986) and Mn oxide reduction (Balistieri and Murray, 1986). In reducing sediments Cd is undoubtedly precipitated as sulphides (Gong, 1977; Elderfield et al, 1981) probably in solid solution with sphalerite, and thus in the Draupne is probably also to be found overgrowing pyrite framboids.

U is enriched relative to average shale in all of the formations investigated here (Chapter 3). The log transformed U is generally correlated with the organic C variable and the pyrite variables. U deposited in oxic sediments is typically rapidly and almost completely remobilised near the sediment surface (Fischer et al, 1986) probably because of oxidation of the organic phase on which it is adsorbed, although living organic matter can also concentrate U (Mann and Fyfe, 1985). The presence of abundant organic matter in the sediment will allow pore water U to be fixed by adsorption of UO_2^{2+} onto organic matter, probably by ion exchange with H^+ of carboxyl groups (Borovec et al, 1979) which is most effective at a pH of 5-8.5 (Langmuir, 1978), and also by formation of relatively stable organic-U complexes above 45°C (Nakashima et al, 1984). Disnar (1981) has shown that UO_2^{2+} is more strongly adsorbed by organic matter than other divalent cations. Reduction of U(VI) to U(IV) and precipitation as uraninite does not occur until higher temperatures are reached (Nakashima et

al, 1984, Meunier et al, 1990). Cagatay et al (1990) show that in some U rich sediments from the near surface Black Sea about 50% of the total U content is present in the exchangeable form, about 25% is fixed in more stable organic-U complexes, and the remainder is detrital. No uraninite was detected under these near surface conditions. Some U is also probably present in these organic rich sediments by incorporation in the francolite produced during organic matter degradation, where U may substitute for Ca.

8.1.2 Metal mobilisation in diagenesis and catagenesis of mudstones

8.1.2.1 Composition of oilfield brines

The major importance of early diagenesis in controlling the trace element composition of mudstone is illustrated in Chapter 6 and the mechanisms of metal incorporation are discussed above. Organic maturity (and thus the continuing effect of diagenesis) was also shown in Chapter 6 to be of importance in controlling the contents of Pb, Zn, Mo and U where it is enriched. Cd too increases in concentration in the Draupne Formation where it follows Zn, but to avoid duplication of the discussion it is not considered seperately. This work suggests that both Mo and U may have been mobilised from the mudstones studied during burial, and that Pb and Zn appear to have been fixed. In both cases the medium by which concentration changes occur must be the sediment pore waters. To be plausible the pore waters must contain appreciable concentrations of these elements.

Oilfield brines are generally the only samples of deeply buried formation waters available for study, although fluid inclusions may also be of use. No data were available from the areas studied but there is now a small volume of literature concerning trace element concentrations in oilfield brines from elsewhere (Billings et al, 1969; Carpenter et al, 1974; Kharaka et al, 1987; Saunders and Swann, 1990). Further information on the trace element suite present in such brines is also available from the analysis of well scale (Saunders and Rowan, 1990).

Oilfield brines with high metal concentrations are typically very saline (maxima exceed 300,000mg/l TDS) and salinity generally but not always increases with depth (Kharaka et al, 1985; Kharaka et al, 1987). The cations are dominated by Na which makes up 70-90% of the total. Ca is the second most abundant cation and generally increases with increasing salinity but Mg is lower than seawater concentration and decreases with increasing temperature. Cl is the dominant anion increasing as salinity increases, and sulphate is low (<100mg/l). The high salinities are a result of halite dissolution (Kharaka et al, 1987) but the elevated Ca concentrations in some brines, and the low Mg contents, are due to water rock reactions such as dolomitisation (Kharaka et al, 1987) or the organic acid mediated albitisation of feldspar (Morton and Land, 1987; Fisher and Boles, 1990). The role of membrane filtration by shales (Graf, 1982; Kharaka et al, 1985) as means of raising salinity and altering fluid compositions remains controversial (Hanor et al, 1988).

The available data (Billings et al, 1969; Carpenter et al, 1974; Kharaka et al, 1987; Saunders and Swann, 1990) mainly from the Gulf Coast suggest that both Pb and Zn can be present in high concentrations in oilfield brines (eg up to 70mg/l Pb and 245mg/l Zn, Kharaka et al, 1987) although these very high concentrations may be exceptional. Data on Mo and U concentrations in subsurface brines are more limited but Saunders and Swann (1990) report Mo concentrations of up to 0.05mg/l and U contents of up to 0.09mg/l and Saunders and Rowan (1990) report 0.36mg/l Mo from Mississippi. Kraemer and Kharaka (1986) and Kraemer (1981) report U in Gulf Coast brines to be orders of magnitude lower at up to 0.054ug/l at slightly higher temperatures.

In their study of Mississippi well scale Saunders and Rowan (1990) report Pb and Zn contents of up to 10% and 4800ppm respectively. Mo and U were found at up to 90ppm and 1.5ppm respectively. These concentrations do not necessarily reflect the concentrations of the elements in the brines but their presence in well scale does confirm their occurrence in the brines.

8.1.2.2 Oilfield brines and ore deposits

Remarkable similarities have been noted between the temperature ranges, and chemical and isotopic compositions of metal bearing oilfield brines, and the fluids responsible for the deposition of MVT Pb-Zn ore deposits as inferred mainly from fluid inclusion evidence (Sverjensky, 1984). The origin of these deposits is now generally believed to be a result of migrating basinal derived brines transporting metals to the site of ore deposition (Anderson and MacQueen, 1982; Sangster, 1990), the flow of which may be episodic (Cathles and Smith, 1983). The differences between the compositions of the oilfield brines and the ore fluids can be explained by brine evolution due to wall rock reaction in the aquifer during brine migration to the point of ore deposition (Sverjensky, 1984; 1987).

Further support to a link between oilfield brines and MVT Pb-Zn deposits is given by the common occurrence of Pb-Zn mineralisation similar in style to MVT throughout the Gulf Coast area. Kyle and Price (1986) describe Pb-Zn mineralisation in 16 salt dome cap rocks, some of which are commercial ore deposits. These are thought to arise as a result of metal bearing saline formation waters such as those described above episodically ascending up salt dome flanks and encountering reduced S in the vicinity of the cap rocks (Kyle and Price, 1986; Light et al, 1987; Hallager et al, 1990). Smaller scale occurrences of sphalerite have been recorded throughout the Gulf Coast area by Tieh and Ledger (1987) in host rocks of varying lithology, and these have been related to the passage of metal rich formation waters. Trace elements associated with MVT deposits and with salt dome cap rock mineralisation usually include Mo, and in addition U mineralisation is found associated with the cap rocks although its source has not been related to the saline brines responsible for the base metal mineralisation (Kyle and Price, 1986; Light et al, 1987).

8.1.2.3 Speciation and sources of metals in oilfield brines and MVT deposits

Surdam et al (1984) and MacGowan and Surdam (1988) have presented experimental evidence for the efficient complexation of Al by difunctional organic acid anions. Their experiments show that large amounts of Al may be complexed in this manner (eg 33ppm Al in solution after reaction of San Joaquin Basin brines with whole rock sandstone, and higher concentrations when feldspar is leached). Geochemical modelling of oilfield brines under subsurface conditions (Kharaka et al, 1985) however suggest that over 99% of Al is complexed with OH^- and that organic acid complexes were minimal. Surdam and MacGowan (1988) are of the opinion that such results are artefacts of erroneous initial starting conditions of such models, due to underestimates of Al and organic acids in produced brines because of precipitation and analytical difficulties.

Similarly despite evidence for the existence of stable Pb and Zn acetate complexes over the range of diagenetic and MVT temperatures (Yang et al, 1989; Giordano, 1989) studies of the speciation of Pb and Zn suggests that organic acids themselves are not significant in complexing these metals in oilfield brines (Kharaka et al, 1985; Kharaka et al, 1987) or MVT ore solutions (Giordano, 1985). Both metals appear to be dominantly incorporated in chloride complexes although the organic acids are important in controlling Eh and pH and are thus indirect controls over metal concentration. The explanation proposed to account for this apparent anomaly (Kharaka et al, 1985; Kharaka et al, 1986; Kharaka et al, 1987) is competition by other cations (eg Na and Ca) for organic acid anions. The stability of some of the Pb and Zn complexes with the various organic anions is unable to compensate for the much greater concentrations of the major cations in solution.

U too (Kharaka et al, 1986, Kraemer and Kharaka, 1986) is also not appreciably complexed by organic acid anions under subsurface conditions. U complexes are dominated by UO_2^+, UO_2Cl^+, and $UO_2(CO_3)_2^+$, and U is saturated with respect to both uraninite and coffinite. Mo

is probably transported as an oxyacid complex such as H_2MoO_4 under subsurface conditions (Wood et al, 1987).

Sources suggested for these elements in oilfield brines have varied but normal diagenetic processes seem able to account for the observed concentrations. In the Gulf Coast area the dissolution of evaporites has probably been important in generating the high salinities which apparently favour very high metal contents (Saunders and Swann, 1990), and as there is an inverse relationship between dissolved sulphide and metal concentrations the dissolved sulphide concentrations must be low (Kharaka et al, 1987). The source of the metals has been suggested as a result of dissolution of feldspar, or iron oxides, or the leaching of shales (Carpenter et al, 1974; Zeilinski et al, 1983; Kharaka et al, 1987).

The role of the organic acids in feldspar dissolution has been considered above. Dissolution of K-feldspar especially, but also albitisation of plagioclase, will result in liberation of Pb to the pore waters, and laboratory leaching of shales (Hathaway et al, 1972; Long and Angino, 1982; Thornton and Seyfried, 1985) by synthetic and natural brines illustrates that metals including Pb and Zn may be mobilised under laboratory conditions. Similarly Pb, Zn, and U were shown to be leachable from red beds by various solutions (Zielinski et al, 1983). Studies of Mississippi Valley Type Pb-Zn deposits which are believed to be a product of mineralising fluids similar in composition to metal rich oilfield brines produce evidence for multiple sources of Pb and Zn (Deloule et al, 1986; Crocetti et al, 1988), and the genetic models of Sverjensky (1984) suggest that oilfield brines supply much of the Zn in these deposits but that a component of the Pb is derived by water rock reactions in the aquifer as the brine migrates from the basin to the site of ore deposition.

8.1.2.4 Calculations of metal fluxes in the Draupne and Heather Formations during burial

Results presented earlier in this work suggest that the concentrations of both Pb and Zn have increased, and that Mo and (in the Draupne Formation only) U have decreased as burial has

progressed. Calculations may be performed to illustrate the extent of these changes using the path diagrams of Chapter 6. As an example the calculation of the Pb concentration change in the Draupne Formation will be demonstrated. The relevant path diagram is shown below.

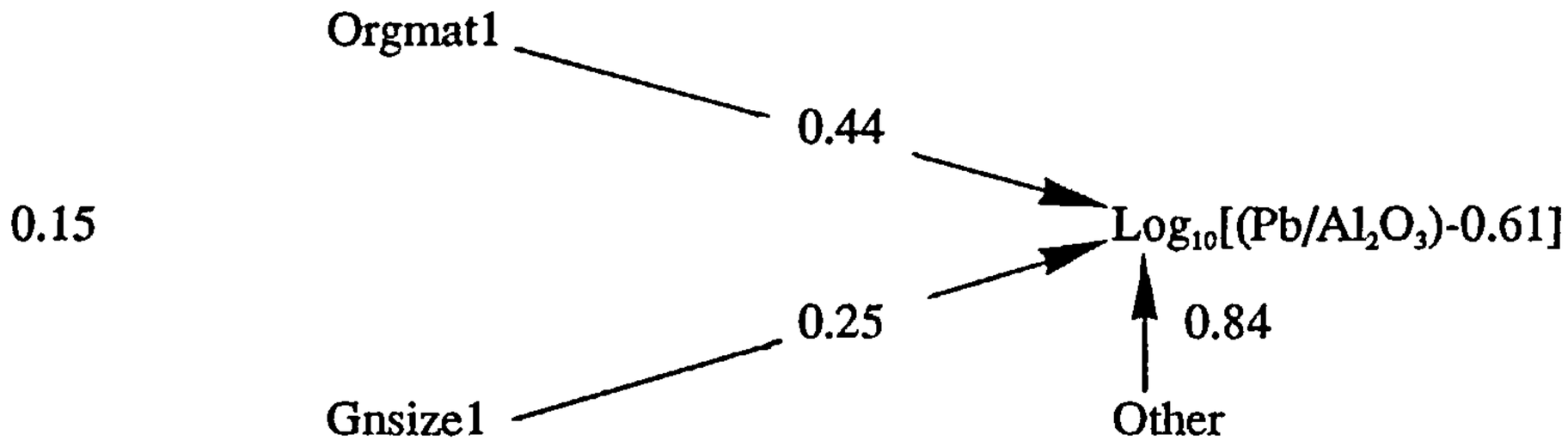

Path diagrams represent the relationships between standardised variables, those in which the mean average is transformed to zero, and the standard deviation to unity. In calculating the change in Pb concentration occurring in an average sample of the Draupne Formation as it is buried from about 1500m (approximately the shallowest burial depth of the Draupne considered in this study) to a depth of about 4000m (deepest Draupne Formation burial studied) only the organic maturity term need be considered. The grain size term is zero as grain size is specified to be the mean for the formation and is hence zero. Note that the average sample referred to is an average Draupne Formation sample, having the average grain size of the Draupne, and having been deposited under average Draupne Formation conditions. These average values will obviously vary between the different formations, the average Draupne depositional environment being considerably more anoxic than that of the Heather Formation for example.

In standardised variables then the Pb content of an average Draupne Formation sample is reduced to the expression:

$$\log_{10}[(Pb/Al_2O_3)-0.61]=0.44*Orgmat1$$

At 1500m burial depth the value of Orgmat1 for the Draupne Formation is -0.12. At 4000m it takes a value of 3.41. Standardising these variables results in values of -0.11 and 3.35 respectively thus at 1500m burial depth the ratio of Pb(ppm) to Al_2O_3(wt%) is 1.36. The corresponding ratio is 4.06 at 4000m. Taking the median Al_2O_3 content of the Draupne (17.1%) results in Pb contents of 23ppm at 1500m rising to 69ppm at 4000m, an increase in 46ppm over this interval after the effects of grain size variation have been removed. The calculated increases in Pb and Zn for the Draupne and Heather Formations over the burial interval 1500m-4000m calculated in the manner described above are summarised in Tables 8.1 and 8.2.

8.1.2.5 The fixing of Pb and Zn during Draupne and Heather Formation burial

The increased content of base metals in the more deeply buried samples of both the Draupne and Heather Formations must arise as a result of interaction with the formation waters. Taking the data of Saunders and Swann (1990) as a basis a typical metal rich formation water of the Gulf Coast area may contain about 100mg/L Zn and 20mg/L Pb. Compared to the less saline waters of the North Sea these concentrations are likely to be high but will give an indication of the minimum volumes of formation water needed to supply the necessary Pb and Zn assuming that all the Pb and Zn in solution may be precipitated. For the Draupne Formation the required water/rock ratios are 3.8L/kg for Zn supply and 2.3L/kg for Pb. The

Table 8.1 Changes in calculated abundance of Pb, Zn Mo, and U in the Draupne Formation as a result of burial.

Draupne Formation

Element	1500m Depth	4000m Depth	Difference
Pb	23ppm	69ppm	+46ppm
Zn	383ppm	764ppm	+381ppm
Mo	77ppm	11ppm	-66ppm
U	24ppm	8ppm	-16ppm

Table 8.2 Changes in the calculated abundance of Pb, Zn, and Mo in the Heather Formation as a result of burial.

	Heather Formation		
Element	1500m Depth	4000m Depth	Difference
Pb	21ppm	30ppm	+9ppm
Zn	132ppm	159ppm	+27ppm
Mo	5.6ppm	3.1ppm	-2.5ppm

corresponding quantities for the Heather Formation are 0.27L/kg and 0.45L/kg. The calculated volumes are similar (about 1 order of magnitude spread) for both Pb and Zn in the Draupne and Heather Formations, the Heather Formation values being noticably lower.

The porosity of an argillaceous rock may be estimated to be about 13% at an intermediate depth of 2500m (Baldwin and Butler, 1985) corresponding to about 0.050L/kg of rock so that the required pore volumes of brine required to supply the necessary Pb and Zn are not excessive, varying between a minimum of 5 and a maximum of about 75, although as stated above these are likely to be minimum values.

If Pb and Zn have been supplied to the Draupne and Heather Formations by compactionally derived brines during their burial from 1500m to 4000m, then these metals must have a source within or adjacent to the Viking Graben system. It is interesting at this point to consider the ratios of Zn to Pb supplied to these two formations. In the former the elemental ratio is about 8 whilst in the latter it is 3. These values are close to the Zn/Pb ratio of about 5 found in most oilfield brines (Carpenter et al, 1974; Kharaka et al, 1987), and used in the calculations above (based on inspection of the data of Saunders and Swann, 1990). A Zn/Pb ratio of 4 is recorded for MVT ore deposits by Sangster (1990), and similar values are apparent in Gulf Coast salt dome mineralisation (Kyle and Price, 1984). Finally Thornton and Seyfried (1985) produced brine solutions with Zn/Pb of between 3 and 8 from an organic rich mudstone and sea water.

As oilfield brines from other areas have such similarities with MVT ore solutions, and because of the similarity in Zn/Pb ratios required here to those of MVT deposits the required metal source is likely to be similar to those of the ore deposits. Three main source types have been proposed for MVT deposits (see discussion above) namely shales, red beds, and feldspar bearing sandstones (Carpenter et al, 1974; Zielinski et al, 1983; Kyle and Price, 1984, Sverjensky, 1984; Thornton and Seyfried, 1985). Likely possible sources of Pb and Zn in the northern North Sea sequence would be the deeply buried and thickly developed mudstones of the Draupne and Heather Formations in the Viking Graben which have sourced much of the North Sea oil. A similar role as both a source of hydrocarbons and possibly metals, and as a reservoir seal has been proposed for the Edale shales in the genesis of the South Pennine Orefield (Mostaghel and Ford, 1984). There also exists abundant evidence for the albitisation of plagioclase feldspar in North Sea reservoirs at 2500-3000m (Morad et al, 1990), which may be followed by the albitisation of K-feldspar (Saigal et al, 1988; Aagaard et al, 1990) which is nearly complete by 3500m. Both of these processes but especially the latter could provide abundant Pb. Finally leaching of the Triassic red beds may have supplied both Pb and Zn to migrating brines.

Panno et al (1988) have documented Zn enrichment in a shale unit adjacent to, and overlying, a MVT Pb-Zn deposit (Pb was not determined) and suggest that the observed distribution of Zn and other elements in the ore deposit and adjacent shale is best explained by repeated episodes of metal enrichment related to episodic release of ore forming solutions. Thus it would appear that even relatively impermeable shales are able to fix Zn from MVT ore forming solutions. Similarly Coveney et al (1987) interpret metal distributions in the Mecca Quarry Shale to be the result of both syndepositional and early diagenetic fixation followed by a period of epigenetic mineralisation due to circulating formation waters expelled by compaction from the deeper parts of the basin. These migrating basinal brines were thought to have supplied a large proportion of the Zn present, the Zn source being the more deeply buried sedimentary sequence, and may have also been responsible for other occurrences of

Pb-Zn mineralisation in the region. This suggestion was also consistent with fluid inclusion studies of sphalerite in the shale which yielded formation temperatures of 80-100°C from saline brines. The model of Coveney et al could be applied with some modification to the Pb and Zn fixation in the Draupne and Heather Formations.

Assuming that there is an adequate supply of Pb and Zn to the Draupne and Heather Formations a suitable precipitation mechanism must be operable if they are to be fixed. The most likely method would for their precipitation as sulphides. This would be consistent with the limited SEM work showing sphalerite overgrowth on early diagenetic pyrite, although this has already been interpreted as reflecting early diagenetic growth of sphalerite. Both processes may have occurred as in the Mecca Quarry shales of Coveney et al (1987). The exact mechanism of metal fixation occuring in these sediments remains a subject for further investigation.

8.1.2.6 The mobilisation of Mo and U during Draupne and Heather Formation burial

Also shown in Tables 8.1 and 8.2 are the decreases predicted for Mo in average Draupne and Heather Formation samples over the burial interval 1500-4000m and the decrease in U in the Draupne Formation only. If it is assumed that the mudstone pore waters can transport these elements at concentrations of 0.03mg/L Mo and 0.02mg/L U (values taken from Saunders and Swann, 1990; U concentrations several orders of magnitude higher than those of Kraemer and Kharaka, 1986) and that they initially contained none we would require water/rock ratios of 2200L/kg and 800L/kg to remove the observed amounts of Mo and U respectively from the Draupne Formation, and 83L/kg to remove Mo from the Heather. The Heather Formation requires the smallest volume once more, but the agreement between these figures is worse than for the supply of Pb and Zn. These calculated volumes are however larger than those necessary to supply the additional Pb and Zn fixed in the respective formations assuming the brine concentrations of these elements are similar to those of the Gulf Coast (see calculations above).

The porosity decrease likely over the interval 1500-4000m is from 20% to 6% (Baldwin and Butler, 1985) corresponding to the expulsion of a little over 0.050L/kg of rock; clearly this is insufficient to account for the observed decrease in these metals unless concentrations are much greater than assumed. As the expulsion of formation waters due to compaction during burial is clearly insufficient, the loss of these elements may also suggest that the Draupne and Heather Formations have been flushed by fluids during burial.

One possibility for the enhanced removal of Mo and to a lesser extent U is transport in a hydrocarbon phase. The Mo content of oils may be as high as 2ppm (Manning and Gize, in preparation; though it is usually less than 0.5ppm; Jones, 1977), resulting in an oil/brine partition coefficient of about 40 (calculated after Manning, 1986) which suggests that in coexisting brine-hydrocarbon systems a large proportion of the Mo might be partitioned into the hydrocarbon phase. This greatly exceeds the corresponding coefficients for Pb (0.019) and Zn (0.28). If petroleum capable of transporting these levels of Mo were to have flushed through the Draupne and Heather Formations the observed Mo losses require only 33L hydrocarbon/kg of rock and 1.25L hydrocarbon/kg respectively. U concentrations in oils reported by Jones (1977) are lower with a reported maximum of 0.43ppm and are commonly less than 0.01ppm. The partition coefficient takes a value of 4.8 suggesting some preference for the petroleum phase, and the calculated U loss in the Draupne Formation would require 37L hydrocarbon/kg. As in the aqueous calculations above these are likely to be minimum values.

The volumes of formation waters required to account for the observed decrease in Mo and U are larger than those required to supply Pb and Zn, although if hydrocarbon transport has occurred the volumes may be lower. The loss need not be related to a fluid influx however, and may be a result of organic maturation. As both the Draupne and Heather Formations are potential hydrocarbon source rocks they have the potential to expel both Mo and U in hydrocarbons generated from their component organic matter, and to release quantities of

fixed metals to the pore water as the kerogen evolves. The Draupne Formation which is the better petroleum source rock has a hydrocarbon generation potential of up to 70g/kg in the Oseberg area (Dahl and Speers, 1985), a value which is higher than the data of this study suggest. The Heather Formation has a potential hydrocarbon yield of up to 15g/kg. The reservoired oil at Oseberg has density of 0.85g/ml. The hydrocarbon generating capacity of the Draupne Formation is thus 0.082L/kg and that for the Heather is 0.017L/kg. These calculated yields seem unable to account for the observed losses in Mo and U in the two formations however even allowing generous estimates for the transportable Mo and U, and assuming that the maximum hydrocarbon generation has occurred from each formation although a small proportion of the Mo loss in the Heather Formation may have occurred in this way.

In sediments where U is greatly enriched such as the Draupne Formation a large proportion is probably adsorbed on organic matter by means of ion exchange with carboxylic groups (Borovec et al, 1979). During burial and diagenesis maturation of organic matter results in loss of these functional groups (Surdam et al, 1984) and hence will reduce the capacity of organic matter to retain U. The acidic nature of the formation waters during burial will decrease the adsorption capacity of the organic phase still further (Langmuir, 1978; Borovec et al, 1979) resulting in even greater release of U. Much of the authigenic U fixed in organic rich sediments such as the Draupne Formation might be expected to be released during diagenesis therefore, although more stable organic-U compounds may form above 45°C (Nakashima et al, 1984). Concentrations of U in the formation waters would have to be very high however to explain the observed losses. Very high U concentrations (up to about 2mg/L) have been observed in reducing (but very shallow) ground waters in the vicinity of U deposits (Spalding et al, 1984), and may be a result of complexation as the concentrations exceed the solubility of both coffinite and uraninite.

Diagenetic release of Mo is more difficult to explain. The Mo in pyrite is probably immobile during diagenesis so that the observed losses may come from organic associated Mo. Other

evidence that Mo is mobile after early diagenesis comes from the high Mo concentrations found in pyrite concretions (see discussion above) although it is likely that these were formed at depths of only a few hundred metres below the sediment surface rather than at depths of kilometres. The occurence of a marginally not significant relationship between organic maturity and the Mo content of the Kimmeridge Clay suggests that Mo may be mobile during burial diagenesis in the onshore formation also despite its different burial history and samples of onshore Kimmeridge Clay have released Mo during low temperature (150°C) laboratory leaching experiments (E Rae, personal communication, 1990) which may suggest that large scale flushing is not a requirement for Mo loss.

8.1.2.7 History of fluid migration in the North Sea

The supply of Pb and Zn to the Draupne and Heather Formations, and the removal of Mo and U, imply that the these formations have behaved as an open system with respect to formation waters. It may at first sight appear paradoxical that these mudstones which form the seal on many North Sea reservoirs are permeable enough to allow such an exchange.

Evidence from a number of studies now suggests that the Brent Group reservoirs underlying the Draupne and Heather Formations have been flushed by compactionally driven fluids migrating from much more deeply buried sediments within the Viking Graben (Sommer, 1978; Liewig et al, 1987; Jourdan et al, 1987; Scotchman et al, 1989; Glasman et al 1989a and b). Petroleum generation began at about 65Ma in the East Shetland Basin (Goff, 1983) and 70-80Ma in the Viking Graben (Goff, 1983; Dahl et al, 1987) and was associated with or preceeded by the expulsion of hot and probably acid compactional brines (Sommer, 1978; Hancock and Taylor, 1978; Liewig et al, 1987; Jourdan et al, 1987; Glasman et al, 1989a and b; Scotchman et al, 1989) which were responsible for a number of the diagenetic phenomena observed in North Sea reservoirs namely feldspar dissolution (Jourdan et al, 1987; Scotchman et al, 1989), and the precipitation of quartz overgrowths and illite, and the illitisation of

kaolinite (Sommer, 1978; Jourdan et al, 1987; Liewig et al, 1987; Glasman et al, 1989a and b).

Fluid inclusion studies on the quartz overgrowths generally suggest precipitation at temperatures of between about 110°C and 155°C which in most cases are above the inferred temperature due to burial at the time of growth and which are occasionally above even present day temperatures (Liewig et al, 1987; Jourdan et al, 1987; Glasman et al, 1989a and b) supporting a model of hot brine migration. Hydrocarbon bearing inclusions are also found in this late diagenetic quartz. K/Ar dating of the illites has allowed the time of growth to be constrained to the period of fluid (both aqueous and hydrocarbon) migration and generally suggests that diagenesis terminates on reservoir filling. Exact timing of reservoir filling varies between fields depending on source area and migration pathway however (Jourdan et al, 1987; Liewig et al, 1987; Glasman et al, 1989a and b).

Furthermore on the basis of K/Ar dating and other techniques applied to the mudstones in the Bergen High area from which many of the samples of this study are drawn Glasman et al (1989c) suggest that the Mesozoic mudstones (ie the Draupne and Heather Formations) were poor seals during early hydrocarbon migration in the late Cretaceous, and that consequently large amounts of fluids (both aqueous and hydrocarbon) may have escaped through these formations during early reservoir filling. Thermal gradients may have been as high as 80-100°C/km at this point. The chemistry of the aqueous fluids flushing the shales was such that rapid smectite dissolution and illite authigenesis occurred (Glasman, 1989c). Migration is believed to have ceased in the later Tertiary as the mudstone seal improved, allowing reservoir filling by hydrocarbons.

The flushing of the mudstones above the Brent reservoirs with migrating compactional brines and early generated hydrocarbons (Glasman, 1989c) may have been responsible for both the supply of Pb and Zn and also possibly the removal of Mo from the Draupne and Heather Formations and U from the Draupne Formation only. Glasman et al (1989c) however

observed that the brine flushing episode has had little effect on the regional thermal maturity. If this is the case then why is there a correlation between the noted metal contents and organic maturity if the flushing which is possibly responsible for the metal flux is not related to maturity? One explanation may be that the fields nearest to the sources of the expelled brine (mainly the Viking Graben) are more likely to be thoroughly flushed early in their history (while their seals are still relatively permeable) than those which are located at a greater distance. A consequence of basin geometry is that the fields adjacent to the Viking Graben are also those most likely to be relatively deeply buried and hence to have the highest organic maturity. Furthermore as the distance between the source of the metal rich brines increases so the likelihood that metals will have already precipitated before encountering low maturity basin margin samples increases.

8.1.3 Summary of discussion

The high contents of the enriched metals in the mudrocks studied can be related to processes of metal fixation which may currently be observed in modern sediments. Sea water is probably the ultimate source of these elements and no anomalous metal supply has been invoked. The increase in Pb and Zn observed with increasing burial in these two North Sea mudrock formations is probably related to their flushing by metal rich compactional fluids escaping from the deeply buried Viking Graben sediments. The observed decrease in Mo in both formations and U in the Draupne Formation only may be related in part to the same episodes of fluid flushing which supplied Pb and Zn, but may also be directly related to the maturation of organic matter and the generation of hydrocarbons within the two sediments. The exact mechanism by which these elements are mobilised remains unclear.

8.2 Conclusions

The geochemistry of three Upper Jurassic mudstone formations, the Draupne and Heather Formations from the Norwegian sector of the North Sea, and The Kimmeridge Clay from the

English outcrop and subcrop has been studied with the intention of relating it to the levels of organic maturity reached in each of the formations. The raw data indicate that the major element compositions of the three formations studied are controlled by the mineralogy, but that all are enriched in TOC and S relative to the average. The Draupne and Heather Formations also have much lower carbonate contents (from CaO/Al_2O_3 and CO_2/Al_2O_3 ratios) than do average shales. Thus the Draupne and Heather Formations fit the Curtis (1980) definition of black shale. The Kimmeridge Clay Formation has an excess of carbonate relative to the black shale definition.

Many black shales are rich in a number of trace elements. The Draupne Formation was shown to be enriched in Cd, Cr, Cu, Mo, Nb, Ni, Th, U, V, Y, and Zn on the grounds that 75% of the Draupne Formation samples exceeded the average shale concentration of these elements (Chapter 3). By the same definition the Heather Formation is enriched in Cr, Li, Mo, Nb, U, and Zn, and the Kimmeridge Clay in Cr, Li, Mo, Nb, and U. Thus Cr, Mo, Nb, and U are enriched in all three of the formations studied.

The raw data were transformed to Al_2O_3 normalised logratios (after Aitchison, 1984) to avoid closure problems, and were examined by correlation analysis (Chapter 4) in an attempt to determine the mineralogical residences of the elements. This resulted in the division of the trace elements into three groups. The elements Cd, Co, Cu, Mo, Ni, (Pb in the Heather and Kimmeridge Clay Formations only), U, V, and Zn were seen to be dominantly associated with either organic matter or pyrite, particularly where they were enriched. Cr, Li, Nb, Rb, Th, and Zr were all thought to be mainly associated with detrital silicates and could usually be separated into elements associated with the silt fraction (feldspar and heavy mineral locations) such as Zr and those having a clay mineral residence (eg Rb in the Draupne Formation). Sc, Sr, and Y were correlated with carbonate or phosphate minerals.

In Chapter 5 a number of mineralogical and geochemical indices were employed in order that variations in grain size, sedimentological maturity, and depositional environment could be

examined in addition to organic maturity. Grain size variation was examined by means of the indices SiO_2/Al_2O_3, TiO_2/Al_2O_3, and (quartz+feldspars/clay). Draupne Formation grain size was coarsest in the west of the area studied, and was generally finer in the east. The Heather Formation showed the reverse trend being coarsest to the east, and fining away from the Norwegian Coast. The Heather Formation also showed a wider range in grain size than did the Draupne. The sedimentological maturity indices for both formations (CIA, quartz/feldspar) suggest that maturity increases westwards. The Kimmeridge Clay Formation displayed both grain size variation, and sedimentological maturity variation laterally along the outcrop, and also vertically between the beds sampled. The most thoroughly sampled bed (bed 32) appeared to be relatively fine grained, but became coarser, and less sedimentologically mature in the south midlands area suggesting the possibility of local less weathered clastic sources in this area.

Study of the depositional environment was performed by examination of the indices V/Cr, Ni/Co, authigenic U, pr/ph, and DOP. These gave very consistent patterns which suggested that the Draupne Formation was deposited beneath a probably anoxic/euxinic water column in the Viking Graben, that conditions were restricted in more intermediate areas, and normal in the east of the study area on the Horda Platform. The majority of Draupne Formation samples were believed to have been deposited beneath waters of lower than normal oxygenation. During Heather Formation deposition euxinic conditions were restricted to local occurences in the Viking Graben, but the same general pattern as for the Draupne Formation was observed with conditions becoming more oxygenated eastwards onto the Horda Platform. The bulk of the Heather Formation was probably deposited in normally oxygenated, or only restricted conditions. The Kimmeridge Clay Formation beds sampled appear to have been deposited primarily under aerobic conditions, the exception being Bed 32. This is associated with restricted conditions which locally may have become anoxic/euxinic.

These studies suggested that variation in factors such as grain size and depositional environment could not be neglected when examining the relationship between the trace

element contents of the formations studied and their organic maturity. Path analysis was used in Chapter 6 to investigate the relative importance of different variables in controlling the trace element content of the three formations studied. The variables investigated were linear combinations of the indices used in the previous chapter to illustrate grain size variation, sedimentological maturity, depostional environment, and organic maturity, with the addition of a variable representing the carbonate mineral abundance. These new variables were calculated from the original indices by means of principal components analysis.

The path analyses generally supported the division of the elements in Chapter 4 based on correlation analysis alone. Cd, Cu, Mo, Ni, U, V, and Zn which were all interpreted as being either organic matter or pyrite associated in the earlier chapter were shown to be dominantly controlled by the depositional environment variable reflecting the importance of water oxygenation in determining the concentration of these elements. Cr, Nb, Th, and Zr concentrations were controlled by the grain size variable. This is consistent with the detrital silicate association noted from the correlation analysis, and concentrations of these elements generally increased with increasing grain size. The concentrations of the elements Sc and Sr were mainly controlled by the abundance of carbonate minerals.

Organic maturity was represented by a variable calculated from the vitrinite reflectance, Rock-Eval T_{max}, and SCI values of the samples. The maturity variable was important in controlling the Pb, Zn and Mo content of both the Draupne and Heather Formations, and the U and Cd content of the Draupne Formation only (both of these elements are considerably enriched relative to the average in this formation). Pb, Zn, and Cd increase with increasing depth in the North Sea mudstones examined, whilst Mo and U decrease. The Kimmeridge Clay Formation showed only a small range in organic maturity. The relationship between Mo and organic maturity in the Kimmeridge Clay was marginally not significant at the probability level used but also suggested a decrease in Mo content with increasing maturity.

Applications of the work to exploration for hydrocarbon reserves were outlined in Chapter 7. As the depositional conditions favouring the fixing of trace metals in a sediment are similar to those in which large amounts of hydrogen rich organic matter are preserved a knowledge of the trace element content of mudstone may be used to predict the abundance and type of organic matter present within it with considerable accuracy. When the elements used for such predictive purposes may themselves be measured down hole by logging tools then this predictive ability may become a powerful and cost effective technique for source rock evaluation. As the concentrations of some elements are also controlled by organic maturity the possibility exists of an inorganic index of organic maturity, one which may also possibly be obtained down hole.

Pb and Zn are believed to have been supplied to the Draupne and Heather Formations by brines escaping from the underlying Brent Group reservoirs during an early stage of filling. The exact mechanism by which Mo and U are mobilised is unclear. With currently available data flushing by considerable amounts of brine or hydrocarbons appears to be the only mechanism capable of transporting the required amount of material. Volumes would be much lower if expelled pore waters, or generated hydrocarbons, could transport enhanced concentrations of these elements.

References

Aagard, P., Egeberg, P. K., Saigal, G. C., Morad, S., and Bjorlykke, K., 1990. Diagenetic albitisation of detrital K-feldspars in Jurassic, Lower Cretaceous and Tertiary clastic reservoir rocks from offshore Norway, II. Formation water chemistry and kinetic considerations. Journal of Sedimentary Petrology, 60, 575-581.

Adams, J. A. S., and Weaver, C. E., 1958. Thorium to uranium ratios as indicators of sedimentary processes. Examples of the concept of geochemical facies. American Association of Petroleum Geologists Bulletin, 42, 387-430.

Afifi, A., and Clark, V., 1984. Computer aided multivariate analysis. Lifetime Learning, Belmont California, 458p.

Aitchison, J., 1981. A new approach to null correlations of proportions. Journal of Mathematical Geology, 13, 175-189.

Aitchison, J., 1982. The statistical analysis of compositional data. Journal of the Royal Statistical Society, B44, 139-177.

Aitchison, J., 1984. The statistical analysis of geochemical compositions. Journal of Mathematical Geology, 16, 531-564.

Aitchison, J., 1986. The statistical analysis of compositional data. Methuen Inc, New York, 416p.

Anderson, G. M., 1975. Precipitation of Mississippi Valley-Type ores. Economic Geology, 70, 937-942.

Anderson, G. M., and Macqueen, R. W., 1982. Ore deposit models-6. Mississippi Valley Type lead-zinc deposits. Geoscience Canada, 9, 108-117.

Anderson, T. F., Kruger, J., and Raiswell, R., 1987. C-S-Fe relationships and the isotopic composition of pyrite in the New Albany Shale of the Illinois Basin, U.S.A. Geochimica et Cosmochimica Acta, 51, 2795-2805.

Argast, S., and Donnelly, T. W., 1987. The chemical discrimination of clastic sedimentary components. Journal of Sedimentary Petrology, 57, 813-823.

Arkell. W. J., 1933. The Jurassic System in Great Britain. Clarendon Press, Oxford.

Arveschoug, N. C., 1986. The Market Weighton Carboniferous trough. Yorkshire Geological Society Circular No 393, p3.

Asuen, G. O., 1988. Elemental concentrations and their relationship in Howick Coal Group, England. Chemie der Erde, 48, 321-332.

Badham, J. P. N., 1981. Shale-hosted Pb-Zn deposits: Products of exhalation of formation waters? Transactions of the Institute of Mining and Metallurgy, 90, B70-76.

Badley, M. E., Price, J. D., Rambech Dahl, C., and Agdestein, T., 1988. The structural evolution of the northern Viking Graben and its bearing upon the extensional modes of basin formation. Journal of the Geological Society of London, 145, 455-472.

Baird, R. A., 1986. Maturation and source rock evaluation of Kimmeridge Clay, Norwegian North Sea. American Association of Petroleum Geologists Bulletin, 70, 1-11.

Baldwin, B., and Butler, C. O., 1985. Compaction curves. American Association of Petroleum Geologists Bulletin, 69, 622-626.

Balistieri, L., Brewer, P. G., and Murray, J. W., 1981. Scavenging residence times of trace metals and surface chemistry of sinking particles in the deep ocean. Deep-Sea Research, 28A, 101-121.

Balistieri, L. S., and Murray, J. W., 1986. The surface chemistry of sediments from the Panama Basin: the influence of Mn oxides on metal adsorption. Geochimica et Cosmochimica Acta, 50, 2235-2243.

Barnard, P. C., Collins, A. G., and Cooper, B. S., 1981. Identification and distribution of kerogen facies in a source rock horizon - examples from the North Sea Basin. In Organic Maturation Studies and Fossil Fuel Exploration, Brooks, J., ed, Academic Press, London, 271-282.

Barnard, P. C., and Cooper, B. S., 1983. A review of geochemical data related to the north-west European gas province. In Petroleum Geochemistry and Exploration of Europe, Brooks, J., ed, Geological Society Special Publication 12, 19-33.

Beales, F. W., and Jackson, S. A., 1966. Precipitation of lead-zinc ores in carbonate reservoirs as illustrated by Pine Point ore field, Canada. Transactions of the Institution of Mining and Metallurgy, 75, B278-B285.

Beier, J. A., and Hayes, J. M., 1989. Geochemical and isotopic evidence for palaeoredox conditions during deposition of the Devonian-Mississippian New Albany Shale, Southern Indiana. Geological Society of America Bulletin, 101, 774-782.

Bernas, B., 1968. A new method for decomposition and comprehensive analysis of silicates by atomic absorption spectrometry. Analytical Chemistry, 40, 1682-1686.

Bender, M. L., Fanning, K. A., Froelich, P. N., Heath, G. R., and Maynard, V., 1977. Interstitial nitrate profiles and oxidation of sedimentary organic matter in the Eastern Equatorial Atlantic. Science, 198, 605-609.

Berner, R. A., 1970. Sedimentary pyrite formation. American Journal of Science, 268, 1-23.

Berner, R. A., 1978. Sulfate reduction and the rate of deposition of marine sediments. Earth and Planetary Science Letters, 37, 492-498.

Berner, R. A., 1984. Sedimentary pyrite formation: an update. Geochimica et Cosmochimica Acta, 48, 605-615.

Berner, R. A., and Raiswell, R., 1983. Burial of organic carbon and pyrite sulfur in sediments over Phanerozoic time: a new theory. Geochimica et Cosmochimica Acta, 47, 855-862.

Berner, R. A., and Westrich, J. T., 1985. Bioturbation and the early diagenesis of carbon and sulfur. American Journal of Science, 285, 193-206.

Bertine, K. K., 1972. The precipitation of molybdenum in anoxic waters. Marine Chemistry, 1, 43-53.

Bertine, K. K., and Turekian, K. K., 1973. Molybdenum in marine deposits. Geochimica et Cosmochimica Acta, 37, 1415-1434.

Billings, G. K., Kestler, S. E., and Jackson, S. A., 1969. Relation of zinc-rich formation waters, Northern Alberta, to the Pine Point Ore Deposit. Economic Geology, 64, 385-391.

Bjorlykke, K., 1974. Depositional history and geochemical composition of Lower Palaeozoic epicontinental sediments from the Oslo region. Norges Geologiske Undersoekelse Arsmelding, 305, 1-81.

Bjorlykke, K., Dypvik, H., and Finstad, K. G., 1975. The Kimmeridge Shale, its composition and radioactivity. In Jurassic Northern North Sea Symposium Proceedings, Finstad, K. G., and Selley, R. C., eds, Norwegian Petroleum Society.

Borovec, Z., Kribek, B., and Tolar, V., 1979. Sorption of uranyl by humic acids. Chemical Geology, 27, 39-46.

Bott, M. H. P., 1988. The Market Weighton gravity anomaly-granite or graben. Proceedings of the Yorkshire Geological Society, 47, 47-53.

Bott, M. H. P., Robinson, J., and Kolnstamn, M. A., 1987. Granite beneath Market Weighton east Yorkshire. Journal of the Geological Society of London, 135, 535-543.

Boyle, E. A., Sclater, F., and Edmond, J. M., 1976. On the marine geochemistry of cadmium. Nature, 263, 42-44.

Brewer, P. G., and Spencer, D. W., 1974. Distribution of some trace elements in Black Sea and their flux between dissolved and particulate phases. In The Black Sea-Geology, Chemistry and Biology, Degens, E. T., and Ross, D. A., eds, American Association of Petroleum Geologists Memoir 20, 137-143.

Brongersma-Sanders, M., 1966. Origin of trace metal enrichment in bituminous shales. In Hobson, G. D., and Spears, G. C., eds, Advances in Organic Geochemistry 1966, Pergamon, London, 231-236.

Brosse, E., and Huc, A. Y., 1986. Organic parameters as indicators of thermal evolution in the Viking Graben. In Thermal Modelling in Sedimentary Basins, Burrur, J. ed. Editions Technip, Paris, 517-530.

Bruland, K. W., 1980. Oceanographic distributions of cadmium, zinc, nickel, and copper in the North Pacific. Earth and Planetary Science Letters, 47, 176-198.

Bruland, K. W., 1983. In Chemical Oceanography, Riley, J. P., and Chester, R., eds, Academic, London, 157-220.

Brumsack, H. J., 1980. Geochemistry of Cretaceous black shales from the Atlantic Ocean (D.S.P.D. Legs 11, 14, 36, and 41). Chemical Geology, 31, 1-25.

Brumsack, H. J., and Gieskes, J. M., 1983. Interstitial water trace-metal chemistry of laminated sediments from the Gulf of California, Mexico. Marine Chemistry, 14, 89-106.

Cagatay, M. N., Gedik, A. and Saltoglu, T., 1990. Geochemistry of uranium in the late Pleistocene-Holocene sediments from the southern part of the Black Sea basin. Chemical Geology, 82, 129-144.

Carothers, W. W., and Kharaka, Y. K., 1978. Aliphatic acid anions in oilfield waters-implications for origin of natural gas. American Association of Petroleum Geologists Bulletin, 62, 2441-2453.

Carpenter, A. B., Trout, M. L., and Pickett, E. E., 1974. Preliminary report on the origin and chemical evolution of lead-and zinc-rich oil field brines in Central Mississippi. Economic Geology, 69, 1191-1206.

Cathles, L. M., and Smith, A. T., 1983. Thermal constraints on the formation of Mississippi Valley type lead-zinc deposits and their implications for episodic basin dewatering and deposit genesis. Economic Geology, 78, 983-1002.

Chadwick, R. A., 1985a. Permian, Mesozoic and Cenozoic structural evolution of England and Wales in relation to the principles of extension and inversion tectonics. In the Atlas of Onshore Sedimentary Basins of England and Wales, Whittaker, A., ed, Blackie, Glasgow, 9-25.

Chadwick, R. A., 1985b. Upper Jurassic: Late Oxfordian to Early Portlandian. In the Atlas of Onshore Sedimentary Basins of England and Wales, Whittaker, A., ed, Blackie, Glasgow, 49-51.

Chadwick, R. A., 1986. Extension tectonics in the Wessex Basin, southern England. Journal of the Geological Society of London, 143, 465-488.

Chayes, F., 1960. On correlation between variables of constant sum. Journal of Geophysical Research, 65, 4185-4193.

Chayes, F., 1962. Numerical correlation and petrographic variation. Journal of Geology, 70, 440-452.

Chayes, F., and Kruskal, W., 1966. An approximate statistical test for correlations between proportions. Journal of Geology, 74, 692-702.

Clarke, F. W., 1924. Data of geochemistry. Bulletin of the United States Geological Survey no. 770, 841p.

Claypool G. E., and Kaplan, I. R., 1974. The origin and distribution of methane in marine sediments. In Natural Gases in Marine Sediments, Kaplan, I. R., ed, Plenum Press, New York, 99-139.

Collier, R. W., 1984. Particulate and dissolved vanadium in the North Pacific Ocean. Nature, 309, 441-444.

Contreras, R., Fogg, T. R., Chasteen, N. D., Gaudette, H. E., and Lyons, W. B., 1978. Molybdenum in pore waters of anoxic marine sediments by electron paramagnetic resonance spectroscopy. Marine Chemistry, 6, 365-373.

Cornford, C., 1984. Source rocks and hydrocarbons of the North Sea. In Introduction to the Petroleum Geology of the North Sea, Glennie, K. W., ed, Blackwell Scientific Publications, Oxford, 171-204.

Cosgrove, M. E., 1970. Iodine in the bituminous Kimmeridge Shales of the Dorset Coast, England. Geochimica et Cosmochimica Acta, 34, 830-836.

Coveney, R. M., Jr, and Martin, S. P., 1983. Molybdenum and other heavy metals of the Mecca Quarry and Logan Quarry Shales. Economic Geology, 78, 132-149.

Coveney, R. M., Jr, Leventhal, J. S., Glascock, M. D., and Hatch, J. R., 1987. Origins of metals and organic matter in the Mecca Quarry Shale Member and stratigraphically equivalent beds across the Midwest. Economic Geology, 82, 915-933.

Cox, B. M., and Gallois, R. W., 1979. Description of the standard stratigraphical sequences of the Upper Kimmeridge Clay, Ampthill Clay and West Walton Beds. In Geological investigations for the Wash Water Storage Scheme, Gallois, R. W., Report of the Institute of Geological Sciences, 78/19, 68-72.

Cox, B. M., and Gallois, R. W., 1981. The stratigraphy of the Kimmeridge Clay of the Dorset type area and its correlation with some other Kimmeridgian sequences. Report of the Institute of Geological Sciences, 80/4.

Crocetti, C. A., Holland, H. D., and McKenna, L. W., 1988. Isotopic composition of lead in galenas from the Viburnum Trend Missouri. Economic Geology, 83, 355-376.

Crossey, L. J., Surdam, R., C., and Lahann, R., 1986. Application of organic/inorganic diagenesis to porosity prediction. In Roles of Organic Matter in Sediment Diagenesis, Gautier, D. L., ed, Society of Economic Palaeonologists and Mineralogists Special Publication 38, SEPM, Tulsa, 147-155.

Curtis, C. D., 1977. Sedimentary geochemistry: environments and processes dominated by involvement of an aqueous phase. Philosophical Transactions of the Royal Society London, A286, 353-372.

Curtis, C. D., 1978. Possible links between sandstone diagenesis and depth related geochemical reactions occurring in enclosing mudstones. Journal of the Geological Society of London, 135, 107-117.

Curtis, C. D., 1980. Diagenetic alteration in black shales. Journal of the Geological Society of London, 137, 189-194.

Curtis, C. D., 1983a. Link between aluminium mobility and destruction of secondary porosity. American Association of Petroleum Geologists Bulletin, 67, 380-384.

Curtis, C. D., 1983b. Geochemistry of porosity enhancement and reduction in clastic sediments. In Petroleum Geochemistry and Exploration of Europe, Brooks, J., ed, Geological Society Special Publication, 12, 113-126.

Curtis, C. D., 1987. Mineralogical consequences of organic matter degradation in sediments: inorganic/organic diagenesis. In Marine clastic Sedimentology, Leggett, J. K., and Zuffa, G. G., eds, Graham and Trotman, London, 108-123.

Curtis, C. D., Coleman, M. L., and Love, L. G., 1986. Pore water evolution during sediment burial from isotope and mineral chemistry of calcite, dolomite and siderite concretions. Geochimica et Cosmochimica Acta, 50, 2321-2334.

Curtis, C. D., and Spears, D. A., 1968. The formation of sedimentary iron minerals. Economic Geology, 63, 257-70.

Dahl, B. and Speers, G. C., 1985. Organic geochemistry of the Oseberg Field (I). In Petroleum Geochemistry in Exploration of the Norwegian Shelf, Thomas, B. M. at al, eds, Graham and Trotman, London, 185-196.

Dahl, B., Nysaether, E., Speers, G. C., and Yukler, A., 1987. Oseberg area-integrated basin modelling. In Petroleum Geology of North West Europe, Brooks, J., and Glennie, K, eds, Graham and Trotman, London, 1029-1038.

Deegan, C. E., and Scull, B. J., 1977. A proposed standard lithostatigraphic nomenclature for the Central and Northern North Sea. Report of the Institute of Geological sciences, 77/25.

Deer, W. A., Howie, R. A., Zussman, J., 1983. An Introduction to the Rock Forming Minerals. Longman, Harlow, 528p.

Deloule, E., Allegre, C., and Doe, B., 1986. Lead and sulfur isotope microstratigraphy in galena crystals from Mississippi Valley-type deposits. Economic Geology, 81, 1307-1321.

Demaison, G., Holck, A. J. J., Jones, R. W., and Moore, G. T., 1983. Predictive source bed stratigraphy; a guide to regional petroleum occurrence. In Origin, Migration and Accumulation of Hydrocarbons, 11th world Petroleum Congress, London, 1-13.

Didyk, B. M., Simoneit, B. R. T., Brassell, S. C., and Eglinton, G., 1978. Organic geochemical indicators of palaeoenvironmental conditions of sedimentation. Nature, 272, 216-222.

Dill, H., 1986. Metallogenesis of early Palaeozoic graptolite shales from the Graefenthal Horst (northern Bavaria-Federal Republic of Germany. Economic Geology, 81, 889-903.

Dill, H., Teschner, M., and Wehner, H., 1988. Petrography, inorganic and organic geochemistry of Lower Permian carbonaceous fan sequences ("Brandschiefer Series")-Federal Republic of Germany: constraints to their palaeogeography and assessment of their source rock potential. Chemical Geology, 67, 307-325.

Disnar, J. R., 1981. Etude experimentale de la fixation de metaux par un materiau sedimentaire actuel d'origine algaire-II. Fixation 'in vitro' de UO_2^{2+}, Cu^{2+}, Ni^{2+}, Zn^{2+}, Pb^{2+}, Co^{2+}, Mn^{2+}, ainsi que de VO_3, MnO_4^{2-} et GeO_3^{2-}. Geochimica et Cosmochimica Acta, 45, 363-379.

Douglas, A. G., and Williams, P. F. V., 1981. Kimmeridge Oil Shale a study of organic maturation. In Organic Maturation Studies and Fossil Fuel Exploration, Brooks, J., ed, Academic Press, London, 255-269.

Dore, A. G., Vollset, J., and Hamar, G. P., 1985. Correlation of the offshore sequences referred to the Kimmeridge Clay Formation-relevance to the Norwegian Sector. In Petroleum

Geochemistry in Exploration of the Norwegian Shelf, Thomas, B. M., et al, eds, Graham and Trotman, London, 27-37.

Doyle, L. J., and Feldhausen, P. H., 1981. Bottom sediments of the eastern Gulf of Mexico examined with traditional and multivariate statistical methods. Journal of Mathematical Geology, 13, 93-117.

Dozy, J. J., 1970. A geological model for the genesis of the lead-zinc ores of the Mississippi Valley, U.S.A. Transactions of the Institution of Mining and Metallurgy, 79, B163-B170.

Drummond, S. E. and Palmer, D. A., 1986. Thermal decarboxylation of acetate. Part II. Boundary conditions for the role of acetate in the primary migration of natural gas and the transportation of metals in hydrothermal systems. Geochimica et Cosmochimica Acta, 50, 825-833.

Duncan, O. D., 1966. Path Analysis: sociological examples. American Journal of Sociology, 72, 1-16.

Dunn, C. E., 1974. Identification of sedimentary cycles through Fourier analysis of geochemical data. Chemical Geology, 13, 217-232.

Dypvik, H., 1984. Geochemical compositions and depositional conditions of Upper Jurassic and Lower Cretaceous Yorkshire Clays, England. Geological Magazine, 121, 489-504.

Dypvik, H., and Brunfelt, A. O., 1979. Distribution of rare earth elements in some North Atlantic Kimmeridgian black shales. Nature, 278, 339-341.

Dypvik, H., Rueslatten, H. G., and Throndsen, T., 1979. Composition of organic matter from North Atlantic Kimmeridgian Shales. American Association of Petroleum Geologists Bulletin, 63, 2222-2226.

Ebukanson, E. J., and Kinghorn, R. R. F., 1985. Kerogen facies in the major Jurassic mudrock formations of southern England and the implication on the depositional environments of their precursors. Journal of Petroleum Geology, 8, 435-462.

Ebukanson, E. J., and Kinghorn, R. R. F., 1986. Maturity of organic matter in the Jurassic of southern England and its relation to the burial history of the sediments. Journal of Petroleum Geology, 9, 259-280.

Elderfield, H., McCaffrey, R. J., Luedtke, N., Bender, M., and Truesdale, V. W., 1981. Chemical diageneses in Narragansett Bay sediments. American Journal of Science, 281, 1021-1055.

Erlank, A. J., Smith, H. S., Marchant, J. W., Cardozo, M. P., and Ahrens, L. H., 1978. Zirconium. In The Handbook of Geochemistry, Wedepohl,K.H., ed, Spriger Verlag, Berlin, 40-G1 - 40-G5.

Ernst, T. W., 1970. Geochemical Facies Analysis. Elsevier, Amsterdam.

Espitalie, J., 1986. Use of Tmax as a maturation index for different types of organic matter. Comparisons with vitrinite reflectance. In Thermal Modelling in Sedimentary Basins, Burrus, J. ed. Editions Technip, Paris, 475-496.

Eugster, H. P., 1985. Oil shales, evaporites and ore deposits. Geochimica et Cosmochimica Acta, 49, 619-635.

Farrimond, P., Comet, P., Eglinton, G., Evershed, R. P., Hall, M. A., Park, D. W., and Wardroper, A. M. K., 1984. Organic geochemical study of the Upper Kimmeridge Clay of the Dorset type area. Marine and Petroleum Geology, 1, 340-354.

Field, J. D., 1985. Organic geochemistry in exploration of the northern North Sea. In Petroleum Geochemistry. In Exploration of the Norwegian Shelf, Thomas, B. M., et al, eds, Graham and Trotman, London, 39-57.

Fischer, K., Dymond, J., Lyle, M., Southar, A., and Rau, S., 1986. The benthic cycle of copper: evidence from sediment trap experiments in the eastern tropical North Pacific Ocean. Geochimica et Cosmochimica Acta, 50, 1535-1543.

Fisher, J. B., 1987. Distribution and occurence of aliphatic acid anions in deep subsurface waters. Geochimica et Cosmochimica Acta, 51, 2459-2468.

Fisher, J. B., and Boles, J. R., 1990. Water-rock interaction in Tertiary sandstones, San Joaquin basin, California, U.S.A.: Diagenetic controls on water composition. Chemical Geology, 82, 83-101.

Fisher, M. J., and Miles, J. A., 1983. Kerogen types, organic maturation and hydrocarbon occurrences in the Moray Firth and South viking Graben, North Sea Basin. In Petroleum Geochemistry and Exploration of Europe, Brooks, J., ed, Geological Society Special Publication 12, 195-201.

Froelich, P. N., Klinkhammer, G. P., Bender, M. L., Luedtke, N. A., Heath, G. R., Cullen, D., Hartman, B., and Maynard, V., 1979. Early oxidation of organic matter in pelagic sediments of the Eastern Equatorial Atlantic: suboxic diagenesis. Geochimica et Cosmochimica Acta, 43, 1075-1090.

Frondel, C., 1970. Scandium 21-K. In The Handbook of Geochemistry, Wedepohl,K.H., ed, Springer Verlag, Berlin, 21-K1 -21-K3.

Gad, M. A., Catt, J. A., and Le Riche, H. H., 1968. Geochemistry of the Whitbian (Upper Lias) sediments of the Yorkshire coast. Proceedings of the Yorkshire Geological Society, 37, 105-139.

Gallois, R. W., 1976. Coccolith blooms in the Kimmeridge Clay and origin of North Sea oil. Nature, 259, 473-475.

Gallois, R. W., 1979. Geological investigations for the Wash Water Storage Scheme. Report of the Institute of Geological Sciences, 78/19.

Gallois, R. W., and Cox, B. M., 1974. Stratigraphy of the Upper Kimmeridge Clay of the Wash area. Bulletin of the Geological Survey of Great Britain, 47, 1-28.

Gallois, R. W., and Cox, B. M., 1976. The stratigraphy of the Lower Kimmeridge Clay of eastern England. Proceedings of the Yorkshire Geological Society, 41, 13-26.

Garven, G., 1984. The role of regional fluid flow in the genesis of the Pine Point deposit, Western Canada Sedimentary Basin. Economic Geology, 80, 307-324.

Garven, G., and Freeze, R. A., 1985a. Theoretical analysis of the role of groundwater flow in the genesis of stratabound ore deposits. 1. Mathematical and numerical model. American Journal of Science, 284, 1085-1124.

Garven, G., and Freeze, R. A., 1985b. Theoretical analysis of the role of groundwater flow in the genesis of stratabound ore deposits. 2. Quantitative results. American Journal of Science, 284, 1125-1174.

Gautier, D. L., 1986. Cretaceous shales from the western interior of North America: sulfur/carbon ratios and sulfur isotope composition. Geology, 14, 225-228.

Gautier, D. L., and Claypool, G. E., 1984. Interpretation of methanic diagenesis in ancient sediments by analogy with processes in modern diageneitic environments. In Clastic Diagenesis, McDonald, D. A., and Surdam, R. C., eds, American Association of Petroleum Geologists Memoir 37, 111-123.

Gibson, D. L., 1985. Pyrite-organic matter relationships: Currant Bush Limestone, Georgia Basin, Australia. Geochimica et Cosmochimica Acta, 49, 989-992.

Giordano, T. H., 1985. A preliminary evaluation of organic ligands and metal-organic complexing in Mississippi Valley-type ore solutions. Economic Geology, 80, 96-106.

Giordano, T. H., 1989. Anglesite ($PbSO_4$) solubility in acetate solutions: The determination of stability constants for lead acetate complexes to 85°C. Geochimica et Cosmochimica Acta, 53, 359-366.

Glasman, J. R., Clark, R. A., Larter, S., Briedis, N. A., and Lundegard, P. D., 1989a. Diagenesis and hydrocarbon accumulation, Brent Sandstone (Jurassic), Bergen High area, North Sea. American association of Petroleum Geologists Bulletin, 73, 1341-1360.

Glasman, J. R., Lundegard, P. D., Clark, R. A., Penny, B. K., and Collins, I. D., 1989b. Geochemical evidence for the history of diagenesis and fluid migration: Brent Sandstone, Heather Field, North Sea. Clay Minerals, 24, 255-284.

Glasman, J. R., Larter, S., Briedis, N. A., and Lundegard, P. D., 1989c. Shale diagenesis in the Bergen High Area, North Sea. Clays and Clay Minerals, 37, 97-112.

Glennie, K. W., 1984. Structural framework and pre-Permian history of the North Sea area. In Introduction to Petroleum Geology of the North Sea, Glennie, K. W., ed, Blackwell Scientific Publications, Oxford, 25-62.

Glickson, M., Chappell, B. W., Freeman, R. S., and Webber, E., 1985. Trace elements in oil shales, their source and organic association with particular reference to Australian deposits. Chemical Geology, 53, 155-174.

Goff, J. C., 1983. Hydrocarbon generation and migration from Jurassic source rocks in the East Shetland Basin and Viking Graben of the Northern North Sea. Journal of the Geological Society of London, 140, 445-474.

Goldhaber, M. B., and Kaplan, I. R., 1975. Controls and consequences of sulfate reduction rates in recent marine sediments. Soil Science, 119, 42-55.

Gong, H., Rose, A. W., and Suhr, N. H., 1977. The geochemistry of cadmium in some sedimentary rocks. Geochimica et Cosmochimica Acta, 41, 1687-1692.

Graf, D. L., 1982. Chemical osmosis, reverse chemical osmosis, and the origin of subsurface brines. Geochimica et Cosmochimica Acta, 46, 1431-1448.

Grout, F. F., 1925. Relation of texture and composition of clays. Bulletin of the Geological Society of America, 36, 393-416.

Gustafson, L. B., and Williams, N. L., 1981. Sediment-hosted stratiform deposits of copper, lead, and zinc. Economic Geology 75th Anniversary Volume, 139-178.

Hall, A., 1983. The application of non-parametric statistical methods to studies of trace element distribution in igneous rocks. In The Significance of Trace Elements in Solving

Petrogenic Problems and Controversies, Augustithis, S. S., ed, Threophrastus Publications, Athens, 161-174.

Hall, W. E., and Friedman, I., 1963. Composition of fluid inclusions, Cave-in-Rock flourite district, Illinois and Upper Mississippi Valley zinc-lead district. Economic Geology, 58, 886-911.

Hallager, W. S., Ulrich, M. R., Kyle, J. R., Price, P. E., and Gose, W. A., 1990. Evidence for episodic basin dewatering in salt dome cap rocks. Geology, 18, 716-719.

Hallam, A., 1958. The concept of Jurassic axes of uplift. Science Progress, London, 46, 441-449.

Hallam, A., 1984. Pre-Quaternary sea level changes. Annual Reviews in Earth and Planetary Sciences, 12, 205-243.

Hancock, N. H., and Taylor, A. M., 1978. Clay mineral diagenesis and oil migration in the Middle Jurassic Brent Sand Formation. Journal of the Geological Society of London, 135, 69-72.

Hanor, J. S., Yousif, K. K., and Land, L. S., 1988. Penrose Conference report: Geochemistry of waters in deep sedimentary basins. Geology, 16, 560-561.

Harms, J. C., Tackenberg, P., Pollock, R. E., and Pickles, E., 1981. The Brae oilfield area. In Petroleum Geology of the Continental Shelf of North West Europe, Illing, L. V., and Hobson, G. D., eds, Institute of Petroleum, Heyden, London, 352-357.

Hathaway, L. R., Galle, O. K., and Evans, T., 1972. Brine leaching of the Heebner Shale (Upper Pennsylvanian) of Kansas. Kansas Geological Survey Bulletin, 204, 1-18.

Hathaway, L. R., and Galle, O. K., 1978. Preliminary investigations of trace element mobilization from the Heebner Shale by pure brine solutions. Trace substances in Environmental Health, 12, 99-104.

Heggie, D., Kahn, D., and Fischer, K., 1986. Trace metals in metalliferous sediments, Manop site M: interfacial pore water profiles. Earth and Planetary Science Letters, 80, 106-116.

Heier, K. S. and Billings, G. K., 1970. Rubidium. In the Handbook of Geochemistry, Wedepolil, K. H., ed., Springer Verlag, Berlin, 37-D-1.

Hennet, R. J.-C., and Crerar, D. A., 1988. Organic complexes in hydrothermal systems. Economic Geology, 83, 742-764.

Heroux, Y., Chagnon, A., and Bertrand, R., 1979. Compilation and correlation of major thermal maturation indicators. American Association of Petroleum Geologists Bulletin, 63, 2128-2144.

Herron, M., 1986. Mineralogy from geochemical well logging. Clays and Clay Minerals, 34, 204-213.

Herron, M., 1988. Geochemical classification of terrigenous sands and shales from core or log data. Journal of Sedimentary Petrology, 58, 820, 829.

Herron, M., and Grau., 1987. Clay and framework mineralogy, cation exchange capacity, matrix density, and porosity from geochemical well logging in Kern County, California. American Association of Petroleum Geologists Bulletin, 71, 567.

Hertzog, R., Colson, L., Seeman, B., O'Brien, M., Scott, H., McKeon, D., Wraight, P., Grau, J., Ellis, D., Schweitzer, J., and Herron, M., 1987. Geochemical logging with spectrometry tools. Society of Petroleum Engineers Annual Technical Conference, Dallas Texas, Paper 16792.

Hirst, D. M., 1971. Considerations of a sedimentary source for the heavy metal content of ore-forming fluids. Transactions of the Institution of Mining and Metallurgy, 80, B1-B3.

Hirst, D. M., and Dunham, K. C., 1963. Chemistry and petrography of the Marl Slate of S.E. Durham, England. Economic Geology, 58, 912-940.

Holland, H. D., 1979. Metals in black shales-a reassessment. Economic Geology, 74, 1676-1680.

Holland, H. D., 1984. The chemical evolution of the atmosphere and oceans. Princeton University Press, Princeton, New Jersey, 582p.

House, M. R., 1985. A new approach to an absolute timescale from measurements of orbital cycles and sedimentary microrhythms. Nature, 315, 721-725.

Hower, J., Eslinger, E. V., Hower, M. E., and Perry, E. A., 1976. Mechanism of burial metamorphism of argillaceous sediment: 1. Mineralogical and chemical evidence. Geological Society of America Bulletin, 87, 725-737.

Huc, A. Y., Irwin, H., Schoell, M., 1985. Organic matter quality changes in an Upper Jurassic shale sequence from the Viking Graben. In Petroleum Geochemistry in Exploration of the Norwegian Shelf, Thomas, B. M. et al, eds, Graham and Trotman, London, 179-183.

Irwin, H., 1979. On an environmental model for the type Kimmeridge Clay. Nature, 279, 819.

Irwin, H., Curtis, C. D., and Coleman, M., 1977. Isotopic evidence for source of diagenetic carbonates formed during burial of organic rich sediments. Nature, 269, 209-213.

Jackson, S. A., and Beales, F. W., 1967. An aspect of sedimentary basin evolution: the concentration of Mississippi Valley-Type ores during late stages of diagenesis. Bulletin of Canadian Petroleum Geology, 15, 383-433.

Johnson, K. S., Stout, P. M., Berelson, W. M., and Sakamoto-Arnold, C. M., 1988. Cobolt and copper distributions in the waters of Santa Monica Basin, California. Nature, 332, 527-530.

Jourdan, A., Thomas, M., Brevart, O., Robson, P., Sommer, F., and Sullivan, M., 1987. Diagenesis as the control of the Brent sandstone reservoir properties in the Greater Alwyn area (East Shetland Basin). In Petroleum Geology of North West Europe, Brooks, J., and Glennie, K., eds, Graham and Trotman, London, 951-961.

Kawamura, K., and Kaplan, I. R., 1987. Dicarboxylic acids generated by thermal alteration of kerogen and humic acids. Geochimica et Cosmochimica Acta, 51, 3201-3207.

Kent, P. E., 1949. A structure contour map of the surface of the buried pre-Permian rocks of England and Wales. Proceedings of the Geologists Association, 60, 87-103.

Kharaka, Y. K., Carothers, W. W., and Rosenbauer, J. R., 1983. Thermal decarboxylation of acetic acid: implications for origin of natural gas. Geochimica et Cosmochimica Acta, 47, 397-402.

Kharaka, Y. K., Hull, R. W., and Carothers, W. W., 1985. Water-rock interactions in sedimentary basins. In Relationship of Organic Matter and Mineral Diagenesis, Society of Economic Palaeontologists and Mineralogists Short Course 17, SEPM, Tulsa, 79-176.

Kharaka, Y. K., Law, L. M., Carothers, W. W., and Goerlitz, D. F., 1986. Role of organic species dissolved in formation waters from sedimentary basins in mineral diagenesis. In Roles of Organic Matter in Sediment Diagenesis, Gautier, D. L., ed, Society of Economic Palaeontologists and Mineralogists Special Publication 38, SEPM, Tulsa, 111-122.

Kharaka, Y. K., Maest, A. S., Carothers, W. W., Law, L. M., Lamothe, P. J., and Fries, T. L. 1987. Geochemistry of metal-rich brines from central Mississippi Salt Dome basin, USA. Applied Geochemistry, 2, 543-561.

Kirk, R. H., 1980. Statfjord Field-a North Sea giant. In Giant Oil and Gas Fields of the Decade 1968-1978, Halbouty, M. T., ed, American Association of Petroleum Geologists Memoir 30, 95-116.

Klinkhammer, G. P., 1980. Early diagenesis in sediments from the Eastern Equatorial Pacific 2. Pore water metal results. Earth and Planetary Science Letters, 49, 81-101.

Knauer, G. A., Martin, J. H., and Gordon, R. M., 1982. Cobolt in North-East Pacific waters. Nature, 297, 49-51.

Kraemer, T. F., 1981. ^{234}U and ^{238}U concentration in brine from geopressured aquifers of the northern Gulf of Mexico basin. Earth and Planetary Science Letters, 56, 210-216.

Kraemer, T. F., and Kharaka, Y. K., 1986. Uranium geochemistry in geopressured-geothermal aquifers of the U.S. Gulf Coast. Geochimca et Cosmochimica Acta, 50, 1233-1238.

Krauskopf, K. B., 1979. Introduction to Geochemistry. McGraw-Hill, 617p

Krejci-Graf, K., 1970. Geochemical facies of sediments. Soil Science, 119, 20-23.

Kyle, J. R., and Price, P. E., 1986. Metallic sulphide mineralization in salt-dome cap rocks, Gulf Coast, U.S.A. Transactions of the Institution of Mining and Metallurgy, 95, B6-B16.

Langmuir, D., 1978. Uranium solution-mineral equilibria at low temperatures with applications to sedimentary ore deposits. Geochimica et Cosmochimica Acta, 42, 547-569.

Leadholm, R. H., Ho, T. T. Y., and Sahai, S. K., 1985. Heat flow, geothermal gradients and maturation modelling on the Norwegian continental shelf using computer methods. In Petroleum Geochemistry in Exploration of the Norwegian Shelf, Thomas, B. M., et al, eds, Graham and Trotman, London, 131-143.

Le Maitre, R. W., 1982. Numerical Petrography. Elsevier, Amsterdam, 281p.

Leventhal, J. S., 1983. An interpretation of carbon and sulfur relationships in Black Sea sediments as indicators of environments of deposition. Geochimica et Cosmochimica Acta, 47, 133-138.

Leventhal, J. S., 1987. Carbon and sulfur relationships in Devonian shales from the Appalachian Basin as an indicator of environment of deposition. American Journal of Science, 287, 33-49.

Leventhal, J. S., and Hosterman, J. W., 1982. Chemical and mineralogical analysis of Devonian black-shale samples from Martin County, Kentucky; Carroll and Washington Counties, Ohio; Wise County, Virginia; and Overton County, Tennessee, U.S.A. Chemical Geology, 37, 239-264.

Lewan, M. D., and Maynard, J. B., 1982. Factors controlling enrichment of vanadium and nickel in the bitumen of organic sedimentary rocks. Geochimica et Cosmochimica Acta, 46, 2547-2560.

Liewig, N., Clauer, N., and Sommer, F., 1987. Rb-Sr and K-Ar dating of clay diagenesis in Jurassic sandstone oil reservoir, North Sea. American Association of Petroleum Geologists Bulletin, 71, 1467-1474.

Light, M. P. R., Posey, H. H., Kyle, J. R., and Price, P. E., 1987. Model for the origins of geopressurised brines, hydrocarbons, cap rocks and metallic mineral deposits: Gulf Coast, USA. In Dynamic Geology of Salt and Related Structures, Lerche, I, and O'Brien, J. J., eds, Academic Press, London, 787-830

Long, D. T., and Angino, E. E., 1982. The mobilisation of selected trace metals from shales by aqueous solutions: effects of temperature and ionic strength. Economic Geology, 77, 646-652.

Love, L. G., and Amstutz, G. C., 1966. Review of microscopic pyrite. Fortschritte der Mineralogie, 43, 273-309.

Lydon, J. W., 1983. Chemical parameters controlling the origin and deposition of sediment-hosted stratiform lead-zinc deposits. In Mineralogical Association of Canada, Short Course Handbook Vol. 8, Sediment-hosted stratiform lead-zinc deposits, Sangster, D. F., ed, 175-250.

Lydon, J. W., 1986. Models for the generation of metalliferous hydrothermal systems within sedimentary rocks and their applicability to the Irish Carboniferous Zn-Pb deposits. In Geology and genesis of mineral deposits in Ireland, Andrew, C. J., Crowe, R. W. A., Finlay, S., and Pennell, W. M., and Pyne, J. F., eds, Irish Association for Economic Geology, 711p.

MacGowan, D. B., and Surdam, R. C., 1988. Difunctional carboxylic acid anions in oilfield waters. Organic Geochemistry, 12, 245-259.

Macqueen, R. W, 1979. Base metal deposits in sedimentary rocks: some approaches. Geoscience Canada, 6, 3-9.

Manheim, F. T., and Landergren, S., 1974. Molybdenum 42-D. In The Handbook of Geochemistry, Wedepohl, K. H., ed, Springer Verlag, Berlin, 42-D1 - 42-D8.

Mann, H., and Fyfe, W. S., 1985. Uranium uptake by algae: experimental and natural environments. Canadian Journal of Earth Science, 22, 1899-1903.

Mann, U., and Muller, P. J., 1988. Source rock evaluation by well log analysis (Lower Toarcian, Hils syncline). Organic Geochemistry, 13, 109-119.

Mann, U., Leythaeuser, D., and Muller, P. J., 1986. Relation between source rock properties and wireline log parameters. An example from Lower Jurassic Posidonia Shale, NW-Germany. In Advances in Organic Geochemistry 1985, Leythaeuser, D., and Rullkotter, J., eds, Pergamon Press, Oxford, 1105-1112.

Manning, D. A. C. 1986. Assessment of the role of organic matter in ore transport processes in low-temperature base metal-systems. Transactions of the Institution of Mining and Metallurgy, 95, B195-B200.

Manning, D. A. C., and Gize, A. P. The role of organic matter in ore transport processes. In preparation.

Maynard, J. B., 1982. Extension of Berner's new geochemical classification of sedimentary environments to ancient sediments. Journal of Sedimentary Petrology, 52, 1325-1331.

McKenzie, D., 1978. Some remarks on the development of sedimentary basins. Earth and planetary Science Letters, 40, 25-32.

Merriman, R. J., 1978. X-ray diffraction analysis. In a pilot study of oil shale occurrences in the Kimmeridge Clay, Gallois, R., Report of the Institute of Geological Sciences 78/13, 25-26.

Meunier, J. D., Landais, P., and Pagel, M., 1990. Experimental evidence of uraninite formation from diagenesis of uranium-rich organic matter. Geochimica et Cosmochimica Acta, 54, 809-817.

Meyer, B. L., and Nederlof, M. H., 1984. Identification of source rocks in wireline logs by density/resistivity and sonic transit time/resistivity crossplots. American Association of Petroleum Geologists Bulletin, 68, 121-129.

Moncure, G. K., Lahann, R. W., and Siebert, R. M., 1984. In Clastic Diagenesis, McDonald, D. A., and Surdam, R. C., eds, American Association of Petroleum Geologists Memoir 37, AAPG, Tulsa, 151-161.

Morad, S., Bergan, M., Knarud, R., and Nystuen, P., 1989. Albitization of detrital plagioclase in Triassic reservoir sandstones from the Snorre Field, Norwegian North Sea. Journal of Sedimentary Petrology, 60, 411-425.

Morris, K. A., 1979. A classification of Jurassic marine shale sequences: an example from the Toarcian (Lower Jurassic) of Great Britain. Palaeogeography, Palaeoclimatology, Palaeoecology, 26, 117-126.

Morris, K. A., 1980. Comparison of major sequences of organic-rich mud deposition in the British Jurassic. Journal of the Geological Society of London, 137, 157-170.

Morton, R. A., and Land, L. S., 1987. Regional variations in formation water chemistry, Frio Formation (Oligocene), Texas Gulf Coast. American Association of Petroleum Geologists Bulletin, 71, 191-206.

Mostaghel, M. A., and Ford, T. D., 1984. A sedimentary basin evolution model for ore genesis in the South Pennine Orefield. Mercian Geologist, 10, 209-224.

Myers, K. J., and Wignall, P. B., 1987. Understanding Jurassic organic-rich mudrocks-new concepts using gamma-ray spectrometry and palaeoecology: examples from the Kimmeridge Clay of Dorset and the Jet Rock of Yorkshire. In Marine clastic sedimentology, Legget, J. K., & Zuffa, G. G., eds, Graham and Trotman, London, 172-189.

Nakashima, S., Disnar, J. R., Perruchot, A., and Trichet, J., 1984. Experimental study of mechanisms of fixation and reduction of uranium by sedimentary organic matter under diagenetic or hydrothermal conditions. Geochimica et Cosmochimica Acta, 48, 2321-2329.

Nesbitt, H. W., and Young, G. M., 1982. Early Proterozoic climates and plate motions inferred from major element chemistry of lutites. Nature, 299, 715-717.

Nicholls, G. D., and Loring, D. H., 1962. The geochemistry of some British Carboniferous sediments. Geochimica et Cosmochimica Acta, 26, 181-223.

Nissenbaum, A., and Swaine, D. J., 1976. Organic matter-metal interaction in recent sediments. The role of humic substances. Geochimica et Cosmochimica Acta, 40, 809-816.

Noble, E. A., 1963. Formation of ore deposits by water of compaction. Economic Geology, 58, 1145-1156.

Ohle, E. L., 1980. Some considerations in determining the origin of ore deposits of the Mississippi Valley Type-part II. Economic Geology, 75, 161-172.

Orbigny, A.d'., 1842-1851. Paleontologie Francaise. Terrains Jurassiques I. Cephalopodes. Victor Masson, Paris.

Palmer, D. L. and Drummond, S. E., 1986. Thermal decarboxylation of acetate. Part I. The kinetics and mechanism of reaction in aqueous solution. Geochimica et Cosmochimica Acta, 50, 813-823.

Panno, S. V., Harbottle, G., and Sayre, E. V., 1988.Distribution of selected elements in the shale of the Davis Formation, Buick Mine area, Viburnum Trend, southeast Missouri. Economic Geology, 83, 140-152.

Paropkari, A. L., 1990. Geochemistry of sediments from the Mangalore-Cochin shelf and upper slope off southwest India: geological and environmental factors controlling dispersal of elements. Chemical Geology, 81, 99-119.

Patterson, J. H., 1988. Mineralogy and chemistry over a cycle of oil shale deposition in the Brick Kiln Member, Rundle Deposit, Queensland, Australia. Chemical Geology, 68, 207-219.

Patterson, J. H., Ramsden, A. R., Dale, L. S., and Fardy, J. J, 1986. Geochemistry and mineralogical residences of trace elements in oil shales from Julia Creek, Queensland, Australia. Chemical Geology, 55, 1-16.

Patterson, J. H., Ramsden, A. R., and Dale, L. S., 1988. Geochemistry and mineralogical residences of trace elements on oil shales from the Condor Deposit, Queensland, Australia. Chemical Geology, 67, 327-340.

Pearson, K., 1897. Mathematical contribution to the theory of evolution on a form of spurious correlations which may arise when indices are used in the measurement of organs. Proceedings of the Royal Society of London, Series B, 60, 489-498.

Pearson, M. J., 1979. Geochemistry of the Hepworth Carboniferous sediment sequence and origin of the diagenetic iron minerals and concretions. Geochimica et Cosmochimica Acta, 43, 927-941.

Pearson, M. J., and Small, J. S., 1988. Illite-smectite diagenesis and palaeotemperatures in northern North Sea Quaternary to Mesozoic shale sequences. Clay Minerals, 23, 109-132.

Pearson, M. J., Watkins, D., Pittion, J-L., Caston, D., and Small, J. S., 1983. Aspects of burial diagenesis, organic maturation and palaeothermal history of an area in the South Viking Graben, North Sea. In Petroleum Geochemistry and the Exploration of Europe, Brooks, J., ed, Blackwell, Oxford, 161-173.

Pearson, M. J., Watkins, D., and Small, J. S., 1982. Clay diagenesis and organic maturation in northern North Sea sediments. In Proceedings of the International Clay Conference Pavia and Bologna 1981, Van Olphen, H., & Veniale, F., eds, Developments in Sedimentology 35, Elsevier, Amsterdam, 665-675.

Pedersen, T. F., Vogel, J. S., and Southon, J. R., 1986. Copper and manganese in hemipelagic sediments at 21°N, East Pacific Rise: diagenetic contrasts. Geochimica et Cosmochimica Acta, 50, 2019-2031.

Penn, I. E., Cox, B. M., and Gallois, R. W., 1986. Towards precision in stratigraphy: geophysical log correlation of Upper Jurassic (including Callovian) strata of the Eastern England Shelf. Journal of the Geological Society of London, 143, 381-410.

Pettijohn, F. J., 1975. Sedimentary Rocks. Harper and Row, New York, 628p.

Philip, G. M., and Watson, D. F., 1987. Probabilism in geological data analysis. Geological Magazine, 124, 577-583.

Philip, G. M., and Watson, D. F., 1988. Angles measure compositional differences. Geology, 16, 976-979.

Pilipchuk, M.F., and Volkov, I.I., 1974. Behaviour of molybdenum in processes of sediment formation and diagenesis in Black Sea. In The Black Sea-Geology, Chemistry and Biology, Degens, E. T., and Ross, D. A., eds, American Association of Petroleum Geologists Memoir 20, 542-553.

Premovic, P. I., Pavlovic, M. S., and Pavlovic, N. Z., 1986. Vanadium in ancient sedimentary rocks of marine origin. Geochimica et Cosmochimica Acta, 50, 1923-1931.

Raiswell, R., 1982. Pyrite texture, isotopic composition and the availability of iron. American Journal of Science, 282, 1244-1263.

Raiswell, R., and Al-Biatty, H. J., 1989. Depositional and diagenetic C-S-Fe signatures in early Palaeozoic normal marine shales. Geochimica et Cosmochimica Acta, 53, 1147-1152.

Raiswell, R., and Berner, R. A., 1985. Pyrite formation in euxinic and semi-euxinic sediments. American Journal of Science, 285, 710-724.

Raiswell, R., and Berner, R. A., 1986. Pyrite and organic matter in Phanerozoic normal marine shales. Geochimica et Cosmochimica Acta, 50, 1967-1976.

Raiswell, R., and Berner, R. A., 1987. Organic C losses during burial and thermal maturation of normal marine shales. Geology, 15, 853-856.

Raiswell, R., Buckley, F., Berner, R. A., and Anderson, T. F., 1988. Degree of pyritization of iron as a palaeoenvironmental indicator of bottom water oxidation. Journal of Sedimentary Petrology, 58, 812-819.

Raiswell, R., and Plant, J., 1980. The incorporation of trace elements into pyrite during diagenesis of black shales, Yorkshire, England. Economic Geology, 75, 684-699.

Rawson, P. F., and Riley, L. A., 1982. Latest Jurassic-Early Cretaceous events and the "Late Cimmerian Unconformity" in North Sea area. American Association of Petroleum Geologists Bulletin, 66, 2628-2648.

Rhys, G. H., 1974. A proposed standard lithostratographic nomenclature for the southern North Sea and an outline structural nomenclature for the whole of the (U.K.) North Sea. Report of the Institute of Geological Sciences, 78/4.

Richardson, G., 1979. The Mesozoic stratigraphy of two boreholes near Worlaby, Humberside. Bulletin of the Geological Survey of Great Britain, 58, 24p.

Rogers, J. J. W., and Adams, J. A. S., 1969. Thorium. The Handbook of Geochemistry, Wedepohl, K. H., ed, Springer Verlag, Berlin, 90-D1 - 90-D2.

Rogers, J. J. W., and Adams, J. A. S., 1969. Uranium 92-D. In The Handbook of Geochemistry, Wedepohl, K. H., ed, Springer Verlag, Berlin, 92-D1.

Russell, M. J., 1978. Downward-excavating hydrothermal cells and Irish-type ore deposits: importance of an underlying thick Caledonian prism. Transactions of the Institution of Mining and Metallurgy, , B168-B171.

Saigal, G. C., Morad, S., Bjorlykke, K., Egeberg, P. K., and Aagaard, P., 1988. Diagenetic alteration of detrital K-feldspar in Jurassic, Lower Cretaceous, and Tertiary clastic reservoir rocks from offshore Norway, I. Textures and origin. Journal of Sedimentary Petrology, 58, 1003-1013.

Sangster, D. F., 1990. Mississippi Valley-type and sedex lead-zinc deposits: a comparative examination. Transactions of the Institution of Mining and Metallurgy, 99, B21-B42.

Saunders, J. A., and Rowan, E. L., 1990. Mineralogy and geochemistry of metallic well scale, Raleigh and Boykin Church oilfields, Mississippi, U.S.A. Transactions of the Institution of Mining and Metallurgy, 99, B54-B58.

Saunders, J. A., and Swann, C. T., 1990. Trace-metal content of Mississippi oil field brines. Journal of Geochemical Exploration, 37, 171-183.

Schmoker, J. W., 1979. Determination of organic content of Appalachian Devonian shales from formation-density logs. American Association of Petroleum Geologists Bulletin, 63, 1504-1509.

Schmoker, J. W., 1980. Organic content of Devonian Shale in western Appalachian basin. American Association of Petroleum Geologists Bulletin, 64, 2156-2165.

Schmoker, J. W., 1981. Determination of organic-matter content of Appalachian Devonian shales from gamma-ray logs. American Association of Patroleum Geologists Bulletin, 65, 1285-1298.

Schou, L., Eggen, S., and Schoell, M., 1985. Oil-oil and oil-source rock correlation, northern North Sea. In Petroleum Geochemistry in Exploration of the Norwegian Shelf, Thomas, B. M., et al, eds, Graham and Trotman, London., 101-117.

Scotchman, I. C., 1984. Diagenesis of the Kimmeridge Clay Formation. Unpublished PhD thesis, University of Sheffield.

Scotchman, I. C., 1987a. Relationship between clay diagenesis and organic maturation in the Kimmeridge Clay formation, onshore U.K. In Petroleum Geology of North West Europe, Brooks, J. and Glennie, K., eds, Graham and Trotman, London, 251-261.

Scotchman, I. C., 1987b. Clay diagenesis in the Kimmeridge Clay Formation, onshore U.K., and its relation to organic maturation. Mineralogical Magazine, 51, 535-551.

Scotchman, I. C., 1989. Diagenesis of the Kimmeridge Clay Formation, onshore U.K. Journal of the Geological Society of London, 146, 285-303.

Sellwood, B. W., and Jenkyns, H. S., 1975. Basins and swells and the evolution of an epeiric sea (Pliensbachian-Bajocian of Great Britain). Journal of the Geological Society of London, 131, 373-388.

Sellwood, B. W., and Sladen, C. P., 1981. Mesozoic and Tertiary argillaceous units: distribution and composition. Quarterly Journal of Engineering Geology, 14, 263-275.

Sharp, J. M., 1978. Energy and momentum transport model of the Ouachita Basin and its possible impact on the formation of economic mineral deposits. Economic Geology, 73, 1057-1068.

Shaw, D. B., and Weaver, C. E., 1965. The mineralogical composition of shales. Journal of Sedimentary Petrology, 35, 213-222.

Shaw, T. J., Geiskes, J. M., and Jahnke, R. A., 1990. Early diagenesis in differing depositional environments: the response of transition metals in pore water. Geochimica et Cosmochimica Acta, 54, 1233-1246.

Shimmield, G. B., and Price, N. B., 1986. The behaviour of molybdenum and manganese during early sediment diagenesis-offshore Baja California, Mexico. Marine Chemistry, 19, 261-280.

Shock, E. L., 1988. Organic acid metastability in sedimentary basins. Geology, 16, 886-890.

Siebert, R. M., Moncure, G. K., and Lahann, R. W., 1984. A theory of framework grain dissolution in sandstones. In Clastic Diagenesis, McDonald, D. A. and Surdam, R. C., eds, American Association of Petroleum Geologists Memoir 37, AAPG, Tulsa 163-175.

Smart, J. G. O., Bisson, G., and Worssam, B. C., 1966. Geology of the country around Canterbury and Folkestone. Memoir of the Geological Survey.

Sommer, F., 1978. Diagenesis of Jurassic sandstones in the Viking Graben. Journal of the Geological Society of London, 135, 63-67.

Spalding, R. F., Druliner, A. D., Whiteside, L. S., and Struempler, A. W., 1984. Uranium geochemistry in groundwater from Tertiary sediments. Geochimica et Cosmochimica Acta, 48, 2679-2692.

Spears, D. A., and Amin, M. A., 1981. Geochemistry and mineralogy of marine and non-marine Namurian Black Shales from the Tansley Borehole, Derbyshire. Sedimentology, 28, 407-417.

Spears, D. A., and Kanaris-Sotiriou, R., 1976. Titanium in some Carboniferous sediments from Great Britain. Geochimica et Cosmochimica Acta, 40, 345-351.

Stow, D. A. V., and Atkin, B. P., 1987. Sediment facies and geochemistry of Upper Jurassic mudrocks in the central North Sea area. In Petroleum Geology of North West Europe, Brooks, J., and Glennie, K., eds, Graham and Trotman, London, 797-808.

Stow, D. A. V., Bishop, C. D., and Mills, S. J., 1982. Sedimentology of the Brae oilfield, North Sea: fan models and controls. Journal of Petroleum Geology, 5, 129-148.

Suess, E., 1979. Mineral phases formed in anoxic sediments by microbial decomposition of organic matter. Geochimica et Cosmochimica Acta, 43, 339-352.

Surdam, R. C., Boese, S. W., and Crossey, L. J., 1984. The chemistry of secondary porosity. In Clastic Diagensis, McDonald, D. A., and Surdam, R. C., eds, American Association of Petroleum Geologists Memoir 37, AAPG, Tulsa, 127-149.

Surdam, R. C., and Crossey, L. J., 1985a. Organic-inorganic reactions during progressive burial: key to porosity and permeability enhancement and preservation. Philosophical Transactions of the Royal Society London, A315, 135-156.

Surdam, R. C., and Crossey, L. J., 1985b. Mechanisms of organic/inorganic interactions in sandstone/shale sequences. In Relationship of Organic Matter in Mineral Diagenesis. Society of Economic Palaeontologists and Mineralogists Short Course 17, 177-232

Surdam, R. C., Crossey, L. J., Hagen, E. S., and Heasler, H. P., 1989. Organic-inorganic interactions and sandstone diagenesis. American Association of Petroleum Geologists Bulletin, 73, 1-23.

Surdam, R. C., and MacGowan, D. B., 1987. Oilfield waters and sandstone diagenesis. Applied Geochemistry, 2, 613-619.

Sverjensky, D. A., 1984. Oil field brines as ore-forming solutions. Economic Geology, 79, 23-37.

Sverjensky, D. A., 1987. The role of migrating oil field brines in the formation of sediment-hosted Cu-rich deposits. Economic Geology, 82, 1130-1141.

Sweeney, M., Turner, P., and Vaughan, D. J., 1987. The Marl Slate: a model for the precipitation of calcite, dolomite and sulphides in a newly formed anoxic sea. Sedimentology, 34, 31-38.

Sweeney, R. E., and Kaplan, I. R., 1980a. Stable isotope composition of dissolved sulfate and hydrogen sulfide in the Black Sea. Marine Chemistry, 9, 145-152.

Sweeney, R. E., and Kaplan, I. R., 1980b. Diagenetic sulfate reduction in marine sediments. Marine Chemistry, 9, 145-152.

Telnaes, N., Van Veen, P., Jacobsen, T., Jones, B. and Steen, A., 1990. Molecular stratigraphy of a core through the Upper Jurassic in the northern North Sea. Submitted to Organic Geochemistry.

Thomas, B. M., Moller-Pedersen, P., Whitaker, M. F., and Shaw, N. D., 1985. Organic facies and hydrocarbon distribution in the Norwegian North Sea. In Petroleum Geochemistry in Exploration of the Norwegian Shelf, Thomas, B. M., et al, eds, Graham and Trotman, London, 3-26.

Thornton, E. C., and Seyfried, W. E., Jr, 1985. Sediment-sea-water interaction at 200 and 300°C, 500 bars pressure: The role of sediment composition in diagenesis and low-grade metamorphism of marine clay. Geological Society of America Bulletin, 96, 1287-1295.

Tieh, T. T., and Ledger, E. R., 1987. Sphalerite in sandstone and limestones of the Gulf Coast and North Texas. Economic Geology, 82, 1064-1069.

Till, R., and Colley, H., 1973. Thoughts on the use of principal components analysis in petrogenetic problems. Mathematical Geology, 5, 341-350.

Turekian, K. K., and Bertine, K. K., 1971. Deposition of molybdenum and uranium along the major ocean ridge systems. Nature, 229, 250-251.

Turekian, K. K., and Wedepohl, K. H., 1961. Distribution of elements in some major units of the earth's crust. Geological Society of America Bulletin, 72, 175-192.

Tyson, R. V., Wilson, R. C. L., and Downie, C., 1979. A stratified water column environmental model for the type Kimmeridge Clay. Nature, 277, 377-380.

Vine, J. D., and Tourtelot, E. B., 1970. Geochemistry of black shale deposits-A summary report. Economic Geology, 65, 253-272.

Vollset, J., and Dore, A. G., eds. A revised Triassic and Jurassic lithostratographic nomenclature for the Norwegian North Sea. Norwegian Petroleum Directorate Bulletin, 3.

Walters, L. J., Jr, Owen, D. E., Henley, A. L., Winsten, M. S., and Valek, K. W., 1987. Depositional environments of the Dakota Sandstone and adjacent units in the San Juan Basin utilizing discriminant analyses of trace elements in shales. Journal of Sedimentary Petrology, 57, 265-277.

Wedepohl, K. H., 1972. Zinc. The Handbook of Geochemistry, Wedepohl, K. H. ed, Springer Verlag, Berlin, 30-K-6.

Welrli, B., and Stumm, W., 1989. Vanadyl in natural waters: Adsorption and hydrolysis promote oxygenation. Geochimica et Cosmochimica Acta, 53, 69-77.

Weir, A. H., Ormerod, E. C., and El Mansey, I. M. I., 1975. Clay mineralogy of sediments of the western Nile Delta. Clay Minerals, 10, 369-386.

Wendlandt, R. F., and Bhuyan, K., 1990. Estimation of mineralogy and lithology from geochemical log measurements. American Association of Petroleum Geologists, 74, 837-856.

Wignall, P. B., 1989. Sedimentary dynamics of the Kimmeridge Clay: tempests and earthquakes. Journal of the Geological Society London, 146, 273-284.

Wignall, P. B., and Myers, K. J., 1988. Interpreting bethnic oxygen levels in mudrocks: a new approach. Geology, 16, 452-455.

Williams, P. F. V., 1986. Petroleum geochemistry of the Kimmeridge Clay of onshore southern and eastern England. Marine and Petroleum Geology, 3, 258-281.

Williams, P. F. V., and Douglas, A. G., 1980. A preliminary organic geochemical investigation of the Kimmeridge oil shales. In Advances in Organic Geochemistry 1979, Douglas, A. G., and Maxwell, J. R., eds, Pergamon, Oxford, 531-545.

Wood, S. A., Crerar, D. A., and Borcsik, M. P., 1987. Solubility of the assemblage pyrite-pyrrhotite-magnetite-sphalerite-galena-gold-stibnite-bismuthinite-argentite-molybdenite in H_2O-NaCl-CO_2 solutions from 200° to 350°C. Economic Geology, 82, 1864-1887.

Yang, M. M., Crerar, D. A., and Irish, D. E., 1989. A Raman spectroscopic study of lead and zinc acetate complexes in hydrothermal solutions. Geochimica et Cosmochimica Acta, 53, 319-326.

Ziegler, P. A., 1981. Evolution of sedimentary basins in north-west Europe. In Petroleum Geology of the Continental Shelf of North West Europe, Illing, L. V., and Hobson, G. D., eds, Institute of Petroleum, Hayden, London, 3-39.

Zielinski, R. A., Bloch, S., and Walker, T. R., 1983. The mobility and distribution of heavy metals during the formation of first cycle red beds. Economic Geology, 78, 1574-1589.

Appendix A

Analytical Methods

A.0 Analytical Methods

A.1 Initial sample preparation

With the exception of electron probe microanalysis, all of the techniques described below required the specimens to be crushed to a fine powder prior to analysis. The methods necessary to achieve this varied according to the initial condition of the samples. Those supplied by Norsk Hydro had already been crushed and required no further preparation. The onshore Kimmeridge Clay samples from boreholes were small and unweathered, and were crushed by hand using an agate pestle and mortar.

A.2 Atomic absorption spectrophotometry

A.2.1 Principles

Elemental analysis by the atomic absorption method has only been widely used in chemistry and geochemistry since the first commercial machines were produced in the early 1960's although it was originally employed some 100 years before. Its advantages include the ability to determine over 50 of the elements present in rocks and minerals, the robust and relatively inexpensive nature of the instruments, and the simplicity of the procedures involved in analysis.

Atomic absorption is a process in which ground state atoms of an element in an atomic vapour absorb light of a wavelength specific to that element, and which is identical to the light emitted from the element when its atoms are excited. This property is due to the arrangement of electrons within an atom where each electron has a discrete set of energy levels available to it. Electrons have a different set of energy levels to others in the same atom but corresponding electrons in different atoms of the same element all have the same energy level arrangement. Atoms with all electrons in the lowest (or ground state) energy

levels may absorb a photon if the energy provided by the photon is exactly that required to raise one or more electrons to higher energy levels. The outer electrons of an atom require least .energy for excitation, but for non-conducting elements and for most of the electrons in conducting elements the energy required is still large, needing UV light or X-rays for excitation. Only metals and semi-metallic elements contain electrons which can be excited by photons in the visible light range, these being the valence electrons.

As the energy required for excitation is different for different elements, light of a particular wavelength will only be absorbed by atoms of one element even in a complex mixture hence interferences are usually minimal. The name resonance wavelength is given to a wavelength at which an atom in the ground state can absorb radiation. If a parallel beam of light at the resonance frequency (nu) of a particular element, and intensity I_0, is passed through an atomic vapour of the element, the absorbance is defined as $\log(I_o/I_{nu})$, where I_{nu} is the intensity of the transmitted radiation. The absorbance is proportional to the concentration of atoms in the vapour (Beers Law).

For absorption to occur the atoms must be in the ground state. The number of atoms in the ground and first excited states can be calculated from the general expression of the Maxwell-Boltzmann law. The fraction of atoms in the excited state is small at the temperatures likely to be found in flames eg at 3000K only 1 in 138 Cs atoms, 1 in 1600 Na atoms, 1 in 27,100 Ca atoms, and 1 in 10^9 Zn atoms is excited.

Although interferences in atomic absorption are minimal they may arise for a number of reasons. If two elements in a solution being analysed have very similar resonance lines then both may absorb a particular wavelength leading to an over large absorbance. A simple way to avoid this problem would be to use a different, non-overlapped resonance line for the analyses. In the flame most atoms reside in the ground state but some easily ionised elements may exist to an appreciable extent as ions, especially in high temperature flames, leading to a low analysis. To prevent this a quantity of easily ionised atoms must be added to the solution

in order to suppress the ionisation of the element being analysed. Other negative interferences may arise if molecules are not broken down to constituent atoms by the flame. A solution here is to use a hotter flame to ensure complete dissociation.

A.2.2 The atomic absorption spectrophotometer

The main components of an atomic absorption spectrophotometer are a light source, a nebulizer, a burner, and a monochromator and photomultiplier. A deuterium lamp for background correction may also be present. Light from the source passes through the flame where the sample has been atomized due to the high temperature and some is absorbed. The light then passes to the monochromator and photomultiplier for measurement.

The light source is usually a hollow cathode lamp which consists of two electrodes sealed in a glass tube with a silica or UV glass window facing the cathode. The cathode itself is made from the element it is wished to analyse and the lamp is filled with argon or neon at 4-10torr. Application of a current (2-15mA, 300-400V) causes the metal cathode to be bombarded by ions from the filler gas, which excites the metal atoms and causes emission of very narrow resonance lines, typically 0.001nm bandwidth as they decay to the ground state. Several lines are produced and any one not interfered with by the filler gas may be used for analysis.

The sample solution is mixed with the oxidant and fuel below the burner before being fed into the flame. The oxidant flow into the nebulizer causes a drop in pressure and draws up the sample solution via a capillary tube. On entering the nebulizer the solution is dispersed as a fine mist before being thoroughly mixed with the fuel gas in a spray chamber. Large droplets of solution are drained from the spray chamber into a waste container located below the machine and the fuel, oxidant, and solution mixture is fed into the burner.

It is in the flame that the sample solution is atomized. The flame temperature is important as it must be high enough to ensure that all molecules are broken down, but not so hot that ionisation becomes a problem. Two flames are used at Newcastle, these being air/acetylene which burns at about 2350K and nitrous oxide/acetylene which gives a temperature of about 2950K. Other flame types may be used and may improve the sensitivity of some elements.

After traversing the atomised sample in the flame and being partially absorbed the light enters a monochromator set to allow only the narrow region of the spectrum (eg 5nm bandpass) about the wavelength of the resonance line of the element being analysed to pass through into the photomultiplier. This is an evacuated tube containing a light sensitive cathode and a series of dynodes which increase the initial signal by up to 1,000,000 times. The absorbance is calculated by comparison to a reference beam and then output to a recording device, or as at Newcastle to a digital display.

A.2.3 Sample preparation

Atomic absorption spectrophotometry was used to determine the following elements in solutions of the rock samples studied: SiO_2, Al_2O_3, Fe_2O_3, MgO, CaO, Na_2O, K_2O, MnO, TiO_2, Cu, Li, Co, Zn, Cd, Cr, Pb, Ag, Ni, V, Sc, Rb, and Sr. Two separate solutions were made, one, the major element solution was used to analyse for SiO_2, Al_2O_3, Fe_2O_3, MgO, CaO, Na_2O, K_2O, and MnO and the other, known as the trace element solution was used for TiO_2, Cu, Li, Co, Zn, Cd, Cr, Pb, Ag, Ni, V, Sc, Rb, and Sr.

The major element solution procedure involves an acid dissolution of the sample at high temperature and pressure and is based on the method of Bernas (1968). The samples (fine powder) are dried in an oven at 110°C for 2 hours. About 100mg of sample is weighed into a Teflon bomb liner and each sample is moistened with 0.5ml of aqua regia (1:3 mixture of nitric and hydrochloric acids). Effervescence may occur at this point and should be noted. 5ml of hydrofluoric acid (Analar 48%) is added and the samples are agitated to break up

aggregates. Lids are added, the Teflon bomb liners are placed in their stainless steel cases, and the stainless steel caps are screwed tightly on. The bombs are placed in an oven at 110°C for 5-6 hours after which they are removed and allowed to cool. The Teflon liners are removed from their cases and the contents transferred to 100ml polystyrene vials containing about 2g of boric acid to complex the fluoride. The lids and sides of the liners are scrubbed with a polythene tube and rinsed with hot water to a maximum volume of 70ml of solution and washings. The vials are put in a warm place with lids on until any remaining boric acid and any precipitate dissolves. When cool the samples are diluted to 200ml in a volumetric flask and transferred to plastic bottles, carbonaceous material being removed at this time by filtering through a number 541 filter paper. Ten times dilutions are made using an automatic diluter into polystyrene vials. Further dilutions are made as necessary depending on sample composition.

The trace element solution preparation procedure involves an acid take up in open beakers. The silica is removed as the volatile silicon tetrafluoride resulting in lower dissolved solids than would otherwise be the case. The method is as follows: Weigh accurately about 0.500g of finely powdered sample into a 50ml Teflon beaker. Moisten each with a few drops of distilled water and add 1ml of nitric acid (Aristar, S.G. 1.42), 1ml of hydrochloric acid (Aristar, S.G. 1.18), and 3ml of hydrofluoric acid (Aristar, 48%). Heat on the hotplate at setting of low 3.5 with lids on for 1 hour to dissolve the silicates then remove lids and turn hotplate to high 3.5. Evaporate the liquid to a volume of about 1ml. Add a further 1ml of nitric acid (Aristar, S.G. 1.42), 3ml of hydrofluoric acid (Aristar, 48%) and 2ml of perchloric acid (Aristar, 60%), evaporate to fumes of perchloric acid, and fume with lids on for 5 minutes. Check lids for evidence of droplets and repeat if necessary. Allow to cool, scrub beaker sides with a polythene tube to remove any build up of carbonaceous material and rinse sides with a few ml of water. Evaporate to fumes of perchloric acid and fume with lids on for 15 minutes, or longer to remove any carbonaceous residues. Check lids as above then allow to cool and add about 25ml of water. Boil for 1 hour to dissolve salts and transfer to 125ml conical or 150ml tall form glass beakers and boil as necessary until a minimum of

residue remains. Cool and dilute to 50ml in a volumetric flask and transfer to polystyrene vials. Remove any residue by filtration (540 paper). Further dilutions may be needed depending on sample composition.

Many samples had a heavy white precipitate remaining even after several hours boiling. These precipitates were removed from some samples by filtration or centrifugation for identification by X-ray diffraction. In all cases the precipitate was $BaSO_4$.

A.2.4 Operating conditions

All of the atomic absorption analyses were performed in the Department of Geology at Newcastle University, using the Varian AA-575 double beam atomic absorption spectrophotometer. Machine operating conditions used for the elements determined are shown in the accompanying table (Table A.1).

Atomic absorption, like many other instrumental methods of analysis is comparative, and the accuracy of the results depends to a large extent on the calibration. It has been shown that absorbance is proportional to the concentration of absorbing atoms in the flame (Beers Law), hence the calibration line (absorbance vs concentration) should be straight. In practice however some curvature is usually apparent and may become serious at high absorbances. The major cause of such curvature is stray light from the hollow cathode lamp entering the photomultiplier. In cases where the absorbance is low and the calibration approaches linearity a single standard may be used for calibration, and the unknown is given by the simple relationship: $C_s=(C_c*A_s)/A_c$ where C_s and C_c are the concentrations of the element in the sample and calibration standard respectively, and A_s and A_c are the respective absorbances. Often however, the use of two, or even three standards is necessary in order that the calibration line be accurately determined. Depending on machine stability re-standardisation was performed at a frequency that varied between re-standardising after every sample to only re-standardising after every eight samples.

For calibration in major element determinations international standard rocks were used. These were prepared in the same manner and at the same time as the samples. Blank samples were also processed with each batch. Approximately five different standard rocks were used for each set of analyses allowing one or two to be used for calibration and leaving the remainder to serve as a check on accuracy.

For trace element determinations synthetic standards were used except for TiO_2 which also used standard rocks. For Zn, Cu, Ni, Cr, Li, Pb, and Co a series of five multi-element

Table A.1 Atomic Absorption Operating Conditions

Element	Lamp	Wavelength/nm	Bandpass/nm	Flame	Background Correction
SiO2	Si	251.6+0.2	0.2	N2O/C2H2 50:99	None
Al2O3	Al	309.3	0.5	N2O/C2H2 60:96	None
EFe2O3	Fe	248.3	0.2	Air/C2H2 52:16	None
MgO	Ca/Mg	285.2	0.5	N2O/C2H2 46:75	None
CaO	Ca/Mg	422.7	0.5	N2O/C2H2 46:75	None
Na2O	Na	589.0	0.5	Air/C2H2 62:16	None
K2O	K	766.5	1	Air/C2H2 62:16	None
MnO	Mn	279.5	0.2	Air/C2H2 52:16	None
Cu	Cu	324.7	0.5	Air/C2H2 50:10	None
Li	Li	670.8	1	Air/C2H2 66:10	None
Co	Co	240.7	0.2	Air/C2H2 48:8	Deuterium lamp
Zn	Zn	213.9	1	Air/C2H2 47:8	Deuterium lamp
Cd	Cd	228.8	0.5	Air/C2H2 46:6	Deuterium lamp
Cr	Cr	357.9	0.2	N2O/C2H2 53:85	None
Pb	Pb	217.0	1	Air/C2H2 40:11	Manual at 220.3nm
Ag	Ag	328.1	0.5	Air/C2H2 50:10	None
Ni	Ni	232.0	0.2	Air/C2H2 50:9	Manual at 231.5nm
V	V	318.5	0.2	N2O/C2H2 43:89	None
Sc	Sc	391.2	0.2	N2O/C2H2 43:92	None
Rb	Rb	780.0	0.2	Air/C2H2 48:10	None
Sr	Sr	460.7	0.5	N2O/C2H2 52:72	None
TiO2	Ti	364.3	0.5	N2O/C2H2 50:93	None

standards were used, covering the commonly found concentration ranges. These were made from solutions of the pure salts of the elements. Cd and Ag standards were made by successive dilution of the appropriate master stock solutions. Standards for Rb, Sr, V, and Sc required an addition of sodium (see below) and were made up from the respective master stock solutions with the addition of 5% of 100mg/ml Na solution.

Not all of the light absorption in the flame need be due to atoms of the element being analysed. Other sources of attenuation may be molecules of the flame gases, or the anions present in the solution. These may lead to a positive error in the calculated absorption and hence to an analysis which is too high. Two methods for correcting this were applied as necessary (Table A.1). The deuterium lamp provides a continuum light source whose output is almost continuous across the monochromator bandpass. Any absorption of the deuterium lamp output due to the analyte element is insignificant hence attenuation must be due to background effects. The absorption due to the background can then be automatically removed from the absorption of the resonance line, as measured by the machine, which outputs the corrected value. In cases where this method gives poor results (Ni and Pb) a manual background correction method is employed. The absorbance is measured first at the resonance line being used and then at a nearby but non-absorbing line produced by the lamp. This second reading is the absorbance due to the background only and is manually subtracted from the first absorbance reading to give the true atomic absorbance.

As discussed above some easily ionised elements may exist to a large part as ions in the flame leading to erroneous results. This effects Rb, Sr, V, and Sc of the elements analysed. To minimise the effect Na is added to the solutions of these elements prior to analysis: Pipette 20ml of trace element solution into a 25ml volumetric flask, add 1.25ml of Na base solution (100mg/ml of Na) from a burette and make up to volume with distilled water (this results in a dilution of 1.25 times).

Some of the more volatile trace elements may be lost during the fuming stage of the trace element procedure. To account for this the Li result from the machine is given a correction factor of 10/9. Any samples which show a high Cr content are repeated using the major element solutions as a check against Cr loss. As an indication of precision and accuracy results of standard rock analyses are shown in Tables A.2 and A.3.

A.3 Carbon, sulphur and phosphorous.

A.3.1 Carbon.

Carbon analyses were performed using the Leco CS244 carbon and sulphur analyser at the Norsk Hydro Research Centre in Bergen, and the Leco CS125 carbon and sulphur analyser in the Department of Soil Science of Newcastle University. In both machines the sample is ignited in an induction furnace and the resulting gases are passed through detector cells which measure the carbon dioxide and sulphur dioxide. Total carbon analyses were performed on bulk rock samples, and total organic carbon analyses were performed on decarbonated samples, the difference in carbon contents between the two analyses giving carbonate carbon. The methods used were similar for both machines and simply involved weighing the required amount of sample into a ceramic crucible, inserting this into the furnace and initiating the analysis cycle.

Table A.2 Results of Repeat Analyses of BM Standard

Oxide	Standard Value(%)	Measured Values(%)
SiO_2	49.5	49.4
Al_2O_3	16.2	16.2 16.2 16.4 16.5 16.1
EFe_2O_3	9.68	9.68 9.68 9.64 9.20
MgO	7.46	7.64 7.58
CaO	6.44	6.18
Na_2O	4.64	4.64 4.16
K_2O	0.20	0.34 0.18 0.18 0.18 0.14
MnO	0.15	0.15 0.15 0.14 0.14

Table A.3 Results of Repeat Analyses of WS1 Standard

Element	Standard Value(ppm)	Measured Value(ppm)		
Ag	-	1	0	2
Cd	-	0	0	0
Co	59	54	55	53
Cr	85	76	89	68
Cu	62	59	61	62
Li	10	10	12	9
Ni	58	60	52	60
Pb	-	8	8	18
Rb	-	20	21	21
Sc	25	23	28	8
Sr	-	344	350	343
V	380	359	363	345
Zn	118	122	130	120

For determination of total organic carbon, carbonate minerals in the sample were removed by an acid leach performed as follows: Weigh out sample (0.7-1.0g) into a 125ml conical beaker and add 20ml of 30% hydrochloric acid (Analar). Heat for two hours on a hotplate at setting 3. Cool and transfer by washing into centrifuge tubes and separate solids by centrifugation at 4000rpm for five minutes. Rinse three times with distilled water, recentrifuging, transfer solids to weighed petri dishes and allow to settle, then remove as much water as possible by pipette. Dry sample on top of oven and weigh petri dish plus sample. Weigh out required amount of decarbonated sample into a ceramic crucible and treat as normal sample. The measured organic carbon in the decarbonated sample is greater than the true total organic carbon and is corrected to its whole rock value.

Calibration of the Norsk Hydro machine was performed using a coke standard of 68.49% carbon, and checked using standards 502063 and $CaCO_3$ of 2.72% and 12% carbon respectively. The Newcastle machine was also checked using a $CaCO_3$ standard of 12% carbon. Appropriate correction factors were calculated from the multiple analyses of these standards. Replicate analyses of standards are shown in Table A.4.

Table A.4 Repeat Analyses of Carbon Standards

Leco Std	$CaCO_3$ Norway	$CaCO_3$ N'castle
2.72% C	12.00% C	12.00% C
2.90	12.57	12.5
2.92	12.54	12.4
3.04	12.50	12.3
2.99	12.46	12.2
2.99	12.63	11.9
2.95		12.4
2.91		12.4
2.90		
2.99		
2.93		

A.3.2 Sulphur

Sulphur analyses were performed by two different methods, both of which are described below. The method used at Newcastle involves heating samples in a furnace in a stream of oxygen to a temperature of 1420°C. Tin chippings or foil in the combustion boats increase the temperature further during combustion, and the sulphur in the samples is evolved as sulphur dioxide. This is swept from the furnace tube due to the oxygen flow, and is bubbled through

a solution of potassium iodide which is reduced by the sulphur dioxide. Sulphur is determined by titration with potassium iodate until the evolution of sulphur dioxide is complete and a stable blue colour is shown by the starch indicator. Solutions required are: Potassium iodide, 40g (Analar) made up to 1l in water, this must be stored in a dark place; 0.2N hydrochloric acid, 20ml of hydrochloric acid (Analar, S.G. 1.18) diluted to 1l; and potassium iodate, 0.8917g of potassium iodate (Analar) dissolved in 1l of water, this must also be kept dark.

The method is as follows: Weigh out the required quantity of sample into a previously ignited ceramic combustion boat. The amount needed varies according to the expected sulphur content but was usually 50-100mg. Spread the sample evenly throughout the boat and cover with about 1g of tin chips. Flush the furnace tube with oxygen at a fast bubble rate for 10 minutes then take a 250ml conical beaker and add 25ml of the 0.2N hydrochloric acid, 5ml of potassium iodide solution, and 0.2g of iodine indicator. Dilute to about 100ml and mix well. Place in position with the exit tube of the furnace immersed in the solution. Slowly insert the combustion boat into the tube and reinsert the oxygen feed. Maintain a constant gas flow. Titrate the sulphur dioxide as it is collected, the end point being given by a faint blue colour. Allow 5 minutes after peak gas generation before ceasing the analysis.

To account for the less than 100% sulphur recovery the method was calibrated using a sulphide standard with 12.04% sulphur. This gave raw values of about 11% sulphur which were used to calculate an appropriate correction factor to apply to the samples. This was normally about 1.1. An indication of the precision results for the standard are shown in Table A.5.

Most of the Norsk Hydro samples were also analysed for sulphur using the Leco CS244 carbon and sulphur analyser and Leco HF100 induction furnace at the Norsk Hydro Research Centre, Bergen, Norway. This method involves combustion of the sample in the induction furnace, following which the evolved gas is passed through detection cells which analyse for

Table A.5 Sulphur Standards and Correction Factors

Raw Sulphur Value (%)	Correction Used	Resulting Sulphur Value (%)
11.00	1.11	12.21
10.80	1.11	11.99
10.64	1.11	11.81
10.77	1.11	11.95
10.88	1.11	12.08
10.90	1.11	12.10
10.86	1.11	12.05
10.50	1.14	11.97
10.25	1.14	11.69
11.08	1.09	12.08

sulphur dioxide and carbon dioxide. The method has the advantage of speed when compared to the wet chemical method described above, each analysis taking only a few minutes, with little preparation needed. The procedure is described below: Weigh about 50mg of each sample into a ceramic ignition crucible.. Add 1 scoop each of iron and tungsten accelerator to the crucibles and place in the furnace loading tube. Type the sample weight into the machine and initiate the analysis cycle. After about 1 minute the machine prints out the sample weight, and the percentage of carbon and sulphur. These are recorded in the machine log book. After every 20 samples the furnace tube is cleaned out.

The machine was calibrated using a coke standard containing 4.11% sulphur. Other standards were run about every 15 samples to check for machine drift, but these had very low sulphur values (0.026%) and do not provide a good indication of precision and accuracy within the sample range. When compared with the results on the same samples using the wet chemical method there is a very good agreement and results from both methods have been used.

A.3.3 Phosphorous

Phosphorous was determined by a colorimetric method using the blue colour (molybdenum blue) developed by the selective reduction of molybdophosphoric acid by ascorbic acid. The intensity of the blue colour is proportional to the concentration of phosphorous in the solution. Interference from silica was avoided by using trace element solutions, in which silica was absent, for the analyses.

Four solutions are required: 3N sulphuric acid; ammonium molybdate solution (5g of powdered ammonium molybdate (Analar) dissolved in 250ml of water); ascorbic acid solution (4.4g of ascorbic acid dissolved in 250ml of water); and 50ug/ml standard phosphorous solution. The reducing solution is made by mixing 125ml of the sulphuric acid with 38ml of the ammonium molybdate solution and then adding 60ml of the ascorbic acid solution. The mixture is then diluted to 250ml. The procedure is as follows: Calculate the amount of reducing solution required, and prepare this amount plus a small excess. Take dry 100ml beakers and add 2ml of trace element solution and 18ml of water using the variable diluter. Add 20ml of reducing solution and 10ml of water to each beaker. Mix the solutions and leave for 24 hours while the colour develops. Any solutions which show obvious signs of high phosphorous concentrations after a few hours colouring can be repeated at higher dilutions. Read the absorbance at 827nm using 1cm cells.

To calibrate the analysis two standards are used. The 100ug standard is prepared as a sample except that 2ml of 50ug/ml standard phosphorous solution is used in place of the trace solution aliquot. 50ug standards are prepared using 2ml of 50ug/ml phosphorous solution and 18ml of water from the variable diluter, to which 40ml of reducing solution and 40ml of water is added using the solution dispenser. Standard blanks are prepared as samples using 2ml water aliquots in place of the trace element solution. The P_2O_5 content of the samples is then given by the equation: $\%P_2O_5=(Ab_{sample})/(4*Ab_{standard})$ where Ab_{sample} is the sample absorbance, and $Ab_{standard}$ is the absorbance of the 50ug standard.

As an indication of the precision and accuracy of the method standard rock results are shown in Tąble A.6

A.4 X-Ray Fluorescence Analysis

A.4.1 Principles

In the discussion of atomic absorption spectrophotometry it was stated that most electrons in most elements required UV or X-ray wavelength radiation for excitation. This is what occurs in X-ray fluorescence analysis, the sample is irradiated by a primary X-ray beam which excites the atoms of the sample and causes them to emit X-rays with characteristic wavelengths. These secondary X-rays are then used to estimate the concentration of the analyte elements in the sample. In a similar way to atomic absorption spectrophotometry, X-ray fluorescence analysis had been known for a considerable time before the production of suitable commercial devices enabled the method to become a widespread analytical procedure. Most available machines can measure the concentration of over 80 elements with atomic numbers above 10 (Na and above), with good accuracy over wide concentration ranges, and the method has the advantage of being non destructive.

Table A.6 Analyses of Standards WS1, BOB1, and NIMN for Phosphorous

Sample	Actual Phosphorous (%)	Recorded Phosphorous (%)
WS1	0.28	0.28, 0.28; 0.27
BOB1	0.16	0.16, 0.16, 0.16
NIMN	0.03	0.02

X-rays are produced when an element is bombarded by electrons (primary X-rays) or by primary X-rays (secondary, or fluorescent X-rays). The X-ray spectrum produced is composed of two portions, the first of which is a broad band of continuous X-ray radiation known as white radiation by analogy with light, and the second of which consists of narrow X-ray peaks superimposed on this band and known as the characteristic, or line spectrum.

The continuous radiation is caused by interactions between the incident, exciting electrons and the electrons of the irradiated element. These interactions decelerate the incoming electrons and cause them to emit X-rays. The energy of these white X-rays varies from the lower limit of X-ray intensities up to a maximum value which corresponds to the total energy of an incoming electron being emitted as an X-ray photon in a single interaction. This maximum X-ray photon energy is a function only of the energy of the incoming electrons, and is independent of the target element. The intensity of the white X-ray spectrum is at a maximum at a wavelength of 1.5-2 times the wavelength of the most energetic photons, and while the overall intensity increases with increasing current, accelerating potential, and atomic number of the target, the distribution of intensities remains relatively unchanged. For a given current the intensity of the white spectrum is proportional to ZV^2, where Z is the atomic number and V is the potential. The spectrum emitted by an X-ray tube however differs from that produced by its target because the longer wavelength photons are reduced by absorption both in the target and in the tube window. Other complications arise because increasing the potential causes an increase in absorption by the target resulting in output rising somewhat less than proportionally with V^2, and because increasing absorption by higher atomic number elements causes output to increase less than proportionally with Z.

The characteristic, or line spectra are produced when incident electrons remove one or more electrons from an inner shell of a target atom. This requires that the incident electrons have sufficient energy to remove electrons from a target atom, the potentials necessary to give this energy being called excitation potentials. The resulting atom with a missing electron is said to be excited, and the vacancy in its electronic structure is soon occupied by an electron from an

outer shell in the atom. As the outer electron has a higher energy before its transition than after excess energy is emitted as an X-ray photon during the transition. Depending on the origin of the transferred electron further re-arrangements may occur as other outer electrons occupy the new vacancy caused by the first re-arrangement, and these will also cause X-ray emission. As the energies of the electrons in the atoms of a particular element are unique to that element, the energy changes during transitions and hence the energy and wavelengths of emitted X-rays are characteristic of particular elements.

In practice the process is not as simple as outlined above because the energy of an electron is governed not just by its shell but by all four of the quantum numbers describing it, and some transitions are not possible. The transitions are controlled by rules known as selection rules and it is these which determine whether a transition is possible or not. For allowed transitions the relative line intensities are governed by the probability of each transition occuring. Characteristic lines which are predicted by the selection rules are known as diagram lines, but other lines are found which are not predicted, and these are known as non-diagram lines. These are thought to occur when vacancies simultaneously occur in two shells and the energy from the double electron jump is emitted as a single photon. Non-diagram lines are most common in the lighter elements.

The characteristic spectrum is divided into a number of series called K, L, M etc, and the position of the initial vacancy determines the series to which a particular line is assigned. Which lines are produced depends on whether the excitation potential of incident electrons is great enough to remove electrons from a particular shell. In general K lines have the highest energies because they have the greatest energy differences with the outer electrons, but they also require the greatest excitation potential. The wavelength of a particular characteristic line is a function of the atomic number of the emitting element (Mosely's Law)

The emission of X-rays because of excitation caused by other X-rays (fluorescence) is similar to that caused by electrons with one major difference, this being that no continuous spectra

occur. The atoms are excited by X-ray photons, and electron transitions occur as described above. In X-ray fluorescence analysis it is these fluorescent X-rays which are analysed and which give information on the composition of a sample.

A.4.2 The X-ray fluorescence spectrometer

The main components of an X-ray fluorescence spectrometer are an X-ray tube to to generate the primary X-rays used for sample excitation, a collimator to produce a parallel beam, a diffracting crystal to resolve the fluorescent X-rays produced by the sample, and a detection system to measure the intensity of the selected lines..

In a conventional X-ray tube X-rays are produced by heating a tungsten filament in an evacuated tube, to produce electrons which are accelerated by a high voltage applied between the filament and an anode. The electrons strike the anode and produce X-rays by the processes described above. The resulting X-rays are then emitted through a beryllium window. Only about 1% of the energy of the electrons is emitted as X-rays, the majority being heat, which requires that the tube be cooled, usually by water.

The main difference between different X-ray tubes is in the choice of anode material. This can be any of a number of elements but the most common anodes are of Cr, Cu, Mo, Rh, Ag, W, Pt, or Au. The choice of material depends on several factors. As the continuous spectrum of a tube is many times as intense as its characteristic radiation, it is the continuous spectrum which is responsible for exciting the atoms in the sample. To obtain a good continuous spectrum a high atomic number is needed, and the tube should be operated at a high voltage to enable as many of the elements in the sample to be excited as possible. A tube cannot be used for the determination of the same element as its anode is composed of, nor can it be used for elements which are interfered with by characteristic lines from the tube. If the analysis of light elements is desired some types of tube eg Cr are available with

thinner windows causing less attenuation of longer wavelengths. The tube requires a stable source of high voltage electricity capable of up to 100kV and 50mA.

The collimators of most machines are of the Soller slit variety. These are composed of a series of regularly spaced metal plates placed in the X-ray beam to ensure that it is parallel on entering the diffracting crystal, (primary collimator), and the detector, (secondary collimator). Increasing the collimation by reducing the spacing of the plates has the effect of increasing the resolution at a cost of reducing the X-ray intensity. The primary collimator is usually adjustable, but a coarse setting is suitable for most analyses.

In order to disperse the fluorescent X-rays for analysis a diffracting crystal is used. Diffraction is discussed in greater detail in the section on X-ray diffraction. Several crystal types are available and those such as LiF, KAP, and PE are amongst the most widely used. For the analysis of a wide range of elements a number of crystals are needed. Crystals cannot diffract X-rays of a wavelength greater than their 2d measurement and so for long wavelengths such as those emitted by light elements crystals with a large spacing are required. These cannot be used for short wavelength samples however. Crystals vary in the efficiency with which they diffract X-rays, and where possible those with a high diffraction efficiency should be used. Crystals should also be chosen so that fluorescence by any of their constituent atoms will not affect the analysis, although this is usually only a problem with light elements.

Two detector types are commonly used in X-ray fluorescence analysis, these being the scintillation counter and the proportional counter. Both types produce a signal which is proportional to the energy of the measured X-ray photons, and both have short dead times. The scintillation counter is most effective when used to detect radiation from from heavy elements, which produce short wavelength X-rays. It is composed of a thalium activated NaI phosphor mounted in a photomultiplier. Scintillations from the phosphor are thus amplified by the action of the photomultiplier, but the noise of the photomultiplier and the absorption by

the casing prevent its use with longer wavelengths. Proportional counters, in contrast, are best used for measuring low energy (long wavelength) X-rays. To enable this they use very thin windows which are usually made of Be, Al, mylar, or polypropylene. The counter is filled with gas such as a 90:10 mixture of argon and methane which is ionised by X-ray photons and which produces a pulse on a central wire anode. To measure intermediate wavelengths either type of detector may be used, or for best results both in parallel.

Even with an input of monochromatic radiation both types of detector will record pulses with a spread of voltages. This spread will be greater for longer wavelengths, and when using a scintillation counter. Pulse height selection is a method which rejects pulses of unwanted energies, and its use becomes increasingly necessary as concentrations decrease. The method involves defining an energy window to pass about 90% of the X-ray beam about the desired peak which will cut out peaks due to harmonics or fluorescence from the diffracting crystal. The count output from the detector is then displayed in digital form on the machine, or is recorded for later analysis.

A.4.3 Sample preparation

X-ray fluorescence analysis was used to determine Pb, Th, Rb, U, Sr, Y, Zr, Nb, and Mo. Samples were presented to the machine in the form of pressed powder pellets which were made using a stainless steel die set and a small hydraulic press. The method is described below. Weigh out the finely powdered sample into the correct sized die (sample weights and die sizes are discussed below). Insert the piston into the die and place on the hydraulic press. Pump to a pressure of 13 tons and leave for 1 minute, then relieve the pressure, remove the die, and press out the pellet onto a piece of paper.

Pellets were made with weights varying between 12g and 3g depending on the size of the sample available. Two different diameter pellets were used which to some extent offset the difference in thickness caused by weight variations. For pellets of 6g or more a 40mm

diameter die was used, while for samples of less than 6g, 32mm diameter pellets were made. Effects on the calibration due to differing pellet size and weight are discussed below.

A.4.4 Operating conditions

All X-ray fluorescence analyses were performed in the Department of Geology of Newcastle University using the Philips PW1410 X-ray spectrometer and PW1730 generator. A Rh X-ray tube was used and was operated at 60kV and 40mA. Fluorescent lines counted were the K_a lines for Rb, Sr, Y, Zr, Nb, and Mo, the L_a for U and Th, and the L_b for Pb. Backgrounds were measured at 5 positions. The spectrometer is connected to a BBC microcomputer on which the X-ray counts are recorded, and from which the analysis is controlled. The control system is menu driven and when the analysis option is chosen prompts the user to enter the operating conditions being used. These are shown in Table A.7.

The 'spinner on' option causes the samples to be rotated in the X-ray beam and helps to achieve a more representative analysis by the averaging process. The collimator is set to coarse as increased resolution is not required and a fine setting would reduce the counts unnecessarily. The LiF200 crystal with a 2d of 0.0403nm is chosen as the diffracting crystal, and the window and lower level values are the pulse height selection parameters used. The vacuum system was used throughout, though it was not strictly necessary. Four samples were

Table A.7 XRF Operating Conditions

Prompt	Reply
Spinner	On
Collimator	Coarse
Crystal	LiF200
Window	255
Lower Level	345
Period	40
Counts/Angle	1
No Samples	Usually 4
No Angles	14

usually run in each analysis (this is the maximum that the machine can hold) and each of the 14 angles was counted for a period of 40s. Detection was by scintillation counter. ...

At the completion of each analysis the recorded counts for the samples are printed out and new samples loaded for the next analysis. The raw count data are transferred from the microcomputer to the university MTS system by the Kermit program or by hand. Once on the MTS system the data is converted to elemental concentrations using the calibration program GLA9:PJO.PROG.O. The program GLA9:PJO.PROG.O uses the raw count data from the fluorescent lines and the measured backgrounds to calculate the concentrations of the various trace elements analysed. The calculation process involves correcting each peak for any overlaps due to other elements, calculating the background at each peak position, and then determining the true peak to background ratio. This ratio is then used to determine the concentration of the element. Matrix effects are controlled by calibrating for a number of different rock types, covering a range of heavy to light element ratios.

The various factors required by the program are provided by a calibration process which is repeated approximately once per year. The calibration first determines the shape of the background curve using pellets made from pure substances such as SiO_2, Al_2O_3, and $CaCO_3$. The ratios of background counts at peak positions to background counts at the measured background positions can then be calculated. Overlap factors are determined using pellets spiked with known concentrations of the overlapping element and measuring the counts at overlapped angles. Finally the calibration factors themselves are determined for the different rock types using spiked pellets of basalt, diorite, granite etc.

As a check on the precision and accuracy of the analyses standard rock pellets were run in amongst the samples. Their results are shown in Table A.8. Sample weights used varied between 12g and 3g, and two different pellet sizes were used. To check the effect of these variations on the calibration which had been performed entirely with 12g, 40mm pellets a number of samples were run with a series of decreasing weights from 12g down to 3g. These

Table A.8 Repeat Analyses of TS Standard

Element	Actual Value(ppm)	Measured Values(ppm)
Mo	132	116 117 116 115 117
Nb	-	16 16 16 15 16
Pb	33	31 30 31 32 31
Rb	222	228 230 230 229 227
Sr	93	87 90 88 88 88
Th	-	15 15 16 14 13
U	22?	38 39 41 39 41
Y	180?	132 135 136 134 137
Zr	279	281 280 286 283 282

showed no consistent changes over the weight ranges used (Table A.9).

The elements Rb, Sr, and Pb were analysed by both atomic absorption spectrophotometry and by X-ray fluorescence. The results of standard rock analyses for both methods show that the greatest accuracy and precision for these elements is given by the X-ray method, and it is these results which are given in Appendix B.

Table A.9 Effect of Sample Weights on XRF Analyses

Element	12g	10g	8g	6g	4g	3g
Pb	25	24	23	23	22	25
Th	13	15	15	14	14	14
Rb	153	155	155	155	154	156
U	10	11	11	10	8	13
Sr	144	146	145	145	148	147
Y	35	35	35	35	35	35
Zr	143	144	141	142	144	142
Nb	17	18	17	18	18	18
Mo	27	28	28	27	27	26

A.5 X-Ray Diffraction

A.5.1 Principles

In X-ray diffraction analysis a monochromatic beam of X-rays, usually a K_a line, is incident on a sample, and the nature of the resulting diffraction provides information about the mineralogy of the sample. The principles and practice of X-ray generation were discussed in the section on X-ray fluorescence and will not be discussed again except where differences occur between the methods. The output from an X-ray tube consists of a continuous white spectrum with the characteristic line spectrum superimposed. Before this can be used for X-ray diffraction analysis however the spectrum must be modified so that only the desired monochromatic line exists. This is achieved by passing the X-ray beam through a thin metal foil known as a filter (or beta filter).

When a beam of X-rays passes through a metal foil such as this the differing X-ray energies are absorbed to different extents. When the incident X-rays are just energetic enough to remove electrons from the inner shells of atoms in the foil, much of their energy, and that of shorter wavelength X-rays also will be absorbed by such excitations, whereas those with too little energy will pass through with much less absorption. This rapid change in absorption is known as an absorption edge, and if it is chosen so that it falls between the desired K_a peak and the unwanted K_b peak of an X-ray tubes output, such that the K_b peak is of slightly shorter wavelength than the absorption edge, then this will be substantially reduced in intensity along with the short wavelength white radiation while the K_a will pass with little attenuation. The K_a peak itself exists as a closely spaced doublet K_{a1} and K_{a2} but these cannot be separated by filtering and are not always resolved by commercially available machines.

When a beam of X-rays strikes a crystalline sample, and its wavelength is less than the interplane spacing as in X-ray diffraction, the process that actually occurs is diffraction, with each atomic electron cloud in the sample acting as a new source of X-rays in a manner

analogous to a beam of light passing through a diffraction grating. The process can be regarded however as reflection, where the angle of incidence is equal to the angle of reflection, from the series of atomic planes present in the sample. The reflections will have a maximum intensity when there is constructive interference between the reflections from successive layers, and this will occur when the path difference between rays from adjacent layers is a whole number of wavelengths. In this case it can be shown that n*lambda=2dsin(theta), where n is an integer, lambda is the wavelength, d is the interplane spacing, and theta is the angle between the incident ray and the plane. Different sets of atomic planes in a crystalline mineral will cause different reflections, and analysing the positions of the X-ray reflections allows the identification of the minerals present in the sample. The intensity of the reflections to some extent allows the proportions of different minerals to be estimated.

A.5.2 The X-ray diffractometer

The main elements of an X-ray diffractometer are a source of X-rays, a monochromator and collimator to remove unwanted radiation and produce a parallel beam, and a detection system to measure the peaks produced. Many of these components are similar to those of an X-ray fluorescence spectrometer and are not discussed again in detail.

The X-ray source is a conventional X-ray tube as in X-ray fluorescence spectrometry but the factors governing the choice of tube target are different. In X-ray fluorescence spectrometry obtaining a good white spectrum is important, but in X-ray diffraction studies a tube must be chosen which is not likely to cause fluorescence in the sample as this will cause a high background. For this reason Cu tubes are not recommended for the analysis of Fe rich samples. Those targets producing shorter wavelength radiation will generally allow more reflections to be seen but longer wavelength tubes will allow better resolution. Probably the most commonly used target is Cu, but other popular ones are Co, Fe, and Cr.

The X-ray output from the tube is reduced to a monochromatic beam by a metal filter and then passes through a series of slits and collimators to produce a parallel beam as in X-ray fluorescence. The beam is then incident on the sample which is slowly rotated by a small motor. At certain angles Bragg reflections will occur and these are passed through further collimators and slits before being measured by a detector which is also driven by a motor at twice the speed of the sample. The detector outputs its signal to either a chart recorder, or as a count number to a computer.

A.5.3 Bulk X-ray diffraction: methods and conditions

The bulk mineralogy of the Norsk Hydro samples was determined using unoriented packed powder samples run on the Philips PW1700 X-ray diffractometer at the Norsk Hydro Research Centre in Bergen, Norway. The machine was fitted with an automatic sample loader and recorded the data directly onto a PDP 11/24 computer, allowing rapid sample analysis. Operating conditions were 40kV, 50mA using Ni filtered Cu K_α radiation, with a 12.5mm divergence slit and 0.1mm receiving slit. Scanning interval was 0.05° and the counting time of 2.5s gives an overall speed of 1.2° 2theta per minute. Samples were scanned from 1.5 to 65°2theta.

Packed powder samples were used to produce a random orientation of particles, although because of the platy nature of some of the clay and mica minerals present a truly random orientation is probably impossible to achieve. Circular aluminium cavity mounts with detachable bases were used to house the samples. The preparation procedure was as follows: Remove the base of the sample holder and place the top part face down on a clean smooth tile. Fill the sample cavity from the rear with the finely powdered sample and compress by tamping with a glass rod, avoiding any shearing movements, add further powder as necessary until the sample cavity is full. Clip on the sample mount base, invert the tile and mount, and place the filled mount in the loading magazine.

Some samples were too small to produce packed powder cavity mounts in this way and were prepared in a different manner. A small glass disc was used which was of the correct size to fit the sample cavity of the aluminium mount. The disc was smeared with a thin layer of petroleum jelly and a small amount of sample was sprinkled evenly over the surface to produce the required random orientation.

In order to quantitatively determine the mineralogy of the samples the diffractogram data were transferred to a Vax 11/785 computer at the Norsk Hydro Research Centre and processed by a method developed at Norsk Hydro and fully described in Karstang and Eastgate (1987). This is based on peak intensities and outputs the percentage of each of 13 common sedimentary minerals present in the sample.

A.5.4 Clay X-ray diffraction methods and conditions.

Selected Norsk Hydro samples were also subjected to a more detailed analysis of the clay mineralogy, with the aims of studying the illite/smectite mixed layer minerals, and producing a semi-quantitative clay mineral analysis. This was performed at Newcastle using the Hilton Brooks/Philips X-ray diffractometer. This operates with Fe filtered Co K_α radiation at 40kV and 20mA. The divergence slit was 1mm, the receiving slit, 0.1mm, and the scatter slit 1mm. Scan speeds and ranges varied and are discussed below.

For the clay mineral analyses the sub 2 micron fraction was analysed. This excludes most of the non clay minerals, which in these samples are quartz, feldspars, carbonates, and pyrite. This fraction was separated from the finely crushed sample by sedimentation in water. The terminal settling time being calculated from Stokes' Law. As the presence of exchangeable ions can alter some of the properties of expandable minerals such as smectites, and mixed layer clays with smectite components, it was necessary to ensure that the exchangeable ions were known and uniform. This was achieved by treating the separated clay fraction with a solution of Mg in order that the Mg^{2+} ions would displace other exchangeable ions present.

The study of clay minerals is best performed on highly oriented specimens. These will show a series of 001 basal reflections which give information on the clay minerals present. These oriented specimens are probably easier to obtain than the random specimens required for the bulk analyses, and a number of methods exist for producing them, such as smearing the clays onto a glass slide, vacuum filtration onto a porous tile, or sedimentation from a slurry onto a glass slide.

Methods have both advantages and disadvantages. The best orientation is provided by sedimentation onto the slide from a slurry, but this suffers from a concentration of the smaller particles (usually smectite) in the upper layers of the sample which can cause errors in quantitative analysis. The method in this study involves the evaporation of a thin slurry pipetted onto a glass slide, and is thought to provide intense peaks for the study of smectite/illite interstratification, without introducing too much error into the semi-quantitative mineralogical interpretation because of settling of larger particles during drying.

The method used to prepare samples for clay analysis is described below. Take the finely crushed rock powder and place in a glass beaker, add 5ml of calgon solution, mix well, and then add 50ml of distilled water. Transfer to a 100ml sedimentation tube and make up to volume. Leave for about 30 minutes then transfer to centrifuge tubes and centrifuge at 4000rpm for 10 minutes. Discard the liquid and resuspend the sample in the sedimentation tube. This is to remove soluble salts which may cause flocculation. Assuming a density of 2.65g/cm^3 for the clays, and a temperature of 20°C the clay suspension is allowed to stand for 4 hours after which the top 5cm is removed by pipette. This contains the sub 2 micron fraction. Centrifuge the sub 2 micron aliquot for 10 minutes at 4000rpm to recover the clays. Resuspend the clays in 0.5m $MgCl_2$ solution and leave overnight. Centrifuge this suspension at 4000rpm for 10 minutes to recover the clays, and discard the Mg solution. Wash and centrifuge the clays repeatedly until no cloudiness remains with $AgNO_3$, usually 3 washes are sufficient. Very long centrifugation times may be necessary to recover the clays during the

final rinses. Add a few drops of water to the clays and mix well to avoid any size separation then pipette the resulting slurry thinly over the surface of a glass slide and allow to dry.

The slides were run in the air dried state, after glycolation (4 hours in a preheated glycolation chamber at 60°C), after heating for 1 hour at 300°C, and after 1 hour at 550°C. Scan speeds of 1° per minute were used.

A.6 Rock-Eval

A.6.1 Principles

Rock-Eval is a whole rock procedure designed to allow the rapid analysis of the solvent extractable hydrocarbon content of a rock, and of the hydrocarbons produced by pyrolysis of the rock kerogen. The CO_2 evolved is also usually measured. In the analysis the sample is subjected to a programmed heating cycle during which it is first heated at 250°C for 3 minutes after which the temperature increases from 250°C to 550°C at a rate of 25°C per minute. On reaching 550°C the temperature is held constant for a period of 3 minutes following which the oven is switched off and cools to a temperature of 250°C in preparation for the next sample.

At low temperatures the free hydrocarbons in the rock are driven from the sample and analysed by a Flame Ionisation Detector (FID). This is able to detect virtually all organic compounds, is sensitive, yet does not respond to common carrier gas impurities and gives a stable baseline from which to work. This first peak is labelled P1. As the temperature rises the kerogen in the rock sample is pyrolised and the hydrocarbons produced are measured by the FID to give a second peak, P2. In most machines the CO_2 produced is trapped up to a temperature of 390°C, and released by heating later for measurement by a Thermal Conductivity Detector (TCD), to give a third peak P3. CO_2 produced above 390°C is not measured due to the probability of contamination by CO_2 from the thermal decomposition of

carbonates. In addition to P1, P2, and P3, the temperature at which the maximum pyrolitic yield of hydrocarbons occurs is also noted, this being T_{max}, which increases with increasing maturity.

Several useful parameters may be derived from the raw Rock-Eval output. If the total organic carbon is known the values of P2 and P3 can be used to determine the hydrogen index (HI), and oxygen index (OI) respectively by the equations: HI=(P2*100)/TOC and OI=(P3*100/TOC). The hydrogen and oxygen indices are related to the H/C and O/C ratios of the kerogen as determined by elemental analysis, and can be used in their place in Van Krevelen type diagrams. The value of P2/P3 gives an indication of the source rock type, and P1/(P1+P2), known as the transformation ratio provides information on the evolution of the source rocks (in effect it is the proportion of the total hydrocarbons which exist in the free state).

A.6.2 Operation and calibration

Rock-Eval was performed at Newcastle using the Girdel Rock-Eval machine in the Organic Geochemistry Unit. The TCD had been disconnected and the machine could only measure the P1 and P2 peaks. In order to collect peak area data the machine was connected to an integrating device. Most of the Norsk Hydro samples were supplied with Rock-Eval data and these were not repeated at Newcastle.

Prior to each days use the gas feeds to the machine: air for the pneumatic systems; hydrogen for the FID; and the helium carrier gas were opened and one or more blank samples were run. These were followed by one or more standards, the first of which usually gave very low results and which were discarded. In addition to the standards run in the mornings a further standard was usually run in the afternoon or at the end of the days use. Each sample analysed was run two or more times on the machine and the value used in Appendix C is an average of the individual analyses. The operating procedure was as follows: Approximately 20mg of

the sample was weighed into the previously ignited crucible, making sure that the correct crucible was being used. Handling the crucible only with tweezers to avoid any possibility of contamination from skin oils, the lid was tightly replaced. The crucible was inserted into the machine, the sample holder was raised to initiate the analysis, and the integrator start switch was simultaneously depressed. When the analysis was complete the crucible was removed, emptied of contents, and ignited in a bunsen flame until glowing faintly to remove the possibility of carry over between samples.

To relate the peak areas printed by the integrator, P1 and P2, to hydrocarbon contents S1 and S2 required a calibration curve to be produced. Ideally a number of different standards would have been used for this, but as only three were available this could not be done. Instead one standard, Blue Lias 3 (S1=0.8mg/g, S2=35.3mg/g) was chosen and was run at different weights allowing the relationship between peak area and hydrocarbon content to be determined.

The results of 11 repeats of Blue Lias 3 are illustrated in Table A.10.

A.7 Electron probe microanalysis.

The electron probe is essentially a device for focussing a beam of electrons onto a small area on the surface of a specimen, and analysing the X-rays produced. The processes involved in the production of X-rays, and in their detection have already been discussed in the section on X-ray fluorescence and will not be repeated. Quantitative analyses may be made by

Table A.10 Repeat Analyses of Blue Lias 3 Standard

S1	0.82, 0.89, 0.88, 0.92, 0.54, 0.73, 0.78, 0.69, 0.22, 0.81, 0.98
S2	36.9, 38.2, 35.1, 37.9, 35.6, 41.0, 39.3, 37.8, 35.0, 39.9, 37.6

comparison of the intensity of a particular characteristic line from the specimen with that from a standard, but in this study the machine was used in its element mapping mode. This involves scanning the beam over the surface of the sample in order to build up an image on the monitor of the surface in which the brightness of any spot is proportional to the concentration of the element being analysed. When the scan is complete the picture on the screen is photographed to produce a permanant image.

The microprobe used for this study was the CAMECA Camebax at the Department of Geology, Manchester University. The specimens were prepared at Manchester as polished thin sections and were carbon coated in order to carry the current of the electron beam. The CAMECA microprobe has a Link Systems 860-500 energy dispersive analytical system and two spectrometers for wavelength dispersive measurements. The elements mapped were Si, Al, Ca, Fe, and S using the energy dispersive system, and Zn and occasionally Mo using wavelength dispersive analysis. Operating conditions were 15kV accelerating potential, 40 degree take off angle, and a 14.5nA beam current.

Appendix B

Inorganic Geochemical and Mineralogical Results

Agreement between the mineralogy determined by XRD and the chemical analyses is good for the bulk of the samples. It has been noted however that the XRD results tend to overestimate the abundance of pyrite relative to their chemically determined sulphur contents. Discrepencies are also apparent in those samples with abundant carbonate or phosphate minerals. In all cases the chemical data are considered to be more reliable being supported by analyses of international standard rocks. The likely error in the XRD determinations in these samples is probably a result of the extrapolation of the XRD calibration to compositional extremes outside the range of the training data set, and the inclusion of minerals in the samples which were not included in the calibration.

WELL	30/6-9	30/6-14	30/6-14	30/6-14	30/6-14
DEPTH	2448.00	2300.00	2315.90	2322.00	2325.20
FMN.	Heather	Draupne	Draupne	Draupne	Draupne
SIO2	41.4	53.2	54.9	57.5	50.9
AL2O3	14.7	14.4	14.8	14.4	14.8
FE2O3	15.7	6.44	5.45	4.94	7.36
MGO	1.65	2.21	1.48	1.53	1.27
CAO	5.78	1.97	0.60	1.16	1.03
NA2O	0.80	0.89	0.54	0.84	0.56
K2O	2.19	3.82	3.28	3.76	3.39
MNO	0.06	0.03	0.03	0.02	0.04
TIO2	0.55	0.54	0.58	0.58	0.56
P2O5	0.14	0.24	0.21	0.26	0.30
LOI	17.5	15.1	18.4	15.7	20.9
S	9.97	3.59	2.72	2.45	3.41
C-ORG	3.70	5.40	8.50	7.00	9.00
C-MIN	0.66	0.39	0.00	0.00	0.00
SUM	100.47	98.84	100.27	100.69	101.11
AG	0	0	0	0	1
CD	0	6	6	8	6
CO	25	29	20	19	20
CR	89	149	280	241	182
CU	58	74	96	90	82
LI	78	50	61	59	54
MO	4			56	97
NB	24			17	16
NI	150	186	139	148	164
PB	44			43	50
RB	57			137	118
SC	14	6	9	11	9
SR	247			280	244
TH	15			14	13
U	2			19	29
V	225	675	888	844	590
Y	31			41	34
ZN	143	510	610	690	480
ZR	159			143	156
QUARTZ	14.62	15.04	20.45	20.75	18.06
KSPAR	3.88	5.27	5.00	6.24	4.25
PLAG	2.21	4.30	2.79	2.51	2.63
MUSC.	0.00	0.00	0.19	0.38	0.00
BIOTITE	0.00	0.00	0.00	0.00	0.00
CHLORITE	0.63	0.33	0.29	0.49	0.05
SMECTITE	6.73	14.71	13.89	13.35	13.14
ILLITE	19.81	34.02	31.00	32.30	31.62
KAOL.	12.58	5.90	7.90	7.63	8.55
CALCITE	3.76	0.32	0.07	1.94	2.62
DOLOMITE	4.72	2.79	1.73	2.17	2.46
SIDERITE	0.42	0.70	0.22	0.45	0.64
PYRITE	26.22	10.59	10.46	7.03	11.08
AMORPH.	4.61	5.83	5.93	5.19	5.65
SUM	99.63	99.52	99.35	100.05	99.78

WELL	30/6-14	30/6-14	30/6-14	30/7-7	30/7-7
DEPTH	2331.00	2350.00	2394.00	3895.00	3899.00
FMN.	Draupne	Draupne	Draupne	Draupne	Draupne
SIO2	48.4	57.5	54.8	52.8	50.9
AL2O3	14.7	18.4	19.0	14.9	14.3
FE2O3	9.10	6.73	6.28	7.37	9.68
MGO	0.96	1.66	1.48	1.54	1.17
CAO	0.78	1.04	0.66	1.54	0.75
NA2O	0.66	0.90	0.92	0.94	0.91
K2O	3.31	3.22	3.10	2.04	1.81
MNO	0.01	0.06	0.03	0.03	0.02
TIO2	0.62	0.84	0.89	0.51	0.53
P2O5	0.24	0.16	0.14	0.14	0.10
LOI	22.0	8.81	13.4	15.5	18.1
S	5.74	1.85	1.78	5.08	6.72
C-ORG	6.40	1.40	4.70	5.96	4.01
C-MIN	0.23	0.00	0.00	0.00	0.50
SUM	100.78	99.32	100.7	97.31	98.27
AG	0	0	0	0	0
CD	1	0	0	22	22
CO	22	16	10	12	16
CR	220	481	319	116	109
CU	87	44	45	111	97
LI	71	114	134	41	43
MO	111			56	52
NB	17			15	16
NI	213	61	54	98	118
PB	31			38	33
RB	118			90	80
SC	8	11	9	14	13
SR	218			282	273
TH	16			15	15
U	32			16	17
V	488	175	200	688	563
Y	28			33	26
ZN	291	104	97	1890	1570
ZR	155			103	113
QUARTZ	17.02	25.39	19.76	15.52	13.35
KSPAR	4.21	9.88	8.91	6.40	5.40
PLAG	1.90	3.35	3.96	5.03	5.00
MUSC.	0.00	0.00	0.28	0.00	0.00
BIOTITE	0.00	0.05	0.17	0.00	0.00
CHLORITE	0.00	0.77	1.05	0.33	0.09
SMECTITE	11.48	8.48	10.24	12.10	11.55
ILLITE	26.51	24.32	25.6	25.61	25.57
KAOL.	9.46	11.62	13.67	9.79	8.49
CALCITE	3.06	0.35	0.15	1.99	1.97
DOLOMITE	2.17	1.69	1.68	4.19	2.69
SIDERITE	0.87	0.70	0.79	1.83	1.43
PYRITE	19.19	8.13	8.21	13.41	20.65
AMORPH.	5.25	4.87	5.66	5.41	5.12
SUM	100.21	99.53	100.14	100.5	100.41

WELL	30/7-7	30/7-7	30/7-7	30/7-7	30/7-7
DEPTH	3902.00	3910.00	3928.00	3945.00	3985.00
FMN.	Draupne	Draupne	Heather	Heather	Heather
SIO2	53.1	47.9		42.3	11.7
AL2O3	14.3	14.3		15.8	2.28
FE2O3	7.86	5.17		6.25	5.27
MGO	1.55	4.49		2.10	1.29
CAO	1.43	6.05		11.0	42.5
NA2O	1.27	0.80		0.63	0.52
K2O	1.90	1.84		2.22	0.30
MNO	0.02	0.09		2.08	0.54
TIO2	0.52	0.47		0.68	0.18
P2O5	0.12	0.07		0.21	0.38
LOI	18.5	15.8		16.5	31.8
S	5.18	3.22	6.73	1.91	2.40
C-ORG	6.48	3.20	4.60	2.50	0.40
C-MIN	0.00	2.77	0.54	2.86	9.80
SUM	100.57	96.98		99.77	96.76
AG	0	0		0	0
CD	22	18		0	0
CO	12	9		15	11
CR	112	104		113	18
CU	89	78		58	16
LI	41	46		118	17
MO	69	33			
NB	15	16			
NI	127	106		108	27
PB	32	28			
RB	85	82			
SC	8	6		18	20
SR	251	296			
TH	14	16			
U	19	11			
V	689	563		238	38
Y	32	19			
ZN	1660	970		104	32
ZR	110	99			
QUARTZ	12.65	13.10	9.72	8.30	0.80
KSPAR	7.15	5.23	5.40	8.93	3.69
PLAG	6.50	5.50	6.73	9.10	2.84
MUSC.	0.00	0.00	0.00	0.00	0.00
BIOTITE	0.00	0.00	0.00	0.11	0.34
CHLORITE	0.41	0.66	0.76	1.24	0.44
SMECTITE	12.78	12.37	11.97	12.74	3.42
ILLITE	26.05	25.43	25.80	32.97	7.79
KAOL.	9.39	10.13	10.44	6.88	1.87
CALCITE	1.24	0.47	4.79	3.34	67.17
DOLOMITE	2.97	10.03	3.56	5.72	5.21
SIDERITE	1.99	1.47	1.73	0.00	2.52
PYRITE	14.89	11.01	14.91	5.47	5.34
AMORPH.	5.71	5.61	5.39	5.44	0.81
SUM	100.52	100.38	100.35	99.30	101.66

WELL	30/7-7	30/7-7	30/7-7	30/7-7	30/7-7
DEPTH	3990.00	4035.00	4070.00	4080.00	4145.00
FMN.	Heather	Heather	Heather	Heather	Heather
SIO2	7.82	40.1	46.0	48.9	
AL2O3	2.27	15.1	16.4	17.9	
FE2O3	20.3	7.20	9.65	6.84	
MGO	6.22	2.34	2.50	2.11	
CAO	22.6	10.8	6.91	7.40	
NA2O	0.30	0.79	1.66	1.24	
K2O	0.28	2.30	2.46	2.57	
MNO	2.79	1.17	1.14	0.78	
TIO2	0.16	0.61	0.64	0.65	
P2O5	3.00	0.18	0.20	0.19	
LOI	30.9	17.0	14.1	13.7	
S	1.02	2.62	1.63	2.08	
C-ORG	1.10	3.30	3.70	3.10	
C-MIN	9.40	2.67	1.89	1.69	
SUM	96.64	97.59	101.66	102.28	
AG	0	0	0	0	
CD	0	0	0	0	
CO	7	20	20	26	
CR	44	99	103	107	
CU	20	47	51	63	
LI	27	110	111	130	
MO		2			
NB		30			
NI	45	114	82	122	
PB		32			
RB		96			
SC	11	8	4	1	
SR		291			
TH		17			
U		4			
V	281	225	283	200	
Y		28			
ZN	122	240	110	132	
ZR		113			
QUARTZ	0.00	7.46	6.55	9.22	5.28
KSPAR	7.80	9.01	8.66	7.30	6.90
PLAG	12.70	8.49	8.25	7.20	7.76
MUSC.	0.02	0.00	0.00	0.00	0.00
BIOTITE	1.56	0.17	0.00	0.00	0.00
CHLORITE	1.69	1.29	1.51	1.31	1.83
SMECTITE	5.61	12.24	12.45	12.16	13.84
ILLITE	24.89	31.21	33.05	33.56	33.31
KAOL.	0.00	6.26	6.27	7.61	8.60
CALCITE	1.59	5.73	4.26	5.04	3.31
DOLOMITE	28.84	4.88	3.63	3.85	2.63
SIDERITE	17.59	0.61	5.71	0.93	3.54
PYRITE	0.84	7.38	4.89	5.72	7.32
AMORPH.	0.08	5.24	5.08	5.71	6.02
SUM	99.99	99.43	99.59	99.25	99.96

WELL	30/7-7	30/7-7	30/7-7	30/7-7	30/7-7
DEPTH	4165.00	4167.00	4205.00	4230.00	4275.00
FMN.	Heather	Heather	Heather	Heather	Heather
SIO2		47.4		50.5	53.5
AL2O3		19.5		22.4	24.1
FE2O3		9.89		7.69	7.16
MGO		2.02		1.87	1.90
CAO		4.52		2.21	1.31
NA2O		1.59		1.21	1.69
K2O		2.30		2.64	2.68
MNO		0.95		0.28	0.22
TIO2		0.67		0.78	0.82
P2O5		0.21		0.34	0.17
LOI		11.0		9.94	9.80
S	2.18	2.51	2.41	1.92	2.04
C-ORG	2.30	3.10	1.40	1.80	1.70
C-MIN	1.97	1.10	3.15	0.68	0.35
SUM		100.05		99.86	103.35
AG		0		0	0
CD		0		0	0
CO		22		26	25
CR		118		134	133
CU		56		62	63
LI		157		182	230
MO					2
NB					26
NI		114		88	102
PB					47
RB					133
SC		13		5	10
SR					203
TH					24
U					3
V		316		188	194
Y					32
ZN		130		183	127
ZR					140
QUARTZ	3.85	5.68	3.88	6.35	5.05
KSPAR	9.37	6.89	7.48	5.63	7.42
PLAG	9.96	7.52	7.77	6.08	6.72
MUSC.	0.00	0.00	0.00	0.00	0.00
BIOTITE	0.00	0.00	0.00	0.07	0.00
CHLORITE	2.10	1.93	1.49	1.69	2.00
SMECTITE	13.48	12.85	11.70	13.86	14.62
ILLITE	32.28	33.57	31.25	34.05	33.46
KAOL.	8.34	8.97	7.15	11.65	12.32
CALCITE	1.98	2.14	10.24	1.34	0.00
DOLOMITE	2.96	2.92	3.90	1.65	1.98
SIDERITE	4.05	3.75	4.10	3.53	2.56
PYRITE	6.46	8.04	7.10	6.95	7.36
AMORPH.	5.98	5.98	5.09	6.75	7.37
SUM	99.87	99.74	100.05	99.44	99.51

WELL	30/7-7	30/7-7	30/7-7	30/7-7	30/7-7
DEPTH	4285.00	4302.00	4305.00	4330.00	4381.00
FMN.	Heather	Heather	Heather	Heather	Heather
SIO2	53.0	45.7	51.3	49.7	49.9
AL2O3	23.7	17.4	21.4	19.4	16.0
FE2O3	5.90	13.8	8.51	8.69	14.8
MGO	1.72	2.47	1.75	2.02	2.70
CAO	1.10	1.29	0.94	2.75	1.77
NA2O	1.10	0.99	1.08	1.52	1.13
K2O	2.72	2.29	2.59	2.42	2.01
MNO	0.22	1.07	0.40	0.97	0.58
TIO2	0.85	0.65	0.71	0.62	0.58
P2O5	0.15	0.15	0.14	0.18	0.20
LOI	9.24	13.6	10.5	11.0	11.7
S	1.26	2.25	2.85	2.89	2.50
C-ORG	1.60	2.10	2.10	2.60	2.30
C-MIN	0.50	1.74	0.50	0.92	2.09
SUM	99.7	99.41	99.32	99.27	101.37
AG	0	0	0	0	0
CD	0	0	0	0	0
CO	20	45	28	39	16
CR	128	106	123	110	100
CU	68	59	64	67	47
LI	206	153	180	144	122
MO	3				2
NB	24				17
NI	69	115	110	140	60
PB	30				39
RB	138				87
SC	10	14	5	8	10
SR	239				251
TH	24				15
U	6				5
V	225	213	225	256	340
Y	36				39
ZN	131	233	193	490	213
ZR	144				91
QUARTZ	7.34	4.66	12.36	12.13	14.44
KSPAR	8.57	8.32	4.59	5.13	3.89
PLAG	7.46	7.18	4.19	5.53	3.01
MUSC.	0.00	0.00	0.55	0.33	1.68
BIOTITE	0.00	0.00	0.00	0.00	0.45
CHLORITE	1.78	1.26	1.22	0.98	1.51
SMECTITE	14.04	13.80	11.48	11.99	10.20
ILLITE	33.18	30.54	34.11	32.65	24.90
KAOL.	11.43	7.95	10.25	8.70	8.08
CALCITE	0.00	0.28	0.00	0.00	0.14
DOLOMITE	2.30	3.02	1.81	2.53	2.76
SIDERITE	2.67	11.93	4.85	4.07	16.8
PYRITE	5.52	6.67	8.36	10.29	7.39
AMORPH.	6.98	5.28	6.05	5.66	4.08
SUM	99.54	99.91	98.65	98.78	99.33

WELL	30/7-7	30/7-7	30/7-7	30/7-7	30/7-7
DEPTH	4450.00	4500.00	4515.00	4530.00	4720.00
FMN.	Heather	Heather	Heather	Heather	Heather
SIO2	50.7	12.6			
AL2O3	22.3	4.24			
FE2O3	7.28	37.6			
MGO	1.93	8.09			
CAO	1.67	7.13			
NA2O	1.29	1.02			
K2O	2.41	0.52			
MNO	0.46	1.39			
TIO2	0.74	0.23			
P2O5	0.16	1.50			
LOI	11.5	29.3			
S	2.34	0.82			
C-ORG	2.80	0.30			
C-MIN	0.23	9.14			
SUM	100.44	103.62			
AG	0	0			
CD	0	0			
CO	21	6			
CR	127	44			
CU	56	20			
LI	158	56			
MO					
NB					
NI	77	23			
PB					
RB					
SC	14	5			
SR					
TH					
U					
V	210	114			
Y					
ZN	244	74			
ZR					
QUARTZ	11.64	3.48	9.52	6.79	12.50
KSPAR	6.07	5.76	7.06	9.70	5.62
PLAG	4.09	0.00	5.99	9.55	5.56
MUSC.	0.57	3.38	0.00	0.00	0.00
BIOTITE	0.00	4.87	0.67	0.14	0.00
CHLORITE	2.43	3.78	2.11	2.49	1.22
SMECTITE	11.59	9.47	13.35	13.27	13.66
ILLITE	32.17	16.60	31.04	30.01	33.69
KAOL.	10.88	1.10	8.71	10.38	8.20
CALCITE	0.00	0.00	0.00	0.15	0.73
DOLOMITE	2.46	1.92	6.05	2.87	2.67
SIDERITE	0.67	48.89	5.29	2.50	1.64
PYRITE	10.28	0.00	5.36	6.47	9.16
AMORPH.	6.54	2.05	5.87	6.30	5.61
SUM	98.63	98.11	99.09	99.94	99.66

WELL	30/7-7	30/9-1	30/9-1	30/9-1	30/9-1
DEPTH	4804.00	2497.00	2529.00	2606.00	2646.00
FMN.	Heather	Heather	Heather	Heather	Heather
SIO2		61.4	60.2	55.5	56.1
AL2O3		17.1	17.6	18.6	17.9
FE2O3		5.51	5.98	7.55	5.04
MGO		1.22	1.89	1.52	1.44
CAO		0.68	1.20	0.94	4.36
NA2O		1.08	1.10	1.38	0.64
K2O		3.03	3.51	2.88	3.34
MNO		0.05	0.06	0.03	0.03
TIO2		0.82	0.86	0.82	0.82
P2O5		0.12	0.11	0.11	0.11
LOI		9.79	8.81	13.00	11.00
S		2.08	0.53	2.79	1.28
C-ORG		1.90	2.40	3.30	2.90
C-MIN		0.00	0.04	0.00	0.21
SUM		100.8	101.32	102.33	100.78
AG		1	1	4	8
CD		0	0	0	0
CO		14	14	14	16
CR		118	83	90	106
CU		49	27	58	53
LI		89	109	108	123
MO		10	4	9	4
NB		19	19	20	43
NI		82	42	56	79
PB		264	18	21	37
RB		87	115	99	113
SC		13	13	11	14
SR		418	194	209	277
TH		11	8	12	17
U		0	2	5	4
V		173	141	169	230
Y		26	19	25	25
ZN		119	151	106	163
ZR		350	232	248	255
QUARTZ	8.44	30.40	31.26	23.51	22.91
KSPAR	8.17	7.98	10.94	8.11	5.41
PLAG	8.63	3.56	5.01	4.43	2.53
MUSC.	0.00	1.03	1.76	0.52	0.41
BIOTITE	0.00	0.15	0.50	0.00	0.00
CHLORITE	1.45	1.25	2.41	1.01	1.28
SMECTITE	13.70	6.80	3.52	8.14	8.12
ILLITE	30.56	19.50	18.94	21.93	29.18
KAOL.	8.78	14.15	12.60	15.31	13.34
CALCITE	0.89	1.61	1.27	2.15	6.53
DOLOMITE	3.15	1.36	0.59	0.28	1.71
SIDERITE	2.02	1.05	1.95	1.05	0.00
PYRITE	10.00	6.92	5.94	7.85	3.02
AMORPH.	5.49	4.49	3.37	5.68	5.65
SUM	100.55	100.27	100.07	99.97	99.01

WELL	30/9-1	31/3-2	31/3-2	31/3-2	31/4-5
DEPTH	2680.00	1541.20	1545.00	1550.00	2063.40
FMN.	Heather	Draupne	Draupne	Draupne	Draupne
SIO2	60.7	45.3	56.0	50.5	53.4
AL2O3	20.0	18.4	21.0	17.0	17.4
FE2O3	5.89	6.25	5.20	6.74	6.89
MGO	1.72	1.37	1.42	2.41	2.18
CAO	0.48	6.19	0.54	2.03	0.91
NA2O	0.88	0.48	0.60	0.84	0.75
K2O	3.36	3.86	4.40	4.33	3.87
MNO	0.03	0.04	0.02	0.04	0.03
TIO2	0.91	0.50	0.79	0.63	0.58
P2O5	0.14	0.40	0.08	0.18	0.09
LOI	8.34	16.1	11.7	16.4	16.6
S	0.91	2.74	1.69	2.39	2.58
C-ORG	0.90	1.90	2.50	4.90	6.10
C-MIN	0.00	2.05	0.00	0.00	0.00
SUM	102.45	98.89	101.75	101.1	102.7
AG	3	0	1	0	0
CD	0	3	0	1	2
CO	24	21	13	24	22
CR	112	175	168	180	120
CU	36	50	46	56	57
LI	120	111	96	74	82
MO	4	36	8	48	79
NB	21	19	33	20	20
NI	62	119	54	132	163
PB	27	24	27	22	23
RB	124	152	182	163	167
SC	11	10	11	14	13
SR	130	314	182	257	201
TH	11	15	16	15	14
U	4	12	6	14	16
V	160	398	210	376	670
Y	28	48	28	31	22
ZN	171	178	78	118	147
ZR	241	125	189	138	117
QUARTZ	28.18	10.90	16.09	13.73	12.38
KSPAR	8.72	3.59	3.95	5.48	5.18
PLAG	2.69	1.89	2.41	2.98	3.12
MUSC.	1.53	0.00	0.15	0.19	0.00
BIOTITE	0.03	0.00	0.00	0.00	0.00
CHLORITE	1.77	0.32	0.53	0.56	0.18
SMECTITE	4.15	13.15	12.42	13.82	16.71
ILLITE	23.11	34.67	37.80	37.61	37.76
KAOL.	16.63	11.24	13.01	9.38	6.02
CALCITE	0.00	8.67	0.00	1.33	1.97
DOLOMITE	1.03	2.82	1.95	3.59	2.27
SIDERITE	0.58	0.21	0.00	0.81	0.49
PYRITE	6.47	6.38	4.35	4.14	6.86
AMORPH.	5.08	6.63	6.91	6.37	6.93
SUM	99.21	99.46	98.56	99.40	99.07

WELL	31/4-5	31/4-5	31/4-5	31/4-5	31/4-5
DEPTH	2064.30	2064.90	2065.20	2065.50	2066.10
FMN.	Draupne	Draupne	Draupne	Draupne	Draupne
SIO2	55.0	52.2	52.9	49.5	54.4
AL2O3	17.8	18.0	17.4	16.3	17.3
FE2O3	6.59	6.65	6.50	6.97	6.13
MGO	2.29	2.40	2.27	2.20	2.61
CAO	0.90	1.10	1.08	1.14	1.58
NA2O	1.23	0.72	0.92	0.80	0.96
K2O	3.60	3.75	3.63	3.58	3.85
MNO	0.03	0.03	0.03	0.03	0.04
TIO2	0.61	0.62	0.58	0.53	0.59
P2O5	0.10	0.12	0.13	0.14	0.27
LOI	16.4	14.4	16.8	19.0	16.1
S	2.76	2.60	2.71	3.22	2.30
C-ORG	5.90	5.10	6.40	4.00	7.00
C-MIN	0.00	0.00	0.00	2.89	0.00
SUM	104.55	99.99	102.24	100.19	103.83
AG	0	0	1	1	0
CD	2	5	2	4	16
CO	20	20	21	23	20
CR	123	130	121	110	124
CU	56	58	52	62	73
LI	86	88	79	73	72
MO	103	73	80	101	71
NB	20	21	29	23	20
NI	159	148	156	180	152
PB	23	21	19	21	21
RB	166	173	167	161	176
SC	8	10	14	15	11
SR	204	213	216	214	228
TH	15	16	15	16	17
U	33	28	23	30	32
V	534	600	529	571	773
Y	31	33	36	33	41
ZN	185	295	212	253	810
ZR	123	127	129	126	126
QUARTZ	13.11	13.36	12.53	11.84	11.10
KSPAR	5.58	5.66	6.42	6.77	6.78
PLAG	2.96	3.06	3.84	3.83	4.13
MUSC.	0.00	0.32	0.20	0.13	0.54
BIOTITE	0.00	0.00	0.00	0.00	0.00
CHLORITE	0.46	0.57	0.42	0.50	0.92
SMECTITE	15.54	13.31	15.19	15.00	14.07
ILLITE	35.94	36.58	35.82	35.19	34.19
KAOL.	7.46	7.36	6.11	4.96	6.14
CALCITE	2.21	0.67	2.01	2.06	0.48
DOLOMITE	2.20	3.57	2.41	2.44	3.73
SIDERITE	0.60	0.13	0.82	1.06	0.58
PYRITE	7.26	8.63	7.79	10.08	11.07
AMORPH.	6.77	6.33	6.45	6.20	5.94
SUM	99.47	98.76	99.38	99.58	99.48

WELL	31/4-5	31/4-6	31/4-6	31/4-6	31/4-6
DEPTH	2066.60	2132.20	2132.30	2132.50	2132.70
FMN.	Draupne	Draupne	Draupne	Draupne	Draupne
SIO2	52.5	49.3	51.1	50.7	48.9
AL2O3	17.2	17.1	16.9	17.7	17.3
FE2O3	7.31	7.48	7.07	6.02	6.93
MGO	2.53	2.76	2.75	2.84	2.93
CAO	1.56	1.94	1.73	2.28	3.22
NA2O	0.88	0.95	0.82	0.86	0.76
K2O	3.75	3.83	3.84	3.92	3.84
MNO	0.03	0.05	0.05	0.07	0.10
TIO2	0.60	0.52	0.56	0.60	0.55
P2O5	0.21	0.20	0.13	0.31	0.40
LOI	16.6	16.6	15.6	15.7	15.0
S	3.41	3.26	3.05	2.04	2.73
C-ORG	6.30	6.70	7.00	6.80	5.70
C-MIN	0.00	0.00	0.00	0.20	0.39
SUM	103.17	100.73	100.55	101.00	99.93
AG	1	5	2	2	0
CD	4	8	9	10	4
CO	20	24	23	17	23
CR	132	113	130	172	146
CU	58	62	67	70	62
LI	69	76	74	80	80
MO	90	85	78	53	77
NB	20	20	19	19	19
NI	190	187	169	141	188
PB	19	22	18	19	20
RB	167	172	173	184	178
SC	16	19	23	15	18
SR	229	246	227	240	247
TH	13	15	16	15	16
U	26	20	18	26	27
V	538	631	668	688	613
Y	38	30	20	34	45
ZN	234	520	610	530	263
ZR	120	118	118	128	121
QUARTZ	11.08	10.03	9.06	9.57	8.93
KSPAR	5.38	5.39	5.87	6.61	6.11
PLAG	3.90	3.59	3.52	3.74	3.28
MUSC.	0.18	0.05	0.47	0.18	0.20
BIOTITE	0.00	0.00	0.00	0.00	0.00
CHLORITE	0.56	0.39	0.74	0.52	0.55
SMECTITE	13.74	14.27	15.02	14.00	14.10
ILLITE	35.96	36.62	34.23	38.20	36.58
KAOL.	5.80	5.45	5.99	6.27	6.49
CALCITE	0.25	0.12	0.43	0.05	0.65
DOLOMITE	3.07	4.20	3.82	4.86	4.93
SIDERITE	0.34	0.00	0.56	0.02	0.05
PYRITE	12.97	13.30	13.56	8.68	11.38
AMORPH.	6.19	6.30	6.27	6.29	6.24
SUM	98.83	98.70	99.22	98.36	98.95

WELL	31/4-9	31/4-9	31/4-9	31/4-9	31/4-9
DEPTH	2105.15	2106.75	2107.15	2109.75	2110.05
FMN.	Draupne	Draupne	Draupne	Draupne	Draupne
SIO2	42.8	55.4	51.8	53.3	49.0
AL2O3	18.5	19.0	18.6	18.2	18.3
FE2O3	6.30	4.89	5.88	6.08	6.35
MGO	1.81	2.16	2.01	2.01	1.86
CAO	5.08	1.54	0.95	1.58	4.18
NA2O	0.90	1.16	0.93	1.06	1.26
K2O	3.01	3.55	3.40	3.43	3.22
MNO	0.05	0.03	0.03	0.03	0.03
TIO2	0.55	0.58	0.61	0.54	0.53
P2O5	0.27	0.19	0.31	0.21	0.12
LOI	19.5	16.5	15.6	16.0	16.4
S	3.17	1.92	2.72	2.90	3.25
C-ORG	6.80	6.86	6.86	6.37	5.40
C-MIN	0.76	0.03	0.00	0.01	0.49
SUM	98.77	105.00	100.12	102.44	101.25
AG	1	0	1	0	0
CD	21	26	11	2	3
CO	19	14	16	18	21
CR	160	165	184	131	140
CU	94	93	81	56	58
LI	139	104	94	84	88
MO	204	53	41	116	100
NB	27	23	27	21	27
NI	143	115	125	146	147
PB	25	21	25	25	22
RB	150	185	174	180	158
SC	13	19	14	11	16
SR	279	244	266	288	267
TH	19	17	16	17	16
U	27	18	18	31	19
V	875	825	586	526	430
Y	34	37	54	32	23
ZN	930	1080	520	194	183
ZR	134	139	160	117	120
QUARTZ	4.95	10.65	11.90	8.65	9.34
KSPAR	3.72	4.71	4.98	4.67	4.03
PLAG	2.25	2.48	2.22	2.47	2.11
MUSC.	0.00	0.30	0.11	0.03	0.00
BIOTITE	0.00	0.00	0.00	0.00	0.00
CHLORITE	0.67	0.80	0.35	0.56	0.22
SMECTITE	13.77	16.26	15.59	16.35	13.57
ILLITE	32.96	35.08	35.70	33.87	32.96
KAOL.	10.74	10.18	9.41	8.94	9.72
CALCITE	7.00	0.46	0.00	0.53	4.57
DOLOMITE	2.60	1.35	2.28	1.90	2.83
SIDERITE	0.08	0.16	0.16	0.41	0.04
PYRITE	14.76	9.28	10.63	14.24	14.26
AMORPH.	6.51	7.33	7.10	6.90	6.48
SUM	99.45	98.70	98.51	99.35	99.15

WELL	31/4-9	31/4-9	31/4-9	31/4-9	31/4-9
DEPTH	2110.60	2111.50	2112.10	2112.90	2113.25
FMN.	Draupne	Draupne	Draupne	Draupne	Draupne
SIO2	8.20	51.7	55.6	54.7	55.7
AL2O3	2.82	17.2	18.2	17.6	17.9
FE2O3	1.27	6.90	5.67	6.83	6.23
MGO	1.15	2.27	2.28	2.11	2.30
CAO	48.13	1.35	1.43	0.93	1.10
NA2O	0.48	1.01	1.71	0.89	1.28
K2O	0.34	3.52	3.73	3.40	3.49
MNO	0.10	0.04	0.03	0.03	0.03
TIO2	0.14	0.59	0.59	0.59	0.63
P2O5	0.05	0.16	0.18	0.12	0.10
LOI	37.9	16.3	15.6	16.2	15.3
S	0.59	3.39	2.31	3.41	2.75
C-ORG	0.34	6.84	6.36	6.80	5.97
C-MIN	10.5	0.36	0.00	0.00	0.00
SUM	100.58	101.04	105.02	103.4	104.06
AG	0	0	0	1	1
CD	0	1	20	2	7
CO	1	16	19	22	22
CR	29	153	140	135	157
CU	10	90	80	59	63
LI	8	79	83	81	83
MO	8	43	72	97	77
NB	12	20	25	21	21
NI	8	105	141	182	151
PB	3	19	21	19	22
RB	8	154	173	171	173
SC	23	8	15	14	14
SR	331	258	244	220	209
TH	3	13	18	17	15
U	6	13	25	29	26
V	74	494	875	496	590
Y	7	28	40	34	33
ZN	24	154	780	199	410
ZR	27	129	129	122	128
QUARTZ	0.00		10.30	10.53	12.48
KSPAR	2.61		5.09	4.44	4.40
PLAG	1.77		2.91	2.67	2.89
MUSC.	0.00		0.04	0.07	0.09
BIOTITE	0.00		0.00	0.00	0.00
CHLORITE	0.00		0.34	0.61	0.53
SMECTITE	4.47		15.10	14.80	14.09
ILLITE	4.89		36.27	32.76	34.68
KAOL.	2.45		8.93	8.77	9.04
CALCITE	89.28		0.01	0.00	0.00
DOLOMITE	3.38		3.01	2.18	2.98
SIDERITE	0.00		0.08	0.36	0.00
PYRITE	0.00		10.64	16.41	12.47
AMORPH.	1.22		6.78	6.50	6.59
SUM	103.57		98.79	99.29	98.90

WELL	31/4-9	31/4-9	31/4-9	31/4-9	31/4-9
DEPTH	2114.00	2114.10	2114.20	2114.20	2114.30
FMN.	Draupne	Draupne	Draupne	Draupne	Draupne
SIO2	51.7	53.1	51.5	50.2	50.1
AL2O3	16.9	18.0	17.5	17.4	17.1
FE2O3	7.07	7.27	6.87	6.92	6.81
MGO	2.24	2.34	2.35	2.20	2.22
CAO	1.35	1.14	1.35	1.21	1.10
NA2O	0.99	0.96	1.37	0.97	0.92
K2O	3.59	3.59	3.55	3.63	3.51
MNO	0.03	0.04	0.03	0.03	0.03
TIO2	0.55	0.60	0.61	0.58	0.58
P2O5	0.14	0.13	0.15	0.16	0.13
LOI	16.5	15.1	17.5	17.5	17.2
S	3.33	3.20	3.21	3.14	3.26
C-ORG	7.18	5.66	7.10	7.24	8.25
C-MIN	0.46	0.67	0.90	0.00	0.32
SUM	101.06	102.27	102.78	100.80	99.70
AG	0	0	0	0	0
CD	4	4	6	2	4
CO	25	26	25	20	25
CR	121	107	118	143	109
CU	64	60	60	61	61
LI	77	89	84	81	82
MO	98	80	91	104	100
NB	25	25	25	28	25
NI	195	161	175	175	176
PB	19	20	23	19	22
RB	155	162	153	168	153
SC	15	16	13	18	13
SR	238	245	252	230	241
TH	13	13	13	15	11
U	18	19	19	28	17
V	519	688	559	641	569
Y	32	34	34	38	32
ZN	234	272	410	146	242
ZR	135	137	138	129	138

QUARTZ	10.54
KSPAR	4.43
PLAG	2.50
MUSCOVITE	0.00
BIOTITE	0.00
CHLORITE	0.40
SMECTITE	14.64
ILLITE	34.36
KAOLINITE	7.97
CALCITE	0.00
DOLOMITE	3.16
SIDERITE	0.08
PYRITE	15.31
AMORPHOUS	6.57
SUM	98.70

WELL	31/4-9	31/4-9	31/4-9	31/4-9	31/4-9
DEPTH	2114.40	2114.50	2114.60	2114.70	2114.80
FMN.	Draupne	Draupne	Draupne	Draupne	Draupne
SIO2	53.7	53.4	49.1	51.6	49.4
AL2O3	17.8	17.7	17.2	18.1	17.1
FE2O3	6.43	6.95	7.77	6.41	7.73
MGO	2.31	2.24	2.07	2.04	2.08
CAO	1.14	1.02	0.91	0.94	1.12
NA2O	1.18	0.98	0.91	0.90	1.06
K2O	3.55	3.53	3.40	3.46	3.52
MNO	0.03	0.03	0.03	0.03	0.03
TIO2	0.61	0.61	0.62	0.58	0.58
P2O5	0.14	0.11	0.14	0.16	0.18
LOI	16.2	16.1	18.2	17.0	18.2
S	2.85	3.40	4.09	2.92	4.17
C-ORG	7.42	6.91	7.25	7.70	7.41
C-MIN	0.19	0.25	0.63	0.14	0.03
SUM	103.09	102.67	100.35	101.22	101.00
AG	0	1	0	1	0
CD	6	8	4	19	6
CO	24	26	29	22	27
CR	120	121	118	115	120
CU	61	63	65	69	70
LI	87	86	81	89	80
MO	87	87	111	85	111
NB	26	23	23	27	36
NI	169	180	215	164	230
PB	21	22	22	22	21
RB	164	157	151	161	150
SC	14	11	15	13	18
SR	250	234	223	239	231
TH	15	14	12	13	14
U	19	19	20	19	20
V	675	613	586	749	673
Y	33	29	33	34	36
ZN	400	480	255	970	360
ZR	151	141	139	145	150
QUARTZ					
KSPAR					
PLAG					
MUSCOVITE					
BIOTITE					
CHLORITE					
SMECTITE					
ILLITE					
KAOLINITE					
CALCITE					
DOLOMITE					
SIDERITE					
PYRITE					
AMORPHOUS					
SUM					

WELL	31/4-9	31/4-9	31/4-9	31/4-9	31/4-9
DEPTH	2114.90	2114.90	2116.50	2117.50	2118.60
FMN.	Draupne	Draupne	Draupne	Draupne	Draupne
SIO2	45.0	52.8	50.4	49.9	52.9
AL2O3	23.8	18.9	17.0	16.9	18.3
FE2O3	6.93	6.91	7.12	7.55	5.29
MGO	1.33	2.16	1.89	2.14	2.55
CAO	0.72	1.06	0.86	1.12	1.32
NA2O	0.98	1.14	1.18	1.08	1.04
K2O	2.23	3.43	3.57	3.64	4.05
MNO	0.04	0.03	0.03	0.03	0.04
TIO2	0.53	0.57	0.49	0.51	0.61
P2O5	0.10	0.13	0.15	0.13	0.18
LOI	17.8	15.7	15.7	15.2	13.8
S	4.39	3.40	3.54	3.38	1.30
C-ORG	5.22	6.10	6.93	6.36	6.21
C-MIN	0.13	0.00	0.00	0.01	0.05
SUM	99.46	102.83	98.39	98.20	100.08
AG	0	0	0	0	2
CD	0	4	5	3	2
CO	20	23	23	24	10
CR	58	112	144	130	225
CU	42	57	58	66	68
LI	87	86	79	77	82
MO	81	98	104	106	19
NB	50	49	43	28	24
NI	148	179	204	210	91
PB	22	23	21	20	22
RB	85	170	169	174	197
SC	13	16	10	11	16
SR	244	247	194	194	258
TH	21	17	16	19	19
U	18	30	28	30	22
V	506	823	615	806	656
Y	31	38	41	37	30
ZN	67	223	393	240	191
ZR	208	163	150	137	141
QUARTZ		10.04	11.53	8.34	9.23
KSPAR		4.07	4.53	4.71	5.58
PLAG		2.38	2.47	2.82	2.79
MUSC.		0.00	0.00	0.00	0.00
BIOTITE		0.00	0.00	0.00	0.00
CHLORITE		0.23	0.26	0.54	0.57
SMECTITE		14.34	13.04	14.51	15.67
ILLITE		35.30	35.23	34.12	40.96
KAOL.		8.95	7.64	8.02	8.59
CALCITE		0.00	0.00	0.00	0.00
DOLOMITE		2.74	3.10	2.65	3.60
SIDERITE		0.00	0.00	0.10	0.00
PYRITE		15.01	16.12	17.40	6.12
AMORP.		6.73	6.12	6.39	7.09
SUM		98.52	98.41	99.10	98.78

WELL	31/4-9	31/4-9	31/4-9	31/4-9	31/4-9
DEPTH	2119.00	2120.00	2120.80	2121.40	2124.50
FMN.	Draupne	Draupne	Draupne	Heather	Heather
SIO2	47.5	48.2	25.5	64.3	57.5
AL2O3	16.7	18.5	9.72	14.8	17.1
FE2O3	8.13	5.50	9.54	5.94	6.43
MGO	2.17	2.50	7.15	1.42	1.50
CAO	1.71	1.54	14.4	0.72	0.56
NA2O	1.00	1.24	0.80	1.22	1.36
K2O	3.57	3.84	2.01	3.82	3.60
MNO	0.04	0.04	0.34	0.05	0.05
TIO2	0.50	0.57	0.30	0.85	0.87
P2O5	0.32	0.13	0.76	0.08	0.06
LOI	16.3	14.6	17.0	7.59	10.9
S	3.93	1.66	5.67	1.93	2.17
C-ORG	6.67	6.33	3.44	1.94	3.37
C-MIN	0.02	0.15	4.36	0.00	0.00
SUM	97.94	96.66	87.52	100.79	99.93
AG	1	3	0	0	0
CD	4	8	2	0	0
CO	24	13	59	12	13
CR	155	223	141	260	172
CU	69	68	39	21	29
LI	83	93	51	81	121
MO	116	25	182	8	6
NB	19	22	15	19	20
NI	249	113	436	81	54
PB	18	22	6	14	17
RB	168	196	97	110	110
SC	8	15	15	8	9
SR	214	229	276	144	148
TH	15	16	9	9	10
U	36	20	76	7	7
V	593	748	468	91	94
Y	43	27	39	22	26
ZN	450	276	421	89	98
ZR	118	137	81	448	335
QUARTZ	9.00	8.33	6.23	35.59	25.03
KSPAR	4.71	5.13	7.14	12.36	10.15
PLAG	2.77	2.41	5.00	4.07	7.39
MUSC.	0.00	0.14	0.00	1.19	1.35
BIOTITE	0.00	0.00	0.96	0.03	0.10
CHLORITE	0.44	0.80	0.69	0.99	1.37
SMECTITE	13.96	15.10	8.02	4.28	5.35
ILLITE	32.97	38.78	25.36	18.43	20.34
KAOL.	8.55	9.53	1.96	7.94	12.34
CALCITE	0.00	0.00	0.00	0.07	0.20
DOLOMITE	3.12	3.91	18.70	1.64	0.00
SIDERITE	0.30	0.07	0.00	0.84	0.55
PYRITE	18.43	8.06	25.25	9.69	11.66
AMORPH.	6.39	7.09	2.67	2.79	3.83
SUM	99.08	98.44	97.99	99.91	99.59

WELL	31/4-9	31/4-9	31/4-9	31/4-9	31/4-9
DEPTH	2130.50	2137.80	2145.60	2155.40	2158.60
FMN.	Heather	Heather	Heather	Heather	Heather
SIO2	56.5	53.4	59.6	57.0	59.5
AL2O3	17.2	18.5	18.3	19.5	18.3
FE2O3	6.61	7.15	6.13	6.31	7.73
MGO	1.76	1.77	1.61	1.72	1.61
CAO	0.78	0.73	0.60	0.60	0.50
NA2O	1.26	1.17	1.30	1.24	1.17
K2O	3.60	3.30	3.53	3.32	3.39
MNO	0.05	0.05	0.05	0.04	0.03
TIO2	0.81	0.83	0.80	0.84	0.86
P2O5	0.11	0.09	0.08	0.12	0.08
LOI	8.99	12.8	8.37	10.6	9.58
S	2.04	2.43	1.57	1.48	2.66
C-ORG	2.25	4.56	2.14	3.33	1.72
C-MIN	0.00	0.00	0.00	0.00	0.00
SUM	97.67	99.79	100.37	101.29	102.75
AG	0	0	0	0	0
CD	0	0	0	4	0
CO	13	12	14	14	15
CR	172	160	240	154	218
CU	27	28	26	30	33
LI	115	107	115	139	127
MO	6	6	4	3	4
NB	19	21	20	26	20
NI	56	51	46	52	56
PB	16	20	15	18	18
RB	118	123	119	120	115
SC	14	11	6	6	9
SR	134	156	143	149	136
TH	9	13	10	13	10
U	5	5	5	6	3
V	120	131	115	119	133
Y	27	29	25	35	25
ZN	109	97	95	109	100
ZR	311	273	313	295	319
QUARTZ	24.78	18.74	29.39	21.37	24.73
KSPAR	12.94	11.33	12.33	11.50	13.41
PLAG	6.77	4.96	4.00	4.15	4.15
MUSC.	1.42	0.26	0.88	0.92	0.81
BIOTITE	0.50	0.28	0.09	0.34	0.28
CHLORITE	1.43	0.97	1.32	1.52	1.15
SMECTITE	4.96	7.41	5.56	8.01	6.57
ILLITE	17.72	24.45	20.78	21.98	20.83
KAOL.	12.03	12.41	11.65	14.59	12.18
CALCITE	1.48	0.00	0.00	0.00	0.00
DOLOMITE	0.29	1.29	0.57	0.44	0.39
SIDERITE	1.41	0.36	1.16	1.03	0.72
PYRITE	10.21	12.57	8.00	9.15	10.92
AMORPH.	3.77	5.00	4.00	5.17	4.27
SUM	99.71	99.27	99.63	99.72	99.63

WELL	31/4-9	31/6-1	31/6-1	31/6-1	31/6-1
DEPTH	2160.40	1324.00	1326.00	1335.00	1337.00
FMN.	Heather	Draupne	Draupne	Draupne	Heather
SIO2	63.0	52.1	51.4	59.5	56.0
AL2O3	17.0	16.7	17.3	16.7	12.4
FE2O3	5.34	6.44	6.07	4.95	13.6
MGO	1.50	2.76	2.55	1.20	1.93
CAO	0.50	3.40	2.28	2.41	0.72
NA2O	1.32	0.78	0.82	1.04	0.91
K2O	3.54	4.78	4.85	4.05	6.66
MNO	0.03	0.05	0.04	0.03	0.04
TIO2	0.93	0.64	0.65	0.78	0.67
P2O5	0.09	0.28	0.17	0.35	0.28
LOI	7.50	12.6	12.5	10.6	7.69
S	0.90	1.69	1.65	1.23	1.79
C-ORG	1.21	2.30	2.70	2.50	0.60
C-MIN	0.00	0.22	0.02	0.05	0.00
SUM	100.75	100.53	98.63	101.61	100.9
AG	0	1	1	0	0
CD	0	1	1	0	0
CO	15	25	17	12	13
CR	260	145	143	241	335
CU	28	36	41	44	16
LI	113	82	82	96	56
MO	5	14	17	10	5
NB	21	20	19	21	14
NI	48	85	73	61	33
PB	18	22	39	19	13
RB	114	160	164	125	196
SC	8	13	16	14	15
SR	139	186	338	148	79
TH	12	13	15	15	6
U	5	6	7	13	1
V	115	195	200	138	96
Y	22	37	34	41	36
ZN	94	153	101	115	96
ZR	402	150	138	375	480
QUARTZ	34.55	16.43	14.14	28.49	13.26
KSPAR	14.41	5.25	5.74	8.11	4.80
PLAG	5.26	2.39	3.94	2.96	0.48
MUSC.	0.75	0.00	0.00	0.40	0.00
BIOTITE	0.10	0.00	0.00	0.00	0.00
CHLORITE	0.96	0.62	0.59	0.80	0.00
SMECTITE	6.07	12.95	13.11	8.76	12.51
ILLITE	20.68	38.11	39.34	26.33	52.50
KAOL.	8.64	8.01	7.75	10.69	1.66
CALCITE	0.00	1.40	1.51	2.58	1.65
DOLOMITE	0.38	5.54	4.33	2.32	3.87
SIDERITE	0.00	0.86	0.31	0.75	0.00
PYRITE	4.06	2.18	3.22	3.63	4.09
AMORPH.	3.82	6.03	5.98	4.50	5.81
SUM	99.15	99.08	99.03	100.12	97.36

WELL	31/6-1	31/6-1	31/6-1	31/6-1	31/6-1
DEPTH	1340.00	1343.00	1346.00	1349.50	1350.00
FMN.	Heather	Heather	Heather	Heather	Heather
SIO2	63.0	60.3	55.7	32.2	8.92
AL2O3	16.7	16.9	18.4	8.71	1.68
FE2O3	5.01	6.02	7.01	20.7	8.05
MGO	1.10	0.97	1.22	1.97	0.65
CAO	0.34	0.52	0.50	12.43	37.1
NA2O	0.98	0.97	0.92	0.50	0.71
K2O	4.03	3.63	3.95	3.08	1.15
MNO	0.03	0.03	0.03	0.30	0.14
TIO2	0.98	0.92	0.84	0.48	0.13
P2O5	0.11	0.11	0.14	0.34	19.8
LOI	8.83	10.6	12.3	17.7	12.2
S	0.99	2.03	2.42	0.86	2.26
C-ORG	0.90	1.20	1.50	0.50	2.70
C-MIN	0.00	0.02	0.00	3.59	2.76
SUM	101.11	100.97	101.01	98.41	90.53
AG	0	0	0	3	1
CD	0	0	0	0	2
CO	10	12	15	12	890
CR	347	390	192	765	115
CU	27	31	34	27	20
LI	118	123	138	59	13
MO	4	4	6	3	10
NB	33	21	20	25	12
NI	45	55	58	50	1395
PB	16	21	18	41	76
RB	103	88	98	60	12
SC	11	10	10	9	24
SR	96	113	107	462	1251
TH	12	13	15	15	2
U	4	7	6	0	73
V	113	124	119	346	175
Y	28	27	29	41	206
ZN	101	89	109	208	6720
ZR	480	575	291	227	177
QUARTZ	34.51	30.12	22.67	10.98	5.30
KSPAR	10.86	10.46	7.34	5.95	9.22
PLAG	3.18	3.17	4.35	0.95	5.07
MUSC.	0.54	0.00	0.07	0.00	0.00
BIOTITE	0.19	0.01	0.03	0.34	0.19
CHLORITE	0.99	0.65	0.66	0.82	0.00
SMECTITE	7.12	7.64	10.21	8.76	5.26
ILLITE	21.53	20.88	23.68	28.22	18.06
KAOL.	10.59	12.04	12.99	3.00	0.00
CALCITE	1.14	2.03	3.70	18.89	18.39
DOLOMITE	1.41	0.80	0.68	4.87	4.61
SIDERITE	1.19	1.28	1.95	10.49	23.12
PYRITE	3.03	6.64	6.33	5.80	19.32
AMORPH.	3.87	4.39	5.57	2.95	0.34
SUM	100.15	99.92	100.23	100.62	103.6

WELL	31/6-3	31/6-3	31/6-3	31/6-3	31/6-3
DEPTH	1385.00	1395.00	1405.00	1415.00	1478.00
FMN.	Draupne	Draupne	Draupne	Draupne	Draupne
SIO2	54.5	56.0	51.9	53.4	52.4
AL2O3	18.9	17.0	15.9	18.1	17.8
FE2O3	6.17	6.38	6.18	6.70	6.66
MGO	2.19	2.70	3.41	2.46	2.82
CAO	1.11	2.01	3.17	1.43	2.52
NA2O	0.82	0.85	0.89	0.95	0.80
K2O	3.88	4.15	4.84	4.98	4.08
MNO	0.03	0.03	0.04	0.03	0.04
TIO2	0.81	0.71	0.77	0.74	0.66
P2O5	0.16	0.31	0.16	0.16	0.18
LOI	11.1	8.58	10.2	9.45	8.48
S	1.46	1.03	0.98	0.94	1.12
C-ORG	3.10	1.90	1.80	2.50	2.30
C-MIN	0.00	0.34	0.85	0.13	0.35
SUM	99.67	98.72	97.46	98.40	96.44
AG	0	0	1	0	0
CD	0	0	0	0	0
CO	16	14	15	18	21
CR	239	201	178	161	162
CU	42	30	35	50	33
LI	83	69	56	69	69
MO	20	4	10	10	16
NB	26	23	21	22	19
NI	51	58	60	67	82
PB	43	28	69	83	27
RB	160	166	138	167	190
SC	10	13	13	11	13
SR	285	201	295	286	237
TH	15	17	6	17	21
U	9	6	0	10	17
V	306	150	143	169	240
Y	32	40	33	33	35
ZN	117	114	134	135	119
ZR	162	182	159	152	145
QUARTZ	15.39	17.02	15.02	11.51	14.19
KSPAR	5.07	4.44	4.92	5.13	4.05
PLAG	1.86	2.06	2.68	2.30	1.94
MUSC.	0.00	0.00	0.20	0.11	0.00
BIOTITE	0.00	0.00	0.00	0.00	0.00
CHLORITE	0.67	0.52	0.78	0.86	0.78
SMECTITE	14.40	13.74	13.41	14.70	14.43
ILLITE	38.49	39.99	37.40	40.20	40.37
KAOL.	9.97	7.85	7.01	9.58	8.10
CALCITE	0.18	0.06	0.50	0.73	0.77
DOLOMITE	2.36	4.71	8.36	4.43	5.22
SIDERITE	0.06	0.00	0.00	0.00	0.13
PYRITE	4.16	2.31	4.18	3.66	2.58
AMORPH.	6.80	6.59	5.69	6.54	6.72
SUM	98.75	98.29	99.36	99.20	98.49

WELL	31/6-3	31/6-3	31/6-3	31/6-3	31/6-3
DEPTH	1495.00	1498.85	1503.00	1506.15	1508.80
FMN.	Draupne	Heather	Heather	Heather	Heather
SIO2	68.0	64.7	62.1	65.1	50.5
AL2O3	14.6	15.8	16.9	14.5	8.31
FE2O3	5.07	6.11	6.85	7.34	5.37
MGO	1.12	1.46	1.58	1.71	1.11
CAO	1.14	1.30	0.64	0.68	15.9
NA2O	1.18	1.16	1.10	1.11	0.68
K2O	2.73	2.91	2.84	3.10	2.54
MNO	0.03	0.03	0.02	0.02	0.19
TIO2	0.75	0.79	0.85	0.76	0.57
P2O5	0.21	0.12	0.13	0.26	0.17
LOI	6.04	5.44	6.50	5.41	13.6
S	1.21	0.79	0.70	0.69	0.33
C-ORG	1.00	0.60	0.80	0.20	0.20
C-MIN	0.00	0.08	0.00	0.30	3.50
SUM	100.87	99.82	99.51	99.99	98.94
AG	0	0	0	1	0
CD	0	0	0	0	0
CO	12	13	16	13	16
CR	101	160	128	133	215
CU	21	22	25	18	12
LI	77	92	103	95	38
MO	5	3	4	3	3
NB	20	20	22	18	18
NI	44	44	50	37	34
PB	15	17	18	15	12
RB	102	118	119	133	105
SC	10	9	10	10	14
SR	179	185	183	193	232
TH	10	10	12	10	10
U	1	4	5	4	3
V	90	104	113	90	180
Y	34	25	27	30	22
ZN	114	89	91	89	149
ZR	353	344	337	376	381
QUARTZ	35.92	35.60	30.01	33.67	23.70
KSPAR	8.66	9.42	9.13	10.06	6.05
PLAG	4.53	1.85	2.88	1.66	0.75
MUSC.	0.66	0.74	0.63	0.37	0.00
BIOTITE	0.09	0.41	0.40	0.00	0.03
CHLORITE	1.03	1.90	2.14	1.61	0.91
SMECTITE	4.58	6.39	6.48	7.01	4.28
ILLITE	19.59	19.88	21.02	25.23	22.12
KAOL.	13.04	11.74	14.92	9.30	3.50
CALCITE	0.69	1.61	0.16	0.69	30.84
DOLOMITE	0.40	0.71	0.33	0.88	1.75
SIDERITE	0.35	1.02	0.57	0.55	0.00
PYRITE	5.43	4.24	5.98	3.28	4.73
AMORPH.	4.31	4.27	5.10	4.62	2.58
SUM	99.27	99.78	99.77	98.86	99.71

WELL	34/8-2	34/8-2	34/8-2	34/8-2	34/10-18
DEPTH	2898.50	2902.00	2911.00	2917.00	2351.40
FMN.	Draupne	Draupne	Draupne	Heather	Draupne
SIO2	23.0	51.6	56.3	54.7	59.1
AL2O3	8.10	18.3	14.7	17.9	14.9
FE2O3	29.2	5.78	7.51	5.71	7.39
MGO	0.68	2.14	1.21	1.64	1.17
CAO	4.69	1.05	0.91	0.60	0.85
NA2O	0.56	0.69	0.91	0.68	1.15
K2O	1.33	4.06	2.70	3.56	3.29
MNO	0.17	0.07	0.04	0.06	0.04
TIO2	0.23	0.73	0.69	0.83	0.60
P2O5	0.27	0.13	0.22	0.11	0.20
LOI	24.1	12.0	15.7	7.47	11.6
S	24.9	2.19	4.08	2.20	3.30
C-ORG	1.60	4.40	7.20	1.30	3.44
C-MIN	0.59	0.00	0.00	0.00	0.25
SUM	92.33	96.55	100.89	93.26	100.29
AG	1	0	0	0	1
CD	4	10	8	0	3
CO	41	19	27	17	37
CR	147	283	414	269	118
CU	30	80	105	41	60
LI	22	83	43	138	67
MO	609			4	95
NB	16			17	18
NI	315	149	189	62	170
PB	6			30	20
RB	28			114	125
SC	9	11	9	10	10
SR	169			1293	153
TH	7			15	14
U	12			1	17
V	273	623	863	200	389
Y	27			28	26
ZN	400	700	530	145	256
ZR	35			205	216
QUARTZ	5.03	15.06	23.49	23.78	24.73
KSPAR	0.14	4.66	3.87	4.28	6.81
PLAG	0.61	3.95	3.15	5.29	4.85
MUSC.	0.00	0.00	0.49	0.00	0.74
BIOTITE	0.00	0.00	0.00	0.00	0.00
CHLORITE	0.00	0.36	0.48	0.46	0.64
SMECTITE	2.50	13.06	9.97	10.71	9.01
ILLITE	8.13	37.07	23.15	29.37	23.77
KAOL.	3.00	7.51	9.07	8.03	9.56
CALCITE	3.56	1.33	0.00	3.57	0.52
DOLOMITE	3.77	2.89	1.34	1.44	1.68
SIDERITE	0.58	0.00	0.24	0.00	0.25
PYRITE	72.54	9.74	19.85	9.98	12.72
AMORPH.	1.33	5.46	4.86	4.06	4.73
SUM	99.75	99.23	99.49	100.18	99.80

WELL	34/10-18	34/10-18	34/10-18	34/10-18	34/10-18
DEPTH	2351.65	2351.75	2352.30	2352.60	2352.80
FMN.	Draupne	Draupne	Draupne	Draupne	Draupne
SIO2	52.8	50.9	47.0	48.1	50.1
AL2O3	13.0	14.1	13.6	13.4	13.5
FE2O3	9.57	8.76	11.0	10.4	8.85
MGO	1.00	1.07	1.22	1.35	1.12
CAO	0.86	0.79	0.90	1.05	1.42
NA2O	0.78	0.73	0.84	0.77	0.94
K2O	2.89	2.32	2.99	2.97	2.92
MNO	0.04	0.03	0.04	0.05	0.05
TIO2	0.57	0.60	0.57	0.63	0.55
P2O5	0.32	0.41	0.35	0.53	0.84
LOI	16.7	22.2	20.4	20.5	18.9
S	6.50	5.83	6.96	6.23	5.81
C-ORG	4.51	4.37	5.47	5.45	6.30
C-MIN	0.40	2.33	0.29	0.02	0.00
SUM	98.53	101.91	98.91	99.75	99.19
AG	1	0	1	0	2
CD	3	18	7	6	8
CO	58	44	52	56	50
CR	123	178	113	160	122
CU	60	98	76	82	70
LI	54	63	43	51	33
MO	160		175	150	186
NB	17		16	18	18
NI	235	259	267	280	324
PB	16		16	16	14
RB	107		113	124	110
SC	6	8	15	11	12
SR	162		172	182	238
TH	15		13	13	14
U	20		25	38	44
V	457	700	575	700	683
Y	32		36	42	66
ZN	281	1110	676	520	657
ZR	193		137	136	157
QUARTZ	22.61	19.84	14.39	15.47	21.91
KSPAR	5.76	4.69	4.84	3.64	4.34
PLAG	3.05	2.08	3.31	2.17	2.17
MUSC.	0.09	0.10	0.00	0.00	0.08
BIOTITE	0.00	0.00	0.00	0.00	0.00
CHLORITE	0.00	0.24	0.01	0.00	0.00
SMECTITE	9.04	10.17	11.95	12.06	9.83
ILLITE	22.29	21.56	25.90	27.35	28.47
KAOL.	7.37	11.18	7.93	7.10	8.88
CALCITE	0.83	1.83	2.68	3.17	2.41
DOLOMITE	2.21	2.60	1.77	1.98	4.84
SIDERITE	0.73	1.29	0.63	1.30	0.59
PYRITE	22.11	20.44	22.50	22.46	13.27
AMORPH.	4.39	4.94	5.33	5.09	4.81
SUM	99.78	100.43	100.46	100.56	98.98

WELL	34/10-18	34/10-18	34/10-18	34/10-18	34/10-18
DEPTH	2353.70	2354.10	2354.50	2354.90	2355.05
FMN.	Draupne	Draupne	Draupne	Draupne	Heather
SIO2	49.9	51.6	46.1	47.9	52.6
AL2O3	14.6	15.2	13.4	14.4	20.0
FE2O3	7.51	6.49	10.5	6.23	7.39
MGO	1.21	1.21	1.03	1.22	1.37
CAO	0.73	0.62	0.56	2.34	0.80
NA2O	1.27	0.84	0.74	0.86	0.90
K2O	2.84	3.02	2.57	2.96	3.27
MNO	0.03	0.03	0.03	0.04	0.04
TIO2	0.51	0.41	0.38	0.39	0.88
P2O5	0.28	0.28	0.29	0.26	0.35
LOI	23.4	20.2	23.2	20.8	12.9
S	5.06	4.17	5.86	3.45	3.05
C-ORG	11.2	8.98	8.28	9.87	3.11
C-MIN	0.00	0.37	0.64	0.33	0.02
SUM	102.28	99.9	98.8	97.4	100.5
AG	2	1	1	2	0
CD	17	19	12	17	0
CO	50	26	40	26	19
CR	126	99	104	129	143
CU	123	107	102	117	45
LI	40	38	38	41	144
MO	157	159	201	119	6
NB	16	15	14	16	20
NI	327	208	320	211	91
PB	20	17	16	18	30
RB	116	134	114	128	116
SC	8	10	12	15	15
SR	226	218	207	238	194
TH	16	15	15	13	23
U	44	39	35	33	4
V	1087	925	853	992	246
Y	45	44	42	39	44
ZN	1237	1057	776	1180	131
ZR	130	116	103	110	165
QUARTZ	18.81	17.60	17.65	15.64	19.86
KSPAR	4.74	4.48	4.89	5.96	7.18
PLAG	4.25	3.69	3.03	3.30	2.94
MUSC.	0.00	0.39	0.00	0.00	0.85
BIOTITE	0.00	0.00	0.00	0.00	0.00
CHLORITE	0.01	0.38	0.18	0.32	1.37
SMECTITE	12.89	13.86	13.50	16.56	9.22
ILLITE	25.70	27.52	25.76	28.26	24.74
KAOL.	8.74	9.66	9.09	8.53	16.49
CALCITE	0.48	0.66	1.60	2.28	0.64
DOLOMITE	2.69	2.35	2.45	2.11	1.66
SIDERITE	0.52	0.46	1.37	1.17	0.96
PYRITE	15.85	12.97	15.68	10.14	8.33
AMORPH.	5.83	6.19	5.67	6.55	5.98
SUM	99.59	99.60	100.34	100.07	100.04

WELL	34/10-18	34/10-18	34/10-18	34/10-18	34/10-18
DEPTH	2355.20	2355.40	2355.60	2355.80	2355.90
FMN.	Heather	Heather	Heather	Heather	Heather
SIO2	51.8		50.5	52.0	44.9
AL2O3	15.9		15.2	13.7	14.8
FE2O3	7.65		7.68	10.1	11.1
MGO	1.05		1.03	0.84	0.92
CAO	0.46		0.58	0.44	0.50
NA2O	0.74		0.67	0.62	0.70
K2O	2.31		2.34	2.01	2.37
MNO	0.05		0.02	0.03	0.03
TIO2	0.62		0.52	0.60	0.45
P2O5	0.24		0.28	0.21	0.20
LOI	21.4		22.2	23.3	22.8
S	0.96?	6.52	5.10	6.48	7.22
C-ORG	0.59?	7.30	6.22	7.62	7.71
C-MIN	0.29?	0.03	2.54	0.00	0.04
SUM	102.22		101.02	103.85	98.77
AG	8		2	0	4
CD	0		5	17	27
CO	170		22	17	15
CR	75		157	163	134
CU	249		100	94	127
LI	1		48	52	47
MO			15		34
NB			22		21
NI	78		94	85	129
PB			24		25
RB			86		78
SC	?		11	8	9
SR			139		117
TH			17		20
U			13		13
V	85		752	661	678
Y			57		45
ZN	15		184	840	1037
ZR			114		99
QUARTZ	20.21	19.17	19.81	20.36	16.24
KSPAR	3.76	3.53	4.55	3.73	4.08
PLAG	2.55	2.12	3.43	2.03	2.40
MUSC.	0.14	0.00	0.00	0.00	0.00
BIOTITE	0.00	0.00	0.00	0.00	0.00
CHLORITE	0.34	0.02	0.34	0.25	0.10
SMECTITE	11.38	10.26	9.51	9.36	8.61
ILLITE	23.20	22.76	23.09	18.20	20.58
KAOL.	14.64	13.16	13.04	12.25	12.54
CALCITE	0.48	1.45	1.28	1.37	1.02
DOLOMITE	1.73	2.66	2.82	2.08	2.67
SIDERITE	0.86	1.12	1.38	1.65	1.20
PYRITE	15.13	19.19	16.08	24.98	26.64
AMORPH.	6.12	5.50	5.40	4.80	4.88
SUM	100.09	100.04	100.10	100.70	100.30

WELL	34/10-18	34/10-18	34/10-18	34/10-18	34/10-18
DEPTH	2361.00	2361.30	2361.70	2361.90	2362.50
FMN.	Heather	Heather	Heather	Heather	Heather
SIO2	51.7	48.0	53.2	53.5	49.5
AL2O3	22.1	18.8	19.9	22.1	21.3
FE2O3	6.93	8.64	6.16	6.13	8.01
MGO	1.31	1.17	1.36	1.19	1.18
CAO	0.42	0.68	0.70	0.36	0.46
NA2O	0.80	0.72	0.88	0.70	0.78
K2O	2.99	2.81	2.91	2.83	2.92
MNO	0.04	0.03	0.03	0.02	0.02
TIO2	0.81	0.79	0.79	0.89	0.89
P2O5	0.22	0.31	0.37	0.17	0.26
LOI	11.9	16.9	14.2	12.6	13.6
S	2.27	4.72	2.23	2.45	3.55
C-ORG	2.64	5.05	4.46	3.09	2.90
C-MIN	0.11	0.00	0.12	0.00	0.00
SUM	99.22	98.85	100.50	100.49	98.92
AG	0	0	0	1	0
CD	0	0	0	0	0
CO	22	20	17	26	23
CR	136	126	113	142	147
CU	47	44	33	49	50
LI	169	134	141	164	168
MO	5	4	4	7	6
NB	20	18	20	22	20
NI	111	106	77	105	120
PB	29	36	25	33	35
RB	118	99	110	116	111
SC	17	12	12	14	17
SR	370	222	253	242	428
TH	23	21	21	26	22
U	4	5	4	6	4
V	238	258	261	265	281
Y	48	38	44	42	44
ZN	225	131	138	122	167
ZR	176	169	187	185	164
QUARTZ	16.92	14.64	19.65	18.78	18.34
KSPAR	6.71	6.37	7.68	6.07	5.14
PLAG	2.49	4.13	2.78	2.94	0.74
MUSC.	0.89	0.39	0.84	0.76	0.33
BIOTITE	0.00	0.25	0.00	0.00	0.00
CHLORITE	2.09	1.50	1.58	1.73	0.08
SMECTITE	8.18	9.62	7.78	6.90	7.55
ILLITE	25.31	21.96	24.52	24.12	29.52
KAOL.	21.30	16.39	17.35	21.48	18.96
CALCITE	0.00	0.69	0.60	0.48	1.38
DOLOMITE	1.35	1.43	2.30	1.08	4.71
SIDERITE	1.64	1.55	1.17	0.93	0.13
PYRITE	6.01	15.56	7.75	6.23	6.47
AMORPH.	6.87	5.95	5.96	6.65	6.28
SUM	99.25	100.43	99.77	97.99	98.14

WELL	34/10-18	34/10-18	34/10-18	34/10-18	34/10-18
DEPTH	2363.00	2363.20	2364.00	2364.30	2364.85
FMN.	Heather	Heather	Heather	Heather	Heather
SIO2	52.3	52.2	55.8	54.8	52.4
AL2O3	21.0	23.5	20.0	18.94	20.6
FE2O3	6.31	6.87	6.88	6.50	7.43
MGO	1.26	1.62	1.34	1.26	1.38
CAO	0.44	0.85	0.70	0.52	0.60
NA2O	0.82	1.58	0.80	0.88	0.82
K2O	3.01	3.07	3.18	3.12	3.12
MNO	0.03	0.05	0.07	0.04	0.04
TIO2	0.86	0.85	0.78	0.73	0.83
P2O5	0.18	0.34	0.36	0.19	0.25
LOI	13.9	11.9	11.5	11.9	12.9
S	2.27	2.00	2.58	2.39	3.38
C-ORG	3.49	3.06	2.31	2.46	2.60
C-MIN	0.65	0.12	0.01	0.05	0.04
SUM	100.11	102.83	101.41	98.88	100.37
AG	0	0	0	0	0
CD	0	0	0	0	0
CO	21	23	19	17	19
CR	144	144	158	144	171
CU	46	50	35	35	49
LI	146	156	131	120	154
MO	5	5	4	4	
NB	21	21	20	18	
NI	93	102	81	71	85
PB	27	27	29	26	
RB	111	118	120	118	
SC	19	11	11	9	10
SR	215	299	148	129	
TH	24	25	20	20	
U	5	4	6	6	
V	242	288	215	188	188
Y	40	58	48	30	
ZN	190	151	152	111	155
ZR	166	160	171	182	
QUARTZ	21.42	18.85	26.23	28.87	22.03
KSPAR	5.38	6.18	6.73	6.80	5.54
PLAG	1.55	1.63	1.32	2.50	1.08
MUSC.	0.07	0.53	0.36	0.79	0.29
BIOTITE	0.00	0.00	0.00	0.00	0.00
CHLORITE	0.02	0.67	0.00	0.34	0.00
SMECTITE	7.16	6.61	5.78	6.23	6.68
ILLITE	31.07	31.11	30.05	25.78	30.66
KAOL.	19.08	20.65	14.98	14.33	16.43
CALCITE	0.62	0.43	1.34	2.08	1.32
DOLOMITE	5.15	4.28	4.73	3.83	5.34
SIDERITE	0.18	0.50	0.21	0.45	0.07
PYRITE	1.68	1.50	2.45	2.77	4.76
AMORPH.	6.28	6.50	5.29	5.08	5.69
SUM	97.85	97.93	97.71	98.61	97.98

WELL	34/10-18	34/10-18	34/10-18	34/10-18	34/10-18
DEPTH	2365.50	2365.90	2366.30	2366.80	2367.00
FMN.	Heather	Heather	Heather	Heather	Heather
SIO2	52.4	51.1	52.5	46.7	39.6
AL2O3	19.4	17.9	18.3	18.5	14.4
FE2O3	7.65	11.4	8.37	10.8	12.00
MGO	1.31	1.07	1.31	1.35	0.79
CAO	0.72	0.59	0.42	0.74	0.26
NA2O	0.82	0.83	0.78	0.78	0.95
K2O	3.25	3.03	3.19	3.26	2.16
MNO	0.09	0.08	0.17	0.07	0.04
TIO2	0.71	0.76	0.70	0.61	0.63
P2O5	0.37	0.31	0.17	0.34	0.10
LOI	12.6	14.8	13.4	15.0	29.3
S	3.61	6.51	4.40	5.66	8.55
C-ORG	1.97	2.03	2.49	2.08	7.51
C-MIN	0.40	0.02	0.00	0.00	0.34
SUM	99.32	101.87	99.31	98.15	100.23
AG	0	0	0	0	0
CD	0	0	0	0	12
CO	19	17	19	27	45
CR	122	154	114	120	169
CU	38	38	34	54	107
LI	125	126	120	92	87
MO	4	4	5	5	56
NB	19	18	18	19	22
NI	80	83	80	112	261
PB	29	26	25	25	30
RB	117	109	114	117	66
SC	14	9	8	13	8
SR	150	137	126	173	55
TH	19	18	20	17	11
U	3	4	5	7	9
V	195	210	180	291	371
Y	48	38	31	60	24
ZN	163	138	137	89	1120
ZR	161	149	160	112	107
QUARTZ	19.90	20.70	20.75	14.04	15.33
KSPAR	5.64	4.01	6.20	3.98	3.65
PLAG	1.29	1.18	2.18	1.19	1.97
MUSC.	0.06	0.32	0.45	0.00	0.00
BIOTITE	0.00	0.00	0.00	0.00	0.00
CHLORITE	0.00	0.00	0.23	0.00	0.00
SMECTITE	7.98	6.30	6.78	10.40	7.89
ILLITE	30.07	28.51	28.45	33.90	24.53
KAOL.	14.81	12.47	13.98	13.83	11.74
CALCITE	1.28	2.04	1.75	1.76	1.72
DOLOMITE	4.28	5.55	4.80	5.62	5.47
SIDERITE	0.63	0.20	0.57	0.14	1.07
PYRITE	8.41	14.36	8.86	10.41	24.44
AMORPH.	5.65	4.75	5.12	6.23	4.80
SUM	98.44	98.21	98.93	98.36	99.32

WELL	34/10-18	34/10-18	34/10-18	34/10-18
DEPTH	2367.40	2367.60	2367.90	2368.00
FMN.	Heather	Heather	Heather	Heather
SIO2	20.7	48.2		
AL2O3	7.66	15.5		
FE2O3	28.9	9.10		
MGO	0.52	0.98		
CAO	0.16	0.52		
NA2O	0.38	0.74		
K2O	1.30	2.75		
MNO	0.06	0.03		
TIO2	0.20	0.51		
P2O5	0.07	0.26		
LOI	30.1	20.8		
S	24.2	6.27		
C-ORG	1.26	6.22		
C-MIN	0.46	0.76		
SUM	90.05	99.39		
AG	1	2		
CD	0	9		
CO	20	20		
CR	90	140		
CU	19	89		
LI	32	51		
MO	10	15		
NB	9	30		
NI	69	96		
PB	16	25		
RB	39	88		
SC	5	13		
SR	53	125		
TH	10	18		
U	0	13		
V	65	661		
Y	11	49		
ZN	80	562		
ZR	41	124		
QUARTZ	9.73	23.13	12.91	18.82
KSPAR	0.67	4.28	7.43	6.96
PLAG	0.57	1.12	4.98	4.16
MUSC.	0.00	0.00	0.00	0.00
BIOTITE	0.00	0.00	0.00	0.00
CHLORITE	0.00	0.00	0.00	0.23
SMECTITE	3.20	7.15	10.64	10.40
ILLITE	20.55	26.39	26.02	21.64
KAOL.	7.14	11.89	10.67	11.01
CALCITE	1.89	2.35	1.44	1.37
DOLOMITE	7.49	5.39	5.19	4.13
SIDERITE	0.00	0.79	2.30	2.25
PYRITE	49.05	14.15	15.32	15.78
AMORPH.	2.50	4.63	5.25	5.13
SUM	98.27	98.78	99.95	100.32

WELL	Nth Wootton	Nth Wootton	Nth Wootton	Nth Wootton	Hartwell
DEPTH	29.70	60.30	66.30	98.10	34.75
SIO2	33.7	45.4	46.1	38.4	56.2
AL2O3	12.1	15.1	15.4	15.2	19.5
FE2O3	4.42	10.1	4.98	4.99	6.49
MGO	1.22	1.72	1.84	2.44	1.69
CAO	22.7	4.63	10.4	15.5	3.86
NA2O	0.40	0.77	0.68	0.56	1.11
K2O	1.92	2.67	2.66	2.80	3.16
MNO	0.02	0.02	0.02	0.04	0.03
TIO2	0.54	0.48	0.60	0.63	0.73
P2O5	0.19	0.17	0.15	0.07	0.18
LOI	21.3	15.8	16.2	16.6	9.52
S	1.42	5.99	1.74	1.18	1.31
C-ORG	1.34	4.53	3.71	0.76	1.25
C-MIN	4.83	0.78	2.79	3.75	0.67
SUM	98.51	96.86	99.03	97.23	102.47
AG	3	2	2	2	1
CD	0	0	0	0	0
CO	10	15	13	15	22
CR	90	153	123	118	151
CU	23	43	36	29	27
LI	65	84	96	75	121
MO	4	11	10	2	4
NB	15	16	17	16	25
NI	42	102	64	61	59
PB	14	19	16	22	28
RB	109	147	161	141	186
SC	9	8	8	15	8
SR	318	231	375	424	342
TH	10	15	13	13	17
U	7	5	8	7	3
V	95	135	165	173	169
Y	23	25	27	22	30
ZN	60	134	71	87	89
ZR	97	122	127	108	160

WELL	Hartwell	Hartwell	Hartwell	Hartwell	Marton
DEPTH	48.25	50.75	60.68	62.25	20.85
SIO2	47.8	56.3	31.9	48.9	33.1
AL2O3	15.0	17.1	12.1	17.4	13.0
FE2O3	6.48	4.98	4.01	5.52	4.68
MGO	1.29	1.43	2.34	2.86	2.32
CAO	7.25	5.34	22.7	5.14	19.0
NA2O	0.77	1.71	0.52	0.77	0.38
K2O	2.50	2.77	2.18	3.91	1.79
MNO	0.02	0.02	0.04	0.04	0.03
TIO2	0.56	0.59	0.50	0.64	0.53
P2O5	0.17	0.28	0.08	0.11	0.48
LOI	12.0	14.8	22.1	12.9	22.0
S	2.02	1.87	1.00	1.27	0.79
C-ORG	3.32	6.14	0.31	3.38	2.55
C-MIN	1.49	1.14	5.65	1.63	4.93
SUM	93.84	105.32	98.47	98.19	97.31
AG	2	1	1	1	2
CD	1	0	0	0	0
CO	10	14	11	12	8
CR	112	135	82	124	98
CU	29	45	21	37	33
LI	90	102	55	89	57
MO	14	13	3	7	4
NB	19	10	13	19	15
NI	49	61	32	57	45
PB	19	21	13	20	13
RB	145	160	109	200	104
SC	11	11	13	14	19
SR	438	322	521	330	213
TH	15	15	12	15	11
U	7	5	4	4	5
V	113	144	130	150	119
Y	30	28	18	27	30
ZN	103	79	47	93	80
ZR	175	161	89	143	87

WELL	Marton	Marton	Marton	Don. on Bain	Don. on Bain
DEPTH	122.30	132.15	139.29	38.00	86.25
SIO2	40.2	36.3	43.2	40.8	43.6
AL2O3	16.7	13.9	14.2	13.7	16.3
FE2O3	11.4	6.25	7.50	4.63	6.14
MGO	2.90	1.17	1.08	2.02	1.30
CAO	4.28	14.4	6.04	17.2	8.79
NA2O	1.08	1.43	1.44	0.38	0.58
K2O	1.42	1.29	2.20	2.30	2.15
MNO	0.04	0.02	0.02	0.03	0.02
TIO2	0.55	0.46	0.43	0.63	0.51
P2O5	0.18	0.27	0.19	0.20	0.18
LOI	18.1	23.4	23.8	18.5	16.4
S	1.91	2.98	5.52	1.27	3.06
C-ORG	6.15	10.1	15.2	1.00	6.23
C-MIN	2.91	3.60	2.10	4.01	1.90
SUM	96.85	98.89	100.1	100.39	95.97
AG	2	3	1	1	1
CD	0	7	13	0	0
CO	14	15	37	15	16
CR	130	100	100	100	149
CU	55	73	143	25	50
LI	74	49	61	62	71
MO	10	69	182	3	21
NB	19	14	16	17	19
NI	69	98	259	20	133
PB	24	24	53	19	23
RB	94	78	122	131	137
SC	15	13	10	13	11
SR	231	268	201	501	333
TH	15	11	14	13	14
U	5	13	13	5	7
V	164	165	860	113	150
Y	27	30	27	25	27
ZN	114	430	460	68	120
ZR	108	85	113	115	128

WELL	Don. on Bain	Don. on Bain	Don. on Bain	Reighton	Reighton
DEPTH	94.75	113.75	154.75	116.43	124.75
SIO2	36.9	49.3	39.4	46.1	53.8
AL2O3	15.1	18.1	12.9	17.3	19.3
FE2O3	4.60	4.76	15.4	6.50	4.78
MGO	1.56	1.44	3.43	1.19	1.59
CAO	16.0	8.83	9.84	7.67	4.01
NA2O	0.63	1.05	0.92	1.35	0.81
K2O	2.31	2.51	2.23	2.08	2.86
MNO	0.02	0.02	0.09	0.02	0.02
TIO2	0.62	0.69	0.51	0.54	0.75
P2O5	0.08	0.09	0.09	0.15	0.09
LOI	17.1	12.9	17.3	15.4	11.0
S	1.44	1.33	1.77	3.29	1.22
C-ORG	1.80	2.88	1.49	7.08	2.32
C-MIN	3.70	1.83	4.49	1.77	0.95
SUM	94.92	99.69	102.11	98.30	99.01
AG	2	2	1	2	1
CD	0	0	0	0	0
CO	11	14	11	17	14
CR	106	134	97	125	141
CU	27	39	24	71	38
LI	81	104	60	74	92
MO	5	7	5	40	5
NB	15	21	15	26	24
NI	51	60	54	85	62
PB	17	20	18	27	24
RB	150	168	123	133	190
SC	9	8	10	6	10
SR	500	373	363	312	311
TH	11	16	10	15	17
U	3	6	6	11	6
V	135	166	133	171	156
Y	23	29	28	27	31
ZN	139	77	78	74	239
ZR	109	149	105	135	180

WELL	Reighton	Tisbury	Tisbury	Tisbury	Tisbury
DEPTH	152.50	142.50	228.00	237.50	268.75
SIO2	50.9	41.9	52.6	40.2	53.9
AL2O3	19.7	15.6	17.8	16.7	13.6
FE2O3	5.35	5.77	5.63	4.41	4.47
MGO	1.86	1.23	1.38	1.34	1.25
CAO	2.08	10.7	6.45	9.34	9.47
NA2O	0.99	0.50	1.58	0.68	1.05
K2O	3.39	2.26	2.86	2.63	2.46
MNO	0.02	0.02	0.03	0.02	0.02
TIO2	0.74	0.59	0.61	0.53	0.66
P2O5	0.12	0.16	0.13	0.17	0.15
LOI	12.1	17.8	14.3	19.8	12.6
S	1.42	2.02	1.47	1.75	1.17
C-ORG	5.00	5.88	4.86	7.89	3.28
C-MIN	0.45	2.58	1.46	2.01	2.01
SUM	97.25	96.53	103.37	95.82	99.63
AG	1	2	2	1	1
CD	0	0	0	0	5
CO	16	12	12	17	10
CR	156	115	129	113	111
CU	61	36	40	58	36
LI	97	84	96	91	75
MO	7	20	11	12	9
NB	22	19	20	16	19
NI	88	58	62	65	48
PB	27	24	19	21	16
RB	218	140	169	166	144
SC	9	9	11	15	15
SR	269	292	341	388	434
TH	16	13	15	12	14
U	8	6	6	3	4
V	213	148	160	186	115
Y	32	23	29	32	32
ZN	104	61	74	194	770
ZR	161	121	147	109	204

WELL	Kimm. Bay	Kimm. Bay	Nth Runcton	Nth Runcton	Nth Runcton
DEPTH	59.25	64.75	17.50	45.25	51.50
SIO2	60.7	55.1	40.5	55.9	48.1
AL2O3	19.8	18.4	13.3	18.8	18.6
FE2O3	4.25	4.66	4.45	5.41	5.04
MGO	0.97	1.33	1.31	1.93	1.87
CAO	0.83	4.66	20.2	5.07	5.68
NA2O	1.49	1.47	0.95	1.11	0.64
K2O	2.92	2.97	2.42	3.60	3.20
MNO	0.02	0.02	0.03	0.03	0.02
TIO2	0.78	0.65	0.58	0.67	0.54
P2O5	0.11	0.17	0.23	0.12	0.11
LOI	13.6	13.3	19.3	10.5	15.1
S	1.51	1.30	1.30	1.85	2.16
C-ORG	5.98	5.52	1.53	2.27	5.76
C-MIN	0.06	1.29	4.03	0.67	1.24
SUM	105.47	102.73	103.27	103.14	98.9
AG	0	0	1	1	1
CD	0	0	0	0	0
CO	14	11	8	14	13
CR	157	143	97	144	144
CU	49	37	22	33	48
LI	69	97	73	107	120
MO	14	6	4	6	5
NB	25	20	16	20	20
NI	67	58	35	59	73
PB	25	18	16	20	21
RB	190	189	123	194	193
SC	16	14	10	10	9
SR	157	209	324	273	276
TH	17	15	10	17	15
U	5	4	3	8	3
V	151	131	88	155	166
Y	28	31	23	26	27
ZN	96	50	58	83	91
ZR	181	161	104	158	161

WELL	Nth Runcton	Nth Runcton	Denver Sluice	Denver Sluice	Denver Sluice
DEPTH	73.75	87.50	16.70	19.30	34.20
SIO2	43.6	54.3	50.6	29.5	48.3
AL2O3	14.6	18.9	18.0	9.18	13.1
FE2O3	4.40	5.36	5.09	8.74	3.47
MGO	1.96	2.70	1.86	0.97	1.84
CAO	15.8	3.50	2.84	22.0	14.9
NA2O	1.39	1.23	0.46	1.40	1.07
K2O	2.91	4.05	3.30	1.86	2.61
MNO	0.03	0.03	0.03	0.03	0.02
TIO2	0.61	0.71	0.53	0.26	0.60
P2O5	0.13	0.10	0.18	0.30	0.13
LOI	16.9	10.4	16.2	19.3	16.8
S	0.72	0.84	2.43	5.44	0.61
C-ORG	1.37	3.72	7.33	7.22	2.36
C-MIN	3.73	0.64	0.63	4.88	3.37
SUM	102.33	101.27	99.09	93.54	102.84
AG	1	1	1	1	1
CD	0	0	2	0	1
CO	10	14	16	8	11
CR	118	159	126	80	112
CU	27	40	61	37	27
LI	80	105	120	56	78
MO	4	7	27	10	6
NB	17	21	17	10	16
NI	42	66	80	50	42
PB	16	17	31	12	15
RB	160	226	187	86	141
SC	13	8	5	6	8
SR	399	270	241	380	354
TH	13	17	16	10	13
U	5	5	5	6	8
V	109	146	154	64	119
Y	21	28	29	30	24
ZN	68	126	102	600	69
ZR	131	153	135	63	168

WELL	Denver Sluice	W. Lavington	W. Lavington	W. Lavington	W. Lavington
DEPTH	43.40	153.25	159.50	185.75	197.50
SIO2	43.7	51.5	52.5	38.0	45.3
AL2O3	13.9	15.0	19.3	12.8	16.9
FE2O3	3.91	7.42	5.35	3.69	5.18
MGO	2.26	1.30	1.65	1.17	1.85
CAO	15.9	9.33	4.62	18.1	8.73
NA2O	0.83	2.11	0.77	0.67	0.70
K2O	2.82	2.71	3.07	2.14	3.21
MNO	0.03	0.03	0.02	0.02	0.02
TIO2	0.63	0.44	0.65	0.53	0.54
P2O5	0.07	0.17	0.13	0.19	0.10
LOI	16.6	13.0	11.4	21.3	14.9
S	0.57	2.82	1.51	0.74	1.30
C-ORG	1.28	6.09	3.79	3.77	4.11
C-MIN	3.65	1.30	1.04	4.22	2.01
SUM	100.65	103.01	99.46	98.61	97.43
AG	1	1	0	1	1
CD	0	0	0	0	0
CO	9	26	13	8	12
CR	112	166	146	105	107
CU	26	43	38	34	40
LI	77	74	112	68	76
MO	3	26	11	6	8
NB	16	19	21	14	17
NI	42	309	60	46	61
PB	13	25	19	14	21
RB	146	144	196	133	185
SC	9	9	9	11	9
SR	447	349	348	433	365
TH	13	15	16	9	14
U	5	6	8	9	6
V	121	115	163	119	115
Y	21	28	27	28	26
ZN	76	87	79	70	69
ZR	133	157	153	122	124

WELL	Portesham	Portesham	Portesham	Portesham	Swindon
DEPTH	35.00	134.49	144.49	203.00	77.25
SIO2	50.5	59.5	55.4	53.4	40.8
AL2O3	15.8	15.4	18.5	13.6	10.3
FE2O3	5.10	5.19	5.42	4.24	16.5
MGO	1.42	1.10	1.08	1.12	0.93
CAO	9.38	7.91	3.15	10.0	8.38
NA2O	1.11	1.24	1.56	1.31	1.25
K2O	3.17	2.20	2.93	2.15	1.87
MNO	0.03	0.02	0.02	0.02	0.05
TIO2	0.62	0.53	0.64	0.64	0.40
P2O5	0.17	0.19	0.14	0.14	0.19
LOI	14.7	16.9	13.5	14.3	17.1
S	1.55	2.12	2.27	0.77	8.85
C-ORG	4.49	7.20	5.78	2.16	2.42
C-MIN	1.69	1.51	0.46	2.77	0.84
SUM	102.00	110.18	102.34	100.92	97.77
AG	1	1	1	1	1
CD	0	0	0	0	0
CO	12	12	12	10	48
CR	127	111	127	103	247
CU	33	41	42	26	32
LI	80	86	88	74	50
MO	5	16	14	7	43
NB	20	20	20	19	15
NI	49	64	56	39	727
PB	19	23	23	13	21
RB	165	146	178	131	91
SC	9	8	9	8	9
SR	320	366	243	264	261
TH	13	15	17	13	12
U	5	7	4	5	7
V	101	104	150	100	71
Y	25	29	29	29	25
ZN	78	54	60	43	284
ZR	144	144	165	206	159

WELL	Swindon	Swindon	Encombe	Warlingham	Warlingham
DEPTH	81.35	89.75	106.00	745.45	829.06
SIO2	46.0	39.5	38.4	10.1	53.3
AL2O3	16.5	12.2	11.9	2.86	19.4
FE2O3	5.50	3.85	4.35	1.18	5.33
MGO	1.69	1.34	1.89	2.64	2.14
CAO	10.1	18.0	18.5	42.6	2.63
NA2O	1.57	0.71	0.74	0.44	0.88
K2O	2.93	2.13	2.17	0.60	3.69
MNO	0.02	0.02	0.02	0.02	0.03
TIO2	0.54	0.55	0.57	0.17	0.68
P2O5	0.16	0.10	0.23	0.15	0.16
LOI	18.2	20.3	20.3	37.3	11.6
S	1.63	0.83	0.58	0.28	1.37
C-ORG	6.87	3.36	1.46	0.52	4.41
C-MIN	2.02	4.08	4.53	10.6	0.71
SUM	103.21	98.7	99.07	98.06	99.84
AG	1	2	2	2	1
CD	0	0	0	0	0
CO	13	11	7	5	11
CR	129	94	97	27	151
CU	47	34	21	10	31
LI	94	65	53	14	120
MO	17	8	3	1	8
NB	16	15	15	5	20
NI	67	41	35	12	65
PB	20	16	13	4	23
RB	170	129	127	27	214
SC	8	11	10	6	8
SR	437	577	400	546	218
TH	14	11	10	2	15
U	10	5	3	0	6
V	150	109	101	31	155
Y	26	21	22	9	30
ZN	94	52	53	20	75
ZR	115	121	114	27	149

WELL	Warlingham	Warlingham
DEPTH	832.10	905.56
SIO2	51.8	50.7
AL2O3	19.8	11.4
FE2O3	5.47	6.24
MGO	1.91	4.63
CAO	2.17	12.2
NA2O	0.80	1.53
K2O	3.40	3.10
MNO	0.03	0.05
TIO2	0.65	0.60
P2O5	0.09	0.13
LOI	13.6	12.9
S	1.97	1.50
C-ORG	5.40	0.66
C-MIN	0.05	3.50
SUM	99.72	103.48
AG	1	2
CD	0	0
CO	13	9
CR	24	90
CU	40	17
LI	109	41
MO	7	4
NB	19	15
NI	67	38
PB	27	36
RB	183	118
SC	6	5
SR	188	211
TH	17	11
U	4	3
V	158	85
Y	23	22
ZN	69	49
ZR	143	175

Clay Mineral Results

Well	30/7-7	30/7-7
Depth	3895-3902	3895-3902(2)
Formation	Draupne	Draupne
%Illite	29.6	42.3
%I-S	53.5	43.6
%Kaolinite	16.9	14.1
%Chlorite	-	-
%I in I-S	>65	>65

Well	30/9-1	30/9-1
Depth	2497-2529	2527-2529(2)
Formation	Heather	Heather
%Illite	15.9	17.5
%I-S	44.6	40.3
%Kaolinite	36.3	34.1
%Chlorite	3.2	8.1
%I in I-S	48	48

Well	30/9-1	30/9-1
Depth	2646-2680	2646-2680(2)
Formation	Heather	Heather
%Illite	37.4	41.8
%I-S	23.0	16.1
%Kaolinite	31.4	37.9
%Chlorite	8.1	4.3
%I in I-S	>65	80

Well	31/3-2	31/3-2
Depth	1545	1545(2)
Formation	Draupne	Draupne
%Illite	43.5	49.9
%I-S	27.0	14.7
%Kaolinite	24.8	31.1
%Chlorite	4.7	4.3
%I in I-S	>65	>65

Well	31/4-5	31/4-5
Depth	2065.2	2065.2(2)
Formation	Draupne	Draupne
%Illite	36.0	33.6
%I-S	52.9	55.9
%Kaolinite	11.0	10.5
%Chlorite	-	-
%I in I-S	63	59

Well	31/4-6	31/4-6
Depth	2132.2	2132.2(2)
Formation	Draupne	Draupne
%Illite	30.7	30.8
%I-S	53.0	55.3
%Kaolinite	7.8	7.6
%Chlorite	8.5	6.4
%I in I-S	60	65

Well	31/4-9	31/4-9
Depth	2211.50	2114.10
Formation	Draupne	Draupne
%Illite	37.8	39.1
%I-S	44.8	40.2
%Kaolinite	12.4	14.1
%Chlorite	5.0	6.6
%I in I-S	65	54

Well	31/4-9	31/4-9
Depth	2114.50	2114.80
Formation	Draupne	Draupne
%Illite	31.2	40.4
%I-S	46.5	27.6
%Kaolinite	13.0	19.3
%Chlorite	9.3	12.7
%I in I-S	65	-

Well	31/4-9	31/4-9
Depth	2145.60	2155.40
Formation	Heather	Heather
%Illite	12.9	30.1
%I-S	36.7	17.3
%Kaolinite	40.5	37.2
%Chlorite	9.9	15.5
%I in I-S	-	-

Well	31/4-9	31/6-1
Depth	2155.40(2)	1324-1326(2)
Formation	Heather	Draupne
%Illite	24.1	34.1
%I-S	25.8	47.2
%Kaolinite	38.5	11.4
%Chlorite	11.6	7.3
%I in I-S	-	58

Well	31/6-1	31/6-3
Depth	1340-1346	1395
Formation	Heather	Draupne
%Illite	33.2	38.2
%I-S	20.4	37.8
%Kaolinite	46.4	15.5
%Chlorite	-	8.4
%I in I-S	-	57

Well	31/6-3	31/6-3
Depth	1395(2)	1478
Formation	Draupne	Draupne
%Illite	40.5	35.6
%I-S	37.4	43.9
%Kaolinite	13.8	13.8
%Chlorite	8.3	6.7
%I in I-S	59	49

Well	31/6-3	31/6-3
Depth	1478(2)	1506.15
Formation	Draupne	Heather
%Illite	42.2	27.7
%I-S	33.2	27.0
%Kaolinite	15.4	30.8
%Chlorite	9.2	14.6
%I in I-S	59	80

Well	34/10-18	34/10-18
Depth	2351.65	2354.10
Formation	Draupne	Draupne
%Illite	35.7	22.8
%I-S	37.2	68.4
%Kaolinite	23.3	8.8
%Chlorite	3.9	-
%I in I-S	>65	43

Well	34/10-18	34/10-18
Depth	2354.10(2)	2354.90
Formation	Draupne	Draupne
%Illite	18.8	19.9
%I-S	71.2	70.7
%Kaolinite	10.0	9.4
%Chlorite	-	-
%I in I-S	45	43

Well	34/10-18	34/10-18
Depth	2354.90(2)	2355.60
Formation	Draupne	Heather
%Illite	25.9	23.6
%I-S	65.3	42.5
%Kaolinite	8.9	34.0
%Chlorite	-	-
%I in I-S	42	-

Well	34/10-18	34/10-18
Depth	2361.30	2361.30(2)
Formation	Heather	Heather
%Illite	30.4	28.2
%I-S	28.8	23.7
%Kaolinite	40.8	40.7
%Chlorite	-	7.4
%I in I-S	-	-

Well	34/10-18	34/10-18
Depth	2364.30	2367.60
Formation	Heather	Heather
%Illite	29.9	26.8
%I-S	32.8	39.3
%Kaolinite	37.3	33.9
%Chlorite	-	-
%I in I-S	-	-

Appendix C

Organic Geochemical Results

The bulk of the maturity data (R_o, SCI, and T_{max}) used in this study were not determined as a part of this project. In order to ensure the validity of these data T_{max} and SCI versus depth plots were compared with those produced for Viking Group sediments in a large study by Brosse and Huc (1986). In both cases the data used in here were found to be representative of the trends found by these authors. A plot of R_o versus depth for the Viking Group sediments was compared with a similar plot from drawn from Brosse and Huc (1986) for the Brent Group coals (Viking Group data were not supplied by the authors) again showing a good agreement. The precision of the three maturity indices used is estimated to be: R_o +/- 10%; SCI +/-1 unit (both JM Jones, personal communication); T_{max} +/-7°C (Espitalie, 1986).

WELL	30/6-9	30/6-14	30/6-14	30/6-14	30/6-14
DEPTH	2448.00	2300.00	2315.90	2322.00	2325.20
RO	0.52			0.47	
SCI					
TMAX	432	421	417	421	417
S1	0.35	0.49	0.76	0.62	0.75
S2	2.28	18.68	33.92	21.19	28.59
S3	1.41	1.36	1.33	1.14	1.97
HI	62	346	399	303	318
OI	38.1	25.2	15.6	16.3	21.9

WELL	30/6-14	30/6-14	30/6-14	30/7-7	30/7-7
DEPTH	2331.00	2350.00	2394.00	3895.00	3899.00
RO					
SCI					
TMAX	412	425	424	433	430
S1	0.81	0.09	0.27	2.60	1.20
S2	15.41	0.71	4.65	4.50	1.60
S3	1.11	1.27	0.72	0.60	1.00
HI	241	51	99	76	40
OI	17.3	90.7	15.3	10.1	24.9

WELL	30/7-7	30/7-7	30/7-7	30/7-7	30/7-7
DEPTH	3902.00	3910.00	3928.00	3945.00	3985.00
RO		0.77			
SCI	7.50		8.00		
TMAX	429	438	441	448	452
S1	1.20	0.05	3.20	0.09	0.300
S2	3.5	1.3	3.3	1.6	0.1
S3	1.4	1.0	1.9	1.0	1.5
HI	54	41	72	64	25
OI	21.6	31.3	40.5	40.0	375.0

WELL	30/7-7	30/7-7	30/7-7	30/7-7	30/7-7
DEPTH	3990.00	4035.00	4070.00	4080.00	4145.00
RO			0.92		
SCI					
TMAX	451	453	455	454	457
S1	0.6	1.1	1.4	0.9	2.7
S2	0.6	2.0	2.0	1.6	2.1
S3	2.6	0.6	2.5	0.6	1.1
HI	55	61	54	52	52
OI	236.4	18.2	67.6	19.4	28.1

WELL	30/7-7	30/7-7	30/7-7	30/7-7	30/7-7
DEPTH	4165.00	4167.00	4205.00	4230.00	4275.00
RO					
SCI					
TMAX	465	462	458	458	458
S1	1.1	1.3	0.6	1.3	0.7
S2	0.9	1.4	0.6	0.8	0.7
S3	0.9	1.1	0.7	0.8	0.2
HI	39	45	43	44	41
OI	39.1	35.5	50.0	44.4	11.8

WELL	30/7-7	30/7-7	30/7-7	30/7-7	30/7-7
DEPTH	4285.00	4302.00	4305.00	4330.00	4381.00
RO					1.08
SCI					
TMAX	452	470	459	459	478
S1	0.5	0.4	0.5	0.5	0.6
S2	0.6	0.7	0.8	0.9	0.9
S3	0.6	0.9	0.6	0.4	1.6
HI	38	33	38	35	39
OI	37.5	42.9	28.6	15.4	69.6

WELL	30/7-7	30/7-7	30/7-7	30/7-7	30/7-7
DEPTH	4450.00	4500.00	4515.00	4530.00	4720.00
RO					
SCI					
TMAX	461	519	479	491	550
S1	0.3	0.1	0.5	0.3	0.7
S2	0.6	0.2	0.4	0.3	0.4
S3	0.1	2.0	1.2	0.2	0.7
HI	21	67			
OI	3.6	666.7			

WELL	30/7-7	30/9-1	30/9-1	30/9-1	30/9-1
DEPTH	4804.00	2497.00	2529.00	2606.00	2646.00
RO			0.46		
SCI		4.50	4.50	4.50	5.00
TMAX	472	421	438	430	439
S1	1.40	0.18	0.10	0.26	0.10
S2	0.50	1.16	2.14	2.08	1.31
S3	0.60	0.35	1.01	0.23	0.91
HI		61	89	63	45
OI		18.4	47.8	7.0	31.4

WELL	30/9-1	31/3-2	31/3-2	31/3-2	31/4-5
DEPTH	2680.00	1541.20	1545.00	1550.00	2063.40
RO	0.48	0.45			
SCI	6.00	3.50	3.50	3.75	3.50
TMAX	431	427	420	425	412
S1	0.12	0.31	0.69	0.96	0.30
S2	0.81	9.35	7.19	15.63	19.61
S3	0.06	3.45	0.94	1.59	0.80
HI	90	492	288	319	321
OI	6.7	181.6	37.6	32.4	13.1

WELL	31/4-5	31/4-5	31/4-5	31/4-5	31/4-5
DEPTH	2064.30	2064.90	2065.20	2065.50	2066.10
RO			0.40		
SCI	3.50	3.50	3.75	4.00	4.00
TMAX	419	424	422	421	426
S1	0.25	0.15	0.30	0.22	0.16
S2	20.21	21.52	22.77	27.60	31.30
S3	0.62	0.68	0.58	0.76	0.82
HI	343	422	356	690	447
OI	10.5	13.3	9.1	19.0	11.9

WELL	31/4-5	31/4-6	31/4-6	31/4-6	31/4-6
DEPTH	2066.60	2132.20	2132.30	2132.50	2132.70
RO				0.52	
SCI	4.00	4.25	4.25	4.25	4.50
TMAX	427	426	428	424	419
S1	0.16	0.17	0.15	0.17	0.18
S2	25.7	28.63	31.52	29.14	21.71
S3	0.88	1.20	1.23	1.25	1.34
HI	408	427	450	429	381
OI	14.0	17.9	17.6	18.4	23.5

WELL	31/4-9	31/4-9	31/4-9	31/4-9	31/4-9
DEPTH	2105.15	2106.75	2107.15	2109.75	2110.05
RO	0.41				
SCI	4.00				
TMAX	423	423	424	425	426
S1	1.31	1.14	1.06	1.18	0.93
S2	46.07	39.24	37.66	36.34	31.95
S3	1.27	0.80	0.71	0.81	0.95
HI	678	572	549	570	592
OI	18.7	11.7	10.4	12.7	17.6

WELL	31/4-9	31/4-9	31/4-9	31/4-9	31/4-9
DEPTH	2110.60	2111.50	2112.10	2112.90	2113.25
RO					
SCI					
TMAX	510		421	417	421
S1	0.01		1.13	1.37	1.09
S2	0.003		32.98	36.27	30.76
S3	0.41		0.84	0.79	0.69
HI	1		519	533	515
OI	120.6		13.2	11.6	11.6

WELL	31/4-9	31/4-9	31/4-9	31/4-9	31/4-9
DEPTH	2114.00	2114.10	2114.20	2114.20	2114.30
RO					
SCI					
TMAX				420	
S1				1.53	
S2				39.7	
S3				0.86	
HI				548	
OI				11.9	

WELL	31/4-9	31/4-9	31/4-9	31/4-9	31/4-9
DEPTH	2114.40	2114.50	2114.60	2114.70	2114.80
RO					
SCI					
TMAX					
S1					
S2					
S3					
HI					
OI					

WELL	31/4-9	31/4-9	31/4-9	31/4-9	31/4-9
DEPTH	2114.90	2114.90	2116.50	2117.50	2118.60
RO					0.46
SCI					4.00
TMAX		421	417	420	424
S1		1.17	1.45	1.15	1.19
S2		30.78	37.64	31.48	33.44
S3		0.48	0.60	0.73	0.65
HI		505	543	495	538
OI		7.9	8.7	11.5	10.5

WELL	31/4-9	31/4-9	31/4-9	31/4-9	31/4-9
DEPTH	2119.00	2120.00	2120.80	2121.40	2124.50
RO					
SCI					
TMAX	423	423	416	412	415
S1	1.43	1.59	0.95	1.01	0.69
S2	32.33	36.52	10.88	4.02	7.21
S3	0.83	0.76	1.08	0.46	0.42
HI	485	577	316	207	214
OI	12.4	12.0	31.4	23.7	12.5

WELL	31/4-9	31/4-9	31/4-9	31/4-9	31/4-9
DEPTH	2130.50	2137.80	2145.60	2155.40	2158.60
RO	0.44		0.44		0.44
SCI	4.50		4.50		4.50
TMAX	420	419	428	426	431
S1	0.36	0.79	0.16	0.30	0.17
S2	4.82	11.1	3.39	6.54	3.86
S3	0.37	0.56	0.46	0.57	0.45
HI	214	243	158	196	224
OI	16.4	12.3	21.5	17.1	26.2

WELL	31/4-9	31/6-1	31/6-1	31/6-1	31/6-1
DEPTH	2160.40	1324.00	1326.00	1335.00	1337.00
RO					0.51
SCI		4.00	4.00	4.00	4.50
TMAX		424	424	414	422
S1	0.09	0.20	0.26	0.24	0.26
S2	3.33	3.36	5.68	2.91	1.97
S3	0.45	1.58	1.76	1.37	0.53
HI	275	146	210	116	328
OI	37.2	68.7	65.2	54.8	88.3

WELL	31/6-1	31/6-1	31/6-1	31/6-1	31/6-1
DEPTH	1340.00	1343.00	1346.00	1349.50	1350.00
RO					
SCI		4.50			
TMAX	429	402	409	431	423
S1	0.26	0.23	0.30	0.05	0.14
S2	1.90	1.34	1.09	0.37	0.79
S3	0.33	0.58	0.58	7.11	4.80
HI	211	112	73	74	29
OI	36.7	48.3	38.7	1422	177.8

WELL	31/6-3	31/6-3	31/6-3	31/6-3	31/6-3
DEPTH	1385.00	1395.00	1405.00	1415.00	1478.00
RO			0.44		
SCI	3.00	3.75	3.75	3.75	4.00
TMAX	428	431	428	430	429
S1	0.23	0.06	0.18	0.22	0.24
S2	7.07	2.49	2.36	4.57	3.65
S3	0.81	0.66	2.36	1.58	1.45
HI	228	131	131	183	159
OI	26.1	34.7	131.1	63.2	63.0

WELL	31/6-3	31/6-3	31/6-3	31/6-3	31/6-3
DEPTH	1495.00	1498.85	1503.00	1506.15	1508.80
RO					
SCI	4.00			4.25	4.00
TMAX	425	420	425	415	427
S1	0.16	0.08	0.15	0.07	0.00
S2	0.93	0.31	0.88	0.47	0.14
S3	0.09	0.14	0.00	0.19	0.95
HI	93	52	110	235	70
OI	9.0	23.3	0.0	95.0	475

WELL	34/8-2	34/8-2	34/8-2	34/8-2	34/10-18
DEPTH	2898.50	2902.00	2911.00	2917.00	2351.40
RO			0.5		
SCI			4.75		
TMAX	427	432	427	437	418
S1	0.04	0.12	0.19	0.07	2.78
S2	1.90	13.59	24.78	1.20	8.00
S3	1.34	1.03	1.06	0.98	
HI	119	309	344	92	233
OI	83.8	23.4	14.7	75.4	

WELL	34/10-18	34/10-18	34/10-18	34/10-18	34/10-18
DEPTH	2351.65	2351.75	2352.30	2352.60	2352.80
RO					
SCI					
TMAX	414	417	413		425
S1	3.60	3.37	1.60		5.75
S2	11.68	11.44	13.38		17.1
S3					
HI	259	262	245		271
OI					

WELL	34/10-18	34/10-18	34/10-18	34/10-18	34/10-18
DEPTH	2353.70	2354.10	2354.50	2354.90	2355.05
RO					
SCI					
TMAX	416	416	414	414	428
S1	3.26	2.18	2.30	2.16	0.51
S2	40.51	36.23	31.88	39.06	3.33
S3					
HI	362	403	385	396	107
OI					

WELL	34/10-18	34/10-18	34/10-18	34/10-18	34/10-18
DEPTH	2355.20	2355.40	2355.60	2355.80	2355.90
RO					
SCI					
TMAX			416	425	414
S1			1.15	1.85	1.05
S2			15.47	10.60	12.77
S3					
HI			249	139	166
OI					

WELL	34/10-18	34/10-18	34/10-18	34/10-18	34/10-18
DEPTH	2361.00	2361.30	2361.70	2361.90	2362.50
RO					
SCI					
TMAX	428	426	428	424	422
S1	0.14	0.28	0.25	0.29	0.41
S2	1.08	1.86	2.10	1.11	0.81
S3					
HI	41	37	47	36	28
OI					

WELL	34/10-18	34/10-18	34/10-18	34/10-18	34/10-18
DEPTH	2363.00	2363.20	2364.00	2364.30	2364.85
RO					
SCI					
TMAX	428	427	429	424	430
S1	0.24	0.22	0.33	0.15	0.40
S2	1.44	1.02	2.71	0.73	3.44
S3					
HI	41	33	117	30	132
OI					

WELL	34/10-18	34/10-18	34/10-18	34/10-18	34/10-18
DEPTH	2365.50	2365.90	2366.30	2366.80	2367.00
RO					
SCI					
TMAX			428	425	
S1			0.34	0.29	
S2			3.04	4.44	
S3					
HI			122	213	
OI					

WELL	34/10-18	34/10-18	34/10-18	34/10-18
DEPTH	2367.40	2367.60	2367.90	2368.00
RO				
SCI				
TMAX	423	419		
S1	0.20	0.77		
S2	1.09	10.67		
S3				
HI	87	172		
OI				

WELL	A	A	A	A	B
DEPTH	29.7	60.3	66.3	98.1	34.75
RO			0.58		
SCI					
TMAX	434	422	430	425	426
S1	0.31	1.04	1.39	0.20	0.19
S2	4.50	15.60	17.9	1.57	2.23
S3					
HI	336	344	482	207	178
OI					

WELL	B	B	B	B	C
DEPTH	48.25	50.75	60.68	62.25	20.85
RO		0.44	0.15		
SCI					
TMAX	436	432	0	435	443
S1	0.10	0.04	0.00	0.12	0.56
S2	12.7	28.0		11.5	9.42
S3					
HI	383	456		340	369
OI					

WELL	C	C	C	D	D
DEPTH	122.30	132.15	139.29	38.00	86.25
RO					
SCI					
TMAX	439	434	432	428	433
S1	2.74	7.40	11.80	0.18	1.11
S2	26.0	45.7	69.5	0.93	26.2
S3					
HI	423	452	457	93	421
OI					

WELL	D	D	D	E	E
DEPTH	94.75	113.75	154.75	116.43	124.75
RO	0.45				0.52
SCI					
TMAX	435	438	436	431	437
S1	0.24	0.21	0.13	1.56	0.23
S2	6.64	10.6	4.35	31.0	9.13
S3					
HI	369	368	292	438	394
OI					

WELL	E	F	F	F	F
DEPTH	152.50	142.50	228.00	237.50	268.75
RO				0.54	
SCI					
TMAX	439	431	434	430	437
S1	0.45	1.11	1.07	1.29	0.36
S2	19.2	26.9	22.4	35.1	11.8
S3					
HI	384	457	461	445	360
OI					

WELL	G	G	H	H	H
DEPTH	59.25	64.75	17.50	45.25	51.50
RO	0.49			0.52	
SCI					
TMAX	436	438	432	428	423
S1	2.40	1.60	0.28	0.43	0.76
S2	25.3	23.5	3.00	8.43	29.6
S3					
HI	423	426	196	371	514
OI					

WELL	H	H	I	I	I
DEPTH	73.75	87.50	16.70	19.30	34.20
RO				0.59	
SCI					
TMAX	433	435	423	425	433
S1	0.20	0.25	1.05	1.82	0.23
S2	3.63	12.9	33.6	27.8	7.22
S3					
HI	265	347	458	385	306
OI					

WELL	I	J	J	J	J
DEPTH	43.40	153.25	159.50	185.75	197.50
RO		0.47			
SCI					
TMAX	430	431	434	433	435
S1	0.29	0.81	0.81	0.57	0.54
S2	3.61	25.7	16.2	17.3	18.0
S3					
HI	282	422	427	459	438
OI					

WELL	K	K	K	K	L
DEPTH	35.00	134.49	144.49	203.00	77.25
RO					0.46
SCI					
TMAX	437	427	429	438	423
S1	0.35	1.81	1.11	0.39	0.28
S2	18.7	32.9	23.5	9.47	7.05
S3					
HI	416	457	407	438	291
OI					

WELL	L	L	M	N	N
DEPTH	81.35	89.75	106.00	745.45	829.06
RO					
SCI					
TMAX	430	436	439	439	434
S1	0.00	0.12	0.29	0.15	1.43
S2	30.4	12.0	4.81	2.17	20.7
S3					
HI	443	357	329	417	469
OI					

WELL	N	N
DEPTH	832.10	905.56
RO		
SCI		
TMAX	427	431
S1	1.78	0.28
S2	25.1	2.11
S3		
HI	465	320
OI		